# Determination of the Role of Group G *Streptococcus* in the Pathogenesis of Rheumatic Heart Disease Using a Rat Model

**Suchandan Sikder**
Doctor of Veterinary Medicine (DVM)
Master of Science (MS) in Medicine


Submitted in fulfilment of the requirements for
the degree of Doctor of Philosophy
in the College of Public Health, Medical and Veterinary Sciences
James Cook University
May 2018

## ELECTRONIC COPY

I, the undersigned, the author of this work, know that this thesis will be available at James Cook University Library and, Australian Digital Theses Network. Here, I declare that the electronic copy of this thesis is an accurate copy of the print thesis submitted, within the limits of the technology available.

I understand that, as an unpublished work, this thesis has significant protection under the Copyright Act and I do not wish to place any further restriction on access to this work.

Suchandan Sikder
May 2018

**STATEMENT OF SOURCES**

**DECLERATION**

I declare that this thesis is my own work and has not been submitted in any form for another degree or diploma at any university or other institution of tertiary education. Information derived from the published or unpublished work of others has been acknowledged in the text and a list of references given.

Suchandan Sikder

May 2018

## DECLARATION OF ETHICS

The research presented and reported in this thesis was conducted in accordance to the institutional guidelines according to the requirements of the James Cook University Animal Ethics Committee (Approval number #A2083) and in accordance with the National Health and Medical Research Council's (NHMRC) Australian Code of Practice for the Care and Use of Animals for Scientific Purposes.

Suchandan Sikder
May 2018

## ACKNOWLEDGEMENTS

I must begin by thanking all those people who have helped me during the entire course of my PhD and those who have inspired me thru. I might not be able to mention each of them here, but I am thankful and touched, and hope to cross-paths again someday.

I express my deepest gratitude to my supervisors, Associate Professors Catherine Rush and Brenda Govan for valuable technical advice and constructive critique during my entire project.

I would like to thank my former primary supervisor Professor Natkunam Ketheesan, for accepting me a PhD student and giving me the opportunity to work in this project. Many thanks for your support, advice and encouragement throughout my entire thesis.

I must thank my fellows within the 'Infectious Disease and Immunopathogenesis Research Group' to share practical knowledge and 'hands on' assistance with me over the last four years. Here, I should mention specially Dr Natasha Williams, Md Abdul Alim, Georgina Price, Dr Jodie Morris and Dr Alanna Sorenson.

I wish to thank the students, staffs in the reception, administration, techies and laboratories within the College of Public Health, Medical and Veterinary Sciences who all worked hard and spent time for me to keep my journey running smoothly. Special thanks to Laurie Reilly, Karen Reeks, Sherie Everingham, Dr Lisa Chilton, Chris Wright, Harindra Sathkumara, Paula Clancy, Scott Blyth, Grace Stanton, Katy Christi, Christine Hall and many others.

I wish to acknowledge Associate Professor Jeffrey Warner, Dean of College Dr Maxine Whittaker, and Associate Dean of Research Education Dr Kerrianne Watt for their valuable advice, motivation, suggestions and consultation especially after Ketheesan left from JCU.

Last but not least, I would like to express my gratitude and gratefulness to my parents for their sacrifice and nurturing my thought and my family. Especial thanks to my beloved wife Eti and my angel Yanti for their continuous support and accompany.

I look forward to a new journey with more adventures and challenges!

## STATEMENT OF THE CONTRIBUTION OF OTHERS

| Nature of assistance | Contribution | Names, titles and affiliations |
|---|---|---|
| **Intellectual support** | Proposal writing<br>Editorial assistance | Natkunam Ketheesan, Professor, University of New England<br>Catherine Rush, A/Professor, JCU<br>Brenda Govan, A/Professor, JCU<br>Dr David McMillan, University of the Sunshine Coast<br>Professor Kadaba Sriprakash, QIMR<br>Dr Nicole moreland, University of Auckland<br>Professor Madeleine Cunningham, University of Oklahoma |
| **Laboratory support** | Bacterial culture, purified protein preparation, lab animal handling-culling-organ collection.<br>ELISA, lymphocyte proliferation assay, histology.<br>ECG, echocardiography.<br>Flow cytometry. | Natkunam Ketheesan<br>Catherine Rush<br>Brenda Govan<br>Dr Natasha Williams, JCU<br>Md Abdul Alim<br>Georgina Price<br>Harindra Sathkumara<br>Dr Miranda Vidgen, University of the Sunshine Coast<br>Dr Scott Simpson, Dr Anil Goutam, Townsville Hospital |
| **Financial support** | Research costs<br><br>Stipend | NHMRC project grant (1026753) awarded to Natkunam Ketheesan and Catherine Rush<br>Australian Government for Endeavour Post Graduate Scholarship |
| **Data collection** | Data analysis | Dr Rabiul Alam Beg, JCU<br>A/Professor Leigh Owens, JCU<br>Catherine Rush<br>Brenda Govan |

## PUBLICATIONS

**Publications directly arising from this thesis:**

**Sikder S**, Williams NL, Sorenson AE, Alim MA, Vidgen ME, Moreland NJ, Rush CM, Simpson RS, Govan BL, Norton RE, Cunningham MW, McMillan DJ, Sriprakash KS and N Ketheesan 2017. Group G *Streptococcus* induces an autoimmune IL-17A/IFN-γ mediated carditis in the Lewis rat model of rheumatic heart disease. *Journal of Infectious Diseases*: PMID: 29236994 (Epub ahead of print, accepted as Cover Photo).

Rush CM, Govan BL, **Sikder S**, Williams NL and N Ketheesan 2014. Animal models to investigate the pathogenesis of rheumatic heart disease. *Front Pediatr* 2:116. doi: 10.3389/fped.2014.00116.

**Sikder** et al. Adoptive transfer of group A *Streptococcus* memory splenocytes and serum induces carditis in a Lewis rat autoimmune valvulitis model. (*In preparation*).

**Sikder** et al. Group G *Streptococcus* induces upregulation of VCAM-1 and ICAM-1 and facilitate transmigration of T-cells into the heart tissues during development of autoimmune carditis. (*In preparation*).

**Additional publications contributed to during this thesis period:**

Alim MA, **Sikder S**, Bridson TL, Rush CM, Govan BL, and N Ketheesan 2017. Anti-microbial function of macrophages is impaired in a diet induced model of type 2 diabetes. *Tuberculosis (Edinb)*: 102:47-54. PMID: 28061952.

Gorton D, **Sikder S**, Williams NL, Chilton L, Rush CM, Govan BL, Cunningham MW, and N Ketheesan 2016. Repeat exposure to group A streptococcal M protein exacerbates cardiac damage in a rat model of rheumatic heart disease. *Autoimmunity*: 1-8.2016.

O'Donohoe TJ, **Sikder S**, Surve N, Rudd D, Schrale RG and N Ketheesan 2018. Significance of anti-myosin antibody formation in patients with myocardial infarction: A prospective observational study. Heart, Lung and Circulation (accepted, manuscript no. HLC-D-17-00497).

## ABSTRACT

Acute rheumatic fever and rheumatic heart disease (ARF/RHD) have long been described as autoimmune sequelae of *Streptococcus pyogenes* or group A streptococcal (GAS) infection characterised by inflammatory changes to heart, joint, brain, blood vessel and skin tissue. In ARF/RHD both antibody and T-cell responses against immunodominant GAS virulence factors including M-proteins, cross-react with host tissue proteins. The M-protein antibodies activate heart endothelial cells by upregulation of adhesion molecules such as VCAM-1 and ICAM-1 to trigger an inflammatory response. Repeat exposure to GAS perpetuates the autoimmune process leading to permanent cardiac damage. However, in some ARF/RHD endemic regions, throat carriage of GAS is low but carriage of the related *Streptococcus dysgalactiae* subspecies *equisimilis* (SDSE), also known as β-haemolytic groups C and G streptococci (GCS/GGS) is high. As SDSE also express M-protein, it has been postulated that streptococci other than GAS may have the potential to initiate or exacerbate ARF/RHD. Further investigation of this hypothesis was limited due to the unavailability of an appropriate experimental model for this uniquely human disease. Using an animal model initially developed to investigate *S. pyogenes* associated ARF/RHD, we have now discovered that GGS does indeed cause both myocarditis and valvulitis, hallmarks of ARF/RHD.

We injected Lewis rats with whole-killed GGS or GGS M-protein Stg480 with or without whole-killed GAS and GAS rM5 protein to induce carditis. Carditis development was determined by electrocardiographic and echocardiographic examination of rats, and histological examination after heart retrieval. Antibody and T-cell reactivity to M-proteins and antibody cross-reactivity to host cardiac myosin and collagen I has been demonstrated. Remarkably the histological, immunological and functional changes in the hearts of rats exposed to GGS are identical to those exposed to GAS. Furthermore, antibody cross-reactivity to cardiac myosin was comparable in both GGS and GAS exposed animals providing additional evidence that GGS can induce and/or exacerbate ARF/RHD. The results provide further evidence that the heterologous GAS and GGS antigen combinations are equally as effective as homologous antigens at inducing heart pathology, heart conduction and valve abnormalities and potentially autoreactive immune responses.

The role of GAS and GGS M-protein specific antibodies and T-cells in upregulation of VCAM-1 and ICAM-1 has been investigated *in vitro* using cultured rat aortic endothelial

cells, and *in vivo* in tissue sections taken from Lewis rats immunised with GAS and GGS M-proteins. Upregulation of VCAM-1 and ICAM-1 was observed in an endothelial cell line stimulated with antibodies and/or T-cells, and in heart sections of rats injected with GAS and GGS M-proteins. Using a Transwell cell culture system, we observed that T-cells from M-protein immunised animals migrated through the endothelial monolayer. Furthermore, we observed the development of carditis in Lewis rats following injection of serum and/or splenocytes from rats previously immunised with GAS rM5 protein.

Our findings suggest that group G *Streptococcus* (GGS) and its M-protein has the potential to induce autoimmune mediated carditis in the Lewis rat model of RHD. The data provides further direct evidence that M-protein specific lymphocytes and antibodies facilitate migration of inflammatory cells to the heart and likely contribute to heart pathology in this animal model as well in human RHD.

## TABLE OF CONTENTS

## LIST OF TABLES

## LIST OF FIGURES

## COMMONLY USED ABBREVIATIONS

| | |
|---|---|
| ABC | : avidin-biotin complex |
| ABTS | : 2,2'-azino-bis(3-ethylbenzothiazoline-6-sulphonic acid) |
| AFS | : attachment factor solution |
| ANOVA | : analysis of variance |
| APC | : allophycocyanine |
| APS | : ammonium persulfate |
| AR | : aortic regurgitation |
| ARF | : acute rheumatic fever |
| ASO | : anti-streptolysin O |
| ATSI | : Aboriginal and Torres Strait Islander |
| BCA | : bicinchoninic acid assay |
| BSA | : bovine serum albumin |
| CAMs | : cell adhesion molecules |
| CD | : cluster of differentiation |
| CFU | : colony forming unit |
| CM | : cardiac myosin |
| ConA | : concanavalin A |
| cpm | : counts per minute |
| DAB | : 3,3'-diaminobenzidine |
| DNA | : deoxyribonucleic acid |
| ECG | : electrocardiography |
| ELISA | : enzyme-linked immunosorbent assay |
| CFA | : complete Freund's adjuvant |
| CINC | : cytokine-induced neutrophil chemoattractant |
| DMSO | : dimethyl sulfoxide |
| Echo | : echocardiography |
| FACS | : fluorescence-activated cell sorting |
| FFPE | : formalin fixed paraffin embedded |
| FITC | : fluorescein isothiocyanate |
| f.p. | : foot pad |
| IFA | : incomplete Freund’s adjuvant |
| GAS | : group A *Streptococcus* |
| GBS | : group B *Streptococcus* |
| GCS | : group C *Streptococcus* |
| GES | : group E *Streptococcus* |
| GGS | : group G *Streptococcus* |
| GlcNAc | : N-acetylglucosamine |
| GM | : growth medium |
| HBSS | : Hank’s balanced salt solution |
| H&E | : haematoxylin and eosin |
| HLA | : human leukocyte antigen |
| HMM | : heavy meromyosin |
| HRP | : horseradish peroxidase |
| ICAM | : inter-cellular adhesion molecule |
| IFN-γ | : interferon-gamma |
| Ig | : immunoglobulin |
| IL | : interleukin |

| | |
|---|---|
| i.m. | : intra-muscular |
| i.p. | : intra-peritoneal |
| IPTG | : isopropyl β-D-1-thiogalactopyranoside |
| IU | : international unit |
| JCU | : James Cook University |
| kDa | : kilodaltons |
| LB | : Luria-Bertani |
| LFA | : leukocyte function antigen |
| LGT | : lateral genetic transfer |
| LMM | : light meromyosin |
| LTA | : lipoteichoic acid |
| mAb | : monoclonal antibody |
| MHC | : major histocompatibility complex |
| MFI | : median fluorescence intensity |
| MNC | : mono-nuclear cells |
| MR | : mitral regurgitation |
| MS | : mitral stenosis |
| NHMRC | : National Health and Medical Research Council |
| NK | : natural killer |
| OD | : optical density |
| PBS | : phosphate buffer saline |
| PE | : phycoerythrin |
| PECAM | : platelet endothelial cell adhesion molecule |
| PMNCs | : poly-morphonuclear cells |
| QIMR | : Queensland Institute of Medical Research |
| RAOEC | : rat aortic endothelial cell |
| RAV | : rat autoimmune valvulitis |
| RHD | : rheumatic heart disease |
| rM5 | : recombinant M5 protein |
| RNA | : ribonucleic acid |
| SA node | : sinoatrial node |
| SBA | : sheep blood agar |
| s.c. | : sub-cutaneous |
| SDSE | : *Streptococcus dysgalactiae* subspecies *equisimilis* |
| SDS-PAGE | : sodium dodecyl sulfate polyacrylamide gel electrophoresis |
| SEM | : standard error of means |
| SI | : stimulation index |
| SOF | : serum opacity factor |
| TCR | : T-cell receptor |
| Th | : T-helper |
| TNF-α | : Tumour necrosis factor-alpha |
| VCAM | : vascular cell adhesion molecule |
| VLA | : very late antigen |
| WBC | : white blood corpuscles |
| WK | : whole killed |

# CHAPTER 1
# GENERAL INTRODUCTION

## 1.1 BACKGROUND

Rheumatic heart disease (RHD) is the most common acquired cause of cardiac damage in humans worldwide during the first 25 years of life (Horstkotte, et al. 1991; Marcus, et al. 1994; Murray and Lopez 1996; Carapetis, et al. 2016). The most commonly affected age group is 5-15 years old (Steer, et al. 2002; Umapathy and Saxena 2018). After single or repeated attacks of acute rheumatic fever, about 30-45% of patients develop RHD as a complication (Carapetis, et al. 2005a; Katzenellenbogen, et al. 2017). Acute rheumatic fever (ARF) is an autoimmune disease possibly caused by inflammatory responses triggered by the immune system to the group A *Streptococcus* (GAS) that cross-reacts with host tissues (Guilherme, et al. 2006; Carapetis, et al. 2016). In ARF/RHD, the patients develop a widespread inflammation in the joints, skin, brain and incurable mitral fibrosis in the heart (Carapetis and Currie 1998; Penm 2008; Parnaby and Carapetis 2010; Umapathy and Saxena 2018).

In 2015, approximately 297,300-337,300 people died of RHD and there were 33.4 million people living with it worldwide (Watkins, et al. 2017). The overall prevalence of RHD was estimated as the highest in sub-Saharan Africa, South Asia and Oceania where 10-15 per 1000 people have had RHD (Karthikeyan and Mayosi 2009; Beaton, et al. 2014; GBDS 2015). An earlier report of 2005 published that approximately 471,000 new cases of ARF are diagnosed each year (Carapetis, et al. 2005b). The incidence rate exceeds 50 per 100,000 people in developing countries although currently decreasing in the developed world (Carapetis, et al. 2005b; Parnaby and Carapetis 2010; Seckeler, et al. 2010; Lawrence, et al. 2013; Carapetis, et al. 2016). However, the communities in some high-income countries that live in poverty, have high rates of ARF/RHD, including the Indigenous populations of Australia and New Zealand (Lawrence, et al. 2013). Globally, the observed prevalence of RHD is highest in Aboriginal and Torres Strait Islander (ATSI) people in the Kimberley (1.02%) and Far North Queensland (1.14%) of Northern Australia, contributed by GAS infections (Carapetis, et al. 1996; AIHW 2004; Rothstein, et al. 2007; Seckeler and Hoke 2011; Remond, et al. 2013).

*Streptococcus pyogenes* or group A *Streptococcus* (GAS) is an opportunistic pathogen of the human pharynx and skin which is associated with a wide spectrum of diseases ranging from uncomplicated pharyngitis to severe invasive and debilitating diseases such as ARF/RHD and glomerulonephritis (Lancefield 1933; Cunningham 2000; Sims, et al. 2016). The cell surface antigens and toxins produced by GAS play a significant role in the induction of these diseases. The M-proteins of certain strains of GAS are the most extensively studied factors that are associated with ARF/RHD (Cunningham 2012; Williamson, et al. 2015; Carapetis, et al. 2016; Williamson, et al. 2016; Brahmadathan 2017; Guilherme, et al. 2017). M-proteins are fibrous coiled-coil dimer of α-helices extending from the surface of GAS that share structural homology with α-helical coiled-coil human proteins like cardiac myosin, tropomyosin, keratin, vimentin, laminin, collagen etc. (Vashishtha and Fischetti 1993; Pruksakorn, et al. 1994; Cunningham 2000; Lymbury, et al. 2003; Guilherme, et al. 2006; Guilherme and Kalil 2010). In addition to GAS, M or M-like proteins have also been reported in the related streptococci of group B (GBS), C (GCS), E (GES), and G (GGS) (Maxted 1949; Maxted and Potter 1967; Daynes and Armstrong 1973; Woolcock 1974; McNeilly and McMillan 2014). However, the association of non-group-A streptococci in the development of ARF/RHD remains underexplored.

Autoimmune molecular mimicry mechanisms initiated between streptococcal M-proteins and host tissue proteins are believed to be responsible for the development of ARF/RHD (Guilherme, et al. 2006; Jaseja, et al. 2010). Molecular mimicry between GAS and host cardiac antigens is the key event in the development of carditis (Kaplan 1963; Zabriskie 1967; Galvin, et al. 2000; Kirvan, et al. 2003). Antibody cross-reactivity between GAS M-protein and cardiac myosin has been reported (Kaplan, et al. 1964; Krisher and Cunningham 1985; Cunningham 2000; Galvin, et al. 2000; Dinkla, et al. 2003b; Cunningham 2014). Using purified anti-myosin antibodies from patients with ARF, cross-reactive epitopes were found on cardiac myosin and the M5 and M6-proteins of GAS (Cunningham, et al. 1989). Anti-collagen I antibodies also reported in patients' sera though the cross-reactivity with GAS antigens has not been confirmed (Martins, et al. 2008). In fact, GAS antigen specific T-cells could also recognise endothelial basement membrane laminin due to homology between cardiac myosin and laminin (Galvin, et al. 2000; Mertens, et al. 2000). It is believed that the cross-reactive antibodies bind to the cardiac endothelial surface and activate endothelium. The activated endothelia express and upregulate vascular cell adhesion molecule (VCAM)-1 and intercellular adhesion molecule (ICAM)-1 that bind with GAS antigen specific activated

T-cells. The binding between adhesion molecules and T-cells facilitates transmigration of T-cells into the valves and myocardium (Galvin, et al. 2000; Roberts, et al. 2001; Guilherme, et al. 2013b). However, the precise mechanisms by which cross-reactive antibodies to cardiac myosin result in cardiac lesions is not entirely clear (Fae, et al. 2005).

The inflammatory process of ARF/RHD has structural and functional effects on the heart. The characteristic histological features of ARF/RHD include mitral valvulitis and granulomatous myocarditis called Aschoff bodies with infiltration of T-cells, macrophages, fibroblasts and neutrophils (Roberts, et al. 2001; Pahlman, et al. 2006). There are reports of predominantly CD4+ T-cell infiltration than CD8+ T-cells during the development of carditis (Ganguly, et al. 1982; Lue, et al. 1983; Bhatia, et al. 1989; Morris, et al. 1993b; Narin, et al. 1995; Guilherme, et al. 2001a; Roberts, et al. 2001; Ellis, et al. 2005; Toor and Vohra 2012). Among the CD4+ T-cells, Roberts, et al. (2001) identified more Th1 T-cells than Th2 cells. The T-cells are major functional phenotypes responsible for formation of Aschoff bodies beneath the endocardium which is considered as hallmark histological finding of rheumatic heart (Chopra, et al. 1988; Fraser, et al. 1995). Chronic inflammation of mitral valve and myocardium leads to mitral stenosis and regurgitation and myocardial conduction abnormalities (Cunningham 2012; Carapetis, et al. 2016). Electrocardiographic (ECG) detection of prolonged P-R intervals in an ECG trace is commonly used as a Jones minor criterion for the detection of myocardial conduction abnormality (Gewitz, et al. 2015). Furthermore, echocardiographic (echo) demonstration of suspected patients enabled early diagnosis, and monitor disease progression (Carapetis, et al. 2016). Common echo findings are mitral valvular thickness, presence of nodules and regurgitation (Jain and Mankad 2013; Wunderlich, et al. 2013).

Various animal models have been used to investigate the rheumatogenic potential of GAS M-proteins (Norlin 1959; Dale and Beachey 1986; Sargent, et al. 1987; Haidan, et al. 2000; Burova, et al. 2004; Burova, et al. 2005; Gorton, et al. 2009; Guilherme, et al. 2011b; Gorton, et al. 2016). Guinea pigs injected with heat killed or lysed GAS or GAS M-protein induced myocarditis and valvulitis with increased T-cell and B-cell, macrophage and fibroblast infiltration in the myocardium and mitral valve (Gross, et al. 1929; Yang, et al. 1977). New Zealand White rabbits injected with GAS M1, M5 or M22 expressing strains induced degeneration of myocardium with verrucous endocarditis and infiltration of macrophage, lymphocytes, and granulocytes (Norlin 1959; Dale and Beachey 1986; Sargent, et al. 1987;

Burova, et al. 2004; Burova, et al. 2005). BALB/c and Swiss mice injected with GAS M3-strain or cell wall fragments produced cross-reacted antibodies to basement membrane collagen (Ohanian, et al. 1969; Dinkla, et al. 2003b). However, Lewis rat autoimmune valvulitis (RAV) model has been used successfully to study pathogenesis of ARF/RHD (Galvin, et al. 2002; Rush, et al. 2014; Gorton, et al. 2016). Repeated injections of Lewis rats with whole killed GAS or purified M-proteins (M5, MT4, MT6, MT7) developed mitral valvulitis and myocarditis with infiltration of mononuclear cells, neutrophils, and fibroblasts. There was increased opsonic serum IgG titres against GAS M-proteins and cardiac myosin with high concentrations of antigen specific T-cell derived cytokines such as; IL-2, IL-6, IL-10, IL-12, IFN-γ and TNF-α (Quinn, et al. 2001; Lymbury, et al. 2003; Li, et al. 2004; Gorton, et al. 2006; Gorton, et al. 2009; Huang, et al. 2009; Gorton, et al. 2010; Xie, et al. 2010; Kirvan, et al. 2014; Gorton, et al. 2016). The cytokines regulate the heart damage in ARF/RHD.

Having the highest documented rates of ARF/RHD in the Indigenous population of Northern Australia the pharyngeal carriage rates of GAS was reported low; only 4% throat swabs were positive to GAS (Carapetis and Currie 1997; McDonald, et al. 2004). Classic rheumatic M-serotypes were absent in these populations (Hartas, et al. 1995). Similar patterns of throat carriage have been reported in Ethiopia, Jamaica and Southern India that have high burden of ARF/RHD (Steer, et al. 2002; Brahmadathan, et al. 2005). However, Indigenous people of the Northern Territory of Australia often suffer from GAS skin sores rather than throat infections (McDonald, et al. 2004). Furthermore, high carriage rates of group C (GCS) and G (GGS) streptococci have been documented in the Indigenous communities of Australia and New Zealand (Haidan, et al. 2000; O'Sullivan, et al. 2017). Such findings have led to the hypothesis that ARF/RHD may arise from GAS pyoderma or from pharyngitis due to non-GAS strains that have inherited certain GAS virulence factors important for initiating ARF/RHD (McDonald, et al. 2004).

Group C (GCS) and G (GGS) streptococci are closely related to GAS. The GCS and GGS are grouped together because some species of streptococci hold both Lancefield group C and G carbohydrates for example; *Streptococcus dysgalactiae* subspecies *equisimilis*, SDSE (McMillan, et al. 2010). In addition, they share the same tissue niche in humans and cause a similar spectrum of diseases such as pharyngitis, impetigo, cellulitis, bacteraemia and necrotising fasciitis. Significantly, GCS/GGS and GAS have similar virulence factors and are

known to exchange genetic material (Bisno, et al. 1987; Bisno, et al. 1996; Sriprakash and Hartas 1996; Williams 2003; Towers, et al. 2004; Davies, et al. 2005; McNeilly and McMillan 2014). Some GCS and GGS are known to possess M-proteins with high sequence and structural homology to the M-types of ARF-associated GAS (Jones and Fischetti 1987; Collins, et al. 1992; Bisno, et al. 1996). Furthermore, GCS and GGS were recovered from children after recurrent severe pharyngitis who subsequently developed ARF (Davies, et al. 2005; Chandnani, et al. 2015). Development of ARF following GAS pyoderma and GGS pharyngitis also reported recently in an Indigenous Maori boy in New Zealand (O'Sullivan, et al. 2017). Antibodies against GGS strains have also been shown to react with human heart myosin (Haidan, et al. 2000). Similar to GAS, GGS possesses M-proteins that bind human collagen IV and are required for the establishment of infection (Dinkla, et al. 2003b; Dinkla, et al. 2007). Collectively, these observations strongly suggest that GGS possesses many of the GAS characteristics which are linked to the pathogenesis of ARF/RHD.

Animal model studies have not yet determined a role for GCS in inducing ARF/RHD (Cromartie, et al. 1977; Yang, et al. 1977). Yang, et al. (1977) demonstrated that GCS possesses non-rheumatogenic antigens that did not induce antibodies and T-cells cross-reactive to cardiac myosin. Cromartie, et al. (1977) did not find any significant changes in the heart sections of Sprague-Dawley rat injected with GCS. However, the association of GGS in the development of ARF/RHD has also not been demonstrated previously (Collins, et al. 1992; Haidan, et al. 2000; Davies, et al. 2005; McDonald, et al. 2006; Dinkla, et al. 2007). Therefore, further studies are warranted to explore the rheumatogenic potential of GGS in the pathogenesis of ARF/RHD (WHO 1988; Taranta and Markowitz 1989; Bisno 1996; Carapetis, et al. 1999).

## 1.2 SIGNIFICANCE OF THE STUDY

Several key questions regarding the involvement of GGS in the pathogenesis of ARF/RHD need to be answered. Does GGS and/or its M-protein have the potential to cause autoimmune mediated carditis? Do GGS M-proteins exacerbate GAS-triggered carditis? Do GAS M-proteins exacerbate GGS M-protein triggered carditis? Do GGS M-protein specific antibodies and splenocytes activate vascular endothelia and facilitate T-cell transmigration to the heart tissues? Do the pathological changes in the heart detectable by electro-physical and echocardiographic examination? In addition, to demonstrate the role of antibodies and T-cells whether the GAS M-protein specific antibodies and splenocytes could passively transfer the

disease into the syngeneic naïve animals was also be explored in this study. The Lewis rat autoimmune valvulitis (RAV) model of ARF/RHD is a suitable animal model to investigate the questions as it is known to develop carditis in earlier animal studies (Quinn, et al. 2001; Galvin, et al. 2002; Gorton, et al. 2009; Rush, et al. 2014; Gorton, et al. 2016).

The specific Aims of this project were:

1. To determine the reactivity of sera from GGS and/or GAS injected rats with whole-killed or M-proteins of GAS and GGS, and cross-reactivity with cardiac myosin and collagen I (outlined in Chapter 5 and 7).
2. To measure memory T-cell proliferative response and the phenotype of proliferating T-cells from rats using *ex vivo* re-stimulation with GGS Stg480 and GAS rM5 and by measuring cytokines respectively (outlined in Chapter 5 and 7).
3. To demonstrate the effect of whole-killed and M-protein of GGS and/or GAS on heart tissue using histology (outlined in Chapter 6 and 7).
4. To determine GAS rM5 protein specific serum and splenocytes induced heart pathology following passive transfer (outlined in Chapter 8).
5. To examine cardiac dysfunction and pathology by performing electrocardiography and echocardiography (outlined in Chapter 6, 7 and 8).
6. To demonstrate expression of VCAM-1 and ICAM-1 *in vitro* in cultured endothelial cells following exposure to GAS and GGS M-protein specific serum and/or splenocytes and *in vivo* in heart tissues from rats injected with GAS and GGS M-proteins (outlined in Chapter 9).
7. To determine T-cell transmigration across endothelial cell monolayers using a Transwell culture system (outlined in Chapter 9).

A final chapter (Chapter 10) will discuss the general findings of this study, including its successful outcomes and its limitations. Future directions which may supplement the body of this work and provide further insights into the mechanisms that initiate development of ARF/RHD are also put forward.

# CHAPTER 2
# LITERATURE REVIEW

## 2.1 INTRODUCTION

Acute rheumatic fever (ARF) and rheumatic heart disease (RHD) are autoimmune diseases following *Streptococcus pyogenes* or group A *Streptococcus* (GAS) infection of throat or skin (Beattie 1907; Carapetis, et al. 2016; Umapathy and Saxena 2018). Following GAS infections, immune responses in particular the T-cells and antibodies generated against antigens of GAS cross-react with host antigens of skin, joints, muscle, central nervous system, and heart (Carapetis, et al. 2016). Repeated exposure to GAS ends with life threatening long term sequela such as chronic, untreatable rheumatic heart disease or glomerulonephritis. ARF/RHD are the most common acquired cause of cardiac damage during early stage of life (Cunningham 2014). In 2015, RHD alone caused 297,300-337,300 deaths with an approximate prevalence of 33.4 million worldwide (Watkins, et al. 2017). Although ARF/RHD are prevalent mostly in low and middle-income countries, the highest prevalence rates are reported in Indigenous communities of Australia and New Zealand may be due to similar socio-economic status (Carapetis, et al. 1996; AIHW 2004; Rothstein, et al. 2007; Seckeler and Hoke 2011; Lawrence, et al. 2013; Remond, et al. 2013). Irrespective of the highest documented rates of ARF/RHD in these pacific communities, throat carriage rates of GAS were reported to be low, with absence of rheumatogenic M-types (Hartas, et al. 1995; Carapetis and Currie 1997; Haidan, et al. 2000). Such findings have led to the hypothesis that ARF may arise from GAS skin infections or from pharyngitis due to non-GAS strains that inherited certain GAS antigens that are important for triggering ARF/RHD (McDonald, et al. 2004).

Epidemiological studies from Australian and Indian communities have provided the rationale for the involvement of non-GAS in the development of ARF/RHD (Carapetis and Currie 1997; Haidan, et al. 2000; Steer, et al. 2002; McDonald, et al. 2004; Brahmadathan, et al. 2005; McDonald, et al. 2006). High carriage rates of *Streptococcus dysgalactiae* subspecies *equisimilis* or group G *Streptococcus* (GGS) that have both Lancefield's group C and G carbohydrates has been documented in the resource poor setting areas of developing countries and Indigenous communities of Australia and New Zealand (Haidan, et al. 2000). Both GGS and GAS are related species and share similar characteristics such as colonisation, disease spectrums and virulence factors for example M-proteins (Bisno, et al. 1987; Jones and

Fischetti 1987; Collins, et al. 1992; Bisno 1996; Bisno, et al. 1996; Sriprakash and Hartas 1996; Carapetis, et al. 1999; Haidan, et al. 2000; Williams 2003; Davies, et al. 2005). However, an association between GGS and ARF/RHD has never been established (Collins, et al. 1992; Haidan, et al. 2000; Davies, et al. 2005; McDonald, et al. 2006; Dinkla, et al. 2007). Hence, further studies are necessary to explore the rheumatogenic potential of group G *Streptococcus* in the development of ARF/RHD (WHO 1988; Taranta and Markowitz 1989; Bisno 1996; Carapetis, et al. 1999).

## 2.2 AETIOLOGICAL AGENT(S) OF ARF/RHD

Over the last century, *Streptococcus pyogenes* or group A *Streptococcus* (GAS) is reported as the only triggering cause of ARF/RHD (Beattie 1907; Carapetis, et al. 2016). The host immune responses induced by untreated GAS infections of throat and/or less reported skin, mistakenly cross-react with self-proteins located in skin, joints, nervous system, muscles, and heart tissues causing acute rheumatic fever (ARF) (Carapetis and Currie 1998; Stewart, et al. 2007; Kerdemelidis, et al. 2010; Parnaby and Carapetis 2010). Repeated or sometimes a single attack of ARF may result in irreparable chronic carditis (RHD) (Carapetis, et al. 2016).

### 2.2.1 Group A *Streptococcus* (GAS)

Streptococci are spherical, Gram-positive bacteria that grow in chains or pairs. Based on their haemolytic properties, streptococci are classified into α-, β- and γ-haemolytic groups. The β-haemolytic streptococci are further classified into 20 serotypes by Lancefield based on the specific carbohydrates present on the cell wall (Lancefield 1933). Among the 20 described serotypes groups A-V (excluding I and J), groups A-D, and F-H have variable degrees of clinical significance in human including ARF/RHD. However, the β-haemolytic group A *Streptococcus* or GAS is the only documented aetiological agent that triggers ARF/RHD (Beattie 1907; Carapetis, et al. 2016).

Group A *Streptococcus* is part of the normal flora of pharynx and skin along with other non-GAS streptococci such as group C *Streptococcus* (GCS) and group G *Streptococcus* (GGS) that have many characteristics similar to GAS. Although the prevalence of ARF/RHD is reported to be the highest in the Indigenous communities of Australia and New Zealand, pharyngeal carriage rates of GAS are reported to be lower than GCS and GGS (Hartas, et al. 1995; Carapetis and Currie 1997; Haidan, et al. 2000; McDonald, et al. 2004; O'Sullivan, et al. 2017). Developing countries like Ethiopia, Jamaica and Southern India also have similar

patterns of throat carriage of streptococci (Steer, et al. 2002; Brahmadathan, et al. 2005). Therefore, the epidemiological findings questioned the role of GAS skin infections or non-GAS throat infections in triggering ARF/RHD (McDonald, et al. 2004).

#### 2.2.1.1 Spectrum of diseases caused by GAS

The scale of infection caused by GAS is ranges from uncomplicated pharyngitis to severe invasive and debilitating diseases such as rheumatic fever and glomerulonephritis (Cunningham 2000). Pharyngitis or sore throat is the most common manifestation of GAS infection (Ferretti, et al. 2016). Approximately 30% of sore throats in children are diagnosed as being associated with GAS (Ebell, et al. 2000; Shaikh, et al. 2010). The highest incidence of GAS pharyngitis occurs in children of school age (Danchin, et al. 2007). Pharyngitis is often associated with skin rash on the trunk and extremities known as scarlet fever. GAS pharyngitis may lead to complications that include peritonsillar cellulitis, peritonsillar abscess, retropharyngeal abscess, suppurative cervical lymphadenitis, mastoiditis, acute sinusitis, and otitis media (Dajani, et al. 1995). This organism also attacks the superficial keratin layer of the skin causing impetigo that leads to glomerulonephritis. Infection of the superficial epidermis causes mild to severe erysipelas. Erysipelas may extend to the subcutaneous tissue causing cellulitis, or the fascia causing life-threatening necrotising fasciitis, or even deeper into muscle causing myositis and myonecrosis (Ferretti, et al. 2016). It also causes streptococcal toxic shock syndrome. GAS also contribute to the occurrence of perianal cellulitis and vulvo-vaginitis in children (Mogielnicki, et al. 2000; Petersen, et al. 2003). Untreated or poorly treated GAS infections may lead to complications like glomerulonephritis and chronic RHD.

Group A streptococcal infection of skin or pharynx may extend to chronic, debilitating glomerulonephritis within 10-14 days of infection. However, groups C and G streptococci may also have a role in this disease sequelae (Ferretti, et al. 2016). Nephritogenic strains of streptococci induce formation of immune complexes that are found in the circulation and deposited in the glomeruli. Alternately, the antigen and antibody deposit separately in the glomerular basement membrane and form immune complexes, causing *in situ* immune complex disease (Poon-King, et al. 1993; Nordstrand, et al. 2000; Yoshizawa, et al. 2004; Batsford, et al. 2005; Oda, et al. 2010).

However, acute rheumatic fever (ARF) is the most common sequelae that occurs several weeks to several months after GAS pharyngitis (Stollerman 1997; Stollerman 2011). Acute rheumatic fever is a global disease which includes major manifestations of the heart, brain, joints, and skin (Steer, et al. 2002; McDonald, et al. 2004; Carapetis, et al. 2016). In susceptible individuals, infection with GAS generate antibodies and T-cells which also recognise host antigens located in the heart, brain, joints, and skin (Galvin, et al. 2000; Ellis, et al. 2005; Fae, et al. 2006; Kirvan, et al. 2006; Ben-Pazi, et al. 2013; Cunningham 2014). As a result, the patients suffer from migratory polyarthritis due to the formation and deposition of immune complexes. Polyarthritis is the most common manifestation of ARF. The cross-reactive antibodies may bind to the basal ganglia and neuronal cells causing Sydenham chorea (Taranta and Stollerman 1956). The antibodies may also bind to the keratin of skin that lead to erythema marginatum and subcutaneous nodules. However, the autoreactive antibodies and T-cells bind with many antigens of the heart resulting in inflammation of both heart valves and the myocardium. The myocardium may heal after inflammation, however there may be permanent damage to the valves, which leads to chronic carditis known as rheumatic heart disease (RHD) (Carapetis, et al. 2016).

#### 2.2.1.2 Virulence factors of GAS

Group A streptococcal surface antigens and toxins have significant roles in the establishment of infection into a host. Important virulence factors of GAS include M-proteins and lipoteichoic acid that help in attachment; a hyaluronic acid capsule that inhibits phagocytosis. Other extracellular products, such as pyrogenic toxin, which causes the rash of scarlet fever; and streptokinase, streptodornase, and streptolysins. However, M-proteins are the most extensively studied virulence factors for ARF/RHD (Markowitz and Gerber 1987; Johnson, et al. 1992; Shikhman, et al. 1994; Stollerman 1997; Cunningham 2000; Shulman, et al. 2006).

**M-protein**

Streptococcal M-proteins are the best-defined virulence factors and are also vaccine candidate antigens (Suyama, et al. 2006; Yang 2007). M-proteins extend from the surface of the streptococci and share sequence homology with human heart proteins (Cunningham 2014; Carapetis, et al. 2016).

*Structure of M-protein*

Streptococcal M-proteins have fibrous coiled-coil dimer of α-helices structures (Swanson, et al. 1969; Phillips, et al. 1981). M-proteins share a common framework having a conserved signal peptide (Phillips, et al. 1981; Haanes-Fritz, et al. 1988). M-proteins have a hyper variable N-terminus, a less variable central domain and a highly conserved C-terminus (Figure 2.1&2.2). The N-terminus is directed outward from the bacteria and is antigenically highly variable with more than 80 different defined serotypes (Fischetti 1989). The C-terminal region binds to the peptidoglycan of the cell wall (Fischetti, et al. 1985). The degree of sequence homology between serotypes increases as the sequence approaches the C-terminus (Fischetti 1989). Nearly the whole protein forms a coiled coil, the only exception is being the first 10-20 amino acids at the N-terminus and cell wall associated residues at the C-terminus (Fischetti 1989). Like most coiled coil proteins, M-proteins contain repeated sequences of heptad periodicity. These repeat regions within the M-proteins are grouped into four domains such as A, B, C and D (Hallas and Widdowson 1983; Fischetti 1989; Proft, et al. 1999; Stevens and Kaplan 2000). The three common patterns correlate with the host colonisation site. Pattern A-C strains were reported in throat colonisation. The D and E strains recovered mostly from pyoderma and both pharyngitis and pyoderma, correspondingly (Shulman, et al. 2004; Bessen and Lizano 2010).

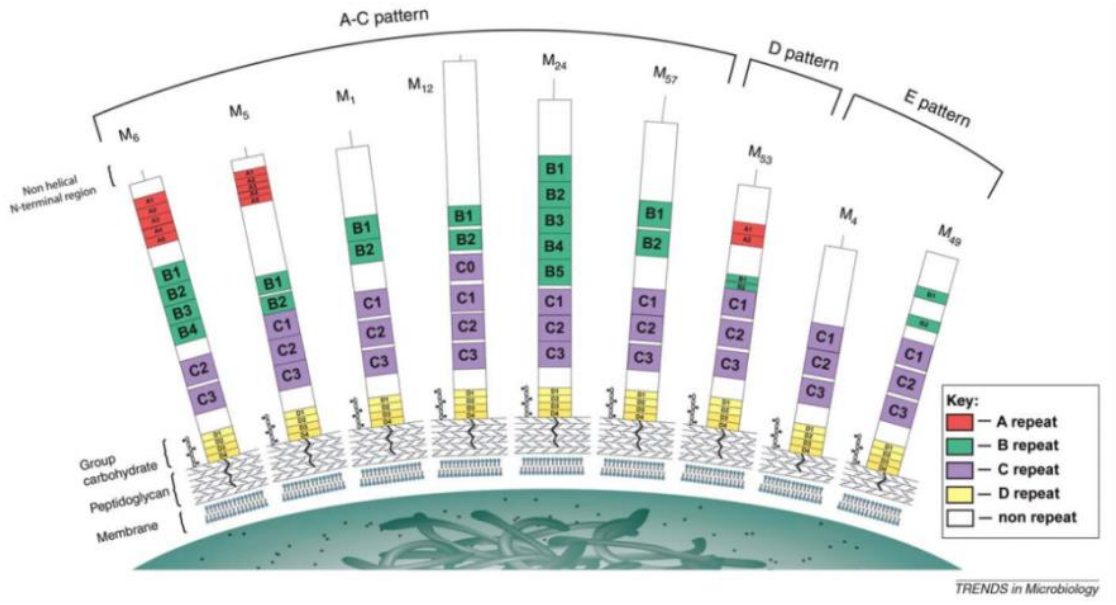


**Figure 2.1** The most-reported M-proteins of group A *Streptococcus*. Each M-protein is represented with hyper-variable N-terminus (outer end), conserved C-region (attached to the cell wall), and less-variable B-region (between N- and C-termini). The patterns A-E have been isolated from different colonisation sites. The image is adapted from Smeesters, et al. (2010).

The N-terminus is the best studied fragment regarding the structure and immunochemistry, and little is known about the C-terminal half of the molecule from any M-serotype (Beachey, et al. 1977). M-proteins from different streptococcal strains may vary in molecular weight and antigenicity (Fischetti, et al. 1985). The M6-protein represents characteristics of a typical rheumatogenic M-protein (Figure 2.2). The non-helical part of the hypervariable region of the M6-protein possesses 11 amino acids. The A repeat region consists of five repeats of 14 amino acids each and the B, C and D repeats of four, two and four repeats of 25, 35 and seven residues each correspondingly (Hollingshead, et al. 1986; Fischetti 1989). Sequence conservation increases from the A repeats to D repeats. The wall-spanning domain of M6 contains 48 residues (Fischetti, et al. 1988).

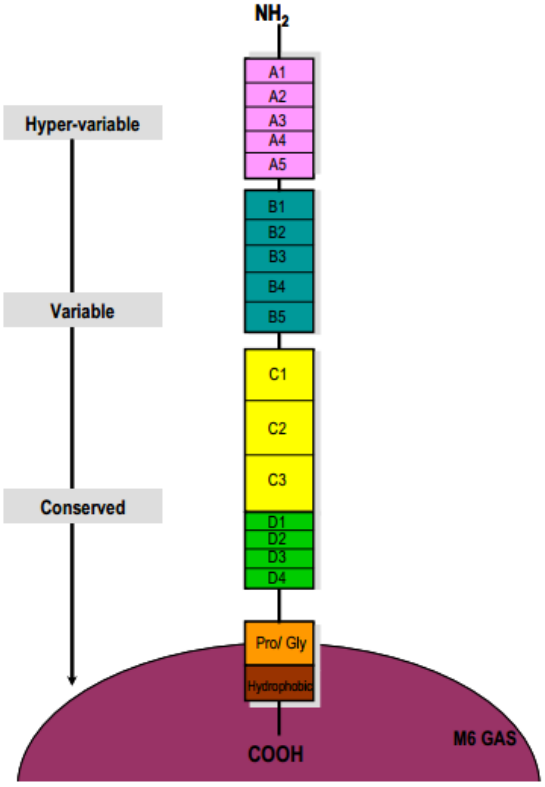


**Figure 2.2** Structure of group A streptococcal M6-protein. The molecule is anchored in the cell wall via the C-terminus and exists as a coiled coil structure. The M6-protein consists of A, B, C and D repeats with capacity to bind several human plasma proteins. The A, B and D repeats may not be present in all M-proteins. The image is adapted from Smeesters, et al. (2010).

*Functions of M-protein*

The structure and sequence of the M-proteins are probably the key contributors for the induction of host cross-reactive responses. The M-proteins can inhibit phagocytosis in the absence of opsonising antibodies in non-immune human host (Lancefield 1962). The N-terminal part is responsible for antigenic variations and efficient serotyping and nucleotide

based *emm*-typing schemes (Fischetti 1989; Facklam, et al. 1999; Cunningham 2000). It also elicits protective antibodies in a type specific manner and is therefore considered as a GAS vaccine candidate (McNeil, et al. 2005). Similarly, the C-terminal region has binding capability to many host molecules (Fischetti 1989; Cunningham 2000; Smeesters, et al. 2008). It also offers an opportunity to develop a broad coverage vaccine (Batzloff, et al. 2003). The C-repeat region consists of 35-42 amino acid repeat units that display high sequence homology with cardiac myosin. SV1 is a GAS vaccine candidate that is constructed from the C-repeat region. Injection of SV1 in Lewis rats did not induce carditis and T-cell response to cardiac myosin, but induced antibodies that recognise majority of GAS M-types demonstrating SV1 as a potentially safe vaccine candidate (McNeilly, et al. 2016). In contrast, the central region has received less attention, although it has been reported to have rheumatogenic epitopes in some *emm*-types. Cross-reactive epitopes against myocardium, synovia and brain are located between the B and C repeat regions. Based on whether M-proteins react with a monoclonal antibody that targets epitopes in the C repeat region of the M6 molecule, streptococci are often classified into Class I or II. The majority of Class I strains are implicated in ARF/RHD. Due to circulation of homologous anti-M-protein antibodies, reinfections with the same serological M-type are relatively less common. Limited clinical evidence exists supporting the involvement of these anti-M-protein antibodies in disease pathogenesis. However, antibodies purified from the sera of patients with ARF/RHD have been shown to react with both M-proteins and host cardiac myosin (Cunningham, et al. 1988; Cunningham, et al. 1989).

*Molecular mimicry*

Molecular mimicry is the sharing of antigenic epitopes by the microbes and the host tissues. In ARF/RHD, streptococcal M-proteins share structural homology with α-helical coiled-coil proteins of host heart such as cardiac myosin, laminin, vimentin, collagen, tropomyosin, keratin, etc. to which they cross-react (Zabriskie and Freimer 1966; Dale and Beachey 1985b; Dale and Beachey 1986; Oldstone 1987; Sargent, et al. 1987; Cunningham, et al. 1988; Damian 1989; Fischetti 1989; Veasy and Hill 1997; Cunningham 2000; Cunningham 2004; Carapetis, et al. 2005a; Fae, et al. 2005; Guilherme, et al. 2006; Guilherme and Kalil 2008; Guilherme and Kalil 2010; Jaseja, et al. 2010). Among the host tissue proteins, cardiac myosin seems to be the major target of cross-reactivity.

Previous studies demonstrated that the cross-reactive antibodies to streptococcal membrane antigens were present in sera of patients with ARF/RHD (Zabriskie 1967; Zabriskie, et al. 1970). Several studies reported anti-M protein antibodies in the sera of patients with ARF/RHD that have cross-reacted with cardiac myosin and vimentin, suggesting these proteins were the target autoantigens recognised in the heart (Dale and Beachey 1985a; Krisher and Cunningham 1985; Cunningham, et al. 1986; Cunningham and Swerlick 1986; Baird, et al. 1991). Krisher and Cunningham (1985) also reported high molecular weight proteins in the human heart tissue extracts that have reacted with GAS specific antibody and monoclonal antibody (mAb) to ventricular myosin. Adsorption of the anti-GAS antibody with GAS reduced reactivity of the antibody for both GAS and cardiac myosin at the same time. Using anti-myosin antibodies in sera from patients with ARF, purified by affinity chromatography Cunningham, et al. (1989) observed that the cross-reactive epitopes were on cardiac myosin and the N-acetylglucosamine (GlcNAc) epitope of the N-terminus of the M5 or M6-proteins of GAS. In the same study, the authors also observed that the murine mAb reactions with M5-peptides were inhibited by overlapping M-protein peptides SM5(164-197)C and SM5(184-197)C. The authors summarised that majority of the mouse and human myosin cross-reactive antibodies could react with an epitope within the C terminus of GAS M5-peptide. Advanced studies demonstrated that the potential rheumatogenic epitopes of cardiac myosin are located in the S2 region (Figure 2.3). Ellis, et al. (2010) reported that regardless of the infecting GAS M serotype, the cardiac myosin epitopes target the S2 region of cardiac myosin and are similar among RHD populations worldwide. Garcia, et al. (2016) studied immunodominant epitopes of cardiac myosin to monitor the epitope response pattern in acute and convalescent rheumatic fever. Using ELISA, the authors analysed the serum cross-reactive antibodies in the patients with ARF/RHD and observed the disease-specific epitopes were identified as S2-1, 4 and 8.

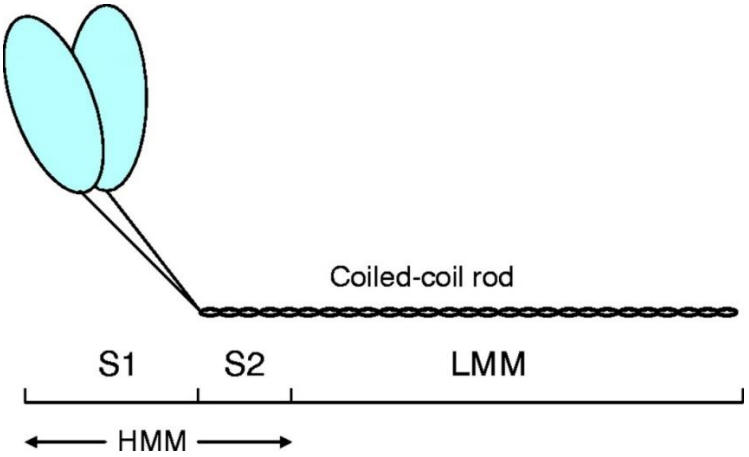


**Figure 2.3** Structure of human cardiac myosin. The coiled-coil structure has high sequence homology with GAS M-proteins. Heavy meromyosin (HMM) and light meromyosin (LMM) can be obtained by proteolytic cleavage. Further cleavage at the neck of HMM separates the single-headed S1 fragments from the S2 fragment. The S2 fragment is the most studied region and reported to contain epitopes cross-reactive with M-proteins. Image is adapted from Hutagalung, et al. (2002).

Furthermore, Ellis, et al. (2005) reported that the T-cells isolated from patients with RHD could potentially recognise GAS M-protein and cardiac myosin, representing one of the most well-defined examples of T-cell mimicry in human autoimmune disease.

In addition to cardiac myosin, antibodies against different types of collagen fibres have been reported in serum of patients with ARF/RHD (Martins, et al. 2008; Chaudhary, et al. 2018). Group A *Streptococcus* uses collagen binding protein (Cpa) and collagen-like protein (Scl) in its pathogenicity. Collagen-like protein has similarities with human collagen and therefore may contribute to induce autoimmunity. In host, collagen fibres form the core structure of mitral valves and chordae tendineae intermixed with elastic fibres (McCarthy, et al. 2010). Collagen in myocardium form the blood vessel wall and strata between myocardial fibres to provide strength to resist mechanical stress (Iyer, et al. 2007). Streptococcal proteins similar to collagen have been reported, although no immunological cross-reactivity has been observed (Lukomski, et al. 2000; Lukomski, et al. 2001). Anti-collagen I antibodies have been reported in sera of patients with ARF/RHD, although the cross-reactivity with GAS has not been proven (Martins, et al. 2008). Antibodies against collagen may be induced following immune responses against certain streptococcal serotypes (Dinkla, et al. 2003a; Tandon, et al. 2013). Otherwise, they might also be due to the release of collagen from injured valves (Tandon, et al. 2013). Banerjee, et al. (2014) reported significantly higher levels of C terminal propeptide of type I procollagen and N terminal propeptide of type III procollagen in

the plasma of patients with ARF/RHD with mitral stenosis and regurgitation. In a separate study, immunohistochemical and confocal microscopy analysis of mitral valves from patients with ARF/RHD revealed that there was disrupted patterns of abundant expression of vimentin and collagen VI (Martins, et al. 2017). Demonstration of antibodies against vimentin, collagen and GAS antigens might add more information about molecular mimicry with GAS and host heart collagen. Chaudhary, et al. (2018) demonstrated high level of antibody titres against collagen binding protein (Cpa) and collagen-like protein (Scl) of GAS in the sera from patients with pharyngitis and ARF compared to healthy controls. The isolates also showed high binding affinity toward host collagen I and IV, which further indicates a potential host pathogen interaction.

Laminin is an extracellular matrix protein of heart valves and cross-reactive antibodies against laminin induced by GAS carbohydrate epitope GlcNAc have been reported (AHA 1992; Cunningham 2000). It has been considered that an antibody binding to laminin is the key to the development of valve damage in RHD (Cunningham 2012). Galvin, et al. (2000) reported that the mAb from serum of patients with ARF/RHD reacted with valvular endothelium and laminin. The authors concluded that anti-GAS/anti-myosin antibodies may produce valvular endothelial injury to expose laminin to the immune system. However, in a separate study, Wahid, et al. (2005) demonstrated that antibodies in the sera from patients with pharyngitis and ARF had significantly higher binding affinity to a recombinant laminin-binding protein of GAS (rGAS-Lmb) compared to serum antibody from healthy controls. The higher antibody response to rGAS-Lmb suggests that high expression of this protein is necessary for colonisation, establishment of infection as well as valve damage.

Furthermore, an immunoproteomic approach with endothelial cell-surface membrane proteins demonstrated anti-vimentin antibodies in sera from half of the patients with RHD (n=140) that have cross-reacted with streptococcal proteins (Delunardo, et al. 2013). The study also demonstrated that the cross-reactive antibodies were able to activate cardiac endothelium by inducing expression of vascular cell adhesion molecule-1 and release of proinflammatory cytokines to amplify the inflammatory response in RHD. In a previous study, (Fae, et al. 2008) it was reported that the T-cells from chronic RHD patients proliferated in the presence of vimentin using a lymphocyte proliferation assay.

Several animal model studies also reported that the antibodies specific for GAS antigens reacted with cardiac myosin (Afanasyeva, et al. 2001; Quinn, et al. 2001; Gorton, et al. 2006; Gorton, et al. 2009; Kirvan, et al. 2014; Gorton, et al. 2016). Cunningham, et al. (1997) identified T-cell cross-reactive epitopes of M5-protein in mice after injection with human cardiac myosin. Later, Quinn, et al. (2001) demonstrated that the GAS rM6-protein induce T-cells in Lewis rats that have proliferated in the presence of purified cardiac myosin. In separate studies, Gorton and colleagues reported that the antibodies and T-cells generated in Lewis rats after injection with a peptide from B-repeat region of rM5-protein (M5-B.6) have responded to cardiac myosin (Gorton, et al. 2009; Gorton, et al. 2016). A proteomic analysis of acute RHD with the iTRAQ labelling based 2D LC-ESI-MS/MS quantitative technology revealed that there was increased expression of myosin and collagen I and V in the mitral valves of Lewis rats injected with GAS that might act as potential biomarker for ARHD (Li, et al. 2015). The cross-reactive antibodies bind to the valvular endothelial surface leading to inflammation, cellular infiltration, and valve scarring (Galvin, et al. 2000; Roberts, et al. 2001; Guilherme and Kalil 2010).

*Association of M proteins with ARF/RHD*

To date, more than 200 M-types (*emm* types) of GAS have been reported. Among them, serotypes 1, 2, 3, 5, 6, 14, 18, 19 and 24 have been reported to be associated with outbreaks of ARF/RHD (Markowitz and Gerber 1987; Johnson, et al. 1992; Stollerman 1997; Guilherme, et al. 2001b; Shulman, et al. 2006). In addition, M serotypes different from those in the United States have been associated with ARF/RHD in Trinidad and Hawaii (Potter, et al. 1982; Read, et al. 1986; Erdem, et al. 2007). The epidemiological studies suggest that the prevalence and incidence of ARF/RHD does not necessarily correlate with the distribution of rheumatogenic M-types of GAS.

**Other key virulence factors**

Streptococcal infection is established by sequential events of adhesion, colonisation and invasion of tissues. Previous damage to tissue may facilitate skin attachment and colonisation. A minimum of 11 adhesins that facilitate adhesion to epithelial cells have been described for GAS including M-proteins, lipoteichoic acid (LTA), protein F/Sfb, fibronectin binding protein, glyceraldehyde-3-phosphate dehydrogenase, galactose-binding protein, vitronectin-binding protein, collagen-binding protein, serum opacity factor, and hyaluronate capsule (Ellen and Gibbons 1972; Ellen and Gibbons 1974; Ofek, et al. 1975; Simpson, et al.

1980; Simpson and Beachey 1983; Valentin-Weigand, et al. 1988; Caparon, et al. 1991; Courtney, et al. 1992a; Courtney, et al. 1992b; Hanski and Caparon 1992; Pancholi and Fischetti 1992; Courtney, et al. 1994a; Courtney, et al. 1994b; Dale, et al. 1994; Okada, et al. 1994; Wang and Stinson 1994a; Wessels and Bronze 1994; Kreikemeyer, et al. 1995; Visai, et al. 1995; Winram and Lottenberg 1996). Streptococci may adhere to endothelial cell or keratinocytes and induce localised inflammatory responses (Courtney, et al. 1997; Wang, et al. 1997). The epithelial cell and keratinocyte proteins help in adherence to GAS include; fibronectin, fibrinogen, collagen, vitronectin, fucosylated glycoprotein, several membrane proteins, and hyaluronate binding receptor (Sanford, et al. 1982; Simpson and Beachey 1983; Valentin-Weigand, et al. 1988; Courtney, et al. 1992a; Wang and Stinson 1994b; Okada, et al. 1995; Visai, et al. 1995; Schrager, et al. 1998). Table 2.1 summarises the streptococcal adhesins that bind with host receptors.

**Table 2.1** GAS antigens that bind with respective host cell receptors during establishment of infection

| GAS antigens | Host cell receptors |
|---|---|
| Lipoteichoic acid (LTA) | Epithelial cell, fibronectin receptor (Courtney, et al. 2002; Neuhaus and Baddiley 2003; Grundling and Schneewind 2007; Courtney, et al. 2009; Percy and Grundling 2014) |
| Protein F/SfbI | Epithelial cell, fibronectin, CD46 receptor on keratinocytes (Talay, et al. 2000; Rodriguez-Ortega, et al. 2006) |
| Fibronectin-binding protein (FBP54) | Fibronectin, fibrinogen (Bessen and Kalia 2002; Kreikemeyer, et al. 2004; Rodriguez-Ortega, et al. 2006; Falugi, et al. 2008; Yamaguchi, et al. 2013) |
| Serum opacity factor (SOF) | Fibronectin (Oehmcke, et al. 2004; Rodriguez-Ortega, et al. 2006) |
| Hyaluronic acid capsule | Keratinocyte, CD44 (hyaluronate receptor) (Stollerman and Dale 2008; Flores, et al. 2012) |
| Glyceraldehyde-3-phosphate dehydrogenase | Pharyngeal epithelium, fibronectin, cytoskeletal proteins, plasminogen-plasmin |
| Vitronectin-binding protein | Fibronectin |
| 70-kDa galactose-binding protein | Galactose |
| Collagen-binding protein | Collagen (Bessen and Kalia 2002; Humtsoe, et al. 2005; Rodriguez-Ortega, et al. 2006; Caswell, et al. 2007; Caswell, et al. 2008; Falugi, et al. 2008; Chen, et al. 2010) |

### 2.2.2 Non-group A *Streptococcus*

Although ARF/RHD is well reported as an autoimmune sequelae of GAS pharyngitis, there are many reports of low GAS carriage rates throughout the world. Several epidemiological studies reported low pharyngeal carriage rate of GAS in school-age children of temperate counties; only 15-30% positive to GAS (Anthony, et al. 1976; Quinn, et al. 1978; Nicolle, et al. 1990; Danchin, et al. 2004; Martin, et al. 2004). The picture is more varied in tropical and subtropical regions; only 4-17% (Rajkumar and Krishnamurthy 2001; Bassili, et al. 2002). On the contrary, recovery rates in pharynx *of Streptococcus dysgalactiae* subspecies *equisimilis* (SDSE) or group G *Streptococcus* (GGS) that have Lancefield's C and G carbohydrates on the cell wall, were high-up-to 20% of cases in some of the Indigenous communities of Australia (Haidan, et al. 2000). Investigations in these communities of Northern Australia revealed that high rates of ARF/RHD was not driven by symptomatic GAS pharyngitis (Kaplan 1993; McDonald, et al. 2006). The median point prevalence for pharyngeal carriage in this population was only 3.7% for GAS (McDonald, et al. 2006). By contrast, the group G (GGS) and C (GCS) β-haemolytic streptococcal carriage rates recorded were 5.1% and 0.7%, respectively (McDonald, et al. 2006). Similar findings have been reported in several Indian studies (Gupta, et al. 1992; Gonzalez-Lama, et al. 2000; Haidan, et al. 2000; Lloyd, et al. 2006). The isolation rate of GGS is as high as 70% from asymptomatic carriers in many tropical countries (WHO 1988; Taranta and Markowitz 1989; Kaplan 1996; Pruksakorn, et al. 2000). A recent study in Southern India reported 32.1% prevalence of GAS, 49.1% GGS and 9.8% GCS (Gowda, et al. 2012). The role of GGS/GCS in streptococcal disease burden is under-recognised by clinicians and microbiologists. However, recent epidemiological data reported that β-haemolytic streptococci belonging to Lancefield group C and G are an emerging threat to human health (Nitsche-Schmitz, et al. 2007). Therefore, pre-exposure to GGS/SDSE may also be an important but overlooked aetiological factor in the pathogenesis of ARF/RHD.

#### 2.2.2.1 Group G *Streptococcus* (GGS)

The β-haemolytic *Streptococcus dysgalactiae* subspecies *equisimilis* (SDSE) or group G *Streptococcus* (GGS) possesses group C or G antigens and rarely A antigen (Vandamme, et al. 1996). It is a normal inhabitant of the lower respiratory tract, skin, gastrointestinal tract, and female genital tract with a capacity to cause opportunistic infections in individuals with underlying medical conditions (Vartian, et al. 1985; Baracco and Risno 2004; Cohen-Poradosu, et al. 2004; Liao, et al. 2008). Although GGS was first isolated from human

puerperal sepsis in 1935, its role in disease has often been ignored (Lancefield and Hare 1935; Barnham 1983; Lindbaek, et al. 2005).

#### 2.2.2.2 Spectrum of diseases caused by group GGS

Although GGS is part of the normal flora, it may cause both non-invasive and invasive diseases in human. In fact, 3-4% of cases of streptococcal bacteraemia resulted from GGS infections (Watsky, et al. 1985). Other diseases associated with GGS include pharyngitis, erysipelas, neonatal sepsis, arthritis, cellulitis, suppurative thrombophlebitis, osteomyelitis, empyema, peritonitis, endometritis, ARF, endocarditis and acute post-infectious glomerulonephritis (Bouza, et al. 1978; Dyson and Read 1981; Stryker, et al. 1982; Auckenthaler, et al. 1983; Lam and Bayer 1983; Nakata, et al. 1983; Finch and Aveline 1984; Vartian, et al. 1985; Watsky, et al. 1985; Craven, et al. 1986; Venezio, et al. 1986; Carstensen, et al. 1988; Brahmadothan and Koshi 1989; Brandt and Spellerberg 2009; Kittang, et al. 2010; Harrington and Clarridge 2013; Kakuya, et al. 2017; Lother, et al. 2017). A recent study reported that children in Japan suffered from GGS pharyngitis following food-poisoning (Yamaguchi, et al. 2018).

Case reports have indicated that GGS also could also cause other life-threatening complicated infections (Venezio, et al. 1986; Mohan, et al. 1989; Burkert and Watanakunakorn 1991; Liao, et al. 2008; Nei, et al. 2012). Bacteraemia with pharyngitis with or without endocarditis have been the most commonly reported presentations of GGS infections (Rantz, et al. 1946; Barnham 1980; Lam and Bayer 1983; Nakata, et al. 1983; Dickie, et al. 1984). GGS has also been recovered from blood of patients suffering from subungual haematoma, systolic murmur and aortic valve abscess and vegetations (Venezio, et al. 1986). A similar case was found with viridans streptococcal endocarditis (Venezio, et al. 1986). There is also a report of recovery of GGS in a patient suffering from fever, asymptomatic murmur of mitral valve prolapse and vegetations (Venezio, et al. 1986). Vegetations are treated as one of the major complications of GGS bacteraemia, occur most often in endocarditis patients and lead to congestive heart failure necessitating valve replacement. A recent study in New Zealand reported ARF in an adolescent following GAS pyoderma and GGS pharyngitis indicating the potential for ARF/RHD following both GAS skin infection and/or GGS pharyngitis (O'Sullivan, et al. 2017).

#### 2.2.2.3 Virulence factors of GGS

Group G *Streptococcus* possesses heterogeneous surface associated virulence factors (Craven, et al. 1986; Bisno, et al. 1987). The important virulence factors enhance bacterial attachment to the host, escape from phagocytosis and ultimate establishment of infection (Kalia and Bessen 2004). The major structures and products of GGS are toxins, proteases and regulatory factors and M-proteins (Davies, et al. 2007a).

**M-proteins**

There are ample studies to prove that GGS possesses M-proteins on its cell wall. M-proteins or M-like proteins are also possessed by group B, C, and E streptococci (Maxted 1949; Maxted and Potter 1967; Daynes and Armstrong 1973; Woolcock 1974). Maxted and Potter (1967) reported the presence of the M12-protein in three GGS strains isolated from the throat and skin sores of Trinidadian children. Swanson, et al. (1969) reported seven strains of GGS that exhibited an abundance of surface fimbriae similar to those present in M-proteins of GAS. Beachey, et al. (1974) reported that the antibodies to pepsin-extracted peptides ranging from 31-45 kDa (the range of peptides of GAS M-proteins) were type-specifically opsonic for GGS strains. Electron microscopic examination observed surface fimbriae on GGS resembling M-proteins. In addition, resistance to phagocytosis with luxuriant growth in fresh human blood, type-specific opsonisation by hyperimmune rabbit sera and immunoprecipitation in agar gel studies confirmed the presence of M-proteins (Lawal, et al. 1982). Moreover, a strain of GGS has been shown to contain DNA which hybridised with a probe encoding the M6-protein of GAS (Scott, et al. 1985). DNA sequencing of the protein genes from GGS clinical isolate revealed structural similarity with M-proteins of both GGS and GAS (Johansson, et al. 2004; Steer, et al. 2009b; Sunaoshi, et al. 2010; Tseng, et al. 2010; Leitner, et al. 2015).

*Function*

Despite GGS colonising the throat, causing clinically significant pharyngitis and its production of M-proteins, little is known about the distribution or clinical significance of these proteins (Bisno, et al. 1987). The GGS M-proteins also have never been reported to directly cause ARF/RHD (Collins, et al. 1992). However, several studies reported that GGS strains grow well in human blood and resist phagocytosis, contributed by M-protein (Bisno, et al. 1987; Jones and Fischetti 1987; Simpson, et al. 1987; Martin, et al. 1990; Collins, et al. 1992; Bisno, et al. 1994; Schnitzler, et al. 1995).

*Association with ARF/RHD*

Several studies have shown that GGS may have the potential to elicit autoimmune responses that may trigger ARF/RHD (Bisno, et al. 1996; Sriprakash and Hartas 1996; Haidan, et al. 2000; Davies, et al. 2005). As described previously M-proteins have a significant role in host cell attachment or escape from immune responses. Five GGS isolates from throat swabs of asymptomatic Indigenous children expressed high levels of M6-type protein: M6 protein has previously been shown to have rheumatogenic potential (Haidan, et al. 2000). In this study, antibodies against the GGS M-types were raised in mice by standard immunisation procedures. The antibodies against GGS throat isolates reacted against human heart myosin, however, the antibodies to five skin isolates showed very low reactivity (Haidan, et al. 2000).

**Other key GGS virulence factors**

In addition to M-proteins, Group G *Streptococcus* produces distinct streptokinase, streptococcal C5a peptidase, hyaluronidase, fibronectin binding protein, collagen binding protein and laminin binding proteins, all of which have potential roles in the establishment of infection. Streptolysin S (sagA), streptolysin O (slo) and haemolysin (hlyIII, helA1) represent toxins or proteases, and CovR and CovS control gene expression (Geyer and Schmidt 2000; Humar, et al. 2002; Hashikawa, et al. 2004). Human GGS strains possess a C5a-peptidase that resists phagocytosis by inhibiting chemotaxis and neutrophil migration (Ikebe, et al. 2004). However, compared to GAS, GGS were reported to express low levels of these C5a-peptidases and hence are less able to resist phagocytosis (Cleary, et al. 1991). Streptokinase dissolves human fibrin, facilitating invasion of GGS (Ikebe, et al. 2004). Similar to GAS, fibronectin-binding proteins (GfbA/SfbI) of GGS act as an invasin to invade human respiratory epithelial cells (Haidan, et al. 2000; Palmieri, et al. 2007).

### 2.2.2.4 Comparison to GAS, similarities and differences

Although GGS is not considered major human pathogen, it has many characteristics similar to GAS (Chhatwal and Talay 2000). GGS and GAS share the same tissue niche, many virulence factors including M-proteins and cause a similar spectrum of disease (Bisno, et al. 1996; Haidan, et al. 2000; Davies, et al. 2005; Dinkla, et al. 2007). M-proteins of GAS and GGS isolated from human infections have similar biological, immunochemical, and structural features (Bisno, et al. 1987; Jones and Fischetti 1987; Simpson, et al. 1987; Martin, et al. 1990; Collins, et al. 1992; Bisno, et al. 1994). The biological and immunochemical identity

between M-proteins of GAS and GGS has been studied extensively (Jones and Fischetti 1987). Colonisation and overlapping clinical presentation are two major forms of evidence for evolutionary interspecies relatedness between GAS and GGS. The rRNA sequence based phylogenetic analysis and other molecular clocks also support the close relatedness between these bacteria (Vandamme, et al. 1996; Poyart, et al. 1998; Facklam 2002; Tapp, et al. 2003). As described previously, several studies have shown that GGS possesses genes for M-proteins, C5a peptidase, streptokinase, streptococcal pyrogenic exotoxins and fibronectin binding proteins, all of which are essential virulence determinants in GAS (Maxted and Potter 1967; Malke, et al. 1985; Walter, et al. 1989; Cleary, et al. 1991; Sachse, et al. 2002; Igwe, et al. 2003; Kalia and Bessen 2003; Towers, et al. 2004). The mosaic structure of some of these GAS and GGS genes strongly suggests lateral genetic transfer has occurred between the two streptococci (Davies, et al. 2005). In addition, it has been suggested that bacteriophages might have contributed to the transfer of genes encoding proteins with rheumatogenic properties from GAS to GGS (Haidan, et al. 2000; Davies, et al. 2007b).

Based on hybridisation profiles, Collins, et al. (1992) reported that GGS M-protein has structural features analogous to class I M-proteins of GAS. The authors also published that there are minimum of four different *emm* alleles associated with GGS. Comparison of GGS *emmL* (*emm* 656) gene sequence with GAS *emm* 12 and 57 revealed that there was 85% homology between them (Robbins, et al. 1987; Manjula, et al. 1991; Podbielski, et al. 1991; Podbielski, et al. 1993; Podbielski, et al. 1994; Whatmore and Kehoe 1994). In addition, the GGS strain 480 *emmL* gene sequence showed 85% homology with the GAS *emm* 57 sequence (Schnitzler, et al. 1995).

In one study, crude mutanolysin (an N-acetyl-muramidase) extracts from GGS strains showed marked similarity to GAS M-proteins based on protein size and immunoblot reactivity with the GAS M6 mAb 10F5 (Hamada, et al. 1978). The GGS mutanolysin extracts had a multiple banding pattern characteristic of and very similar to those of the proteins in the GAS extract (Figure 2.4). The GGS extracts also possessed diffuse upper bands similar to the M-protein extract of GAS (Fischetti, et al. 1985) which represent M-proteins bound to cell wall fragments containing the GAS specific carbohydrate (Fischetti, et al. 1985). This suggests a mechanism of attachment of the GGS M-protein to the cell wall similar to that of the GAS M-protein (Fischetti, et al. 1985; Hollingshead, et al. 1986). A pepsin-derived fragment from

GGS strain D886 stimulates opsonic antibodies demonstrating GGS M-proteins as primary virulence factor as in GAS (Jones and Fischetti 1987).

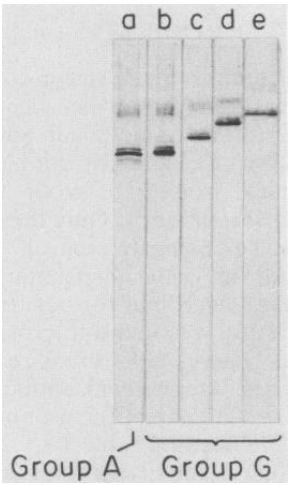


**Figure 2.4** GGS possess M-protein similar to GAS M-protein. SDS-PAGE and Western blot analysis of crude GAS and GGS mutanolysin showed protein bands in GGS extracts that are similar to those in GAS extracts. Lane a, GAS strain D471; lanes b-e, GGS strains D862, D884, D959, and D851, respectively (Jones and Fischetti 1987).

Immunological cross-reactivity of monoclonal antibodies with GAS serotype M6-protein and hybridisation data suggested that the GGS M-proteins are structurally similar to GAS M-proteins (Scott, et al. 1985; Jones and Fischetti 1987). Gene sequences for the M-proteins from several GGS isolates revealed significant similarity with GAS M-proteins at the C terminus and only limited similarity at the N terminus (Collins, et al. 1992; Schnitzler, et al. 1995). Expression of M12 antigen of GAS by GGS suggests that gene transfer between GGS and GAS can make GGS more virulent for humans (Simpson, et al. 1992). Sequence data in fact demonstrated similarity between some *emm*Gs and *emm*12 or *emm*57 from GAS (Schnitzler, et al. 1995). Group G streptococcal isolates-6 (*emm*GGS6) from the Northern Territory of Australia showed 99% identity to *emm*LG935 and *emm* of STDONALD, a GAS isolate (Schnitzler, et al. 1995). These data are consistent with ongoing cross-species gene transfer between GGS and GAS. Although GAS and GGS have many characteristics common to each other, GGS and its M-proteins are still less characterised and studied in terms of their roles in causing disease and in particular their involvement in the aetiology of ARF/RHD.

## 2.3 RISK FACTORS OF ARF/RHD

The prevalence and incidence of ARF/RHD around the world is dependent on the environment, the socio-economic standard and genetic factors. The relative contribution of each of these individual risks is difficult to elucidate given that many of them overlap and most are associated with poverty and economic disadvantage (Steer, et al. 2002; Diao, et al. 2011; Rothenbuhler, et al. 2014).

### 2.3.1 Environmental risk factors

F. J. Poynton, a paediatrician at the Hospital for Sick Children in London, said that risk factors associated with ARF/RHD included 'climatic and local surroundings, sanitations and conditions of housing' and declared that 'it is to *prevention*, then that we look for some advance from this grievous state of affairs' (Campbell 1944). Overcrowding due to industrialisation is an important factor of poor hygiene leading to streptococcal pharyngitis or skin infection. In many developing regions, rapid industrialisation has brought a population shift from rural to urban areas leading to crowded urban slums (Markowitz 1991). In Kinshasa town in the Democratic Republic of Congo, the risk of RHD was found to be far higher (risk ratio: 4.1) in semi-urban areas (22.2 per 1000) compared to urban areas (4 per 1000) (Longo-Mbenza, et al. 1998). In these semi-urban areas, 81.1% of subjects lived in houses with more than eight people. The rise in the standard of living in Denmark has seen the incidence of ARF fall astonishingly between 1862 and 1962 (Kaplan 1985; Kumar 1995). Crowded living conditions with close interpersonal contacts contribute to the persistence and spread of virulent streptococcal strains. During the 1950s, a study conducted on US Air Force Base barracks revealed that acquisition of streptococcal infections increased when beds were moved closer together (Wannamaker 1954). In a study on ARF patients in Baltimore, it was demonstrated that overcrowding was the predominant cause of the higher incidence rate among non-white peoples (Gordis, et al. 1969). However, the situation is less clear in developing countries due to the lack of appropriate studies. In contrast, Adanja, et al. (1988) found that crowding was not associated with ARF/RHD in Serbia. In a study in Northern India, the prevalence of RHD was recorded to be 3.8 per 1000 in rural areas and 1.3 per 1000 in urban areas (Berry 1972). The apparently reduced association between overcrowding and ARF/RHD in Serbia and Northern India suggest that there is a threshold above which extra crowding has little effect. Effects of seasonal variation closely mimic the incidence of streptococcal infections. High incidence in early autumn, late winter and early spring are

particularly pronounced in temperate climates but are not significant in the tropics (WHO 2004).

### 2.3.2 Social risk factors

Over the past 150 years, socioeconomic and environmental factors have been playing an indirect but important role in the prevalence and incidence of ARF/RHD in both developed and developing countries (Carapetis, et al. 2016). Discussing the importance of socio-economic status in the prevalence of ARF/RHD, Glover (1930) suggested that 'no disease has a clearer social incidence than acute rheumatism which falls perhaps 30 times as frequently upon the poorer children of the industrial town, as upon the children of the well-to-do'.

Poverty, malnutrition, overcrowding and poor housing are recorded as the most significant determinants of ARF/RHD by enabling rapid spread of streptococci throughout a population (Kaplan 1980; WHO 1988; Taranta and Markowitz 1989; Narula, et al. 1999; Stevens and Kaplan 2000; WHO 2004). Evidence suggests that malnutrition in early childhood plays a significant role in susceptibility to ARF/RHD (Coburn 1961). In a study in Serbia, children patients with a bodyweight of 10% below average had a 42% increased risk of ARF/RHD (Adanja, et al. 1988). Subjects with lower albumin levels showed a significantly higher risk when compared with normal subjects (Zaman, et al. 1998). Protein-calorie malnutrition causes lymphopenia, thymic atrophy and altered cell-mediated and antibody responses that may predispose to ARF (Fraker, et al. 2000).

Moreover, inadequate health-systems may lead to misdiagnosis, inadequate or late diagnosis and treatment of streptococcal pharyngitis and ARF/RHD. Shortage of resources for providing quality health care, inadequate expertise of healthcare providers and low-level awareness of the disease in the community are major constraints in RHD endemic regions (WHO 1987; WHO 1988; Taranta and Markowitz 1989; Bisno 1996; Kaplan 1996; WHO 2004). Some authors suggest that the difference in prevalence between developed and developing countries is due to the difference in access to medical services (Kumar 1995). The incidence of ARF/RHD decreased in USA by one-third between 1960 and 1970 after the introduction of 'Comprehensive Care Programs' (Gordis 1973). In Costa Rica, the incidence rate fell with a National Health Strategy of primary benzathine penicillin prophylaxis by the 1970s (Arguedas and Mohs 1992). Remarkably, 78% and 74% reduction in the incidence occurred as a result of a 10-year educational programme directed at healthcare workers and

the public in Martinique and Guadeloupe, respectively (Bach, et al. 1996). Primary prophylaxis programmes effectively increase public concern about ARF/RHD and access to medical services as well as the treatment for pharyngitis. High rates of ARF/RHD in Indigenous people of New Zealand and Australia are likely to be related to poor hygiene, inadequate clean water and sewerage system and inaccessible health services rather than genetic susceptibility (Carapetis and Currie 1998; Carapetis, et al. 2000; Couzos and Carapetis 2003; Penm 2008; Parnaby and Carapetis 2010; White, et al. 2010).

### 2.3.3 Host genetic factors

The genetic pattern of susceptibility to ARF/RHD has been sought for more than a century. Many studies have been conducted that aim to define the pattern of inheritance responsible for susceptibility. Recent studies have tried to uncover specific markers for susceptibility to ARF/RHD (Kaplan 1980; WHO 1988; Taranta and Markowitz 1989; Guilherme, et al. 1991; Ramasawmy, et al. 2007; Guilherme, et al. 2011b). Pedigree studies suggested that the immune reactions are genetically controlled with high responsiveness to the streptococcal cell wall antigens being expressed through a single recessive gene and low responsiveness through a single dominant gene. However, single nucleotide polymorphisms in a number of genes affect patients with RHD (Guilherme, et al. 2011b).

Genes controlling the low level response to the streptococcal antigen is closely linked to the Class II human leukocyte antigen (HLA; corresponding to MHC class II) (Sasazuki, et al. 1980). The molecular mechanism by which HLA class II molecules confer susceptibility to autoimmune disease is not clear. The role of the molecules is to present antigens to the T-cell receptor (TCR), leading to the recruitment of large numbers of CD4+ T-cells that specifically recognise antigenic peptides from extracellular pathogens and the activation of adaptive immune responses. Therefore, the associated alleles probably encode molecules that facilitate the presentation of some streptococcal peptides to T-cells that later trigger autoimmune reactions mediated by molecular mimicry (Guilherme, et al. 2011b).

The HLA molecules are encoded by the HLA genes (-A, -B, -C, -DR, -DQ and -DP) which are located on the short arm of human chromosome 6. Early studies pointed out the association of ARF/RHD with several HLA class II alleles, for example, DR4 was present more frequently in Caucasian ARF patients, DR2 in African-American populations, DR1 and DRw6 in ARF patients from South Africa, and HLA-DR3 in Indian patients who also had a

low frequency of DR2 (Ayoub, et al. 1986; Roberts, et al. 2001). In addition, DQW2 was reported more frequently in Asian ARF patients. Moreover, the HLA-DR7 allele found in Brazilian, Turkish, Egyptian and Latvian patients could be considered with ARF/RHD. HLA-DQB or -DQA alleles may be related to the development of multiple valvular lesions in RHD patients in Egypt and in Latvia (Guedez, et al. 1999; Visentainer, et al. 2000; Stanevicha, et al. 2007).

## 2.4 IMMUNE RESPONSES AND PATHOGENESIS OF ARF/RHD

The pathogenesis of ARF/RHD is complex. Although significant progress has been made in understanding the autoimmune processes, the precise mechanism has not been understood completely (Cunningham 2004; Guilherme, et al. 2006). Antibodies, T-cells generated and upregulation of major histocompatibiltiy antigens during and immediately after streptococcal infection are being investigated as potential factors in the pathogenesis of the disease. In fact, molecular mimicry between M-proteins of rheumatogenic strains of streptococci and human cardiac proteins is the most studied and identified event in the pathogenesis of rheumatic carditis (Stevens and Kaplan 2000; Guilherme and Kalil 2010). Evidence from many clinical and experimental animal studies suggest that auto-reactive antibodies and T-cells initiate ARF/RHD by triggering endothelial inflammation in the heart (Kaplan, et al. 1964; Kaplan and Svec 1964; Beachey, et al. 1988; Bronze, et al. 1988; Cunningham, et al. 1989; Lehmann, et al. 1992; Quinn, et al. 1995; Cunningham, et al. 1997; Galvin, et al. 2000; Guilherme, et al. 2000; Brandt, et al. 2001; Galvin, et al. 2002; Guilherme and Kalil 2002; Cunningham 2003; Ellis, et al. 2005; Fae, et al. 2006; Guilherme, et al. 2006).

### 2.4.1 Human studies

The auto-reactive antibodies and T-cells can recognise streptococcal and host antigens due to structural similarities, or similar amino acid sequences (Guilherme, et al. 2011a).

#### 2.4.1.1 Antibody responses

The past few decades of study have shown the presence of cross-reactivity between human proteins and streptococcal antigens recognised by antibodies (Carapetis, et al. 2016). After pharyngeal or skin infection, the immune system responds to GAS by antibody production and T-cell priming and differentiation (Kaplan, et al. 1964; Roberts, et al. 2001; Gorton, et al. 2009; Cunningham 2014; Gorton, et al. 2016). The antibodies are believed to be directed against the M-proteins of certain strains of the streptococci that cross-react with glycoprotein

antigens in heart, joints, skin and brain leading to pathology of the organs (Svartman, et al. 1975; Husby, et al. 1976; Cromartie, et al. 1977; Fenderson, et al. 1989; Fischetti 1989; Froude, et al. 1989; Gulizia, et al. 1991; Khanna, et al. 1997).

In chronic RHD, GAS M-proteins are the antigens most frequently reported to trigger autoimmune reactions against cardiac myosin that lead to the development of carditis (Cunningham, et al. 1989; Cunningham, et al. 1997; Quinn, et al. 2001). Previous studies from the 1960s demonstrated antibody deposition in human heart tissues from patients with ARF/RHD (Kaplan, et al. 1964). The findings of this study were later supported using mouse and human mAbs against GAS that reacted with both myocardial and valvular tissues (Krisher and Cunningham 1985; Cunningham 2000; Cunningham 2014). Antibody cross-reactivity between GAS M-proteins and cardiac myosin suggests that cardiac myosin is the target autoantigens recognised in the heart (Dale and Beachey 1985a; Krisher and Cunningham 1985; Cunningham, et al. 1986; Cunningham and Swerlick 1986; Baird, et al. 1991). Moreover, using anti-myosin antibodies purified by affinity chromatography from ARF patients' sera, cross-reactive epitopes were found on cardiac myosin and the M5 or M6 proteins of GAS (Cunningham, et al. 1989). Demonstration of antibodies against cardiac myosin S2 peptides is reported in many recent studies to monitor disease progression or heart damage (Galvin, et al. 2002; Ellis, et al. 2010; Gorton, et al. 2011; Garcia, et al. 2016). Antibodies in sera from patients with ARF/RHD also reacted with collagen I molecule (Dinkla, et al. 2003a; Tandon, et al. 2013). Antibodies against collagen I are reported in patients with ARF/RHD although no immunological cross-reactivity has been observed (Martins, et al. 2008). It is possible that the cross-reactive antibodies bind to the valvular endothelial surface and upregulate vascular cell adhesion molecules including VCAM-1 that leads to inflammation and leucocyte infiltration into the valves and myocardium (Galvin, et al. 2000; Roberts, et al. 2001).

#### 2.4.1.2 T-cell responses in ARF/RHD

In ARF/RHD, there is strong evidence of the recognition of heart proteins by autoreactive T-cells via molecular mimicry (Cunningham 2003; Fae, et al. 2006; Guilherme, et al. 2006; Carapetis, et al. 2016). T-cell clones isolated from patient with ARF/RHD could recognise both streptococcal and host proteins suggesting epitope mimicry (Ellis, et al. 2005). In a separate study, heart infiltrating T-cell clones from ARF/RHD patients demonstrated simultaneous recognition of streptococcal M5-protein and heart tissue proteins including

peptides from the light meromyosin (LMM) and S2 regions of human cardiac myosin (Fae, et al. 2006). It was observed that 16 LMM peptides were exclusively recognised by T-cell clones from the mitral valve whereas only eight peptides were recognised by clones derived from the myocardium (Fae, et al. 2006). The recognition of human LMM regions and M5-protein sequences by both myocardium and valve-derived intra-lesional T-cell clones suggest that mimicry contributes to the development of RHD. During development of carditis, the autoreactive T-cells probably enter the rheumatic valves through the activated valve surface endothelium (Roberts, et al. 2001). Therefore, it was hypothesised that myosin is not a predominant autoantigen in the valves, rather the myosin cross-reactivity with valvular proteins might occur first through mimicry, and then by an epitope-spreading mechanism to the valvular tissues (Lehmann, et al. 1992; Guilherme, et al. 1995; Ellis, et al. 2005). The autoreactive T-cells infiltrate the valve and the myocardium, and form Aschoff nodules (Raizada, et al. 1983; Dale and Beachey 1987; Guilherme, et al. 1995; Guilherme, et al. 2001b; Carapetis, et al. 2016).

Peripheral blood MNCs from children with ARF/RHD have been shown to produce more TNF-α than healthy controls (Miller, et al. 1989). TNF-α has a proinflammatory effect that induces and exacerbates the inflammatory responses in ARF/RHD patients (Miller, et al. 1989; Morris, et al. 1993a; Narin, et al. 1995; Yegin, et al. 1997; Settin, et al. 2007). Significant number of TNF-α-producing cells in the throat and valves was also reported in patients with ARF/RHD (Guilherme, et al. 2004). Polymorphisms in other cytokine-encoding genes have also been investigated and seem to be involved with the disease. These include TGF-β1, IL-1Ra and IL-10 (Chou, et al. 2004; Settin, et al. 2007; Azevedo, et al. 2010; Kamal, et al. 2010). ARF/RHD patients from Egypt and Brazil with severe carditis showed low levels of IL-1Ra expression suggesting the absence of control of the inflammatory process (Settin, et al. 2007; Azevedo, et al. 2010). Human IL-10, which regulates the functions of many different immune cells is overrepresented in Egyptian ARF/RHD patients (Sabat, et al. 2010). IL-10 is associated with the development of multiple valvular lesions (Settin, et al. 2007). Polymorphism in the cytotoxic T-cell lymphocyte antigen-4 (CTLA-4), which is a negative regulator of T-cell proliferation, has also been shown in Turkish ARF/RHD patients (Duzgun, et al. 2009).

In addition to this, high TNF-α, IFN-γ and low IL-4 levels have been found in the rheumatic valve suggesting an imbalance between Th1 and Th2 cytokines and probably contributing to

the progressive and permanent valve damage (Guilherme, et al. 2011a). Heart-infiltrating T-cells isolated from the heart valves of ARF/RHD patients have previously been shown to be predominantly IFN-γ-producing. The high number of IL-4 producing T-cells in the myocardium might be the reason why myocarditis heals with the progression of valvulitis (Guilherme, et al. 2004; Fae, et al. 2006; Guilherme and Kalil 2007; Guilherme, et al. 2011a).

Th-17 cells and IL-17A were discovered only relatively recently but have become a very important immune mediator in extracellular bacterial infections and appear to play a pathological role in numerous autoimmune diseases where fibrosis is a thematic endpoint (Bettelli, et al. 2006; Bilik, et al. 2016). A role for Th-17 cells and IL-17A has been reported previously in the context of murine GAS infections (Wang, et al. 2010; Dileepan, et al. 2016). In another study, high concentrations of IL-17 in the serum of Lewis rats injected with GAS M-protein and a high expression of IL-17 in the mitral valves of rats and human patients with ARF/RHD were observed (Wen, et al. 2015). Elevated levels of IL-17A have also been reported in ARF/RHD sera compared to healthy controls (Bilik, et al. 2016). IL-17 is important in recruiting neutrophils and macrophages to the site of infection, and is a relatively new finding in the development of autoimmune carditis (Ivanov, et al. 2006; Annunziato, et al. 2007).

#### 2.4.1.3 Mechanism of migration of immune cells into heart tissues

Interaction between valvular endothelial cells and circulating leukocytes is the key initial event in the targeting of sites of inflammation. Adhesion between leukocytes and endothelial cells or with extracellular matrix components mediates by cell adhesion molecules (CAMs) expressed on the vascular endothelium and on immune and inflammatory cells. They also help in the transmigration of leukocytes across the vascular endothelium. The intercellular adhesion molecule-1 (ICAM-1), vascular endothelial cell adhesion molecule-1 (VCAM-1) and endothelial selectin (E-selectin) are expressed on the vascular endothelium and serve as ligands for counter receptors on circulating inflammatory cells (Ley, et al. 2007). The expression of VCAM-1 acts as the hallmark of inflammation and heralds for cellular infiltration. VCAM-1 interacts with very late antigen (VLA)-4 expressed on T-cells leading to an influx of activated CD4+ and CD8+ cells (Figure 2.5). The extracellular or soluble portions of CAMs are detectable at low levels in the serum of healthy individuals but at significantly higher levels in ARF/RHD patients (Gearing and Newman 1993).

It has been shown previously that anti-M-protein or anti-cardiac myosin antibodies lead to an up-regulation of VCAM-1 and other adhesion molecules on endothelial cells (Roberts, et al. 2001; Carapetis, et al. 2016). A break in the endothelial continuity of a heart valve would expose sub-endothelial structures (vimentin, laminin and valvular interstitial cells) and lead to a "chain reaction" of valvular destruction. Once valve leaflets are inflamed through the valvular surface endothelium, new vascularisation occurs. This newly formed microvasculature allows T-cells to infiltrate and perpetuate the cycle of valvular damage. Aschoff bodies or granulomatous lesions may form beneath the endocardium containing macrophages and T-cells (Roberts, et al. 2001). The presence of T-cell infiltration, even in old mineralised lesions is indicative of persistent and progressive disease in the valves. Valvular interstitial cells and other valvular constituents under the influence of inflammatory cytokines perpetuate aberrant repair (WHO 2004). As a result, the valve becomes progressively scarred, causing regurgitation and congestive heart failure (Kemeny, et al. 1989).

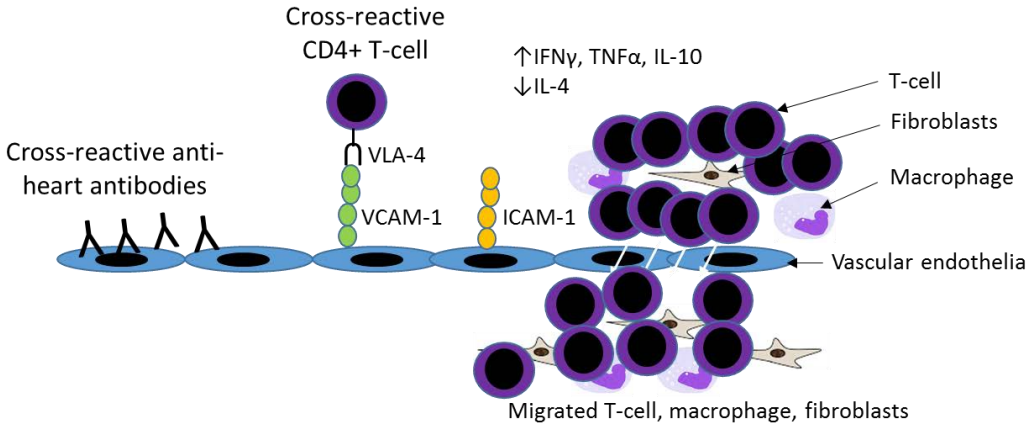


**Figure 2.5** Activation of endothelial cell and migration of inflammatory cells into heart tissue. Cross-reactive antibodies to streptococci and heart proteins activate endothelial cells by inducing expression of VCAM-1 and ICAM-1. Activated VCAM-1 reacts with VLA-4 of cross-reactive T-cells. Expression of ICAM-1 facilitates migration of autoreactive T-cells. Macrophages and fibroblast cells migrate into the heart tissue and form Aschoff nodules and cause mitral valve fibrosis. The image is modified from Guilherme, et al. (1995), Galvin, et al. (2000), Roberts, et al. (2001) and Guilherme, et al. (2004).

Several studies have demonstrated elevated concentrations of adhesion molecules in the serum of ARF/RHD patients with residual valvular lesions. Yaman, et al. (2003) found that serum levels of ICAM-1 were increased in patients at the onset of ARF, reaching a peak in the active phase and declining during remission to the inactive phase of the disease (Yaman,

et al. 2003). The authors considered ICAM-1 as an important factor contributing to the pathogenesis of ARF. They also commented that improvement of ARF management might best be determined by monitoring serum ICAM-1 levels, even when clinical and other laboratory test results have returned to normal. The authors also demonstrated high serum levels of VCAM-1 and ICAM-1 in patients with rheumatic mitral stenosis. However, Chen, et al. (2004) verified that the plasma level of soluble VCAM-1 fell significantly in patients with mitral stenosis after percutaneous transluminal mitral valvuloplasty. Hafez, et al. (2013) assayed the serum levels of ICAM-1, VCAM-1 and E-selectin from 50 children with ARF/RHD. The level of these molecules was significantly higher in patients than in healthy children. In addition, the serum levels of these molecules were significantly higher in patients with severe carditis than in patients with mild to moderate carditis. Remarkably, high levels of molecules were also recorded among those with heart failure than those without heart failure. The authors also reported that the pre-treatment serum levels of ICAM-1 and VCAM-1 were markedly higher in the patients with residual valve lesions than normal valve patients.

#### 2.4.1.4 Characteristic histological features of rheumatic heart

The characteristic histological features of ARF/RHD include extensive inflammation of myocardium and valves with infiltration of T-cells, macrophages, fibroblasts, neutrophils and deposition of collagen fibres (Fae, et al. 2004; Pahlman, et al. 2006). Guilherme, et al. (1995) detected a high proportion of CD4+ T-cells in valvular lesions, and this was further confirmed by studies carried out on heart valves from patients by Roberts, et al. (2001). Fraser, et al. (1995) observed aggregated macrophages in the mitral valves during the early stages of inflammation, followed by lymphocytic infiltration and neovascularisation in 15 patients with ARF/RHD. Further studies on rheumatic hearts detected infiltration of T-cells and B-cells due to delayed type hypersensitivity inflammation and autoimmune progression (Kay 1997; Abbas and Lichtman 2003; Sampaio, et al. 2007). Immunohistochemical determination performed on fragments of mitral valve and papillary muscle of RHD patients showed predominantly CD4+ cells. Intralesional T-cell lines generated from these tissues revealed predominantly CD3+TCRαβ+CD4+ T cells (Fae, et al. 2004). It has been proposed that neovascularisation arises with infiltration of fibroblasts, Anitschkow cells and neutrophils (Guilherme, et al. 2001b; Kirvan, et al. 2003; Sampaio, et al. 2007; Guilherme and Kalil 2010).

In addition, Aschoff bodies (Figure 2.6) are granulomatous structures commonly present beneath the endocardium and contain Anitschkow cells, Aschoff cells and T-cells (Roberts, et al. 2001; Carapetis, et al. 2016). The myocardial Aschoff bodies are believed to be formed following injury of the interstitial non-myogenic collagen fibres (Murphy 1952). Formation of exudative, granulomatous or fibrotic Aschoff bodies leads to dysfunction of the myocardium and mitral valves (Cunningham 2012; Carapetis, et al. 2016). Further inflammation leads to fibrinous vegetation (verrucae) of the leaflets and subsequent scarring, which might ultimately lead to valvular stenosis (Veasy and Tani 2005; Carapetis, et al. 2016). Although the myocardium may heal following inflammation, there can be permanent damage to the mitral valves.

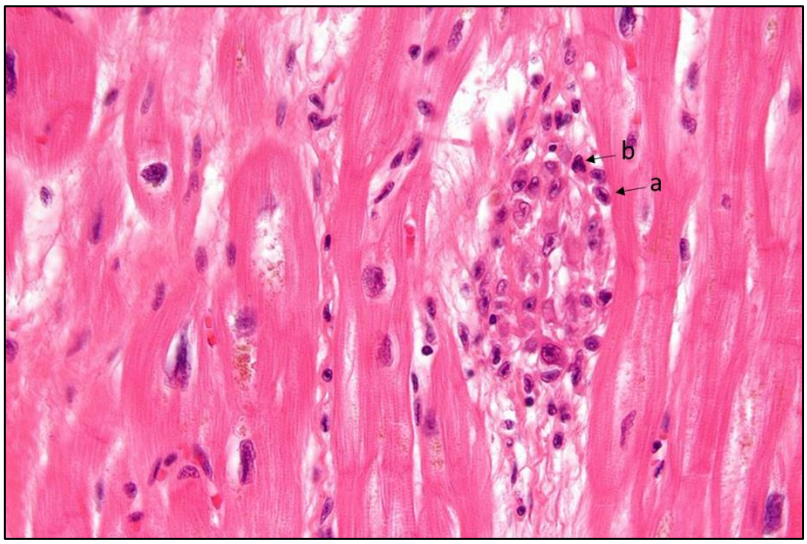


**Figure 2.6** A typical Aschoff nodule in myocardium of patient with ARF/RHD. Granulomatous structure has fibrinoid deposition, lymphocytic infiltration, and characteristically abnormal macrophages surrounding necrotic centres. Some of these macrophages are with condensed chromatic and called Anitschkow cells or "caterpillar cells" (a). Others may fuse to form multinucleated giant cells (b). Image adapted from Virmani and Roberts (1977) and Love and Restrepo (1988).

Fibrosis of heart tissues is the hallmark of structural remodelling, resulting from the chronic inflammatory rheumatic process in ARF/RHD. Fibrosis results from extensive deposition of collagen typically induced by mechanical overload or tissue damage (Towbin 2007). Lis, et al. (1987) reported that in ARF/RHD there is an approximately three-fold increase in the total amount of collagen fibre in heart valves. Excessive collagen deposition leads to thickening of the mitral valve leaflets and fusion of commissures and chordae tendinea and ultimately to mitral stenosis (Banerjee, et al. 2014). Mitral stenosis induces mitral regurgitation, with increase in compensatory dilatation of ventricle. Progressive ventricular dilatation causes

increase in wall stress with tissue damage and contractile dysfunction and eventually heart failure (Marciniak, et al. 2007; Gaasch and Meyer 2008; Carapetis, et al. 2016).

#### 2.4.1.5 Characteristic functional changes of rheumatic heart

The inflammatory responses in ARF/RHD have functional effects on various parts of the heart valves that can lead to cardiac dysfunction and ultimately heart failure. Excessive deposition of inflammatory cells and collagen induce thickening of the mitral leaflets. The thickening of mitral valves leads to limited leaflet movement and excessive leaflet tip motion, lack of coaptation, compensatory dilatation of the left atrium and ventricle, and mitral regurgitation (Carapetis, et al. 2016). The dilation of valve annuli and elongation of chordae tendinea also result in inadequate coaptation of the valve leaflets and resulting valvular regurgitation (Veasy and Tani 2005). Further inflammation leads to fibrinous vegetations along the edges of the leaflets and scarring, which might ultimately lead to valvular stenosis, in which the valve becomes narrowed, stationary and is unable to fully open (Carapetis, et al. 2016). Moreover, mitral stenosis is the most frequent occurrence in patients with ARF/RHD (Hollenberg 2017). However, subclinical systolic dysfunction exists due to desynchrony of myofibrils contraction, even while the left ventricular functions are normal with conventional echocardiography (Guven, et al. 2014). Inflammation of the myocardium leads to a delay in the electrical impulse conduction from the sinoatrial node (SA node) to the ventricle. This functional change can be determined by using electrocardiogram (ECG). Prolongation of P-R interval in a typical ECG trace represents the contractile dysfunction from the atrium to the ventricle (Gewitz, et al. 2015).

### 2.4.2 Studies in animal models

Humans are the unique hosts for GAS infections and ARF/RHD. Animal models showing typical signs, pathogenesis and pathology specific to particular human disease are necessary for a deeper understanding of the mechanisms underlying diseases such as ARF/RHD. Several studies have been performed in mice, rats, rabbits, non-human primates, pigs, sheep, goats, cattle and even in dogs and cats to find a suitable animal model to examine the autoimmune process in ARF/RHD (Gross, et al. 1929; Baker, et al. 1935; Yang, et al. 1977; Burova, et al. 2004; Burova, et al. 2005; Gorton, et al. 2009; Huang, et al. 2009; Xie, et al. 2010; Kirvan, et al. 2014; Gorton, et al. 2016). Among them, different strains of rat, mouse and guinea pig showed changes that mimic ARF/RHD. Upon injection of antigens derived from GAS, or cardiac myosin, these animals developed myocarditis and/or valvulitis similar

to patients with ARF/RHD. They also showed antibody and T-cell responses that cross-react with host cardiac proteins. The rodent and small animal models used previously to model autoimmune mediated carditis and the antibody and T-cell responses to streptococcal and host antigens, histological changes in the mitral valve and myocardium in the animals are summarised in the Table 2.2 and 2.3.

**Table 2.2** Immunopathological changes in rodents investigated as model for experimental autoimmune carditis

| Antigen and route of injection | Histological changes in the host | Antibody response | T-cell response | Host cross-reactivity | References |
|---|---|---|---|---|---|
| **Lewis rat** (*Rattus norvegicus*) | | | | | |
| Whole GAS (f.p.) | **Myocarditis** Monocyte, fibroblast, Aschoff-like cell **Valvulitis** Lymphocyte, monocyte, macrophages, fibroblast, giant cell | Anti-myocardial IgG, anti-streptolysin O (ASO) | | Valvular protein, myocardial protein | (Cavelti 1947; Huang, et al. 2009; Xie, et al. 2010) |
| Cell wall fragments of GAS (s.c., i.p.) | **Myocarditis, valvulitis** T-cell, monocyte, other MNCs, PMNCs, Anitschkow cell | Anti-GAS IgG | CD3+, CD4+, CD8+, IFN-γ, TNF-α | Myosin, LMM | (Cromartie, et al. 1977; Lymbury, et al. 2003; Gorton, et al. 2009; Kirvan, et al. 2014) |
| Recombinant proteins or peptides of GAS (s.c., f.p.) | **Myocarditis, valvulitis** T-cell, other MNCs, PMNCs, Anitschkow cell | Anti-myosin IgG | CD3+, CD4+, CD8+, CD68+, TCR-ab+ | Myosin, valvular protein | (Quinn, et al. 2001; Gorton, et al. 2006; Gorton, et al. 2010; Gorton, et al. 2016) |
| Cardiac protein (s.c., f.p.) | **Myocarditis** Lymphocyte, PMNCs, giant cell, fibroblast, MNCs, macrophages, dendritic cells, fibrin, collagen | Anti-myosin IgG | CD4+, CD8+, CD11c+, CD45+, NK cell, ED-1+, Th17, IL-1α, | Myosin, laminin, LMM | (Friedman, et al. 1970; Kodama, et al. 1990; Okura, et al. 1998; Tsujimura, |

| | | | | | |
|---|---|---|---|---|---|
| | **Valvulitis**<br>MNCs, Anitschkow cell, increased peripheral WBC | | IL-1β, IL-1ra, IL-2, IL-6, IL-10, IL-12, IFN-γ, IP-10, IP-1α, TNF-α, CINC-1, CINC-3, MMP-1 | | et al. 2000; Galvin, et al. 2002; Li, et al. 2004; Gorton, et al. 2006; Tanaka, et al. 2011; Nakagawa, et al. 2012) |
| **Mice** (*Mus musculus*) | | | | | |
| Cell wall fragments of GAS (i.p.) | **Myocarditis**<br>MNCs, Anitschkow myocyte<br>**Valvulitis**<br>MNCs, PMNCs Epicarditis, sub-epicarditis | Collagen IV, reactive IgG, IgG1, IgG2a | CD44+, CD62L- | Basement membrane collagen | (Ohanian, et al. 1969; Dinkla, et al. 2003b; Guilherme, et al. 2013a) |
| Cardiac protein (s.c., i.p., i.v., f.p.) | **Myocarditis, pericarditis, endocarditis**<br>MNCs, PMNCs, plasma cell, lymphocyte, Anitschkow myocyte, giant cell, eosinophil | IgG1, IgE, anti-myosin Ig, anti-myelommal Ig, anti-sarcolemmal IgG, normal level of IgM | CD4+, CD8+, B220+ B-cell, IL-4 | Cardiac myosin, sarcolemma | (Gray 1949; Izumi, et al. 1987; Neu, et al. 1987; Kodama, et al. 1990; Smith and Allen 1991; Afanasyeva, et al. 2001) |
| No antigen. Mice lacking genes for FcγRI, FcγRIII & FcγRIV | **Mitral valvulitis**<br>T-cell, macrophages | IgG1, IgG2b, IgG2c | CD11c, CD16, CD32, CD64, DC, F4/80 | | (Hobday, et al. 2014) |
| **Guinea pig** (*Cavia porcellus*) | | | | | |
| Whole GAS (s.c., f.p., i.m., i.v.) | **Myocarditis, valvulitis**<br>B-cell, T-cell, macrophages, MNCs, fibroblast | IgG | CD8+ | Cardiac myofibre, sarcolemma | (Gross, et al. 1929; Yang, et al. 1977) |
| Cell wall fragments of GAS (s.c., f.p., i.m.) | **Myocarditis, valvulitis**<br>B-cell, T-cell, macrophages, fibroblast | IgG | CD8+ | Cardiac myofibre, sarcolemma | (Yang, et al. 1977) |
| Cardiac protein (s.c., | **Myocarditis**<br>Lymphocyte, | Anti-myosin-β IgG | CD3 | | (Hosenpud, et al. 1985; |

| | | | | | |
|---|---|---|---|---|---|
| f.p., i.v.) | PMNCs, fibroblast | | | | Kodama, et al. 1990; Radhakrishnan 1996) |

f.p.: foot pad, i.v.: intra-venous, i.m.: intra-muscular, s.c.: sub-cutaneous, i.p.: intra-peritoneal, MNC: mono-nuclear cell, PMNC: poly-morpho-nuclear cell, WBC: white blood corpuscles, Ig: immunoglobulin, CD: cluster differential, IFN: interferon, TNF: tumour necrosis factor, TCR: T-cell receptor, NK: natural killer, Th: helper T-cell, IL: interleukin, CINC: cytokine-induced neutrophil chemoattractant, MMP: matrix metallo-proteinases, ED-1+: rat macrophage specific marker, LMM: light meromyosin.

**Table 2.3** Immunopathological changes in small animals investigated as model for experimental autoimmune carditis

| Antigen and route of injection | Histological changes in the host | Antibody response | T-cell response | Host cross-reactivity | References |
|---|---|---|---|---|---|
| **Rabbit** | | | | | |
| Whole GAS (s.c., f.p., i.m., i.v., i.d., i.p.) | **Myocarditis, valvulitis** Lymphocyte, MNCs, giant cell, leukocyte, Aschoff bodies, fibroblast, fibrin, collagen | | | Skeletal muscle | (Gross, et al. 1929; Moon and Stewart 1931; Baker, et al. 1935; Norlin 1959; Yang, et al. 1977) |
| Cell wall fragments of GAS (s.c., f.p., i.m., i.v., i.d.) | Myofibrosis with degeneration of sarcoplasm, myofibril, endothelia and basement membrane Lymphocyte, macrophages, granulocyte | Anti-myosin IgG, anti-sarcolemmal Ig | T-cell, IL-6, C3 | Sarcolemmal membrane protein, myosin, aortic glycoprotein, skeletal muscle | (Yang, et al. 1977; Goldstein, et al. 1983; Dale and Beachey 1985b; Dale and Beachey 1986; Jones and Fischetti 1987; Sargent, et al. 1987; Burova, et al. 2004; Burova, et al. 2005) |
| Cardiac | **Myocarditis** | Anti-rabbit | | | (Kaplan |

| | | | | | |
|---|---|---|---|---|---|
| protein (s.c., f.p., i.v.) | MNCs, PMNCs, eosinophil | cardiac IgG | | | and Craig 1963) |
| **Dog** | | | | | |
| Whole GAS (i.p. followed by i.v.) | Controversial myocardial and valvular lesions similar to RHD | | | | (Gross, et al. 1929; Moon and Stewart 1931) |
| **Cat, sheep, calf, pig** | | | | | |
| Whole GAS (i.p. followed by i.v.) | **Myocarditis and valvulitis** Lymphocyte, MNCs, PMNCs | | | | (Gross, et al. 1929) |

i.v.: intra-venous, i.m.: intra-muscular, s.c.: sub-cutaneous, i.d.: intra-dermal, i.p.: intra-peritoneal, f.p.: foot pad, MNC: mono-nuclear cell, PMNC: poly-morpho-nuclear cell, Ig: immunoglobulin, IL: interleukin.

Other than the above described animal models, two studies using non-human primate (rhesus monkey, *Macaca mulatta*) model showed typical RHD lesions. following pharyngeal spray of GAS organisms, Vanace (1960) demonstrated pericarditis, myocarditis and valvulitis with infiltration of lymphocytes, histiocytes, Anitshkow cells and plasma cells. Later, Anand, et al. (1983) reported similar histological changes with endocardial and subendocardial infiltration of MNCs after subcutaneous injection of GAS membrane antigen.

Most of the animal models studied only showed evidence of myocarditis and valvulitis lesions that poorly represent the ARF/RHD (Unny and Middlebrooks 1983). However, in the past decade, the Lewis rat autoimmune valvulitis (RAV) model has been used and shown to induce experimental myocarditis and valvulitis, contributing towards understanding the pathogenesis of ARF/RHD (Kodama, et al. 1990; Wegmann, et al. 1994; Li, et al. 2004; Guilherme, et al. 2011b; Rush, et al. 2014; Gorton, et al. 2016). In response to different streptococcal antigens, Lewis rats developed typical histological lesions with activation and infiltration of inflammatory cells and antibody responses similar to human RHD patients (Table 2.2 and 2.4). In a study of Lewis rats, myocarditis lesions developed in 80% of rats with focal inflammatory cell infiltration near small vessels. Valvulitis were induced in 40% of Lewis rats following immunisation with formalin killed GAS (Huang, et al. 2009). In addition, immunostaining of cellular infiltrates in valvular and myocardial tissue revealed that heart damage observed in streptococcal M-protein-immunised rats is mediated by CD4+ cells and macrophages, in agreement with human studies (Guilherme, et al. 2001b). Following immunisation with rM6, Quinn, et al. (2001) reported the induction of valvulitis and focal

myocarditis in Lewis rats which were histologically similar to human RHD lesions. In support of these studies, lesions and cellular infiltration predominantly of CD4+ cells, CD68+ macrophages and Anitschkow cells (caterpillar cells) were observed in mitral and aortic valves as well as the tricuspid valve of rats immunised with rM5 (Quinn, et al. 2001; Gorton, et al. 2009). A functional study of rheumatic rat hearts also showed ultrasonographic findings similar to human RHD patients (Zachary, et al. 2002).

**Table 2.4** Comparative pathological features between patients with RHD and the RAV model

| RHD (Human) | RAV model |
|---|---|
| **Gross anatomical changes** | |
| Hypertrophy or stenosis of mitral valve (Becker and Murphy 1969; Marijon, et al. 2007) | Cardiac hypotrophy (Cavelti 1947) |
| **Functional changes** | |
| **ECG**<br>Diffuse T-wave inversions, saddle shaped ST segment elevations, prolonged QT or PR interval (Taran and Szilagyi 1951; Thomas 1953; Feldman and McNamara 2000) | **ECG**<br>Prolongation of PR interval (Gorton, et al. 2016). |
| **Echocardiography**<br>Left atrial and ventricular cardiomegaly, vegetation and thickened leaflet (Hubbard, et al. 1987). Mitral, aortic valve regurgitation, restricted leaflet mobility, valvular thickening (Brand, et al. 1992; Narula and Kaplan 2001; Marijon, et al. 2007; Goel, et al. 2013; Jain and Mankad 2013; Shivaram, et al. 2013) | **Echocardiography**<br>Left atrial and ventricular cardiomegaly (Zachary, et al. 2002) |
| **Histological changes** | |
| **Cellular infiltrate**<br>CD4+, CD8+, macrophages, dendritic cells, MNCs, PMNCs (Kaplan and Frederick 1961; Becker and Murphy 1969; Marboe, et al. 1985; Amoils, et al. 1986; Chow, et al. 1989; Kemeny, et al. 1989; Fraser, et al. 1997; Roberts, et al. 2001; Shioji, et al. 2001; Fae, et al. 2005; Fairweather, et al. 2006; Guilherme, et al. 2011a) | **Cellular infiltrate**<br>CD3+, CD4+, CD8+, CD11c+, Th17, CD45+, CD68+, αβTCR+, macrophages, dendritic cells, MNCs, PMNCs, WBC, NK cell, neutrophil, giant cell, fibroblast, ED-1+, histiocyte (Cavelti 1947; Friedman, et al. 1970; Kodama, et al. 1990; Okura, et al. 1998; Galvin, et al. 2000; Quinn, et al. 2001; Lymbury, et al. 2003; Gorton, et al. 2006; Gorton, et al. 2009; Gorton, et al. 2010; Tanaka, et al. 2011; Nakagawa, et al. 2012; Kirvan, et al. 2014; Gorton, et al. 2016) |
| **Inflammatory pathology**<br>Granulomatous myocarditis, myocardial | **Inflammatory pathology**<br>Granulomatous, fibrinous and necrotic |

| | |
|---|---|
| necrosis and fibrosis, valvulitis, valvular fibrosis with neovascularisation, perivascular deposition of connective tissue, Anitschkow cell, Aschoff bodies, interstitial degeneration and oedema (Kaplan and Frederick 1961; Kemeny, et al. 1989; Narula, et al. 1993; Fraser, et al. 1995; Galvin, et al. 2000; Roberts, et al. 2001) | mitral, tricuspid and aortic valvulitis, myocardial necrosis, Anitschkow cell, Aschoff bodies, interstitial and perivascular deposition of collagen and connective tissue (Cavelti 1947; Okura, et al. 1998; Galvin, et al. 2000; Tsujimura, et al. 2000; Quinn, et al. 2001; Lymbury, et al. 2003; Li, et al. 2004; Gorton, et al. 2009; Nakagawa, et al. 2012; Gorton, et al. 2016) |
| **Immunological changes** | |
| **Antibody responses**<br>Antistreptolysin-O, anti-streptococcal Ig, anti-myosin Ig (Becker and Murphy 1969; Galvin, et al. 2000) | **Antibody responses**<br>Anti-GAS IgG, anti-myocardial IgG, anti-myosin IgG (Kodama, et al. 1990; Tsujimura, et al. 2000; Quinn, et al. 2001; Li, et al. 2004; Gorton, et al. 2006; Gorton, et al. 2009; Huang, et al. 2009; Gorton, et al. 2010; Nakagawa, et al. 2012) |
| **Cytokine production**<br>IL-1, IL-2, IL-4, IL-6, IL-8, IFN-γ, TNF-α, (Fraser, et al. 1997; Fae, et al. 2005; Zhang, et al. 2009; Guilherme, et al. 2011a) | **Cytokine production**<br>IL-2, IL-6, IL-10, IL-12, IL-17, IL-1β, IL-1ra, IFN-γ, TNF-α, CINC-1, CINC-3, IP-10, LIX, MIP-1α (Okura, et al. 1998; Quinn, et al. 2001; Li, et al. 2004; Tanaka, et al. 2011; Nakagawa, et al. 2012; Kirvan, et al. 2014) |
| **Upregulation of receptors**<br>TLR-2, TLR-7, TLR-8, VCAM-1 (Springer 1994; Roberts, et al. 2001; Zhang, et al. 2009) | **Upregulation of receptors**<br>VCAM-1, ICAM-1, MMP, tissue inhibitor of MMP-1 (Nakagawa, et al. 2012; Gorton, et al. 2016) |

MMP: matrix metalloproteinases, IP: IFN-γ-induced protein, CINC: cytokine induced neutrophil chemoattractant, MIP: macrophage inflammatory protein, ICAM: intercellular adhesion molecule, LIX: a neutrophil chemoattractant, MNC: mono-nuclear cell, PMNC: polymorphonuclear cell, WBC: white blood corpuscles, Ig: immunoglobulin, CD: cluster differential, IFN: interferon, TNF: tumour necrosis factor, TCR: T-cell receptor, NK: natural killer, Th: helper T-cell, IL: interleukin, ED-1+: rat macrophage specific marker.

## 2.5 DIAGNOSIS OF RHD

Clinically ARF/RHD are frequently diagnosed based on clinical signs and symptoms with a previous history of throat or skin infection by GAS (Carapetis, et al. 2016; Gottlieb, et al. 2018). Jones criteria were first introduced in 1944 for diagnosis of ARF/RHD (Jones 1944). After that, several modifications have been made for effective diagnosis with latest update at 2015 (Gewitz, et al. 2015). The diagnostic criteria are divided into major and minor categories within the Jones criteria. A patient is confirmed ARF/RHD if either two major or one major and at least one minor manifestation are evident. Evidence of previous GAS infection is usually confirmed by using streptococcal serology. Recently, Licciardi, et al.

(2018) introduced high-risk (HR) criteria which increased 20% patients with diagnosis of ARF.

### 2.5.1 General criteria

Fever and arthritis are the most common clinical symptoms and are seen in >90% and 75% of patients respectively (Carapetis, et al. 2016). Both fever and arthritis are difficult to differentiate from other diseases. Arthritis of ARF/RHD is very responsive to non-steroidal anti-inflammatory drugs. In addition, painless sub-cutaneous round nodules of 0.5-2 cm in diameter are also seen in patients with ARF/RHD although less common than fever and arthritis (Carapetis and Currie 2001; Steer, et al. 2009a). Moreover, bright pink-blanching macules or papules known as erythema marginatum are usually observed around the trunk and in the proximal limbs. In some cases, the patients with ARF develop involuntary movements of skeletal muscles known as Sydenham chorea. Sydenham chorea is a self-limiting symptom which usually diminishes over time with some exceptions where patients may suffer even beyond two years (Cardoso, et al. 1999).

However, carditis is observed in >50% of patients with ARF and is characterised by inflammation, stenosis and regurgitation of the mitral valve and less frequently of the aortic valve, and myocarditis (Veasy, et al. 1987; Veasy, et al. 1994; Vijayalakshmi, et al. 2008). Unusual manifestations that are not part of the Jones criteria include reactive arthritis, indolent carditis or the involvement of all four heart valves (Taranta and Stollerman 1956; Guvenc and Cimen 2017; Nishibukuro, et al. 2018). Carditis development in patients can be assessed using different imaging techniques such as electrocardiography (ECG) and echocardiography (Echo).

### 2.5.2 Imaging techniques

The immunopathology of a heart with rheumatic carditis can be demonstrated by different imaging tools. Chest X-ray was used in the mid twentieth century for the diagnosis of cardiac pathology in ARF/RHD (Holt 1946; Streda, et al. 1971). Chest X-rays may show left atrial enlargement and redistribution of pulmonary vascular flow to the upper lungs fields, pericardial calcification, pulmonary oedema, pulmonary ossification: due to mitral valve disease, cardiomegaly, left atrial enlargement from mitral valve disease, diffuse alveolar haemorrhage can result from severe mitral stenosis (Woolley and Stark 1999). In lateral

projections, calcification of the mitral valve apparatus may be visible. If the patient has developed heart failure, pulmonary congestion will be visible on the chest X-rays.

Later, electrocardiographic (ECG) assessment of cardiac dysfunction was introduced. A typical ECG trace consists of waveform components which indicate electrical events during one heartbeat. These waveforms are labelled as P, Q, R, S, T and U. P wave is the first short upward movement of an ECG trace (Figure 2.7). It indicates that the atria are contracting, pumping blood into the ventricles. The QRS complex, normally begins with a downward deflection, Q; a larger upwards deflection, a peak R; and then a downwards S wave. The QRS complex represents ventricular depolarisation and contraction. The P-R interval indicates the transit time for the electrical signal to travel from the sinoatrial (SA) node to the ventricles. In human, prolongation of the P-R interval is observed in 30-35% patients with ARF/RHD (Homer and Shulman 1991; Cunningham 2012). In Jones criteria, prolonged P-R interval is included as a minor manifestation (Gewitz, et al. 2015). ECG data based on peak P and R values have also been published in an earlier study where prolonged P-R interval was reported in Lewis rats following injection with GAS rM5-protein (Gorton, et al. 2016).

The QTc interval has also been recognised as a useful sign of active carditis. The abnormal prolongation of the QT interval in patients is shown to be a function of the severity of the carditis and not of the cardiac rate. Severe clinical carditis lengthens the electrical systole relative to diastole. This disturbance in the sequence of electrical events in the cardiac cycle is considered to be a characteristic of carditis. This event might be used as a valuable diagnostic criterion for recognising carditis in rheumatic patients (Taran and Szilagyi 1947; Abrahams 1949). QT, QTc and P-wave dispersions are significantly greater and permanent in both the acute and chronic RHD patients. Severity of mitral regurgitation (MR) and left atrial enlargement are found to be positively correlated with P-wave dispersion (Alp, et al. 2014). T-wave changes are rare expect as a sequel to pericarditis (Thomas 1953).

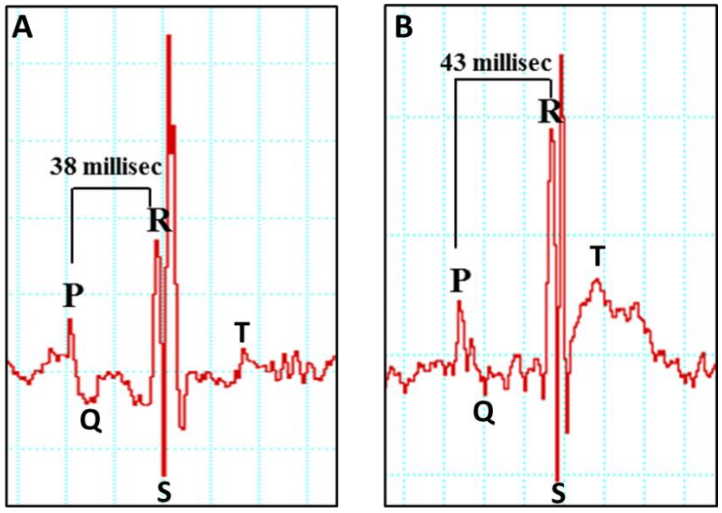


**Figure 2.7** ECG in Lewis rat. ECG trace consists of waveform labelled P, Q, R, S, T. Normal P-R interval in healthy control rat (A). (B) Prolongation of P-R interval in GAS rM5 immunised rats.

Echocardiography (Echo) is the primary imaging modality in rheumatic mitral stenosis. It is essential for diagnosis, serial follow up, therapeutic procedural guidance and prognostication. In large scale population screening, echocardiography is a useful tool for early identification of RHD and prevention of chronic sequelae. Echocardiography has considerably enhanced the clinical assessment and management of patients with ARF/RHD compared to simple auscultation (Gewitz, et al. 2015). Echo is now considered essential for large scale population screening, early detection of ARF/RHD, for serial follow up and for therapeutic procedural guidance (Abernethy, et al. 1994; Minich, et al. 1997; Figueroa, et al. 2001; Narula and Kaplan 2001; Vijayalakshmi, et al. 2008). Echocardiographic findings that feature in ARF/RHD include changes to mitral valvular morphology, especially valvular thickening and slow or impaired valvular leaflet movement (Jain and Mankad 2013; Wunderlich, et al. 2013). Thickening of the mitral valve with limited movement and excessive leaflet tip motion, thickening and fusion of chordae, lack of coaptation, compensatory dilatation of left atrium and ventricle and mitral regurgitation are salient findings of patients with rheumatic heart (Figure 2.8) (Carapetis, et al. 2016). A two-dimensional (2D) echo is commonly used to detect these findings (Chauvaud, et al. 2001; Carabello 2005; Jain and Mankad 2013; Wunderlich, et al. 2013).

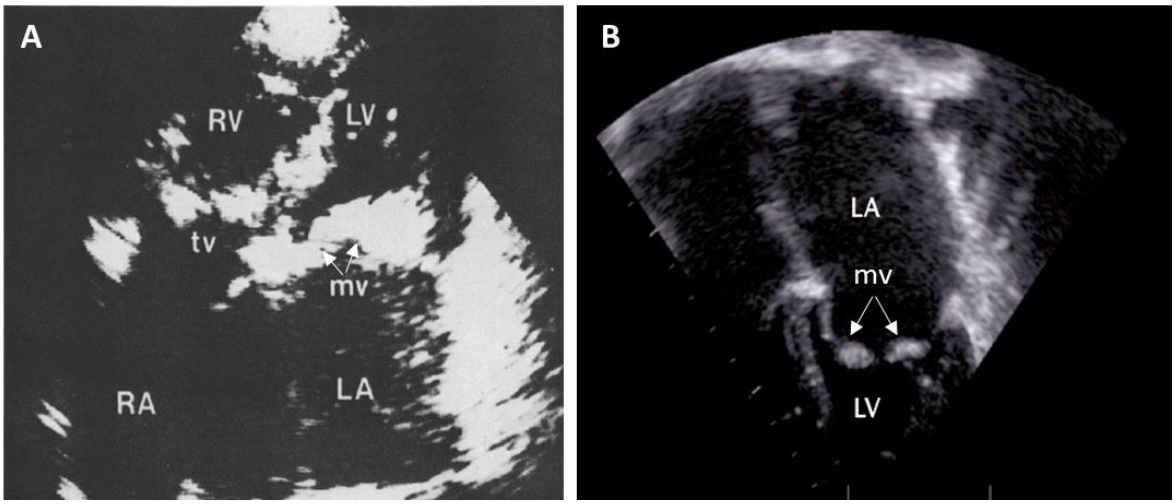


**Figure 2.8** Apical four-chamber views in black and white Doppler showing gross thickening of the mitral valve in patients with RHD (A-B) (Hubbard, et al. 1987; Carapetis, et al. 2016). Left atria are severely dilated. LA: left atrium, LV: left ventricle, RA: right atrium, RV: right ventricle, mv: mitral valve.

In addition, Doppler echocardiography is more sensitive in detecting valvular lesions that are missed in clinical examination (Carabello 2005). In patients with RHD, mitral regurgitation (MR) (Figure 2.9) is the commonest murmur followed by aortic regurgitation (AR). Overriding or prolapse of the anterior (less commonly of the posterior) mitral valve leaflet due to elongation of chordae is the main echocardiographic feature of pure MR in young people (Marcus, et al. 1989; Camara, et al. 2004; Kamblock, et al. 2005). Chordal rupture can lead to flail leaflet in more severe cases (Marcus, et al. 1989). Dilation of the posterior mitral annulus is also a common finding (Marcus, et al. 1989; Kamblock, et al. 2005). Apparent masses may be detected as echo-dense structures, frequently mobile and described according to their situation, shape, size and how they interfere with the motion of the mitral valve. In addition, irregular outlines and oscillatory motion of valvular leaflets demonstrated different kinds of vegetations (Hubbard, et al. 1987).

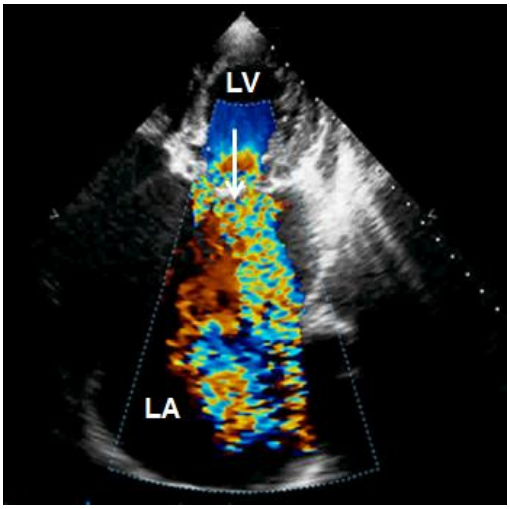


**Figure 2.9** Mitral regurgitation in patient with RHD assessed using Doppler echo (Srinivas, et al. 2013). LV: left ventricle, LA: left atrium

In adult patients, valvular and/or chordal thickening and tethering of either or both leaflets can be present even in mild disease and is the predominant mechanism of MR (Chauvaud, et al. 2001). Patients with MR and mitral stenosis (MS) show characteristic 'elbow' appearance of the anterior mitral leaflet due to the restricted leaflet motion. The Doppler echo is very significant in detecting regurgitation lesions, especially MR and in the setting of multivalvular involvement (Marijon, et al. 2007; Shivaram, et al. 2013). The lengthening of QT dispersion on the echo Doppler cardiogram reflects cardiac involvement in ARF and be a new important parameter in diagnosis and therapeutic decision making for RHD (Remigio de Aguiar, et al. 2010).

The effective prevention and control of ARF/RHD requires a more complete understanding of the aetiology and pathogenesis of this significant disease. The current epidemiological studies on the prevalence and incidence of ARF/RHD and streptococcal carriage in the host has questioned the role of non-group A streptococci, especially group G *Streptococcus* (GGS) in the aetiology of these conditions. Therefore, there is an urgent need to investigate the involvement of GGS in the pathogenesis of ARF/RHD. Furthermore, the common epitopes shared by GAS, GGS and host heart proteins also may be relevant to the early diagnosis of ARF/RHD and should be considered in the design of effective vaccine candidates to eradicate this disease.

# CHAPTER 3
# GENERAL MATERIALS AND METHODS

The general materials and methods used in this project are described in this Chapter. The materials and methods which are specific to a particular chapter are described in the relevant chapter. The details for buffers are described in Appendix 1 and suppliers/distributors are included in Appendix 2.

## 3.1 MATERIALS

### 3.1.1 General chemicals and consumables

Chemicals of the highest grade available were purchased from *Sigma* (*Australia*) unless otherwise stated. Media for bacterial culture were purchased from *Sigma* and *Acumedia* (*Australia*). Plastic ware including microfuge tubes, centrifuge tubes, and petri dishes were purchased from *Sarstedt* (*Australia*). Non-sterile 96 well flat-bottom micro plates for ELISA and sterile flat-bottom plates and flasks for cell culture were purchased from *Thermo Scientific* (*Australia*).

#### 3.1.1.1 Reagents for protein expression

Antibiotics used for bacterial culture, ampicillin (#A9518) and kanamycin (#K1377), HIS-select nickel affinity gel (#H0537) for M-protein purification and acrylamide (#A9926) for sodium dodecyl sulfate polyacrylamide gel electrophoresis (SDS-PAGE) were purchased from *Sigma* (*Australia*). Isopropyl β-D-1-thiogalactopyranoside (IPTG, #R0392) and Tris-HEPES SDS-PAGE sample buffer (#28398) and 20× running buffer (#28368) was from *Thermo Scientific* (*Australia*). Disposable polypropylene (10ml) desalting/buffer exchange columns (#34964) for protein purification was from *Qiagen* (*Australia*). Chromatography columns were purchased from *Amersham Bioscience* (*Australia*). BCA protein assay kit (#A53225) was from *Pierce Biotechnology* (*USA*). Lysozyme (#1243004), protease inhibitors (#P-1543) and ammonium persulfate (APS, #161-0700) were from *Roche*, *Bio-rad* (*Australia*). Centrifugal filter units (Ultracel-10k, #UFC801008) were purchased from *Millipore Corporation* (*Australia*).

### 3.1.1.2 Antigens

Calcium activated myosin from porcine heart (buffered aqueous solution, 12.9 mg/ml, #M0531) and Collagen I from human placenta (5 mg vial, Bornsteein and Traub type I, #C7774) was purchased from *Sigma* (*Australia*).

### 3.1.1.3 Adjuvants

Complete and incomplete Freund's adjuvant (CFA, #F5881 and IFA, #F5506) were purchased from *Sigma* (*Australia*). Lyophilised *Bordetella pertussis* toxin (#PHZ1174) was purchased from *Gibco* (*USA*).

### 3.1.1.4 Reagents for lymphocyte culture and proliferation assays

RPMI medium 1640 (#R7388), HEPES buffer (1M, #15630-080), L-glutamine (200mM, #21051-024) and penicillin/streptomycin solution (10,000 units/ml of penicillin and 10,000 µg/ml of streptomycin, #15140-122) were purchased from *Life Technologies* (*Australia*). Autologous rat serum was sourced from Lewis rats at the Small Animal Facility at James Cook University. Pooled rat sera were heat-treated for complement inactivation by heating at 56°C for 30 min in a water bath. Samples of heat-inactivated rat sera was spread on sheep blood agar (SBA) plates and incubated at 37°C for 48 h to confirm sterility. Ficoll-Paque Plus (#17-1440-03) density gradient solution was purchased from *GE Healthcare* (*Australia*).

### 3.1.1.5 Reagents for ELISA

Flat bottomed 96 well Maxisorp plates (#44-2404-21) were purchased from *Nunc* (*Denmark*). To prepare carbonate-bicarbonate coating buffer, $Na_2CO_3$ (#463) was purchased from *Thermo Fisher Scientific* (*Australia*), $NaHCO_3$ (#S5761) was from *Sigma* (*Australia*) and $NaN_3$ (#SA189) was from *Chem-Supply Pty Ltd* (*Australia*). To prepare wash buffer, $Na_2HPO_4$ (#ALF011592.36) and NaCl (#CM0982B) were purchased from *Thermo Fisher Scientific* (*Australia*), KCl (#10198) and $KH_2PO_4$ (#10203) were from *AnalaR* (*Australia*) and Tween20 (#P1379) was from *Sigma* (*Australia*). Bovine serum albumin (#A2153) for blocking was purchased from *Sigma* (*Australia*). Goat anti-rat peroxidase conjugated IgG (#112-005-003) was purchased from *Jackson Immunoresearch* (*USA*). 2,2'-azino-bis (ABTS, #50-66-06) peroxidase substrate was purchased from *KPL* (*USA*).

#### 3.1.1.6 Reagents for histology

Rat heart tissues were preserved in 10% neutral buffered formalin (#AFAA.25ML, *Australian Biostain*), and stained using Haematoxylin and Eosin (H&E) and Masson's trichrome stain prepared in house.

#### 3.1.1.7 Reagents for immunohistochemistry

Mouse anti-rat CD106/VCAM-1 (#MCA4633GA) was purchased from *Biorad* (*USA*). Mouse anti-rat CD54/ICAM-1 (#202403) was from *BioLegend* (*USA*). Peroxidase labelled Horse anti-mouse IgG (H+L, #PI-2000), avidin-biotin Complex (ABC, #PK-6100), 3, 3'-diaminobenzidine (DAB, #SK-4100) were purchased from *Vector Laboratories* (*USA*).

### 3.1.2 Animals

Lewis rats (LEW/SsN; Albino: a,h,c: RT1) bred by sibling mating in the Small Animal House at James Cook University (Townsville, Australia) were used throughout and randomly allocated to groups. A sample size of ≥4 per group was considered adequate to achieve a power of >70% based on our previous findings in this rat model (Gorton, et al. 2009; Gorton, et al. 2016). The Lewis rat was chosen as a model as it is highly susceptible to develop autoimmune carditis (Lymbury, et al. 2003; Gorton, et al. 2009; Rush, et al. 2014; Gorton, et al. 2016). Female rats were selected for experiments as the higher prevalence and incidence rates of ARF/RHD and more severe forms of RHD have been reported in females (AIHW 2004). Rats of 8-14 weeks and 150-250 gm body weight were used for all experiments. Rats were maintained in standard rat cages with wire lids and wood shavings as bedding in 12 h light/dark cycles. Pelleted protein-rich commercial diet has minimum crude protein 18%, maximum crude fibre 5%, minimum fat 3%, maximum salt 0.5% and calcium 1.5% was purchased from *Goldmix Stockfeeds* (*Australia*) and tap water were provided *ad libitum*. Bedding was changed weekly. Experimental rats were checked daily, and a log was maintained to monitor animal well-being.

#### Animal ethics

All experiments were carried out in accordance to the institutional guidelines according to the requirements of the James Cook University Animal Ethics Committee (Approval number #A2083) and in accordance with the National Health and Medical Research Council's (NHMRC) Australian Code of Practice for the Care and Use of Animals for Scientific Purposes.

### 3.1.3 Bacterial strains and culture

#### 3.1.3.1 Streptococci

Cultures of *Streptococcus pyogenes* (group A *Streptococcus*, GAS) M type 5 strain (stock: M5 GAS, M5T5.2A, 01.02.2008) and *Streptococcus dysgalactiae* subsp. *equisimilis* (group G *Streptococcus*, GGS; stock: GGS NS3396, 07.07.2011) were provided by Pathology Queensland at The Townsville Hospital, Townsville and Queensland Institute of Medical Research (QIMR), Brisbane respectively. To culture GAS and GGS for injection and as coating antigen for ELISA, frozen stocks (-80°C in glycerol) were plated on sheep blood agar (SBA) using a sterile loop and incubated overnight at 37°C with 5% $CO_2$. Gram staining was done on the following day to confirm Gram positive cocci. A single colony of GAS or GGS was inoculated into a 1 L of Todd Hewitt yeast broth and incubated overnight at 37°C with 5% $CO_2$. To determine the total colony forming units (CFU) in 1 L, the broth culture was serially diluted from 1:10 to $1:10^{12}$ and plated in triplicate on SBA and incubated as before. The concentration of the bacteria was adjusted after counting the colonies from serial dilutions plates to $1\times10^{11}$ CFU/ml, allowing $1\times10^{10}$ CFU in 100 µl for injections. The broth culture was centrifuged at 4000 ×g for 10 min. The bacterial pellet was washed three times with PBS, resuspended in 10 ml PBS and added 1% (of total volume) neutral buffered formalin, incubated at 4°C for 48 h to kill the bacteria. To confirm bacteria had been killed, 50 µl of each GAS and GGS was spread on SBA plates and incubated for another 48 h at 37°C with 5% $CO_2$.

#### 3.1.3.2 *Escherichia coli*

An *E. coli* strain BL21 (*Qiagen, Australia*) harbouring a plasmid (pREP4) with the cloned M5 gene (*E. coli* BL21/pREP4/pQE-30.m5) (Gorton, et al. 2009) was used for the production of GAS rM5 protein. Frozen stocks were prepared in Luria-Bertani (LB) broth at 37°C supplemented with, ampicillin (100 µg/ml) and kanamycin (25 µg/ml) and stored in 15% (v/v) glycerol at -80°C for further use.

An *E. coli* strain (*E. coli* pJ404) containing a cloned M-protein gene (*emm*-type *Stg480*) from *Streptococcus dysgalactiae* subsp. *equisimilis* clinical isolate NS3396 was kindly provided by David McMillan from University of the Sunshine Coast, Queensland, Australia. LB medium containing ampicillin (100 µg/ml) was used to culture bacteria for M-protein expression and purification.

## 3.2 METHODS

### 3.2.1 Protein preparation

#### 3.2.1.1 GAS and GGS recombinant M-protein expression

Recombinant M-proteins from GAS and GGS were prepared as previously described (Robinson, et al. 1991; Gorton, et al. 2009) using the procedure described in QIAexpressionist™ Handbook (*Qiagen*). Briefly, each *E. coli* expression strain containing recombinant plasmid (*E. coli* BL21-rM5 for GAS rM5 protein and BL21/pJ404_*Stg480* for GGS Stg480 protein) was streaked onto on appropriate agar (LB/ampicillin/kanamycin for GAS rM5 and LB/ampicillin for GGS Stg480) and incubated overnight at 37°C.

The following day, a single colony was inoculated into 20 ml LB medium with 100 µg/ml ampicillin and 25 µg/ml kanamycin (for GAS) or 100 µg/ml ampicillin alone for GGS and incubated overnight at 37°C in an orbital shaker with 200 ×rpm. After approximately 24 h, bacteria were pelleted, the pellet was washed in PBS and resuspended in 20 ml fresh LB prior to 1:50 dilution into 1 L of fresh LB with appropriate antibiotics. Cultures were grown at 37°C with shaking until an $OD_{600nm}$ of between 0.4 and 0.6 was reached. A 1 ml aliquot was then removed, pelleted and stored at -20°C as the un-induced control (UC) for SDS-PAGE analysis. Expression of the 6×histidine-tagged GAS rM5 or GGS Stg480 protein was induced by the addition of isopropyl β-D-thiogalactopyranoside (IPTG) to a final concentration of 1 mM and growth allowed to continue for a further 4 h at the same temperature with shaking. A post-induction sample (induced control, IC) was removed for SDS-PAGE analysis as above.

An alternative method was used to induce expression of M-protein. A single colony of *E. coli* BL21-rM5 or BL21/pJ404_*Stg480* was spread onto appropriate agar plate filling the available agar and incubated overnight at 37°C. The following day, the plate was divided into four quadrants and each quadrant of *E. coli* was scrapped into 500 ml terrific broth with appropriate antibiotics and incubated at 37°C with shaking at 200 rpm until $OD_{600nm}$ of between 0.4 and 0.6. An un-induced control (UC) sample for SDS-PAGE was reserved. IPTG was then added and the temperature of the incubator was dropped to 16°C with shaking at 100 ×rpm for a further 48 h. An induced control (IC) sample was taken before the bacteria were pelleted by centrifugation at 4000 ×g for 20 min at 4°C. The cell pellet was weighed and kept frozen at -20°C until extraction.

### 3.2.1.2 Preparation of protein lysates

Frozen cell pellets were thawed on ice for 15-20 min and resuspended in Lysis Buffer (Appendix 1) at 2-5 ml lysis buffer per gram wet weight. A protease inhibitor cocktail was added using 1 tablet per 25 ml cell suspension. Lysozyme at 1 mg/ml was added and the suspension was incubated on ice for a further 30 min. The suspension was then sonicated (*Biosonic III, Thermo Fisher Scientific*) at 300W for 20 sec bursts with 20 sec intervals 3 times or passed through French press twice at 1000 psi. For SDS-PAGE, 10 µl of lysate sample was taken apart. RNase A at 10 µg/ml and DNase1 at 1 µg/ml was added to the remaining lysate to reduce viscosity by nucleic acid degradation. Following 15 min incubation on ice, the lysate was centrifuged at 10000 ×g for 30 min at 4°C to pellet the cell debris. A 10 µl of supernatant sample (clear lysate, CL) was removed for SDS-PAGE analysis and stored at -20°C. The remaining supernatant was filtered (0.45 µm) and mixed with a Ni-NTA resin slurry (*Qiagen, Australia*) in a 4:1 ratio, then mixed gently in a rotating wheel for 60 min at 4°C. The mixture was loaded into Ni-NTA Superflow Columns (*Qiagen, Australia*) and the flow-through was collected by gravity flow. A 10 µl of flow-through sample (flow through, FT) was removed for SDS-PAGE analysis and stored at -20°C. The mixture was then washed 3 times with 4 times the resin bed volume of wash buffer and 10 µl of each wash was collected (W1-W4) for SDS-PAGE analysis. Finally, a volume of elution buffer equivalent to a quarter of the resin bed volume was added. It was repeated 8 times and each one was collected. A 10 µl of each elution (E1-E8) was removed for SDS-PAGE analysis.

### 3.2.1.3 SDS-PAGE analysis

The samples removed at different steps of recombinant M-protein expression and extraction (UC, IC, lysate, CL, FT, W1-W4, E1-E8) were analysed by SDS-PAGE using a Mini-Protein III system (*BioRad, Australia*). The samples were mixed with an equal volume of SDS-PAGE sample buffer (#84788, *Thermo Fisher Scientific*) followed by heating at 100°C for 5 min. A 10 µl of each heated sample was loaded onto 0.75 mm 12% acrylamide gels (Appendix 1) following the inner and outer chambers being filled with 1× Tris-HEPES-SDS running buffer. In some experiments, protein was resolved on 1.0 mm 12% LongLife™ Tris-HEPES precast gels (*Gradipore, Australia*). Electrophoresis was performed at 120-150V for ~45 min or until the dye front reached the end of the gel. A 10 µl of PageMark TriColour protein ladder (#786-419, *G-Biosciences, USA*) and a known GAS rM5 protein sample were loaded into Well 1 and 2 respectively for comparison (Figure 3.1). Gels were stained with

Coomassie Blue stain (#SG-010, *NuSep, Australia*) overnight and destained with a 6% acetic acid solution. The expected size of recombinant M-proteins of GAS and GGS is 47 kilodalton (kDa) and samples that showed bands of this size were considered positive. In most cases, elution fractions 3 to 7 (E3-E7) contained proteins of the expected size (Figure 3.1). Positive elution fractions were pooled and further processed for rM protein purification and concentration.

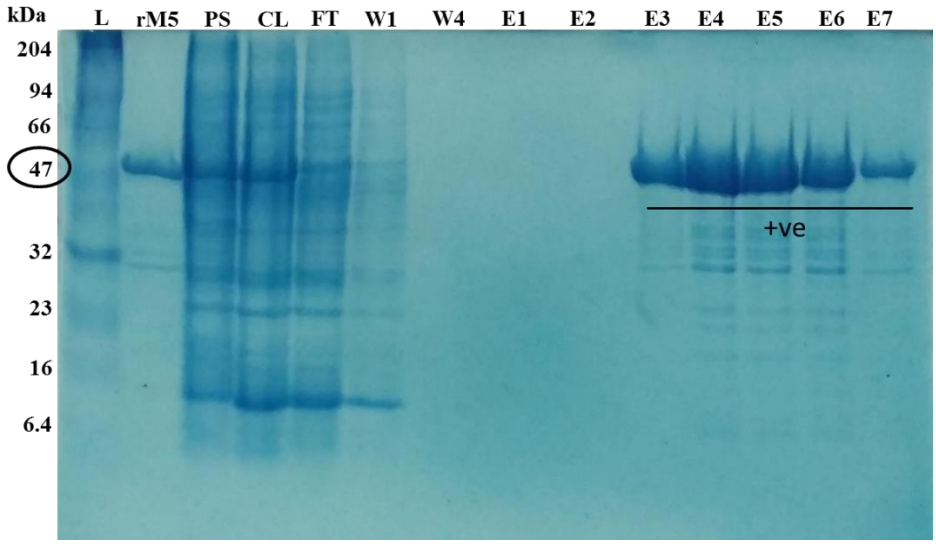


**Figure 3.1** Expression profile of GAS rM5 protein. The ladder (L) has proteins of various molecular size, from 6.4-204 kDa including a protein having similar size of GAS rM5, 47 kDa. The known purified rM5 sample (rM5) was used as positive control. The post lysis (PS), clear lysate (CL), flow through (FT) and wash 1 (W1) had rM5 protein with a lot of contaminated proteins and excluded for further purification. The wash 4 (W4) and elution 1-2 (E1-2) did not contain any rM5. However, the elution samples 3-7 (E3-7) had the maximum GAS rM5 protein with minimum contaminated proteins and were used for purification.

### 3.2.1.4 Purification and concentration of M-protein

Imidazole was removed from positive samples by buffer exchange using 1× PBS (pH 7.4) in a chromatography column (Section 3.1.1.1). The flow-through rM protein in PBS was collected for further purification and concentration using a centrifugal filter unit (Section 3.1.1.1). Ultrafiltration removes the smaller fractions (<14 kDa) of proteins. Ultrafiltration was performed at 4000 ×g for 20 min at 4°C. This was repeated 2-3 times followed by freezing at -80°C until protein estimation by bicinchoninic acid (BCA) assay.

Alternatively, each positive eluted protein fraction was mixed with an equal volume of saturated ammonium sulphate and incubate for 1 h at 4°C on rocker or rotator. The protein was precipitated by centrifugation at 18000 ×g for 20 min at 4°C. The supernatants were

discarded and the pellets were pooled by resuspension in 1× PBS (pH 7.4). The entire process was performed twice and the final pellets were washed with 1 ml PBS at 18000 ×g for 5 min at 4°C and frozen at -80°C for BCA analysis.

#### 3.2.1.5 BCA protein assay for determining M-protein concentration

The rM protein concentration was measured using a BCA Protein Assay kit (#A53225, *Pierce Biotechnology*). Bovine serum albumin (BSA) standards and protein samples were prepared according to the instructions provided by the manufacturer. The working reagent was prepared by mixing Part A containing bicinchoninic acid and Part B containing 4% cupric sulphate at a ratio of 50:1. The samples were diluted 2-fold from 1:4 to 1:64. A 25 µl aliquot of each standard (range 0-2000 µg/ml) or sample was mixed with 200 µl of working reagent were added (in triplicate) into the wells of a 96 well microtitre plate. The microtitre plate was incubated at 37°C for 30 min, cooled to room temperature and absorbance was measured at 562 nm using EZ Read 2000 spectrophotometer (*Biochrom*). A BSA standard third degree polynomial curve was generated using GraphPad Prism 7 software (Figure 3.2). The concentration of rM protein in each sample was determined from the standard curve and the dilution factor was incorporated to calculate the final concentration.

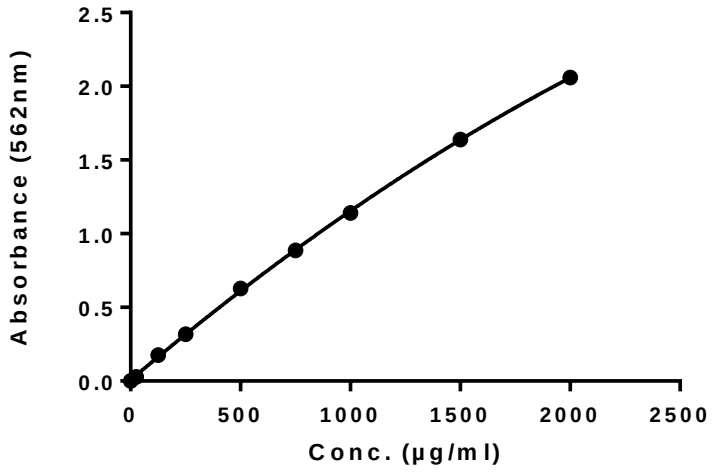


**Figure 3.2** A standard curve of BCA protein assay. Standard curve was used to calculate the total amount of GAS rM5 and GGS Stg480 proteins in the total volume of samples.

### 3.2.2 Animal experiment procedures

#### 3.2.2.1 Anaesthesia

Experimental rats were anaesthetised during subcutaneous (hock) injections and whilst performing electrocardiography (ECG) and echocardiography (echo). Animals were not

anaesthetised for intraperitoneal injections or blood collection. General anaesthesia was performed using gaseous anaesthetic machine (#VETT3 695, *AD Instrument*, *Power Laboratories*) with isoflurane (#26675-46-7, *LASER Animal Health*). Anaesthesia was induced using a dog nose cone (source) with 5% isoflurane and 1-2 L/min $O_2$. Proper induction of anaesthesia was monitored by no eye blinking, no response to noise when tapping the nose cone or following toe pinch. After induction, the isoflurane level was adjusted to 2% for maintenance of anaesthesia. After injections or completion of ECG or echo, the animals were removed into a recovery cage and observed throughout recovery.

#### 3.2.2.2 Animal Sacrifice

Experimental rats were killed humanely at the end of each experiment for the purposes of tissue collection and analysis. The rats were killed by $CO_2$ asphyxiation according to institutional procedures. The Animal Care and Ethics Committee guidelines were maintained during killing procedures.

#### 3.2.2.3 Sample collection

**Collection of blood**

*Blood collection from tail vein*

Blood was collected from the lateral tail vein of all animals prior to any injections (baseline serum). The rats were warmed by keeping them in an incubator at 40-42°C for 20 min prior to blood collection. Rat restraints were used to restrain the rats during blood collection. Rat tails were disinfected with cyclohexidine. About 0.5 to 1 ml of blood was collected from each rat into 1.5 ml microcentrifuge tubes by puncturing the tail vein with 22G ¾ inch gauge needle. Serum was separated from clotted blood (30 min at room temperature) following centrifugation at 2000 ×g for 10 min.

*Blood collection from caudal vena cava*

At the endpoint of each experiment, blood was collected from the caudal vena cava for separation of sera. After spraying 70% ethanol on rats, the abdomen and thorax were dissected and opened. Blood from caudal vena cava was collected directly using 22G ¾inch needle. Alternatively, the vena cava was bled into the thoracic cavity and blood was collected into serum clot activator tubes (#454067, *Vacuette*) using a sterile transfer pipette. The blood samples were left at least 30 min at room temperature followed by separation of sera by

centrifugation at 2000 ×g for 10 min. Each serum was aliquoted into 3 separate sterile microcentrifuge tubes, and stored at -80°C temperature until required.

**Heart retrieval**

For histological staining (H&E and Masson's trichrome) and immunohistochemistry, hearts were retrieved from rats keeping the aortic arch intact. The hearts were gently flushed with 1× PBS (pH 7.4) mixed with 1 mM $CaCl_2$ through the aorta to remove excess blood from the blood vessels and heart chambers. The hearts were preserved overnight in 10% neutral buffered formalin (NBF) for further processing for histological staining and immunohistochemistry examination.

**Collection of spleen**

After opening the left abdomen, the stomach was lifted to expose the spleen. The excess fat was removed from the spleen and the excised spleen put into ice cold transport medium (RPMI with streptomycin/penicillin) using sterile forceps. The spleen samples were kept on ice prior to separation of mononuclear cells (MNCs) for *in vitro* assays.

*Separation of mononuclear cells from spleen*

Spleen cell suspensions were prepared by maceration of the spleen through a fine mesh metal screen into RPMI medium supplemented with 100 IU/ml penicillin and 100 µg/ml streptomycin. After debris was allowed to settle for about 20 min, the MNCs were isolated by the density gradient method. The cell suspension was layered onto Ficoll-Paque Plus and centrifuged at 500 ×g for 20 min at room temperature. The buffy coat at the interface of the Ficoll-Paque Plus and RPMI medium was collected and the cells washed by centrifugation at 500 ×g for 10 min 3 times in fresh RPMI medium before counting.

*Enumeration of mononuclear cells*

Splenic MNCs were counted after addition of trypan blue to count viable cells. The trypan blue viability test is based on the principle that live cells possess an intact cell membrane that excludes trypan blue, whereas dead cells take up the dye. Cell suspensions were mixed with an equal volume of trypan blue (0.4% in PBS) and examined using bright microscopy in an improved Neubauer haemocytometer. Viable cells had a clear cytoplasm and were observed as transparent, non-viable PBMCs were stained blue and excluded from counts. Contaminating erythrocytes were excluded based on their appearance. Cells were counted

from all 25 central squares if the cells count was low otherwise cells from only 5 squares (4 corners and 1 central) were counted (Figure 3.3, green squares) and multiplied by 5. The total number of cells per ml was calculated as cell count × dilution factor (2 for trypan blue) × $10^4$ (volume of the haemocytometer). For culture, the cells were re-suspended into RPMI to a concentration of $5\times10^6$ cells/ml.

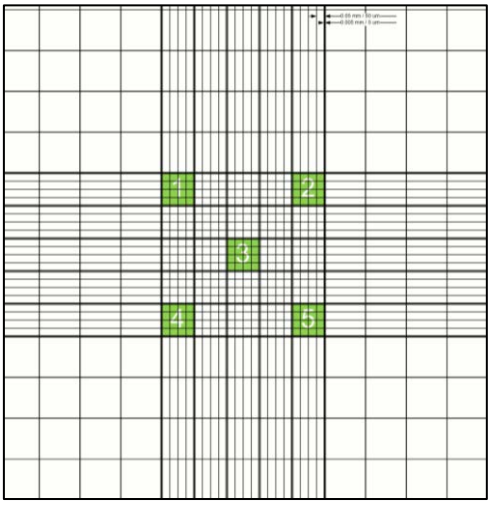


**Figure 3.3** Cell counting using a Neubauer haemocytometer. The cells of the green squares in the 4 corners and 1 central were enumerated and multiplied by 5 to calculate total number of cells in 25 small squares.

### 3.2.3 Animal methods

#### 3.2.3.1 Preparation of antigens for injection

Each rat was injected with 500 µg of GAS rM5 or GGS Stg480 or $1\times10^{10}$ CFU of whole killed GAS M5 (WK-GAS) or whole killed GGS NS3396 (WK-GGS) in 100 µl of sterile 1× phosphate buffer saline (PBS, pH 7.4). An equal volume (100 µl) of Complete Freund's Adjuvant (CFA) or Incomplete Freund's Adjuvant (IFA) was added to the antigen solution and mixed using a vortex until a water-in-oil emulsion formed that did not diffuse when a drop was placed on the surface of water. The control group rats were injected with sterile 100 µl 1× PBS (pH 7.4), mixed with equal volume of CFA/IFA as above.

#### 3.2.3.2 Injection protocols

The injection schedule using during experiments is outlined in Table 3.1. The injections were administered using a 1 ml syringe (#TER00223, *Terumo*) fitted with a 25G ¾ inch needle. Prime and booster injections were administered subcutaneously (s.c.) under general

anaesthesia (Section 3.2.2.1). *Bordetella pertussis* toxin was administered via intraperitoneal (i.p.) injection.

**Table 3.1** Standard injection regime

| Treatment | Antigen, adjuvant and dose (in 200 µl PBS) | Route of administration |
|---|---|---|
| **Priming injection** | • GAS rM5 or GGS Stg480 500 µg in CFA 'or'<br>• WK-GAS or WK-GGS $1\times10^{10}$ CFU in CFA | s.c. at hock |
| ***B. pertussis* toxin** | 0.3 µg per rat | i.p. |
| **Boost injections** | • GAS rM5 or GGS Stg480 500 µg in IFA 'or'<br>• WK-GAS or WK-GGS $1\times10^{10}$ CFU in IFA | s.c. at flank |

PBS: phosphate buffer saline, GAS: group A *Streptococcus*, GGS: group G *Streptococcus*, CFA: complete Freund's adjuvants, IFA: incomplete Freund's adjuvant, CFU: colony forming units, s.c: sub-cutaneous, i.p: intra-peritoneal.

The priming injections were given s.c. in the hock region (Gorton, et al. 2010). Before administering antigens, the ankle area of skin was sprayed with 70% ethanol and the antigen-adjuvant emulsion was injected s.c. bevel upwards into the lateral side of the foot directly above the heel and into the groove between the fibularis longus and soleus muscles. Once the emulsion was injected, the rats were monitored in an isolation cage until fully recovered. The booster injections were administered s.c. in the flank region.

### 3.2.4 Immunological assays

#### 3.2.4.1 Lymphocyte proliferation assays

Lymphocyte proliferation assays were used to assess the ability of memory lymphocytes to proliferate in response to various non-specific (mitogen) and specific (recall antigen) stimuli. The specificity and reactivity of lymphocytes from immunised rats were determined by measuring proliferative responses to antigen in a [$^3$H] thymidine incorporation assay (Gorton, et al. 2009). Optimum concentration of each stimulating antigen was determined by several initial experiments. Typically, MNCs extracted from individual rat spleens (Section 3.2.2.3) were cultured in triplicate wells in U96-well culture plates (#163320, *Nunc, Denmark*) in the presence of antigen stimulants followed by incubation in a humidified atmosphere for 72-120 h at 37°C in 5% $CO_2$. MNCs were added to each well at a concentration of $10^5$ cells/well in RPMI-1640 medium, supplemented with 2.5% heat-inactivated rat serum, 100 IU/ml

penicillin, 100 µg/ml streptomycin, 2 mM L-glutamine and 10 mM HEPES buffer. Test cells were stimulated with 10 µg/ml of GAS rM5 or GGS Stg480. Cells stimulated with 1 µg/ml of concanavalin A (ConA, #C2272, *Sigma*) were used as the positive control. Baseline readings were obtained from unstimulated cells in culture medium only. After 72-120 h of culture, cells were pulsed for 20 h with 0.25 µCi $^{3}$H-thymidine (#NET027E005MC, *GEHealthcare, Australia*) before harvesting onto filter mats (#6005409, *Perkin Elmer*, USA) using Wallac MicroBeta® Trilux scintillation counter (*Perkin Elmer, USA*). When dry, scintillation fluid was applied to the filter mats and counts per minute (cpm) were measured in a Wallac MicroBeta® Trilux schintillation counter. The proliferative response was evaluated using the stimulation index (SI), calculated as a ratio of mean cpm in stimulated cells and cpm in unstimulated cells (cpm of test wells/cpm of control wells). A stimulation index of ≥3 was considered significant.

#### 3.2.4.2 Enzyme linked immunosorbent assay

Immunoglobulin G (IgG) reactivity in sera from rats was determined by enzyme linked immunosorbent assay (ELISA). The coating concentrations of different antigens and starting dilutions of rat sera were titrated with several initial experiments (Section 4.3). Briefly, F96-well plates (*Nunc, Denmark*) were coated overnight at 4°C with 500 µg/ml of WK-GAS or WK-GGS, 1 µg/ml of GAS rM5 or GGS Stg480, 10 µg/ml cardiac myosin or collagen I. The wells were washed four times with Wash Buffer (1× PBS at pH 7.4, 0.05% Tween 20) and blocked with 200 µl of Blocking Buffer (Wash Buffer, 1% bovine serum albumin) overnight at 37°C. After washing, the plates were kept inverted and blotted on paper to remove residual blocking solution. Individual rat sera were applied in duplicate using two-fold dilutions across the plate. A 1:100 starting serum dilution was used for PBS injected rats. A 1:400 starting dilution was used for serum from animals injected with whole killed bacteria and rM proteins. For cardiac myosin and collagen I ELISAs, sera from rats injected with WK-GAS, WK-GGS, GAS rM5, GGS Stg480 and PBS was diluted at 1:100 and applied in duplicate. Plates were incubated for 2 h at 37°C. After washing, goat anti-rat IgG (H+L) conjugated with horseradish-peroxidase was added at 1:5000 dilution for 1 h at 37°C. After washing, 2-2'–azino-di(3-ethylbenzthiazoline)-6-sulphonate (ABTS) was added for 30 min before the optical density (OD) was measured at dual wavelengths 414 nm (ABTS absorption maximum) with 492 nm (reference) Controls included a positive serum sample from rats injected with WK-GAS, GAS rM5, cardiac myosin and collagen I, pooled baseline rat serum (diluted 1:100) as the negative control and enzyme conjugated secondary antibody alone.

Titres were calculated as the highest dilution of serum that gave an absorbance of more than three standard deviations above the mean absorbance of negative control wells on each plate. For cardiac myosin and collagen I ELISAs, the OD values between sera from rats injected with WK-GAS, WK-GGS, GAS rM5, GGS Stg480 and PBS were compared to test the difference.

### 3.2.5 Histology

#### 3.2.5.1 Preparation of heart tissue

Hearts fixed overnight in 10% neutral buffer formalin (NBF) were bisected along the base of aorta (Figure 3.4) for processing and preparation of paraffin-embedded sections. The preserved heart samples were processed by a 6-h cycle using a Shandon Citadel 2000 Tissue Processor (*Shandon Southern Products Ltd, United Kingdom*). Heart sections were cut at 5 µm on a microtome, placed on glass slides and dried at 60°C until staining.

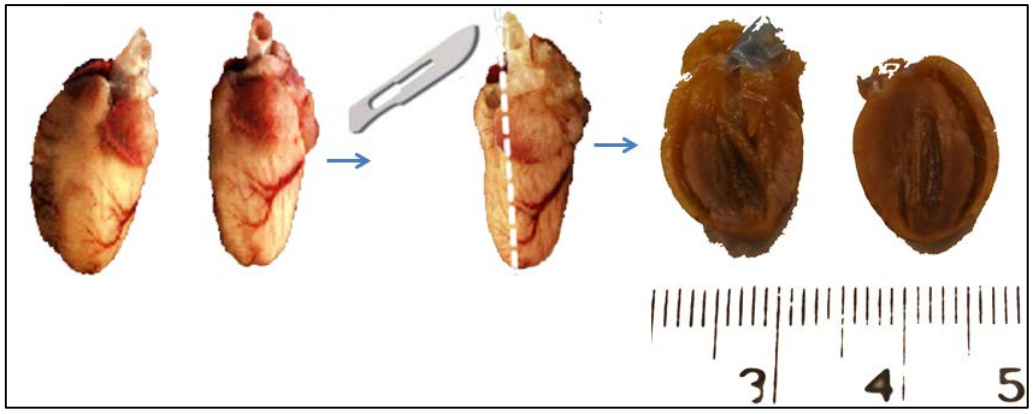


**Figure 3.4** Standard procedure of cutting rat heart for histological examination. The heart samples were hold tight using a forceps and cut into 2 equal pieces using a surgical blade directed lateral to the aorta and along the left atrium and ventricle.

#### 3.2.5.2 Haematoxylin and eosin staining of heart sections

Formalin fixed paraffin embedded sections were stained with haematoxylin and eosin (H&E) following standard protocols (Appendix 3). Stained tissue sections containing mitral valves (usually 2 sections per rat) were examined microscopically using an Olympus BH2 microscope fitted with a QImaging camera for evidence of mitral valvulitis and myocarditis, including inflammatory cell infiltration, fibrosis and necrosis, and scored as described in Table 3.2. Histological examination was also performed by a second experienced observer blinded to the sample identity. The mitral valvulitis and myocarditis scores from each rat were summed to achieve a "carditis" score.

**Table 3.2** Mitral valvulitis and myocarditis severity scores (H&E staining)

| Score | Mitral valve | Myocardium |
|---|---|---|
| **0** | No inflammatory cells associated with valves | Diffuse, individual cells throughout tissue |
| **1** | <5 isolated cells in/on valves | 1-2 small foci |
| **2** | >5 cells on valve surface only | >2 small foci |
| **3** | Focal lesion in valve | Large focal lesion |
| **4** | >1 lesion | Aschoff-type lesion |

Examples of scores are shown later in Chapter 6, Figure 6.1.

#### 3.2.5.3 Masson's trichrome staining of heart sections

Masson's trichrome staining was performed following standard procedures (Appendix 3) to observe deposition of collagen fibres in the mitral valve and myocardium. In this technique, the haematoxylin was used to stain cell nuclei black or blue, the acid fuchsin was used to stain muscle cells red, whereas the methyl blue was used to stain the collagen fibres blue. The heart sections were examined using a light microscope (*BX43 Olympus*). Percentage of collagen deposition (stained blue colour) in the mitral valve and myocardium was determined on the digital images using the CellSens image analysis software® (*Olympus*). A minimum of 5 photographed areas of mitral valve and myocardium were used to analyse data.

### 3.2.6 Imaging techniques

#### 3.2.6.1 Electrocardiography

Electrocardiography (ECG) was performed on all experimental rats prior to antigen injections and before experimental end points. The ECG machine used was from *AD Instruments* (*Power Laboratories*). This instrument has a data acquisition and analysis system with 16 bit resolution (hardware and software supported), and is capable of recording at speeds of up to 200,000 samples per sec (400 kHz aggregate). ECG was performed under isoflurane induced maintenance anaesthesia (Section 3.2.2.1) with 1-1.5 L/min of oxygen. The 3 standard limb leads were constructed from electrodes of 26 gauge, water-proof, stainless steel needles (LL911; *Lead-Lok,* USA). The negative electrode had a red wire to differentiate from the ground electrode which was green and the positive electrode which was yellow. The leads were placed subcutaneously for 1 cm at the right and left forepaws and the medial left thigh

region keeping the rats in supine position (Figure 3.5). The blue electrode (negative) was placed carefully in the left wrist, green one (ground) in the right wrist and yellow electrode (positive) in the left ankle. The electrical potentials were recorded for 30 sec with *LabChart 6* software provided by *AD Instruments* (*Power Laboratories*). Time at peak points of P and R waves were noted and P-R interval was calculated. ECG traces were analysed and the average of 15 P-R intervals (5 each from the beginning, middle and end) was calculated for each rat. Group data was then expressed as mean ± standard errors of mean (SEM).

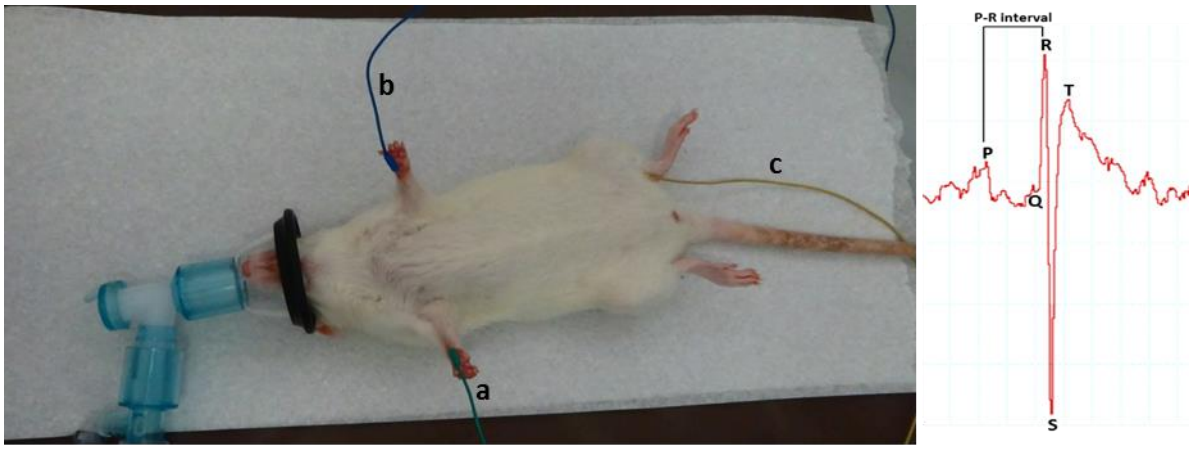


**Figure 3.5** Performance of ECG in a rat. All ECG procedure was performed in rats with general anaesthesia. The standard limb lids were inserted s.c. into the fore limbs and left hind limb when the rat was in supine position. ECG traces were recorded for at least 30 sec. The ECG trace in the right shows normal P-R interval (38 millisec) of a rat before starting immunisations, a: ground electrode, b: negative electrode, c: positive electrode.

### 3.2.6.2 Echocardiography

Echocardiography (echo) was performed by an experienced researcher/clinician blinded to the sample identity (Dr Scott Simpson, The Townsville Hospital). Dr Simpson has extensive experience in preterm, neonatal and paediatric human echocardiography. A day prior to echocardiography assessment, the chest fur of each rat was shaved under maintenance anaesthesia (2% isoflurane). The machine used for echocardiography was a Philips CX50 portable ultrasound (*Bothwell*, *USA*) with a L15-7iO; 15Hz phased linear array probe with 128 elements, designed for mid to high frequency superficial imaging at high resolution with lens footprint: elevation 10 mm, scan plane 32 mm and transducer length 89 mm. The echo probe was directed towards the heart from left side and ultrasound frequency was adjusted until clearly visible the mitral valve and mitral valve movements (Figure 3.6). The images of the mitral valves and a short video of movement were recorded. Areas of abnormal or pathological heart valve appearance were identified as echo-dense structures and described

according to the number, density, size and whether these structures appeared to interfere with the motion of the mitral valves. Each rat was scored based on the mitral valvular pathology on echocardiography examination as described in Table 3.3. The thickness and nodular scores of each rat were summed and expressed as mean ± standard errors of mean (SEM).

**Table 3.3** Echocardiographic scores

| Score | Valvular thickness | Nodules on the leaflets |
|---|---|---|
| **0** | No inflammatory thickening | No nodules |
| **1** | Moderately thick | 1-2 foci/nodule(s) |
| **2** | Distinctly thick | >2 foci/nodules |

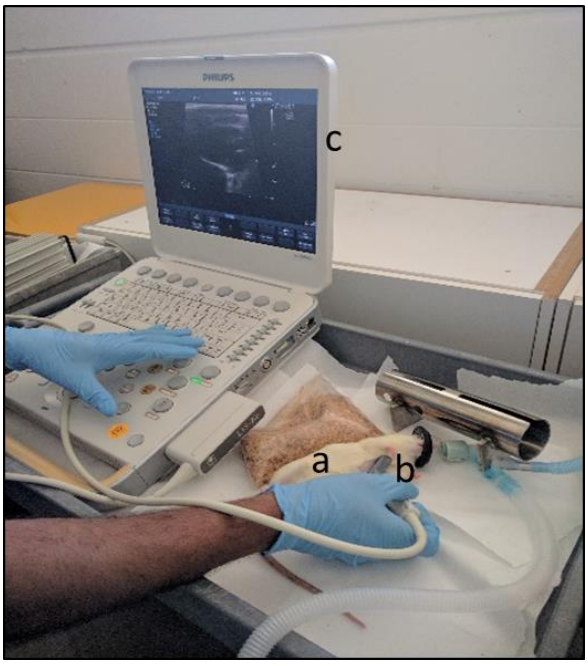


**Figure 3.6** Performance of echocardiography in a rat. General anaesthesia of rat was maintained using 2% isoflurane. The rat was held in supine position. Echo probe was directed to heart of rat is a position so that the left atrium and ventricle and mitral valves can be examined. The mitral valves were detected as white leaflets directed towards the left ventricle. a: Lewis rat, b: echo probe, c: monitor of echo machine.

### 3.2.7 Statistical analysis

Confirmation of normal distribution of data sets was established using D'Agostino & Pearson normality test in GraphPad Prism 7 statistical software. The data sets from experimental and control groups that passed D'Agostino & Pearson normality test was compared and tested using one-way analysis of variance (ANOVA) with Tukey's multiple comparisons test or t-test. Non-parametric Kruskal-Wallis tests and Mann-Whitney tests were performed to

compare data that weren't normally distributed. The results are reported as mean ± standard error (SEM). A p value of $\leq 0.05$ was considered significant.

# CHAPTER 4
# OPTIMISATION AND VALIDATION OF EXPERIMENTAL METHODOLOGIES

In this chapter, the optimisation of various laboratory techniques is described. Existing techniques and assays used previously in the Lewis rat autoimmune carditis model (e.g. electrocardiography (ECG), ELISA, lymphocyte proliferation assays) have been re-evaluated to ensure competency, assay precision and validity. New techniques, not previously used in this model (e.g. echocardiography) required establishment, evaluation and optimisation prior to their use as experimental outcome measurements are described.

In this chapter the following experimental methodologies were optimised:

1. Electrocardiography (ECG) was evaluated by analysing ECG data generated by two independent investigators. Used in Chapters 6-8.
2. Echocardiography (echo) techniques were established and validated by an experienced paediatrician/researcher blinded to the animal treatment group. Used in Chapters 6 and 8.
3. ELISAs were optimised by chequerboard titration of all reagents to optimise antigen coating concentrations, blocking conditions and serum dilutions. Used in Chapters 5, 7 and 8.
4. Lymphocyte proliferation assay conditions were optimised to determine optimal antigen stimulation conditions and culture period. Used in Chapters 5, 7 and 8.
5. Rat aortic endothelial cell (RAOEC) culture conditions were established and standardised. RAOEC were used in Chapter 9.

## 4.1 OPTIMISATION OF ELECTROCARDIOGRAPHY (ECG)

The P and R points of measurement on electrocardiograms are of interest in this thesis as prolongation of the P-R interval reflects electrical conduction abnormalities of the myocardium (Gewitz, et al. 2015) and is one of the minor manifestations of Jones Criteria for the diagnosis of ARF/RHD (Saxena 2000; Carapetis, et al. 2016). Prolongation of the P-R interval on ECG is present in 30-35% of ARF patients (Homer and Shulman 1991) and was used to measure cardiac dysfunction in immunised Lewis rats in a previous study (Gorton, et al. 2016). In humans a typical P-R interval is measured as the period that extends from the beginning of the P wave (the onset of atrial depolarisation) until the beginning of the QRS complex (the onset of ventricular depolarisation). However, the rapid heart rate of the rat

makes it difficult to select P and R points. Instead, objective and reproducible measurements can be achieved using the peaks of the P wave and R wave (Farraj, et al. 2011). Nevertheless, the consistency of P and R peak value extraction from each ECG signal recorded by the ECG software needed to be verified. This was done by repeating the measurements by both the same operator (intra-observer variation) and/or a second operator (inter-observer variation) skilled in ECG.

### 4.1.1 Materials and methods

All rat experiments were approved and conducted under James Cook University Animal Ethics approval A2083. For optimisation of ECG, female Lewis rats of 12-14 weeks age injected with whole killed GAS M5 (WK-GAS, n=1) or whole killed GGS NS3396 (WK-GGS, n=1) or PBS (n=4) were used. The lower number of animals (n=1) used was due to unavailability of animal stock (Gorton, et al. 2016). The schedule for priming and booster injections and adjuvant preparation is described in Section 5.2.3 and Table 5.1 (Whole-killed long term). The rats were assessed with ECG as described in Section 3.2.6.1 at day 230 prior to cull. To verify the consistency of data analysis, the peak P and R point values were independently extracted twice from the ECG trace using LabChart 8 Reader software (to determine intra-observer variation). The initial and the second P-R interval values were analysed by non-linear regression using GraphPad Prism 7.

For further verification of consistency of data analysis, a second operator experienced in rat ECG was asked to extract the data from the same ECG traces (to determine inter-observer variation). The initial and the second operator data were analysed by non-linear regression using GraphPad Prism 7.

### 4.1.2 Results

The two values of intra-observational and inter-observer variation analysis are plotted on the X-axis and Y-axis (Figure 4.1). It was observed that the XY values were approximately linear and the $R^2$ values approached 1. This indicates the consistency of the P and R values irrespective of different times of measurement and different operators.

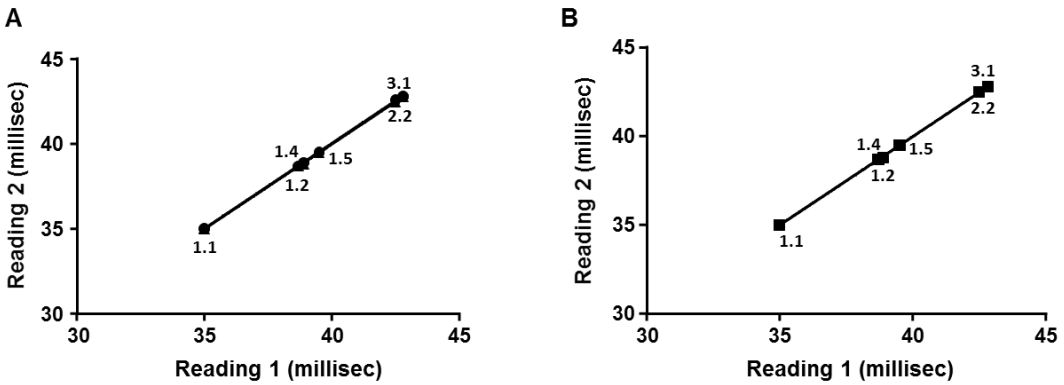


**Figure 4.1** Intra- (A) and inter- (B) observer variation analysis of ECG. The P-R intervals shown here are from PBS injected rats (n=4; 1.1-1.2, 1.4-1.5), GAS M5 injected rat (n=1; 2.2) and GGS NS3396 injected rat (n=1; 3.1). A: $R^2 = 0.9999$, B: $R^2 = 0.9998$.

### 4.1.3 Discussion and interpretation

In ECG, the peak P and R values were chosen to make the data extraction procedure simple and consistent. Hence, while this measurement is slightly different from the commonly accepted measurement in humans, this modification has been used previously for other rodent ECG studies (Gorton, et al. 2009; Gorton, et al. 2016) and is the accepted methodology for rodents.

The normal range for the P-R interval in rat ECG varies according to the rat strain and the type and level of anaesthesia used (Konopelski and Ufnal 2016). Very few studies have recorded ECGs from conscious rodents due to the difficulty in preventing movement during the ECG trace recordings. In a study on healthy Sprague-Dawley rats of body weight 174-292 gm, the P-R interval was recorded as 48-70±47 millisec under ether anaesthesia (Normann, et al. 1961). In another study, healthy 4-12 month old Long-Evans rats had an average P-R interval of 50 millisec under light ether anaesthesia (Sambhi and White 1960). In a separate study on Albino rats of either sex (n=15, 200-300 gm), P-R intervals were between 43±01 and 45±02 millisec (Kumar, et al. 2009). P-R interval in rats has been shown to differ with medications and in different disease conditions such as hypertension (Bestetti, et al. 1987; Detweiler 1997; Berne and Levy 2001; Konopelski and Ufnal 2016).

In the current study, we observed prolonged P-R interval in rats injected with WK-GAS and WK-GGS (>40 millisec) compared to PBS injected control rats (<40 millisec). As reference range values are not available for rats, we took care to record ECGs from rats by the same operator, using the same level and method of anaesthesia. Comparing our values to those

published by others would be more difficult to interpret, as other studies might have employed different conditions and used different strains of rats. However, the consistency of P-R interval values in two different observations by the same operator and between different operators suggests that the method described in this Chapter and throughout this thesis is reliable and an appropriate measurement of cardiac function/dysfunction.

## 4.2 OPTIMISATION OF ECHOCARDIOGRAPHY (ECHO)

Echocardiography is commonly used for clinical diagnosis of ARF/RHD, serial follow up of patients and provides therapeutic procedural guidance and prognostic information (Gewitz, et al. 2015). It is also useful in large scale population screening for early detection of ARF/RHD (Abernethy, et al. 1994; Minich, et al. 1997; Figueroa, et al. 2001; Narula and Kaplan 2001; Vijayalakshmi, et al. 2008). Salient echocardiographic features include mitral valvular morphology, especially valvular thickening and impaired valvular leaflet movement (Figure 4.2) (Jain and Mankad 2013; Wunderlich, et al. 2013; Carapetis, et al. 2016). To our knowledge echo of rat hearts has not been previously used to detect heart valve pathology. Therefore, the rat echo procedure required setup and optimisation prior to use of this technique in the assessment of rat valve pathology.

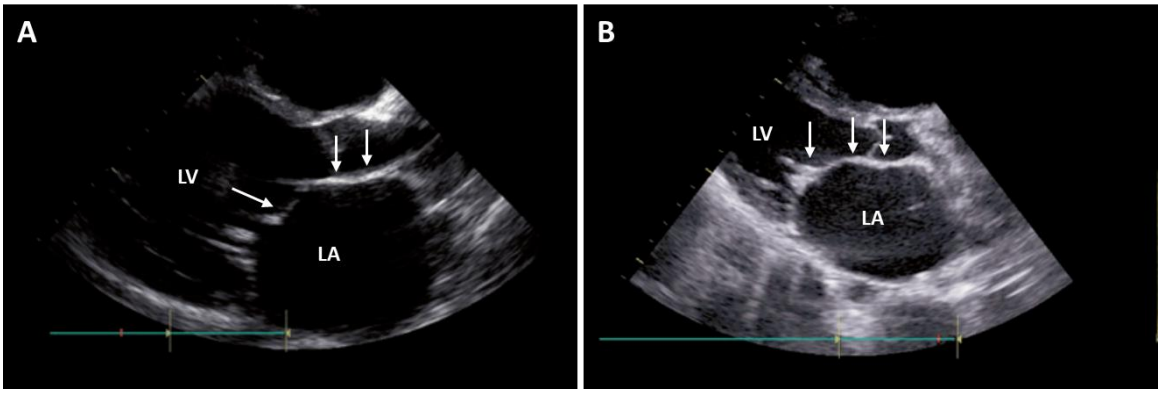


**Figure 4.2** Echocardiogram from a child with mitral valvular pathology (parasternal long-axis view). A: the mitral valve is thickened with excessive leaflet tip motion and lack of coaptation; B: the mitral valve is thickened with limited motion and the left atrium is severely dilated. Arrows (→) indicate mitral valve leaflets. LA: left atrium, LV: left ventricle. The images are extracted from Carapetis, et al. (2016).

### 4.2.1 Materials and Methods

The Lewis rats injected with whole-killed GAS (n=7) and the control rats (n=7) injected with PBS were used. The immunisation procedure described in Section 5.2.3 (Whole-killed long term) was followed to optimise the echo process. The echo was performed on rats at day 230

of post priming injection under isoflurane anaesthesia (Section 3.2.6.2). Echo setup and training was performed by a clinician/researcher (Dr Scott Simpson, The Townsville Hospital) with extensive experience in paediatric heart sonography for the detection of ARF/RHD. The rats were scored from '0' to '2' based on degree of leaflet thickness and presence of nodules (Section 3.2.6.2, Table 3.3).

### 4.2.2 Results

During echo, blinded measurements of mitral valve morphologies were recorded i.e. the operator was blinded to the identity/injection group of individual rats. The mitral valves of PBS injected control rats were uniform with no abnormal thickening or focal lesions (Figure 4.3, A). However, the mitral valves of rats injected with WK-GAS were dense white and thick structures with circular, white nodules (Figure 4.3, B-E). The findings from rats injected with WK-GAS were similar to the echo findings of children during screening for ARF/RHD (Figure 4.2).

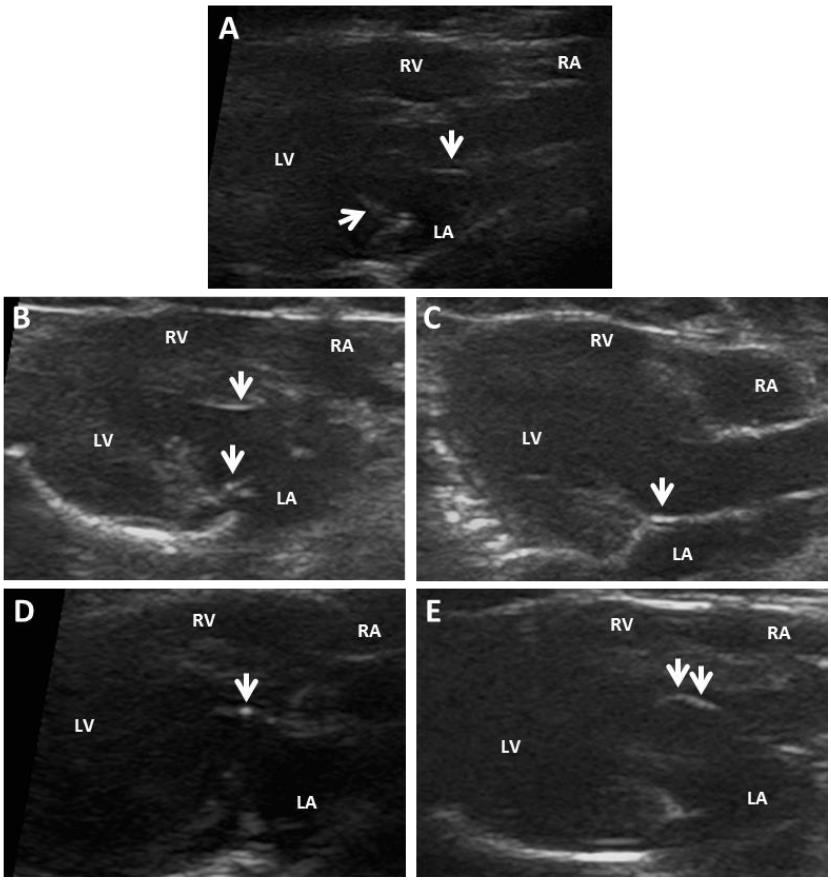


**Figure 4.3** Examination of mitral valves of rats using echocardiography. (A) Score 0, normal mitral valve leaflets with no inflammatory thickening or nodules, (B) Score 1, moderately thick mitral valve, (C) Score 2, distinctly thick leaflets, (D) Score 1, 1 focus/nodule, (E) Score 2, >2 foci/nodules. Arrows (→) indicate mitral valve leaflets, LA: left atrium, LV: left ventricle, RA: right atrium, RV: right ventricle.

### 4.2.3 Discussion and interpretation

In the revised Jones Clinical Criteria (2015) for the diagnosis of ARF/RHD, the echocardiographic assessment was added as a mandatory tool, even in the absence of classical auscultatory findings (Gewitz, et al. 2015). Echocardiographic screening is now common practice for the early diagnosis of ARF/RHD (Carapetis, et al. 2016). To our knowledge, this is the first echocardiographic assessment of rats for the detection of valvular pathology. As there are no baseline values available for rats, we took care for the same operator to assess all rats, using the same level and means of anaesthesia and keeping the animal identity blinded to the operator. Hence, it was applied in both control and experimental rats and therefore presents a valid and reliable measurement of mitral valvular pathology in rats demonstrating symptoms characteristic of ARF/RHD. The scoring system of echo findings is particularly important for data analysis.

## 4.3 OPTIMISATION OF SERUM ANTIBODY ELISA

Indirect ELISAs were performed to detect reactivity in sera from rats injected with WK-GAS, WK-GGS, GAS rM5 and GGS Stg480 against streptococcal (WK-GAS, WK-GGS, GAS rM5 and GGS Stg480) and host tissue antigens (cardiac myosin and collagen I). Optimisation of antigen (WK-GAS, WK-GGS, GAS rM5 and GGS Stg480) coating concentrations was required prior to assessment of antibody titres. The coating concentration of cardiac myosin and collagen I used was as described in an earlier study (Gorton, et al. 2009). The time required for effective blocking on non-specific antibody binding also required optimisation. Determination of appropriate serum starting dilutions was also required.

### 4.3.1 Materials and methods

The pooled sera samples used to optimise the coating concentration of WK-GAS, WK-GGS, GAS rM5 and GGS Stg480 antigens for ELISA were from experiments where rats were injected with WK-GAS, WK-GGS and GAS rM5 and GGS Stg480 (Section 5.2.3, whole-killed and M-protein short term experiments). The same sera samples also used to titrate the starting concentration of serum.

The ELISA procedure described in Section 3.2.4.2 was used with modifications as described below. WK-GAS and WK-GGS, prepared as described in Section 3.1.3.1 were added to wells of microtitre plates at 2 mg/ml and diluted 2-fold across the plate. To ensure optimum blocking was achieved, plates were incubated for 3 h or kept overnight at 37°C. Sera from

rats injected with WK-GAS and WK-GGS were applied in duplicate at 1:100 dilution followed by goat anti-rat secondary antibody and chromogen/substrate. To optimise the coating concentration of GAS rM5 and GGS Stg480, microtitre plates were coated with 2 µg/ml of GAS rM5 or GGS Stg480 and diluted 2-fold across the plate before adding sera (at 1:100 dilution) from rats injected with WK-GAS, WK-GGS, GAS rM5 and GGS Stg480. Sera from PBS injected control rats were used as negative controls.

To optimise the serum starting dilution, microtitre plates were coated with 1 µg/ml of GAS rM5 or GGS Stg480 (the concentration used from the optimisation of coating concentration). After overnight blocking, the serum samples were diluted 2-fold down the plate with an initial starting dilution 1:100.

### 4.3.2 Results

Optimisation of coating concentration of WK-GAS, WK-GGS, GAS rM5 and GGS Stg480 was determined by the lowest concentration or highest dilution of the antigen giving the highest comparable OD values between sera (at 1:100 dilution) from rats injected with WK-GAS, WK-GGS, GAS rM5 and GGS Stg480 and PBS. Here, the absorbance values of pooled serum from rats injected with PBS and WK-GAS or WK-GGS against WK-GAS and WK-GGS were observed to be very similar when the microtitre plates incubated for 3 h (Figure 4.4, A&B, left panels). However, overnight blocking of microplates made a visible difference in absorbance values between sera from rats injected with PBS and WK-GAS or WK-GGS against both WK-GAS and WK-GGS (Figure 4.4, A&B, right panels). Hence, overnight blocking was found superior to 3 h blocking. Nevertheless, the greatest difference in absorbance values was observed when the WK-GAS and WK-GGS samples were diluted at 0.5 mg/ml (indicated by red arrows).

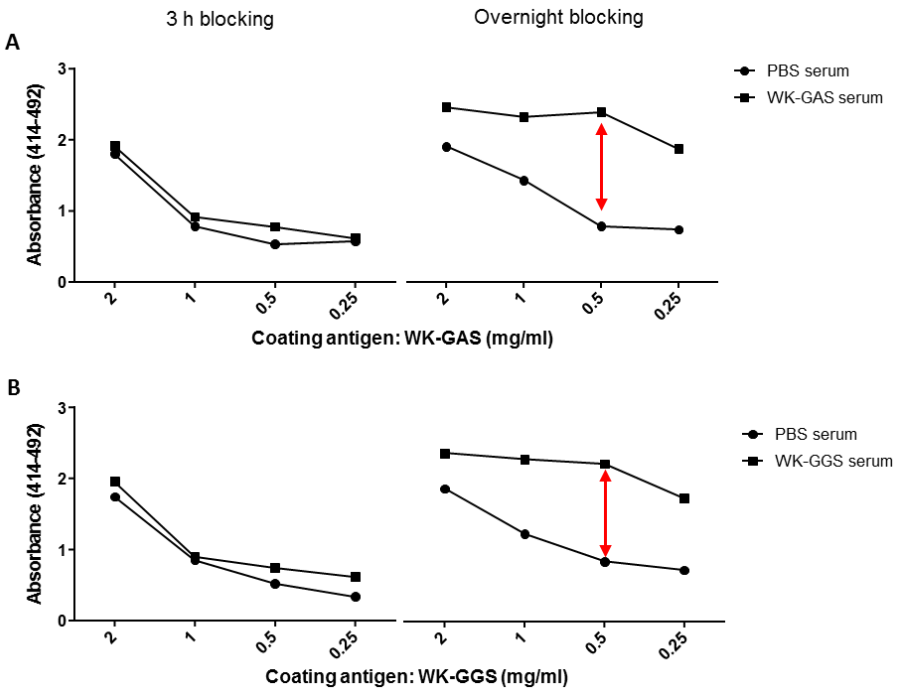


**Figure 4.4** Optimisation of coating concentration of WK-GAS and WK-GGS. Absorbance values of sera antibodies from rats injected with PBS (n=6), WK-GAS (n=7) and WK-GGS (n=7) against WK-GAS (A) and WK-GGS (B). Left panel: 3 h incubation for blocking, right panel: overnight blocking. Red arrows indicate the lowest concentration of WK-GAS and WK-GGS with the highest difference in OD values.

While titrating the coating concentration of GAS rM5 and GGS Stg480, the OD values of pooled sera from rats injected with WK-GAS, WK-GGS, GAS rM5 and GGS Stg480 was found to be higher in comparison to OD values of pooled sera from PBS injected control rats, irrespective of the coating concentration of antigens (Figure 4.5). However, the highest difference in OD values was observed (indicated by red arrows) when the microplate was coated with 1 µg/ml of GAS rM5 (Figure 4.5, A-D) and GGS Stg480 (Figure 4.5, E-H).

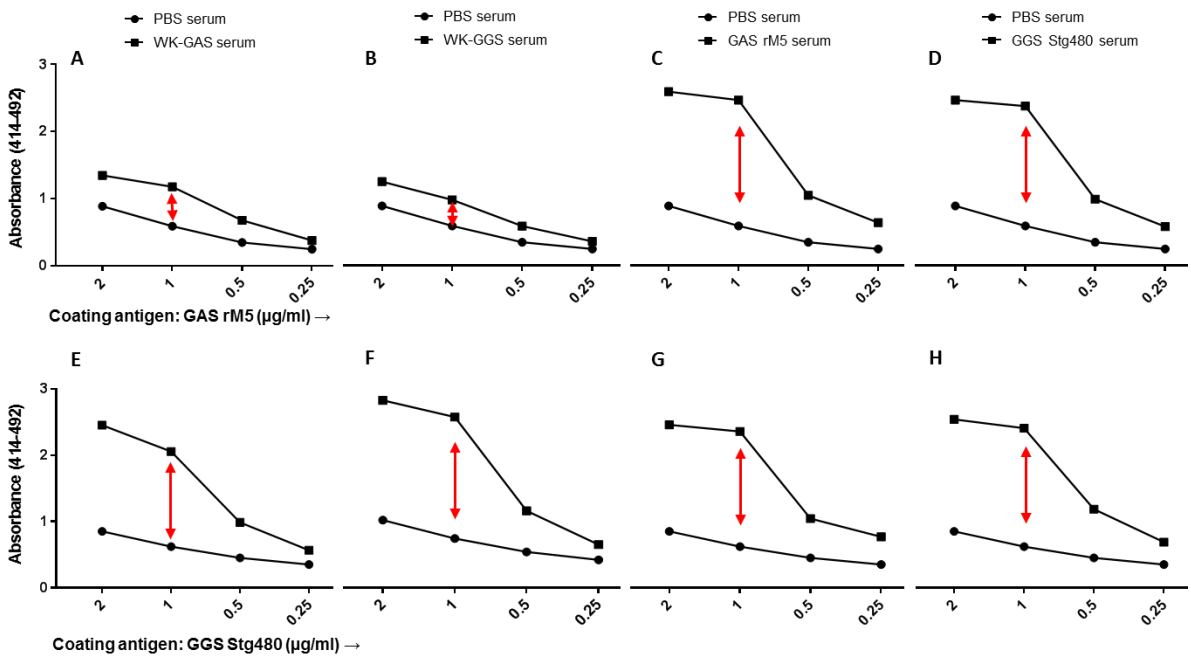


**Figure 4.5** Optimisation of coating concentration of GAS rM5 and GGS Stg480. Absorbance values of pooled sera from rats injected with WK-GAS (A, n=7), WK-GGS (B, n=7), GAS rM5 (C, n=6) and GGS Stg480 (D, n=6) against GAS rM5. The absorbance values of respected sera antibodies against GGS Stg480 (E-H). Red arrows indicate the lowest concentration of GAS rM5 and GGS Stg480 with the highest difference in OD values.

To determine the serum IgG titre against GAS and GGS antigens within a single plate, it was important to optimise the starting concentration of sera. The OD values of pooled sera from rats injected with WK-GAS, WK-GGS, GAS rM5 and GGS Stg480 against GAS rM5 (Figure 4.6, A-D) and GGS Stg480 (Figure 4.6, E-H) were found to be higher compared to pooled sera from PBS injected control rats. However, consistently higher difference in OD values was observed in all sera diluted from 1:100 to 1:800 (indicated by markers '⟷').

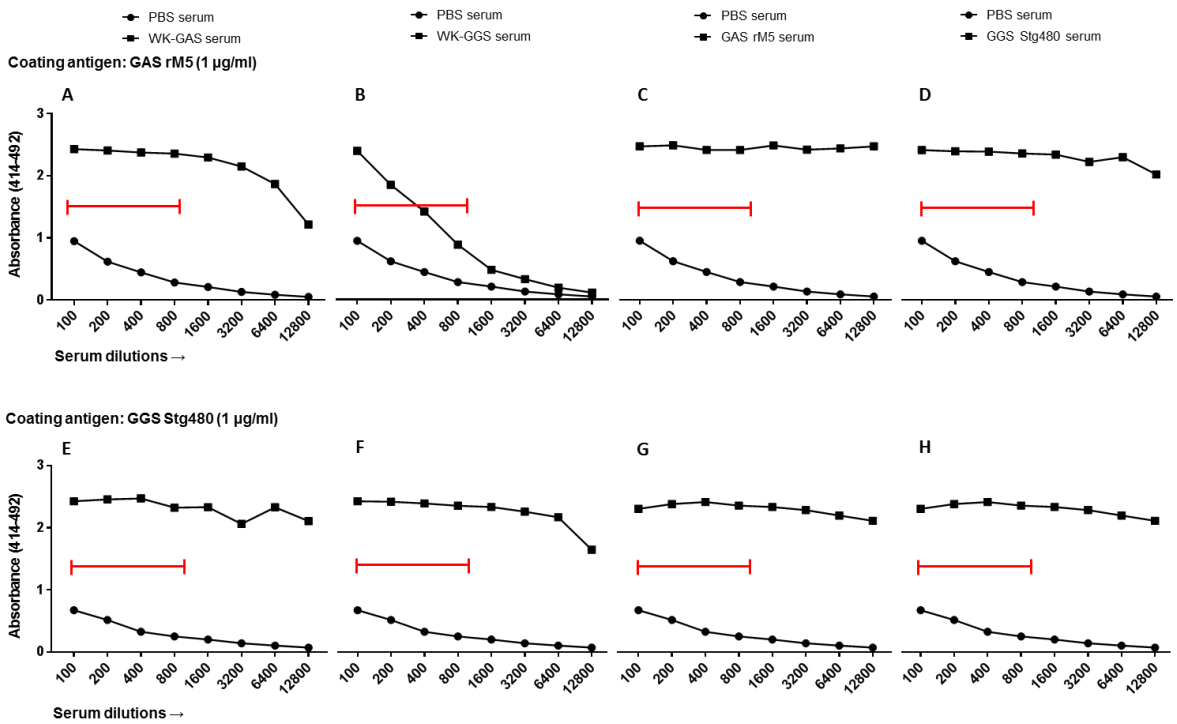


**Figure 4.6** Optimisation of serum starting concentration for detection of IgG reactivity against GAS rM5 and GGS Stg480. Absorbance values of antibodies in pooled sera (2-fold diluted from 1:100 to 1:12800) from rats injected with WK-GAS (A, n=7), WK-GGS (B, n=7), GAS rM5 (C, n=6) and GGS Stg480 (D, n=6) against GAS rM5. The absorbance values of respected sera antibodies against GGS Stg480 (E-H). Markers (⟷) indicate the lowest dilutions of sera that have given higher OD values in all sera from rats injected with WK-GAS, WK-GGS, GAS rM5 and GGS Stg480 compared to sera from PBS injected control rats (n=6).

### 4.3.3 Discussion and interpretation

Coating concentrations of WK-GAS and WK-GGS were determined by the lowest concentration or highest dilution of the antigen that has given highest comparable OD values between pooled sera from rats injected with WK-GAS or WK-GGS and PBS. The highest comparable OD values between the sera from rats injected with WK-GAS or WK-GGS and PBS was observed when the microtitre plate was coated with WK-GAS or WK-GGS at 0.5 mg/ml concentration and incubated overnight for blocking. Therefore, in all experiments described in this thesis the IgG reactivity of sera from GAS and GGS injected (either whole killed bacteria or rM proteins) rats was determined to be optimal using 0.5 mg/ml of WK-GAS and WK-GGS as the antigen coating concentration with overnight background blocking of plates.

Similarly, during optimisation of coating concentration of GAS rM5 and GGS Stg480, higher OD values was observed in sera from rats injected with WK-GAS, WK-GGS, GAS rM5,

GGS Stg480 compared to PBS injected control sera. However, the difference in OD values was found to be higher when the microplate was coated with GAS rM5 and GGS Stg480 at 2 μg/ml and 1 μg/ml and decreased thereafter. Therefore, 1 μg/ml concentration of GAS rM5 and GGS Stg480 was used in all experiments.

Greater differences between the OD values of sera from PBS injected rats and sera from rats injected with whole killed or rM proteins of GAS or GGS were observed in the lower dilutions of sera (from 1:100 to 1:800). Therefore, during original experiments rat sera was diluted from 1:400/800 with 2-fold dilutions across the plate to get to able to determine the endpoint titres of samples within a single plate.

## 4.4 OPTIMISATION OF LYMPHOCYTE PROLIFERATION ASSAY

Lymphocyte proliferation assays (LPA) were used to detect antigen-specific memory lymphocyte proliferative response following stimulation with GAS and GGS antigens. However, prior to using these assays, different batches of normal, heat-inactivated rat sera and different concentrations of heat-inactivated commercial foetal bovine sera were evaluated for their ability to support rat lymphocyte proliferation. The culture time for maximal proliferation was determined simultaneously.

### 4.4.1 Materials and methods

Two male Lewis rats (8 weeks) were used in this experiment. The rats were culled and mononuclear cells was separated from splenocyte suspension as described in Section 3.2.2.2 and Section 3.2.2.3. The sera samples used in this study are described in the Table 4.1. The proliferation of lymphocytes was measured by [$^3$H]thymidine incorporation as described in Section 3.2.4.1. The T-cell mitogen Concanavalin A (ConA) was used as the stimulant to assess the influence of each batch/type of sera on T lymphocyte proliferation.

**Table 4.1** Sources and description of sera tested

| Serum ID | Comments |
|---|---|
| **S1** | Serum stored for 2 years, heat inactivated, sterile |
| **S2** | Fresh rat serum, heat inactivated |
| **S3** | Foetal bovine serum (FBS) 20% |
| **S4** | FBS 10% |

### 4.4.2 Results

The stimulation index for freshly collected rat serum (S2) and 20% FBS (S3) supplemented cells was higher than stored serum (S1) or 10% FBS (S4) supplemented cells (Figure 4.7). In addition, it was observed that the longer incubation of cell culture (from 72 h to 120 h) reduced the cell proliferation.

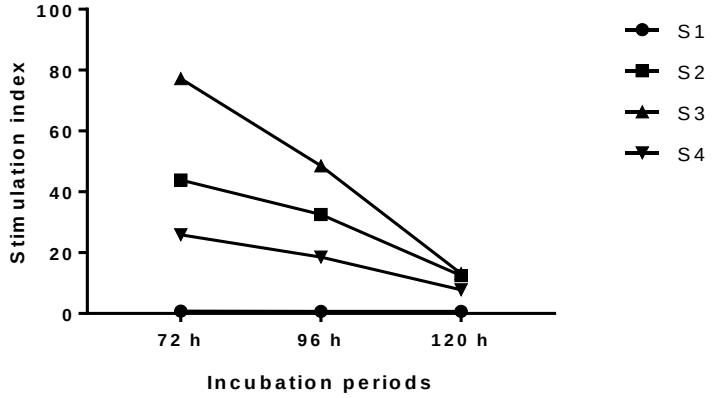


**Figure 4.7** Proliferative responses of splenocytes using different sera supplementations and incubation periods**.** 'S1-S4' indicates serum samples 1-4 as described in Table 4.1.

### 4.4.3 Discussion and interpretation

Concanavalin A (ConA) is a plant-derived T-cell mitogen, and is extensively used for *in vitro* stimulation and proliferation assays (Dwyer and Johnson 1981). Here, the maximum lymphocyte proliferative response was observed after 72 h incubation followed by a decline when further incubated to 120 h. The result indicates that splenocytes should be cultured at least for 72 h. This time point is also suitable for antigen-specific T-cell proliferation as proliferating cells are at much lower frequency when stimulated with specific antigen. Therefore, during antigen specific cell proliferation assay, the lymphocytes should be cultured minimum for 72 h. In addition, splenocytes cultured with freshly prepared heat inactivated rat serum and 20% FBS showed a higher stimulation index irrespective of incubation period compared to the stocks of heat inactivated rat serum that have been stored and 10% FBS. These results indicate that long term storage of rat sera for use as a growth supplement is inappropriate. Therefore, freshly prepared heat inactivated rat serum is the optimal serum supplement to use during lymphocyte culture.

## 4.5 OPTIMISATION OF RAT ENDOTHELIAL CELL CULTURE

Rat aortic endothelial cells (RAOECs) were used in Chapter 9 in *in vitro* cell culture experiments to investigate the role of serum antibodies compared to T-cells in driving heart valve inflammation. The experiments described below aimed to optimise RAOEC culture conditions and determine the optimal concentration of rat test serum to be added to activate RAOEC. Cell activation was determined by measuring the expression of two endothelial cell adhesion molecules; vascular cell adhesion molecule (VCAM)-1 and intercellular adhesion molecule (ICAM)-1 using flow cytometry.

### 4.5.1 Materials and methods

Rat aortic endothelial cells (RAOEC) at passage six were grown in multiwell cell culture plates (12 well) as described in Section 9.2.6. When cells were sub-confluent (~80%), the growth medium was changed to Hank's balanced salt solution (HBSS) for 24 h to achieve cell quiescence prior to performing activation assays.

RAOEC were stimulated for 2 h and 6 h with 2% or 5% heat-inactivated sera taken from rats injected with GAS rM5, GGS Stg480 and PBS (Section 5.2.3, M-protein short term). Controls included unstimulated RAOEC (negative control) or RAOEC stimulated with 10 ng/ml TNF-α (positive control). All samples were tested with five replicates. After 2 h and 6 h of stimulation, RAOEC were washed in staining buffer (Appendix 1), harvested and stained for 30 min on ice in the dark with mouse monoclonal IgG1 anti-rat CD31-FITC (clone TLD-3A12, #MA516952, *Invitrogen*) and FITC-conjugated mouse IgG1a, κ isotype control, (clone MOPC-21, #400107, *BioLegend*) to identify endothelial cells. Biotin-conjugated mouse anti-rat CD54 (clone 1A29, #202403, *BioLegend*) followed by streptavidin APC (#17-4317-82, *eBioscience*) and APC-conjugated mouse IgG1, κ isotype control (clone OX33, #17-0462-80, *eBioscinece*) were used to detect ICAM-1. PE-conjugated mouse anti-rat CD106 (clone MR106, #200403) and PE-mouse IgG1, κ isotype control (clone MOPC-21, #400111, *BioLegend*) were used to detect VCAM-1 expression. After washing in staining buffer, cells were resuspended in BD FACS Flow and immediately acquired for flow cytometry. Data was acquired using a BD FACSCanto II flow cytometer using FACs DIVA 8.0.1 software. Cell debris, characterised by low forward and side scatter, were excluded from analysis and cells stained with isotype control antibodies were used to set VCAM-1 and ICAM-1 positive gates. For each sample, 100,000 total events were recorded.

The data distribution of percentage and MFI of VCAM-1/ICAM-1 and percentage of CD3+ cells was checked using GraphPad Prism 7 statistical software. All the data from experimental and control groups passed D'Agostino & Pearson omnibus normality test and therefore were compared and tested using unpaired t test. The results are reported as mean ± standard error (SEM), $p \leq 0.05$ was considered significant.

### 4.5.2 Results

Expression of adhesion molecules (VCAM-1 and ICAM-1) was determined following appropriate gating of endothelial cells in forward and side scatters (Figure 4.8, A). The unstimulated cells showed very little expression of VCAM-1 and ICAM-1 (Figure 4.8, B&G). However, the positive control cells stimulated with TNF-α showed significant expression of adhesion molecules (Figure 4.8, C&H). The representative histogram plots of endothelial cells stimulated with serum from rats injected with PBS, GAS rM5 and GGS Stg480 are shown in the Figure 4.8, D-F&I-K.

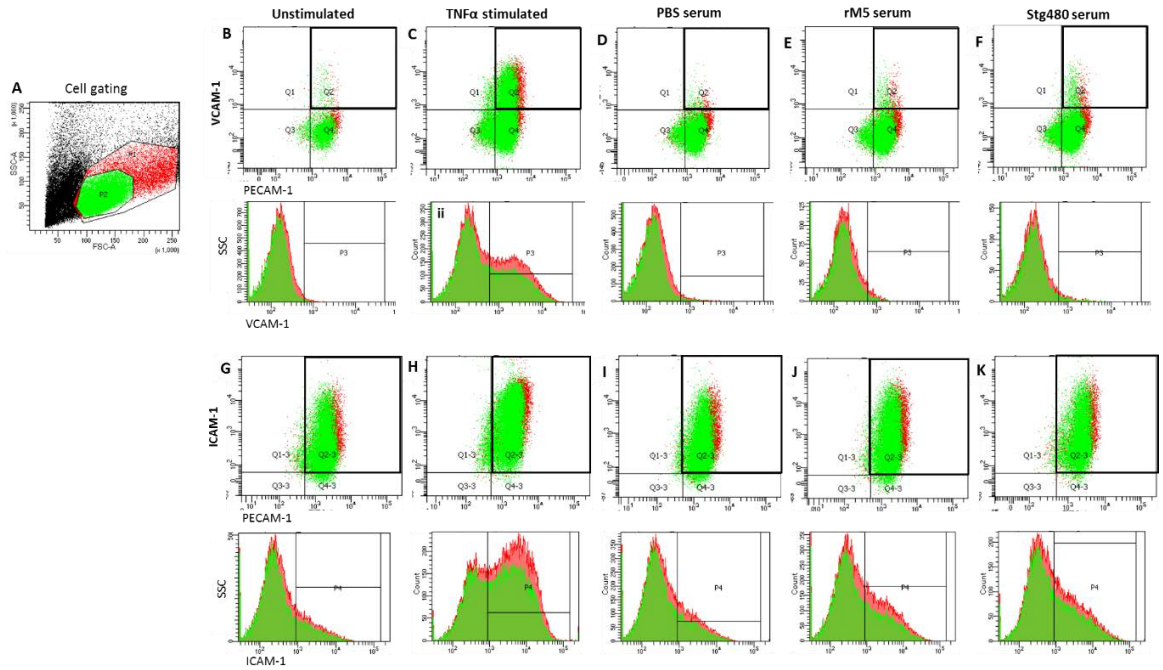


**Figure 4.8** VCAM-1 and ICAM-1 expression on the surface of rat aortic endothelial cell. (A) Dot plot showing the gating strategy used to determine VCAM-1/ICAM-1 positive endothelial cells. Quiescent cells were stimulated for 2 h or 6 h with pooled sera (2% or 5%) from rats injected with PBS, GAS rM5 and GGS Stg480. Unstimulated endothelial cells (negative control) showed low VCAM-1 (B) and ICAM-1 (G) expression. However, TNF-α stimulation (positive control) increased expression of VCAM-1 (C) and ICAM (H). Heat inactivated (HI) pooled serum from rats injected with GAS rM5 and GGS Stg480 induced VCAM-1 (E&F) and ICAM-1 (J&K) expression in a larger percentage of endothelial cells compared to serum from PBS injected control rats (D&I).

VCAM-1 and ICAM-1 expression was observed to be higher in cells stimulated with 5% serum from rats injected with GAS rM5, GGS Stg480 or PBS compared to 2% serum (Figure 4.9) though some of the differences were not significant. Moreover, cells incubated with 5% serum for 6 h had greater expression of VCAM-1 and ICAM-1 compared to cells with a 2 h incubation (Figure 4.10). Unstimulated endothelial cells had low expression of VCAM-1/ICAM-1 whereas, TNF-α was shown to strongly upregulate VCAM-1 and ICAM-1 expression as a positive control.

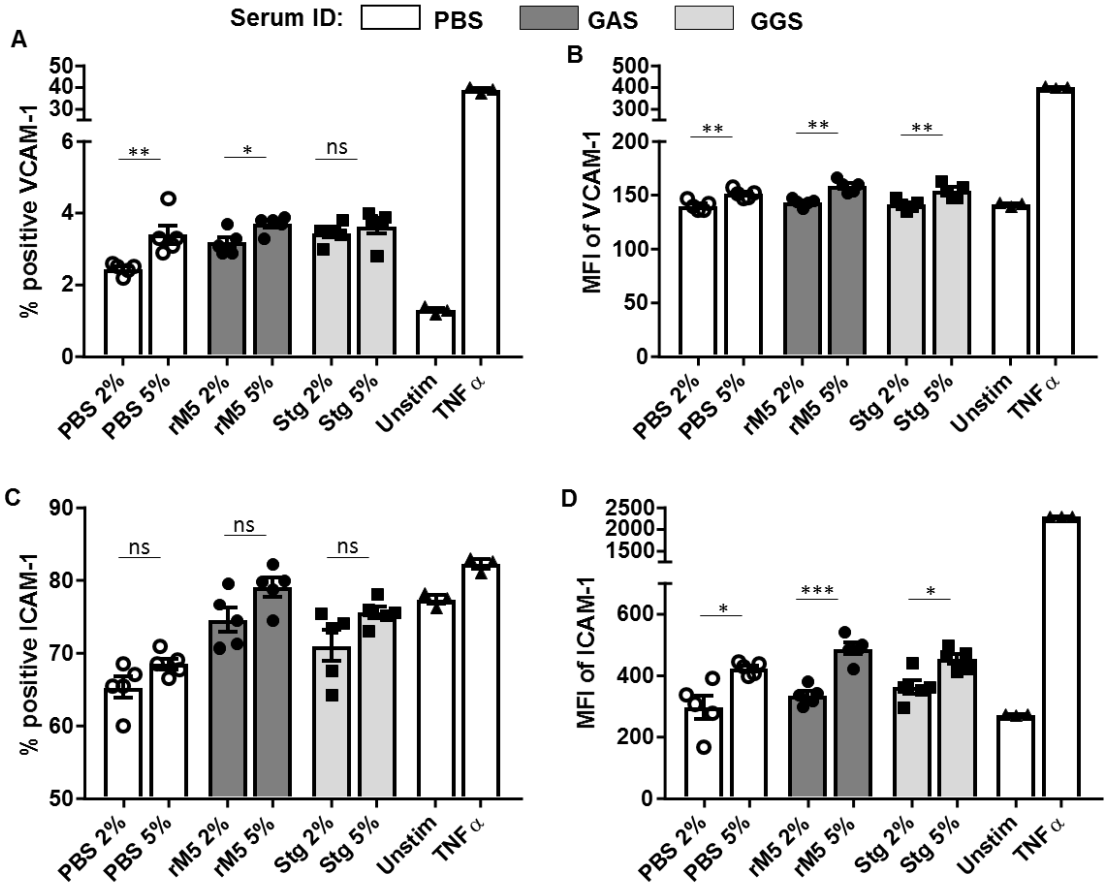


**Figure 4.9** Optimisation of rat sera concentration used for VCAM-1 and ICAM-1 expression. VCAM-1 (A&B) and ICAM-1 (C&D) expression is more in endothelial cells stimulated with 5% non-immune (PBS) or immune (rM5 and Stg480) sera compared to 2% sera. The level of VCAM-1 and ICAM-1 expression is lowest in the unstimulated cells (A-D, Unstim). However, the highest expression of adhesion molecules is observed in the cells stimulated with TNF-α (A-D). Error bars represent standard errors of the means (SEM). Statistical difference tested by t test; *p<0.05, **p<0.01, ***p<0.001, ns: not significant.

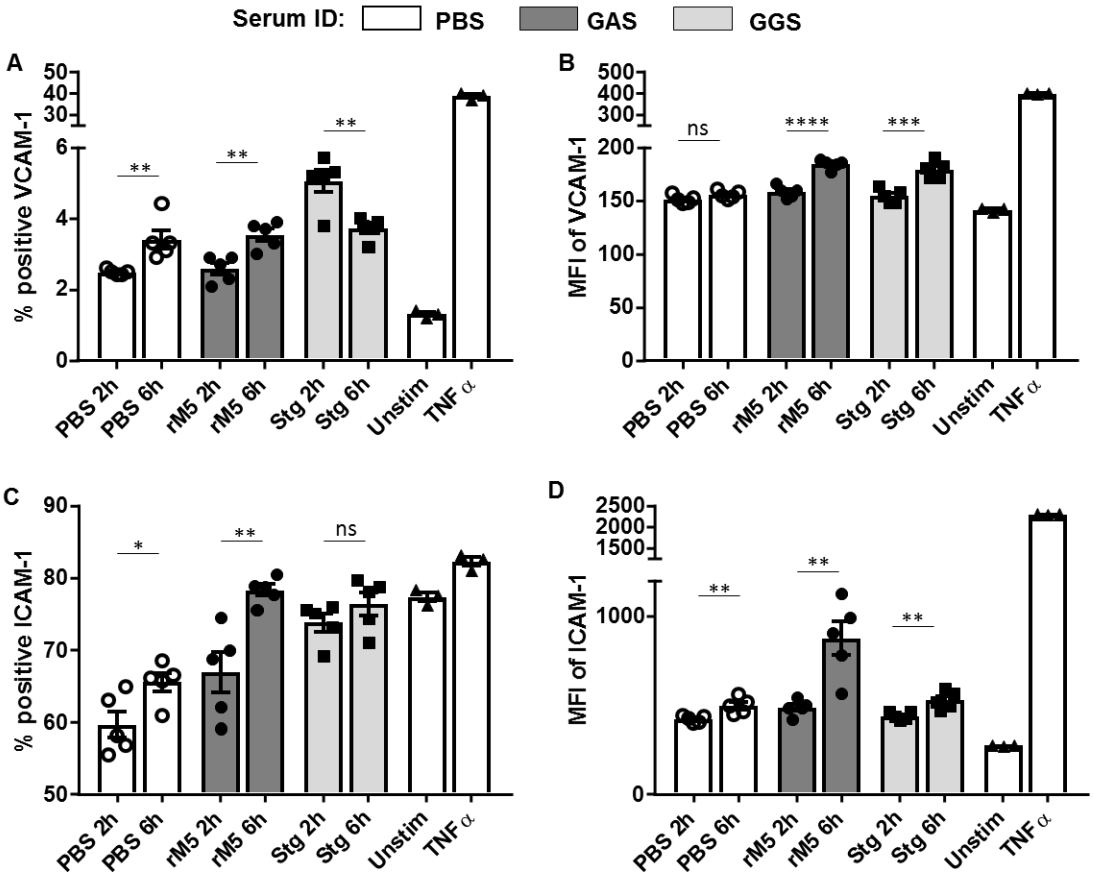


**Figure 4.10** Optimisation of incubation period of endothelial cell culture to induce expression of VCAM-1 and ICAM-1. VCAM-1 (A&B) and ICAM-1 (C&D) expression is higher in RAOE cells cultured for 6 h compared to 2 h with 5% non-immune (PBS) or immune (rM5 and Stg480) sera. The level of VCAM-1 and ICAM-1 expression is lowest in the unstimulated cells (A-D, Unstim). However, the highest expression of adhesion molecules was in the cells stimulated with TNF-α irrespective of a 2 h or 6 h incubation period (A-D). Error bars represent standard errors of the means (SEM). Statistical difference tested by t test; *p<0.05, **p<0.01, ***p<0.001, ****p<0.0001, ns: not significant.

### 4.5.3 Discussion and interpretation

Studies have demonstrated the VCAM-1 expression on valve endothelium is a probable pathway of T-cell infiltration into the mitral valves in patients with ARF/RHD (Roberts, et al. 2001). Expression of VCAM-1 by rat aortic endothelial cells (RAOEC) following *in vitro* culture also demonstrated after stimulation with serum from rats injected with GAS rM5 (Gorton, et al. 2016). However, different concentrations of serum and different incubation periods for adhesion molecule expression was used in different studies (Krankel, et al. 2011; Gorton, et al. 2016). In the current study, 5% and 2% serum concentrations were used based on earlier studies to optimise the concentration of rat sera to obtain optimum expression of VCAM-1 and ICAM-1. Tumour necrosis factor (TNF)-α was used as a positive control stimulant as it stimulates leukocyte adhesion to the endothelium by upregulating VCAM-1

and ICAM-1 (Pober, et al. 1987; Carlos, et al. 1990). The results of this study showed that 5% rat sera could induce VCAM-1 and ICAM-1 better than 2% sera, regardless of whether it was immune and non-immune sera. The 5% sera may contain enough antibodies or other soluble serum components to contribute to a higher expression of VCAM-1 and ICAM-1.

In addition, the incubation period of RAOEC culture after stimulation was also optimised by culturing the RAOEC for 2 h and 6 h after addition of stimulants. The results of this study showed that VCAM-1 and ICAM-1 were better expressed in the cells incubated for 6 h. This may be due to the slow rate of VCAM-1 and ICAM-1 expression by endothelial cells, resulting in a higher expression after 6 h of incubation. Therefore, VCAM-1 and ICAM-1 expression was optimal when endothelial cells were stimulated with 5% serum for 6 h.

# CHAPTER 5
# ANTIBODY AND T-CELL RESPONSES TO GROUP G *STREPTOCOCCUS* IN A LEWIS RAT AUTOIMMUNE VALVULITIS MODEL

## 5.1 INTRODUCTION

In acute rheumatic fever (ARF) and rheumatic heart disease (RHD), the antibody and T-cell responses generated following *Streptococcus pyogenes* (group A *Streptococcus,* GAS) infection are thought to cross-react with host tissues (Guilherme, et al. 2006). During GAS infections, antigen presenting cells present antigens to T-cells. T-cell (predominantly CD4+) activation enhances the activities of B-cells and macrophages to clear the infection. GAS-antigen specific B-cells differentiate into IgM and IgG secreting plasma cells. In individuals susceptible to ARF/RHD, the host immune response to GAS triggers autoimmune reactions to host tissues mediated by both GAS-specific antibodies and T-cells through a process called molecular mimicry by four different mechanisms; (i) identical amino acid sequences, (ii) homologous but non-identical sequences, (iii) common or similar amino acid sequences of different molecules (proteins, carbohydrates), and (iv) structural similarities (Guilherme, et al. 2011a; Carapetis, et al. 2016). Molecular mimicry between GAS and host cardiac antigens is supported by evidence from previous studies (Kaplan 1963; Zabriskie 1967; Galvin, et al. 2000; Kirvan, et al. 2003).

The GAS M-protein shares structural homology with α-helical coiled-coil host proteins such as cardiac myosin, tropomyosin, keratin, vimentin, valvular laminin and collagen (Cunningham 2000; Guilherme, et al. 2006; Guilherme and Kalil 2010; Carapetis, et al. 2016; Martins, et al. 2017). In patients with ARF/RHD, antibody cross-reactivity between GAS M-protein and cardiac myosin has been well documented (Galvin, et al. 2000; Dinkla, et al. 2003b). Early studies from the 1960s demonstrated antibody deposition in human valve and myocardial tissues from patients who had died of ARF/RHD (Kaplan, et al. 1964). The findings of this study were later confirmed using mouse (Krisher and Cunningham 1985; Cunningham 2000) and human monoclonal antibodies (Cunningham 2014) against GAS that reacted with both myocardial and valvular tissues. Antibody cross-reactivity between GAS M-proteins and cardiac myosin suggests that M-proteins were the target autoantigens recognised in the heart (Dale and Beachey 1985a; Krisher and Cunningham 1985; Cunningham, et al. 1986; Cunningham and Swerlick 1986; Baird, et al. 1991). Using anti-myosin antibodies purified by affinity chromatography from ARF patients' sera, cross-

reactive epitopes were found on cardiac myosin and the M5/M6 proteins of GAS (Cunningham, et al. 1989). Studies in animal models reported that the New Zealand White rabbits injected with GAS M1, M5 or M22 expressing strains showed increased levels of IgG antibody reactivity against cardiac myosin (Norlin 1959; Dale and Beachey 1986; Sargent, et al. 1987; Burova, et al. 2004; Burova, et al. 2005). Antibodies against collagen I also reported in patients with ARF/RHD though the cross-reactivity with GAS antigens hasn't been proven (Martins, et al. 2008). It is hypothesised that the antibodies bind with heart endothelium, and activate endothelial cells (Carapetis, et al. 2016). Activated endothelium facilitate infiltration of antigen specific immune cells into the heart tissues.

In ARF/RHD inflammation and autoimmune responses lead to infiltration of T-cells and B-cells into heart tissues (Kay 1997; Abbas and Lichtman 2003; Sampaio, et al. 2007). Immuno-histochemical examination of sections of mitral valve of ARF/RHD patients showed predominantly CD4+ T-cells (Fae, et al. 2004). Animal model studies have revealed a role for antibodies and T-cells in the development of ARF/RHD (Gorton, et al. 2009; Rush, et al. 2014). Guinea pigs injected with different GAS antigens, including heat killed whole bacteria, lysed cells, trypsinised cell wall extracts, M-proteins or protoplast membranes, exhibited myocarditis and valvulitis with increased T-cell, B-cell, macrophage and fibroblast infiltration in the myocardium and mitral valve (Gross, et al. 1929; Yang, et al. 1977). Moreover, Lewis rats injected with GAS M5 protein and peptides showed infiltration of T-cell and macrophages in heart tissues with histological changes similar to the changes seen in the hearts of patients with ARF/RHD (Gorton, et al. 2009; Gorton, et al. 2016). However, understanding the type of T-cells and cytokines produced by T-cells are important to explore deep into the how T-cells are trafficked into the heart tissues.

Despite the highest worldwide prevalence rates of ARF/RHD being in the Indigenous communities of Australia and New Zealand, very low pharyngeal carriage rates of GAS (only 4% throat swabs positive) are reported in these communities (Carapetis and Currie 1997; McDonald, et al. 2004). Similar patterns of throat carriage have been reported in other resource poor developing countries with a high burden of ARF/RHD (Steer, et al. 2002; Brahmadathan, et al. 2005). In Indigenous communities of Australia however, GAS is often associated with skin sores rather than throat infections (McDonald, et al. 2004). These findings have led to the hypothesis that ARF/RHD may arise from GAS pyoderma or from

pharyngitis due to non-GAS strains that have inherited particular GAS virulence factors important for the initiation of ARF/RHD (McDonald, et al. 2004).

Group G *Streptococcus* (*Streptococcus dysgalactiae* subspecies *equisimilis*, SDSE or GGS) possesses many features similar to GAS. It shares the same tissue niche as GAS. GGS causes a similar spectrum of disease and has similar virulence factors to GAS (Bisno, et al. 1987; Williams 2003). GGS and GAS are also known to exchange genetic material (Bisno, et al. 1996; Sriprakash and Hartas 1996; Davies, et al. 2005). Some GGS isolates possess M-proteins such as Stg485, Stg480, Stg6 with high sequence and structural homology to the M-types of ARF-associated GAS strains (Jones and Fischetti 1987; Collins, et al. 1992; Bisno, et al. 1996; Jensen and Kilian 2012). Indeed GGS, but not GAS, has been recovered from an Indigenous Australian child after recurrent severe pharyngitis which was followed by ARF (Davies, et al. 2005). Moreover, antibodies against GGS strains have been shown to react with human heart myosin (Haidan, et al. 2000). However, GGS antigen specific antibody recognition of GAS could interpolate a hypothesis that GGS possess identical immunogenic antigens of GAS. Interestingly, collagen binding motifs that are similar to GAS M-proteins were also seen in some GGS M-proteins (Dinkla, et al. 2007). Collectively, these observations strongly suggest GGS possesses many of the same characteristics as GAS that are linked to the pathogenesis of ARF/RHD.

However, the association of GGS with ARF/RHD has not been proven as it is not considered a major human pathogen (Collins, et al. 1992; Haidan, et al. 2000; Davies, et al. 2005; McDonald, et al. 2006; Dinkla, et al. 2007). Therefore, further studies are warranted into the rheumatogenic potential and role of GGS in the pathogenesis of ARF/RHD (WHO 1988; Taranta and Markowitz 1989; Bisno 1996; Carapetis, et al. 1999). In this chapter, the antibody and T-cell responses to whole-killed GGS NS3396 and GGS M-protein (Stg480) in a Lewis rat autoimmune valvulitis (RAV) model are described.

### 5.1.1 Aims

The overall Aim of this study is to investigate streptococcal and host tissue antigen specific antibody and T-cell responses in rats injected with whole-killed GGS NS3396 and GGS Stg480.

The specific Aims are:

1. To determine the immunogenicity of GGS M-protein and whole-killed GGS bacteria and determine the reactivity of sera from GGS injected rats with GAS M-protein and whole-killed GAS.
2. To determine cross-reactivity of sera from GGS injected rats with the host proteins cardiac myosin and Collagen I.
3. To measure memory T-cell proliferative response from rats using *ex vivo* re-stimulation with GGS Stg480 and GAS rM5.
4. To characterise the phenotype of proliferating T-cells by measuring cytokines.

## 5.2 MATERIALS AND METHODS

### 5.2.1 Experimental animals

The Lewis rat was chosen as a model as it is highly susceptible to develop autoimmune carditis (Li, et al. 2004). Female Lewis rats used for immunisation experiments were obtained from Small Animal Breeding Facility at James Cook University, Townsville, Australia and details of these animals are described in Section 3.1.2.

### 5.2.2 Antigens and adjuvants

Formalin treated whole-killed GGS NS3396 (WK-GGS) and whole-killed GAS M5 (WK-GAS) were prepared as described in Section 3.1.3.1 and the concentration was adjusted to $10^{11}$ CFU/ml to inject $10^{10}$ CFU/rat in 100 µl of PBS. Recombinant M-protein of GGS (Stg480) and GAS (rM5) used in this study were prepared as described in Section 3.2.1. Sterile phosphate buffer saline (PBS, pH 7.4) was used to inject control rats. Complete and incomplete Freund's adjuvants and commercial *Bordetella pertussis* toxin were injected into rats as described in Section 3.1.1.3 and Section 3.2.3.2. Calcium activated porcine cardiac myosin and human collagen I (Section 3.1.1.2) were used in ELISA to demonstrate cross-reactive IgG antibodies in sera from rats injected with GGS and GAS antigens as described in Section 3.2.4.2.

### 5.2.3 Experimental design

In all immunisation experiments, rats (n=5-8 per group) were injected with GGS and GAS antigens under general anaesthesia (Section 3.2.2.1). A sample size of ≥4 was considered adequate to achieve a power of >70% based on our previous findings (Gorton, et al. 2009; Gorton, et al. 2016). The injection protocol described in Section 3.2.3.2 was followed. In all

whole-killed bacteria immunisation experiments, rats were injected with either $10^{10}$ CFU WK-GGS or WK-GAS with CFA (1:1) subcutaneously (s.c.) in the hock as described previously (Gorton, et al. 2010). In all experiments using purified M-proteins, rats were injected with 0.5 mg/100 µl of GGS Stg480 or GAS rM5 emulsified in CFA s.c. in the hock. Control rats were injected with PBS in CFA. The dose rates of bacteria and protein have been designed based on previous studies (Quinn, et al. 2001; Lymbury, et al. 2003; Gorton, et al. 2009; Huang, et al. 2009). At day 1 and day 3 after the priming injection, each rat was injected intraperitoneally (i.p.) with 0.3 µg *B. pertussis* toxin in 200 µl PBS. The schedule for booster injections is shown in Table 5.1. Boost antigen preparations contained $10^{10}$ CFU of WK-GGS or WK-GAS or 0.5 mg/100 µl of GGS Stg480 or GAS rM5 in IFA instead of CFA.

In some experiments, animals were culled after 35/60 days (short term) whereas in other experiments animals were culled after 225/240 days (long term). For short term experiments, rats were boosted at days 7, 14 and 21 following the priming injection. The experimental endpoint for short term experiments was 35-60 days. For long term experiments, additional boost injections were given at days 120, 150 or 210 prior to the experimental endpoint on day 225-240.

**Table 5.1** Injection schedule

| Experimental design | Group size (n=) | Prime | Boosts | Experiment endpoint |
|---|---|---|---|---|
| **Whole-killed short term** | 7 | WK-GAS | Day 7, 14, 21 | 60 days |
| | 7 | WK-GGS | Day 7, 14, 21 | |
| | 6 | PBS | Day 7, 14, 21 | |
| **Whole-killed long term** | 7 | WK-GAS | Day 7, 14, 21, 120, 210 | 240 days |
| | 8 | WK-GGS | Day 7, 14, 21, 120, 210 | |
| | 7 | PBS | Day 7, 14, 21, 120, 210 | |
| **M-protein short term** | 6 | GAS rM5 | GAS rM5 on day 7, 14, 21 | 35 days |
| | 6 | GGS Stg480 | GGS Stg480 on day 7, 14, 21 | |
| | 6 | PBS | PBS on day 7, 14, 21 | |
| **M-protein long term** | 5 | GAS rM5 | GAS rM5 on day 7, 14, 21, 150 | 225 days |
| | 5 | GGS Stg480 | GGS Stg480 on day 7, 14, 21, 150 | |
| | 5 | PBS | PBS on day 7, 14, 21, 150 | |

WK: whole killed, GAS: group A *Streptococcus*, GGS: group G *Streptococcus*, PBS: phosphate buffer saline.

M-protein-injected short term and long term experiments were repeated twice each with n=5 group sizes. The schedule for antigen-adjuvant injections was similar with the exception of the long term experiment endpoint where the experimental endpoint was at day 180 rather than day 225 as shown in Table 5.1.

### 5.2.4 Culling of rats and collection of blood and spleens

The rats were culled according to the procedure described in Section 3.2.2.2 and blood and spleen samples were collected and processed as described in Section 3.2.2.3.

### 5.2.5 Serum antibody detection by ELISA

The reactivity of IgG in individual rat sera was evaluated against surface antigens of WK-GGS and WK-GAS and purified M-proteins of GGS Stg480 and GAS rM5 using an indirect ELISA. The cross-reactivity of serum IgG with porcine cardiac myosin and human collagen I was also evaluated. The antigen coating concentration for WK-GGS and WK-GAS ELISAs was 500 µg/ml, whereas 1 µg/ml was used for GGS Stg480 and GAS rM5 ELISAs (Section 4.3). The coating concentration of porcine cardiac myosin and human collagen I was 10 µg/ml as described previously by Gorton, et al. (2009). Antigens were coated onto Nunc Maxisorp F96 plates in carbonate bicarbonate coating buffer, pH 9.6 (Appendix 1). The ELISA procedure was as described in Section 3.2.4.2.

### 5.2.6 Lymphocyte proliferation assay

The ability of memory lymphocytes to proliferate in response to GGS Stg480 and GAS rM5 was measured by a [$^3$H]thymidine incorporation lymphocyte proliferation assay. Mononuclear cells from splenocyte suspensions were separated according to the procedure described in Section 3.2.2.3 and the proliferation assay method described in Section 3.2.4.1 was followed. Purified GGS Stg480 and GAS rM5 were used at concentrations of 10 µg/ml to stimulate antigen-specific lymphocyte proliferation. Plates were harvested after 96 h at 37°C in 5% $CO_2$ [$^3$H]thymidine added for the last 20 h of culture.

### 5.2.7 Analysis of antigen-specific cytokine production

To characterise the phenotype of proliferating T-cells, splenocytes were cultured for 72 h as described above (Section 5.2.6). Cell culture supernatants were collected by centrifugation at 500 ×g for 10 min at room temp and stored at -80°C prior to analysis. Quantitative measurements of IFN-γ (#ab46107), IL-17A (#ab119536) and IL-4 (#ab46073) were done using *Abcam* ELISA kits. Cytokine concentrations in culture supernatants were determined from standard curves using non-linear fit methods (i.e. second order polynomial, quadratic).

### 5.2.8 Statistical analysis

The data distribution of endpoint titres, OD values, stimulation indices and cytokine concentrations was checked using GraphPad Prism 7 statistical software. The data from experimental and control groups that passed D'Agostino & Pearson omnibus normality test were compared and tested using one-way analysis of variance (ANOVA) with Tukey's post hoc multiple comparisons test. Non-parametric Kruskal-Wallis test or Mann-Whitney test (two tailed) were performed to compare median values that weren't normally distributed. The specific statistical test used for each data set is presented in the figure legends. The results are reported as mean ± standard error (SEM), $p \leq 0.05$ was considered significant.

## 5.3 RESULTS

The results of whole-killed GGS and whole-killed GAS injected short term and long term experiments and M-protein injected short term and long term experiments are presented in this Chapter. The results of repeat experiments are provided in Appendix 5. The details of statistical analysis also provided in the Appendix 5.

### 5.3.1 Antibodies produced following GGS antigen injection also recognise GAS antigens

In this study, we analysed rat sera to detect IgG responses to surface antigens of whole-killed GAS M5 (WK-GAS) and whole-killed GGS (NS3396). In both short and long term experiments, significantly higher IgG response to WK-GAS was observed in the sera from rats injected with WK-GGS compared to PBS injected control rats (Figure 5.1 A). Anti-WK-GAS antibodies also reacted significantly with WK-GGS compared to IgG reactivity from control rats (Figure 5.1 C). Sera from rats injected with GGS Stg480 or GAS rM5 also had a similar spectrum of reactivity (Figure 5.1 B&D).

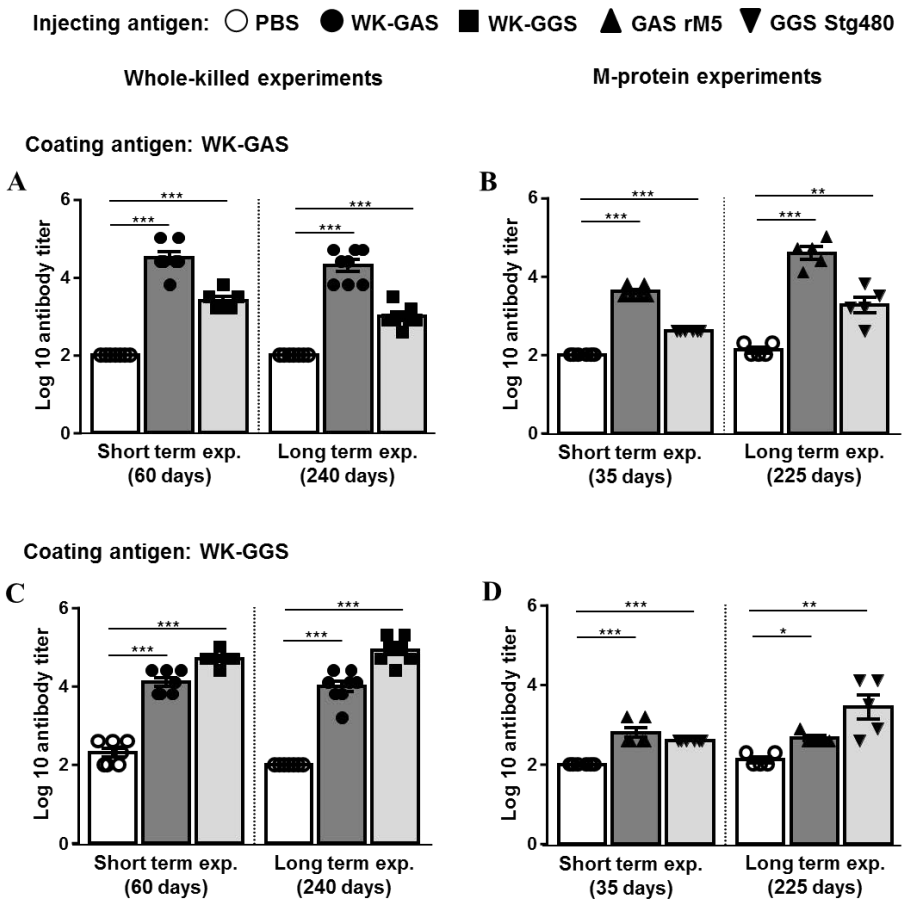


**Figure 5.1** Antibody responses to whole-killed GAS and GGS in whole-killed and M-protein injected rats. Serum IgG from rats injected short term and long term with WK-GGS (n=7-8) reacted with surface antigens of WK-GAS (A). Similarly, serum IgG from rats injected with WK-GAS (n=7) reacted with WK-GGS (C). Anti-GGS Stg480 antibodies also reacted against WK-GAS (B) and anti-GAS rM5 antibodies reacted against WK-GGS (D). In all experiments, serum from PBS injected rats (n=6-7) was used as control. Error bars represent standard errors of the mean (SEM). Statistical difference by one-way ANOVA with Tukey's post hoc multiple comparison; *p<0.05, **p<0.001, ***p<0.0001.

Here, we have demonstrated serum IgG responses against GAS rM5 in rats injected with WK-GGS or GGS Stg480. Moreover, serum IgG response from rats injected with WK-GAS or GAS rM5 also demonstrated reactivity against GGS Stg480. Significantly higher IgG responses against GAS rM5 were observed in rats injected short term or long term with WK-GGS (Figure 5.2 A) and GGS Stg480 (Figure 5.2 B) compared to IgG response from rats injected with PBS. Similar IgG reactivity was observed against GGS Stg480 in the sera from rats injected with WK-GAS (Figure 5.2 C) and GAS rM5 (Figure 5.2 D). The PBS injected control rats showed a very low serum IgG response to GAS rM5 and GGS Stg480.

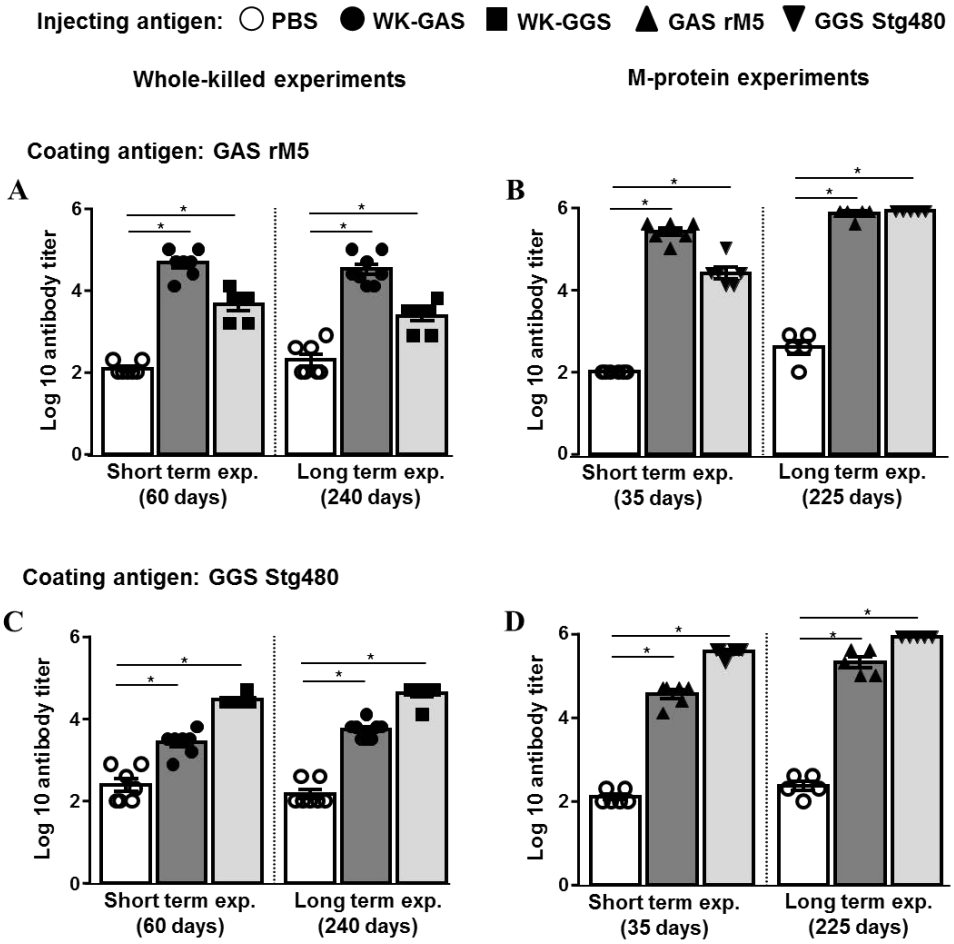


**Figure 5.2** Antibodies generated following exposure to GGS and GAS reacted with GGS and GAS M-proteins. IgG antibody in the sera from rats injected with WK-GGS (n=7-8) reacted with GAS rM5 (A). Similarly, serum IgG from rats injected with WK-GAS (n=7) reacted with GGS Stg480 (C). IgG response to GAS rM5 (B) and GGS Stg480 (D) was also found significantly higher in rats injected with GGS Stg480 and GAS rM5 compared to PBS injected control rats (n=6-7). Error bars represent standard errors of the mean (SEM). Statistical difference by one-way ANOVA with Tukey's post hoc multiple comparison; *p<0.0001.

### 5.3.2 Antibodies produced following GGS antigen injection recognise host proteins

In this study, we have demonstrated cardiac myosin and collagen I specific serum IgG responses in rats injected with WK-GGS, WK-GAS, GGS Stg480 and GAS rM5. A significantly higher IgG response to cardiac myosin was observed in sera from rats injected with WK-GGS or WK-GAS (Figure 5.3 A) and GAS or GGS M-proteins (Figure 5.3 B) compared to PBS injected control rats. IgG reactivity to human collagen I in the sera of rats injected short term with WK-GAS and short term or long term with GGS Stg480 or GAS rM5 was higher compared to sera from PBS injected control rats (Figure 5.3 C&D). The IgG response to collagen I in sera from rats injected short term or long term with WK-GGS and

long term with WK-GAS was higher than the IgG response in sera from PBS injected control rats although the difference was not significant (Figure 5.3 C).

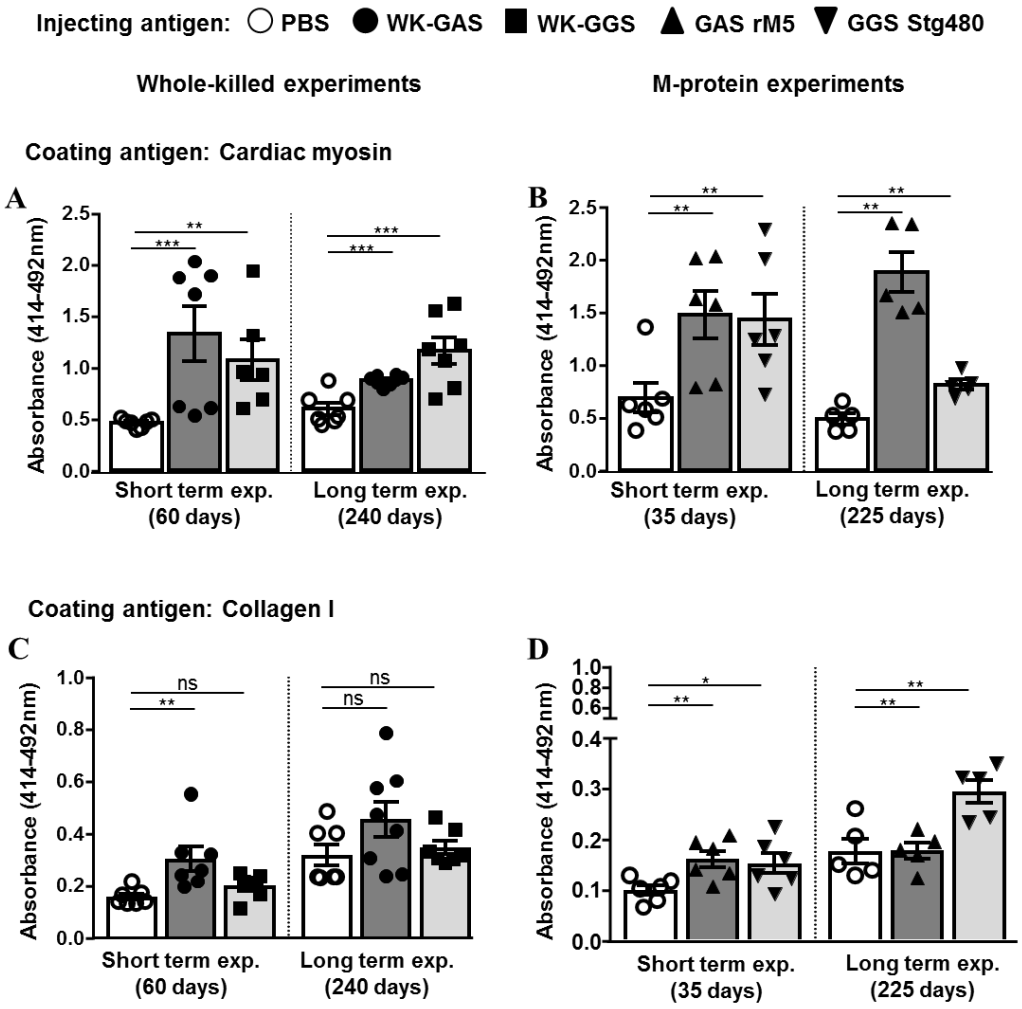


**Figure 5.3** Antibodies generated following exposure to GGS and GAS cross-reacted with cardiac myosin and collagen I. Antisera (at 1:100 dilution) raised in rats following injection with WK-GGS (n=7-8) and WK-GAS (n=7) (A), GGS Stg480 (n=5-6) and GAS rM5 (n=5-6) (C) reacted against cardiac myosin. (B&D) Reactivity to collagen I was also observed in the rats though the sera from WK-GGS injected short term and long term rats and WK-GAS injected long term rats were not found significant. In all experiments PBS injected control rats (n=5-7) were included. Error bars represent standard errors of the mean (SEM). Statistical difference by Mann-Whitney test; *p<0.05, **p<0.01, ***p<0.001, ns: not significant.

### 5.3.3 T-cells generated following exposure to GGS antigens recognise streptococcal antigens

In this study, we have demonstrated the splenic T-cell proliferative response to GAS rM5 and GGS Stg480 in rats injected long term with WK-GGS and WK-GAS and short term and long term with M-proteins of GGS and GAS. A significantly higher T-cell proliferative response

to GAS rM5 was observed in rats injected with WK-GGS (Figure 5.4 A) or GGS Stg480 (Figure 5.4 B) compared to PBS injected control rats. The anti-GAS (both whole-killed and rM5) T-cells also proliferated in response to GGS Stg480 (Figure 5.4 C&D). The T-cells from PBS injected control rats showed very low proliferative response to GAS rM5 and GGS Stg480.

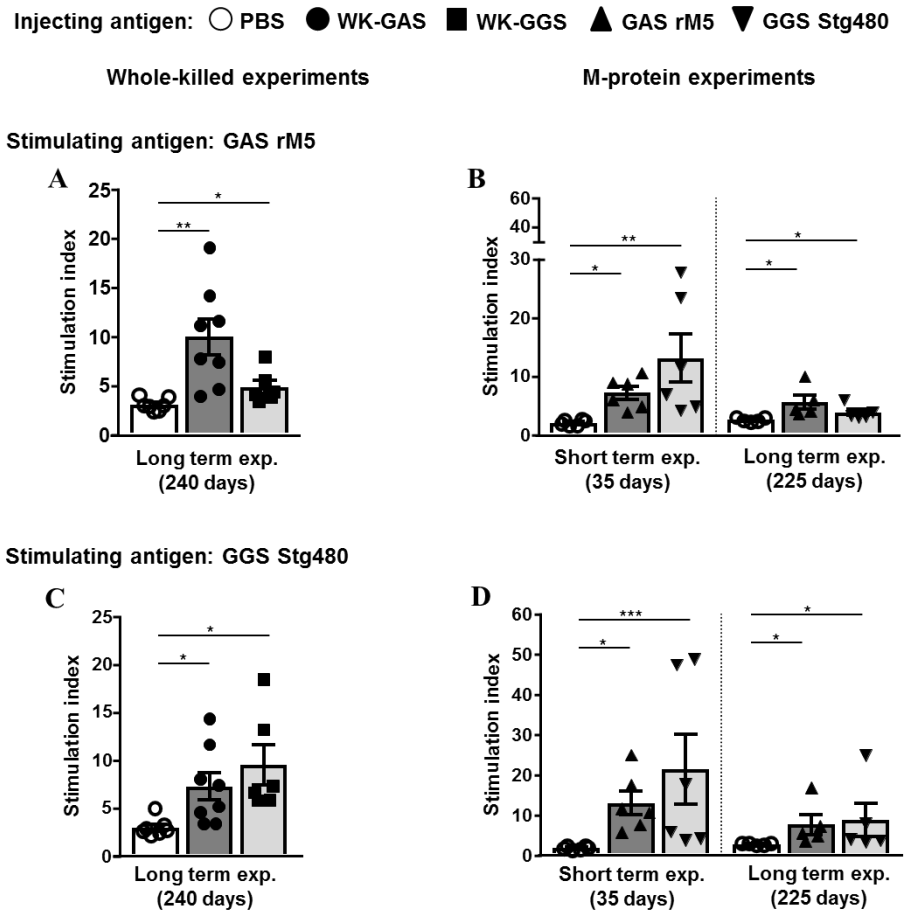


**Figure 5.4** Splenic T-cells from GGS and GAS injected rats proliferate in response to GGS and GAS M-proteins. The T-cells from rats injected long term with WK-GGS (n=8) (A) and short term and long term with GGS Stg480 (n=5-6) (B) proliferated in response to GAS rM5. The T-cells from rats injected with WK-GAS (n=7) and GAS rM5 (n=5-6) also proliferated in response to GGS Stg480 (C&D). The T-cell proliferative response to GAS rM5 and GGS Stg480 was minimal in control rats injected with PBS (n=5-7). Error bars represent standard errors of the mean (SEM). Statistical difference by one-way ANOVA with Tukey's post hoc multiple comparison; *p<0.05, **p<0.01, ***p<0.0001.

### 5.3.4 GGS and GAS specific Th17/Th1/Th2 cells are produced in response to GAS and GGS antigen injection

In this study, we analysed IFN-γ, IL-17A and IL-4 production by splenic T-cells upon *ex vivo* re-stimulation with GAS rM5 and GGS Stg480. Significantly higher levels of IFN-γ were

produced by T-cells from rats injected long term with WK-GGS (Figure 5.5 A) and short term and long term with GGS Stg480 (Figure 5.5 B) in response to GAS rM5 compared to PBS injected control rats. Similarly, T-cells from rats injected with WK-GAS and GAS rM5 produced significantly higher amounts of IFN-γ in response to GGS Stg480 compared to controls (Figure 5.5 C&D). Similar to IFN-γ, significantly high levels of IL-17A and IL-4 production were observed in rats injected with WK-GAS, WK-GGS, GAS rM5 and GGS Stg480 in response to GAS rM5 and GGS Stg480 (Figure 5.6 and Figure 5.7) compared to controls.

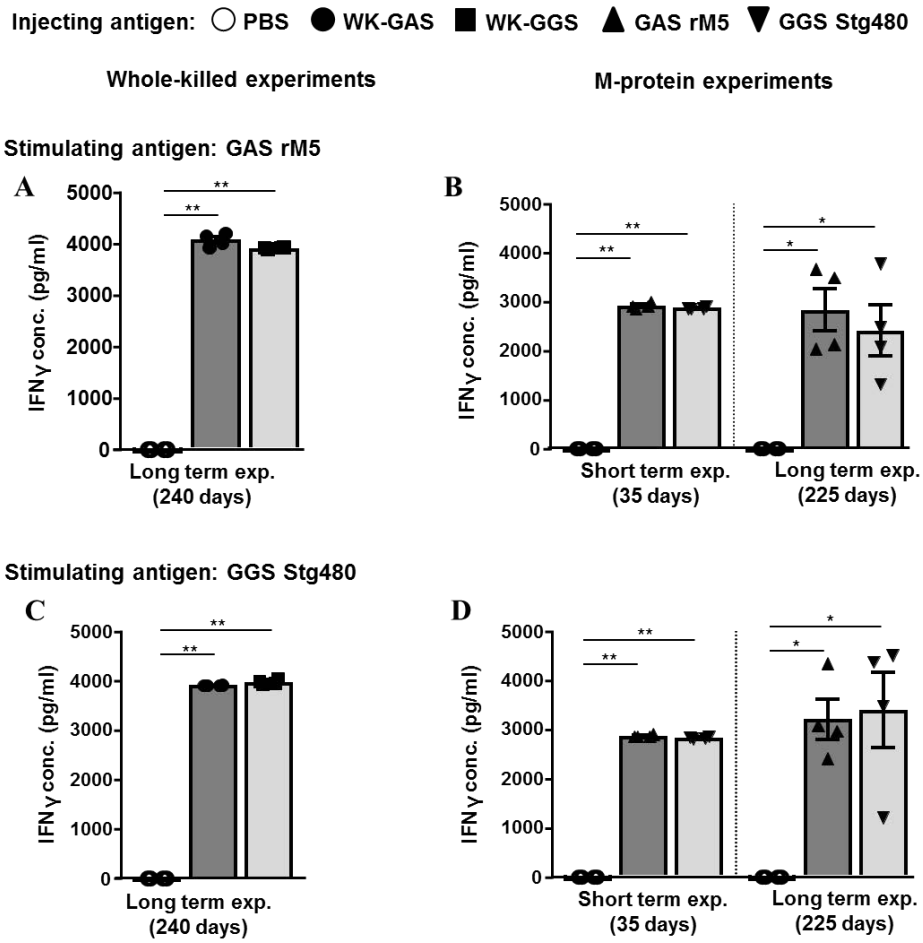


**Figure 5.5** GGS and GAS specific memory T-cells produce high amounts of IFN-γ upon ex vivo re-stimulation with GGS and GAS antigens. After 72 h culture, splenic T-cells from rats long term injected with WK-GGS (n=8) and WK-GAS (n=7) produced high amounts of IFN-γ in response to GAS rM5 (A) and GGS Stg480 (C) re-stimulation. High levels of IFN-γ were also produced by T-cells from the rats injected short and long term with GGS Stg480 (n=5-6) and GAS rM5 (n=5-6) following stimulation with GAS rM5 (B) and GGS Stg480 (D). In all experiments, rats injected with PBS were used as controls (n=5-7). Error bars represent standard errors of the mean (SEM). Statistical difference by one-way ANOVA with Tukey's post hoc multiple comparison; *$p<0.005$, **$p<0.0001$.

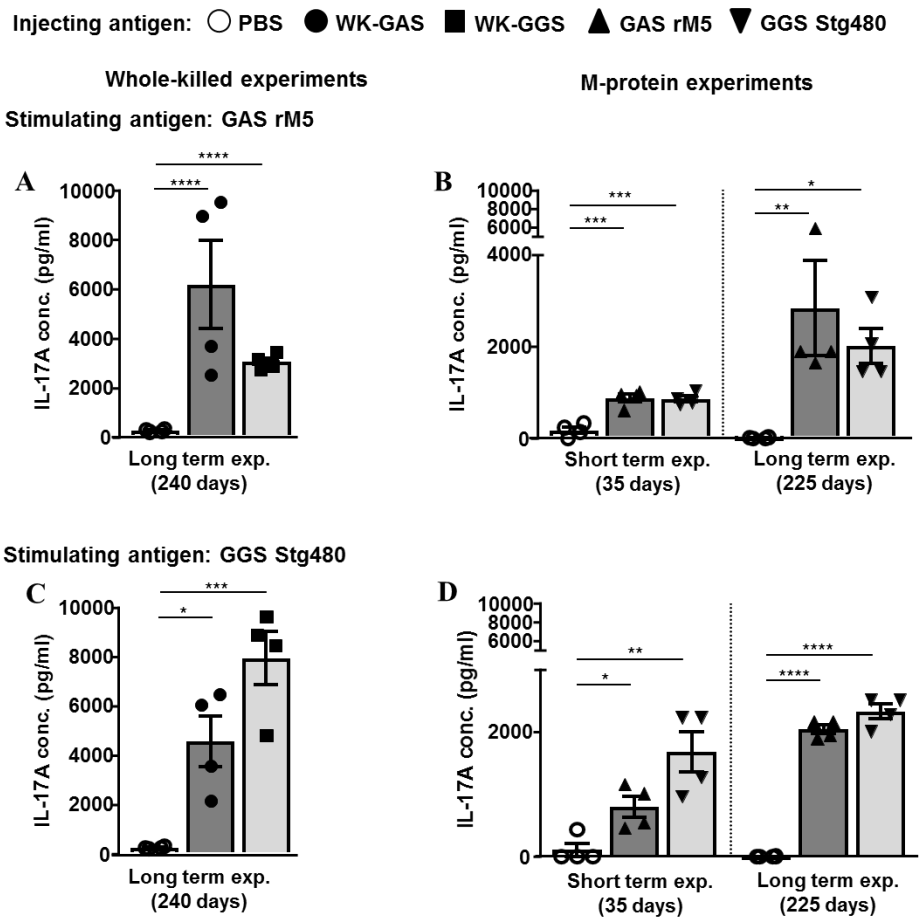


**Figure 5.6** GGS and GAS specific memory T-cells produce high amounts of IL-17A. Splenic T-cells from rats injected long term with WK-GGS (n=8) and WK-GAS (n=7) produced high amounts of IL-17A cytokine in response to GAS rM5 (A) and GGS Stg480 (C). High levels of IL-17A were also produced by T-cells from rats injected short and long term with GGS Stg480 (n=5-6) and GAS rM5 (n=5-6) following stimulation with GAS rM5 (B) and GGS Stg480 (D). In all experiments, rats injected with PBS (n=5-7) were used as controls. Error bars represent standard errors of the mean (SEM). Statistical difference tested by one-way ANOVA with Tukey's post hoc multiple comparison; *p<0.05, **p<0.01, ***p<0.001, ****p<0.0001.

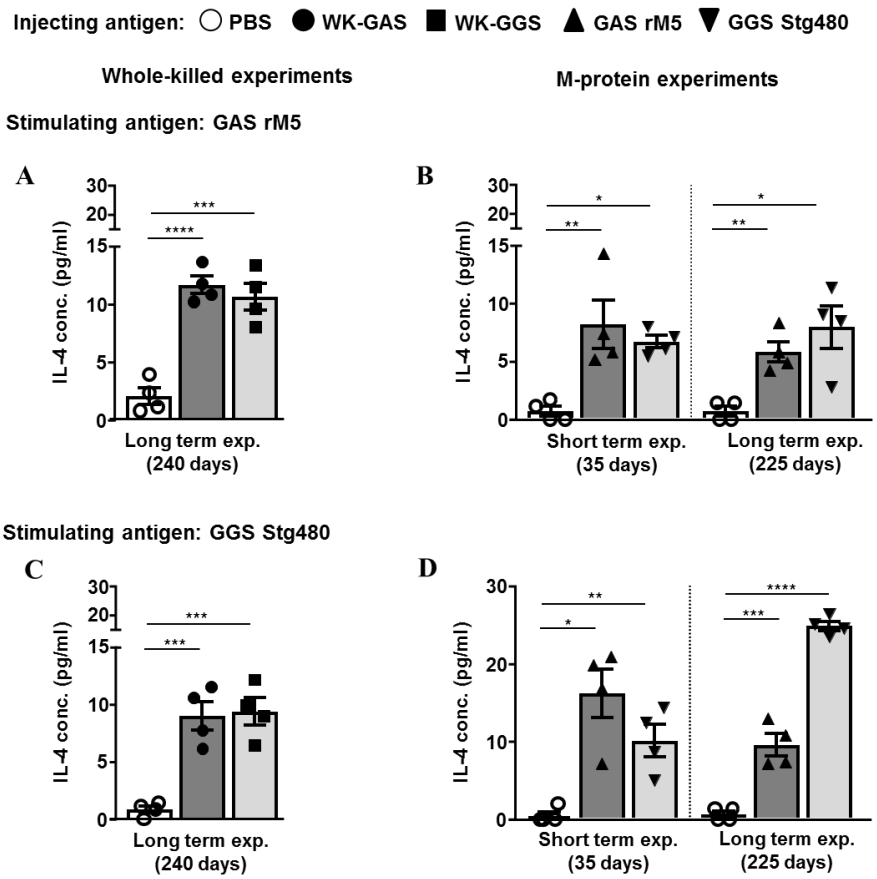


**Figure 5.7** GGS and GAS specific memory T-cells produce IL-4. Splenic T-cells from rats injected long term with WK-GGS (n=8) and WK-GAS (n=7) produced IL-4 in response to GAS rM5 (A) and GGS Stg480 (C). Significantly higher amounts of IL-4 were also produced by T-cells from rats injected short and long term with GGS Stg480 (n=5-6) and GAS rM5 (n=5-6) following stimulation with GAS rM5 (B) and GGS Stg480 (D). In all experiments, rats injected with PBS (n=5-7) were used as controls. Error bars represent standard errors of the mean (SEM). Statistical difference tested by one-way ANOVA with Tukey's post hoc multiple comparison; *p<0.05, **p<0.01, ***p<0.001, ****p<0.0001.

## 5.4 DISCUSSION

The Lewis rat autoimmune valvulitis (RAV) model is an appropriate animal model to study acute rheumatic fever and rheumatic heart disease. In several previous studies of ARF/RHD, the RAV model has been used successfully to induce and demonstrate carditis and observe autoimmune responses (Quinn, et al. 2001; Galvin, et al. 2002; Lymbury, et al. 2003; Gorton, et al. 2009; Gorton, et al. 2010; Gorton, et al. 2016). Moreover, this Lewis rat model is the first in which valvular changes akin to human heart pathology have been demonstrated and impaired heart function demonstrated. Whilst the RAV model has been useful in characterising key aspects involved in the autoimmune processes in RF/RHD pathogenesis, the limitations in the use of this model include: (1) species differences in rat versus human predisposition and character of the immune response; (2) the use of inbred strains; the use of

outbred or alternate MHC types has not been investigated and; (3) the restriction to one sex. Further studies are required to determine its suitability to comprehensively model this complex human disease.

In ARF/RHD, after pharyngeal or skin infection, the immune system responds to group A *Streptococcus* by antibody production (IgM followed by IgG) and T-cell priming and differentiation (Kaplan, et al. 1964; Roberts, et al. 2001; Gorton, et al. 2009; Cunningham 2014; Gorton, et al. 2016). The group A streptococcal M-protein is the major virulence determinant and an immunodominant GAS antigen and is most frequently reported to trigger autoimmune reactions against heart proteins that lead to the development of carditis (Cunningham, et al. 1989; Cunningham, et al. 1997; Quinn, et al. 2001). Anti-GAS M-protein antibodies have been reported in many clinical and experimental animal studies as potential auto-antibodies (Beachey, et al. 1988; Bronze, et al. 1988; Cunningham, et al. 1989; Quinn, et al. 1995; Brandt, et al. 2001). GGS M-proteins share significant sequence and structural features with the M-proteins of well-established rheumatogenic group A streptococcal serotypes like GAS M5. However, immunological similarities between GAS and GGS might be explained by antibody mediated cross-recognition. In the current study, antibodies induced in rats following exposure to WK-GGS and GGS Stg480, reacted with surface antigens of WK-GAS and the GAS rM5 protein (Figure 5.1 and Figure 5.2). Conversely, the anti-WK-GAS and anti-GAS rM5 antibodies also reacted with surface antigens of WK-GGS and GGS Stg480 protein (Figure 5.1 and Figure 5.2). Antibody reactivity in the sera of PBS injected control rats was minimal. We did not include a negative background control which is a limitation of the current study. We have demonstrated and published previously that the protein preparation methods used here removed contaminating proteins (Section 3.2.1.4 and Figure 3.1) and *E. coli* endotoxin (Gorton, et al. 2016). The results indicate that GGS induces antibodies that cross react with GAS and the converse; GAS induces antibodies that cross react with GGS. Anti-GAS and anti-GGS antibodies have been reported in patients with ARF/RHD (Kaplan, et al. 1964; Kaplan and Svec 1964; Galvin, et al. 2000; Sikder, et al. 2018). Cross-recognition of GGS by anti-GAS antibodies and *vice versa* indicates structural similarity between GAS and GGS antigens and shared potential for rheumatogenicity.

The GAS M-protein shares structural homology with several α-helical coiled-coil host proteins including cardiac myosin and collagen I. (Cunningham 2000; Guilherme, et al. 2006; Guilherme and Kalil 2010; Carapetis, et al. 2016; Martins, et al. 2017). In ARF/RHD,

antibody cross-reactivity between GAS M-proteins and cardiac myosin has been well documented (Galvin, et al. 2000; Ellis, et al. 2005). In several studies using Lewis rats, anti-GAS M-proteins antibodies have been reported to cross-react with cardiac myosin (Quinn, et al. 2001; Lymbury, et al. 2003; Gorton, et al. 2009; Gorton, et al. 2016). Previously in murine experiments it was observed that antibodies raised against cardiac myosin had greater reactivity to GGS than GAS M-proteins (Haidan, et al. 2000). Importantly in the current study, serum from rats injected with WK-GGS or GGS Stg480 reacted with cardiac myosin. This provides further evidence that GGS is capable of initiating an autoimmune process similar to GAS-induced ARF/RHD. Dale and Beachey (1985a) observed the cross-reactive antibodies to GAS M5 protein bound to the heavy chains region of myosin (Dale and Beachey 1985a). Cunningham, et al. (1997) reported that the N-terminus, B-repeat region and C-terminus of GAS M5 protein have high amino acid similarities with conserved regions of cardiac myosin (Cunningham, et al. 1997). However, to predict the epitopes of GGS M-protein and cardiac myosin involved in the antibody cross-reactivity, the amino acid sequencing is necessary.

In the current study, serum IgG from rats injected with WK-GGS and GGS Stg480 also showed reactivity to human collagen I (Figure 5.3). The results were similar to the IgG reactivity from rats injected with WK-GAS and GAS rM5. Collagen is an important structural protein of the heart valve and GAS surface protein similar to human collagen have been reported (Lukomski, et al. 2000; Lukomski, et al. 2001). Antibodies in rat sera reacting with collagen may be simply able to bind to B-cell epitopes within the collagen I molecule (Dinkla, et al. 2003a; Tandon, et al. 2013) or alternatively, collagen-specific antibodies may have been induced due to the release of collagen from damaged valves during the inflammation associated with carditis and a breakdown of immune tolerance (Tandon, et al. 2013). BALB/c and Swiss mice vaccinated with the M3 strain or cell wall fragments of GAS produced IgG that cross-reacted with endocardial basement membrane collagen (Ohanian, et al. 1969; Dinkla, et al. 2003b; Guilherme, et al. 2013a). Antibodies against collagen I have been reported in patients with ARF/RHD although no immunological cross-reactivity has been observed (Martins, et al. 2008). This absence of cross-reactivity raises the possibility of an alternative pathogenic pathway in ARF that produces an antibody-mediated response to collagen in the valve that does not rely on molecular mimicry. Currently, only cardiac myosin and M-protein (but not collagen) have been shown to induce valvulitis when injected into experimental animals (Quinn, et al. 2001; Galvin, et al. 2002). It is possible that the cross-

reactive antibodies bind to the valvular endothelial surface and upregulate vascular cell adhesion molecules including VCAM-1 that leads to inflammation and leukocyte infiltration into the valves and myocardium (Galvin, et al. 2000; Roberts, et al. 2001).

In ARF/RHD, there is strong evidence of the recognition of heart proteins by autoreactive T-cells via molecular mimicry (Cunningham 2003; Fae, et al. 2006; Guilherme, et al. 2006; Carapetis, et al. 2016). The autoreactive T-cells infiltrate the valve and the myocardium, and form Aschoff nodules (Raizada, et al. 1983; Dale and Beachey 1987; Guilherme, et al. 1995; Guilherme, et al. 2001b; Carapetis, et al. 2016). In the current study, splenic T-cells from rats injected with WK-GGS and GGS Stg480 proliferated in response to GAS rM5. Conversely, anti-GAS T-cells also proliferated in response to GGS Stg480. Several animal studies have reported that the anti-GAS T-cells proliferate in response to GAS M-proteins and peptides (Lymbury, et al. 2003; Ellis, et al. 2005; Fae, et al. 2005; Guilherme, et al. 2007; Gorton, et al. 2009; Gorton, et al. 2016). However, the phenotype of T-cell involved in the ARF/RHD is a matter of dispute. There are controversial reports of increase of CD4+ and CD8+ T-cells during the course of development of carditis. Increase of CD8+ T-cells has been reported in few studies (Ganguly, et al. 1982; Lue, et al. 1983) whereas, many studies reported a comparative increase of CD4+ T-cells (Bhatia, et al. 1989; Morris, et al. 1993b; Narin, et al. 1995; Guilherme, et al. 2001a; Roberts, et al. 2001; Ellis, et al. 2005; Toor and Vohra 2012). Among the CD4+ T-cells, Roberts, et al. (2001) identified more Th1 T-cells than Th2 cells (Roberts, et al. 2001). T-cells activated by streptococcal M-protein derived peptides and co-stimulators secrete cytokines to stimulate activation and proliferation of antigen-specific T-cell and B-cells (Abbas 2008).

Our model of ARF/RHD valvulitis has provided new evidence for an IL-17A/IFN-γ signature in this disease and suggests that this may be an important pathway in RHD. In addition, high levels of M-protein specific IFN-γ and IL-17A in this study suggested that a Th1/Th17 dominated immune response may drive heart pathology. Heart-infiltrating T-cells isolated from the heart valves of ARF/RHD patients have previously been shown to be predominantly IFN-γ-producing. IL-4 producing T-cells however, were demonstrated in the myocardium (Guilherme, et al. 2004; Fae, et al. 2006; Guilherme and Kalil 2007; Guilherme, et al. 2011a) but IL-4 was not a dominant cytokine in the rat model although seen at low concentrations.

Our data suggests that both GAS and GGS and their M-proteins induce high levels of IL-17A. Th-17 cells and IL-17A were discovered only relatively recently (Bettelli, et al. 2006) but have become a very important immune mediators in extracellular bacterial infections and appear to play a pathological role in numerous autoimmune diseases where fibrosis is a thematic endpoint (Bilik, et al. 2016). A role for Th-17 cells and IL-17A has been reported previously in the context of murine GAS infections (Wang, et al. 2010; Dileepan, et al. 2016). In another study, high concentrations of IL-17 in the serum of Lewis rats and high expression of IL-17 in the mitral valves of rats and human patients were observed (Wen, et al. 2015). Elevated level of IL-17A has also been reported in ARF/RHD sera compared to healthy controls (Bilik, et al. 2016). IL-17 is important in recruiting neutrophils and macrophages to the site of infection (Ivanov, et al. 2006; Annunziato, et al. 2007) and is a relatively new finding in the development of autoimmune carditis. Although there is some previous indirect evidence for involvement of IL-17A and Th17 cells in the pathogenesis of ARF/RHD, no previous animal studies have reported a role for these cytokine and cellular mediators. Our findings suggest that the altered balance between Th1/Th2/Th17 cytokines may drive pathology in ARF/RHD.

Our findings suggest that group G *Streptococcus* (GGS) and its M-protein has the potential to generate autoreactive antibodies and T-cells to group A *Streptococcus*. Most importantly, the GGS induced autoantibodies to host cardiac myosin and collagen I. Current hypotheses relating to the development of ARF/RHD suggest that multiple separate GAS infections are required for development of ARF/RHD (Cunningham 2014; Carapetis, et al. 2016). There is no evidence however that strains causing these repeat infections need to be of the same M-type. Our results suggest that GGS may also contribute in this model of disease. This is particularly relevant in those regions of the world where ARF/RHD is endemic, and GAS is rarely recovered from the throat.

# CHAPTER 6
# REPEAT EXPOSURE TO GROUP G *STREPTOCOCCUS* INDUCES CARDITIS IN LEWIS RAT AUTOIMMUNE VALVULITIS MODEL

## 6.1 INTRODUCTION

Experiments described in Chapter 5 of this thesis showed that antibody and T-cell responses were induced in Lewis rats following injection with whole-killed group G *Streptococcus* NS3396 (GGS) and GGS M-protein (Stg480). The inflammatory process of acute rheumatic fever (ARF) has structural and functional effects on the heart that can lead to acute inflammatory damage and ultimately to chronic rheumatic heart disease (RHD). Inflammation of myocardium and particularly the mitral valves are common findings in ARF/RHD (Roberts, et al. 2001). Inflammation and fibrotic changes may cause dilation of the mitral annulus (junction between the left atrium and left ventricle and insertion site for valve leaflets) and elongation of chordae tendinae, and papillary muscle resulting in mitral valve incompetence, mitral regurgitation and ultimately heart failure (Carapetis, et al. 2016). It is postulated that GAS M-protein-specific T-cells and B-cells are autoreactive against host antigens due to homology between streptococcal M-proteins and host tissue proteins (Guilherme, et al. 2011a). The auto-reactive antibodies and T-cells upregulate cell adhesion molecules on the valvular endothelium (Lehmann, et al. 1992; Roberts, et al. 2001) leading to inflammation, cellular infiltration and valve fibrosis and scarring (Quinn, et al. 1995; Guilherme, et al. 2000; Galvin, et al. 2002; Guilherme and Kalil 2002; Cunningham 2003; Ellis, et al. 2005; Fae, et al. 2006).

The characteristic histological features of ARF/RHD include extensive inflammation of myocardium and valves with infiltration of T-cells, macrophages and neutrophils, fibroblasts accumulation and deposition of collagen fibres (Pahlman, et al. 2006). In addition, Aschoff bodies are granulomatous structures commonly present beneath the endocardium and contain Anitschkow cells, Aschoff cells and T-cells (Roberts, et al. 2001; Carapetis, et al. 2016). The myocardial Aschoff bodies are believed to be formed following injury of the interstitial non-myogenic collagen fibres (Murphy 1952). Formation of exudative, granulomatous or fibrotic Aschoff bodies leads to dysfunction of myocardium and mitral valves (Cunningham 2012). Further inflammation leads to fibrinous vegetation (verrucae) of the leaflets and subsequent scarring, which might ultimately lead to valvular stenosis (Veasy and Tani 2005). The

myocardium may heal over time, there can be permanent damage to the mitral valves (Carapetis, et al. 2016).

In ARF/RHD, the inflammation-driven pathological changes in the heart can be demonstrated using various imaging techniques (Cunningham 2012). Abnormalities in the conduction of electrical impulses through the heart are recorded with an electrocardiogram (ECG). Prolongation of the P-R interval in ECG is used to demonstrate these heart conduction anomalies (Cunningham 2012). Prolonged P-R interval denotes the delay in the electrical impulse conduction from sinoatrial node (SA node), to the ventricle and is also a minor Jones Clinical Criterion for the diagnosis of ARF/RHD (Gewitz, et al. 2015). Moreover, echocardiography (Echo) has considerably enhanced the clinical assessment and management of patients with ARF/RHD compared to simple auscultation (Gewitz, et al. 2015). Echo is now considered essential for large scale population screening, early detection of ARF/RHD, for serial follow up and for therapeutic procedural guidance (Abernethy, et al. 1994; Minich, et al. 1997; Figueroa, et al. 2001; Narula and Kaplan 2001; Vijayalakshmi, et al. 2008). Echocardiographic findings that feature in ARF/RHD include changes to mitral valvular morphology, especially valvular thickening and slow or impaired valvular leaflet movement (Jain and Mankad 2013; Wunderlich, et al. 2013).

The relationship between group A *Streptococcus* and damage to the mitral valve and myocardium has been established by many clinical and animal model studies (Galvin, et al. 2000; Quinn, et al. 2001; Lymbury, et al. 2003; Gorton, et al. 2009; Kirvan, et al. 2014; Bright, et al. 2016; Carapetis, et al. 2016; Gorton, et al. 2016). In this study, we report that the histological and functional changes observed in the heart of rats exposed to whole-killed GGS NS3396 and GGS M-protein Stg480 are indistinguishable to those exposed to whole-killed GAS M5 and GAS M-protein rM5.

### 6.1.1 Aims

The overall Aim of the research presented in this chapter was to examine the effect of group G *Streptococcus* on the development of cardiac pathology in the Lewis rat model.

The specific Aims are:

1. To demonstrate the effect of whole-killed GGS NS3396 and GGS M-protein Stg480 on heart tissue using histology.

2. To examine cardiac dysfunction and pathology by performing electrocardiography and echocardiography.

## 6.2 MATERIALS AND METHODS

Experimental design, animals, antigens and adjuvants and short and long term antigen injection schedules were as described in Chapter 5 (Section 5.2). Rats were culled according to the procedures described in Section 3.2.2.2 and heart samples collected as described in Section 3.2.2.3. Rat heart histological staining using haematoxylin and eosin (H&E) stain and Masson's trichrome stain was performed as described in Section 3.2.5. Histological scoring for carditis was performed as described in Table 6.1.

**Table 6.1** Mitral valvulitis and myocarditis severity scores (H&E staining)

| Score | Mitral valve | Myocardium |
|---|---|---|
| **0** | No inflammatory cells associated with valves | Diffuse, individual cells throughout tissue |
| **1** | <5 isolated cells in/on valves | 1-2 small foci |
| **2** | >5 cells on valve surface only | >2 small foci |
| **3** | Focal lesion in valve | Large focal lesion |
| **4** | >1 lesion | Aschoff-type lesion |

Assessment of cardiac dysfunction and pathology by ECG and echo was as described in Section 3.2.6.

### 6.2.1 Statistical analysis

The normality of pooled histology, ECG and echo data was evaluated using GraphPad Prism 7 statistical software. All data from experimental and control groups passed D'Agostino & Pearson omnibus normality tests and were therefore compared and tested using one-way analysis of variance (ANOVA) with Tukey's post hoc multiple comparisons test. The results are reported as mean ± standard error (SEM), $p \leq 0.05$ was considered significant.

## 6.3 RESULTS

The results of histological examination and functional assessment of heart of rats injected with whole-killed and M-proteins of GAS and GGS are described in this chapter.

### 6.3.1 GGS NS3396 and GAS M5 and their respective M-proteins (GGS Stg480 and GAS rM5) cause carditis

Previously studies demonstrated that both GAS rM5 protein and GAS strains induced inflammatory and other RHD-like symptoms in a rat model of valvulitis (Gorton, et al. 2009; Huang, et al. 2009; Xie, et al. 2010; Gorton, et al. 2016). To determine whether GGS NS3396 could invoke similar pathology, rats were injected with whole-killed GGS NS3396 (WK-GGS) or GGS M-protein (Stg480), and compared to whole-killed GAS M5 (WK-GAS) and GAS rM5-protein. Representative H&E stained heart section images are shown below (Figure 6.1) with individual images from all rats shown in Appendix 6. In all experiments, heart sections from all rats injected with WK-GGS, WK-GAS and M-protein of GGS and GAS, showed marked infiltration of mononuclear cells (MNCs) into myocardial and valvular tissues (Figure 6.1 and Appendix 6 Supplementary Figure 6.4B&6.4C, 6.4E&6.4F, 6.5B&6.5C, 6.5E&6.5F, 6.6B&6.6C, 6.6E&6.6F, 6.8B&6.8C and 6.8E&6.8F). Variable degrees of verrucae and oedema were also observed into mitral valve leaflets. Inflammatory changes were observed in rats at both 60 and 240 days post primary injection with whole-killed bacteria (Figure 6.1 A and Appendix 6 Supplementary Figure 6.4B&6.4C, 6.4E&6.4F, 6.5B&6.5C and 6.5E&6.5F). Inflammatory changes were also observed in rats at both 35 and 225 days post primary injection with GAS rM5 and GGS Stg480 (Figure 6.1 B and Appendix 6 Supplementary Figure 6.6B&6.6C, 6.6E&6.6F, 6.8B&6.8C and 6.8E&6.8F). In contrast, the mitral valve and myocardium tissues of PBS injected control rats showed little or no evidence of inflammation (Figure 6.1 C&D and Appendix 6 Supplementary Figure 6.4A&6.4D, 6.5A&6.5D, 6.6A&6.6D and 6.8A&6.8D). All rats injected with whole-killed bacteria or M-protein had variable degrees of MNC infiltration in the mitral valves (Figure 6.1 E&G) and myocardium (Figure 6.1 F&H). Higher magnification (1000×) of inflammatory foci within the mitral valve and myocardium revealed the presence of scarcely distributed polymorphonuclear cells (Figure 6.1 I&J z). Cells similar in appearance to "Aschoff cells" (Figure 6.1 I&J x) and "Anitschkow cells" (Figure 6.1 I&J y) were also observed. Moreover, an interstitial focal myocarditis with granulomatous structures resembling "Aschoff nodule like" structures (Figure 6.1 J) were observed in rats injected with whole-killed bacteria or M-proteins of GGS and GAS. The combined mitral valvulitis and myocarditis (carditis) severity scores were significantly higher in rats injected with whole-killed bacteria (Figure 6.1 A) and GAS and GGS M-proteins (Figure 6.1 B).

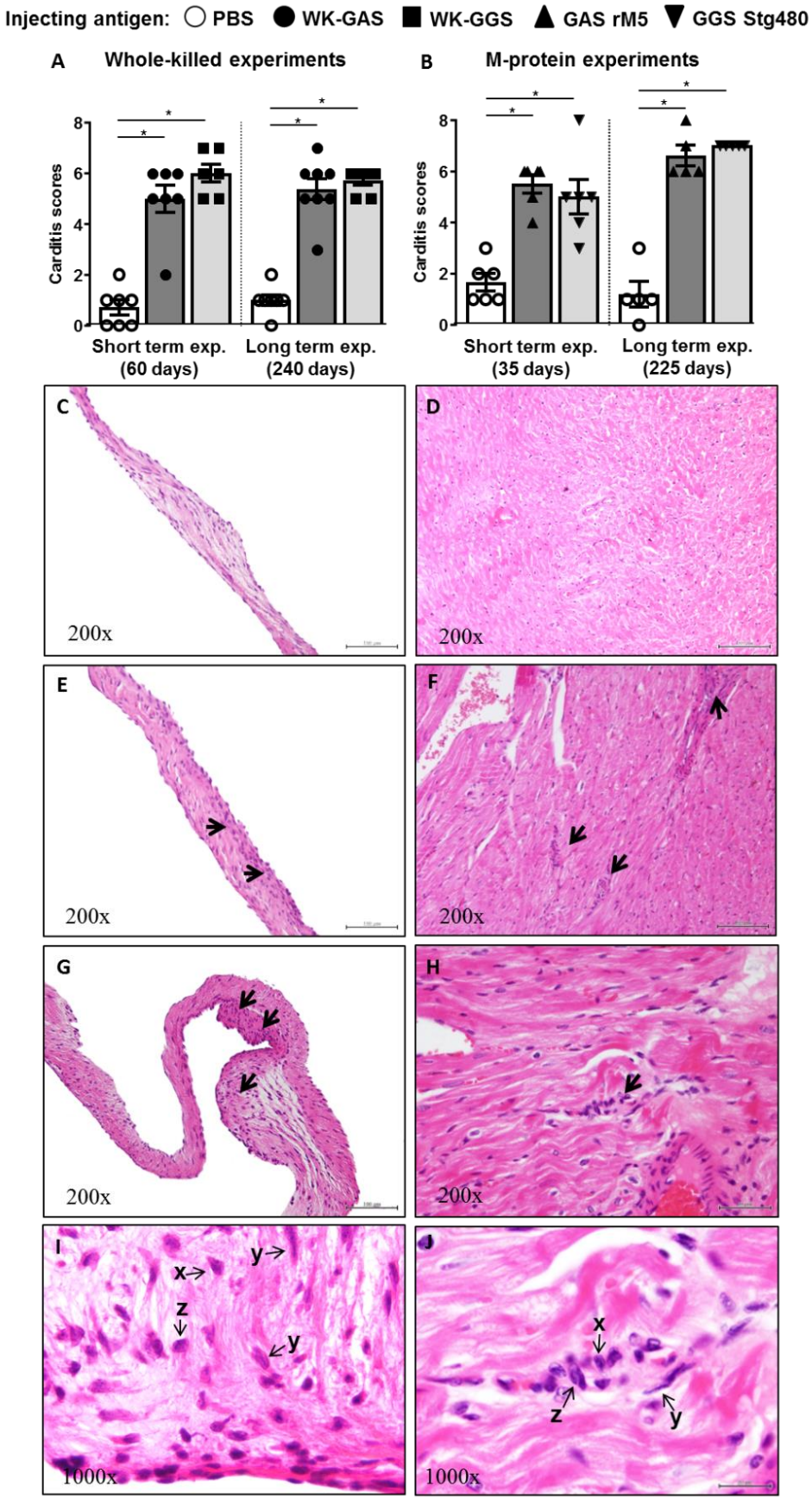


**Figure 6.1** Histological changes in cardiac tissues are identical following exposure to either GGS or GAS. Carditis scores were determined in Lewis rats injected with WK-GGS (n=7-8)

and WK-GAS (n=7) (A) and M-proteins of GGS (n=5-6) and GAS (n=5-6) (B) compared to control rats (PBS injected, n=5-7). There was no evidence of inflammation in the mitral valves (C) and myocardium (D) observed in control rats. Inflammatory focal lesions (arrows, E&G), verrucae (arrows, G) and oedematous mitral valves in rats injected with whole-killed and M-protein of GGS and GAS. Rats injected with whole-killed bacteria or M-proteins had interstitial focal myocarditis with granulomatous structures evident (arrows, F&H). Scale bars as indicated, C&D: score 0, E&F: score 2, G-J: score 4, x: Aschoff like cells, y: Anitschow like cells, z: polymorphonuclear cell. Error bars represent standard errors of the mean (SEM). Statistical difference by 1-way ANOVA with Tukey's post hoc multiple comparison test; *$p<0.0001$.

The M-protein injected short and long term experiments were repeated in full and showed similar inflammatory pathology; the results from experimental repeats are shown in Appendix 6, Supplementary Figure 6.1, 6.7 and 6.9.

### 6.3.2 GGS and GAS promote deposition of collagen fibres in heart tissues

Mitral valvular fibrosis leading to valvular stenosis and regurgitation is a key feature in the pathogenesis of ARF/RHD (Lis, et al. 1987). In the current study Masson's trichrome staining was performed to demonstrate collagen fibre deposition in rat myocardium and mitral valve tissues. The distribution of collagen within the mitral leaflets of control rats injected with PBS was confined to discrete areas (Figure 6.2 C and Appendix 6 Supplementary Figure 6.10A, 6.11A, 6.12A and 6.14A). Small amounts of collagen were also observed surrounding blood vessels throughout the myocardial tissues of control rats (Figure 6.2 F and Appendix 6 Supplementary Figure 6.10D, 6.11D, 6.12D and 6.14D). In contrast, extensive deposition of collagen and thickening of mitral leaflets was observed in rats injected with WK-GAS (Figure 6.2 D and Appendix 6 Supplementary Figure 6.10B&6.11B) and WK-GGS (Figure 6.2 E and Appendix 6 Supplementary Figure 6.10C&6.11C). Moreover, the myocardium of whole-killed bacteria injected rats showed widespread collagen deposition in the areas of inflammation (Figure 6.2 G&H and Appendix 6 Supplementary Figure 6.10E&6.10F and 6.11E&6.11F). Similar lesions were observed in the mitral valves and myocardium of rats injected with GGS Stg480 and GAS rM5 (Appendix 6 Supplementary Figure 6.12B&6.12C, 6.12E&6.12F, 6.14B&6.14C and 6.14E&6.14F). The combined percentage of collagen deposition in mitral valve and myocardium was found to be significantly higher in rats injected with whole-killed bacteria (Figure 6.2 A) or M-proteins (Figure 6.2 B) of GAS and GGS.

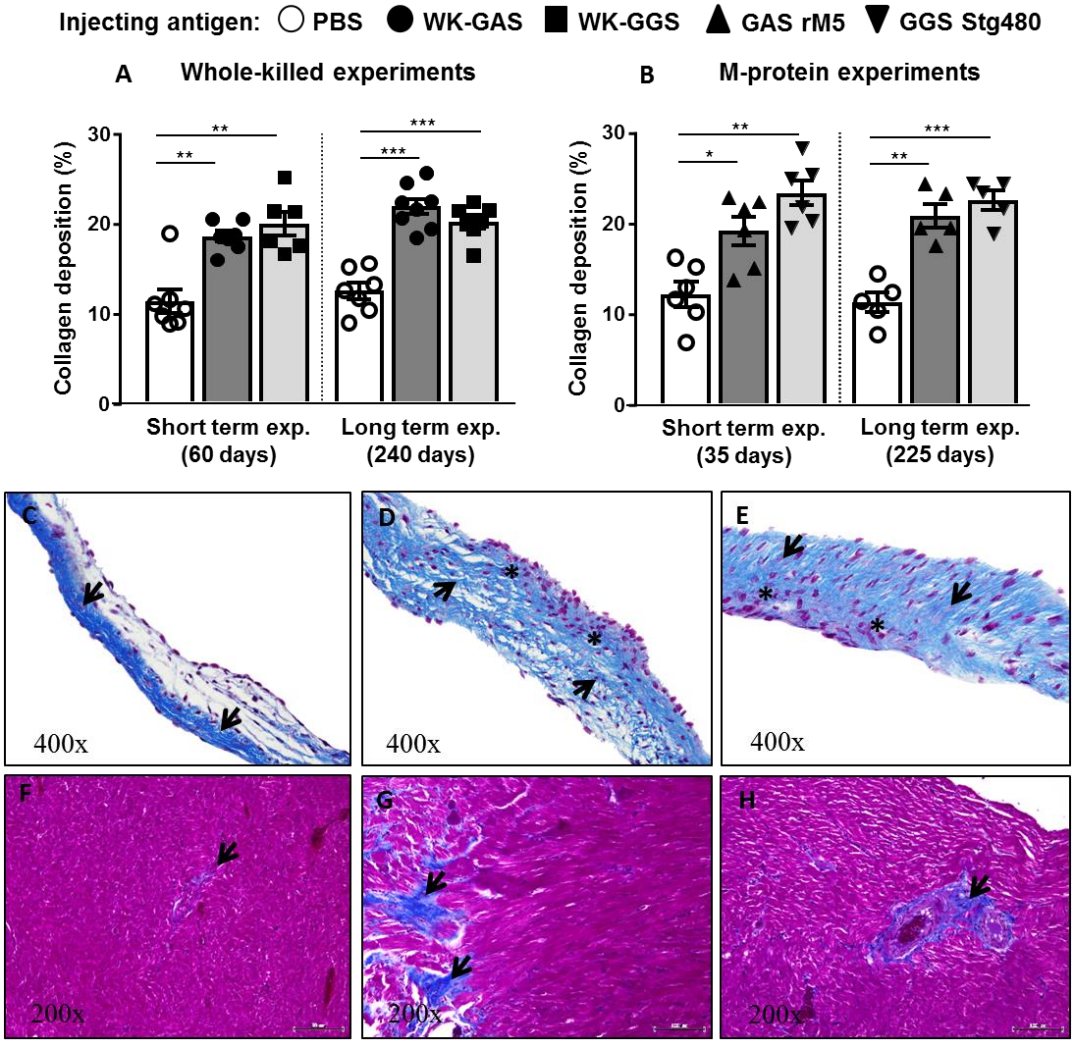


**Figure 6.2** Group G and A streptococci induce collagen deposition in the mitral valve and myocardium. Extensive collagen deposition (blue) was demonstrated in Lewis rats injected with WK-GGS (n=7-8) and WK-GAS (n=7) (A) and M-proteins of GGS (n=5-6) and GAS (n=5-6) (B) compared to PBS injected control rats (n=5-7). There was uniform distribution of collagen fibre in the mitral valve of control rats (C). Extensive deposition of collagen was observed in the mitral valves of rats injected with WK-GAS (D) and WK-GGS (E). In myocardium of control rats, scanty amounts of collagen were observed surrounding the blood vessels (F). Widespread deposition of collagen was observed in the myocardium of rats injected with WK-GAS (G) and WK-GGS (H). Collagen fibre is stained blue (indicated by arrows) in Masson's trichrome staining. Scale bars as indicated, asterisks (*) indicate inflammatory foci. Error bars represent standard errors of the mean (SEM). Statistical difference by 1-way ANOVA with Tukey's post hoc multiple comparison test; *p<0.05, p**<0.001, ***p<0.0001.

The M-protein injected short and long term experiments were repeated and similarly showed extensive deposition of collagen fibres in the mitral valves and myocardium; the results from experimental repeats are shown in Appendix 6 Supplementary Figure 6.2, 6.13 and 6.15.

### 6.3.3 Electrocardiographic changes are identical following exposure to GAS and GGS antigens

Prolongation of the P-R interval on ECG reflects conduction abnormalities of the myocardium (Gewitz, et al. 2015). In the current study, P-R intervals were prolonged in rats injected with WK-GAS and WK-GGS at 60 days and 240 days after priming injections, as compared to PBS injected control rats (Figure 6.3 A). The rats injected with GAS rM5 and GGS Stg480 also revealed similar results at 35 days and 225 days after antigen priming (Figure 6.3 B). The ECG changes of GAS rM5 and GGS Stg480 injected rats were reproduced in repeat experiments (Appendix 6 Supplementary Figure 6.3).

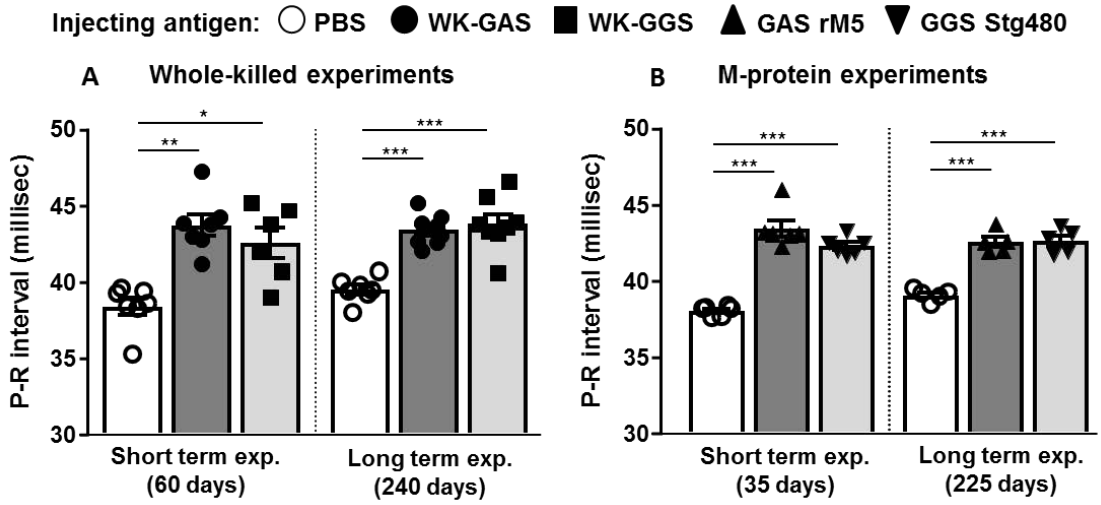


**Figure 6.3** Electrocardiographic changes demonstrate functional impairment following exposure to GAS and GGS. Prolongation of P-R interval in rats injected with WK-GAS (n=7) and WK-GGS (n=7-8) was observed 60 days (A, short term exp.) and 240 days (A, long term exp.) after priming injections compared to the PBS injected control rats (n=6-7). Similar findings were recorded in M-protein of GAS (n=5-6) and GGS injected rats (n=5-6) at 35 days (B, short term exp.) and 225 days (B, long term exp.) after priming, when compared to controls (n=5-6). Error bars represent standard errors of the mean (SEM). Statistical difference by 1-way ANOVA with Tukey's post hoc multiple comparison test; *$p<0.01$, **$p<0.001$, ***$p<0.0001$.

### 6.3.4 Group G *Streptococcus* induces echocardiographic changes similar to GAS

Echocardiographic assessment helps in the clinical diagnosis and monitoring of patients with ARF/RHD (Carapetis, et al. 2016). In the current study, impairment of cardiac function was further demonstrated by echocardiography (echo). Echo scores were generated based on mitral valvular thickening and the presence of nodules on the valve leaflets. Using echo, we found uniform valvular structures in the control rats injected with PBS (Figure 6.4 B and Appendix 6 Supplementary Figure 6.16A&6.17A). In contrast, valvular thickening and

nodules were observed in rats injected with WK-GAS, WK-GGS, GAS rM5 and GGS Stg480 (Figure 6.4 C-F and Appendix 6 Supplementary Figure 6.16B&6.16C and 6.17B&6.17C). The higher echo scores were observed in rats injected with WK-GAS, WK-GGS, GAS rM5 and GGS Stg480 compared to PBS injected control rats (Figure 6.4 A).

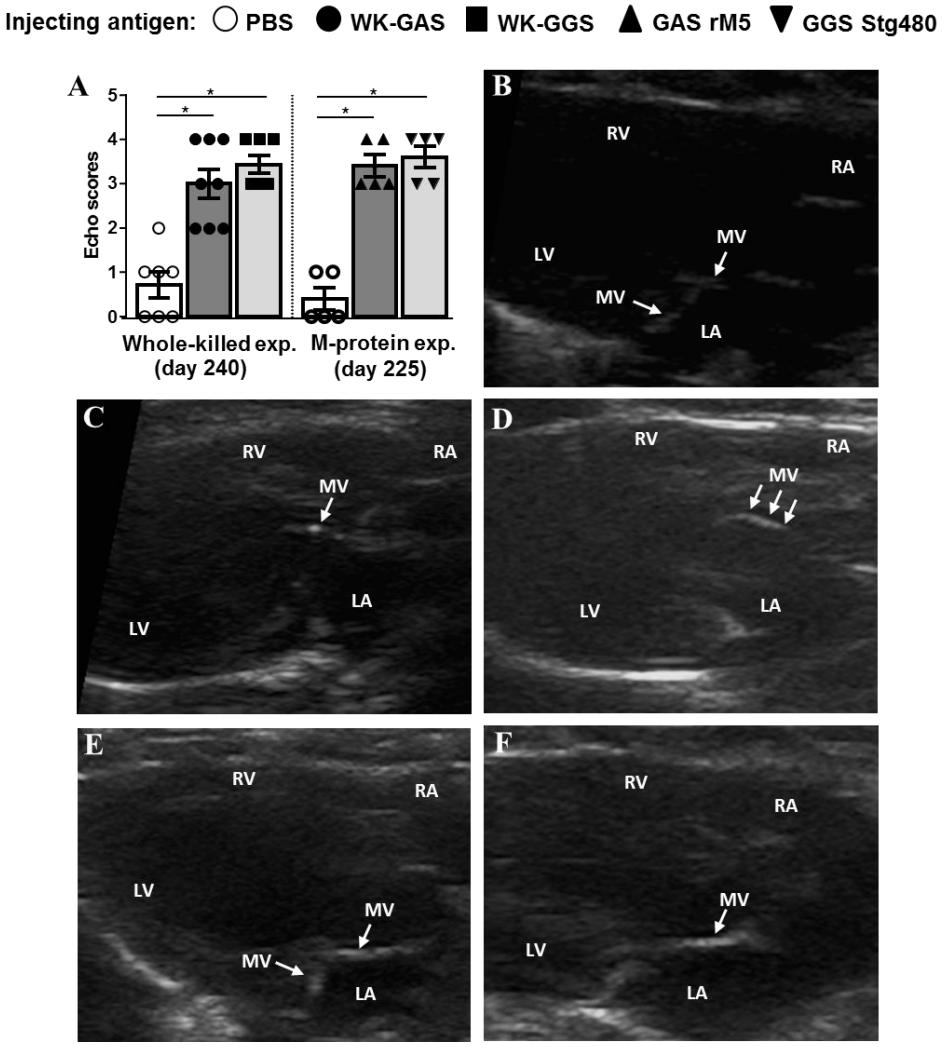


**Figure 6.4** Echocardiographic changes demonstrate mitral valve pathology following exposure to GAS and GGS. Echocardiographic scores were determined based on mitral valvular thickening and the presence of valve nodules. The mitral valves of PBS treated animals (n=5-7) had a uniform valvular structure (B, score 0). Pathological changes were observed with nodules on the mitral valves indicated by arrows in panel C (score 1) and D (score 2). Fibrotic thickening of the valve leaflet was observed as white opaque areas as indicated by arrows in panel E (score 1) and F (score 2). (A) Higher scores on echo were observed in the rats injected with WK-GAS (n=7), WK-GGS (n=8), GAS rM5 (n=5) and GGS Stg480 (n=5) compared to PBS treated controls (n=5-7). Arrows indicate mitral leaflets, MV: mitral valves, LA: left atrium, RA: right atrium, LV: left ventricle, RV: right ventricle. Error bars represent standard errors of the mean (SEM). Statistical difference by 1-way ANOVA with Tukey's post hoc multiple comparison test; *p<0.0001.

## 6.4 DISCUSSION

Classically, throat infection by GAS has been considered a prerequisite for the development of ARF/RHD. However, in ARF/RHD endemic areas, pharyngeal carriage of GAS in these populations is relatively low and GGS can be recovered from this niche more frequently (Haidan, et al. 2000; McDonald, et al. 2006; O'Sullivan, et al. 2017). Based on these epidemiological observations it has been postulated that GAS throat infection may not necessarily be the only trigger for the disease sequelae (McDonald, et al. 2004; McDonald, et al. 2006). Here for the first time we provide *in vivo* evidence that the injection of rats with either a GGS M-protein or a strain of GGS circumstantially associated with ARF/RHD (Towers, et al. 2004; Davies, et al. 2005), induce valvulitis and cardiac inflammation similar to GAS and GAS M-protein. The current study only focussed on the pathological changes that occur in the heart tissues. The study design did not include demonstration of changes in other organs e.g. kidney, joints etc as occurs in ARF. The changes observed in this model (prolonged P-R intervals, cardiac inflammation and presence of Aschoff nodules) when Stg480 or GGS were used as the injecting antigen are all consistent with features of ARF/RHD in humans.

Inflammation of the heart with mitral valvular fibrosis is a hallmark of patients with ARF/RHD (Roberts, et al. 2001). Inflammation of the mitral valve and myocardium occurs in >50% of patients (Veasy, et al. 1987; Veasy, et al. 1994; Roberts, et al. 2001; Vijayalakshmi, et al. 2008). In this study, rats injected with Stg480, a M-protein only found in specific GGS isolates, or those injected with whole-killed GGS NS3396 showed evidence of mitral valvulitis and myocarditis. These findings were consistent with those following injection of GAS or recombinant M5 protein. GAS isolates of M-type 5 are classic “rheumatogenic” type strains, are associated with ARF/RHD and have been previously shown to induce autoimmune valvulitis in this rat model (Quinn, et al. 2001; Lymbury, et al. 2003; Gorton, et al. 2009; Huang, et al. 2009; Xie, et al. 2010; Kirvan, et al. 2014). Infiltrating cells in both the mitral valve and myocardium were predominantly mononuclear cells. However, macrophages similar to the ‘Aschoff giant cell’ and polymorphonuclear cells were also observed in focal areas of inflammation. In support of these observations, Gorton, et al. (2009) suggested that CD4+ T-cells and CD68 macrophages infiltrating the mitral valves and myocardium mediate valvular and myocardial tissue damage in GAS rM5-protein injected rats. Quinn, et al. (2001) reported the induction of valvulitis and focal myocarditis in Lewis rats following injection with GAS rM6 protein which were histologically identical to human RHD lesions.

Guilherme, et al. (1995) detected a high proportion of CD4+ T-cells in valvular lesions, and this was further confirmed by studies carried out on heart valves from patients by Roberts, et al. (2001). Fraser, et al. (1995) observed aggregated macrophages in the mitral valves during the early stages of inflammation, followed by lymphocytic infiltration and neovascularisation in 15 patients. However, the effect of non-specific stressor(s) related to the dose of protein/bacteria injection in cardiac pathology and dysfunction were not evaluated in this study.

In patients with ARF/RHD, Aschoff nodules composed of Anitschkow cells and Aschoff cells have been described in cardiac tissue (Fraser, et al. 1995). In this study, all rats treated with either M-protein or whole-killed bacteria developed myocarditis with granulomatous structures with an "Aschoff nodule like" appearance. Cells similar to "Anitschkow cells" and "Aschoff cells" were also observed in both myocardial and valvular tissues. Similar lesions were observed by Quinn, et al. (2001) in GAS rM6 treated rats and Lymbury, et al. (2003) in rats injected with pooled conserved region peptides of GAS rM5 protein. In addition, Kirvan, et al. (2014) identified cardiopathogenic epitopes of M5-protein in the Lewis rat and passively transferred valvulitis with peptide specific T-cell lines. The inflammatory responses have structural and functional effects on various parts of the heart valves that may lead to acute inflammatory damage and ultimately to chronic fibrosis. This includes dilation of valve annuli; rings that surround the valve and that help close leaflets during systole, and elongation of chordae tendinae, which connect leaflets of the mitral and tricuspid valves to the left and right ventricles, respectively. Together these changes result in inadequate coaptation of the valve leaflets, which in turn causes regurgitation (Veasy and Tani 2005). Further inflammation leads to fibrinous vegetations along the edges of the leaflets and scarring, which might ultimately lead to valvular stenosis, in which the valve becomes narrowed, stationary and is unable to fully open (Carapetis, et al. 2016).

Mitral valve leaflets are composed mostly of collagen fibres. Collagen tissues intermixed with elastic fibres form the extracellular matrix of the valvular apparatus covered by a layer of endothelial cells (McCarthy, et al. 2010). Collagen is a major component of chordae tendinae and the fibrous skeleton which anchors and supports the valves. In normal myocardium, collagen is found beneath the endothelial layer, around blood vessels, in the basement membrane and also forming narrow strata between muscle fibres, thus providing strength to the heart against mechanical stress (Iyer, et al. 2007). Fibrosis of heart tissues is

the hallmark of structural remodelling in ARF/RHD, resulting from chronic inflammatory rheumatic processes. Fibrosis results from extensive deposition of collagen typically induced by mechanical overload or tissue damage (Towbin 2007). In the current study, extensive deposition of collagen was observed in the mitral valve leaflets and myocardial tissues of rats injected with either bacteria or M-proteins. The fibrotic lesions were mostly observed in the areas of inflammation. Lis, et al. (1987) reported approximately a three-fold increase in the total amount of collagen fibres in the heart valves of ARF/RHD patients. Excessive collagen deposition leads to thickening of the mitral valve leaflets and fusion of commissures and chordae tendinae and ultimately to mitral stenosis (Banerjee, et al. 2014). Mitral stenosis induces mitral regurgitation, with increase in compensatory dilatation of ventricle. Progressive ventricular dilatation causes increase in wall stress with tissue damage and contractile dysfunction and eventually heart failure (Marciniak, et al. 2007; Gaasch and Meyer 2008; Carapetis, et al. 2016).

The inflammatory cascade in ARF has structural and functional effects on the heart that lead to cardiac dysfunction. The immunopathology of a heart can be investigated by different imaging tools. An electrocardiogram (ECG) shows whether the heart is in sinus rhythm or atrial fibrillation. A typical ECG trace consists of waveform components which indicate electrical events during one heartbeat. These waveforms are labelled P, Q, R, S, T and U. P wave is the first short upward movement of an ECG trace. It indicates that the atria are contracting, pumping blood into the ventricles. The QRS complex, normally begins with a downward deflection, Q; a larger upwards deflection, a peak R; and then a downwards S wave. The QRS complex represents ventricular depolarisation and contraction. The P-R interval indicates the transit time for the electrical signal to travel from the sinoatrial (SA) node to the ventricles. In the current study, ECG was used to demonstrate cardiac dysfunction in rats by measuring P-R intervals. Although the rapid heart rate of the rat made it difficult to select typical P and R points, objective and reproducible measurements was achieved using the peaks of the P wave and R wave (Farraj, et al. 2011). ECG data based on peak P and R values have been published in an earlier study on Lewis rats (Gorton, et al. 2016). In the current study, all rats injected with whole-killed or M-protein of GGS demonstrated prolongation of the P-R interval compared to those injected with PBS, suggesting a delay in ventricular depolarisation. The prolongation of P-R intervals observed were consistent with Gorton, et al. (2016) who reported in Lewis rats following injections with GAS rM5-protein and Bestetti, et al. (1987) who showed similar findings in rats following infection with

*Trypanosoma cruzi*. In humans, prolongation of the P-R interval is observed in 30-35% patients with ARF/RHD (Homer and Shulman 1991; Cunningham 2012). The findings of this study support the current use of ECG as a clinical diagnostic tool in ARF/RHD (Gewitz, et al. 2015).

The thickening of mitral valves with limited movement and excessive leaflet tip motion, thickening and fusion of chordae, lack of coaptation, compensatory dilatation of the left atrium and ventricle and mitral regurgitation are salient findings of patients with RHD (Carapetis, et al. 2016). A two-dimensional (2-D) echo is commonly used to detect these abnormalities (Chauvaud, et al. 2001; Carabello 2005; Jain and Mankad 2013; Wunderlich, et al. 2013). Assessment of cardiac pathology and dysfunction in rats using echo has been performed by many researchers using different echo methods and diverse anaesthesia such as ketamine-xylazine (Saleem, et al. 2017; Watanabe, et al. 2017), sevoflurane (Qiu, et al. 2017), chloral hydrate (Qiu, et al. 2017). Common methods of echo performed in rats are transthoracic echo (Saleem, et al. 2017; Watanabe, et al. 2017; Wu, et al. 2017) and non-invasive surface echo (Qiu, et al. 2017), although non-invasive echo is most suited to assess left ventricular morphology and function in murine models of cardiac disease (Gardin, et al. 1995; Tanaka, et al. 1996; Pacher, et al. 2008). In the current study, 2-D echo was able to detect mitral valvular thickening and the presence of nodules on mitral leaflets in rats injected with bacteria or M-protein using. To our knowledge, this is the first echo assessment of valvular pathology in the RAV model. Functional studies of rheumatic rat hearts also reported echo findings similar to human RHD patients (Zachary, et al. 2002). Future studies could extend the current echo measurements to include the thickness of mitral valve leaflets and the heart wall, internal dimensions of the left atrium and ventricle during systole and diastole and assessment of mitral regurgitation (thereby assessment of total cardiac function) for better explanation of the echocardiographic evaluation in this model (Ono, et al. 2002; Tada, et al. 2010).

The histological and imaging data presented in this chapter suggest that group G *Streptococcus* has the potential to induce autoimmune mediated carditis in the Lewis rat model of RHD. The results further support the findings of Chapter 5, in that carditis development is mediated by autoimmune responses. Further studies could include oropharyngeal infection studies to more closely mimic the accepted pathogenesis of ARF/RHD following streptococcal pharyngitis. Advance studies are recommended to identify

GGS clinical isolates and to demonstrate whether GGS and GAS together contribute to the disease clinically. Our experimental observations suggest that repetitive infections with group G *Streptococcus* may lead to ARF/RHD.

# CHAPTER 7
# GROUP G *STREPTOCOCCUS* CAN INITIATE AND EXACERBATE AUTOIMMUNE CARDITIS

## 7.1 INTRODUCTION

There is a strong epidemiological link between infections with group A *Streptococcus* (GAS) pharyngitis and ARF and RHD (McCarty 1956; Carapetis, et al. 2016) and it is generally accepted that multiple separate infections with GAS are required to trigger ARF and drive disease progression in RHD (Cunningham 2014). However, data is lacking as to whether these repeat infections need to be with the same strain of GAS that initiated ARF or whether subsequent infections with streptococci with similar M-types are sufficient to exacerbate disease. The results of experiments described in Chapter 5 and Chapter 6 of this thesis revealed that whole-killed GAS and GGS and their respective M-proteins can independently trigger autoimmune carditis in our rat model with features that are similar to those of patients with ARF/RHD (Fraser, et al. 1995; Cunningham 2003; Fae, et al. 2006; Guilherme, et al. 2006; Wen, et al. 2015; Bilik, et al. 2016; Carapetis, et al. 2016). As discussed previously, GGS and GAS share many features including sequence similarity in their respective M-proteins, their abilities to colonise similar tissues and the spectrum of diseases caused (Bisno, et al. 1987; Jones and Fischetti 1987; Collins, et al. 1992). The involvement of GGS in the initiation stage of disease versus the exacerbation of GAS–triggered autoimmune processes has not been established. Whether GAS and GGS can combine to cause carditis has not been studied previously.

Based on our previous data we hypothesised that because of similarities in the GAS and GGS M-proteins, GGS and GAS M-proteins may be able to substitute for each other in driving autoimmune carditis. The overall objective of the work described in chapter 7 is to model the potential role of GGS as an initiator and/or an exacerbator of autoimmune-mediated carditis in Lewis rats using heterologous prime/boost antigen injection regimes. This was done by priming with GGS Stg480 followed by boosting with GAS rM5 (initiation) and by priming with GAS rM5 and boosting with GGS Stg480 (exacerbation).

### 7.1.1 Aims

The specific Aims of this study were:

1. To determine antibody responses to GAS and GGS M-proteins and cross-reactivity to cardiac myosin in rats injected with heterologous antigens.
2. To measure memory T-cell responses in rats injected with heterologous antigens.
3. To examine GAS and GGS M-protein induced heart histological changes.
4. To demonstrate cardiac dysfunction in rats injected with heterologous antigens by performing electrocardiography.

## 7.2 MATERIALS AND METHODS

### 7.2.1 Experimental animals

Female Lewis rats bred at James Cook University, Townsville, Australia were used for experiments. The details of these rats are described in Section 3.1.2.

### 7.2.2 Antigens and adjuvants

Recombinant GAS M5 (rM5)-protein and GGS Stg480 protein were prepared for injections as described in Section 3.2.1. Control rats were injected with sterile PBS, pH 7.4 (Appendix 1). Freund's complete and incomplete adjuvants (CFA and IFA) and *B. pertussis* toxin as described in Section 3.1.1.3 were used to prepare antigen-adjuvant emulsions (Section 3.2.3.1). The injection protocols described in Section 3.2.3.2 was followed.

### 7.2.3 Experimental design and immunisation

Prime and boost antigen injections in rats were performed under anaesthesia as described in Section 3.2.2.1. The priming s.c. injection was performed with 0.5 mg/100 µl of GAS rM5 or GGS Stg480 emulsified in CFA in the hock as described previously (Gorton, et al. 2010). Rats were boosted with 0.5 mg/100 µl of heterologous antigens i.e. GAS rM5 protein primed rats were boosted with GGS Stg480 in IFA s.c. in the flank and GGS Stg480 primed rats were boosted with GAS rM5 emulsified in IFA. Control rats were injected with PBS in CFA (prime) or IFA (boost). At day 1 and day 3 after the priming injection, each rat was i.p injected with 0.3 µg *B. pertussis* toxin in 200 µl PBS. The schedule for injections is shown in Table 7.1. For short term experiments, rats were boosted with the heterologous antigen at days 7, 14 and 21 after the priming injection. For long term experiments, an additional heterologous boost injection was given at day 150. The short term experimental rats were culled after 35 days whereas the rats under long term experiments were culled after 180 days.

**Table 7.1** Injection schedule

| Experimental design | Group size (n=) | Prime | Boosts | Experiment endpoint |
|---|---|---|---|---|
| **Short term experiment** | 5<br>4<br>5 | GAS rM5<br>GGS Stg480<br>PBS | GGS Stg480 on day 7, 14, 21<br>GAS rM5 on day 7, 14, 21<br>PBS on day 7, 14, 21 | 35 days |
| **Long term experiment** | 5<br>5<br>5 | GAS rM5<br>GGS Stg480<br>PBS | GGS Stg480 on day 7, 14, 21, 150<br>GAS rM5 on day 7, 14, 21, 150<br>PBS on day 7, 14, 21, 150 | 180 days |

GAS: group A *Streptococcus*, GGS: group G *Streptococcus*, PBS: phosphate buffer saline.

### 7.2.4 Culling of rats and collection of samples

At the end of each experiment, rats were culled as described in Section 3.2.2.2. Peripheral blood, heart and spleens were retrieved as described in Section 3.2.2.3.

### 7.2.5 Serum antibody detection by ELISA

The IgG reactivity of sera from rats was evaluated against surface antigens of whole-killed GAS and whole-killed GGS, GAS rM5 and GGS Stg480 using indirect ELISAs. The IgG cross-reactivity to porcine cardiac myosin was also evaluated. The ELISA procedure was as described in Section 3.2.4.2.

### 7.2.6 Lymphocyte proliferation assay

Rat spleen mononuclear cells rats were prepared as described in Section 3.2.2.3. The proliferative response of splenocytes in the presence of GAS rM5 or GGS Stg480 was measured by lymphocyte proliferation assay as described in Section 3.2.4.1. Plates were harvested after 96 h at 37°C in 5% $CO_2$ with [$^3$H]thymidine added for the last 20 h of culture.

### 7.2.7 Histological examination of rat heart sections

Formalin-fixed rat hearts were processed, embedded in paraffin, sectioned and stained with H&E and Masson's trichrome stain using standard procedures as described in Section 3.2.5. The heart tissue sections were examined for evidence of inflammation as described in Section 3.2.5.2 and the severity of inflammation was scored for analysis as described in Table 3.2.

The extent of collagen fibre deposition in the mitral valve and myocardium of rats was determined as described in Section 3.2.5.3.

### 7.2.8 Electrocardiographic examination of rats

Assessment of cardiac dysfunction of rats was performed under anaesthesia (Section 3.2.2.1) by ECG using the procedure described in Section 3.2.6.1.

### 7.2.9 Statistical analysis

The data distribution of endpoint titres, OD values, stimulation indices, carditis severity scores, percentage of collagen deposition and P-R intervals in ECG was evaluated using GraphPad Prism 7 statistical software. All data from experimental and control rats passed D'Agostino & Pearson omnibus normality tests and therefore were tested using one-way analysis of variance (ANOVA) with Tukey's post hoc multiple comparisons test. The results are reported as mean ± standard error (SEM), $p \leq 0.05$ was considered significant.

## 7.3 RESULTS

The results of short term and long experiments using heterologous antigen injection regimes are presented in this chapter.

### 7.3.1 Antibodies produced following injection with heterologous M-proteins recognise GAS and GGS antigens

In this study, we analysed rat sera to detect IgG response to whole-killed and M-proteins of GAS and GGS (Figure 7.1). In both short term (35 days) and long term (180 days) experiments, significantly higher IgG responses to surface antigens of whole-killed GAS (Figure 7.1 A) and whole-killed GGS (Figure 7.1 B) were observed in the sera from rats primed with GAS rM5 and boosted with GGS Stg480. Similarly, anti-WK-GAS (Figure 7.1 A) and anti-WK-GGS (Figure 7.1 B) IgG responses were also observed in the rats primed with GGS Stg480 and boosted with GAS rM5. Regardless of the prime-boost combinations, the sera IgG from all rats injected with GAS and GGS M-proteins reacted with GAS rM5 (Figure 7.1 C) and GGS Stg480 (Figure 7.1 D) compared to PBS injected control rats.

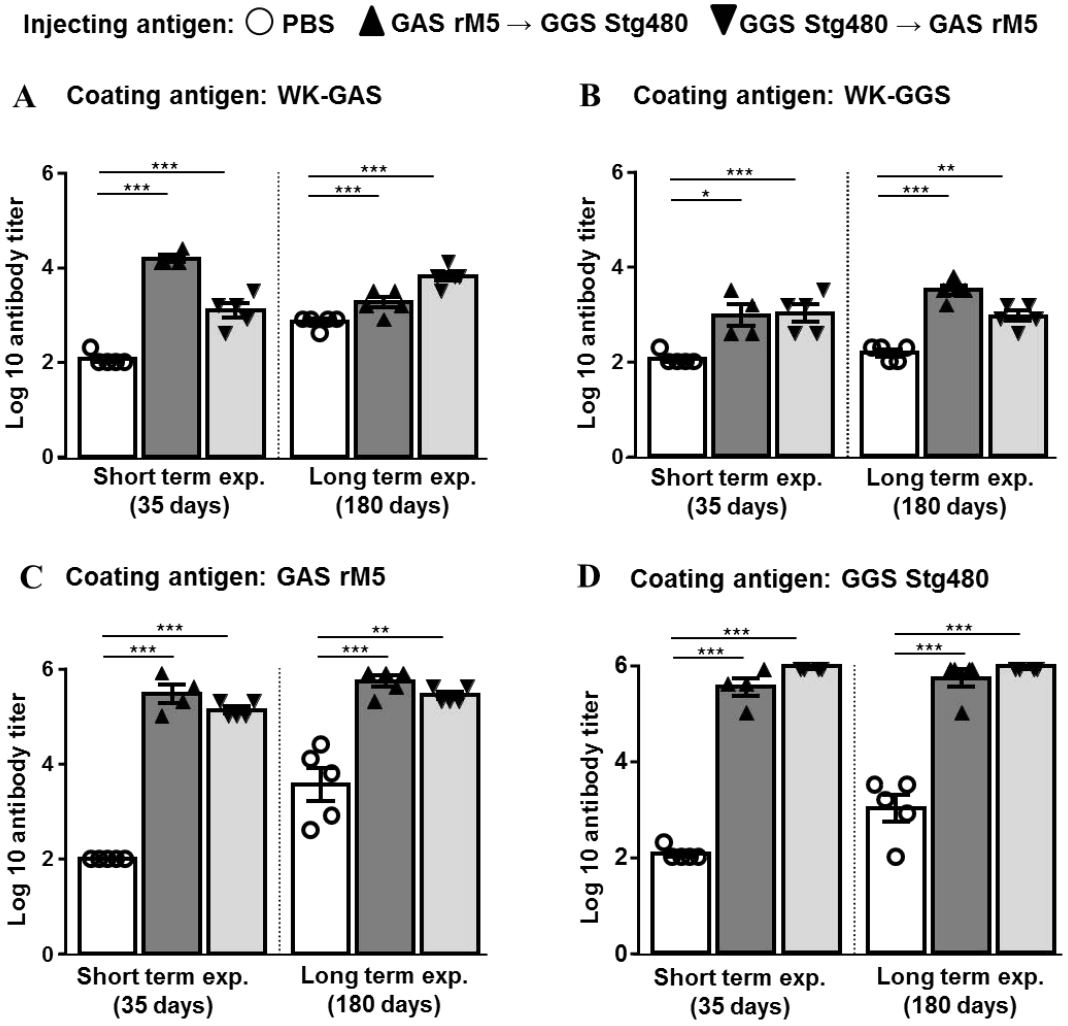


**Figure 7.1** Serum IgG reactivity to whole-killed and M-proteins of GAS and GGS. Serum IgG from rats primed with GAS rM5 and boosted with GGS Stg480 (i.e. GAS rM5 → GGS Stg480, n=5) reacted with whole-killed GAS as coating antigen (A). Similarly, serum IgG reactivity was detected from rats primed with GGS Stg480 and boosted with GAS rM5 (i.e. GGS Stg480 → GAS rM5, n=4-5) (A). IgG reactivity was also observed against surface antigens of whole-killed GGS (B). The serum IgG response to GAS rM5 (C) and GGS Stg480 (D) was significantly higher in the rats primed with GAS rM5 and boosted with GGS Stg480 or alternatively, primed with GGS Stg480 and boosted with GAS rM5 compared to PBS injected control rats (n=5). Error bars represent standard errors of the mean (SEM). Statistical differences were determined using one-way ANOVA with Tukey's post hoc multiple comparisons test; *p<0.05, **p<0.001, ***p<0.0001.

### 7.3.2 Antibodies produced following injection with heterologous M-proteins recognise cardiac myosin

Serum IgG from rats primed with GAS rM5, and boosted with GGS Stg480 analysed after 35 or 180 days (short versus long term), reacted with cardiac myosin in ELISA (Figure 7.2). Similarly, sera from rats primed with GGS Stg480 and boosted with GAS rM5 also reacted

with cardiac myosin. Sera from PBS injected control rats showed significantly less reactivity with cardiac myosin compared to all prime-boost antigen combinations.

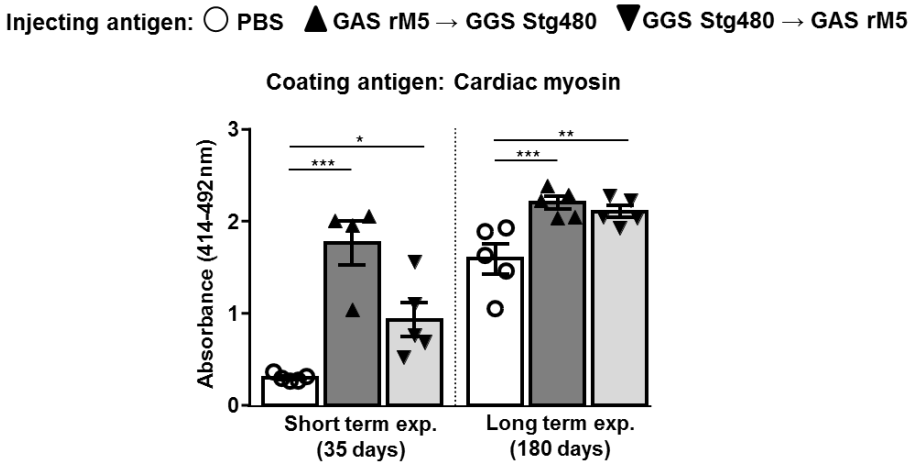


**Figure 7.2** Antibodies induced following exposure to GAS and GGS M-protein reacted with cardiac myosin in ELISA. Sera from rats primed with GAS rM5 and boosted with GGS Stg480 (GAS rM5 → GGS Stg480, n=5) or alternatively, primed with GGS Stg480 and boosted with GAS rM5 (GGS Stg480 → GAS rM5, n=4-5) showed significantly higher absorbance values ($A_{414\text{-}492nm}$) against cardiac myosin compared to PBS injected control rats (n=5). Error bars represent standard errors of the mean (SEM). Statistical differences were determined using one-way ANOVA with Tukey's post hoc multiple comparisons test; *p<0.05, **p<0.01, ***p<0.001.

### 7.3.3 T-cells proliferate in response to heterologous M-proteins

Splenic T-cells from rats primed with GAS rM5 and boosted with GGS Stg480 proliferated *in vitro* when stimulated with both GAS rM5 and GGS Stg480 proteins (Figure 7.3 A&B). This was observed following both short term and long term heterologous prime-boost regimes. Similarly, splenocytes from rats primed with GGS Stg480 and boosted with GAS rM5 proliferated when either GAS rM5 or GGS Stg480 were used as the stimulating antigen (Figure 7.3 A&B). Regardless of the prime-boost combination, splenocytes from all rats injected with GAS and GGS M-proteins proliferated significantly upon incubation with GAS rM5 (Figure 7.3 A) and GGS Stg480 (Figure 7.3 B) compared to PBS injected control rats.

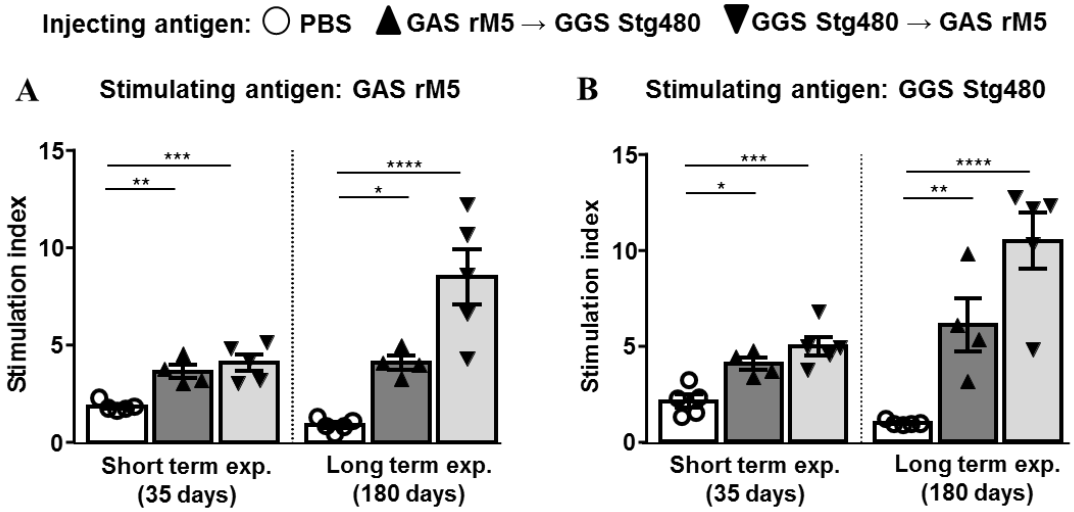


**Figure 7.3** Splenic T-cells from GAS and GGS M-protein injected rats proliferated in response to GAS and GGS M-proteins. Splenic T-cells from rats primed with GAS rM5 and boosted with GGS Stg480 (GAS rM5 → GGS Stg480, n=5) or alternatively, primed with GGS Stg480 and boosted with GAS rM5 (GGS Stg480 → GAS rM5, n=4-5) showed significantly higher proliferative responses to GAS rM5 (A) and GGS Stg480 (B) than PBS injected control rats (n=5). Stimulation index was calculated as average counts per minute (CPM) of test wells/average CPM of unstimulated control wells. Error bars represent standard errors of the mean (SEM). Statistical differences were determined using one-way ANOVA with Tukey's post hoc multiple comparisons test; *p<0.05, **p<0.01, ***p<0.001, ****p<0.0001.

### 7.3.4 Heterologous GAS and GGS M-protein injections induce carditis

To determine whether combined GAS and GGS M-proteins influence mitral valve and myocardial inflammation, heart sections of rats primed with GAS rM5 and boosted with GGS Stg480 or primed with GGS Stg480 and boosted with GAS rM5 were examined after H&E staining. Carditis severity scores were significantly higher in rats injected with GAS and GGS M-proteins regardless of the prime-boost combinations compared to control rats injected with PBS (Figure 7.4 A). Similar results were observed following both short and long term prime-boost antigen injection regimes. Histological staining of heart sections from PBS injected rats revealed uniform mitral valvular structure without the presence of inflammatory cells (Figure 7.4 B and Appendix 7 Supplementary Figure 7.1A&7.2A). Some individual inflammatory cells were observed near blood vessels in the myocardium of control rats (Figure 7.4 C and Appendix 7 Supplementary Figure 7.1D&7.2D). In contrast, heart sections from rats primed with GAS rM5 and boosted with GGS Stg480 showed extensive cellular infiltrates in the mitral valves (Figure 7.4 D and Appendix 7 Supplementary Figure 7.1B&7.2B). Moreover, "Aschoff nodule like" lesions were observed in the myocardium tissues (Figure 7.4 E and Appendix 7 Supplementary Figure 7.1E&7.2E). Rats primed with GGS Stg480 and boosted

with GAS rM5 had similar pathological lesions in the mitral valves (Figure 7.4 F and Appendix 7 Supplementary Figure 7.1C&7.2C) and myocardium (Figure 7.4 G and Appendix 7 Supplementary Figure 7.1F&7.2F). Cells similar in appearance to "Aschoff cells" (Figure 7.4 E&G x) and 'Anitschkow cells" (Figure 7.4 E&G y) as well as polymorphonuclear cells (Figure 7.4 E z) were observed in the myocardium of rats injected with GAS rM5 followed by GGS Stg480 and *vice versa*.

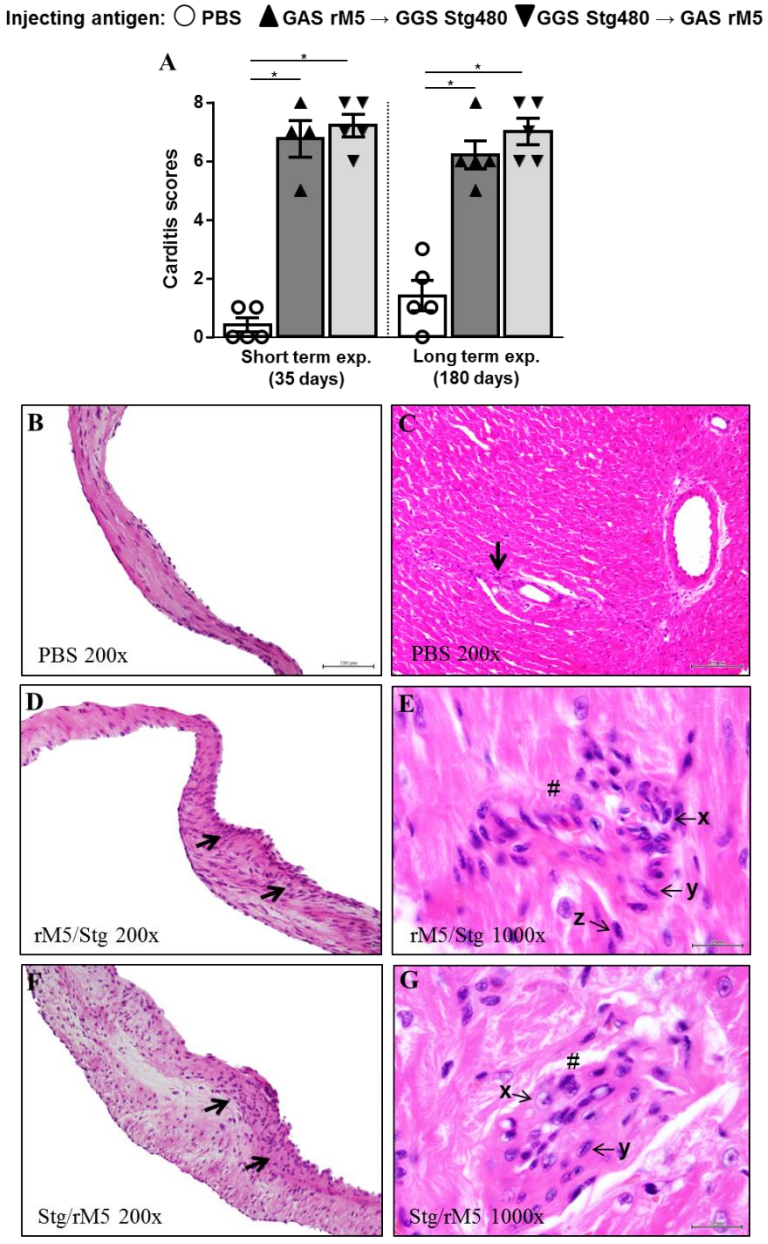


**Figure 7.4** GAS and GGS M-proteins induce mitral valvulitis and myocariditis. (A) Higher carditis scores were found in rats primed with GAS rM5 and boosted with GGS Stg480 (GAS rM5 → GGS Stg480, n=5) and primed with GGS Stg480 and boosted with GAS rM5 (GGS Stg480 → GAS rM5, n=4-5) compared to PBS injected control rats (n=5). (B) The mitral valve from PBS injected rats showed no evidence of inflammation. (C) The myocardium from the control rats showed isolated inflammatory cells surrounding blood vessels. Extensive infiltration of inflammatory cells was observed in mitral leaflets of rats primed

with GAS rM5 and boosted with GGS Stg480 (D; rM5/Stg) and primed with GGS Stg480 and boosted with GAS rM5 (F; Stg/rM5). Interstitial focal inflammation with granulomatous structures similar to Aschoff nodules were observed in the myocardium of rats primed with GAS rM5 and boosted with GGS Stg480 (E; rM5/Stg) and primed with GGS Stg480 and boosted with GAS rM5 (G; Stg/rM5). Scale bars as indicated, x: Aschoff like cells, y: Anitschow like cells, z: polymorphonuclear cell. Error bars represent standard errors of the mean (SEM). Statistical differences were determined using one-way ANOVA with Tukey's post hoc multiple comparison test; *$p<0.0001$.

### 7.3.5 Heterologous GAS and GGS M-protein injections induce collagen deposition in heart tissues

Rat heart sections were stained with Masson's trichrome stain to determine the extent of collagen deposition in the mitral valves and myocardium. The percentage of tissue (combined valve and myocardium) staining positive for collagen was significantly higher in rats injected with GAS and GGS M-proteins, regardless of the prime-boost combination, compared to control rats injected with PBS (Figure 7.5 A). Results were similar at 35 days (short term) and 180 days (long term). Examination of heart sections from rats injected with PBS revealed uniform deposition of collagen fibres throughout the valvular leaflets (Figure 7.5 B and Appendix 7 Supplementary Figure 7.3A&7.4A). Collagen staining in the myocardium sections of control rats was restricted to surrounding blood vessels (Figure 7.5 C and Appendix 7 Supplementary Figure 7.3D&7.4D). In contrast, heart sections from rats primed with GAS rM5 and boosted with GGS Stg480 showed extensive collagen staining throughout the mitral valves (Figure 7.5 D and Appendix 7 Supplementary Figure 7.3B&7.4B) and myocardium (Figure 7.5 E and Appendix 7 Supplementary Figure 7.3E&7.4E). Heart sections from rats primed with GGS Stg480 and boosted with GAS rM5 showed similar collagen staining in the mitral valves (Figure 7.5 F and Appendix 7 Supplementary Figure 7.3C&7.4C) and myocardium (Figure 7.5 G and Appendix 7 Supplementary Figure 7.3F&7.4F).

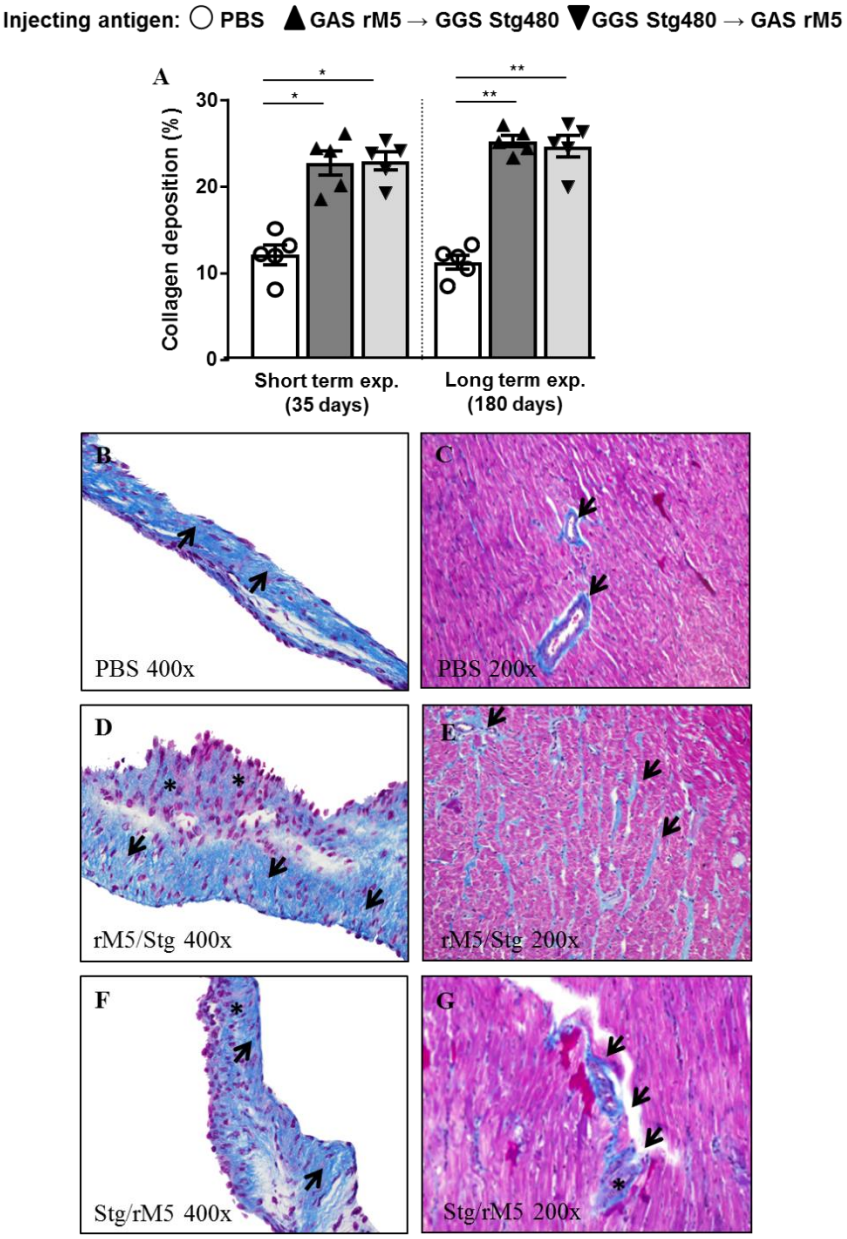


**Figure 7.5** GAS and GGS M-proteins induce collagen deposition in the heart. Extensive collagen deposition was demonstrated in Lewis rats primed with GAS rM5 and boosted with GGS Stg480 (GAS rM5 → GGS Stg480, n=5) and alternatively, primed with GGS Stg480 and boosted with GAS rM5 (GGS Stg480 → GAS rM5, n=4-5) (A). The PBS injected control rats (n=5) demonstrated uniformly distributed collagen in the mitral valves (B) and surrounding the blood vessels in the myocardium (C). Extensive deposition of collagen fibres was also observed in the mitral valves of rats primed with GAS rM5 and boosted with GGS Stg480 (D; rM5/Stg) and primed with GGS Stg480 and boosted with GAS rM5 (F; Stg/rM5). The myocardium of the rats also showed focal fibrosis with collagen deposition (E, G; Stg/rM5). Collagen is stained blue (indicated by arrows) in Masson's trichrome staining. Scale bars as indicated, asterisk (*) indicated infiltration of inflammatory cells. Error bars represent standard errors of the mean (SEM). Statistical differences were determine using by one-way ANOVA with Tukey's post hoc multiple comparison test; *$p<0.001$, **$p<0.0001$.

### 7.3.6 Heterologous GAS and GGS M-protein injections induce prolongation of P-R interval in ECG

ECG was performed on rats to detect abnormalities in the electrical conduction of heart tissue following antigen injection. Regardless of the prime-boost combinations and for both short term and long term injection regimes, significantly prolonged P-R intervals were recorded in rats injected with GAS and GGS M-proteins compared to control rats injected with PBS (Figure 7.6).

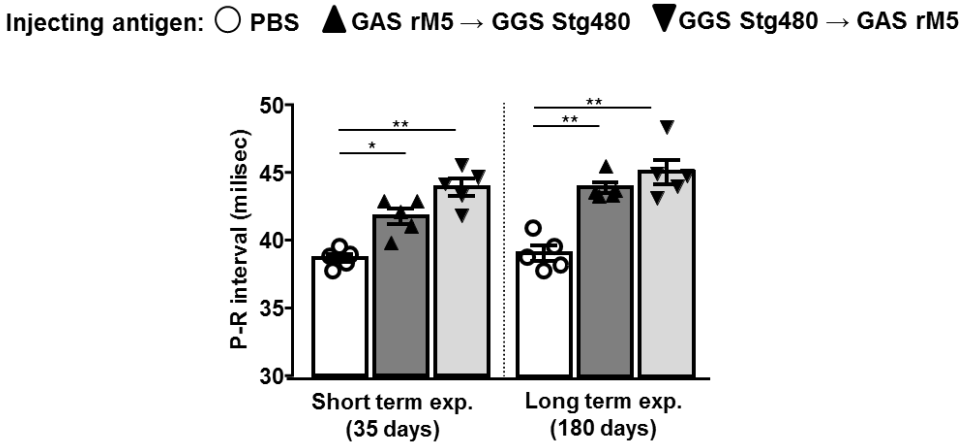


**Figure 7.6** Electrocardiographic assessment demonstrated cardiac dysfunction in rats following heterologous injections with GAS and GGS M-proteins. Prolongation of P-R interval was observed in rats primed with GAS rM5 and boosted with GGS Stg480 (GAS rM5 → GGS Stg480, n=5) or alternatively, primed with GGS Stg480 and boosted with GAS rM5 (GGS Stg480 → GAS rM5, n=4-5), compared to PBS injected control rats (n=5). Similar results were observed at both 35 days (short term exp.) and 180 days (long term exp.) after the priming injection. Error bars represent standard errors of the mean (SEM). Statistical differences were determined using one-way ANOVA with Tukey's post hoc multiple comparison test; *$p<0.01$, **$p<0.0001$.

## 7.4 DISCUSSION

It is now widely accepted that group A *Streptococcus* (GAS) infection is the causative agent of ARF/RHD (Beattie 1907; Carapetis, et al. 2016). Accumulating anecdotal and largely epidemiological evidence from Indian and Australian communities (Carapetis and Currie 1997; Haidan, et al. 2000; Steer, et al. 2002; McDonald, et al. 2004; Brahmadathan, et al. 2005; McDonald, et al. 2006) has questioned this dogma and provided the rationale for the work presented in this thesis. Chapter 5 and Chapter 6 of this thesis, showed that group G *Streptococcus* (GGS) alone can stimulate the production of autoantibodies and autoreactive T-cells that potentially damage rat heart tissues. As these two organisms are often found together, in similar niches in the body and are known to share genetic material (Bisno, et al. 1996; Sriprakash and Hartas 1996; Davies, et al. 2005), a third possibility also exists: that

GAS and GGS may act together in triggering and driving ARF/RHD. Therefore, we hypothesised that immune responses initiated against GAS M5 protein may be boosted by GGS strain with primary sequence homology and/or structural homology in its M-protein and *vice versa*. B- and T-cell epitopes shared by heterologous antigens may mean that related M-proteins could potentially act as either initiators or exacerbators of autoreactive immune responses.

In this chapter we modelled two different scenarios; (1) whether GGS can initiate disease followed by GAS-driven exacerbation or, (2) whether GGS can exacerbate GAS-initiated disease. The results presented in this chapter provide evidence that the heterologous GAS and GGS antigen combinations are equally as effective as homologous antigens at inducing heart pathology, heart conduction and valve abnormalities and potentially autoreactive immune responses. Irrespective of the prime-boost antigen combinations, the serum IgG from rats injected with GAS and GGS M-proteins reacted with surface antigens and M-proteins of GAS and GGS. The splenic T-cells from rats also proliferated in response to heterologous GAS and GGS M-proteins. Cardiac myosin reactivity was also demonstrated in sera from animals following both heterologous prime-boost antigen combinations. The increase of anti-cardiac myosin antibody levels in PBS injected control rats may be related to adjuvant exposure in aged rats.

As discussed previously in Chapters 5&6, the similarities we observed in the immune responses and heart pathology of GAS and GGS M-protein injected rats is likely to be due to homology between GAS and GGS M-proteins. Numerous studies have identified extensive sequence and structural homology between GGS M-proteins and GAS M-proteins (Moody, et al. 1965; Maxted and Potter 1967; Scott, et al. 1985; Bisno, et al. 1987; Jones and Fischetti 1987; Simpson, et al. 1987; Bessen, et al. 1989; Bessen and Fischetti 1990; Collins, et al. 1992). In the current study, we used GAS M5 protein (reported in several studies to induce autoimmune mediated carditis (Galvin, et al. 2002; Gorton, et al. 2009; Gorton, et al. 2016) and the M-protein (Stg480) from GGS strain NS3396. This particular GGS strain has been isolated from several patients with suspected ARF/RHD (Haidan, et al. 2000; Rantala, et al. 2010; Jensen and Kilian 2012). Sikder, et al. (2018) reported that the N-terminus, A-repeat and B-repeat regions of Stg480 and M5 has a primary amino acid identity (21%) and similarity (44%), however identity was greater within the C-repeat region. Sikder and colleagues also predicted that like GAS M-proteins, GGS Stg480 also has a coiled-coil

structure. The irregularities in the α-helix were demonstrated in the heptad coiled-coil motif throughout Stg480 which is consistent with other M-proteins (Sriprakash and Hartas 1996). Further analyses will be required to more precisely define the immunogenic regions of Stg480 and M5 proteins and whether shared B- and T-cell epitopes in the GAS and GGS M-proteins can further explain the findings presented in this chapter.

In Chapter 6 we showed that rats injected with homologous prime-boost GAS or GGS M-proteins developed inflammation in the myocardium and mitral valves. The results presented in this chapter clearly show these inflammatory lesions are reproduced following injection with heterologous M-proteins. Thickening of mitral valve leaflets due to excessive deposition of collagen fibres and infiltration of inflammatory cells was also observed. The myocardium of the M-protein injected rats was demonstrated with granulomatous lesions similar to "Aschoff nodule" and contained cells similar to "Anitschkow cells" and "Aschoff cells". The observations are akin to the findings reported in earlier rat model studies and patients with ARF/RHD (Aschoff 1906; Fraser, et al. 1995; Guilherme, et al. 2001b; Gorton, et al. 2009; Huang, et al. 2009; Xie, et al. 2010; Gorton, et al. 2016). An ECG assessment of rats injected with GAS and GGS M-proteins had prolongation of P-R intervals regardless of prime-boost antigen combinations. Mitral valve fibrosis leads to mitral stenosis and subsequent mitral regurgitation. Mitral regurgitation induces fibrosis of myocardium due to mechanical overload and ultimate heart failure (Carapetis, et al. 2016).

Previous epidemiological studies have postulated that group A streptococcal (GAS) throat infection may not be the only trigger for the disease sequelae in ARF/RHD (McDonald, et al. 2004; McDonald, et al. 2006). We hypothesised that because of similarities in the GAS and GGS M-proteins, GGS and GAS M-proteins may be able to substitute for each other in driving autoimmune carditis. The results of this study suggest that GGS may both trigger and exacerbate autoimmune process to ARF/RHD in association with GAS. Future studies could be designed to identify shared epitopes in both the proteins that may be significant drivers of the autoimmune processes in this disease. Identification of the common epitopes between GAS and GGS isolates will help to develop a more precise serological assay for evidence of preceding GAS/GGS infection. Homologous amino acid sequences in C repeat regions of GAS and GGS M-proteins may have potential in designing a vaccine to prevent GAS and GGS infection (Steer, et al. 2009b). The C-repeat region vaccines are currently under investigation both from the perspective of including peptides homologous across GAS and

GGS but also avoiding those GGS peptide antigens that may potentially generate autoimmunity (Bauer, et al. 2012; McNeilly, et al. 2016; Sekuloski, et al. 2018).

Epidemiological studies may reveal the clinical correlation between GAS and GGS as causative agents of ARF/RHD. In the current project, although we did not aim to compare the effects of homogenous and heterogenous GAS and GGS antigen exposure on the development of carditis and antibody and T-cell response there was variable degrees of additive effects in the carditis development in the rats injected with both GAS and GGS M-proteins. In conclusion, our experimental data suggest that GAS and GGS have synergistic effects in the development of autoimmune carditis and that both could potentially initiate and exacerbate disease.

# CHAPTER 8
# ADOPTIVE TRANSFER OF GROUP A *STREPTOCOCCUS* SPLENOCYTES AND SERUM INDUCES CARDITIS IN A LEWIS RAT AUTOIMMUNE VALVULITIS MODEL

## 8.1 INTRODUCTION

This chapter describes the transfer of carditis to naïve Lewis rats using serum and/or splenocytes from rats injected with the GAS rM5 protein.

The development of RHD is linked to the formation of chronic valvular lesions resulting from cytotoxic antibody deposition and T-lymphocyte infiltration that disrupts cardiac function (Zabriskie, et al. 1970; Krisher and Cunningham 1985; Kemeny, et al. 1989; Fraser, et al. 1995; Guilherme, et al. 1995; Roberts, et al. 2001; Galvin, et al. 2002; Martins, et al. 2008). Following GAS infection, antibodies and T-cells respond to M-protein and other GAS antigens (Carapetis, et al. 2016). The GAS M-protein specific antibodies and T-cells are believed to recognise host cardiac myosin (and other host antigens) through molecular mimicry (Galvin, et al. 2000; Kirvan, et al. 2003; Fae, et al. 2006; Cunningham 2014). The hypothesis of molecular mimicry between GAS and heart antigens is supported by evidence from studies using mAbs (Galvin, et al. 2000), and both peripheral and intralesional T-cell clones from patients with ARF and RHD (Ellis, et al. 2005; Fae, et al. 2006; Cunningham 2014). The anti-GAS antibodies activate heart endothelium and upregulate vascular cell adhesion molecules (CAMs) (Chopra, et al. 1988; Roberts, et al. 2001; Tandon, et al. 2013). An activated endothelium facilitates transmigration of autoreactive T-cells into the valve and myocardium (Guilherme, et al. 1995; Galvin, et al. 2000; Roberts, et al. 2001; Guilherme, et al. 2004). The valves become progressively scarred and thickened causing ultimate stenosis and regurgitation (Kemeny, et al. 1989). Salient myocardial features include: focal infiltration of inflammatory cells, formation of granulomatous lesions known as Aschoff nodules and fibrosis that leads to myocardial dysfunction (Roberts, et al. 2001). Valvular regurgitation and myocardial dysfunction together end with heart failure as a long term sequela (Carapetis, et al. 2016).

The specific role of antibodies versus autoreactive T-cells in ARF/RHD has been studied in patients and in various animal models (Galvin, et al. 2000; Quinn, et al. 2001; Kirvan, et al. 2003; Lymbury, et al. 2003; Li, et al. 2004; Fae, et al. 2006; Gorton, et al. 2006; Gorton, et al.

2009; Huang, et al. 2009; Gorton, et al. 2010; Xie, et al. 2010; Cunningham 2014; Kirvan, et al. 2014). Antibodies that react with GAS and heart proteins have been identified in the sera of patients with ARF and in the sera of rabbits and mice that had been immunised against GAS (Krisher and Cunningham 1985; Galvin, et al. 2000; Ellis, et al. 2005; Fae, et al. 2006; Cunningham 2014). Antibodies and T-cells from patients with ARF/RHD and cells from experimental myocarditis and/or valvulitis induced by cardiac myosin or streptococcal antigens can recognise several cardiac myosin epitopes (Ellis, et al. 2005). Previous studies have shown that CD4+ helper T-cells are the major effectors of autoimmune reactions in the heart tissue of RHD patients with cytokines produced by these cells are the key drivers of inflammation in ARF/RHD (Raizada, et al. 1983; Kemeny, et al. 1989; Guilherme, et al. 1991).

Passive transfer of GAS M5 peptide-specific T-cells into naïve Lewis rats has previously been shown to induce valvulitis (Kirvan, et al. 2014). Wegmann, et al. (1994) reported myocarditis in recipient Lewis rats following adoptive transfer of T-cells stimulated by specific peptides derived from cardiac myosin. Smith and Allen (1991) and Bachmaier, et al. (1999) reported the development of myocarditis in mice following adoptive transfer of myosin-reactive T-cells. Using mAb to deplete CD4+ T-cells, Smith and Allen (1991) also showed that the myosin injected mice did not develop myocarditis providing evidence that the myosin-induced myocarditis is a CD4+ T-cell-mediated disease. Furthermore, the same authors (Smith and Allen (1991)) reported that transfer of high-titre anti-myosin antibody serum to naïve recipient mice did not transfer myocarditis.

While GAS M-protein specific antibodies and T-cells appear to be important mediators of heart damage, their individual or combined roles in the recognition, invasion, and destruction of heart tissue in rheumatic carditis is incompletely understood (Kirvan, et al. 2014). Direct demonstration of *in vivo* effects of antibodies and T-cells in patients with ARF/RHD in heart pathology is challenging, with animal models currently the primary means to investigate these putative mechanisms. The current study investigated the capacity of M-protein specific antibodies and splenocytes to transfer carditis to naïve syngeneic rats. We sought direct *in vivo* evidence that humoral and/or cellular mechanisms drive carditis in this model.

### 8.1.1 Aims

The overall Aim of this study was to investigate development of carditis in Lewis rats following injection of serum and/or splenocytes from rats previously immunised with GAS rM5 protein.

The specific Aims were:

1. To determine GAS rM5 protein specific serum and splenocytes induced heart pathology by histological examination.
2. To demonstrate cardiac dysfunction of recipient rats by performing electrocardiography and echocardiography.
3. To demonstrate M5 protein and cardiac myosin antibody reactivity in serum from recipient rats.
4. To determine memory T-cell proliferative responses from recipient rats upon *ex vivo* re-stimulation with GAS rM5.
5. To characterise the phenotype of proliferating Th-cell subsets in recipient rats.

## 8.2 MATERIALS AND METHODS

### 8.2.1 Experimental animals

Female Lewis rats bred at James Cook University, Townsville, Australia were used. The details of rats are described in Section 3.1.2.

### 8.2.2 Antigens and adjuvants

Carditis was induced in donor rats by repeated injection of GAS rM5 protein mixed with CFA or IFA and *B. pertussis* adjuvant as described in Section 5.2.3. Recombinant GAS M5 protein was prepared as described in Section 3.2.1 and used for ELISA as described in Section 3.2.4.2. Sterile PBS, pH 7.4 (Appendix 1) was used to inject control rats. Freund's complete and incomplete adjuvants (CFA and IFA) and *B. pertussis* toxin described in Section 3.1.1.3 were used. Antigen-adjuvant emulsions were prepared as described in Section 3.2.3.1. Cardiac myosin described in Section 3.1.1.2 was used in ELISA.

### 8.2.3 Experimental design

#### 8.2.3.1 Injection of donor rats

Donor rats (n=4 per group) were injected with GAS rM5 protein to induce carditis (Figure 8.1). Control donor rats were injected with PBS. The injection schedule described in Section

5.2.3 (M-protein short term) and Table 8.1 was followed. Donor rats were culled 35 days after the priming injection.

#### 8.2.3.2 Evaluation of donor serum, splenocyte proliferation, heart function and pathology

The injection schedule shown previously in Chapter 5 (Section 5.2.3) was used to induce carditis, heart dysfunction and antibody and T-cell response in donor rats. To test that donor rats had developed carditis and immune responses similar to patients with ARF/RHD, sera from donor rats were evaluated for serum antibody response to GAS rM5 and cardiac myosin and splenic GAS rM5 specific T-cell responses were measured. Heart pathology was demonstrated using electrocardiography (ECG), echocardiography (echo) and histological examination of heart tissue sections. The donor rats were culled according to the procedure described in Section 3.2.2 35 days after the priming injection. The blood, spleen and heart samples were collected as described in the Section 3.2.2.3. The serum IgG response to GAS rM5 and cardiac myosin was evaluated by ELISA (Section 3.2.4.2). The splenic T-cell proliferative responses and cytokines produced by proliferating T-cells were evaluated by lymphocyte proliferation assay (Section 3.2.4.1) and ELISA (Section 5.2.7) respectively. Assessment of heart function was performed by electrocardiography (Section 3.2.6.1) and echocardiography (Section 3.2.6.2). Carditis was confirmed by microscopic examination of H&E stained heart sections (Section 3.2.5.2).

#### 8.2.3.3 Preparation of serum and lymphocytes from donor rat spleen

Following collection of blood, the serum samples from the donor rats were separated (Section 3.2.2.3) and stored at -80°C. The sera samples were thawed, pooled and warmed to room temperature before being injected into naïve recipient rats. The spleens from the donor rats were collected as described in Section 3.2.2.3. Mononuclear cells from spleens were separated, pooled and enumerated (Section 3.2.2.3). Mononuclear cells from both GAS rM5 and PBS injected rats were cultured (Section 3.2.4.1) and stimulated *in vitro* with GAS rM5 (10 µg/ml) for 72 h to expand M5-specific T-cells. Viable cells were enumerated by trypan blue staining (Section 3.2.2.3) before transfer into naïve recipients.

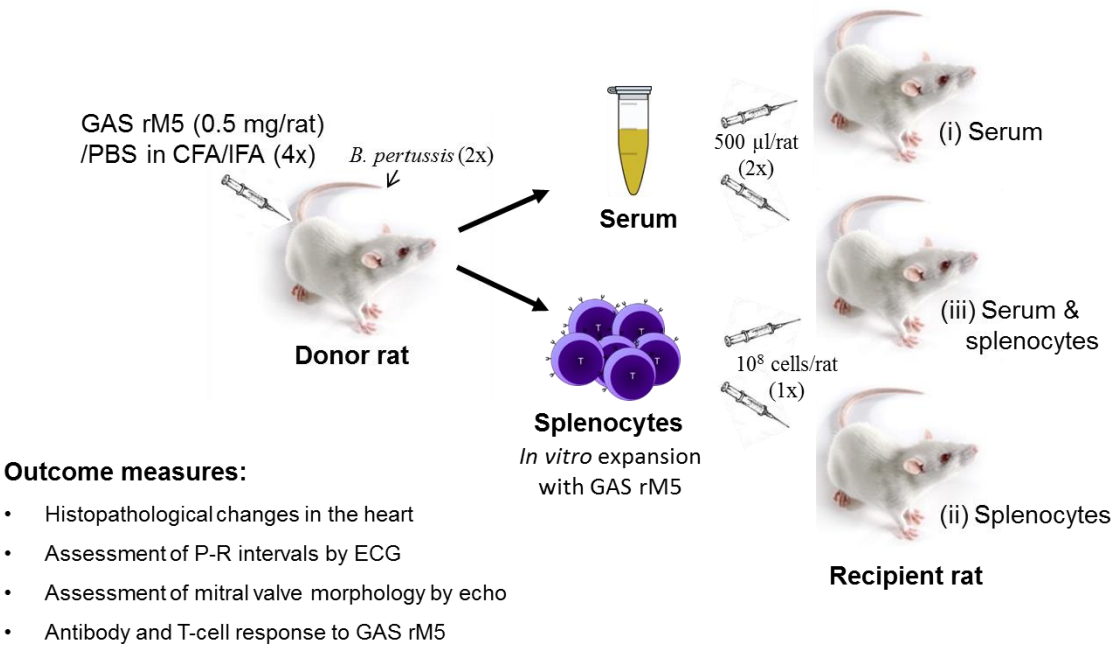


**Figure 8.1** Overview of experimental design for evaluating adoptive transfer of carditis. Priming injection of donor rats (n=4) was performed with 0.5 mg/rat GAS rM5 protein mixed with CFA s.c. in the hock region. Three booster injections were performed with 0.5 mg/rat GAS rM5 in IFA s.c. in the flank. Control donor rats (n=4) were injected with PBS mixed with CFA or IFA. *B. pertussis* toxin (0.3 µg/rat) was injected i.p. 1 and 3 days after the priming injection. Donor rats were culled 35 days after priming, and serum and splenic mononuclear cell (MNC) suspensions were prepared. The splenic MNCs from the donors were cultured *in vitro* with GAS rM5 protein stimulation for 72 h. Recipient syngeneic rats (n=4) were injected i.v. with either; (i) 500 µl of serum and a second dose after a week, (ii) a single dose of $1\times10^8$ MNCs per rat or, (iii) both serum (×2 doses) and $1\times10^8$ MNCs. Cardiac dysfunction was assessed by ECG and echo. Recipient rats were culled at either 21 or 86 days and H&E staining performed on heart sections to assess carditis. The antibody and T-cell responses to GAS rM5 and cardiac myosin were also assessed in donors and recipients. GAS rM5: group A streptococcal recombinant M5 protein, PBS: phosphate buffer saline, CFA: complete Freund's adjuvant, IFA: incomplete Freund's adjuvant.

**Table 8.1** Injection schedule

| Experimental design | Group size (n=) | Prime | Boost/2nd injection | Experiment endpoint |
|---|---|---|---|---|
| **Donor rats:** active induction of carditis | 4 | GAS rM5 | GAS rM5 on day 7, 14, 21 | 35 days |
| | 4 | PBS | PBS on day 7, 14, 21 | |
| **(i) Serum recipient rats** | 4 | GAS rM5 serum | GAS rM5 serum on day 7 | 21 days |
| | 4 | PBS serum | PBS serum on day 7 | |
| **(ii) Splenocyte recipient rats** | 4 | GAS rM5 splenocyte | | |
| | 4 | PBS splenocyte | | |
| **(iii) Serum and splenocyte recipient rats** | 4 | GAS rM5 serum and splenocyte | GAS rM5 serum on day 7 | 86 days |
| | 4 | PBS serum and splenocyte | PBS serum on day 7 | |

#### 8.2.3.4 Injection of serum and splenocytes into recipient rats

Recipient rats were divided into 3 groups; (i) serum recipients, (ii) splenocyte recipients, and (iii) serum and splenocyte recipients (Figure 8.1). All i.v. injections of recipient rats were performed under general anaesthesia (Section 3.2.2.1). For group (i), serum recipient rats, rats (n=4 per group) were injected with 500 µl of serum from GAS rM5 or PBS injected donors and a second dose after 7 days as described previously (Smith and Allen 1991). For group (ii), splenocyte recipients (n=4 per group) were injected with a single dose of $1\times10^8$ splenic MNCs per rat from GAS rM5 or PBS injected donors in 500 µl of RPMI. For group (iii), recipient rats (n=4 per group) were injected with $1\times10^8$ splenic MNCs mixed with 500 µl of serum from GAS rM5 or PBS injected donors. Seven days post-priming, recipients received an additional 500 µl serum from the same donors. Serum or splenic MNCs recipient rats were culled 21 day after the priming injection. Rats that received both serum and splenocytes (group (iii)) were culled 86 days after priming (Table 8.1).

#### 8.2.3.5 Evaluation of recipient serum, splenocyte proliferation, heart function and pathology

Recipient rats were culled according to the procedure described in Section 3.2.2. Blood, spleens and hearts were collected as described in the Section 3.2.2.3. ECG (Section 3.2.6.1), echo (Section 3.2.6.2) and heart histological staining (Section 3.2.5.2) were performed as

described previously. The serum antibody reactivity against GAS rM5 and cardiac myosin was performed using ELISAs as described in Section 3.2.4.2. Splenic MNCs proliferation assays and cytokine analysis (GAS rM5 as stimulant) were performed as described in Section 3.2.4.1 and Section 5.2.7.

### 8.2.4 Statistical analysis

The data distribution of carditis severity scores, P-R intervals in ECG, echo scores, ELISA endpoint titres, ELISA absorbance values, lymphocyte proliferation stimulation indices and cytokine concentrations were determined using GraphPad Prism 7 statistical software. The data from experimental and control group that passed D'Agostino & Pearson omnibus normality tests were compared using parametric unpaired t test. Non-parametric Mann-Whitney test was used to compare data that were not normally distributed. The specific statistical test used for each data set is presented in the figure legends. The results are reported as mean ± standard error (SEM), $p \leq 0.05$ was considered significant.

## 8.3 RESULTS

### 8.3.1 GAS rM5 specific antibodies and splenocytes induce carditis in recipient rats

The current study was designed to determine whether GAS rM5 specific antibodies or T-cells alone or in combination, could induce carditis in naïve recipients. Recipient rats injected with either serum, or splenocytes from immune donors, developed histological carditis, although the carditis scores from the splenocyte only recipients did not reach statistical significance compared to PBS controls (Figure 8.2 A). Hearts from recipient rats injected with combined serum and splenocytes, showed significant evidence of carditis. The pathological findings in recipient rats were similar to donor rats (Appendix 8 Supplementary Figure 8.1A (2.1-2.4) and 8.1B (2.1-2.4)). Recipients with carditis had foci of inflammation within the mitral valve leaflets (Figure 8.2 C&D and Appendix 8 Supplementary Figure 8.2A (2.1-2.4), 8.2C (2.1-2.4) and 8.2E (2.1-2.4)). Moreover, severe inflammation with infiltration of inflammatory cells were observed in the myocardium of recipients (Figure 8.2 F and Appendix 8 Supplementary Figure 8.2B (2.1-2.4), 8.2D (2.1-2.4) and 8.2F (2.1-2.4)). In myocardium granulomatous inflammation similar to ‘Aschoff type nodules’ were observed (Figure 8.2 G and Appendix 8 Supplementary Figure 8.2B (2.1-2.4), 8.2D (2.1, 2.4) and 8.2F (2.1-2.4)). Macrophages similar to ‘Anitshokow cells’ (Figure 8.2 G x) and ‘Aschoff cells’ (Figure 8.2 G y) were also observed in myocarditis areas of serum and/or splenocyte recipients.

The mitral valve and myocardium of control rats contained very few inflammatory cells (Figure 8.2 B and Appendix 8 Supplementary Figure 8.1A (1.1-1.4), 8.2A (1.1-1.4), 8.2C (1.1-1.4) and 8.2E (1.1-1.4)). The myocardium of the control rats also had small number of inflammatory cells that were uniformly distributed (Figure 8.2 E and Appendix 8 Supplementary Figure 8.1B (1.1-1.4), 8.2B (1.1-1.4), 8.2D (1.1-1.4) and 8.2F (1.1-1.4)).

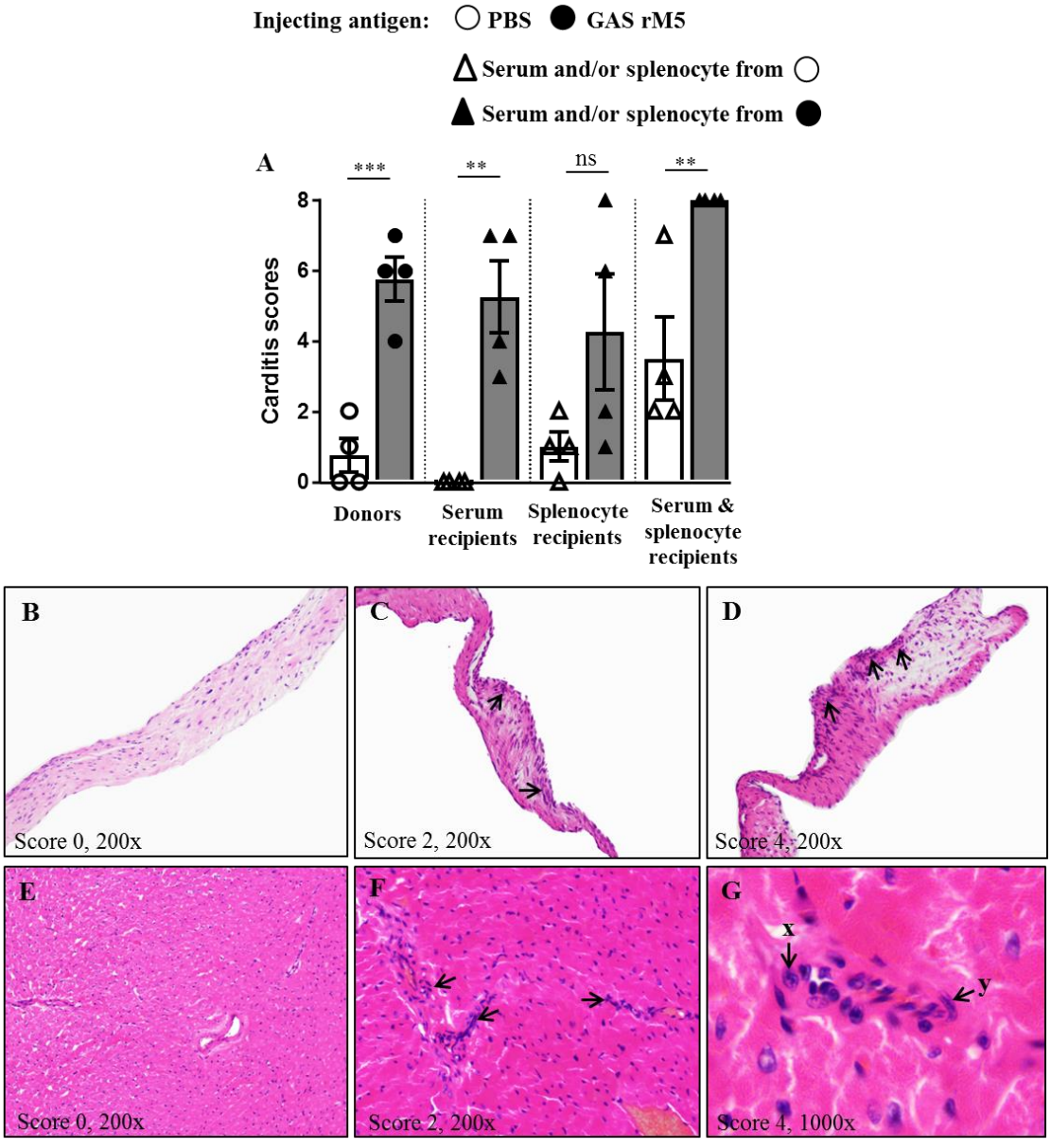


**Figure 8.2** GAS rM5 protein specific serum and splenocytes induce carditis. Higher carditis scores were observed in donor rats injected with GAS rM5 protein (n=4) compared to donor rats injected with PBS (n=4) (A). Recipient rats (n=4) injected with serum or serum plus splenocytes from GAS rM5 injected donor rats had significantly higher carditis scores compared to the recipient rats injected with serum or serum plus splenocytes from donor rats injected with PBS (A). The carditis scores of rats receiving GAS rM5 restimulated splenocytes were also higher than controls although this difference was not statistically significant. Representative histological images of different inflammatory scores of mitral

valve and myocardium are shown in B-G. Control rats had no evidence of inflammation in the mitral valve (B) and myocardium (E). Infiltration of inflammatory cells and/or focal lesions was observed in the mitral valves of donor rats injected with GAS rM5 or recipient rats injected with serum and/or splenocytes from GAS rM5 injected donor rats (C score 2, D score 4). There was interstitial focal myocarditis with granulomatous structures similar to Aschoff nodules in the myocardium of donor rats injected with GAS rM5 or recipient rats injected with serum and/or splenocytes from GAS rM5 injected donor rats (F score 2, G score 4). Scale bars as indicated, x: Aschoff like cells, y: Anitschow like cells. Error bars represent standard errors of the mean (SEM). Statistical difference by unpaired t test; **p<0.01, ***p<0.001, ns: not significant.

### 8.3.2 GAS rM5 immune serum and splenocytes induce prolongation of P-R interval on ECG in recipient rats

ECG was performed and peak P and R points of each ECG trace were recorded from donor and recipient rats. Significant prolongation of P-R intervals was observed in donor rats injected with GAS rM5 compared to PBS injected control rats (Figure 8.3). Moreover, recipients injected with serum and/or splenocytes from the GAS rM5 injected donors, also demonstrated significantly prolonged P-R intervals (Figure 8.3).

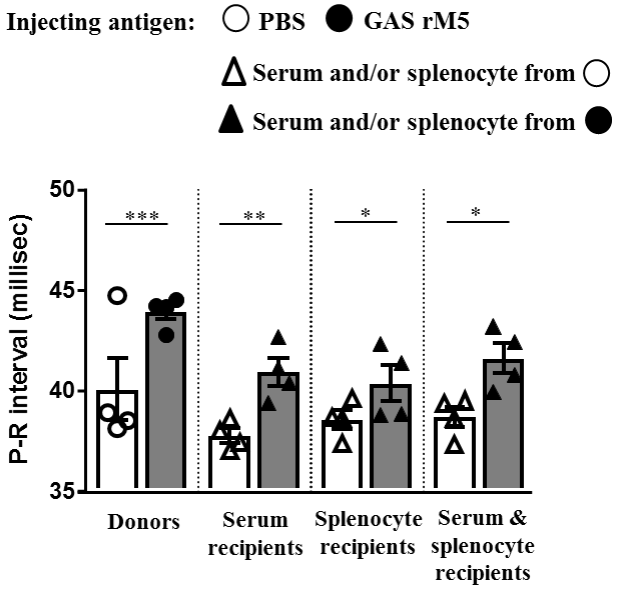


**Figure 8.3** Electrocardiographic assessment demonstrates cardiac dysfunction in recipient rats following immune serum and splenocyte transfer. Significant prolongation of P-R intervals was observed in donor rats injected with GAS rM5 (n=4) compared to PBS injected control rats (n=4). Prolongation of P-R intervals was also observed in recipient rats (n=4) injected with either serum or splenocytes or combined serum and splenocytes from GAS rM5 injected donor rats compared to controls. Error bars represents standard errors of mean (SEM). Statistical difference by unpaired t test; *p<0.05, **p<0.001.

### 8.3.3 GAS rM5 specific antibodies and splenocytes induce mitral valve pathology

Impairment of cardiac function was further assessed using echocardiography (echo). We observed a uniform mitral valvular structure in control donor rats injected with PBS or control recipient rats injected with serum and splenocytes from control donor rats (Figure 8.4 B and Appendix 8 Supplementary Figure 8.3A (1.1-1.4) and 8.3B (1.1-1.4). In contrast, mitral valves of recipient rats injected with combined serum and splenocytes form GAS rM5 injected rats showed variable mitral valve thickness with the presence of nodule(s) (Figure 8.4 C-E and Appendix 8 Supplementary Figure 8.3B (2.1-2.4)). The findings were similar to the donor rats injected with GAS rM5 (Figure 8.4 C-E and Appendix 8 Supplementary Figure 8.3A (2.1-2.4)). Echo was not performed on serum only or splenocyte only transfer groups. The echo scores (based on mitral valvular thickness and nodules) were also significantly higher in donor rats and recipient rats injected with serum and splenocytes from GAS rM5 injected donor rats (Figure 8.4 A).

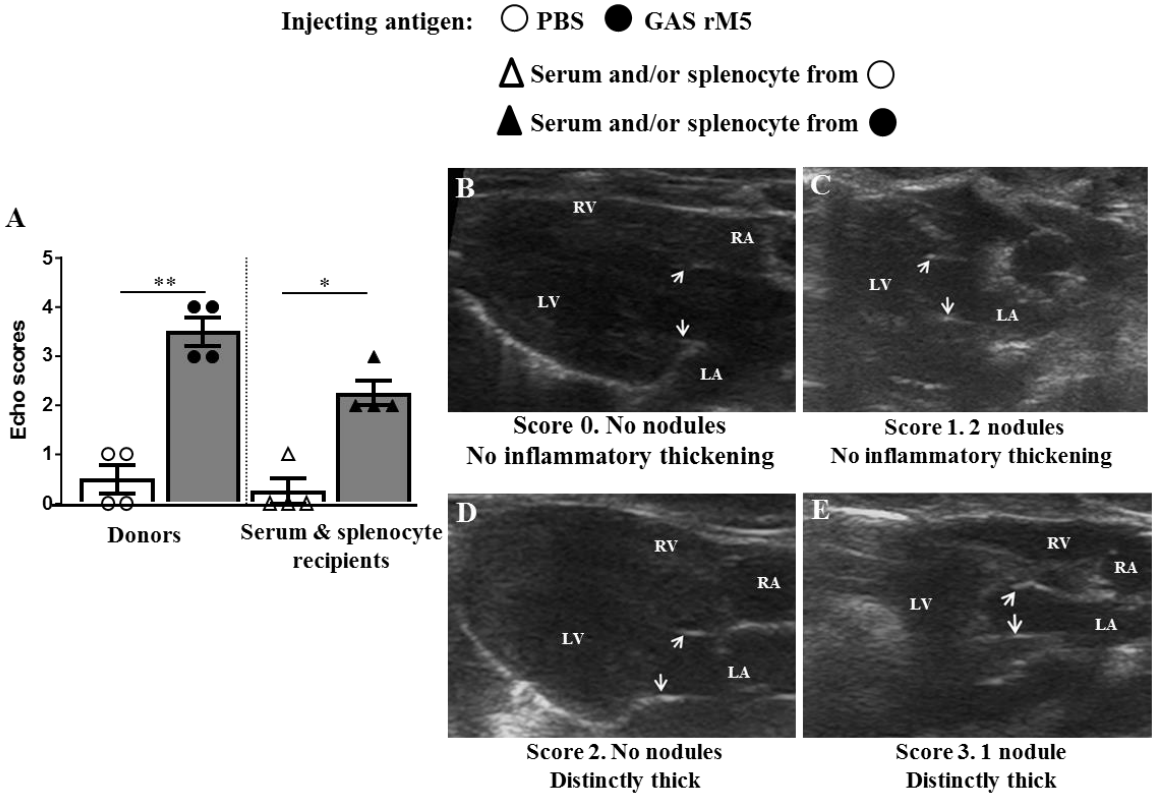


**Figure 8.4** Echocardiographic changes demonstrate mitral valve pathology in immune serum and splenocytes recipient rats. Echo scores were determined based on thickness and number of nodules on mitral valves. Higher scores on echo were observed in donor rats injected with GAS rM5 (n=4) and recipient rats (n=4) injected with serum and splenocytes from GAS rM5 injected donor rats compared to control rats injected with PBS or serum and splenocytes from PBS injected control donor rats (n=4) (A). The control donor and recipient rats had uniform mitral valvular structures without leaflet thickening or valvular nodules (B, score 0).

However, donor rats injected with GAS rM5 and recipient rats injected with serum and splenocytes from GAS rM5 injected donor rats showed variable degrees of mitral valvular thickness and the presence of nodules (C-E, score 1-3). Arrows indicate mitral valve leaflets, LA: left atrium, LV: left ventricle, RA: right atrium, RV: right ventricle. Error bars represent standard errors of the mean (SEM). Statistical difference by unpaired t test; *p<0.05, **p<0.001.

### 8.3.4 Antibodies in serum and/or splenocyte recipient rats recognise GAS rM5

We analysed sera from donor and recipient rats to detect IgG responses to GAS rM5 and cross-reactivity to host cardiac myosin. High-titre M5-specific IgG was demonstrated in donor sera (Figure 8.5 A). Antibodies in donor sera also recognised cardiac myosin (Figure 8.5 B). We detected M5-specific antibodies in the sera of recipient rats injected with serum only and serum plus splenocytes (Figure 8.5 A). Surprisingly, we also detected M5-specific antibodies in the serum of recipients receiving splenocytes only (Figure 8.5 A). We could not demonstrate significant reactivity against cardiac myosin in the sera from any recipient group (Figure 8.5 B). In all experiments, serum from donor rats injected with PBS or recipient rats injected with serum and/or splenocytes from PBS injected donor rats were used as controls and these showed minimal reactivity with rM5 or cardiac myosin.

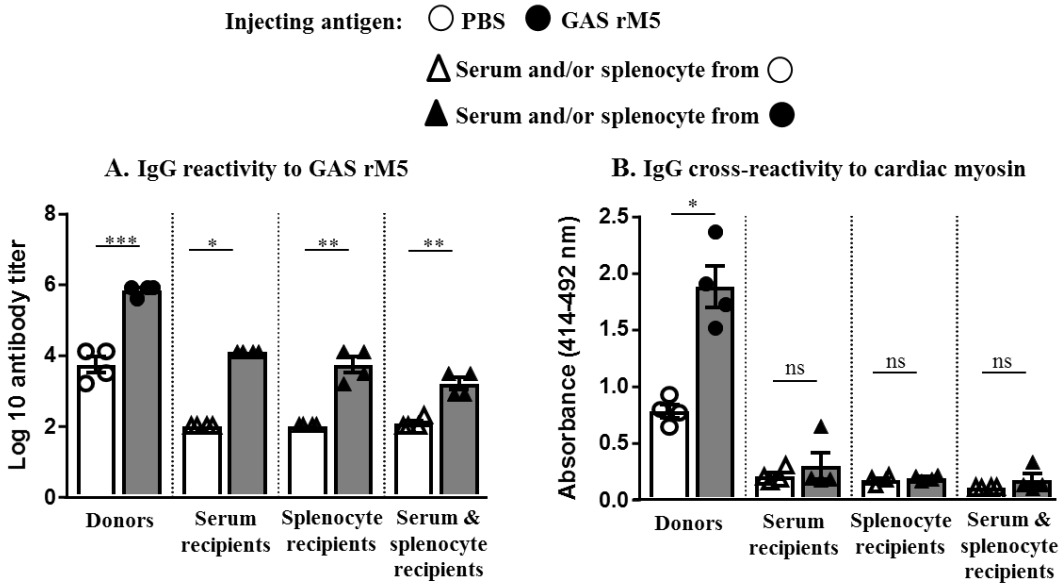


**Figure 8.5** Serum IgG reactivity to GAS rM5 and cross-reactivity to cardiac myosin. Serum IgG from donor rats injected with GAS rM5 (n=4) reacted significantly with GAS rM5 compared to PBS injected control rats (n=4) (A). Serum IgG from recipient rat groups (n=4) receiving immune serum and/or splenocytes reacted with GAS rM5 (A). Sera from donor rats, but not recipient rats, reacted with cardiac myosin (B). Error bars represent standard errors of the mean (SEM). Statistical difference by unpaired t test (Panel A: Donors, Splenocyte recipients, Serum & splenocyte recipients; Panel B: Donors, Splenocyte

recipients) and Mann-Whitney test (Panel A: Serum recipients; Panel B: Serum recipients, Serum & splenocyte recipients); *p<0.05, **p<0.001, ***p<0.0001, ns: not significant.

### 8.3.5 T-cells from serum and splenocyte recipient rats proliferate in response to GAS rM5

Splenocytes from donor rats injected with GAS rM5 proliferated in response to GAS rM5 restimulation (Figure 8.6 A). Splenocytes from recipient rats injected with serum plus splenocytes from GAS rM5 injected donor rats also proliferated in the presence of GAS rM5 (Figure 8.6 A). Lymphocyte proliferation assays were not performed on serum only or splenocyte only transfer groups. The proliferating T-cells from both donor and recipient rats produced significantly more IFN-γ (Figure 8.6 B), IL-17A (Figure 8.6 C) and IL-4 (Figure 8.6 C) than unstimulated cells (not shown) and cultures from control animals. In all experiments, donor rats injected with PBS or recipient rats injected with serum and/or splenocytes from PBS injected donor rats were used as controls.

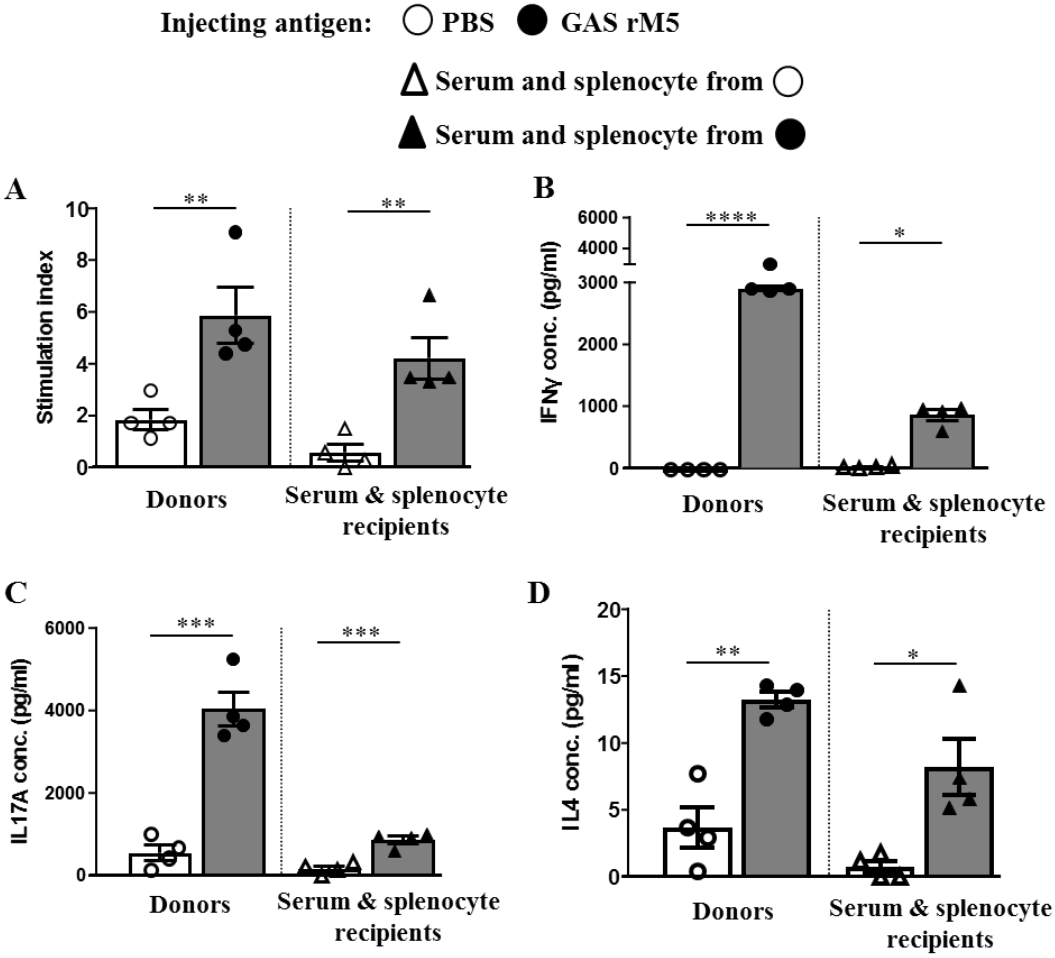


**Figure 8.6** Splenocytes from GAS rM5 specific serum plus splenocyte recipient rats proliferate in response to GAS rM5 and secrete IFN-γ, IL-17A and IL-4. The splenic T-cells

from donor rats injected with GAS rM5 (n=4) proliferate in response to GAS rM5 (A, left panel) and produce significantly higher amounts of IFN-γ (B, left panel), IL-17A (C, left panel) and IL-4 (D, left panel) compared to PBS injected control rats (n=4). The splenic T-cells from recipient rats (n=4) injected with serum and splenocytes from GAS rM5 injected donor rats showed similar proliferative and cytokine production response (A-D, right panels). The recipient rats injected with serum and splenocytes from PBS injected donor rats were used as controls (n=4). Error bars represent standard errors of the mean (SEM). Statistical difference by unpaired t test except IFN-γ production in recipient rats (B, right panel) which was tested by Mann-Whitney test; *p<0.05, **p<0.01, ***p<0.001, ****p<0.0001.

## 8.4 DISCUSSION

The immune mechanisms that mediate the cardiovascular pathology associated with diseases such as RHD are poorly defined (Breed and Binstadt 2015). Carditis is the key feature of ARF, occurring in >50% of patients (Veasy, et al. 1987; Veasy, et al. 1994; Roberts, et al. 2001; Vijayalakshmi, et al. 2008; Mota, et al. 2014). Several clinical and animal model studies have previously suggested that carditis development in ARF/RHD is initiated by anti-GAS antibodies followed by T-cell infiltration of the valve and myocardium (Kaplan, et al. 1964; Roberts, et al. 2001; Gorton, et al. 2009; Cunningham 2014; Carapetis, et al. 2016; Gorton, et al. 2016). However, the antigen inducing autoreactive T-cell and antibody responses against heart tissues are poorly defined (Smith and Allen 1991). It is essential to understand how immune effector cells are targeted to the heart, how these cells are activated, and if their effector functions are antigen specific. This chapter focussed on investigating the relative contributions of antibodies and T-lymphocytes to the induction of autoimmune carditis. Adoptive transfer experiments are often used to definitively determine the respective roles of antibodies versus cells in driving the pathology of immune-mediated diseases. Here we showed that both antibodies (serum) and T-cells (splenocytes) derived from GAS M5-immunised diseased donors could induce valvular and myocardial inflammation and heart dysfunction in naïve recipients. We conclude that both antibodies and T-cells independently and together can initiate and mediate autoimmune valvulitis in Lewis rats. To our knowledge, this is the first report of ARF/RHD-like cardiac dysfunction achieved by adoptive transfer of T-cells and/or serum.

The current study was designed to demonstrate whether rM5 injection induces cross-reactive and pathogenic T-cells and antibodies that could potentially recognise cardiac tissues and induce heart inflammation when transferred into naïve syngeneic rats. GAS rM5-specific lymphocytes and serum were independently capable of inducing valvulitis and myocarditis as early as 21 days after transfer (Figure 8.2). Valvular inflammation was demonstrated in all

serum recipient rats and 50% of splenocyte recipients. Normal splenocytes and serum from PBS injected animals did not induce heart inflammation. We also evaluated whether serum and splenocytes when transferred together could induce carditis. Eighty-six days after transfer we observed higher carditis scores than those observed following either serum only or cell only transfer (Figure 8.2).

Kirvan et al. 2014 reported that passive transfer of T-cell lines specific to the N-terminal region of the M5/M6 protein into naïve rats produced valvulitis characterised by infiltration of CD4+ T-cells. It was unclear however if it was the transferred cells that trafficked directly to the heart, or whether other host cells were responsible for the initiation of disease. Myocarditis development following adoptive transfer of cardiac myosin protein or peptide specific T-cells has been reported in several earlier studies (Smith and Allen 1991; Kodama, et al. 1992; Wegmann, et al. 1994; Bachmaier, et al. 1999). After CD4+ T-cells depletion using mAbs, Smith and Allen (1991) also showed that the myosin-induced myocarditis is a CD4+ T-cell-mediated disease. Histopathologic examination of heart sections from rats received cardiac myosin specific T-cells developed myocarditis with infiltration of lymphocytes, macrophages, and scattered giant cells, associated focally with destruction of myocardial fibres (Kodama, et al. 1992). In animal models of other autoimmune diseases Miller, et al. (1988) showed that a diabetic phenotype could be reproduced in mice following adoptive transfer of antigen-specific CD4+ and CD8+ T-cells. Similarly, Haskins and McDuffie (1990) found that a CD4+ islet-specific T-cell clone could transfer diabetes in a murine model. In experimental autoimmune neuritis models.

Antibodies specific for several autoantigens have been shown to transfer disease to naïve hosts in different autoimmune disease models. For example, passive transfer of muscle nicotinic acetylcholine receptor (AChR) antibodies in mouse models of myasthenia gravis reproduces the clinical phenotype of diseased animals (Toyka, et al. 1975; Tzartos, et al. 1987). Passive transfer of rabbit polyclonal antibodies generated against human epidermal antigen (BP180) into neonatal BALB/c mice developed a subepidermal blistering disease that closely mimicked autoimmune bullous pemphigoid (Liu, et al. 1993). Guinea pigs developed autoimmune tubulointerstitial disease following passive transfer of pure IgG1 or IgG2 fractions of isologous anti-tubular basement membrane (TBM) (Hall, et al. 1977). Mice developed autoimmune autonomic neuropathy following passive transfer of IgG antibodies specific to ganglionic AChR generated in rabbits (Vernino, et al. 2004). Neu, et al. (1990)

and Smith and Allen (1991) reported that transfer of serum with high-titre anti-myosin antibodies to recipient mice did not develop myocarditis. The authors suggested that the antibodies may play a role in accentuating heart damage, possibly by an antibody-dependent cell cytotoxicity mechanism, once the T-cell-mediated recognition of autoreactive myosin epitopes is established. Other studies have shown that passive transfer of affinity-purified anti-heart autoantibodies from sera of patients with myocarditis directly induces experimental myocarditis in naïve mice (Caforio, et al. 2015).

Our findings suggest either an additive effect of antibodies and lymphocytes or that as the inflammatory response becomes chronic over time, valve damage increases. Which of these phenomena is occurring is not clear presently and future experiments that follow the inflammatory response triggered by serum only or cell only transfer over time would help elucidate more precise mechanisms. It is therefore likely that multiple mechanisms could operate to cause immune-mediated tissue destruction.

In ARF/RHD, it has been hypothesised that GAS-specific antibodies activate vascular endothelial cells of heart by inducing the expression of vascular cell adhesion molecules (CAMs) to facilitate transmigration of autoreactive T-cells into the myocardium and valvular tissues (Roberts, et al. 2001; Carapetis, et al. 2016). In the current study, M5-specific donor antibodies may be responsible for driving the observed heart pathology directly by activating the heart endothelium of recipient rats. We observed M5-specific antibodies in day 21 sera of serum recipients and in day 86 sera of serum plus splenocyte recipients. The half-life of rat IgG is reported to be only approximately 63 h (Peppard and Orlans 1980), suggesting that M5-reactive antibodies are being synthesised *de novo* in these serum recipients and that these antibodies are pathogenic. This result implies that antibodies alone can initiate the entire sequence of immune responses and cellular interactions resulting in naïve B-cell priming in naïve recipients. However, this scenario would require either; (i) M5 antigen to be co-transferred with serum to prime the naïve recipient B- (and CD4+ T-) cells or, (ii) recipient antibodies against an unknown host protein can cross-react with the M5 antigen in ELISA. Which of these situations is occurring is presently unclear. Future studies will be required to demonstrate carditis development following passive transfer of T-cells or antibodies with GAS M-proteins to confirm these hypotheses.

Surprisingly, we also detected M5-specific antibodies in day 21 sera of recipients receiving splenocytes only. Memory B-cells, in addition to memory T-cells may have been expanded *in vitro* prior to cell transfer hence M5 antibody-secreting donor B-cells/plasma cells may have seeded secondary lymphoid tissues of recipient animals. Because we transferred splenocyte suspensions into recipients we were unable to definitively separate the specific contributions of heart tissue-reactive splenic memory B-cells versus memory T-cells in triggering inflammation in recipient animals. In an adoptive transfer study, Paque and Miller (1992) demonstrated inflammation of myocardium and coxsackievirus-specific antibodies in the serum of recipient mice 35 days after adoptive transfer of purified B-cells or splenocytes containing 35% memory B-cells. These authors suggested that recipient mice may be able to synthesise anti-virus antibodies as early as 72 h to as late as 35 days following adoptive transfer. Hence, antibodies alone may be able to drive carditis in our model. Further experiments using purified donor B-cells or T-cells, transferred into naïve recipients may help clarify our findings.

Previous studies have demonstrated that GAS M-protein specific antibodies cross-react with cardiac myosin (Cunningham, et al. 1989; Galvin, et al. 2002; Kirvan, et al. 2014). In Chapter 5 of this thesis, we reported low levels of cardiac myosin reactive IgG in the serum of GAS (and GGS) M-protein injected rats. In the study described in this chapter however, the serum collected from recipient rats failed to react with porcine cardiac myosin in ELISA. Any cardiac myosin reactive antibodies in the donor serum may have been diluted once transferred into recipients and these were below the limits of detection of the cardiac myosin ELISA.

In our study, splenocytes from recipient rats proliferated *in vitro* in response to rM5, confirming that these memory lymphocytes were "adopted" into the naive host. Further experiments using purified donor B-cells or T-cells, transferred into naïve recipients may help clarify and extend our findings and determine which lymphocyte type is proliferating. Directly tracking the fate of transferred T/B-cells into heart tissue may also provide definitive evidence as to which lymphocyte type is responsible for heart inflammation. We did however show that T-cells from recipient rats produced very high levels of IL-17A and IFN-γ in response to rM5 stimulation with lower concentrations of IL-4. This pattern was identical to that observed in donor rats and as shown previously in Chapter 5, this pattern of cytokine secretion indicates a dominant Th-1 and Th-17 response which is similar to that reported for

human T-cell clones from RHD patients (Ellis, et al. 2005; Fae, et al. 2006). In ARF/RHD, the majority of T-cells isolated from heart and peripheral blood were found to secrete IFN-γ with fewer cells secreting the Th-2 type cytokine IL-4 (Guilherme, et al. 2004; Guilherme, et al. 2006). Th-1 and Th-17 cells may attach to and traverse the valve endothelium, thereby infiltrating the valve. IFN-γ and other pro-inflammatory cytokines secreted by antigen-activated T-cells may play an important role in the development or maintenance of valvulitis by inducing expression of VCAM-1 on valvular endothelium, which in turn, increases the rate of mononuclear cell recruitment to the valve surface (Kirvan, et al. 2014). The role of the Th-17 cell in the pathogenesis of ARF/RHD is unknown, although high concentrations of IL-17 in the serum of Lewis rats and accompanying high expression of IL-17 in the mitral valves of Lewis rats and human patients has been reported (Wen, et al. 2015). Additional studies will be needed to clarify the cellular, humoral and molecular factors necessary to mediate M-protein specific T-cell infiltration into the heart.

As discussed in earlier chapters, ARF/RHD is clinically diagnosed when a patient presents with two major manifestations or one major and at least two minor manifestations according to the Jones Criteria for the diagnosis of ARF/RHD 2015 (Gewitz, et al. 2015). Prolongation of P-R interval in ECG is one of the Jones Minor Criteria for the diagnosis of rheumatic fever. Moreover, echocardiographic screening of suspected ARF patients is the latest recommendation that has been included in the 2015 Jones Criteria. It is helpful in diagnosing clinical and subclinical carditis even in the absence of classical auscultatory findings (Gewitz, et al. 2015). Prolongation of P-R interval is a minor criterion and in a typical ECG trace indicates delay in ventricular depolarisation due to myocardial pathology. In the current study, rats receiving serum or splenocytes or both serum and splenocytes showed prolonged P-R intervals in ECG. In the current study, thickening of mitral valves of rats transferred with serum and splenocytes from GAS rM5 injected rats was observed as echo-dense white leaflets in echocardiography. Echo dense foci on mitral leaflets were also demonstrated as white and round structures on the leaflets. The results were identical to the echocardiographic findings of donor rats and in patients with ARF/RHD (Carapetis, et al. 2016).

The transfer of carditis to Lewis rats by GAS rM5-stimulated autoreactive T-cells and serum showed the critical role of T-cells and antibodies in ARF/RHD. We did not address the immunogenic epitopes of GAS rM5 protein specific antibodies and T-cells that might have contributed to the carditis. Monitoring the inflammatory responses following transfer of

antibodies and T-cell over time could better explain the source of antibodies and T-cells contributed to the disease. Future studies are suggested to remove pathogenic antibodies and T-cells to prevent development of carditis. The data provides direct evidence that streptococcal M-protein specific lymphocytes and antibodies facilitate migration of inflammatory cells to the heart *in vivo* and likely contribute to heart pathology in this animal model as well in human RHD. Further dissection of the interactions between endothelial cells, serum antibodies and T-cells is the subject of the following chapter.

# CHAPTER 9
# GROUP G *STREPTOCOCCUS* STIMULATES UPREGULATION OF ENDOTHELIAL ADHESION MOLECULES AND FACILITATES T-CELL MIGRATION INTO HEART TISSUE

## 9.1 INTRODUCTION

The vascular endothelium plays an important role in the development of inflammatory heart disease by regulating immune cell trafficking into tissues. The cardiac chambers and valves are lined with a monolayer of endothelial cells. The endothelium regulates vascular integrity, inflammation, thrombosis, and vascular remodelling. Valvular endothelial cell dysfunction results in vascular disorders such as degenerative heart disease, myxomatous or floppy valves, rheumatic heart inflammation, and infective endocarditis (Leask, et al. 2003). Endothelial cell dysfunction may be caused by mechanical overload, bacterial infection, autoantibodies, and circulating endothelial cell modulators (Leask, et al. 2003). In ARF/RHD, interaction of blood mononuclear cells and the endothelium is essential for the development of heart lesions (Galvin, et al. 2000).

Development of rheumatic heart lesions is mediated by sequential events involving interactions between cellular integrins, adhesion molecules and chemokines. Leukocyte transmigration across the valve endothelium initiates early stage heart damage. A number of molecules are involved in the recruitment of leukocytes including T-cells into heart tissue. Vascular cell adhesion molecule (VCAM)-1 is expressed on endothelial cells and has previously been reported to be upregulated by antibodies to group A *Streptococcus* (GAS) that can also bind to human cardiac tissue proteins. Upregulation of VCAM-1 leads to lymphocyte infiltration into heart tissues (Galvin, et al. 2000). Guilherme, et al. (2013b) also described a key role for intercellular adhesion molecule (ICAM)-1, P- and E-selectins and chemokines in the recruitment of inflammatory cells to the heart tissues (Guilherme, et al. 2013b).

Upregulation of VCAM-1 indicates an activation of the endothelium and is also a sign of underlying tissue damage (Springer 1994). The presence of pro-inflammatory cytokines such as TNF-α or binding of cross-reactive antibodies to heart endothelial cells can damage the heart endothelium and up-regulate VCAM-1 (Galvin, et al. 2000; Roberts, et al. 2001; Ellis, et al. 2010; Parks, et al. 2012). In either case, infiltration of the heart by inflammatory cells is

triggered by cytokines. Endothelial cells interact with circulatory lymphocytes by expressing VCAM-1 which interact with very late antigen (VLA)-4 on activated lymphocytes. VCAM-1 and VLA-4 interaction reduces mobility of lymphocytes, increases gaps between endothelial cells and facilitates transmigration of lymphocytes into the heart tissue (Ellis, et al. 2005; Fae, et al. 2006). In a study of patients with RHD, Roberts, et al. (2001) observed CD4+ and CD8+ T-cells adhered to the endothelium of rheumatic valves and penetration through the sub-endothelial layer. The adherence and extravasation of T-cells were attributed to an upregulation of VCAM-1 (Roberts, et al. 2001). The findings of Roberts and colleagues (2001) was supported by Cunningham's group (Galvin, et al. 2000; Roberts, et al. 2001; Ellis, et al. 2005; Fae, et al. 2006; Kirvan, et al. 2014) who described that cross-reactive antibodies mediated the upregulation of VCAM-1 on the valvular endothelial surface and that this facilitated inflammation and T-cell infiltration into the valve tissues. Studies using the Lewis rat model of autoimmune valvulitis further supported this hypothesis and showed that GAS M5-protein specific antibodies induce VCAM-1 upregulation on cultured rat aortic endothelial cells (Gorton, et al. 2016). These studies however did not investigate whether VCAM-1 upregulation influenced T-cell migration across the endothelial cell monolayer.

Interactions between intercellular adhesion molecule (ICAM)-1 expressed by the endothelial cells, and leukocyte function associated antigen (LFA)-1 is critical for leukocyte adhesion to endothelial cells and subsequent transmigration (Jois and Teruna 2003). ICAM-1/LFA-1 interaction is essential for T-cells activation and migration to target tissues (Anderson and Siahaan 2003). Leukocyte chemoattractant cytokines play a role in controlling leukocyte adhesion to endothelial cells (Lukacs, et al. 1995; Tekstra, et al. 1999; Gawaz, et al. 2000; Muller, et al. 2000). In ARF/RHD, the T-cell chemoattractant CXCL9 mediates T-cell recruitment to the myocardium and valve tissues (Fae, et al. 2013). The increased T-cell infiltration modifies the interstitial cell structure and function, causing myocarditis, and valve thickening and fibrosis. These chronic inflammatory processes lead to fibrotic scarring, affecting valve haemodynamics and function.

The interaction of T-cells with the valve (or myocardial vascular endothelium) and their subsequent migration into heart tissues may also be controlled by T-cell attracting chemokines such as CCL1/I-309 and CXCL9/Mig. CXCL9 is an IFN-γ-inducible chemotactic cytokine, and is produced by dendritic cells, B-cells and macrophages (Park, et al. 2002). CXCL9 binds to the receptor CXCR3 expressed predominantly on memory and

effector T-cells (Loetscher, et al. 1996). Fae, et al. (2013) reported that the T-cell line developed from mitral valves of patients with ARF/RHD significantly migrated to the bottom chamber having CXCL9 of Transwell cell culture system. The increased expression of endothelial adhesion molecules and inflammatory chemokines are unsurprising in the inflammatory context of RHD development. However, these have not been widely investigated and furthermore did not explain why valvular tissue is specifically targeted (Bright, et al. 2016).

Rheumatic heart lesions result from chronic inflammation and CD4+ and CD8+ T-cell infiltration. Recurrent acute cardiac inflammation frequently evolves into chronic RHD. Valvular deformities occur as chronic sequelae that lead to mitral and aortic regurgitation and/or stenosis (Guilherme, et al. 2013b). Previous studies have reported that there is a strong association between endothelial cell VCAM-1 expression and rheumatic heart lesion formation (Galvin, et al. 2000; Roberts, et al. 2001; Gorton, et al. 2016). Far less is known about the role of endothelial cells, especially ICAM-1 expression during transmigration of T-cells in valvular disease. Therefore, in the current study the role of GAS and GGS M-protein specific antibodies and T-cells in mediating the upregulation of VCAM-1 and ICAM-1 has been investigated; (i) *in vitro* using cultured rat aortic endothelial cells and; (ii) *in vivo* in tissue sections taken from Lewis rats immunised with GAS and GGS M-proteins. Whether these activated endothelia facilitate T-cell transmigration was also investigated.

### 9.1.1 Aims

The overall Aim of this study is to investigate whether VCAM-1 and ICAM-1 expression by endothelial cells is induced by antibodies and T-cells specific to GAS and GGS M-proteins and results in transmigration of T-cells across an endothelial cell layer.

The specific Aims were:

1. To determine GAS and GGS M-protein specific antibody binding to the rat aortic endothelial cell monolayer.
2. To demonstrate expression of VCAM-1 and ICAM-1 in cultured endothelial cells following exposure to GAS and GGS M-protein specific serum and/or splenocytes.
3. To demonstrate VCAM-1 and ICAM-1 expression *in vivo* in heart tissues from rats injected with GAS and GGS M-proteins.

4. To determine T-cell transmigration across endothelial cell monolayers using a Transwell culture system.

## 9.2 MATERIALS AND METHODS

### 9.2.1 Experimental animals, antigens and adjuvants

Female Lewis rats bred at James Cook University, Townsville, Australia were used. The details of rats are described in Section 3.1.2. Recombinant M-protein of GGS (Stg480) and GAS (rM5) and adjuvants used in this study are described in Section 5.2.2. The injection schedules described in M-protein short term experiment of Section 5.2.3 were followed.

### 9.2.2 Reagents for endothelial cell culture

Rat aortic endothelial cells (RAOEC, #SR30405), rat endothelial growth medium (REGM, #PMR21150), subculture reagent kit (#PR090100K), Hank's balanced salt solution (HBSS, #PR062100), trypsin/EDTA solution (#PR070100), trypsin neutralisation solution (#PR080100), attachment factor solution (AFS, #PR123100) and rat endothelial cell growth supplement (#PMR211GS) were purchased from *Genlantis PrimaPure* (*USA*). Tumor necrosis factor alpha (TNF-α, #000-18181) was from *eBioscience* (*USA*). Rat CXCL9 (#RP0917R) was purchased from *Kingfisher Biotech* (*USA*). Sterile 6.5 mm Transwell plates with 8.0 μm pore polycarbonate membrane inserts (#3422) were purchased from *Corning Costar Corporation* (*USA*). Dimethyl sulfoxide (DMSO, #D2650) for cell cryopreservation was purchased from *Sigma* (*Australia*).

### 9.2.3 Reagents for flow cytometry

Sheath fluid (FACS Flow, #342003) was from *Becton Dickinson Bioscience* (*USA*). FITC-conjugated mouse anti-rat CD31 IgG1, clone TLD-3A12 (#MA516952) was purchased from *Invitrogen* (*USA*). FITC-conjugated mouse IgG1a, κ isotype control, clone MOPC-21 (#400107) was from *BioLegend* (*USA*). Biotin-conjugated mouse anti-rat CD54, clone 1A29 (#202403) from *BioLegend* (*USA*). Streptavidin APC (#17-4317-82) was from *eBioscience* (*USA*). APC-conjugated mouse IgG1, κ isotype control, clone OX33 (#17-0462-80) was from *eBioscinece* (*USA*). PE-conjugated mouse anti-rat CD106, clone MR106 (#200403) and PE-mouse IgG1, κ isotype control, clone MOPC-21 (#400111) were from *BioLegend* (*USA*). 123count eBeads (#01-1234-42), mouse anti-rat CD3 FITC, clone eBioG4.18 (G4.18) (#11-0030-81) and FITC-mouse IgG3, κ isotype control (#14-4742-82) were purchased from *eBioscience* (*USA*).

### 9.2.4 Reagents for immunohistochemistry

Mouse anti-rat CD106, clone MR106 (#MCA4633GA) was purchased from *Biorad* (*USA*). Mouse anti-rat CD54-biotin, clone 1A29 (#202403) was from *BioLegend* (*USA*). Mouse IgG1 κ isotype control, clone P3.6.2.8.1 (#501129514) was from *eBioscience* (*USA*). Goat anti-mouse HRP secondary antibody (#170-6516) was from *Biorad* (*USA*). Avidin-biotin Complex (ABC, #PK-4000), ImmPACT 3, 3'-diaminobenzidine peroxidase (HRP) substrate (DAB, #SK-4105) were purchased from *Vector Laboratories* (*USA*). Haematoxylin stain was prepared in house.

### 9.2.5 Experimental design

Lewis rats (n=3 per group) were injected with GAS rM5 or GGS Stg480 or PBS under general anaesthesia as described previously (Section 3.2.2.1). The immunisation schedules described in M-protein short term experiment of Section 5.2.3 were followed. Rats were culled (Section 3.2.2.2) 35 days after the priming injection to collect serum and splenocytes (Section 3.2.2.3). The serum samples from each rat group were pooled and stored at -80°C until use. The splenocytes from rats were restimulated *in vitro* with 10 μg/ml of rM5 or Stg480 protein stimulation for 72 h (Section 3.2.4.1) before inoculation onto the rat aortic endothelial cell monolayer (Figure 9.1 A).

To determine the GAS rM5 and GGS Stg480 specific antibody binding to endothelial cell surface antigens, rat aortic endothelial cell (RAOEC) monolayers were prepared in 96F-microtitre plates (Figure 9.1 B). Pooled serum from rats injected with rM5 or Stg480 was added at 1:6400 dilution followed by anti-rat secondary antibody and ABTS (details in Section 9.2.8). In separate experiments, RAOEC monolayers were incubated with 5% pooled serum and/or $10^6$ M-protein restimulated splenocytes from rats injected with rM5 or Stg480 for 6 h (Figure 9.1 C). Adherent RAOECs were detached and harvested and the expression of VCAM-1 and ICAM-1 was determined using flow cytometry (details in Section 9.2.9). *In vivo* expression of VCAM-1 and ICAM-1 in rat heart sections was determined using immunohistochemistry (Figure 9.1 D). Heart sections from rats injected with rM5 or Stg480 were treated with anti-VCAM-1 and anti-ICAM-1 antibodies followed by a secondary antibody and DAB. Brown colouration of the endothelial cells indicated positive expression of VCAM-1/ICAM-1 (details in Section 9.2.10).

*In vitro* antibody induced T-cell migration across the RAOEC monolayer was demonstrated in a Transwell plate system (Figure 9.1 E). RAOEC monolayers in Transwell plate upper chambers were treated with 5% pooled serum and $10^6$ splenocytes from rats injected with rM5 or Stg480 for 6 h. Rat T-cell chemoattractant CXCL9 was provided in the lower chambers. The total number of T-cells added to the upper chamber and the number of migrated T-cells in the lower chamber was enumerated using 123count$^{TM}$ eBeads and flow cytometry following staining with anti-rat CD3-FITC (details in Section 9.2.11).

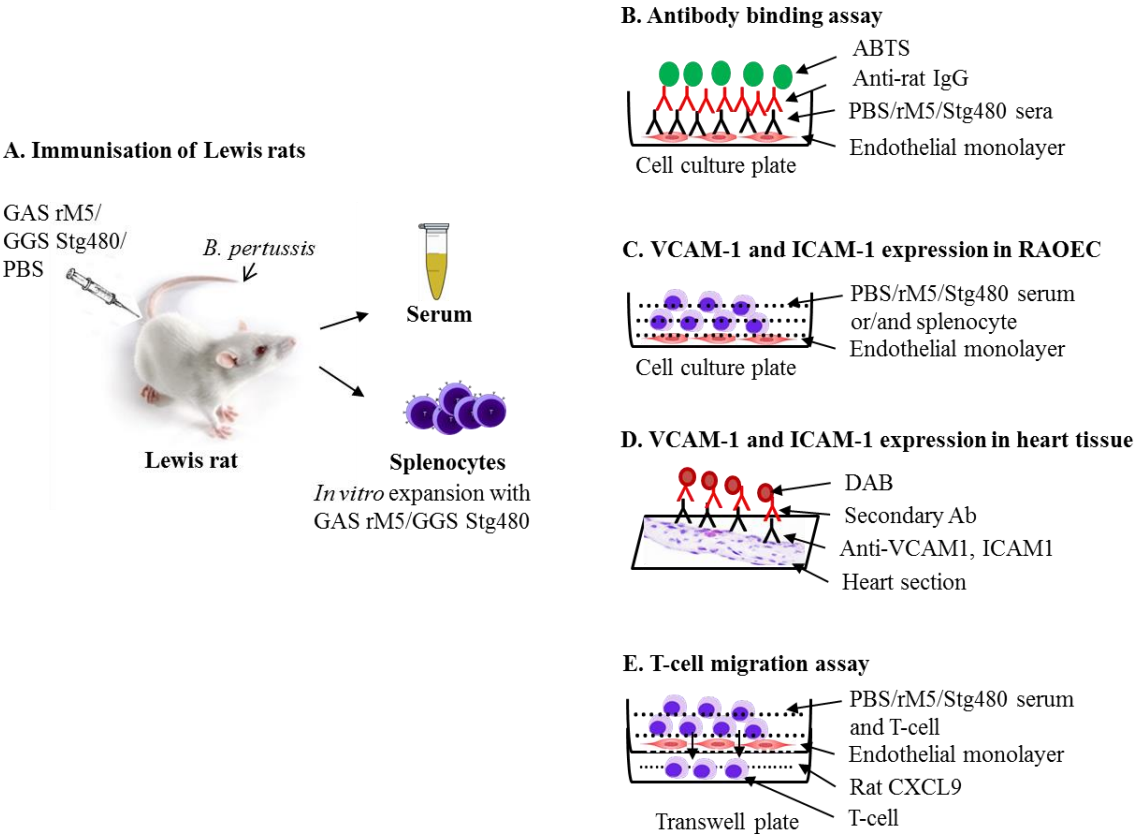


**Figure 9.1** Overview of experimental design for evaluating endothelial cell adhesion molecule expression and T-cell transmigration. (A) Lewis rats (n=3 per group) were injected s.c. with 0.5 mg/rat GAS rM5/GGS Stg480 protein mixed with CFA with 3 booster injections mixed with IFA at 1 week intervals. Control rats (n=3) were injected with PBS mixed with CFA or IFA. *B. pertussis* toxin (0.3 µg/rat) was injected i.p. at day 1 and 3 of priming injection. Rats were culled 35 days after the priming injection, and serum and mononuclear splenocytes were prepared. Splenocytes were restimulated *in vitro* with rM5/Stg480 for 72 h. In-cell ELISA technique was used to assess antibody binding to endothelial cell surface antigens (B). Rat aortic endothelial cell (RAOEC) monolayers were prepared in 96 flat bottomed microtitre plates. Pooled sera (+ heat inactivated, + antigen adsorbed) from either PBS, rM5 or Stg480 injected rats were added at 1:6400 dilution followed by HPR-conjugated anti-rat secondary antibody and ABTS. To assess the influence of serum antibody and T-cells on endothelial VCAM-1 and ICAM-1 expression, (C) RAOEC monolayers were treated with pooled sera and/or splenocytes for 6 h. Cells were detached and the expression of VCAM-1

and ICAM-1 was determined using flow cytometry. (D) VCAM-1 and ICAM-1 expression in the rat heart sections was determined using immunohistochemistry. Rat heart sections were treated with anti-VCAM-1 and anti-ICAM-1 antibodies followed by secondary antibody and DAB. Brown colouration of the cells indicated positive staining for VCAM-1/ICAM-1. T-cell transmigration across endothelial cell monolayers (E) was determined using Transwell plates. Pooled serum and splenocytes were added to the upper chambers and incubated for 6 h. Rat T-cell chemoattractant CXCL9 was added to the bottom chamber. T-cells that had migrated to the lower chamber were enumerated using 123count$^{TM}$ eBeads and flow cytometry.

### 9.2.6 Culture of rat aortic endothelial cells

All endothelial cell culture was performed in a Class II biological safety cabinet. Sterile T-75 or T-25 culture flasks were coated with 7.5 ml or 2.5 ml attachment factor solution (AFS) respectively and flasks were incubated overnight at room temperature (~22°C). After AFS was discarded, the flasks were stored at 4°C and used within 1 month. A cryopreserved rat aortic endothelial cell (RAOEC) line was purchased form *Genlantis PrimaPure* at the third passage (P3) containing $1\times10^6$ cells per 1 ml. The endothelial cell growth medium (GM) was warmed to 37°C and 15 ml was transferred into a T-75 flask (2.5 ml for T-25 flask). Cryopreserved vials of RAOEC were removed from liquid nitrogen storage and the cells thawed immediately by placing the vial in a 37°C water bath for 1 min. The cells were resuspended in the vial by gently pipetting the suspension 5 times with a 1 ml pipette before inoculation into the culture flask containing warmed GM. The flask was rocked gently to evenly distribute the cells and incubated in a 37°C, 5% $CO_2$ humidified incubator. The next day, the supernatant was removed and fresh, warmed GM was added to remove residual dimethyl sulfoxide (DMSO). The GM was changed every second day until the cells reached 80% confluence.

When the monolayer had reached 80% confluence, cells were subcultured into new AFS-coated T-75 or T-25 flasks or sterile multi-well culture plates. To retrieve the cells, the monolayer of T-75 flask was washed with 7.5 ml of Hanks Buffer Salt Solution (HBSS) (2.5 ml for T-25 flask) followed by the addition of 6 ml Trypsin/EDTA solution at room temperature (2 ml for T-25 flask). The flask was rocked gently to ensure the solution covered all cells and 5 ml of Trypsin/EDTA solution (1.5 ml for T-25 flask) removed immediately to avoid permanent cell damage. The trypsinisation process was monitored using an inverted microscope. The bottom of the flask was scraped using a cell-scraper (#83.1830, *Sarstedt*) to detach the cells from the flask. To inhibit trypsin activity, 5 ml of Trypsin neutralisation solution (1.7 ml for T-25 flask) was added to the flask. The cell suspension was removed into

a conical tube and centrifuged at 500 ×g for 5 min at room temperature. The cell pellet was resuspended in 5 ml HBSS and cells were counted using a haemocytometer. New AFS-coated flasks or multi-well plates were seeded at the required cell density for further cultures or experiments as required. The maximum passage number used for all experiments was six passages. For cryopreservation, the cells were suspended in FBS-10% DMSO at 5-10×$10^5$ cells per ml. After overnight freezing at -80°C cryovial containing cells were stored frozen in liquid nitrogen.

### 9.2.7 Splenocyte counts using flow cytometry and 123count$^{TM}$ eBeads

For T-cell migration experiments, the T-cells in pooled splenocyte samples (Section 9.2.5) were counted using 123count$^{TM}$ eBeads counting beads (#01-1234, *Invitrogen*) The counting beads are 7 μm microparticles with a known concentration (1024 beads/μl) that enabled determination of absolute cell count and cell concentration in a particular volume of samples analysed by flow cytometry. The beads are encapsulated with dyes compatible with blue (488 nm) and violet (405 nm) excitation sources and emitting fluorescence between approximately 500 nm and 750 nm. During flow cytometric analysis using the BD FACSCanto II, live endothelial cells (as determined by forward scatter versus side scatter) were gated (P1 region) and the beads were gated (P2 region) using a FITC versus PE plot (Figure 9.2). A minimum of 1000 bead events were acquired to ensure statistically significant determination of cell concentrations according to the manufacturer's instructions. The number of beads counted was then used to determine the cell concentrations. Cell concentrations were calculated using the formula: [Cell count (P1) × eBead volume/ eBead count (P2) × Cell volume] × eBead concentration (1024 beads/μl).

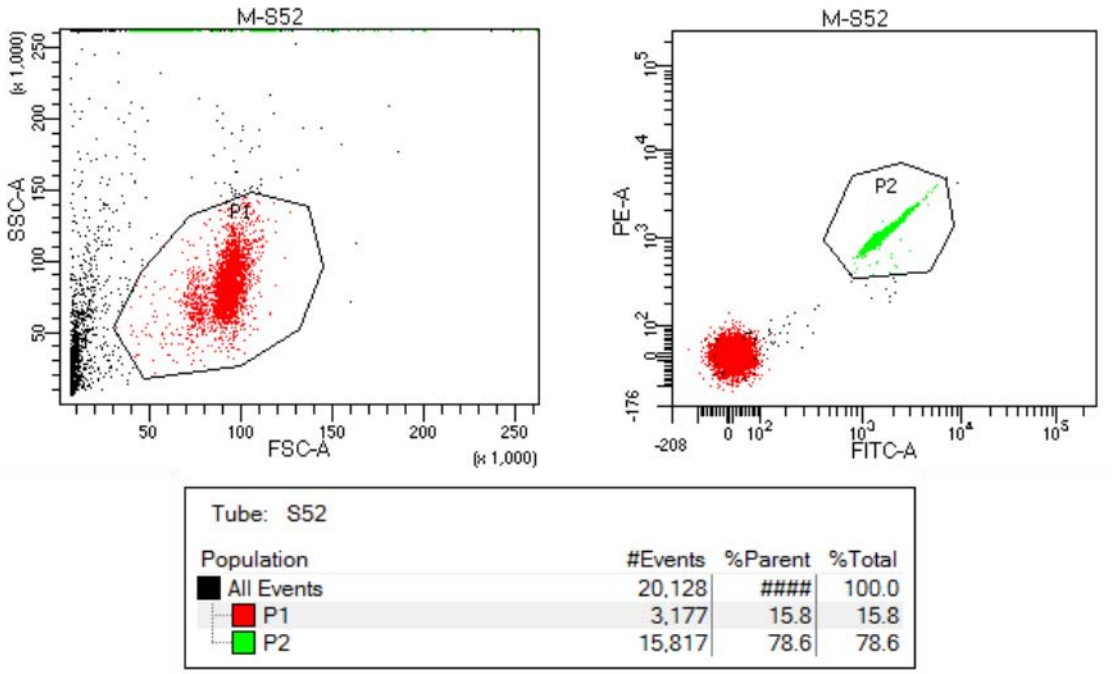


**Figure 9.2** Gating of 123countTM eBeads counting beads for calculating cell concentration. The example FACS plot shows the gating of target cell population (P1) and bead population (P2) from which event numbers are recorded and used to determine cell concentration. FSC: forward scatter, SSC: side scatter.

### 9.2.8 ELISA for detection of antibody binding to cultured endothelial cells

Serum from individual rats in each group were pooled and heated for 20 min at 56°C to inactivate complement. The GAS rM5 and GGS Stg480 specific serum antibody adherence to the surface antigens of RAOEC was determined using ELISA (Figure 9.1 B). The ELISA procedure described in Section 3.2.4.2 was followed with modifications described below. Attachment factor solution treated (32 µl/well, 4°C overnight) Nunc Maxisorp F96 plates were seeded with 7000 cells/well at six passages in 100 µl growth medium. The plates were incubated at 37ºC with 5% $CO_2$ until ~100% confluent. After overnight serum starvation of cells in 100 µl HBSS, the cells were fixed in 100 µl of 4% paraformaldehyde at 25°C for 15-30 min. After 3 washes with PBS (pH 7.4), 1% triton-PBS (Appendix 1) was used to enhance cell permeabilisation for 30 min in a plate shaker at 150 rpm and 37ºC. After washing, 100 µl of pooled serum from rats injected with rM5 or Stg480 or PBS was added at 1:6400 dilution (titrated by several initial experiments) in 5 replicates and incubated overnight at 4°C. After washing, goat anti-rat IgG (H+L) conjugated with horseradish-peroxidase was added at 1:5000 dilution for 2 h at 37°C. After washing, 2-2'–azino-di(3-ethylbenzthiazoline)-6-sulphonate (ABTS) was added for 30 min before the optical density (OD) was measured at

405 nm. A negative serum sample from rats injected with PBS was included as a control. The OD values of sera from rats injected with GAS rM5, GGS Stg480 and PBS were compared.

### 9.2.9 Flow cytometry for detection of surface VCAM-1/ICAM-1 expression

Nunc Maxisorp 6-well plates previously treated with AFS (1 ml/well) were seeded with RAOEC (10000 cells/well) at six passages and grown until ~80% confluent (Figure 9.1 C). After overnight serum starvation of cells in 1 ml HBSS, the cells were stimulated with 1 ml of 5% heat inactivated (56°C 30 min) serum or $10^6$ splenocytes (after *in vitro* expansion with GAS rM5 or GGS Stg480, Section 3.2.4.1) from rats injected with GAS rM5 or GGS Stg480 for 6 h. In a separate experiment, to determine whether rM5 and Stg480-specific antibodies contribute to VCAM-1/ICAM-1 expression, RAOEC were incubated with 5% heat inactivated immune sera, which had been pre-absorbed overnight at 4°C with 100 mg/ml rM5 or Stg480 protein. GAS rM5 or GGS Stg480 protein alone were used as control to determine if antigen alone increases VCAM-1/ICAM-1 expression. Unstimulated RAOEC and the cells stimulated with 5% heat inactivated sera or $10^6$ splenocytes from rats injected with PBS were used as negative controls. Cells stimulated with 10 ng/ml of TNF-α were used as a positive control. All samples were tested in triplicate wells and experiments were repeated twice on different days.

After 6 h of stimulation, RAOEC were washed in staining buffer (PBS/2% FBS/0.05% $NaN_3$, pH 7.4) and harvested using 0.2% EDTA/PBS solution at room temperature. The cells ($10^6$ per tube) were stained for 30 min on ice with mouse anti-rat CD31-FITC (1 µg/$10^6$ cells) to detect endothelial cell marker PECAM-1 or mouse IgG-FITC isotype control, mouse anti-rat CD106-PE (0.5 µg/$10^6$ cells) to detect adhesion molecule VCAM-1 or mouse IgG-PE isotype control and mouse anti-rat CD54-biotin (0.25 µg/$10^6$ cells) to detect adhesion molecule ICAM-1 or mouse IgG-APC isotype control. After washing in staining buffer, streptavidin APC (0.25 µg/$10^6$ cells) was added for 30 min to stain CD54 i.e the ICAM-1 molecule. After washing, cells were resuspended in sheath fluid and immediately subjected to flow cytometry. Data were acquired using a BD FACSCanto II flow cytometer using BD FACSDiva 8.0.1 software. Cell debris, characterised by low forward and side scatter, were excluded from analysis and cells stained with isotype control antibodies were used to set VCAM-1/ICAM-1 positive gates. For each sample, 100,000 cell events were recorded. Data was analysed using two-dimensional dot plots or histograms. The percentage cells positive

for each adhesion molecule and the median fluorescence intensity for both adhesion molecules were determined for the CD31+ gated cells.

### 9.2.10 Immunohistochemistry for detection of VCAM-1/ICAM-1 in heart tissues from M-protein injected rats

All immunohistochemistry procedures were carried out at room temperature using Tris-buffered saline (TBS, pH 7.4) (Appendix 1) for all washing steps. Excised hearts were fixed in 10% neutral buffered formalin for <24 h, processed, embedded in paraffin wax and sectioned (5 μm thickness) as described previously (Section 3.2.5) Sections were deparaffinised in xylene with 2 changes for 5 min each, dehydrated with graded ethanol and rinsed with distilled water. Endogenous peroxidase was blocked with 0.3% (w/v) $H_2O_2$ in methanol for 30 min. Sections were rinsed in TBS 3 times for 5 min each time and incubated with 10% normal bovine serum in TBS for 30 min. Excess serum was removed without rinsing, and sections were incubated 1 h at room temperature with primary antibody against CD106 (mouse anti-rat CD106 unconjugated) and CD54 (mouse anti-rat CD54-biotin conjugated) at 1:100 dilution in TBS (Figure 9.1 D). After washing, CD106 treated sections were incubated with goat anti-rat secondary antibody HRP at 1:100 dilution and CD54 treated sections were incubated with ABC-peroxidase solution for 30 min at room temperature. After washing, positive staining was visualised with DAB for 1-3 min. Haematoxylin for 1 min was used as background stain before examination under microscope (*BX43 Olympus*). The percentage of positive staining in the myocardium using a representative section per rat was determined on the digital images using the CellSens image analysis software® (*Olympus*). Histological analysis of each tissue was conducted on a representative section. To determine the extent of VCAM-1/ICAM-1 expression, a minimum of 3 images of each heart section of each rat were taken at the 1000× magnification.

### 9.2.11 T-cell transmigration assay

The experimental design is shown in Figure 9.1 E. Transwell plate inserts were seeded with $6.7\times10^5$ RAOEC/well (six passage) and grown until 100% confluent followed by overnight serum starvation with HBSS. To activate RAOEC, 100 μl of 5% heat inactivated serum from rats injected with GAS rM5 or GGS Stg480 was added. In a separate experiment, 5% heat inactivated serum pre-adsorbed with rM5 or Stg480 was used to detect rM5 and Stg480 specific antibody induced T-cell migration. The positive control cells were treated with 10 ng/ml of TNF-α. The untreated cells and cells treated with 5% heat inactivated serum PBS

injected rats were used as the negative controls. Rat T-cell chemoattractant CXCL9 (100 ng/ml in 600 µl of RPMI) or RPMI only as vehicle was provided to the wells of the lower chamber of the Transwell plate.

Splenic MNCs (after *in vitro* expansion with GAS rM5 or GGS Stg480 for 72 h, Section 3.2.4.1) from rats injected with GAS rM5 or GGS Stg480 or PBS were enumerated using a Neubauer haemocytometer (Section 3.2.2.3) and added to the respective upper chambers (PBS cells to PBS sera treated well, rM5 cells to the rM5 sera treated well and Stg480 cells to Stg480 sera.) at approximately $10^6$ cells per well in 200 µl RPMI. An aliquot of 200 µl of each cell suspension containing approximately $10^6$ MNCs from rats injected with PBS, rM5 or Stg480 was stained retrospectively with anti-rat CD3-FITC to provide a precise count of the number of CD3+ T-cells actually added from each of the three different MNC suspensions (i.e. from PBS-, rM5- or Stg480-injected rats). The total number of T-cells added in the upper chamber was 180,781 for PBS, 564,718 for rM5 and 594,150 for Stg480. After 6 h of incubation at 37°C and 5% $CO_2$, the transmigrating T-cells were collected from the lower chamber. After washing in staining buffer, the cells were stained for 30 min on ice with mouse anti-rat CD3-FITC (0.5 µg/$10^6$ cells) to detect T-cells or mouse IgG3-FITC as the isotype control and enumerated using 123count$^{TM}$ eBeads and flow cytometry as described in Section 9.2.7. Data were acquired using a BD FACSCanto II flow cytometer using BD FACSDiva 8.0.1 software. One hundred thousand cell events were recorded for each sample. To analyse the data, the percentage of T-cells migrating across the endothelial monolayer was calculated as: number of T-cells added to upper chamber/ number of T-cells collected from lower chamber × 100.

### 9.2.12 Statistical analysis

The data distribution of OD values, percentage of VCAM-1/ICAM-1 and CD3+ cells, and percentage of DAB stained area was checked using GraphPad Prism 7 statistical software. All the data from experimental and control groups passed D'Agostino & Pearson omnibus normality test and therefore were compared and tested using one-way analysis of variance (ANOVA) with Tukey's post hoc multiple comparisons test. The results are reported as mean ± standard error (SEM), $p \leq 0.05$ was considered significant.

## 9.3 RESULTS

The results of interactions between GAS rM5 or GGS Stg480 specific antibodies and/or splenocytes and rat endothelial cells are described in this chapter. The results of repeat experiments are provided in Appendix 9. The details of statistical analysis are also provided in Appendix 9.

### 9.3.1 GAS and GGS M-protein antibodies bind to endothelial cells

In this study, we investigated whether sera from rats injected with GAS and GGS M proteins could bind to RAOECs. Significantly higher IgG binding was observed in the sera from rats injected with GAS rM5 or GGS Stg480 compared to PBS injected control rats (Figure 9.1). The IgG reactivity in immune sera was reduced significantly following adsorption with the corresponding injecting antigen, indicating that antibody-antigen binding was via the antigen binding region of the antibody, rather than interactions between the Fc region.

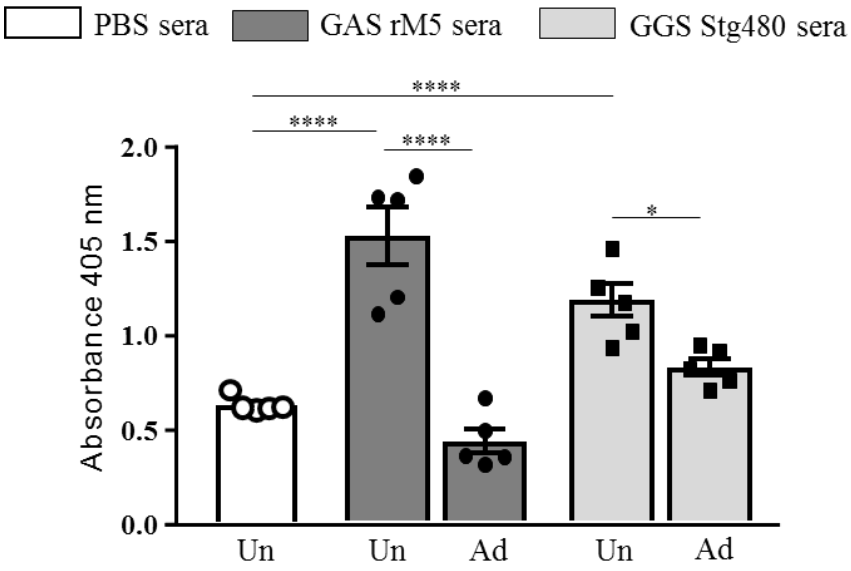


**Figure 9.3** GAS and GGS M-protein specific antibodies bind to the surface antigens of RAOEC in an In-cell ELISA. Pooled heat inactivated sera from rats injected with GAS rM5 (n=3) and GGS Stg480 (n=3) bound to endothelial cells and showed significantly higher absorbance values compared to PBS injected control rats (n=3). Antibody binding to endothelial cells reduced significantly after adsorption of GAS rM5 pooled serum with GAS rM5 and adsorption of GGS Stg480 pooled serum with Stg480. Error bars represent standard errors of the mean (SEM). Statistical differences were determined using one-way ANOVA with Tukey's post hoc multiple comparisons test; *$p<0.05$, ****$p<0.0001$. Un: unadsorbed, Ad: adsorbed.

### 9.3.2 GAS and GGS M-protein specific antibodies and splenocytes induce expression of endothelial cell adhesion molecules in cultured endothelial cells

VCAM-1 and ICAM-1 expression increased in endothelial cells stimulated with 5% heat inactivated serum from GAS rM5 or GGS Stg480 injected rats compared to cells stimulated with non-immune serum (Figure 9.4 B and Figure 9.5 B) although the difference in GAS rM5 serum induced ICAM-1 expression was not significant. Moreover, sera from rM5 injected rats pre-adsorbed with rM5 protein, resulted in partial reduction of VCAM-1 and ICAM-1 expression. Similarly, sera from Stg480 injected rats pre-adsorbed with Stg480 protein also resulted in reduction of ICAM-1 expression. VCAM-1 and ICAM-1 expression was also higher in endothelial cells stimulated with splenocytes from GAS rM5 and GGS Stg480 injected rats alone, or together with the corresponding heat inactivated serum (Figure 9.4 C-D and Figure 9.5 C-D). GAS rM5 or GGS Stg480 protein alone did not induce VCAM-1 or ICAM-1 expression. TNF-α addition (positive control) resulted in significant upregulation of both VCAM-1 and ICAM-1.

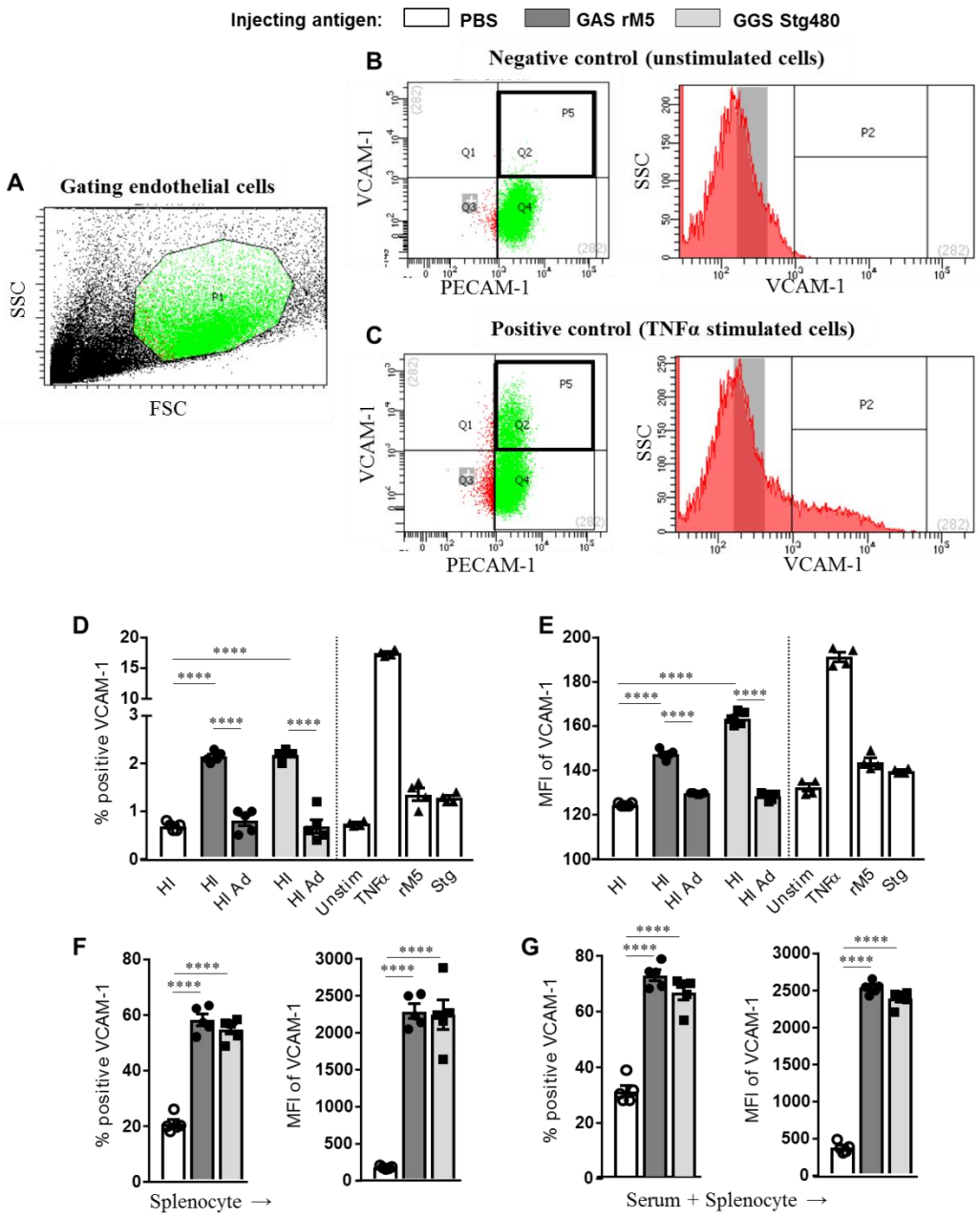


**Figure 9.4** GAS and GGS M-protein specific antibodies and splenocytes induce expression of VCAM-1 in endothelial cells. (A) Dot plot showing the gating strategy used to determine the percentage of VCAM-1 positive endothelial cells. Unstimulated endothelial cells (negative control) showed low VCAM-1 expression (B, D&E). However, TNF-α stimulation (positive control) increased expression of VCAM-1 (C, D&E). Heat inactivated (HI) pooled serum from rats injected with GAS rM5 and GGS Stg480 induced VCAM-1 expression in a larger percentage of endothelial cells compared to serum from PBS injected control rats (D&E). VCAM-1 expression reduced after adsorption of GAS rM5 serum with GAS rM5 and GGS Stg480 serum with Stg480 (HI ad). The addition of rM5 or Stg480 M-proteins to endothelial cells did not influence endothelial cell VCAM-1 expression (D&E). Significantly higher expression of VCAM-1 was observed in the RAOEC stimulated with splenocytes from rats injected with GAS and GGS M-protein compared to controls (F) or when splenocytes and sera were added together (G). Error bars represent standard errors of the mean (SEM). Statistical differences were determined using one-way ANOVA with Tukey's post hoc multiple comparisons test; ****$p<0.0001$.

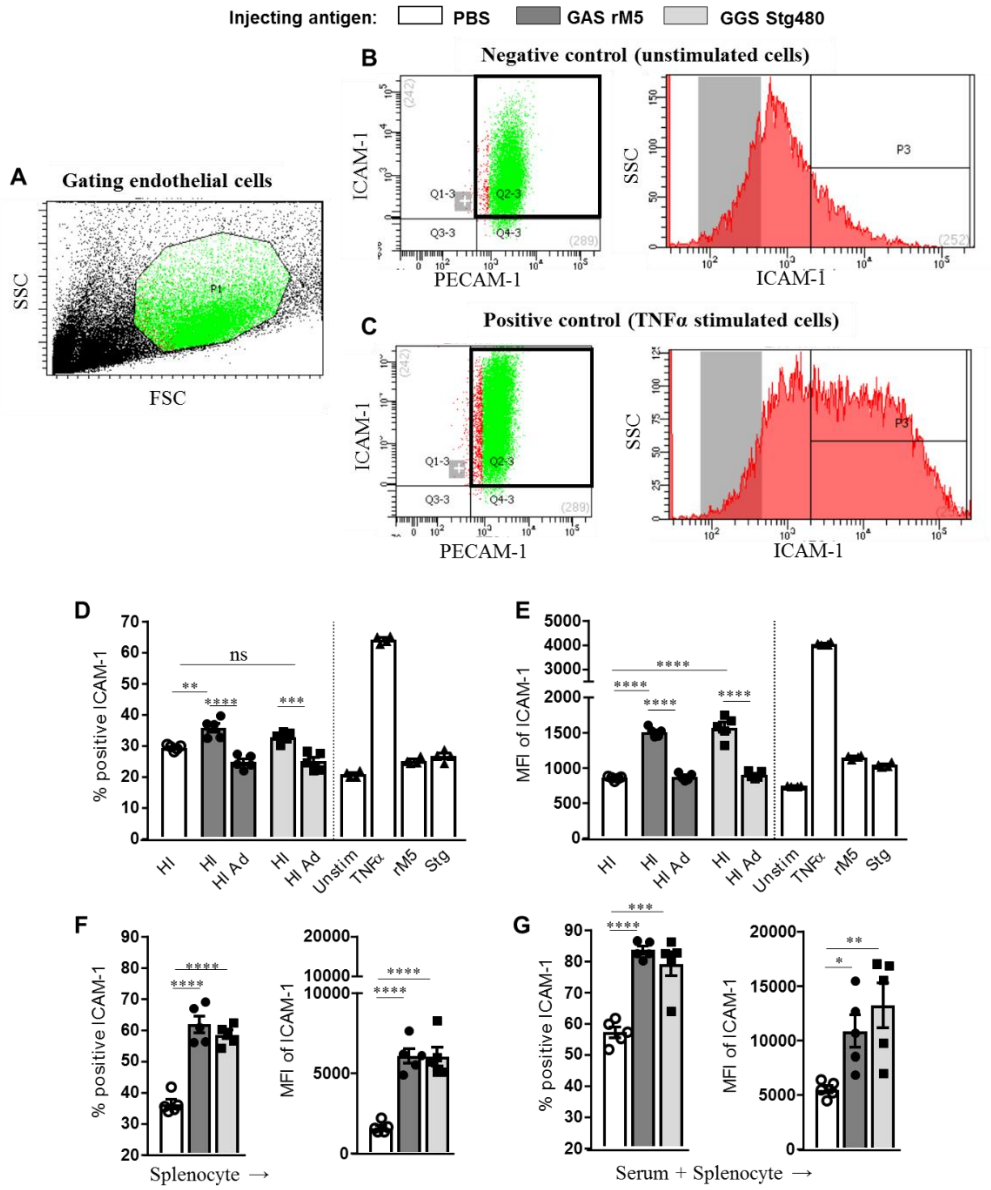


**Figure 9.5** GAS and GGS M-protein specific antibodies and splenocytes induce expression of ICAM-1 in endothelial cells. (A) Dot plot showing the gating strategy used to determine the percentage of ICAM-1 positive endothelial cells. Unstimulated endothelial cells (negative control) showed low ICAM-1 expression (B, D&E). However, TNF-α stimulation (positive control) increased expression of ICAM-1 (C, D&E). Heat inactivated (HI) pooled serum from rats injected with GAS rM5 and GGS Stg480 induced ICAM-1 expression in a larger percentage of endothelial cells compared to serum from PBS injected control rats (D&E). ICAM-1 expression reduced after adsorption of GAS rM5 serum with GAS rM5 and GGS Stg480 serum with Stg480 (HI ad). The addition of rM5 or Stg480 M-proteins to endothelial cells did not influence endothelial cell ICAM-1 expression (D&E). Significantly higher expression of ICAM-1 was observed in the RAOEC stimulated with splenocytes from rats injected with GAS and GGS M-protein compared to controls (F) or when splenocytes and sera were added together (G). Error bars represent standard errors of the mean (SEM). Statistical differences were determined using one-way ANOVA with Tukey's post hoc multiple comparisons test; *p<0.05, **p<0.01, ***p<0.001, ****p<0.0001, ns: not significant.

### 9.3.3 VCAM-1 and ICAM-1 expression is up-regulated in heart tissues of M-protein injected rats

Heart sections from rats were immunostained (Figure 9.6&9.7) and examined to ascertain whether the endothelial lining of mitral valves and myocardium express VCAM-1 and ICAM-1. Only small numbers of VCAM-1 and ICAM-1 positive cells were observed in the lining of mitral valves from rats injected with GAS rM5 (Figure 9.6 D&E) or GGS Stg480 (Figure 9.6 G&H). No VCAM-1 or ICAM-1 positive cells were observed in the mitral valve sections from control rats injected with PBS (Figure 9.6 A&B). Sections stained with isotype control antibodies (Figure 9.6 C, F&I) showed no staining.

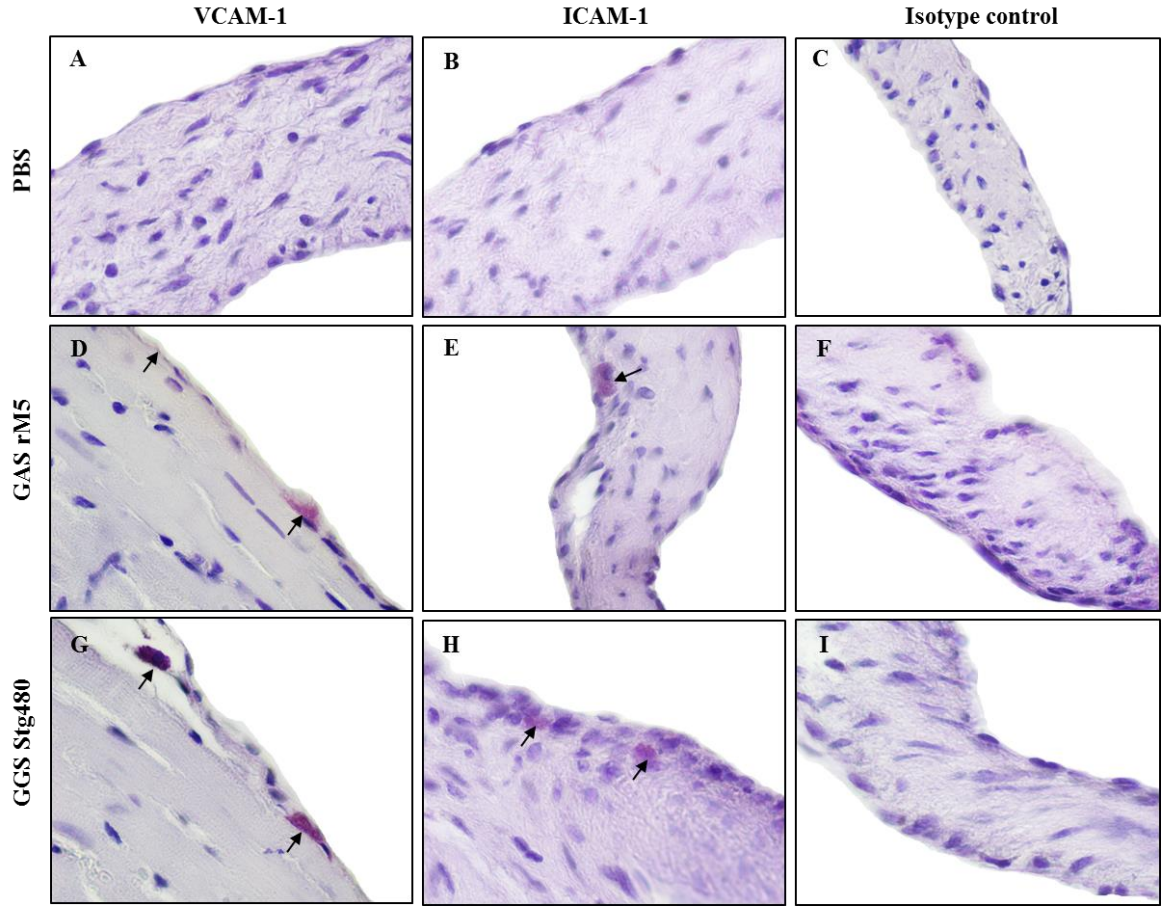


**Figure 9.6** GAS and GGS M-protein injection induces adhesion molecule expression in mitral valves. VCAM-1 and ICAM-1 levels in paraffin sections of heart tissue were assessed by immunohistochemical staining with monoclonal antibodies to VCAM-1 and ICAM-1. VCAM-1 and ICAM-1 stained cells were found in the mitral valve sections of rats injected with GAS rM5 (n=3) and GGS Stg480 (n=3), whereas absent in control rats (n=3). (A-I) Panels show representative sections from each rat groups. Mitral valve sections from rats injected with PBS (A-C) had no evidence of VCAM-1 or ICAM-1 positive cells. Isotype control antibody stained sections from all rat groups also had no positive cells. Valve sections

from rats injected with GAS rM5 and GGS Stg480 and stained with VCAM-1 and ICAM-1 antibodies had positive cells indicated by arrows (D&E, G&H). Magnifications 1000×.

VCAM-1 and ICAM-1 staining was observed within the myocardium of GAS rM5 and GGS Stg480 injected rats, mainly surrounding the blood vessels and endocardial lining (Figure 9.7 E&F and H&I). The myocardium sections from control rats injected with PBS (Figure 9.7 B&C) and the sections stained with isotype control antibodies (Figure 9.7 D, G&J) had no staining. The percentage of VCAM-1/ICAM-1 stained area was found higher in the myocardium sections from rats injected with GAS rM5 or GGS Stg480 compared to PBS injected control rats (Figure 9.7 A).

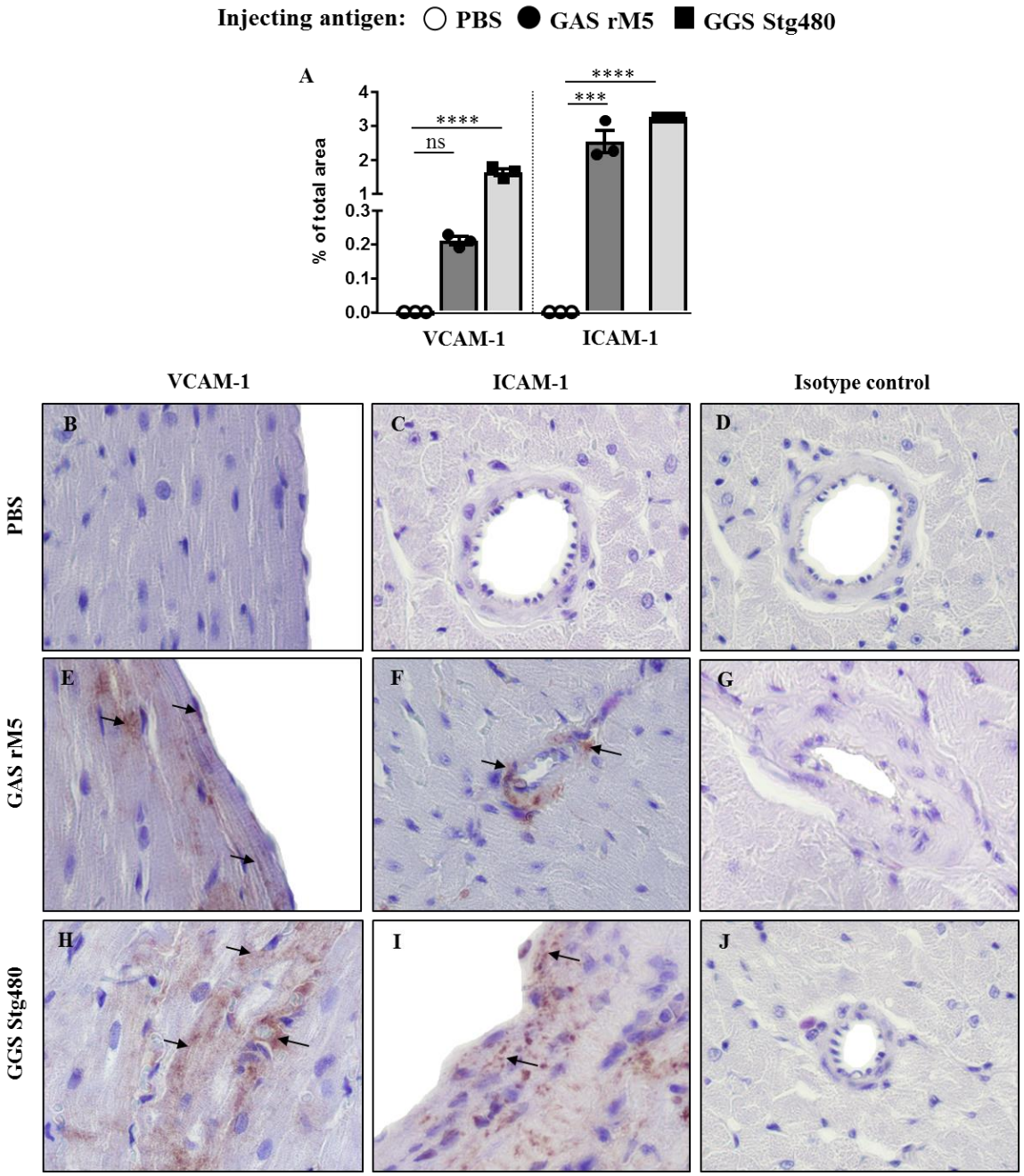


**Figure 9.7** GAS and GGS M-protein injection induces adhesion molecule expression in myocardium. (A) Graphs depict total VCAM-1 and ICAM-1 staining in all myocardium sections examined in the group as a percentage of total pixels. VCAM-1 and ICAM-1 staining were found higher in the myocardium sections of rats injected with GAS rM5 (n=3) and GGS Stg480 (n=3) mainly around blood vessels and endocardial lining compared to control rats (n=3). (B-J) Panels show representative myocardium sections from each of the rat groups. Myocardium sections from rats injected with PBS (B-D) had no evidence of VCAM-1 or ICAM-1 positive cells. Isotype control antibody stained sections from all rat groups had no positive cells. Myocardium sections from rats injected with GAS rM5 and GGS Stg480 and stained with VCAM-1 and ICAM-1 antibodies had positive cells indicated by arrows (E-F, H-I). Magnification is 1000×. Error bars represent standard errors of the mean (SEM). Statistical differences were determined using one-way ANOVA with Tukey's post hoc multiple comparison test; ***p<0.001, ****p<0.0001, ns: not significant.

### 9.3.4 GAS and GGS M-protein specific antibodies facilitate migration of T-cells across endothelial cells

A significantly higher percentage of T-cells migrated across the endothelial monolayer and into the lower chamber when wells were stimulated with serum from rM5- or Stg480-injected rats (Figure 9.8 B). This T-cell migration was reduced after pre-adsorption of serum with the respective injecting antigen. In contrast, far fewer T-cells migrated in wells stimulated with serum from PBS injected rats and in wells lacking stimulant. As expected, T-cell migration was greatest in wells with TNF-α added.

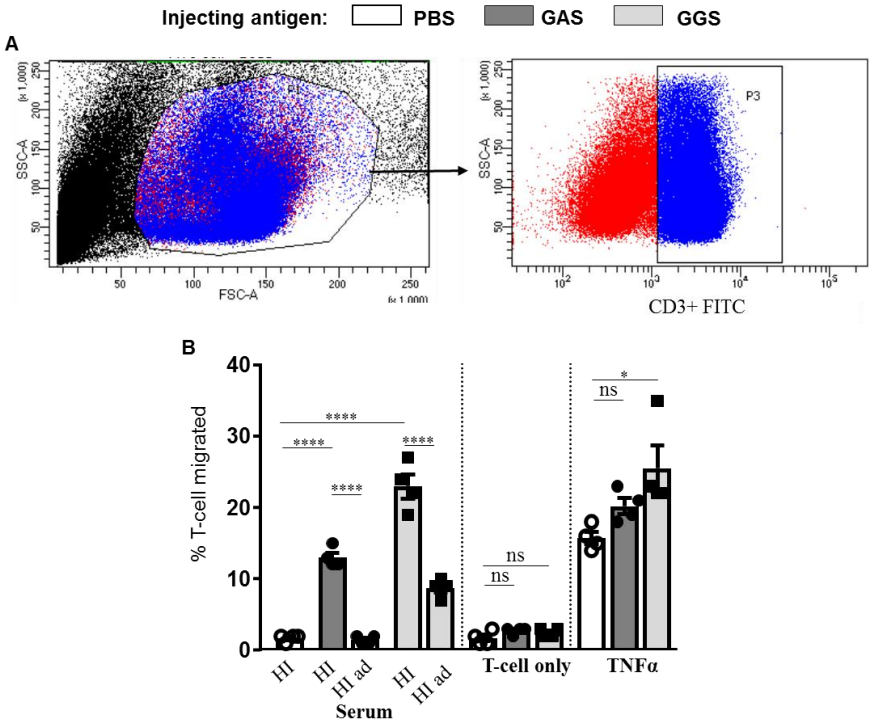


**Figure 9.8** GAS and GGS M-protein specific antibodies induce T-cell migration across endothelial cell monolayers. Splenic MNCs from rats injected with rM5/Stg480/PBS was enumerated using Neubauer haemocytometer and $10^6$ cells were added to the respective upper chambers. The actual number of CD3+ T-cells provided in the upper chamber was enumerated using 123count$^{TM}$ eBeads and flow cytometry. Heat-inactivated serum from rats injected with rM5/Stg480/PBS was added (rM5 serum to rM5 T-cell etc.) to the endothelial monolayer in upper chamber. Pooled serum from rM5 infected animals, pre-adsorbed with rM5 and pre-adsorbed serum from Stg480 injected rats was added in separate wells. Rat chemoattractant CXCL9 was added to the lower chambers. After 6 h of incubation, the total number of T-cells in the lower chamber was counted using 123count$^{TM}$ eBeads. (A) A representative dot plots show gating of MNCs in gate P1 and CD3+ T-cells in gate P3. (B) Heat inactivated (HI) sera from rM5- or Stg480-injected rats induced significantly higher T-cell migration to the lower chamber compared to the HI serum from PBS injected control rats. Pre-adsorption of rM5 serum (HI ad) with rM5 and Stg480 proteins significantly reduced T-cell migration. Few T-cells crossed the unstimulated endothelial monolayer (T-cell only). Stimulation of the endothelial monolayer with TNF-α (positive control) allowed the

highest T-migration. Error bars represent standard errors of the mean (SEM). Statistical difference by one-way ANOVA with Tukey's post hoc multiple comparisons test; *$p<0.05$, ****$p<0.0001$, ns: not significant.

## 9.4 DISCUSSION

The immunopathogenesis of ARF/RHD has not been completely elucidated but existing data suggests that it involves the generation of antibodies against group A streptococcal (GAS) M-protein or carbohydrate antigen N-acetyl-glucosamine, cross-reacting with antigens on the surface of heart endothelial cells. In the current study, we did not investigate precisely which endothelial cell antigens are targeted by GAS/GGS M-proteins specific antibodies and splenocytes. We did however show that anti-M protein antibodies and splenocytes could indeed activate VCAM-1 and ICAM-1 and that this interaction was significantly decreased when sera were absorbed with M protein, suggesting that anti-M protein antibodies are reactive with endothelial cell antigens. Identification of the endothelial target antigen/s was beyond the scope of the current study. It has been hypothesised that antibody or complement binding to the surface of heart endothelial cells, induces an activated endothelial cell phenotype and even damage to the integrity of the endothelium. Endothelial cells lining the heart valves and blood vessels within the myocardium and endocardium become activated, showing increased expression of cell adhesion molecules (CAMs) (Roberts, et al. 2001). The adhesion molecules, VCAM-1, ICAM-1, and endothelial selectin (E-selectin) are expressed on the vascular endothelium serve as ligands for counter-receptors on circulating inflammatory cells. The roles of the LFA-1/ICAM-1 and VLA-4/VCAM-1 pathways in recruiting leukocytes, especially T-cells into tissues have been studied previously (Springer 1995; Sprent, et al. 1997; Rose, et al. 2002; Anderson and Siahaan 2003). They are critical in the targeting of circulating leukocytes to sites of inflammation, in the transmigration of leukocytes across vascular endothelium, and in immune effector functions (Hafez, et al. 2013). The accumulation of leukocytes in the valves and myocardium, results in granulomatous inflammation in these tissues (Roberts, et al. 2001). Damage to cardiac tissues by this initial inflammation has been proposed to release intracellular host antigens including cardiac myosin as new targets of the ongoing autoimmune response.

In the current study, the ability of GAS and GGS specific antibodies and T-cells to activate endothelial cells was investigated using rat endothelial cell monolayers to model the heart endothelium. Furthermore, we investigated whether the activated endothelial layer influenced T-cell transmigration, thereby modelling the recruitment of Ag-specific T-cells into cardiac

tissues in RHD. It was found that serum IgG from rats injected with GAS rM5 or GGS Stg480 protein were able to bind to rat endothelial cells (Figure 9.3). We showed that adsorption of immune sera with M-protein antigens reduced IgG binding indicating that antibody binding was via the antigen binding domain rather than the Fc region of the antibody and subsequent engagement of Fc receptors on endothelial cells. This result supports the current hypothesis that an early event in RHD pathogenesis involves antibody binding to an unknown antigen on the surface of endothelial cells (Roberts, et al. 2001). The results of this experiment are similar to those reported by Del Papa and Colleagues (1999) who observed that serum IgG from systemic lupus erythematosus (SLE) patients bound to human umbilical vein endothelial cell (HUVEC) monolayers. These authors suggested that in SLE the adhesion of monocytes to endothelial cells was initiated by antibodies and followed by upregulation of E-Selectin, ICAM-1, VCAM-1 expression (Del Papa, et al. 1999). Another study reported that aberrations in endothelial cell adhesive interactions occur in patients with autoimmune rheumatic diseases due to overexpression of adhesion molecules (Sfikakis and Tsokos 1995). Future studies could investigate the subsequent steps in endothelial cell activation i.e. how antibodies binding to antigens on the cell surface trigger signalling cascades that induce endothelial cell activation.

In ARF/RHD, expression of CAMs is necessary for the recruitment of pathogenic T-cells to heart tissues (Roberts, et al. 2001). It has been hypothesised that IgG antibodies to GAS or pro-inflammatory cytokines, such as TNF-α or IFN-γ secreted by antigen-activated T-cells, react with the heart endothelium to trigger upregulation of VCAM-1 on the endothelial surface, leading to T-cell infiltration into heart tissues (Chopra, et al. 1988; Roberts, et al. 2001; Tandon, et al. 2013). In the current study, antibodies specific to GAS rM5 and GGS Stg480 induced upregulation of VCAM-1 in rat endothelial cells (Figure 9.4 D&E). All sera were heated prior to experiments, to inactivate complement proteins and therefore exclude their role in endothelial cell activation. Prior adsorption of sera with M-protein antigens diminished the activating effect of immune sera on VCAM-1 expression, again demonstrating antibody binding and subsequent endothelial cell activation was via the IgG antigen binding region. As expected, the positive control TNF-α induced significant upregulation of VCAM-1. M-proteins alone were unable to induce upregulation of VCAM-1. These results confirmed that VCAM-1 upregulation in endothelial cells was due to specific antibody binding rather than complement mediated activation, or influenced by M-proteins directly. The results

support the findings of Gorton, et al. (2016) who reported increased VCAM-1 expression by RAOEC following stimulation with 2% heart inactivated serum from GAS rM5 immunised rats. VCAM-1 interacts with VLA-4 of circulating antigen specific T-cells to facilitate extravasation (Brunner, et al. 2013).

We also observed the splenocyte suspensions restimulated with GAS and GGS M-protein also induced upregulation of VCAM-1 compared to splenocytes from control animals (Figure 9.4 F). The result implies that activated T-cells can themselves influence the endothelium. When splenocytes and serum were added together, VCAM-1 expression was further increased, compared to addition of only antibodies or splenocytes alone (Figure 9.4 G). The results suggest that antibodies and activated T-cells favour each other to enhance endothelial cell activation.

We observed significantly higher ICAM-1 expression in endothelial cells stimulated with antibodies and/or T-cells from rats injected with GAS rM5 or GGS Stg480 proteins compared to PBS injected control rats (Figure 9.5 D-G). Reduced ICAM-1 expression on endothelial cells incubated with adsorbed sera indicated that the antibody binding was via the Fab portion of IgG. Significantly higher ICAM-1 expression following TNF-α stimulation was anticipated as this was used as the positive control. M-proteins alone did not induce ICAM-1, indicated that the upregulation of ICAM was mediated by antibodies and/or T-cells specific to M-proteins. These results confirmed that ICAM-1 upregulation was due to specific antibody binding rather than complement mediated activation. Moreover, ICAM-1 expression was increased when endothelial cells were cultured with GAS and GGS M-protein specific splenocytes (Figure 9.5 F), indicating that activated T-cells can activate the endothelium by themselves. However, ICAM-1 expression was further increased when splenocytes and serum were added together, compared to either serum or splenocytes alone (Figure 9.5 G), suggesting that both antibodies and activated T-cells may work together to enhance endothelial cell activation. In ARF/RHD, ICAM-1 has been evaluated to follow the progression of inflammation, even when clinical and other laboratory test results are normal (Zhang, et al. 2005; Hafez, et al. 2013). Yetkin, et al. (2001) reported a high level of ICAM-1 in the serum of patients with rheumatic mitral stenosis. Increased serum levels of ICAM-1 were observed in patients at the beginning of ARF, with a peak in the active phase followed by a decline during remission to the inactive phase (Yaman, et al. 2003).

In this study, the mitral valve and myocardium sections from rats injected with GAS rM5 and GGS Stg480 were examined to detect *in vivo* expression of VCAM-1 and ICAM-1. Immunostaining of mitral valves from GAS and GGS M-protein injected animals revealed low numbers of VCAM-1 and ICAM-1 positive cells, with no positive staining observed in PBS injected animals. In contrast, sections of the myocardium from M-protein injected rats had increased VCAM-1 and ICAM-1 staining primarily surrounding the blood vessels and in the endocardial lining. Moreover, the cell adhesion molecular expression was higher in the myocardium of rats injected with GGS M-protein compared to GAS M-protein. It is unclear why such differences were observed but this suggests that the GGS M-proteins or the antibodies and T-cells directed to GGS M-proteins might be more able than GAS M-protein to activate endothelial cells to facilitate carditis. No staining was observed in tissues from PBS-injected rats. In a previous study, Kirvan, et al. (2014) reported increased upregulation of VCAM-1 in naïve Lewis rats following passive transfer of an NT5/6-specific T-cell line. In a separate study, Roberts, et al. (2001) reported VCAM-1 expression on the valvular endothelium of patients with valvular heart disease. Benvenuti, et al. (2000) reported similar findings in Chagas disease patients with severe cardiomyopathy.

The migratory abilities of leukocytes are critically dependent on their phenotype and activation state, and shaped by multiple factors including the CAMs, their ligands, and chemoattractant cytokines (Hunt, et al. 1996; Sallusto, et al. 2000; Gerard and Rollins 2001; Moser and Loetscher 2001; Rose, et al. 2002; Marino, et al. 2003; Thomsen, et al. 2003). Although this study did not examine the phenotype of T-cells that crossed the endothelial monolayer, future studies are suggested to demonstrate type of migrated T-cells. In the current study, T-cell transmigration was demonstrated *in vitro* across the endothelial cell monolayer stimulated with serum antibodies from the rats injected with GAS rM5 and GGS Stg480. It was observed that migration was significantly higher for T-cells from M-protein injected than that of the non-immunised T-cells (i.e. PBS injected). We observed significantly higher T-cell migration across the endothelial monolayer stimulated with antibodies from rats injected with GAS rM5 or GGS Stg480 proteins (Figure 9.8). Reduced T-cell migration across endothelial cells incubated with M-protein adsorbed sera indicated that the trafficking of T-cells was facilitated by antibody binding to the endothelial cell. Significantly higher T-cell migration was observed following TNF-α stimulation (positive control) of endothelial monolayers compared to unstimulated monolayers. These results confirmed that T-cell migration to the heart tissues is facilitated by M-protein specific antibody binding to

endothelial cells and subsequent activation of endothelium. The results were supported by Gorton, et al. (2016) who reported increased infiltration of T-cells and macrophages in the myocardium and mitral valve of Lewis rats injected with GAS rM5 protein. Future studies are suggested to demonstrate rM5 or Stg480 specific T-cell adhesion to endothelial cells, transmigration, and infiltration into heart tissues *in vivo* in RAV model and patients with ARF/RHD.

The current study did not analyse the VCAM-1 and ICAM-1 levels in the serum of rats injected with GAS rM5 or GGS Stg480 and endothelial cell culture supernatants following stimulation with rM5 or Stg480 and this could be considered a limitation of our study. The results of this study suggest that the mechanism of pathogenesis in rheumatic carditis begins at the heart endocardium. A significant positive correlation between GAS rM5 and GGS Stg480 specific antibodies and T-cells and cell adhesion molecules was observed. This study was unique in analysing the possible role of antibodies and T-cells in inducing heart lesions. Therefore, further clinical studies should be conducted to identify GAS rM5 or GGS Stg480 specific antibodies and T-cells adhered to the endothelial lining of heart and phenotype of leukocytes migrated into the heart tissues of patients with ARF/RHD. In summary, the present findings support the hypothesis that the heart endothelium is activated by and binds to host antigen specific antibodies and activated T-cells, which then extravasate into the heart tissues potentially driving the inflammation of RHD.

# CHAPTER 10
# GENERAL DISCUSSION AND CONCLUSIONS

Acute rheumatic fever (ARF) and rheumatic heart disease (RHD) are autoimmune mediated diseases of humans caused by undesired immune activity to host tissues following group A *Streptococcus* (GAS) infection of the pharynx or skin. Several epidemiological studies have postulated that group G *Streptococcus* (GGS) might have a similar rheumatogenic potential to GAS and have contributed to the prevalence of ARF and RHD (Sriprakash and Hartas 1996; Haidan, et al. 2000; Davies, et al. 2005; O'Sullivan, et al. 2017). The current project was focused largely to investigate the role of GGS in the development of autoimmune mediated carditis. We investigated whether the response was similar to the immune responses and heart pathology in patients with ARF/RHD using a Lewis rat autoimmune valvulitis (RAV) model. In the current study, the RAV model was used because Lewis rats immunised with rM protein develop the hallmark histological features of human RF/RHD, both in the myocardial and in valvular tissue and these changes are associated with the generation of heart tissue cross-reactive antibodies and T cells. More extensive characterisation of cardiac function in the RAV model may lead to an even greater acceptance of this RAV model amongst researchers working on different aspects of RF/RHD. The studies described herein this thesis provide important scientific information regarding the possible contribution of GGS in causing ARF/RHD in humans.

In children and young adults, ARF/RHD is the major cause of acquired heart disease particularly in the resource poor settings and is responsible for a significant number of child deaths (Remenyi, et al. 2013; Mirabel, et al. 2014). Although ARF/RHD has not been reported for many years in developed countries, discrete records of the disease still exist in Indigenous communities of Australia, New Zealand and many Pacific Island regions (Carapetis, et al. 2005b). A better understanding of the causal agent(s) that contribute to the disease process is important to reduce the burden of ARF/RHD. Understanding the underlying mechanisms involved in the pathogenesis of ARF/RHD will be helpful in taking preventive and therapeutic measures to reduce RHD occurrence. An effective and safe vaccine against streptococci will enable the eradication of RHD and other life-threatening infections caused by the streptococci such as necrotising fasciitis and streptococcal toxic shock syndrome.

The first task undertaken in this project was to explore the possible contribution of group G *Streptococcus* (GGS) in the development of autoimmune mediated carditis in a Lewis rat autoimmune valvulitis (RAV) model. Because GGS is not considered a major human pathogen, although it has many similar characteristics to group A *Streptococcus* or GAS (the only reported trigger for ARF/RHD), we hypothesised that GGS might have similar immunogenic properties to induce antibody and T-cell responses and cause inflammation of the cardiac tissues. We injected Lewis rats with whole-killed (WK) GGS strain NS3396 or GGS M-protein, Stg480. In separate experiments, Lewis rats were primed with Stg480 and boosted with GAS rM5 proteins. GAS rM5 protein has previously been reported to induce carditis in animal model studies (Gorton, et al. 2009; Kirvan, et al. 2014; Gorton, et al. 2016). Alternatively, rats were primed with rM5 and boosted with Stg480.

Classically, throat infection by GAS has been considered a prerequisite for the development of ARF/RHD. However, there are evidence of ARF/RHD to be caused following GAS skin infections (Williamson, et al. 2015; Williamson, et al. 2016; Frost, et al. 2017; Ly, et al. 2017; Suzuki, et al. 2017). To mimic the development of ARF/RHD following skin infections with GAS and/or GGS we injected Lewis rats through the subcutaneous route. However future studies are necessary to demonstrate immune responses to streptococcal and host proteins and development of carditis following pharyngeal infection of GGS.

We report here that WK-GGS or Stg480 protein independently or together with WK-GAS and GAS rM5 induce mitral valvulitis and myocarditis as evidenced by histological examination. This was confirmed by the presence of mitral valvular functional changes and myocardial conduction abnormalities indicated by prolonged P-R intervals using ECG and echo of rats. The antibodies and T-cells from the rats injected with WK-GGS or Stg480 also recognise WK-GAS and rM5 protein. Additionally, these antibodies also could recognise porcine cardiac myosin that has 97% amino acid sequence homology with human cardiac myosin. In ARF/RHD, antibody cross-reactivity between GAS M-proteins and human cardiac myosin is considered as the key event in the development of heart damage (Cunningham 2006; Carapetis, et al. 2016). Together these results indicate that GGS has a similar potential to GAS to trigger carditis. In addition, a recent clinical case study reported RHD in a child with a previous history of group C streptococcal pharyngitis (Chandnani, et al. 2015). Therefore, future studies are suggested to identify other non-group A streptococci that have potential to cause chronic rheumatic carditis. Moreover, isolation and identification of GGS

M-protein specific antibodies and memory T-cells from the serum and heart sections of patients with ARF/RHD are necessary to confirm the link between GGS and RHD. Identification of immunogenic peptides of GAS and GGS having shared cardiogenic epitopes, is proposed to develop a more precise serological assay for evidence of preceding GAS/GGS infection. This will also help to develop an effective vaccine to reduce the prevalence of RHD and other deadly streptococcal infections.

Cytokines reveal the phenotype of immune cells involved in a disease process. In ARF/RHD, majority of the T-cells isolated from the heart valves and myocardium of patients was IFN-γ and IL-4 producing respectively (Guilherme, et al. 2004; Fae, et al. 2006; Guilherme and Kalil 2007; Guilherme, et al. 2011a). Interferon (IFN)-γ helps to recruit macrophages. Higher number of IFN-γ producing T-cells in the mitral valve represented the progression of inflammation and fibrosis. However, predominated IL-4 producing T-cells in the myocardium represented myocardial healing as IL-4 has a regulatory effect (Bilik, et al. 2016). In another study, high concentrations of IL-17 in the serum of Lewis rats injected with inactivated GAS and high expression of IL-17 in the mitral valves of rats and human patients was observed (Wen, et al. 2015). Interleukin (IL)-17 is important in autoimmune diseases where fibrosis is a sequela. High amount of IFN-γ and IL-17A in our study suggest that IFN-γ/IL-17A might be an important pathway to T-cell recruitment to the heart tissues. Therapy aimed at neutralising the effect of these two inflammatory cytokines or enhancement of IL-4 secretion may have potential in preventing the progression of carditis leading to congestive cardiac failure.

Another aim of this project was to establish whether it was possible to passively transfer carditis to naïve syngeneic rats using serum and/or memory T-cells from GAS rM5 injected rats. Subsequently to determine whether these cells traffic to the heart or the antibodies facilitate host immune cell migration to develop carditis. We observed that the recipient rats had inflammation of the mitral valve and myocardium and developed lesions similar to patients with ARF/RHD. However, further *in situ* studies are warranted to identify the inflammatory cells involved in carditis using specific markers, and to understand whether these autoreactive T-cells are from the donor or host rats. One limitation of this study was we were unable to monitor carditis at different time points following passive transfer. This would have enabled us to determine the source of the migrated T-cells, role of antibodies, and time taken to develop carditis. Understanding the antibodies and T-cells that contribute to the

disease process will be essential for designing immunotherapeutic approaches aimed at neutralising or removing the deleterious antibodies or T-cells.

Using *in vivo* experiments, the central role of antibodies and T-cells from rats injected with rM5 or Stg480 proteins, in the activation of endothelial cells and upregulation of adhesion molecules (CAMs) and facilitation of T-cell migration was investigated. Expression and upregulation of CAMs, for example VCAM-1 and ICAM-1 was also studied *in vivo* using rat heart sections. The findings indicated that both the antibodies and T-cells independently could induce upregulation of VCAM-1/ICAM-1. Therefore, we propose that the heart damage in RHD might be mediated by direct interaction of antigen specific effector T-cells to the heart endothelium (Figure 10.1). Alternatively, antigen specific antibodies mediate endothelial cell activation followed by transmigration of T-cells. Advanced studies demonstrating dynamics of CAMs expression at different dosages/concentrations of antibodies and T-cells are suggested. Monitoring CAMs concentration in serum from rats and endothelial cell culture supernatants stimulated with antibodies and/or T-cells could mimic clinical studies to identify markers of heart damage progression (Yetkin, et al. 2001; Yaman, et al. 2003; Zhang, et al. 2005; Hafez, et al. 2013). Neutralisation of VCAM-1 or ICAM-1 may also have therapeutic potential by blocking the pathway of T-cell trafficking to the heart tissues.

The currently accepted mechanism of rheumatic carditis involves generation of antibodies against GAS carbohydrate N-acetylglucosamine (GlcNAc) or M-protein that bind with endothelial cells in the endocardium of the heart (Goldste1N, et al. 1967; Dudding and Ayoub 1968; Cunningham, et al. 1986; Galvin, et al. 2002; Carapetis, et al. 2016; Gorton, et al. 2016; Guilherme, et al. 2017). Antibody binding to endothelial cells induces upregulation of VCAM-1 that subsequently binds with activated T-cells via very late antigen (VLA)-4 and facilitates migration of T-cells into heart tissues (Yamauchi, et al. 2004; Carapetis, et al. 2016). However, our findings propose that the activated T-cells against GAS or GGS M-protein also have an independent potential to activate endothelial cells and to induce upregulation of VCAM-1 and ICAM-1 in addition to GAS/GGS specific antibodies (Figure 10.1). A recent clinical study reported the occurrence of ARF/RHD following GGS pharyngitis supporting our hypothesis (O'Sullivan, et al. 2017). The VCAM-1/VLA-4 and ICAM-1/LFA-1 binding may facilitate transmigration of M-protein specific T-cells into the valve and myocardium tissues.

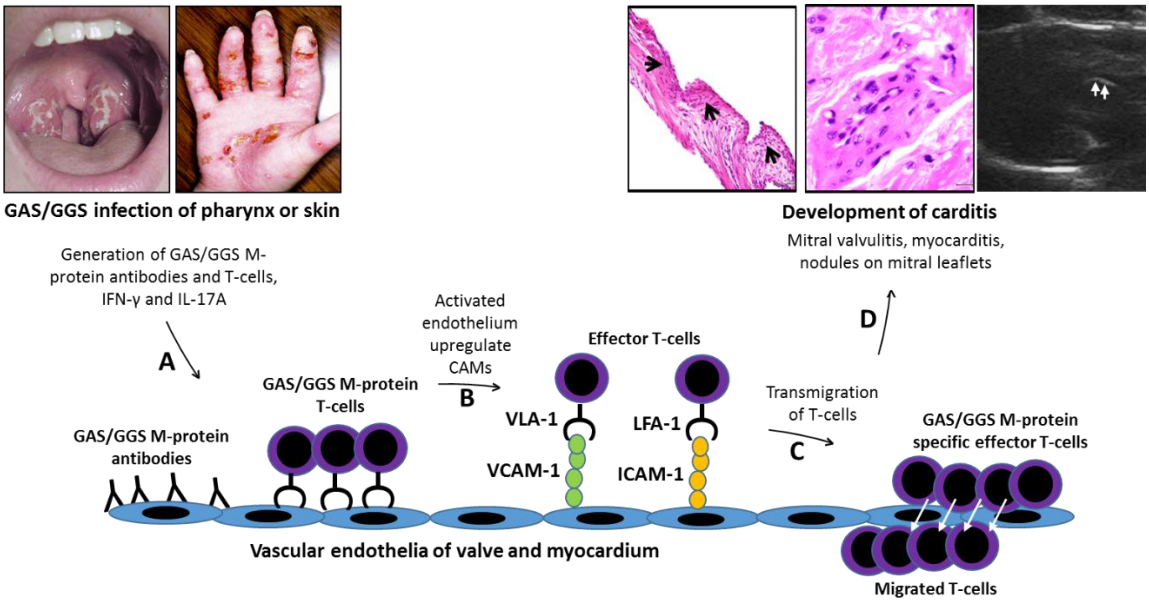


**Figure 10.1** Proposed mechanism of development of carditis in ARF/RHD. (A) The antibodies and/or T-cells generated following GAS/GGS infection of pharynx or skin bind with vascular endothelial layer of the valve and myocardium and activate endothelium. IFN-γ and IL-17A mediate T-cell reactivity with endothelial cells. (B) The activated endothelial cells upregulate VCAM-1 and ICAM-1 that bind with very late antigen (VLA)-4 and lymphocyte function associated antigen (LFA)-1 of effector T-cells. (C) The endothelium-T-cell interaction increases the permeability of endothelial layer and T-cells migrate to the heart tissues through this pathway. (D) Increased T-cell transmigration causes mitral valvulitis, form Aschoff like nodule in the myocardium and nodular lesions in the mitral leaflets that result in mitral regurgitation and cardiac failure.

In developing and middle-income countries, ARF/RHD continue to be significant problems affecting children and young adults. The disease not only causes high mortality but impacts on the quality of life of many more who survive. Unless the precise mechanisms of the disease process are identified, measures to reduce the burden of ARF/RHD including better diagnostics, treatment of disease progression or prevention based vaccine strategies will not be possible. Furthermore, the development of affordable therapeutics and or vaccines against this post streptococcal autoimmune sequelae has to be a priority to deliver equitable health care to the developing world. Currently, for primary prophylaxis of ARF/RHD, only individuals confirmed to have GAS infections are provided with antibiotic therapy (Jack, et al. 2015). Therefore, the lack of awareness that GGS or other potential non-GAS streptococci could trigger ARF/RHD, may result in under treatment of pharyngeal and/or skin infections, increasing the likelihood of ARF/RHD in endemic areas. Our experimental observations suggest that repetitive infections with GAS and/or GGS have the potential to develop autoimmune mediated heart damage.

## REFERENCES


Abbas, A. K. 2008. Diseases of immunity. *In* Robbins and Cotran, Pathologic Basis of Disease. 7 edition. V. Kumar, A.K. Abbas, and N. Fausto, eds. Pp. 218-219. Philadelphia, USA: WB Saunders.

Abbas, A. K., and A. H. Lichtman 2003. Cellular and molecular immunology. 5 edition. Pp. 562. Philadelphia, USA: WB Saunders.

Abernethy, M., N. Bass, N. Sharpe, C. Grant, J. Neutze, P. Clarkson, S. Greaves, D. Lennon, S. Snow, and G. Whalley 1994. Doppler echocardiography and the early diagnosis of carditis in acute rheumatic fever. Aust N Z J Med 24(5):530-535.

Abrahams, D. G. 1949. The Q-T interval in acute rheumatic carditis. Br Heart J 11(4):342-349.

Adanja, B., H. Vlajinac, and M. Jarebinski 1988. Socioeconomic factors in the etiology of rheumatic fever. J Hyg Epidemiol Microbiol Immunol 32(3):329-335.

Afanasyeva, M., Y. Wang, Z. Kaya, S. Park, M. J. Zilliox, B. H. Schofield, S. L. Hill, and N. R. Rose 2001. Experimental autoimmune myocarditis in A/J mice is an interleukin-4-dependent disease with a Th2 phenotype. Am J Pathol 159(1):193-203.

AHA 1992. Guidelines for the diagnosis of rheumatic fever: Jones criteria, 1992 update. Special Writing Group of the Committee on Rheumatic Fever, Endocarditis, and Kawasaki Disease of the Council on Cardiovascular Disease in the Young of the American Heart Association. JAMA 268(15):2069-2073.

AIHW 2004. Rheumatic heart disease: all but forgotten in Australia except among Aboriginal and Torres Strait Islander peoples. Australian Institute of Health and Welfare Bulletin 16: 1-19.

Alp, H., T. Baysal, H. Altin, Z. Karatas, and S. Karaarslan 2014. QT and P-wave dispersions in rheumatic heart disease: Prospective long-term follow up. Pediatr Int 56(5):681-688.

Amoils, B., R. C. Morrison, A. A. Wadee, R. Marcus, D. Ninin, P. King, P. Sareli, S. Levin, and A. R. Rabson 1986. Aberrant expression of HLA-DR antigen on valvular fibroblasts from patients with active rheumatic carditis. Clin Exp Immunol 66(1):88-94.

Anand, I. S., N. K. Ganguly, A. K. Khanna, R. N. Chakravarti, and P. L. Wahi 1983. Pathogenesis of immune-mediated carditis in monkeys. Adv Myocardiol 4:215-226.

Anderson, M. E., and T. J. Siahaan 2003. Targeting ICAM-1/LFA-1 interaction for controlling autoimmune diseases: designing peptide and small molecule inhibitors. Peptides 24(3):487-501.

Annunziato, F., L. Cosmi, V. Santarlasci, L. Maggi, F. Liotta, B. Mazzinghi, E. Parente, L. Fili, S. Ferri, F. Frosali, F. Giudici, P. Romagnani, P. Parronchi, F. Tonelli, E. Maggi, and S. Romagnani 2007. Phenotypic and functional features of human Th17 cells. J Exp Med 204(8):1849-1861.

Anthony, B. F., E. L. Kaplan, L. W. Wannamaker, and S. S. Chapman 1976. The dynamics of streptococcal infections in a defined population of children: serotypes associated with skin and respiratory infections. Am J Epidemiol 104(6):652-666.

Arguedas, A., and E. Mohs 1992. Prevention of rheumatic fever in Costa Rica. J Pediatr 121(4):569-572.

Aschoff, L. 1906. Myocarditisfrage. Verh Dtsch Path Ges 8:46-53.

Auckenthaler, R., P. E. Hermans, and J. A. Washington 1983. Group G streptococcal bacteremia: clinical study and review of the literature. Rev Infect Dis 5(2):196-204.

Ayoub, E. M., D. J. Barrett, N. K. Maclaren, and J. P. Krischer 1986. Association of class II human histocompatibility leukocyte antigens with rheumatic fever. J Clin Invest 77(6):2019-2026.

Azevedo, P. M., R. Bauer, F. Caparbo Vde, C. A. Silva, E. Bonfa, and R. M. Pereira 2010. Interleukin-1 receptor antagonist gene (IL1RN) polymorphism possibly associated to severity of rheumatic carditis in a Brazilian cohort. Cytokine 49(1):109-113.

Bach, J. F., S. Chalons, E. Forier, G. Elana, J. Jouanelle, S. Kayemba, D. Delbois, A. Mosser, C. Saint-Aime, and C. Berchel 1996. 10-year educational programme aimed at rheumatic fever in two French Caribbean islands. Lancet 347(9002):644-648.

Bachmaier, K., N. Neu, L. M. de la Maza, S. Pal, A. Hessel, and J. M. Penninger 1999. Chlamydia infections and heart disease linked through antigenic mimicry. Science 283(5406):1335-1339.

Baird, R. W., M. S. Bronze, W. Kraus, H. R. Hill, L. G. Veasey, and J. B. Dale 1991. Epitopes of group A streptococcal M protein shared with antigens of articular cartilage and synovium. J Immunol 146(9):3132-3137.

Baker, B. M., C. B. Thomas, and R. M. Penich 1935. Experimental carditis: Changes in the myocardium and pericardium of rabbits sensitized to streptococci. American Heart Journal 10(8):1124-1125.

Banerjee, T., S. Mukherjee, S. Ghosh, M. Biswas, S. Dutta, S. Pattari, S. Chatterjee, and A. Bandyopadhyay 2014. Clinical significance of markers of collagen metabolism in rheumatic mitral valve disease. PLoS One 9(3):e90527.

Baracco, G. J., and A. L. Risno 2004. Group C, Group G streptococcal infections: epidemiologic and clinical aspects. *In* Gram positive pathogens. V.A. Fischetti, R.P. Nowick, J.J. Ferreti, D.A. Portnoy, and J.I. Rood, eds. Pp. 222-229. Washington DC: American Society for Microbiology press.

Barnham, M. 1980. Rapidly fatal group B and G streptococcal infections in adults. J Infect 2(3):279-281.

Barnham, M. 1983. The gut as a source of the haemolytic streptococci causing infection in surgery of the intestinal and biliary tracts. J Infect 6(2):129-139.

Bassili, A., S. Barakat, G. E. Sawaf, S. Zaher, A. Zaki, and E. E. Din Saleh 2002. Identification of clinical criteria for group A-beta hemolytic streptococcal pharyngitis in children living in a rheumatic fever endemic area. J Trop Pediatr 48(5):285-293.

Batsford, S. R., S. Mezzano, M. Mihatsch, E. Schiltz, and B. Rodriguez-Iturbe 2005. Is the nephritogenic antigen in post-streptococcal glomerulonephritis pyrogenic exotoxin B (SPE B) or GAPDH? Kidney Int 68(3):1120-1129.

Batzloff, M. R., W. A. Hayman, M. R. Davies, M. Zeng, S. Pruksakorn, E. R. Brandt, and M. F. Good 2003. Protection against group A streptococcus by immunization with J8-diphtheria toxoid: contribution of J8- and diphtheria toxoid-specific antibodies to protection. J Infect Dis 187(10):1598-1608.

Bauer, M. J., M. M. Georgousakis, T. Vu, A. Henningham, A. Hofmann, M. Rettel, L. M. Hafner, K. S. Sriprakash, and D. J. McMillan 2012. Evaluation of novel Streptococcus pyogenes vaccine candidates incorporating multiple conserved sequences from the C-repeat region of the M-protein. Vaccine 30(12):2197-2205.

Beachey, E. H., M. Bronze, J. B. Dale, W. Kraus, T. Poirier, and S. Sargent 1988. Protective and autoimmune epitopes of streptococcal M proteins. Vaccine 6(2):192-196.

Beachey, E. H., G. L. Campbell, and I. Ofek 1974. Peptic digestion of streptococcal M protein. II. Extraction of M antigen from group A streptococci with pepsin. Infect Immun 9(5):891-896.

Beachey, E. H., G. H. Stollerman, E. Y. Chiang, T. M. Chiang, J. M. Seyer, and A. H. Kang 1977. Purification and properties of M protein extracted from group A streptococci with pepsin: covalent structure of the amino terminal region of type 24 M antigen. J Exp Med 145(6):1469-1483.

Beaton, A., E. Okello, T. Aliku, S. Lubega, P. Lwabi, C. Mondo, R. McCarter, and C. Sable 2014. Latent rheumatic heart disease: outcomes 2 years after echocardiographic detection. Pediatr Cardiol 35(7):1259-1267.

Beattie, J. M. 1907. A contribution to the bacteriology of rheumatic fever. J Exp Med 9(2):186-206.

Becker, C. G., and G. E. Murphy 1969. Demonstration of contractile protein in endothelium and cells of the heart valves, endocardium, intima, arteriosclerotic plaques, and Aschoff bodies of rheumatic heart disease. Am J Pathol 55(1):1-37.

Ben-Pazi, H., J. A. Stoner, and M. W. Cunningham 2013. Dopamine receptor autoantibodies correlate with symptoms in Sydenham's chorea. PLoS One 8(9):e73516.

Benvenuti, L. A., M. L. Higuchi, and M. M. Reis 2000. Upregulation of adhesion molecules and class I HLA in the myocardium of chronic chagasic cardiomyopathy and heart allograft rejection, but not in dilated cardiomyopathy. Cardiovasc Pathol 9(2):111-117.

Berne, R. M., and M. N. Levy 2001. The Heart Generates its own pacemaker activity. *In* Cardiovascular Physiology. 8 edition. Pp. 28-38. St Louis, MA.: Mosby, Inc.

Berry, J. N. 1972. Prevalence survey for chronic rheumatic heart disease and rheumatic fever in northern India. Br Heart J 34(2):143-149.

Bessen, D. E., and V. A. Fischetti 1990. Differentiation between two biologically distinct classes of group A streptococci by limited substitutions of amino acids within the shared region of M protein-like molecules. J Exp Med 172(6):1757-1764.

Bessen, D. E., and A. Kalia 2002. Genomic localization of a T serotype locus to a recombinatorial zone encoding extracellular matrix-binding proteins in Streptococcus pyogenes. Infect Immun 70(3):1159-1167.

Bessen, D. E., and S. Lizano 2010. Tissue tropisms in group A streptococcal infections. Future Microbiol 5(4):623-638.

Bessen, D., K. F. Jones, and V. A. Fischetti 1989. Evidence for two distinct classes of streptococcal M protein and their relationship to rheumatic fever. J Exp Med 169(1):269-283.

Bestetti, R. B., E. G. Soares, V. N. Sales-Neto, R. Correa de Araujo, and J. S. Oliveira 1987. Electrocardiographic changes in T. cruzi-infected rats after the ajmaline test. Res Exp Med (Berl) 187(3):185-194.

Bettelli, E., Y. Carrier, W. Gao, T. Korn, T. B. Strom, M. Oukka, H. L. Weiner, and V. K. Kuchroo 2006. Reciprocal developmental pathways for the generation of pathogenic effector TH17 and regulatory T cells. Nature 441(7090):235-238.

Bhatia, R., J. Narula, K. S. Reddy, M. Koicha, A. N. Malaviya, R. B. Pothineni, R. Tandon, and M. L. Bhatia 1989. Lymphocyte subsets in acute rheumatic fever and rheumatic heart disease. Clin Cardiol 12(1):34-38.

Bilik, M. Z., I. Kaplan, N. Polat, M. A. Akil, A. Akyuz, H. Acet, M. Yuksel, U. Inci, F. Kayan, and N. Toprak 2016. Serum Levels of IL-17 and IL-23 in Patients With Rheumatic Mitral Stenosis. Medicine (Baltimore) 95(18):e3562.

Bisno, A. L. 1996. Acute pharyngitis: etiology and diagnosis. Pediatrics 97(6 Pt 2):949-954.

Bisno, A. L., R. E. Campo, and C. M. Collins 1994. M proteins of group G streptococci: structural and functional studies. *In* A. Totolian (ed.), Pathogenic streptocci: present and future. Pp. 225-227. St. Petersburg, Russia: Lancer Publications.

Bisno, A. L., C. M. Collins, and J. C. Turner 1996. M proteins of group C streptococci isolated from patients with acute pharyngitis. J Clin Microbiol 34(10):2511-2515.

Bisno, A. L., D. E. Craven, and W. R. McCabe 1987. M proteins of group G streptococci isolated from bacteremic human infections. Infect Immun 55(3):753-757.

Bouza, E., R. D. Meyer, and D. F. Busch 1978. Group G streptococcal endocarditis. Am J Clin Pathol 70(1):108-111.

Brahmadathan, K. N., B. R. Rajkumari, J. M. Jose, V. Abraham, and A. Joseph 2005. Molecular epidemiology of group A streptococcal infections in South Indian children. Proceedings of the XVI Lancefield International Symposium on Streptococci an Streptococcal Diseases, Palm Cove, Queensland, Australia, 2005.

Brahmadathan, N. K. 2017. Molecular biology of Group A *Streptococcus* and its implications in vaccine strategies. Indian J Med Microbiol 35(2):176-183.

Brahmadothan, K. N., and G. Koshi 1989. Importance of group G streptococci in human pyrogenic infections. J Trop Med Hyg 92:35-38.

Brand, A., S. Dollberg, and A. Keren 1992. The prevalence of valvular regurgitation in children with structurally normal hearts: a color Doppler echocardiographic study. Am Heart J 123(1):177-180.

Brandt, C. M., and B. Spellerberg 2009. Human infections due to *Streptococcus dysgalactiae* subspecies *equisimilis*. Clin Infect Dis 49(5):766-772.

Brandt, E. R., P. J. Yarwood, D. J. McMillan, H. Vohra, B. Currie, L. Mammo, S. Pruksakorn, J. Saour, and M. F. Good 2001. Antibody levels to the class I and II epitopes of the M protein and myosin are related to group A streptococcal exposure in endemic populations. Int Immunol 13(10):1335-1343.

Breed, E. R., and B. A. Binstadt 2015. Autoimmune valvular carditis. Curr Allergy Asthma Rep 15(1):491.

Bright, P. D., B. M. Mayosi, and W. J. Martin 2016. An immunological perspective on rheumatic heart disease pathogenesis: more questions than answers. Heart 102(19):1527-1532.

Bronze, M. S., D. S. McKinsey, E. H. Beachey, and J. B. Dale 1988. Protective immunity evoked by locally administered group A streptococcal vaccines in mice. J Immunol 141(8):2767-2770.

Brunner, S., H. D. Theiss, M. Leiss, U. Grabmaier, J. Grabmeier, B. Huber, M. Vallaster, D. A. Clevert, M. Sauter, R. Kandolf, C. Rimmbach, R. David, K. Klingel, and W. M. Franz 2013. Enhanced stem cell migration mediated by VCAM-1/VLA-4 interaction improves cardiac function in virus-induced dilated cardiomyopathy. Basic Res Cardiol 108(6):388.

Burkert, T., and C. Watanakunakorn 1991. Group G *Streptococcus* septic arthritis and osteomyelitis: report and literature review. J Rheumatol 18(6):904-907.

Burova, L. A., V. A. Nagornev, P. V. Pigarevsky, M. M. Gladilina, E. A. Gavrilova, V. G. Seliverstova, A. A. Totolian, A. Thern, and C. Schalen 2005. Myocardial tissue damage in rabbits injected with group A streptococci, types M1 and M22. Role of bacterial immunoglobulin G-binding surface proteins. APMIS 113(1):21-30.

Burova, L. A., V. A. Nagornev, P. V. Pigarevsky, M. M. Gladilina, I. V. Molchanova, E. A. Gavrilova, A. A. Totolian, A. Thern, and C. Schalen 2004. Induction of myocarditis in rabbits injected with group A streptococci. Indian J Med Res 119 Suppl:183-185.

Caforio, A. L., A. Angelini, M. Blank, A. Shani, S. Kivity, G. Goddard, A. Doria, A. Schiavo, M. Testolina, S. Bottaro, R. Marcolongo, G. Thiene, S. Iliceto, and Y. Shoenfeld 2015. Passive transfer of affinity-purified anti-heart autoantibodies (AHA) from sera of patients with myocarditis induces experimental myocarditis in mice. Int J Cardiol 179:166-177.

Camara, E. J., C. Neubauer, G. F. Camara, and A. A. Lopes 2004. Mechanisms of mitral valvar insufficiency in children and adolescents with severe rheumatic heart disease: an echocardiographic study with clinical and epidemiological correlations. Cardiol Young 14(5):527-532.

Campbell, M 1944. Frederick John Pyonton. British Heart Journal 6:96-98.

Caparon, M. G., D. S. Stephens, A. Olsen, and J. R. Scott 1991. Role of M protein in adherence of group A streptococci. Infect Immun 59(5):1811-1817.

Carabello, B. A. 2005. Modern management of mitral stenosis. Circulation 112(3):432-437.

Carapetis, J. R., A. Beaton, M. W. Cunningham, L. Guilherme, G. Karthikeyan, B. M. Mayosi, C. Sable, A. Steer, N. Wilson, R. Wyber, and L. Zühlke 2016. Acute rheumatic fever and rheumatic heart disease. Nat Rev Dis Primers (2):15084.

Carapetis, J. R., and B. J. Currie 1997. Clinical epidemiology of rheumatic fever and rheumatic heart disease in tropical Australia. Adv Exp Med Biol 418:233-236.

Carapetis, J. R., and B. J. Currie 1998. Preventing rheumatic heart disease in Australia. Med J Aust 168(9):428-429.

Carapetis, J. R., and B. J. Currie 2001. Rheumatic fever in a high incidence population: the importance of monoarthritis and low grade fever. Arch Dis Child 85(3):223-227.

Carapetis, J. R., B. J. Currie, and E. L. Kaplan 1999. Epidemiology and prevention of group A streptococcal infections: acute respiratory tract infections, skin infections, and their sequelae at the close of the twentieth century. Clin Infect Dis 28(2):205-210.

Carapetis, J. R., B. J. Currie, and J. D. Mathews 2000. Cumulative incidence of rheumatic fever in an endemic region: a guide to the susceptibility of the population? Epidemiol Infect 124(2):239-244.

Carapetis, J. R., M. McDonald, and N. J. Wilson 2005a. Acute rheumatic fever. Lancet 366(9480):155-168.

Carapetis, J. R., A. C. Steer, E. K. Mulholland, and M. Weber 2005b. The global burden of group A streptococcal diseases. Lancet Infect Dis 5(11):685-694.

Carapetis, J. R., D. R. Wolff, and B. J. Currie 1996. Acute rheumatic fever and rheumatic heart disease in the top end of Australia's Northern Territory. Med J Aust 164(3):146-149.

Cardoso, F., A. P. Vargas, L. D. Oliveira, A. A. Guerra, and S. V. Amaral 1999. Persistent Sydenham's chorea. Mov Disord 14(5):805-807.

Carlos, T. M., B. R. Schwartz, N. L. Kovach, E. Yee, M. Rosa, L. Osborn, G. Chi-Rosso, B. Newman, R. Lobb, and et al. 1990. Vascular cell adhesion molecule-1 mediates lymphocyte adherence to cytokine-activated cultured human endothelial cells. Blood 76(5):965-970.

Carstensen, H., C. Pers, and O. Pryds 1988. Group G streptococcal neonatal septicaemia: two case reports and a brief review of literature. Scand J Infect Dis 20(4):407-410.

Caswell, C. C., M. Barczyk, D. R. Keene, E. Lukomska, D. E. Gullberg, and S. Lukomski 2008. Identification of the first prokaryotic collagen sequence motif that mediates binding to human collagen receptors, integrins alpha2beta1 and alpha11beta1. J Biol Chem 283(52):36168-36175.

Caswell, C. C., E. Lukomska, N. S. Seo, M. Hook, and S. Lukomski 2007. Scl1-dependent internalization of group A Streptococcus via direct interactions with the alpha2beta(1) integrin enhances pathogen survival and re-emergence. Mol Microbiol 64(5):1319-1331.

Cavelti, P. A. 1947. Studies on the Pathogenesis of Rheumatic Fever. II: Cardiac Lesions Produced in Rats by Means of Autoantibodies. Arch Path 44:13.

Chandnani, H. K., R. Jain, and P. Patamasucon 2015. Group C *Streptococcus* Causing Rheumatic Heart Disease in a Child. J Emerg Med 49(1):12-14.

Chaudhary, P., R. Kumar, V. Sagar, S. Sarkar, R. Singh, S. Ghosh, S. Singh, and A. Chakraborti 2018. Assessment of Cpa, Scl1 and Scl2 in clinical group A *Streptococcus* isolates and patients from north India: an evaluation of the host pathogen interaction. Res Microbiol 169(1):11-19.

Chauvaud, S., J. F. Fuzellier, A. Berrebi, A. Deloche, J. N. Fabiani, and A. Carpentier 2001. Long-term (29 years) results of reconstructive surgery in rheumatic mitral valve insufficiency. Circulation 104(12 Suppl 1):I12-15.

Chen, M. C., H. W. Chang, S. S. Juang, H. K. Yip, C. J. Wu, T. H. Yu, and C. I. Cheng 2004. Percutaneous transluminal mitral valvuloplasty reduces circulating vascular cell adhesion molecule-1 in rheumatic mitral stenosis. Chest 125(4):1213-1217.

Chen, S. M., Y. S. Tsai, C. M. Wu, S. K. Liao, L. C. Wu, C. S. Chang, Y. H. Liu, and P. J. Tsai 2010. Streptococcal collagen-like surface protein 1 promotes adhesion to the respiratory epithelial cell. BMC Microbiol 10:320.

Chhatwal, G. S., and S. R. Talay 2000. Pathogenicity factors in group C and G streptococci. *In* Gram-positive pathogens. V.A. Fischetti, R.P. Novick, J.J. Ferretti, D.A. Portnoy, and J.I. Rood, eds. Pp. 177-183. Washington, DC, USA: American Society for Microbiology.

Chopra, P., J. Narula, A. S. Kumar, S. Sachdeva, and M. L. Bhatia 1988. Immunohistochemical characterisation of Aschoff nodules and endomyocardial inflammatory infiltrates in left atrial appendages from patients with chronic rheumatic heart disease. Int J Cardiol 20(1):99-105.

Chou, H., C. Chen, C. Tsai, and F. Tsai 2004. Association between transforming growth factor-?1 gene C-509T and T869C polymorphisms and rheumatic heart disease. Am Heart J 148(1):181-186.

Chow, L. H., Y. Ye, J. Linder, and B. M. McManus 1989. Phenotypic analysis of infiltrating cells in human myocarditis. An immunohistochemical study in paraffin-embedded tissue. Arch Pathol Lab Med 113(12):1357-1362.

Cleary, P. P., J. Peterson, C. Chen, and C. Nelson 1991. Virulent human strains of group G streptococci express a C5a peptidase enzyme similar to that produced by group A streptococci. Infect Immun 59(7):2305-2310.
Coburn, A. F. 1961. Susceptibility to rheumatic disease. J Pediatr 58:448-451.
Cohen-Poradosu, R., J. Jaffe, D. Lavi, S. Grisariu-Greenzaid, R. Nir-Paz, L. Valinsky, M. Dan-Goor, C. Block, B. Beall, and A. E. Moses 2004. Group G streptococcal bacteremia in Jerusalem. Emerg Infect Dis 10(8):1455-1460.
Collins, C. M., A. Kimura, and A. L. Bisno 1992. Group G streptococcal M protein exhibits structural features analogous to those of class I M protein of group A streptococci. Infect Immun 60(9):3689-3696.
Courtney, H. S., M. S. Bronze, J. B. Dale, and D. L. Hasty 1994a. Analysis of the role of M24 protein in group A streptococcal adhesion and colonization by use of omega-interposon mutagenesis. Infect Immun 62(11):4868-4873.
Courtney, H. S., D. L. Hasty, and J. B. Dale 2002. Molecular mechanisms of adhesion, colonization, and invasion of group A streptococci. Ann Med 34(2):77-87.
Courtney, H. S., D. L. Hasty, J. B. Dale, and T. P. Poirier 1992a. A 28-kilodalton fibronectin-binding protein of group A streptococci. Curr Microbiol 25(5):245-250.
Courtney, H. S., Y. Li, J. B. Dale, and D. L. Hasty 1994b. Cloning, sequencing, and expression of a fibronectin/fibrinogen-binding protein from group A streptococci. Infect Immun 62(9):3937-3946.
Courtney, H. S., I. Ofek, and D. L. Hasty 1997. M protein mediated adhesion of M type 24 *Streptococcus pyogenes* stimulates release of interleukin-6 by HEp-2 tissue culture cells. FEMS Microbiol Lett 151(1):65-70.
Courtney, H. S., I. Ofek, T. Penfound, V. Nizet, M. A. Pence, B. Kreikemeyer, A. Podbielski, D. L. Hasty, and J. B. Dale 2009. Relationship between expression of the family of M proteins and lipoteichoic acid to hydrophobicity and biofilm formation in Streptococcus pyogenes. PLoS One 4(1):e4166.
Courtney, H. S., C. von Hunolstein, J. B. Dale, M. S. Bronze, E. H. Beachey, and D. L. Hasty 1992b. Lipoteichoic acid and M protein: dual adhesins of group A streptococci. Microb Pathog 12(3):199-208.
Couzos, S., and J. Carapetis 2003. Rheumatic fever. *In* Aboriginal primary health care: an evidence-based approach. 2 edition. S. Couzos and R. Murray, eds. Pp. 281-310. South Melbourne: Oxford University Press.

Craven, D. E., A. I. Rixinger, A. L. Bisno, T. A. Goularte, and W. R. McCabe 1986. Bacteremia caused by group G streptococci in parenteral drug abusers: epidemiological and clinical aspects. J Infect Dis 153(5):988-992.

Cromartie, W. J., J. G. Craddock, J. H. Schwab, S. K. Anderle, and C. H. Yang 1977. Arthritis in rats after systemic injection of streptococcal cells or cell walls. J Exp Med 146(6):1585-1602.

Cunningham, M. W. 2000. Pathogenesis of group A streptococcal infections. Clin Microbiol Rev 13(3):470-511.

Cunningham, M. W. 2003. Autoimmunity and molecular mimicry in the pathogenesis of post-streptococcal heart disease. Front Biosci 8:533-543.

Cunningham, M. W. 2004. T cell mimicry in inflammatory heart disease. Mol Immunol 40(14-15):1121-1127.

Cunningham, M. W. 2006. Molecular mimicry, autoimmunity and infection in the pathogenesis of rheumatic fever. International Congress Series 1289(0):14-19.

Cunningham, M. W. 2012. Streptococcus and rheumatic fever. Curr Opin Rheumatol 24(4):408-416.

Cunningham, M. W. 2014. Rheumatic fever, autoimmunity, and molecular mimicry: the streptococcal connection. Int Rev Immunol 33(4):314-329.

Cunningham, M. W., S. M. Antone, M. Smart, R. Liu, and S. Kosanke 1997. Molecular analysis of human cardiac myosin-cross-reactive B- and T-cell epitopes of the group A streptococcal M5 protein. Infect Immun 65(9):3913-3923.

Cunningham, M. W., N. K. Hall, K. K. Krisher, and A. M. Spanier 1986. A study of anti-group A streptococcal monoclonal antibodies cross-reactive with myosin. J Immunol 136(1):293-298.

Cunningham, M. W., J. M. McCormack, P. G. Fenderson, M. K. Ho, E. H. Beachey, and J. B. Dale 1989. Human and murine antibodies cross-reactive with streptococcal M protein and myosin recognize the sequence GLN-LYS-SER-LYS-GLN in M protein. J Immunol 143(8):2677-2683.

Cunningham, M. W., J. M. McCormack, L. R. Talaber, J. B. Harley, E. M. Ayoub, R. S. Muneer, L. T. Chun, and D. V. Reddy 1988. Human monoclonal antibodies reactive with antigens of the group A *Streptococcus* and human heart. J Immunol 141(8):2760-2766.

Cunningham, M. W., and R. A. Swerlick 1986. Polyspecificity of antistreptococcal murine monoclonal antibodies and their implications in autoimmunity. J Exp Med 164(4):998-1012.

Dajani, A., K. Taubert, P. Ferrieri, G. Peter, and S. Shulman 1995. Treatment of acute streptococcal pharyngitis and prevention of rheumatic fever: a statement for health professionals. Committee on Rheumatic Fever, Endocarditis, and Kawasaki Disease of the Council on Cardiovascular Disease in the Young, the American Heart Association. Pediatrics 96(4 Pt 1):758-764.

Dale, J. B., R. W. Baird, H. S. Courtney, D. L. Hasty, and M. S. Bronze 1994. Passive protection of mice against group A streptococcal pharyngeal infection by lipoteichoic acid. J Infect Dis 169(2):319-323.

Dale, J. B., and E. H. Beachey 1985a. Epitopes of streptococcal M proteins shared with cardiac myosin. J Exp Med 162(2):583-591.

Dale, J. B., and E. H. Beachey 1985b. Multiple, heart-cross-reactive epitopes of streptococcal M proteins. J Exp Med 161(1):113-122.

Dale, J. B., and E. H. Beachey 1986. Sequence of myosin-crossreactive epitopes of streptococcal M protein. J Exp Med 164(5):1785-1790.

Dale, J. B., and E. H. Beachey 1987. Human cytotoxic T lymphocytes evoked by group A streptococcal M proteins. J Exp Med 166(6):1825-1835.

Damian, R. T. 1989. Molecular mimicry: parasite evasion and host defense. Curr Top Microbiol Immunol 145:101-115.

Danchin, M. H., S. Rogers, L. Kelpie, G. Selvaraj, N. Curtis, J. B. Carlin, T. M. Nolan, and J. R. Carapetis 2007. Burden of acute sore throat and group A streptococcal pharyngitis in school-aged children and their families in Australia. Pediatrics 120(5):950-957.

Danchin, M. H., S. Rogers, G. Selvaraj, L. Kelpie, P. Rankin, R. Vorich, M. Howson, J. B. Carlin, N. Curtis, T. M. Nolan, and J. R. Carapetis 2004. The burden of group A streptococcal pharyngitis in Melbourne families. Indian J Med Res 119 Suppl:144-147.

Davies, M. R., D. J. McMillan, R. G. Beiko, V. Barroso, R. Geffers, K. S. Sriprakash, and G. S. Chhatwal 2007a. Virulence profiling of *Streptococcus dysgalactiae* subspecies *equisimilis* isolated from infected humans reveals 2 distinct genetic lineages that do not segregate with their phenotypes or propensity to cause diseases. Clin Infect Dis 44(11):1442-1454.

Davies, M. R., D. J. McMillan, G. H. Van Domselaar, M. K. Jones, and K. S. Sriprakash 2007b. Phage 3396 from a *Streptococcus dysgalactiae* subspecies *equisimilis* pathovar may have its origins in streptococcus pyogenes. J Bacteriol 189(7):2646-2652.

Davies, M. R., T. N. Tran, D. J. McMillan, D. L. Gardiner, B. J. Currie, and K. S. Sriprakash 2005. Inter-species genetic movement may blur the epidemiology of streptococcal diseases in endemic regions. Microbes Infect 7(9-10):1128-1138.

Daynes, R. A., and C. H. Armstrong 1973. An antiphagocytic factor associated with group E *Streptococcus*. Infect Immun 7(2):298-304.

Del Papa, N., E. Raschi, G. Moroni, P. Panzeri, M. O. Borghi, C. Ponticelli, A. Tincani, G. Balestrieri, and P. L. Meroni 1999. Anti-endothelial cell IgG fractions from systemic lupus erythematosus patients bind to human endothelial cells and induce a pro-adhesive and a pro-inflammatory phenotype in vitro. Lupus 8(6):423-429.

Delunardo, F., V. Scalzi, A. Capozzi, S. Camerini, R. Misasi, M. Pierdominici, M. Pendolino, M. Crescenzi, M. Sorice, G. Valesini, E. Ortona, and C. Alessandri 2013. Streptococcal-vimentin cross-reactive antibodies induce microvascular cardiac endothelial proinflammatory phenotype in rheumatic heart disease. Clin Exp Immunol 173(3):419-429.

Detweiler, D. K. 1997. Electrocardiography in toxicology studies. *In* Comprehensive Toxicology. I.G. Sipes, C.A. McQueen, and A.J. Gandolfi, eds. Pp. 95-114. New York, USA: Pergamon Press.

Diao, M., A. Kane, M. B. Ndiaye, A. Mbaye, M. Bodian, M. M. Dia, M. Sarr, A. Kane, J. J. Monsuez, and S. A. Ba 2011. Pregnancy in women with heart disease in sub-Saharan Africa. Arch Cardiovasc Dis 104(6-7):370-374.

Dickie, A. S., D. A. Bremner, and P. J. Say 1984. Group G streptococcal septicaemia: report of six cases. J Infect 8(2):173-176.

Dileepan, T., E. D. Smith, D. Knowland, M. Hsu, M. Platt, P. Bittner-Eddy, B. Cohen, P. Southern, E. Latimer, E. Harley, D. Agalliu, and P. P. Cleary 2016. Group A *Streptococcus* intranasal infection promotes CNS infiltration by streptococcal-specific Th17 cells. J Clin Invest 126(1):303-317.

Dinkla, K., D. P. Nitsche-Schmitz, V. Barroso, S. Reissmann, H. M. Johansson, I. M. Frick, M. Rohde, and G. S. Chhatwal 2007. Identification of a streptococcal octapeptide motif involved in acute rheumatic fever. J Biol Chem 282(26):18686-18693.

Dinkla, K., M. Rohde, W. T. Jansen, J. R. Carapetis, G. S. Chhatwal, and S. R. Talay 2003a. *Streptococcus pyogenes* recruits collagen via surface-bound fibronectin: a novel colonization and immune evasion mechanism. Mol Microbiol 47(3):861-869.

Dinkla, K., M. Rohde, W. T. Jansen, E. L. Kaplan, G. S. Chhatwal, and S. R. Talay 2003b. Rheumatic fever-associated Streptococcus pyogenes isolates aggregate collagen. J Clin Invest 111(12):1905-1912.

Dudding, B. A., and E. M. Ayoub 1968. Persistence of streptococcal group A antibody in patients with rheumatic valvular disease. J Exp Med 128(5):1081-1098.

Duzgun, N., T. Duman, F. E. Haydardedeoglu, and H. Tutkak 2009. Cytotoxic T lymphocyte-associated antigen-4 polymorphism in patients with rheumatic heart disease. Tissue Antigens 74(6):539-542.

Dwyer, J. M., and C. Johnson 1981. The use of concanavalin A to study the immunoregulation of human T cells. Clinical and Experimental Immunology 46(2):237-249.

Dyson, A. E., and S. E. Read 1981. Group G streptococcal colonization and sepsis in neonates. J Pediatr 99(6):944-947.

Ebell, M. H., M. A. Smith, H. C. Barry, K. Ives, and M. Carey 2000. The rational clinical examination. Does this patient have strep throat? Jama 284(22):2912-2918.

Ellen, R. P., and R. J. Gibbons 1972. M protein-associated adherence of *Streptococcus pyogenes* to epithelial surfaces: prerequisite for virulence. Infect Immun 5(5):826-830.

Ellen, R. P., and R. J. Gibbons 1974. Parameters affecting the adherence and tissue tropisms of *Streptococcus pyogenes*. Infect Immun 9(1):85-91.

Ellis, N. M., D. K. Kurahara, H. Vohra, A. Mascaro-Blanco, G. Erdem, E. E. Adderson, L. G. Veasy, J. A. Stoner, E. Tam, H. R. Hill, K. Yamaga, and M. W. Cunningham 2010. Priming the immune system for heart disease: a perspective on group A streptococci. J Infect Dis 202(7):1059-1067.

Ellis, N. M., Y. Li, W. Hildebrand, V. A. Fischetti, and M. W. Cunningham 2005. T cell mimicry and epitope specificity of cross-reactive T cell clones from rheumatic heart disease. J Immunol 175(8):5448-5456.

Erdem, G., C. Mizumoto, D. Esaki, V. Reddy, D. Kurahara, K. Yamaga, L. Abe, D. Johnson, K. Yamamoto, and E. L. Kaplan 2007. Group A streptococcal isolates temporally associated with acute rheumatic fever in Hawaii: differences from the continental United States. Clin Infect Dis 45(3):e20-24.

Facklam, R. 2002. What happened to the streptococci: overview of taxonomic and nomenclature changes. Clin Microbiol Rev 15(4):613-630.

Facklam, R., B. Beall, A. Efstratiou, V. Fischetti, D. Johnson, E. Kaplan, P. Kriz, M. Lovgren, D. Martin, B. Schwartz, A. Totolian, D. Bessen, S. Hollingshead, F. Rubin, J. Scott, and G. Tyrrell 1999. emm typing and validation of provisional M types for group A streptococci. Emerg Infect Dis 5(2):247-253.

Fae, K. C., D. D. da Silva, S. E. Oshiro, A. C. Tanaka, P. M. Pomerantzeff, C. Douay, D. Charron, A. Toubert, M. W. Cunningham, J. Kalil, and L. Guilherme 2006. Mimicry in recognition of cardiac myosin peptides by heart-intralesional T cell clones from rheumatic heart disease. J Immunol 176(9):5662-5670.

Fae, K. C., D. Diefenbach da Silva, A. M. Bilate, A. C. Tanaka, P. M. Pomerantzeff, M. H. Kiss, C. A. Silva, E. Cunha-Neto, J. Kalil, and L. Guilherme 2008. PDIA3, HSPA5 and vimentin, proteins identified by 2-DE in the valvular tissue, are the target antigens of peripheral and heart infiltrating T cells from chronic rheumatic heart disease patients. J Autoimmun 31(2):136-141.

Fae, K. C., S. E. Oshiro, A. Toubert, D. Charron, J. Kalil, and L. Guilherme 2005. How an autoimmune reaction triggered by molecular mimicry between streptococcal M protein and cardiac tissue proteins leads to heart lesions in rheumatic heart disease. J Autoimmun 24(2):101-109.

Fae, K. C., S. A. Palacios, L. G. Nogueira, S. E. Oshiro, L. M. Demarchi, A. M. Bilate, P. M. Pomerantzeff, C. Brandao, P. G. Thomaz, M. dos Reis, R. Sampaio, A. C. Tanaka, E. Cunha-Neto, J. Kalil, and L. Guilherme 2013. CXCL9/Mig mediates T cells recruitment to valvular tissue lesions of chronic rheumatic heart disease patients. Inflammation 36(4):800-811.

Fae, K., J. Kalil, A. Toubert, and L. Guilherme 2004. Heart infiltrating T cell clones from a rheumatic heart disease patient display a common TCR usage and a degenerate antigen recognition pattern. Mol Immunol 40(14-15):1129-1135.

Fairweather, D., S. Frisancho-Kiss, D. B. Njoku, J. F. Nyland, Z. Kaya, S. A. Yusung, S. E. Davis, J. A. Frisancho, M. A. Barrett, and N. R. Rose 2006. Complement receptor 1 and 2 deficiency increases coxsackievirus B3-induced myocarditis, dilated cardiomyopathy, and heart failure by increasing macrophages, IL-1beta, and immune complex deposition in the heart. J Immunol 176(6):3516-3524.

Falugi, F., C. Zingaretti, V. Pinto, M. Mariani, L. Amodeo, A. G. Manetti, S. Capo, J. M. Musser, G. Orefici, I. Margarit, J. L. Telford, G. Grandi, and M. Mora 2008. Sequence variation in group A Streptococcus pili and association of pilus backbone types with lancefield T serotypes. J Infect Dis 198(12):1834-1841.

Farraj, A. K., M. S. Hazari, and W. E. Cascio 2011. The utility of the small rodent electrocardiogram in toxicology. Toxicol Sci 121(1):11-30.

Feldman, Arthur M., and Dennis McNamara 2000. Myocarditis. N Engl J Med 343(19):1388-1398.

Fenderson, P. G., V. A. Fischetti, and M. W. Cunningham 1989. Tropomyosin shares immunologic epitopes with group A streptococcal M proteins. J Immunol 142(7):2475-2481.

Ferretti, J. J., D. L. Stevens, and V. A. Fischetti 2016. *In* Streptococcus pyogenes : Basic Biology to Clinical Manifestations. Oklahoma City (OK): University of Oklahoma Health Sciences Center(c) The University of Oklahoma Health Sciences Center.

Figueroa, F. E., M. S. Fernandez, P. Valdes, C. Wilson, F. Lanas, F. Carrion, X. Berrios, and F. Valdes 2001. Prospective comparison of clinical and echocardiographic diagnosis of rheumatic carditis: long term follow up of patients with subclinical disease. Heart 85(4):407-410.

Finch, R. G., and A. Aveline 1984. Group G streptococcal septicaemia: clinical observations and laboratory studies. J Infect 9(2):126-133.

Fischetti, V. A. 1989. Streptococcal M protein: molecular design and biological behavior. Clin Microbiol Rev 2(3):285-314.

Fischetti, V. A., K. F. Jones, S. K. Hollingshead, and J. R. Scott 1988. Structure, function, and genetics of streptococcal M protein. Rev Infect Dis 10(2):S356-359.

Fischetti, V. A., K. F. Jones, and J. R. Scott 1985. Size variation of the M protein in group A streptococci. J Exp Med 161(6):1384-1401.

Flores, A. R., B. E. Jewell, N. Fittipaldi, S. B. Beres, and J. M. Musser 2012. Human disease isolates of serotype m4 and m22 group a streptococcus lack genes required for hyaluronic acid capsule biosynthesis. MBio 3(6):e00413-00412.

Fraker, P. J., L. E. King, T. Laakko, and T. L. Vollmer 2000. The dynamic link between the integrity of the immune system and zinc status. J Nutr 130(5):1399s-1406s.

Fraser, W. J., Z. Haffejee, and K. Cooper 1995. Rheumatic Aschoff nodules revisited: an immunohistological reappraisal of the cellular component. Histopathology 27(5):457-461.

Fraser, W. J., Z. Haffejee, D. Jankelow, A. Wadee, and K. Cooper 1997. Rheumatic Aschoff nodules revisited. II: Cytokine expression corroborates recently proposed sequential stages. Histopathology 31(5):460-464.

Friedman, I., N. Ron, A. Laufer, and A. M. Davies 1970. Experimental myocarditis: enhancement by the use of pertussis vaccine in Lewis rats. Experientia 26(10):1144-1145.

Frost, H. R., D. Laho, M. L. Sanderson-Smith, P. Licciardi, S. Donath, N. Curtis, J. Kado, J. B. Dale, A. C. Steer, and P. R. Smeesters 2017. Immune Cross-Opsonization Within emm Clusters Following Group A *Streptococcus* Skin Infection: Broadening the Scope of Type-Specific Immunity. Clin Infect Dis 65(9):1523-1531.

Froude, J., A. Gibofsky, D. R. Buskirk, A. Khanna, and J. B. Zabriskie 1989. Cross-reactivity between streptococcus and human tissue: a model of molecular mimicry and autoimmunity. Curr Top Microbiol Immunol 145:5-26.

Gaasch, W. H., and T. E. Meyer 2008. Left ventricular response to mitral regurgitation: implications for management. Circulation 118(22):2298-2303.

Galvin, J. E., M. E. Hemric, S. D. Kosanke, S. M. Factor, A. Quinn, and M. W. Cunningham 2002. Induction of myocarditis and valvulitis in lewis rats by different epitopes of cardiac myosin and its implications in rheumatic carditis. Am J Pathol 160(1):297-306.
Galvin, J. E., M. E. Hemric, K. Ward, and M. W. Cunningham 2000. Cytotoxic mAb from rheumatic carditis recognizes heart valves and laminin. J Clin Invest 106(2):217-224.
Ganguly, N. K., I. S. Anand, A. K. Khanna, R. S. Kohli, and P. L. Wahi 1982. T cells and T cell subsets in rheumatic heart disease. Indian J Med Res 76:854-858.
Garcia, A. F., K. M. Yamaga, L. A. Shafer, O. Bollt, E. K. Tam, M. W. Cunningham, and D. K. Kurahara 2016. Cardiac Myosin Epitopes Recognized by Autoantibody in Acute and Convalescent Rheumatic Fever. Pediatr Infect Dis J 35(9):1021-1026.
Gardin, J. M., F. M. Siri, R. N. Kitsis, J. G. Edwards, and L. A. Leinwand 1995. Echocardiographic assessment of left ventricular mass and systolic function in mice. Circ Res 76(5):907-914.
Gawaz, M., K. Brand, T. Dickfeld, G. Pogatsa-Murray, S. Page, C. Bogner, W. Koch, A. Schomig, and F. Neumann 2000. Platelets induce alterations of chemotactic and adhesive properties of endothelial cells mediated through an interleukin-1-dependent mechanism. Implications for atherogenesis. Atherosclerosis 148(1):75-85.
GBDS 2015. Global, regional, and national incidence, prevalence, and years lived with disability for 301 acute and chronic diseases and injuries in 188 countries, 1990-2013: a systematic analysis for the Global Burden of Disease Study 2013. Lancet 386(9995):743-800.
Gearing, A. J., and W. Newman 1993. Circulating adhesion molecules in disease. Immunol Today 14(10):506-512.
Gerard, C., and B. J. Rollins 2001. Chemokines and disease. Nat Immunol 2(2):108-115.
Gewitz, M. H., R. S. Baltimore, L. Y. Tani, C. A. Sable, S. T. Shulman, J. Carapetis, B. Remenyi, K. A. Taubert, A. F. Bolger, L. Beerman, B. M. Mayosi, A. Beaton, N. G. Pandian, and E. L. Kaplan 2015. Revision of the Jones Criteria for the diagnosis of acute rheumatic fever in the era of Doppler echocardiography: a scientific statement from the American Heart Association. Circulation 131(20):1806-1818.
Geyer, A., and K. H. Schmidt 2000. Genetic organisation of the M protein region in human isolates of group C and G streptococci: two types of multigene regulator-like (mgrC) regions. Mol Gen Genet 262(6):965-976.
Glover, J. A. 1930. Milroy Lectures on the Incidence of Rheumatic Diseases. I. The Incidence of Acute Rheumatism. Lancet:499-505.

Goel, P. K., N. Moorthy, and T. Bhatia 2013. Rheumatic severe mitral stenosis with complete heart block. Pediatr Cardiol 34(7):1749-1750.
Goldste1N, I., B. Halpern, and L. Robert 1967. Immunological Relationship between *Streptococcus* A Polysaccharide and the Structural Glycoproteins of Heart Valve. Nature 213:44.
Goldstein, I., L. Scebat, J. Renais, P. Hadjinsky, and J. Dutartre 1983. Rheumatic-like carditis induced in rabbits by cross-reacting antigens: *Streptococcus* A polysaccharide and rabbit aortic glycoproteins. Isr J Med Sci 19(6):483-490.
Gonzalez-Lama, Z., J. J. Gonzalez, P. Lupiola, and M. T. Tejedor 2000. Carriers of beta hemolytic streptococci from groups A, B, and C among schoolchildren in Las Palmas. Enferm Infecc Microbiol Clin 18(6):271-273.
Gordis, L. 1973. Effectiveness of comprehensive-care programs in preventing rheumatic fever. N Engl J Med 289(7):331-335.
Gordis, L., A. Lilienfeld, and R. Rodriguez 1969. Studies in the epidemiology and preventability of rheumatic fever. II. Socio-economic factors and the incidence of acute attacks. J Chronic Dis 21(9):655-666.
Gorton, D., S. Blyth, J. G. Gorton, B. Govan, and N. Ketheesan 2010. An alternative technique for the induction of autoimmune valvulitis in a rat model of rheumatic heart disease. J Immunol Methods 355(1–2):80-85.
Gorton, D. E., B. L. Govan, N. Ketheesan, A. A. Sive, R. E. Norton, B. J. Currie, R. J. Towers, A. I. Mascaro-Blanco, and M. W. Cunningham 2011. Cardiac myosin epitopes for monitoring progression of rheumatic fever. Pediatr Infect Dis J 30(11):1015-1016.
Gorton, D., B. Govan, C. Olive, and N. Ketheesan 2006. A role for an animal model in determining the immune mechanisms involved in the pathogenesis of rheumatic heart disease. Int Congr Ser 1289(0):289-292.
Gorton, D., B. Govan, C. Olive, and N. Ketheesan 2009. B- and T-cell responses in group a streptococcus M-protein- or Peptide-induced experimental carditis. Infect Immun 77(5):2177-2183.
Gorton, D., S. Sikder, N. L. Williams, L. Chilton, C. M. Rush, B. L. Govan, M. W. Cunningham, and N. Ketheesan 2016. Repeat exposure to group A streptococcal M protein exacerbates cardiac damage in a rat model of rheumatic heart disease. Autoimmunity 49(8):563-570.
Gottlieb, M., B. Long, and A. Koyfman 2018. Clinical Mimics: An Emergency Medicine-Focused Review of Streptococcal Pharyngitis Mimics. J Emerg Med.

Gowda, K. .L, M. A. M. Marie, S. R. B. Rani, C. T. Shivannavar, and K. N. Brahmadathan 2012. High throat carriage of Groups G/C streptococci among school children in Bangalore City and its significance. African J Microbiol Res 6(43):7128-7130.

Gray, F. G. 1949. Spontaneous cardiac lesions in mice; their bearing on attempts to produce experimental carditis. Am J Pathol 25(6):1215-1225.

Gross, L., L. Loewe, and B. Eliasoph 1929. Attempts to reproduce rheumatic fever in animals. J Exp Med 50(1):41-65.

Grundling, A., and O. Schneewind 2007. Synthesis of glycerol phosphate lipoteichoic acid in Staphylococcus aureus. Proc Natl Acad Sci U S A 104(20):8478-8483.

Guedez, Y., A. Kotby, M. El-Demellawy, A. Galal, G. Thomson, S. Zaher, S. Kassem, and M. Kotb 1999. HLA class II associations with rheumatic heart disease are more evident and consistent among clinically homogeneous patients. Circulation 99(21):2784-2790.

Guilherme, L., E. Cunha-Neto, V. Coelho, R. Snitcowsky, P. M. Pomerantzeff, R. V. Assis, F. Pedra, J. Neumann, A. Goldberg, M. E. Patarroyo, and et al. 1995. Human heart-infiltrating T-cell clones from rheumatic heart disease patients recognize both streptococcal and cardiac proteins. Circulation 92(3):415-420.

Guilherme, L., E. Cunha-Neto, A. C. Tanaka, N. Dulphy, A. Toubert, and J. Kalil 2001a. Heart-directed autoimmunity: the case of rheumatic fever. J Autoimmun 16(3):363-367.

Guilherme, L., P. Cury, L. M. Demarchi, V. Coelho, L. Abel, A. P. Lopez, S. E. Oshiro, S. Aliotti, E. Cunha-Neto, P. M. Pomerantzeff, A. C. Tanaka, and J. Kalil 2004. Rheumatic heart disease: proinflammatory cytokines play a role in the progression and maintenance of valvular lesions. Am J Pathol 165(5):1583-1591.

Guilherme, L., S. F. de Barros, K. F. Kohler, S. R. Santos, F. M. Ferreira, W. R. Silva, R. Alencar, E. Postol, and J. Kalil 2017. Rheumatic Heart Disease: pathogenesis and vaccine. Curr Protein Pept Sci 18.

Guilherme, L., N. Dulphy, C. Douay, V. Coelho, E. Cunha-Neto, S. E. Oshiro, R. V. Assis, A. C. Tanaka, P. M. Pomerantzeff, D. Charron, A. Toubert, and J. Kalil 2000. Molecular evidence for antigen-driven immune responses in cardiac lesions of rheumatic heart disease patients. Int Immunol 12(7):1063-1074.

Guilherme, L., K. C. Fae, S. E. Oshiro, A. C. Tanaka, P. M. Pomerantzeff, and J. Kalil 2007. T cell response in rheumatic fever: crossreactivity between streptococcal M protein peptides and heart tissue proteins. Curr Protein Pept Sci 8(1):39-44.

Guilherme, L., F. M. Ferreira, K. F. Kohler, E. Postol, and J. Kalil 2013a. A vaccine against *Streptococcus pyogenes*: the potential to prevent rheumatic fever and rheumatic heart disease. Am J Cardiovasc Drugs 13(1):1-4.

Guilherme, L., and J. Kalil 2002. Rheumatic fever: the T cell response leading to autoimmune aggression in the heart. Autoimmun Rev 1(5):261-266.

Guilherme, L., and J. Kalil 2007. Rheumatic fever: from innate to acquired immune response. Ann N Y Acad Sci 1107:426-433.

Guilherme, L., and J. Kalil 2008. Role of autoimmunity in rheumatic fever. Future Rheumatology 3(2):161-167.

Guilherme, L., and J. Kalil 2010. Rheumatic fever and rheumatic heart disease: cellular mechanisms leading autoimmune reactivity and disease. J Clin Immunol 30(1):17-23.

Guilherme, L., J. Kalil, and M. Cunningham 2006. Molecular mimicry in the autoimmune pathogenesis of rheumatic heart disease. Autoimmunity 39(1):31-39.

Guilherme, L., K. F. Kohler, and J. Kalil 2011a. Rheumatic heart disease: mediation by complex immune events. Adv Clin Chem 53:31-50.

Guilherme, L., K. F. Köhler, P. Pommerantzeff, G. Spina, and J. Kalil 2013b. Rheumatic Heart Disease: Key Points on Valve Lesions Development. J Clin Exp Cardiolog 3(6).

Guilherme, L., K. F. Kohler, E. Postol, and J. Kalil 2011b. Genes, autoimmunity and pathogenesis of rheumatic heart disease. Ann Pediatr Cardiol 4(1):13-21.

Guilherme, L., S. E. Oshiro, K. C. Fae, E. Cunha-Neto, G. Renesto, A. C. Goldberg, A. C. Tanaka, P. M. Pomerantzeff, M. H. Kiss, C. Silva, F. Guzman, M. E. Patarroyo, S. Southwood, A. Sette, and J. Kalil 2001b. T-cell reactivity against streptococcal antigens in the periphery mirrors reactivity of heart-infiltrating T lymphocytes in rheumatic heart disease patients. Infect Immun 69(9):5345-5351.

Guilherme, L., W. Weidebach, M. H. Kiss, R. Snitcowsky, and J. Kalil 1991. Association of human leukocyte class II antigens with rheumatic fever or rheumatic heart disease in a Brazilian population. Circulation 83(6):1995-1998.

Gulizia, J. M., M. W. Cunningham, and B. M. McManus 1991. Immunoreactivity of anti-streptococcal monoclonal antibodies to human heart valves. Evidence for multiple cross-reactive epitopes. Am J Pathol 138(2):285-301.

Gupta, R., K. Prakash, and A. K. Kapoor 1992. Subclinical group A streptococcal throat infection in school children. Indian Pediatr 29(12):1491-1494.

Guven, S., T. Sen, O. Tufekcioglu, E. Gucuk, B. Uygur, and E. Kahraman 2014. Evaluation of left ventricular systolic function with pulsed wave tissue Doppler in rheumatic mitral stenosis. Cardiol J 21(1):33-38.

Guvenc, O., and D. Cimen 2017. A rare situation in acute rheumatic carditis: Involvement of all four valves. Turk J Pediatr 59(4):497-500.

Haanes-Fritz, E., W. Kraus, V. Burdett, J. B. Dale, E. H. Beachey, and P. Cleary 1988. Comparison of the leader sequences of four group A streptococcal M protein genes. Nucleic Acids Res 16(10):4667-4677.

Hafez, M., S. Yahia, W. Eldars, H. Eldegla, M. Matter, G. Attia, and S. Hawas 2013. Prediction of residual valvular lesions in rheumatic heart disease: role of adhesion molecules. Pediatr Cardiol 34(3):583-590.

Haidan, A., S. R. Talay, M. Rohde, K. S. Sriprakash, B. J. Currie, and G. S. Chhatwal 2000. Pharyngeal carriage of group C and group G streptococci and acute rheumatic fever in an Aboriginal population. Lancet 356(9236):1167-1169.

Hall, C. L., R. B. Colvin, K. Carey, and R. T. McCluskey 1977. Passive transfer of autoimmune disease with isologous IgG1 and IgG2 antibodies to the tubular basement membrane in strain XIII guinea pigs: loss of self-tolerance induced by autoantibodies. J Exp Med 146(5):1246-1260.

Hallas, G., and J. P. Widdowson 1983. The relationship between opacity factor and M protein in *Streptococcus pyogenes*. J Med Microbiol 16(1):13-26.

Hamada, S., M. Torii, S. Kotani, N. Masuda, T. Ooshima, K. Yokogawa, and S. Kawata 1978. Lysis of *Streptococcus mutans* cells with mutanolysin, a lytic enzyme prepared from a culture liquor of *Streptomyces globisporus* 1829. Arch Oral Biol 23(7):543-549.

Hanski, E., and M. Caparon 1992. Protein F, a fibronectin-binding protein, is an adhesin of the group A streptococcus *Streptococcus pyogenes*. Proc Natl Acad Sci USA 89(13):6172-6176.

Harrington, A. T., and J. E. Clarridge 2013. Impact of identification of *Streptococcus dysgalactiae* subspecies *equisimilis* from throat cultures in an adult population. Diagn Microbiol Infect Dis 76(1):20-23.

Hartas, J., A. M. Goodfellow, B. J. Currie, and K. S. Sriprakash 1995. Characterisation of group A streptococcal isolates from tropical Australia with high prevalence of rheumatic fever: probing for signature sequences to identify members of the family of serotype 5. Microb Pathog 18(5):345-354.

Hashikawa, S., Y. Iinuma, M. Furushita, T. Ohkura, T. Nada, K. Torii, T. Hasegawa, and M. Ohta 2004. Characterization of group C and G streptococcal strains that cause streptococcal toxic shock syndrome. J Clin Microbiol 42(1):186-192.

Haskins, K., and M. McDuffie 1990. Acceleration of diabetes in young NOD mice with a CD4+ islet-specific T cell clone. Science 249(4975):1433-1436.

Hobday, P. M., J. L. Auger, G. R. Schuneman, S. Haasken, J. S. Verbeek, and B. A. Binstadt 2014. Fcγ Receptor III and Fcγ Receptor IV on Macrophages Drive Autoimmune Valvular Carditis in Mice. Arthritis Rheum 66(4):852-862.

Hollenberg, S. M. 2017. Valvular Heart Disease in Adults: Etiologies, Classification, and Diagnosis. FP Essent 457:11-16.

Hollingshead, S. K., V. A. Fischetti, and J. R. Scott 1986. Complete nucleotide sequence of type 6 M protein of the group A *Streptococcus*. Repetitive structure and membrane anchor. J Biol Chem 261(4):1677-1686.

Holt, J. H. 1946. Rheumatic heart disease; the use of x-ray in diagnosis. J Mich State Med Soc 45:197-201.

Homer, C., and S. T. Shulman 1991. Clinical aspects of acute rheumatic fever. The Journal of rheumatology Supplement 29:2-13.

Horstkotte, D., R. Niehues, and B. E. Strauer 1991. Pathomorphological aspects, aetiology and natural history of acquired mitral valve stenosis. Eur Heart J 12:55-60.

Hosenpud, J. D., S. M. Campbell, M. V. Hart, M. S. Paul, J. R. Rowles, and N. R. Niles 1985. Experimental autoimmune myocarditis in the guinea pig. Cardiovasc Res 19(10):613-622.

Huang, J., X. Xie, Z. F. Lin, M. Q. Luo, B. Y. Yu, and J. R. Gu 2009. Induction of myocarditis lesions in Lewis rats by formalin-killed cells of group A *Streptococcus*. J Int Med Res 37(1):175-181.

Hubbard, W. N., C. Westgate, L. M. Shapiro, and R. M. Donaldson 1987. Acquired abnormalities of the tricuspid valve--an ultrasonographic study. Int J Cardiol 14(3):311-318.

Humar, D., V. Datta, D. J. Bast, B. Beall, J. C. De Azavedo, and V. Nizet 2002. Streptolysin S and necrotising infections produced by group G *Streptococcus*. Lancet 359(9301):124-129.

Humtsoe, J. O., J. K. Kim, Y. Xu, D. R. Keene, M. Hook, S. Lukomski, and K. K. Wary 2005. A streptococcal collagen-like protein interacts with the alpha2beta1 integrin and induces intracellular signaling. J Biol Chem 280(14):13848-13857.

Hunt, S. W., E. S. Harris, S. A. Kellermann, and Y. Shimizu 1996. T-lymphocyte interactions with endothelium and extracellular matrix. Crit Rev Oral Biol Med 7(1):59-86.

Husby, G., I. van de Rijn, J. B. Zabriskie, Z. H. Abdin, and R. C. Williams, Jr. 1976. Antibodies reacting with cytoplasm of subthalamic and caudate nuclei neurons in chorea and acute rheumatic fever. J Exp Med 144(4):1094-1110.

Hutagalung, A. H., M. L. Landsverk, M. G. Price, and H. F. Epstein 2002. The UCS family of myosin chaperones. J Cell Sci 115(21):3983-3990.

Igwe, E. I., P. L. Shewmaker, R. R. Facklam, M. M. Farley, C. van Beneden, and B. Beall 2003. Identification of superantigen genes speM, ssa, and smeZ in invasive strains of beta-hemolytic group C and G streptococci recovered from humans. FEMS Microbiol Lett 229(2):259-264.

Ikebe, T., S. Murayama, K. Saitoh, S. Yamai, R. Suzuki, J. Isobe, D. Tanaka, C. Katsukawa, A. Tamaru, A. Katayama, Y. Fujinaga, K. Hoashi, and H. Watanabe 2004. Surveillance of severe invasive group-G streptococcal infections and molecular typing of the isolates in Japan. Epidemiol Infect 132(1):145-149.

Ivanov, II, B. S. McKenzie, L. Zhou, C. E. Tadokoro, A. Lepelley, J. J. Lafaille, D. J. Cua, and D. R. Littman 2006. The orphan nuclear receptor RORgammat directs the differentiation program of proinflammatory IL-17+ T helper cells. Cell 126(6):1121-1133.

Iyer, V., E. R. Edelman, and L. S. Lilly 2007. Basic cardiac structure and function. *In* Pathophysiology of Heart Disease, a collaborative project of medical students and faculty. 4 edition. L.S. Lilly, ed.

Izumi, T., B. Maisch, and K. Kochsiek 1987. Experimental murine myocarditis after immunization with cardiac membranous proteins. European Heart Journal 8(suppl J):419-424.

Jack, S., D. Williamson, Y. Galloway, N. Pierse, R. Milne, G. Mackereth, J. Zhang, J. Oliver, and M.G. Baker 2015. Interim Evaluation of the Sore Throat Component of the Rheumatic Fever Prevention Programme – Quantitative Findings. Pp. 1-175. Porirua, New Zealand: The Institute of Environmental Science and Research Ltd.

Jain, S., and S. V. Mankad 2013. Echocardiographic assessment of mitral stenosis: echocardiographic features of rheumatic mitral stenosis. Cardiol Clin 31(2):177-191.

Jaseja, H., S. Badaya, and P. Tonpay 2010. Immuno-prophylaxis against development of cardiac valvular complications in patients with rheumatic fever: A proposal method. WebmedCentral Immunology 1(9):758.

Jensen, A., and M. Kilian 2012. Delineation of *Streptococcus dysgalactiae*, its subspecies, and its clinical and phylogenetic relationship to *Streptococcus pyogenes*. J Clin Microbiol 50(1):113-126.

Johansson, H. M., M. Morgelin, and I. M. Frick 2004. Protein FOG--a streptococcal inhibitor of neutrophil function. Microbiology 150(12):4211-4221.
Johnson, D. R., D. L. Stevens, and E. L. Kaplan 1992. Epidemiologic analysis of group A streptococcal serotypes associated with severe systemic infections, rheumatic fever, or uncomplicated pharyngitis. J Infect Dis 166(2):374-382.
Jois, S. D., and T. J. Teruna 2003. A peptide derived from LFA-1 protein that modulates T-cell adhesion binds to soluble ICAM-1 protein. J Biomol Struct Dyn 20(5):635-644.
Jones, K. F., and V. A. Fischetti 1987. Biological and immunochemical identity of M protein on group G streptococci with M protein on group A streptococci. Infect Immun 55(3):502-506.
Jones, T. D. 1944. The diagnosis of rheumatic fever. J Am Med Assoc 126:481-484.
Kakuya, F., T. Kinebuchi, H. Okubo, K. Matsuo, M. Kuroda, and H. Fujiyasu 2017. Acute Pharyngitis Associated with *Streptococcus dysgalactiae* Subspecies *equisimilis* in Children. Pediatr Infect Dis J.
Kalia, A., and D. E. Bessen 2003. Presence of streptococcal pyrogenic exotoxin A and C genes in human isolates of group G streptococci. FEMS Microbiol Lett 219(2):291-295.
Kalia, A., and D. E. Bessen 2004. Natural selection and evolution of streptococcal virulence genes involved in tissue-specific adaptations. J Bacteriol 186(1):110-121.
Kamal, H., G. Hussein, H. Hassoba, N. Mosaad, A. Gad, and M. Ismail 2010. Transforming growth factor-beta1 gene C-509T and T869C polymorphisms as possible risk factors in rheumatic heart disease in Egypt. Acta Cardiol 65(2):177-183.
Kamblock, J., L. N'Guyen, B. Pagis, P. Costes, C. Le Goanvic, P. Lionet, B. Maheu, and G. Papouin 2005. Acute severe mitral regurgitation during first attacks of rheumatic fever: clinical spectrum, mechanisms and prognostic factors. J Heart Valve Dis 14(4):440-446.
Kaplan, E. L. 1980. The group A streptococcal upper respiratory tract carrier state: an enigma. J Pediatr 97(3):337-345.
Kaplan, E. L. 1985. Epidemiological approaches to understanding the pathogenesis of rheumatic fever. Int J Epidemiol 14(4):499-501.
Kaplan, E. L. 1993. T. Duckett Jones Memorial Lecture. Global assessment of rheumatic fever and rheumatic heart disease at the close of the century. Influences and dynamics of populations and pathogens: a failure to realize prevention? Circulation 88(4 Pt 1):1964-1972.
Kaplan, E. L. 1996. Recent epidemiology of group A streptococcal infections in North America and abroad: an overview. Pediatrics 97(6 Pt 2):945-948.

Kaplan, M. H. 1963. Immunologic relation of streptooccal and tissue antigens. I. Properties of an antigen in certain strains of group A streptococci exhibiting an immunologic cross-reaction with human heart tissue. J Immunol 90:595-606.
Kaplan, M. H., R. Bolande, L. Rakita, and J. Blair 1964. Presence of bound immunolgobulins and complement in the myocardium in acute rheumatic fever. Association with cardiac failure. N Engl J Med 271:637-645.
Kaplan, M. H., and J. M. Craig 1963. Immunologic studies of heart tissue. VI. Cardiac lesions in rabbits associated with autoantibodies to heart induced by immunization with heterologous heart. J Immunol 90:725-733.
Kaplan, M. H., and D. D. Frederick 1961. Occurence of bound gamma globulin in auricular appendages from rheumatic hearts, relationship to certain histopathologic features of rheumatic heart disease. J Exp Med 113(1):1-16.
Kaplan, M. H., and K. H. Svec 1964. Immunologic relation of streptooccal and tissue antigens. II. Cross-reaction of antisera to mammalian heart tissue with a cell wall constituent of certain strains of group A *Streptococcus*. J Exp Med 119:651-666.
Karthikeyan, G., and B. M. Mayosi 2009. Is primary prevention of rheumatic fever the missing link in the control of rheumatic heart disease in Africa? Circulation 120(8):709-713.
Katzenellenbogen, J. M., A. P. Ralph, R. Wyber, and J. R. Carapetis 2017. Rheumatic heart disease: infectious disease origin, chronic care approach. BMC Health Serv Res 17(1):793.
Kay, A. B. 1997. Concepts of allergy and hypersensitivity. *In* Allergy and allergic diseases. A.B. Kay, ed. Pp. 23-25. Oxford: Blackwell Sciences.
Kemeny, E., T. Grieve, R. Marcus, P. Sareli, and J. B. Zabriskie 1989. Identification of mononuclear cells and T cell subsets in rheumatic valvulitis. Clin Immunol Immunopathol 52(2):225-237.
Kerdemelidis, M., D. R. Lennon, B. Arroll, B. Peat, and J. Jarman 2010. The primary prevention of rheumatic fever. J Paediatr Child Health 46(9):534-548.
Khanna, A. K., Y. Nomura, V. A. Fischetti, and J. B. Zabriskie 1997. Antibodies in the sera of acute rheumatic fever patients bind to human cardiac tropomyosin. J Autoimmun 10(1):99-106.
Kirvan, C. A., J. E. Galvin, S. Hilt, S. Kosanke, and M. W. Cunningham 2014. Identification of streptococcal M-protein cardiopathogenic epitopes in experimental autoimmune valvulitis. J Cardiovasc Transl Res 7(2):172-181.
Kirvan, C. A., S. E. Swedo, J. S. Heuser, and M. W. Cunningham 2003. Mimicry and autoantibody-mediated neuronal cell signaling in Sydenham chorea. Nat Med 9(7):914-920.

Kirvan, C. A., S. E. Swedo, D. Kurahara, and M. W. Cunningham 2006. Streptococcal mimicry and antibody-mediated cell signaling in the pathogenesis of Sydenham's chorea. Autoimmunity 39(1):21-29.

Kittang, B. R., N. Langeland, S. Skrede, and H. Mylvaganam 2010. Two unusual cases of severe soft tissue infection caused by *Streptococcus dysgalactiae* subsp. *equisimilis*. J Clin Microbiol 48(4):1484-1487.

Kodama, M., Y. Matsumoto, and M. Fujiwara 1992. In vivo lymphocyte-mediated myocardial injuries demonstrated by adoptive transfer of experimental autoimmune myocarditis. Circulation 85(5):1918-1926.

Kodama, M., Y. Matsumoto, M. Fujiwara, F. Masani, T. Izumi, and A. Shibata 1990. A novel experimental model of giant cell myocarditis induced in rats by immunization with cardiac myosin fraction. Clin Immunol Immunopathol 57(2):250-262.

Konopelski, P., and M. Ufnal 2016. Electrocardiography in rats: a comparison to human. Physiol Res 65(5):717-725.

Krankel, N., K. Kuschnerus, P. Madeddu, T. F. Luscher, and U. Landmesser 2011. A novel flow cytometry-based assay to study leukocyte-endothelial cell interactions in vitro. Cytometry A 79(4):256-262.

Kreikemeyer, B., M. Klenk, and A. Podbielski 2004. The intracellular status of Streptococcus pyogenes: role of extracellular matrix-binding proteins and their regulation. Int J Med Microbiol 294(2-3):177-188.

Kreikemeyer, B., S. R. Talay, and G. S. Chhatwal 1995. Characterization of a novel fibronectin-binding surface protein in group A streptococci. Mol Microbiol 17(1):137-145.

Krisher, K., and M. W. Cunningham 1985. Myosin: a link between streptococci and heart. Science 227(4685):413-415.

Kumar, R, A Kela, and G Tayal 2009. Effect Of Acute Stress On Rat ECG. The Internet Journal of Pharmacology 8(1).

Kumar, R. 1995. Controlling rheumatic heart disease in developing countries. World Health Forum 16(1):47-51.

Lam, K., and A. S. Bayer 1983. Serious infections due to group G streptoccocci. Report of 15 cases with in vitro-in vivo correlations. Am J Med 75(4):561-570.

Lancefield, R. C. 1933. A serological differentiation of human and other groups of hemolytic streptococci. J Exp Med 57(4):571-595.

Lancefield, R. C. 1962. Current knowledge of type-specific M antigens of group A streptococci. J Immunol 89:307-313.

Lancefield, R. C., and R. Hare 1935. The serological differentiation of pathogenic and non-pathogenic strains of hemolytic streptococci from parturient women. J Exp Med 61(3):335-349.

Lawal, S. F., A. O. Coker, E. O. Solanke, and O. Ogunbi 1982. Serotypes among Lancefield-group G streptococci isolated in Nigeria. J Med Microbiol 15(1):123-125.

Lawrence, J. G., J. R. Carapetis, K. Griffiths, K. Edwards, and J. R. Condon 2013. Acute rheumatic fever and rheumatic heart disease: incidence and progression in the Northern Territory of Australia, 1997 to 2010. Circulation 128(5):492-501.

Leask, R. L., N. Jain, and J. Butany 2003. Endothelium and valvular diseases of the heart. Microscopy Research and Technique 60(2):129-137.

Lehmann, P. V., T. Forsthuber, A. Miller, and E. E. Sercarz 1992. Spreading of T-cell autoimmunity to cryptic determinants of an autoantigen. Nature 358(6382):155-157.

Leitner, E., I. Zollner-Schwetz, G. Zarfel, L. Masoud-Landgraf, M. Gehrer, U. Wagner-Eibel, A. J. Grisold, and G. Feierl 2015. Prevalence of emm types and antimicrobial susceptibility of *Streptococcus dysgalactiae* subsp. *equisimilis* in Austria. Int J Med Microbiol 305(8):918-924.

Ley, K., C. Laudanna, M. I. Cybulsky, and S. Nourshargh 2007. Getting to the site of inflammation: the leukocyte adhesion cascade updated. Nat Rev Immunol 7(9):678-689.

Li, W., Z. Zeng, C. Gui, H. Zheng, W. Huang, H. Wei, and D. Gong 2015. Proteomic analysis of mitral valve in Lewis rat with acute rheumatic heart disease. Int J Clin Exp Pathol 8(11):14151-14160.

Li, Y., J. S. Heuser, S. D. Kosanke, M. Hemric, and M. W. Cunningham 2004. Cryptic epitope identified in rat and human cardiac myosin S2 region induces myocarditis in the Lewis rat. J Immunol 172(5):3225-3234.

Liao, C. H., L. C. Liu, Y. T. Huang, L. J. Teng, and P. R. Hsueh 2008. Bacteremia caused by group G Streptococci, taiwan. Emerg Infect Dis 14(5):837-840.

Licciardi, F., G. Scaioli, R. Mulatero, A. Marolda, M. Delle Piane, S. Martino, D. Montin, and P. A. Tovo 2018. Epidemiologic Impact of the New Guidelines for the Diagnosis of Acute Rheumatic Fever. J Pediatr.

Lindbaek, M., E. A. Hoiby, G. Lermark, I. M. Steinsholt, and P. Hjortdahl 2005. Clinical symptoms and signs in sore throat patients with large colony variant beta-haemolytic streptococci groups C or G versus group A. Br J Gen Pract 55(517):615-619.

Lis, Y., M. C. Burleigh, D. J. Parker, A. H. Child, J. Hogg, and M. J. Davies 1987. Biochemical characterization of individual normal, floppy and rheumatic human mitral valves. Biochem J 244(3):597-603.

Liu, Z., L. A. Diaz, J. L. Troy, A. F. Taylor, D. J. Emery, J. A. Fairley, and G. J. Giudice 1993. A passive transfer model of the organ-specific autoimmune disease, bullous pemphigoid, using antibodies generated against the hemidesmosomal antigen, BP180. J Clin Invest 92(5):2480-2488.

Lloyd, C. A., S. E. Jacob, and T. Menon 2006. Pharyngeal carriage of group A streptococci in school children in Chennai. Indian J Med Res 124(2):195-198.

Loetscher, M., B. Gerber, P. Loetscher, S. A. Jones, L. Piali, I. Clark-Lewis, M. Baggiolini, and B. Moser 1996. Chemokine receptor specific for IP10 and mig: structure, function, and expression in activated T-lymphocytes. J Exp Med 184(3):963-969.

Longo-Mbenza, B., M. Bayekula, R. Ngiyulu, V. E. Kintoki, N. F. Bikangi, K. V. Seghers, L. E. Lukoki, M. F. Mandundu, M. Manzanza, and Y. Nlandu 1998. Survey of rheumatic heart disease in school children of Kinshasa town. Int J Cardiol 63(3):287-294.

Lother, S. A., D. S. Jassal, P. Lagace-Wiens, and Y. Keynan 2017. Emerging group C and group G streptococcal endocarditis: A Canadian perspective. Int J Infect Dis 65:128-132.

Love, G. L., and C. Restrepo 1988. Aschoff bodies of rheumatic carditis are granulomatous lesions of histiocytic origin. Mod Pathol 1(4):256-261.

Lue, H. C., W. P. Tseng, G. J. Lin, K. H. Hsieh, R. P. Hsieh, and J. F. Chiou 1983. Clinical and epidemiological features of rheumatic fever and rheumatic heart disease in Taiwan and the Far East. Indian Heart J 35(3):139-146.

Lukacs, N. W., R. M. Strieter, V. Elner, H. L. Evanoff, M. D. Burdick, and S. L. Kunkel 1995. Production of chemokines, interleukin-8 and monocyte chemoattractant protein-1, during monocyte: endothelial cell interactions. Blood 86(7):2767-2773.

Lukomski, S., K. Nakashima, I. Abdi, V. J. Cipriano, R. M. Ireland, S. D. Reid, G. G. Adams, and J. M. Musser 2000. Identification and characterization of a second extracellular collagen-like protein made by group A *Streptococcus*: control of production at the level of translation. Infect Immun 68(12):6542-6553.

Lukomski, S., K. Nakashima, I. Abdi, V. J. Cipriano, B. J. Shelvin, E. A. Graviss, and J. M. Musser 2001. Identification and characterization of a second extracellular collagen-like protein made by group A *Streptococcus*: control of production at the level of translation. Infect Immun 69(3):1729-1738.

Ly, A. T., J. P. Noto, O. L. Walwyn, R. R. Tanz, S. T. Shulman, W. Kabat, and D. E. Bessen 2017. Differences in SpeB protease activity among group A streptococci associated with superficial, invasive, and autoimmune disease. PLoS One 12(5):e0177784.

Lymbury, R. S., C. Olive, K. A. Powell, M. F. Good, R. G. Hirst, J. T. LaBrooy, and N. Ketheesan 2003. Induction of autoimmune valvulitis in Lewis rats following immunization with peptides from the conserved region of group A streptococcal M protein. J Autoimmun 20(3):211-217.

Malke, H., B. Roe, and J. J. Ferretti 1985. Nucleotide sequence of the streptokinase gene from *Streptococcus equisimilis* H46A. Gene 34(2-3):357-362.

Manjula, B. N., K. M. Khandke, T. Fairwell, W. A. Relf, and K. S. Sriprakash 1991. Heptad motifs within the distal subdomain of the coiled-coil rod region of M protein from rheumatic fever and nephritis associated serotypes of group A streptococci are distinct from each other: nucleotide sequence of the M57 gene and relation of the deduced amino acid sequence to other M proteins. J Protein Chem 10(4):369-384.

Marboe, C. C., D. M. Knowles, 2nd, M. B. Weiss, and J. J. Fenoglio, Jr. 1985. Monoclonal antibody identification of mononuclear cells in endomyocardial biopsy specimens from a patient with rheumatic carditis. Hum Pathol 16(4):332-338.

Marciniak, A., P. Claus, G. R. Sutherland, M. Marciniak, T. Karu, A. Baltabaeva, E. Merli, B. Bijnens, and M. Jahangiri 2007. Changes in systolic left ventricular function in isolated mitral regurgitation. A strain rate imaging study. Eur Heart J 28(21):2627-2636.

Marcus, R. H., P. Sareli, W. A. Pocock, and J. B. Barlow 1994. The spectrum of severe rheumatic mitral valve disease in a developing country. Correlations among clinical presentation, surgical pathologic findings, and hemodynamic sequelae. Ann Intern Med 120(3):177-183.

Marcus, R. H., P. Sareli, W. A. Pocock, T. E. Meyer, M. P. Magalhaes, T. Grieve, M. J. Antunes, and J. B. Barlow 1989. Functional anatomy of severe mitral regurgitation in active rheumatic carditis. Am J Cardiol 63(9):577-584.

Marijon, E., P. Ou, D. S. Celermajer, B. Ferreira, A. O. Mocumbi, D. Jani, C. Paquet, S. Jacob, D. Sidi, and X. Jouven 2007. Prevalence of rheumatic heart disease detected by echocardiographic screening. N Engl J Med 357(5):470-476.

Marino, A. P., M. I. Azevedo, and J. Lannes-Vieira 2003. Differential expression of adhesion moleculesshaping the T-cell subset prevalence during the early phase of autoimmune and Trypanosoma cruzi-elicited myocarditis. Mem Inst Oswaldo Cruz 98(7):945-952.

Markowitz, M. 1991. Streptococcal disease in developing countries. Pediatr Infect Dis J 10(10 Suppl):S11-14.
Markowitz, M., and M. A. Gerber 1987. Rheumatic fever: recent outbreaks of an old disease. Conn Med 51(4):229-233.
Martin, J. M., M. Green, K. A. Barbadora, and E. R. Wald 2004. Group A streptococci among school-aged children: clinical characteristics and the carrier state. Pediatrics 114(5):1212-1219.
Martin, N. J., E. L. Kaplan, M. A. Gerber, M. A. Menegus, M. Randolph, K. Bell, and P. P. Cleary 1990. Comparison of epidemic and endemic group G streptococci by restriction enzyme analysis. J Clin Microbiol 28(9):1881-1886.
Martins, C. O., L. Demarchi, F. M. Ferreira, P. M. Pomerantzeff, C. Brandao, R. O. Sampaio, G. S. Spina, J. Kalil, E. Cunha-Neto, and L. Guilherme 2017. Rheumatic heart disease and myxomatous degeneration: differences and similarities of valve damage resulting from autoimmune reactions and matrix disorganization. PLoS One 12(1):e0170191.
Martins, T. B., J. L. Hoffman, N. H. Augustine, A. R. Phansalkar, V. A. Fischetti, J. B. Zabriskie, P. P. Cleary, J. M. Musser, L. G. Veasy, and H. R. Hill 2008. Comprehensive analysis of antibody responses to streptococcal and tissue antigens in patients with acute rheumatic fever. Int Immunol 20(3):445-452.
Maxted, W. R. 1949. Occurrence of the M. substance of type 28 group A in streptococci of Lancefield groups B, C and G. J Gen Microbiol 3(1):1-6.
Maxted, W. R., and E. V. Potter 1967. The presence of type 12 M-protein antigen in group G streptococci. J Gen Microbiol 49(1):119-125.
McCarthy, K. P., L. Ring, and B. S. Rana 2010. Anatomy of the mitral valve: understanding the mitral valve complex in mitral regurgitation. Eur J Echocardiogr 11(10):i3-9.
McCarty, M. 1956. Nature of rheumatic fever. Circulation 14(6):1138-1143.
McDonald, M., B. J. Currie, and J. R. Carapetis 2004. Acute rheumatic fever: a chink in the chain that links the heart to the throat? Lancet Infect Dis 4(4):240-245.
McDonald, M. I., R. J. Towers, R. M. Andrews, N. Benger, B. J. Currie, and J. R. Carapetis 2006. Low rates of streptococcal pharyngitis and high rates of pyoderma in Australian aboriginal communities where acute rheumatic fever is hyperendemic. Clin Infect Dis 43(6):683-689.
McMillan, D. J., D. E. Bessen, M. Pinho, C. Ford, G. S. Hall, J. Melo-Cristino, and M. Ramirez 2010. Population genetics of *Streptococcus dysgalactiae* subspecies *equisimilis* reveals widely dispersed clones and extensive recombination. PLoS One 5(7):e11741.

McNeil, S. A., S. A. Halperin, J. M. Langley, B. Smith, A. Warren, G. P. Sharratt, D. M. Baxendale, M. A. Reddish, M. C. Hu, S. D. Stroop, J. Linden, L. F. Fries, P. E. Vink, and J. B. Dale 2005. Safety and immunogenicity of 26-valent group A *Streptococcus* vaccine in healthy adult volunteers. Clin Infect Dis 41(8):1114-1122.

McNeilly, C., S. Cosh, T. Vu, J. Nichols, A. Henningham, A. Hofmann, A. Fane, P. R. Smeesters, C. M. Rush, L. M. Hafner, N. Ketheesan, K. S. Sriprakash, and D. J. McMillan 2016. Predicted Coverage and Immuno-Safety of a Recombinant C-Repeat Region Based Streptococcus pyogenes Vaccine Candidate. PLoS One 11(6):e0156639.

McNeilly, C. L., and D. J. McMillan 2014. Horizontal gene transfer and recombination in *Streptococcus dysgalactiae* subsp. *equisimilis*. Front Microbiol 5:676.

Mertens, N. M., J. E. Galvin, E. E. Adderson, and M. W. Cunningham 2000. Molecular analysis of cross-reactive anti-myosin/anti-streptococcal mouse monoclonal antibodies. Mol Immunol 37(15):901-913.

Miller, B. J., M. C. Appel, J. J. O'Neil, and L. S. Wicker 1988. Both the Lyt-2+ and L3T4+ T cell subsets are required for the transfer of diabetes in nonobese diabetic mice. J Immunol 140(1):52-58.

Miller, L. C., E. D. Gray, M. Mansour, Z. H. Abdin, R. Kamel, S. Zaher, and W. E. Regelmann 1989. Cytokines and immunoglobulin in rheumatic heart disease: production by blood and tonsillar mononuclear cells. J Rheumatol 16(11):1436-1442.

Minich, L. L., L. Y. Tani, L. T. Pagotto, R. E. Shaddy, and L. G. Veasy 1997. Doppler echocardiography distinguishes between physiologic and pathologic "silent" mitral regurgitation in patients with rheumatic fever. Clin Cardiol 20(11):924-926.

Mirabel, M., K. Narayanan, X. Jouven, and E. Marijon 2014. Cardiology patient page. Prevention of acute rheumatic fever and rheumatic heart disease. Circulation 130(5):e35-37.

Mogielnicki, N. P., J. D. Schwartzman, and J. A. Elliott 2000. Perineal group A streptococcal disease in a pediatric practice. Pediatrics 106(2 Pt 1):276-281.

Mohan, P. K., J. Shanmugam, A. Nair, and J. Tharakan 1989. Fatal outcome of group-G streptococcal meningitis (a case report). J Postgrad Med 35(1):49-50.

Moody, M. D., J. Padula, D. Lizana, and C. T. Hall 1965. Epidemiologic charaterization of group A streptococci by T-agglutination and M-precipitation tests in the public health laboratory. Health Lab Sci 2:149-162.

Moon, V. H., and H. L. Stewart 1931. Experimental Rheumatic Lesions in Dogs and in Rabbits. Arch Pathol 11(190):1931.

Morris, K., C. Mohan, P. L. Wahi, I. S. Anand, and N. K. Ganguly 1993a. Enhancement of IL-1, IL-2 production and IL-2 receptor generation in patients with acute rheumatic fever and active rheumatic heart disease; a prospective study. Clin Exp Immunol 91(3):429-436.
Morris, K., C. Mohan, P. L. Wahi, I. S. Anand, and N. K. Ganguly 1993b. Increase in activated T cells and reduction in suppressor/cytotoxic T cells in acute rheumatic fever and active rheumatic heart disease: a longitudinal study. J Infect Dis 167(4):979-983.
Moser, B., and P. Loetscher 2001. Lymphocyte traffic control by chemokines. Nat Immunol 2(2):123-128.
Mota, C. C., Z. M. Meira, R. N. Graciano, F. F. Graciano, and F. D. Araujo 2014. Rheumatic Fever prevention program: long-term evolution and outcomes. Front Pediatr 2:141.
Muller, A. M., C. Cronen, L. I. Kupferwasser, H. Oelert, K. M. Muller, and C. J. Kirkpatrick 2000. Expression of endothelial cell adhesion molecules on heart valves: up-regulation in degeneration as well as acute endocarditis. J Pathol 191(1):54-60.
Murphy, G. E. 1952. Evidence that Aschoff bodies of rheumatic myocarditis develop from injured myofibers. J Exp Med 95(3):319-332.
Murray, C. J., and A. D. Lopez 1996. A compendium of incidence, prevalence, and mortality estimates for over 200 conditions. *In* Global Health Statistics. Cambridge: Harvard University Press.
Nakagawa, P., Y. Liu, T. D. Liao, X. Chen, G. E. Gonzalez, K. R. Bobbitt, D. Smolarek, E. L. Peterson, R. Kedl, X. P. Yang, N. E. Rhaleb, and O. A. Carretero 2012. Treatment with N-acetyl-seryl-aspartyl-lysyl-proline prevents experimental autoimmune myocarditis in rats. Am J Physiol Heart Circ Physiol 303(9):H1114-1127.
Nakata, M. M., J. H. Silvers, and W. L. George 1983. Group G streptococcal arthritis. Arch Intern Med 143(7):1328-1330.
Narin, N., N. Kutukculer, R. Ozyurek, A. R. Bakiler, A. Parlar, and M. Arcasoy 1995. Lymphocyte subsets and plasma IL-1 alpha, IL-2, and TNF-alpha concentrations in acute rheumatic fever and chronic rheumatic heart disease. Clin Immunol Immunopathol 77(2):172-176.
Narula, J., P. Chopra, K. K. Talwar, K. S. Reddy, R. S. Vasan, R. Tandon, M. L. Bhatia, and J. F. Southern 1993. Does endomyocardial biopsy aid in the diagnosis of active rheumatic carditis? Circulation 88(5 Pt 1):2198-2205.
Narula, J., and E. L. Kaplan 2001. Echocardiographic diagnosis of rheumatic fever. Lancet 358(9297):2000.

Narula, J., R. Virmani, K. S. Reddy, and R. Tandon 1999. Rheumatic Fever. American Registry of Pathology, Washington DC, USA.

Nei, T., K. Akutsu, A. Shima, I. Tsuboi, H. Suzuki, T. Yamamoto, K. Tanaka, A. Shinoyama, Y. Kojima, Y. Washio, S. Okawa, K. Sonobe, Y. Norose, and R. Saito 2012. A case of streptococcal toxic shock syndrome due to Group G streptococci identified as *Streptococcus dysgalactiae* subsp. *equisimilis*. J Infect Chemother 18(6):919-924.

Neu, N., B. Ploier, and C. Ofner 1990. Cardiac myosin-induced myocarditis. Heart autoantibodies are not involved in the induction of the disease. J Immunol 145(12):4094-4100.

Neu, N., N. R. Rose, K. W. Beisel, A. Herskowitz, G. Gurri-Glass, and S. W. Craig 1987. Cardiac myosin induces myocarditis in genetically predisposed mice. J Immunol 139(11):3630-3636.

Neuhaus, F. C., and J. Baddiley 2003. A continuum of anionic charge: structures and functions of D-alanyl-teichoic acids in gram-positive bacteria. Microbiol Mol Biol Rev 67(4):686-723.

Nicolle, L. E., B. Postl, B. Urias, B. Law, and N. Ling 1990. Group A streptococcal pharyngeal carriage, pharyngitis, and impetigo in two northern Canadian native communities. Clin Invest Med 13(3):99-106.

Nishibukuro, M., N. Tsutsumi, M. Chiyotanda, T. Hijikata, S. Morichi, S. Go, G. Yamanaka, Y. Kashiwagi, and H. Kawashima 2018. Poststreptococcal reactive arthritis in Japan. J Infect Chemother.

Nitsche-Schmitz, D. P., H. M. Johansson, I. Sastalla, S. Reissmann, I. M. Frick, and G. S. Chhatwal 2007. Group G streptococcal IgG binding molecules FOG and protein G have different impacts on opsonization by C1q. J Biol Chem 282(24):17530-17536.

Nordstrand, A., W. M. McShan, J. J. Ferretti, S. E. Holm, and M. Norgren 2000. Allele substitution of the streptokinase gene reduces the nephritogenic capacity of group A streptococcal strain NZ131. Infect Immun 68(3):1019-1025.

Norlin, G. 1959. Experimental heart granulomatosis in rabbits and its relation to rheumatic carditis. Acta Rheumatol Scand 5:85-100.

Normann, S. J., R. E. Priest, and E. P. Benditt 1961. Electrocardiogram in the normal rat and its alteration with experimental coronary occlusion. Circ Res 9:282-287.

O'Sullivan, L., N. J. Moreland, R. H. Webb, A. Upton, and N. J. Wilson 2017. Acute Rheumatic Fever After Group A *Streptococcus* Pyoderma and Group G *Streptococcus* Pharyngitis. Pediatr Infect Dis J 36(7):692-694.

Oda, T., N. Yoshizawa, K. Yamakami, K. Tamura, A. Kuroki, T. Sugisaki, E. Sawanobori, K. Higashida, Y. Ohtomo, O. Hotta, H. Kumagai, and S. Miura 2010. Localization of nephritis-associated plasmin receptor in acute poststreptococcal glomerulonephritis. Hum Pathol 41(9):1276-1285.

Oehmcke, S., A. Podbielski, and B. Kreikemeyer 2004. Function of the fibronectin-binding serum opacity factor of Streptococcus pyogenes in adherence to epithelial cells. Infect Immun 72(7):4302-4308.

Ofek, I., E. H. Beachey, W. Jefferson, and G. L. Campbell 1975. Cell membrane-binding properties of group A streptococcal lipoteichoic acid. J Exp Med 141(5):990-1003.

Ohanian, S. H., J. H. Schwab, and W. J. Cromartie 1969. Relation of rheumatic-like cardiac lesions of the mouse to localization of group A streptococcal cell walls. J Exp Med 129(1):37-49.

Okada, N., M. K. Liszewski, J. P. Atkinson, and M. Caparon 1995. Membrane cofactor protein (CD46) is a keratinocyte receptor for the M protein of the group A *Streptococcus*. Proc Natl Acad Sci USA 92(7):2489-2493.

Okada, N., A. P. Pentland, P. Falk, and M. G. Caparon 1994. M protein and protein F act as important determinants of cell-specific tropism of *Streptococcus pyogenes* in skin tissue. J Clin Invest 94(3):965-977.

Okura, Y., K. Takeda, S. Honda, H. Hanawa, H. Watanabe, M. Kodama, T. Izumi, Y. Aizawa, S. Seki, and T. Abo 1998. Recombinant murine interleukin-12 facilitates induction of cardiac myosin-specific type 1 helper T cells in rats. Circ Res 82(10):1035-1042.

Oldstone, M. B. 1987. Molecular mimicry and autoimmune disease. Cell 50(6):819-820.

Ono, K., T. Masuyama, K. Yamamoto, R. Doi, Y. Sakata, N. Nishikawa, T. Mano, T. Kuzuya, H. Takeda, and M. Hori 2002. Echo doppler assessment of left ventricular function in rats with hypertensive hypertrophy. J Am Soc Echocardiogr 15(2):109-117.

Pacher, P., T. Nagayama, P. Mukhopadhyay, S. Batkai, and D. A. Kass 2008. Measurement of cardiac function using pressure-volume conductance catheter technique in mice and rats. Nat Protoc 3(9):1422-1434.

Pahlman, L. I., M. Morgelin, J. Eckert, L. Johansson, W. Russell, K. Riesbeck, O. Soehnlein, L. Lindbom, A. Norrby-Teglund, R. R. Schumann, L. Bjorck, and H. Herwald 2006. Streptococcal M protein: a multipotent and powerful inducer of inflammation. J Immunol 177(2):1221-1228.

Palmieri, C., I. M. Ratsch, M. S. Princivalli, C. Candelaresi, G. Magi, C. Spinaci, G. V. Coppa, and B. Facinelli 2007. erm(A)-mediated macrolide resistance and ability to invade

human respiratory cells in a *Streptococcus dysgalactiae* subspecies *equisimilis* pharyngeal isolate. J Antimicrob Chemother 60(6):1405-1406.
Pancholi, V., and V. A. Fischetti 1992. A major surface protein on group A streptococci is a glyceraldehyde-3-phosphate-dehydrogenase with multiple binding activity. J Exp Med 176(2):415-426.
Paque, R. E., and R. Miller 1992. Adoptively transferred anti-idiotype pulsed B cells mediate autoimmune myocarditis. Infect Immun 60(8):3396-3404.
Park, M. K., D. Amichay, P. Love, E. Wick, F. Liao, A. Grinberg, R. L. Rabin, H. H. Zhang, S. Gebeyehu, T. M. Wright, A. Iwasaki, Y. Weng, J. A. DeMartino, K. L. Elkins, and J. M. Farber 2002. The CXC chemokine murine monokine induced by IFN-gamma (CXC chemokine ligand 9) is made by APCs, targets lymphocytes including activated B cells, and supports antibody responses to a bacterial pathogen in vivo. J Immunol 169(3):1433-1443.
Parks, T., P. R. Smeesters, and A. C. Steer 2012. Streptococcal skin infection and rheumatic heart disease. Curr Opin Infect Dis 25(2):145-153.
Parnaby, M. G., and J. R. Carapetis 2010. Rheumatic fever in indigenous Australian children. J Paediatr Child Health 46(9):527-533.
Penm, E. 2008. Cardiovascular disease and its associated risk factors in Aboriginal and Torres Strait Islander peoples 2004-05. (Cardiovascular disease series no. 29. Cat. no. CVD 41) Canberra. Australian Institute of Health and Welfare.
Peppard, J. V., and E. Orlans 1980. The biological half-lives of four rat immunoglobulin isotypes. Immunology 40(4):683-686.
Percy, M. G., and A. Grundling 2014. Lipoteichoic acid synthesis and function in gram-positive bacteria. Annu Rev Microbiol 68:81-100.
Petersen, J. P., M. S. Kaltoft, J. C. Misfeldt, H. Schumacher, and H. C. Schonheyder 2003. Community outbreak of perianal group A streptococcal infection in Denmark. Pediatr Infect Dis J 22(2):105-109.
Phillips, G. N., Jr., P. F. Flicker, C. Cohen, B. N. Manjula, and V. A. Fischetti 1981. Streptococcal M protein: alpha-helical coiled-coil structure and arrangement on the cell surface. Proc Natl Acad Sci U S A 78(8):4689-4693.
Pober, J. S., L. A. Lapierre, A. H. Stolpen, T. A. Brock, T. A. Springer, W. Fiers, M. P. Bevilacqua, D. L. Mendrick, and M. A. Gimbrone, Jr. 1987. Activation of cultured human endothelial cells by recombinant lymphotoxin: comparison with tumor necrosis factor and interleukin 1 species. J Immunol 138(10):3319-3324.

Podbielski, A., J. Hawlitzky, T. D. Pack, A. Flosdorff, and M. D. Boyle 1994. A group A streptococcal Enn protein potentially resulting from intergenomic recombination exhibits atypical immunoglobulin-binding characteristics. Mol Microbiol 12(5):725-736.
Podbielski, A., A. Kaufhold, and P. P. Cleary 1993. PCR-Mediated Amplification of Group A Streptococcal Genes Encoding Immunoglobulin-Binding Proteins. ImmunoMethods 2(1):55-64.
Podbielski, A., B. Melzer, and R. Lutticken 1991. Application of the polymerase chain reaction to study the M protein(-like) gene family in beta-hemolytic streptococci. Med Microbiol Immunol 180(4):213-227.
Poon-King, R., J. Bannan, A. Viteri, G. Cu, and J. B. Zabriskie 1993. Identification of an extracellular plasmin binding protein from nephritogenic streptococci. J Exp Med 178(2):759-763.
Potter, E. V., J. B. Vincente, WHite R. T. Mayon, M. A. Shaughnessy, T. Poon-King, and D. P. Earle 1982. Skin infections and immunoglobulin A in serum, sweat, and saliva of patients recovered from poststreptococcal acute glomerulonephritis or acute rheumatic fever and their siblings. Am J Epidemiol 115(6):951-959.
Poyart, C., G. Quesne, S. Coulon, P. Berche, and P. Trieu-Cuot 1998. Identification of streptococci to species level by sequencing the gene encoding the manganese-dependent superoxide dismutase. J Clin Microbiol 36(1):41-47.
Proft, T., S. L. Moffatt, C. J. Berkahn, and J. D. Fraser 1999. Identification and characterization of novel superantigens from *Streptococcus pyogenes*. J Exp Med 189(1):89-102.
Pruksakorn, S., B. Currie, E. Brandt, C. Phornphutkul, S. Hunsakunachai, A. Manmontri, J. H. Robinson, M. A. Kehoe, A. Galbraith, and M. F. Good 1994. Identification of T cell autoepitopes that cross-react with the C-terminal segment of the M protein of group A streptococci. Int Immunol 6(8):1235-1244.
Pruksakorn, S., N. Sittisombut, C. Phornphutkul, C. Pruksachatkunakorn, M. F. Good, and E. Brandt 2000. Epidemiological analysis of non-M-typeable group A Streptococcus isolates from a Thai population in northern Thailand. J Clin Microbiol 38(3):1250-1254.
Qiu, H., H. Wu, J. Ma, H. Cao, L. Huang, W. Qiu, Y. Peng, and C. Ding 2017. DL-3-n-Butylphthalide reduces atrial fibrillation susceptibility by inhibiting atrial structural remodeling in rats with heart failure. Naunyn Schmiedebergs Arch Pharmacol.
Quinn, A., E. E. Adderson, P. G. Shackelford, W. L. Carroll, and M. W. Cunningham 1995. Autoantibody germ-line gene segment encodes VH and VL regions of a human anti-

streptococcal monoclonal antibody recognizing streptococcal M protein and human cardiac myosin epitopes. J Immunol 154(8):4203-4212.
Quinn, A., S. Kosanke, V. A. Fischetti, S. M. Factor, and M. W. Cunningham 2001. Induction of autoimmune valvular heart disease by recombinant streptococcal m protein. Infect Immun 69(6):4072-4078.
Quinn, R. W., P. N. Lowry, and R. V. Zwaag 1978. Significance of hemolytic streptococci for Nashville school children: clinical and serologic observations. South Med J 71(3):242-246.
Radhakrishnan, V. V. 1996. Experimental myocarditis in the guinea-pig. Cardiovasc Res 31(4):651-654.
Raizada, V., R. C. J. Williams, P. Chopra, N. Gopinath, K. Prakash, K. B. Sharma, K. M. Cherian, S. Panday, R. Arora, M. Nigam, J. B. Zabriskie, and G. Husby 1983. Tissue distribution of lymphocytes in rheumatic heart valves as defined by monoclonal anti-T cell antibodies. Am J Med 74(1):90-96.
Rajkumar, S., and R. Krishnamurthy 2001. Isolation of group A beta-hemolytic streptococci in the tonsillopharynx of school children in Madras City and correlation with their clinical features. Jpn J Infect Dis 54(4):137-139.
Ramasawmy, R., K. C. Fae, G. Spina, G. D. Victora, A. C. Tanaka, S. A. Palacios, A. G. Hounie, E. C. Miguel, S. E. Oshiro, A. C. Goldberg, J. Kalil, and L. Guilherme 2007. Association of polymorphisms within the promoter region of the tumor necrosis factor-alpha with clinical outcomes of rheumatic fever. Mol Immunol 44(8):1873-1878.
Rantala, S., S. Vahakuopus, J. Vuopio-Varkila, R. Vuento, and J. Syrjanen 2010. *Streptococcus dysgalactiae* subsp. *equisimilis* Bacteremia, Finland, 1995-2004. Emerg Infect Dis 16(5):843-846.
Rantz, L. A., P. J. Boisvert, and W. W. Spink 1946. Hemolytic streptococcic and nonstreptococcic diseases of the respiratory tract; a comparative clinical study. Arch Intern Med (Chic) 78(4):369-386.
Read, S. E., H. F. Reid, V. A. Fischetti, T. Poon-King, R. Ramkissoon, M. McDowell, and J. B. Zabriskie 1986. Serial studies on the cellular immune response to streptococcal antigens in acute and convalescent rheumatic fever patients in Trinidad. J Clin Immunol 6(6):433-441.
Remenyi, B., J. Carapetis, R. Wyber, K. Taubert, and B. M. Mayosi 2013. Position statement of the World Heart Federation on the prevention and control of rheumatic heart disease. Nat Rev Cardiol 10(5):284-292.

Remigio de Aguiar, M. I., L. C. Saraiva, and C. L. Santos 2010. QT Dispersion predicting acute rheumatic carditis. Cardiol Young 20(5):473-476.
Remond, M. G., K. L. Severin, Y. Hodder, J. Martin, C. Nelson, D. Atkinson, and G. P. Maguire 2013. Variability in disease burden and management of rheumatic fever and rheumatic heart disease in two regions of tropical Australia. Intern Med J 43(4):386-393.
Robbins, J. C., J. G. Spanier, S. J. Jones, W. J. Simpson, and P. P. Cleary 1987. *Streptococcus pyogenes* type 12 M protein gene regulation by upstream sequences. J Bacteriol 169(12):5633-5640.
Roberts, S., S. Kosanke, D. S. Terrence, D. Jankelow, C. M. Duran, and M. W. Cunningham 2001. Pathogenic mechanisms in rheumatic carditis: focus on valvular endothelium. J Infect Dis 183(3):507-511.
Robinson, J. H., M. C. Atherton, J. A. Goodacre, M. Pinkney, H. Weightman, and M. A. Kehoe 1991. Mapping T-cell epitopes in group A streptococcal type 5 M protein. Infect Immun 59(12):4324-4331.
Rodriguez-Ortega, M. J., N. Norais, G. Bensi, S. Liberatori, S. Capo, M. Mora, M. Scarselli, F. Doro, G. Ferrari, I. Garaguso, T. Maggi, A. Neumann, A. Covre, J. L. Telford, and G. Grandi 2006. Characterization and identification of vaccine candidate proteins through analysis of the group A Streptococcus surface proteome. Nat Biotechnol 24(2):191-197.
Rose, D. M., J. Han, and M. H. Ginsberg 2002. Alpha4 integrins and the immune response. Immunol Rev 186:118-124.
Rothenbuhler, M., C. J. O'Sullivan, S. Stortecky, G. G. Stefanini, E. Spitzer, J. Estill, N. R. Shrestha, O. Keiser, P. Juni, and T. Pilgrim 2014. Active surveillance for rheumatic heart disease in endemic regions: a systematic review and meta-analysis of prevalence among children and adolescents. Lancet Glob Health 2(12):e717-726.
Rothstein, J., R. Heazlewood, and M. Fraser 2007. Health of Aboriginal and Torres Strait Islander children in remote Far North Queensland: findings of the Paediatric Outreach Service. Med J Aust 186(10):519-521.
Rush, C. M., B. L. Govan, S. Sikder, N. L. Williams, and N. Ketheesan 2014. Animal models to investigate the pathogenesis of rheumatic heart disease. Front Pediatr 2:116.
Sabat, R., G. Grutz, K. Warszawska, S. Kirsch, E. Witte, K. Wolk, and J. Geginat 2010. Biology of interleukin-10. Cytokine Growth Factor Rev 21(5):331-344.
Sachse, S., P. Seidel, D. Gerlach, E. Gunther, J. Rodel, E. Straube, and K. H. Schmidt 2002. Superantigen-like gene(s) in human pathogenic *Streptococcus dysgalactiae*, subsp

*equisimilis*: genomic localisation of the gene encoding streptococcal pyrogenic exotoxin G (speG(dys)). FEMS Immunol Med Microbiol 34(2):159-167.
Saleem, N., A. Prasad, and S. K. Goswami 2017. Apocynin prevents isoproterenol-induced cardiac hypertrophy in rat. Mol Cell Biochem.
Sallusto, F., C. R. Mackay, and A. Lanzavecchia 2000. The role of chemokine receptors in primary, effector, and memory immune responses. Annu Rev Immunol 18:593-620.
Sambhi, M. P., and F. N. White 1960. The electrocardiogram of the normal and hypertensive rat. Circ Res 8:129-134.
Sampaio, R. O., K. C. Fae, L. M. Demarchi, P. M. Pomerantzeff, V. D. Aiello, G. S. Spina, A. C. Tanaka, S. E. Oshiro, M. Grinberg, J. Kalil, and L. Guilherme 2007. Rheumatic heart disease: 15 years of clinical and immunological follow-up. Vasc Health Risk Manag 3(6):1007-1017.
Sanford, B. A., V. E. Davison, and M. A. Ramsay 1982. Fibrinogen-mediated adherence of group A *Streptococcus* to influenza A virus-infected cell cultures. Infect Immun 38(2):513-520.
Sargent, S. J., E. H. Beachey, C. E. Corbett, and J. B. Dale 1987. Sequence of protective epitopes of streptococcal M proteins shared with cardiac sarcolemmal membranes. J Immunol 139(4):1285-1290.
Sasazuki, T., H. Kaneoka, Y. Nishimura, R. Kaneoka, M. Hayama, and H. Ohkuni 1980. An HLA-linked immune suppression gene in man. J Exp Med 152(2 Pt 2):297s-313s.
Saxena, A. 2000. Diagnosis of rheumatic fever: current status of Jones Criteria and role of echocardiography. Indian J Pediatr 67(3 Suppl):S11-14.
Schnitzler, N., A. Podbielski, G. Baumgarten, M. Mignon, and A. Kaufhold 1995. M or M-like protein gene polymorphisms in human group G streptococci. J Clin Microbiol 33(2):356-363.
Schrager, H. M., S. Alberti, C. Cywes, G. J. Dougherty, and M. R. Wessels 1998. Hyaluronic acid capsule modulates M protein-mediated adherence and acts as a ligand for attachment of group A *Streptococcus* to CD44 on human keratinocytes. J Clin Invest 101(8):1708-1716.
Scott, J. R., W. M. Pulliam, S. K. Hollingshead, and V. A. Fischetti 1985. Relationship of M protein genes in group A streptococci. Proc Natl Acad Sci USA 82(6):1822-1826.
Seckeler, M. D., L. L. Barton, and R. Brownstein 2010. The persistent challenge of rheumatic fever in the Northern Mariana Islands. Int J Infect Dis 14(3):e226-229.
Seckeler, M. D., and T. R. Hoke 2011. The worldwide epidemiology of acute rheumatic fever and rheumatic heart disease. Clin Epidemiol 3:67-84.

Sekuloski, S., M. R. Batzloff, P. Griffin, W. Parsonage, S. Elliott, J. Hartas, P. O'Rourke, L. Marquart, M. Pandey, F. A. Rubin, J. Carapetis, J. McCarthy, and M. F. Good 2018. Evaluation of safety and immunogenicity of a group A streptococcus vaccine candidate (MJ8VAX) in a randomized clinical trial. PLoS One 13(7):e0198658.

Settin, A., H. Abdel-Hady, R. El-Baz, and I. Saber 2007. Gene polymorphisms of TNF-alpha(-308), IL-10(-1082), IL-6(-174), and IL-1Ra(VNTR) related to susceptibility and severity of rheumatic heart disease. Pediatr Cardiol 28(5):363-371.

Sfikakis, P. P., and G. C. Tsokos 1995. Lymphocyte adhesion molecules in autoimmune rheumatic diseases: basic issues and clinical expectations. Clin Exp Rheumatol 13(6):763-777.

Shaikh, N., E. Leonard, and J. M. Martin 2010. Prevalence of streptococcal pharyngitis and streptococcal carriage in children: a meta-analysis. Pediatrics 126(3):e557-564.

Shikhman, A. R., N. S. Greenspan, and M. W. Cunningham 1994. Cytokeratin peptide SFGSGFGGGY mimics N-acetyl-beta-D-glucosamine in reaction with antibodies and lectins, and induces in vivo anti-carbohydrate antibody response. J Immunol 153(12):5593-5606.

Shioji, K., C. Kishimoto, and S. Sasayama 2001. Fc receptor-mediated inhibitory effect of immunoglobulin therapy on autoimmune giant cell myocarditis: concomitant suppression of the expression of dendritic cells. Circ Res 89(6):540-546.

Shivaram, P., M. I. Ahmed, P. T. Kariyanna, H. Sabbineni, and U. M. Avula 2013. Doppler echocardiography imaging in detecting multi-valvular lesions: a clinical evaluation in children with acute rheumatic fever. PLoS One 8(9):e74114.

Shulman, S. T., G. Stollerman, B. Beall, J. B. Dale, and R. R. Tanz 2006. Temporal changes in streptococcal M protein types and the near-disappearance of acute rheumatic fever in the United States. Clin Infect Dis 42(4):441-447.

Shulman, S. T., R. R. Tanz, W. Kabat, K. Kabat, E. Cederlund, D. Patel, Z. Li, V. Sakota, J. B. Dale, and B. Beall 2004. Group A streptococcal pharyngitis serotype surveillance in North America, 2000-2002. Clin Infect Dis 39(3):325-332.

Sikder, S., N. L. Williams, A. E. Sorenson, M. A. Alim, M. E. Vidgen, N. J. Moreland, C. M. Rush, R. S. Simpson, B. L. Govan, R. E. Norton, M. W. Cunningham, D. J. McMillan, K. S. Sriprakash, and N. Ketheesan 2018. Group G Streptococcus Induces an Autoimmune Carditis Mediated by Interleukin 17A and Interferon gamma in the Lewis Rat Model of Rheumatic Heart Disease. J Infect Dis 218(2):324-335.

Simpson, W. A., and E. H. Beachey 1983. Adherence of group A streptococci to fibronectin on oral epithelial cells. Infect Immun 39(1):275-279.

Simpson, W. A., I. Ofek, C. Sarasohn, J. C. Morrison, and E. H. Beachey 1980. Characteristics of the binding of streptococcal lipoteichoic acid to human oral epithelial cells. J Infect Dis 141(4):457-462.

Simpson, W. J., J. M. Musser, and P. P. Cleary 1992. Evidence consistent with horizontal transfer of the gene (emm12) encoding serotype M12 protein between group A and group G pathogenic streptococci. Infect Immun 60(5):1890-1893.

Simpson, W. J., J. C. Robbins, and P. P. Cleary 1987. Evidence for group A-related M protein genes in human but not animal-associated group G streptococcal pathogens. Microb Pathog 3(5):339-350.

Sims, S. A., S. Colquhoun, R. Wyber, and J. R. Carapetis 2016. Global Disease Burden of Group A Streptococcus. *In* Streptococcus pyogenes : Basic Biology to Clinical Manifestations. J.J. Ferretti, D.L. Stevens, and V.A. Fischetti, eds. Oklahoma City, USA: The University of Oklahoma Health Sciences Center.

Smeesters, P. R., P. Mardulyn, A. Vergison, R. Leplae, and L. Van Melderen 2008. Genetic diversity of Group A *Streptococcus* M protein: implications for typing and vaccine development. Vaccine 26(46):5835-5842.

Smeesters, P. R., D. J. McMillan, and K. S. Sriprakash 2010. The streptococcal M protein: a highly versatile molecule. Trends Microbiol 18(6):275-282.

Smith, S. C., and P. M. Allen 1991. Myosin-induced acute myocarditis is a T cell-mediated disease. J Immunol 147(7):2141-2147.

Sprent, J., D. F. Tough, and S. Sun 1997. Factors controlling the turnover of T memory cells. Immunol Rev 156:79-85.

Springer, T. A. 1994. Traffic signals for lymphocyte recirculation and leukocyte emigration: the multistep paradigm. Cell 76(2):301-314.

Springer, T. A. 1995. Traffic signals on endothelium for lymphocyte recirculation and leukocyte emigration. Annu Rev Physiol 57:827-872.

Srinivas, S. K., P. Bhat, M. Hegde, and C. N. Manjunath 2013. Giant left atrium due to rheumatic mitral regurgitation. J Am Coll Cardiol 62(5):e9.

Sriprakash, K. S., and J. Hartas 1996. Lateral genetic transfers between group A and G streptococci for M-like genes are ongoing. Microb Pathog 20(5):275-285.

Stanevicha, V., J. Eglite, D. Zavadska, A. Sochnevs, R. Shantere, and D. Gardovska 2007. HLA class II DR and DQ genotypes and haplotypes associated with rheumatic fever among a clinically homogeneous patient population of Latvian children. Arthritis Res Ther 9(3):R58.

Steer, A. C., J. R. Carapetis, T. M. Nolan, and F. Shann 2002. Systematic review of rheumatic heart disease prevalence in children in developing countries: the role of environmental factors. J Paediatr Child Health 38(3):229-234.

Steer, A. C., J. Kado, A. W. Jenney, M. Batzloff, L. Waqatakirewa, E. K. Mulholland, and J. R. Carapetis 2009a. Acute rheumatic fever and rheumatic heart disease in Fiji: prospective surveillance, 2005-2007. Med J Aust 190(3):133-135.

Steer, A. C., G. Magor, A. W. Jenney, J. Kado, M. F. Good, D. McMillan, M. Batzloff, and J. R. Carapetis 2009b. emm and C-repeat region molecular typing of beta-hemolytic Streptococci in a tropical country: implications for vaccine development. J Clin Microbiol 47(8):2502-2509.

Stevens, D., and E. Kaplan 2000. Streptococcal infections. Clinical aspects, microbiology and molecular pathogenesis. Pp. 102-132. New York: Oxford University Press.

Stewart, T., R. McDonald, and B. Currie 2007. Acute rheumatic fever: adherence to secondary prophylaxis and follow up of Indigenous patients in the Katherine region of the Northern Territory. Aust J Rural Health 15(4):234-240.

Stollerman, G. H. 1997. Rheumatic fever. Lancet 349(9056):935-942.

Stollerman, G. H. 2011. Rheumatic and heritable connective tissue diseases of the cardiovascular system. *In* E. Braunwald, Braunwald's Heart Disease: A Textbook of Cardiovascular Medicine. E. Braunwald, ed. Pp. 1706-1734. Philadelphia, USA: WB Saunders.

Stollerman, G. H., and J. B. Dale 2008. The importance of the group a streptococcus capsule in the pathogenesis of human infections: a historical perspective. Clin Infect Dis 46(7):1038-1045.

Streda, A., D. Kankova, and D. Handlova 1971. X-ray picture of the hand in rheumatic fever. Cas Lek Cesk 110(46):1066-1067.

Stryker, W. S., D. W. Fraser, and R. R. Facklam 1982. Foodborne outbreak of group G streptococcal pharyngitis. Am J Epidemiol 116(3):533-540.

Sunaoshi, K., S. Y. Murayama, K. Adachi, M. Yagoshi, K. Okuzumi, N. Chiba, M. Morozumi, and K. Ubukata 2010. Molecular emm genotyping and antibiotic susceptibility of *Streptococcus dysgalactiae* subsp. *equisimilis* isolated from invasive and non-invasive infections. J Med Microbiol 59(Pt 1):82-88.

Suyama, M., D. Torrents, and P. Bork 2006. PAL2NAL: robust conversion of protein sequence alignments into the corresponding codon alignments. Nucleic Acids Res 34(Web Server issue):W609-612.

Suzuki, T., M. Mawatari, T. Iizuka, T. Amano, S. Kutsuna, Y. Fujiya, N. Takeshita, K. Hayakawa, and N. Ohmagari 2017. An Ineffective Differential Diagnosis of Infective Endocarditis and Rheumatic Heart Disease after Streptococcal Skin and Soft Tissue Infection. Intern Med 56(17):2361-2365.

Svartman, M., E. V. Potter, T. Poon-King, and D. P. Earle 1975. Immunoglobulins and complement components in synovial fluid of patients with acute rheumatic fever. J Clin Invest 56(1):111-117.

Swanson, J., K. C. Hsu, and E. C. Gotschlich 1969. Electron microscopic studies on streptococci. I. M antigen. J Exp Med 130(5):1063-1091.

Tada, Y., S. Kagota, M. Matsumoto, Y. Naito, H. Shibata, N. Nejime, T. Tsujino, M. Koshiba, T. Masuyama, and K. Shinozuka 2010. Characterization of cardiac size and function in SHRSP.Z-Lepr(fa)/IzmDmcr rats, a new animal model of metabolic syndrome. Biol Pharm Bull 33(12):1971-1976.

Talay, S. R., A. Zock, M. Rohde, G. Molinari, M. Oggioni, G. Pozzi, C. A. Guzman, and G. S. Chhatwal 2000. Co-operative binding of human fibronectin to Sfbl protein triggers streptococcal invasion into respiratory epithelial cells. Cell Microbiol 2(6):521-535.

Tanaka, K., M. Ito, M. Kodama, M. Tomita, S. Kimura, M. Hoyano, W. Mitsuma, S. Hirono, H. Hanawa, and Y. Aizawa 2011. Sulfated polysaccharide fucoidan ameliorates experimental autoimmune myocarditis in rats. J Cardiovasc Pharmacol Ther 16(1):79-86.

Tanaka, N., N. Dalton, L. Mao, H. A. Rockman, K. L. Peterson, K. R. Gottshall, J. J. Hunter, K. R. Chien, and J. Ross, Jr. 1996. Transthoracic echocardiography in models of cardiac disease in the mouse. Circulation 94(5):1109-1117.

Tandon, R., M. Sharma, Y. Chandrashekhar, M. Kotb, M. H. Yacoub, and J. Narula 2013. Revisiting the pathogenesis of rheumatic fever and carditis. Nat Rev Cardiol 10(3):171-177.

Tapp, J., M. Thollesson, and B. Herrmann 2003. Phylogenetic relationships and genotyping of the genus *Streptococcus* by sequence determination of the RNase P RNA gene, rnpB. Int J Syst Evol Microbiol 53(Pt 6):1861-1871.

Taran, L. M., and N. Szilagyi 1947. The duration of the electrical systole, Q-T, in acute rheumatic carditis in children. Am Heart J 33(1):14-26.

Taran, L. M., and N. Szilagyi 1951. The Q-T interval in rheumatic disease in children. Br Heart J 13(1):10-16.

Taranta, A., and M. Markowitz 1989. Rheumatic fever. Boston: Kluwer Academic Publishers.

Taranta, A., and G. H. Stollerman 1956. The relationship of Sydenham's chorea to infection with group A streptococci. Am J Med 20(2):170-175.
Tekstra, J., H. Beekhuizen, J. S. Van De Gevel, I. J. Van Benten, C. W. Tuk, and R. H. Beelen 1999. Infection of human endothelial cells with *Staphylococcus aureus* induces the production of monocyte chemotactic protein-1 (MCP-1) and monocyte chemotaxis. Clin Exp Immunol 117(3):489-495.
Thomas, G. 1953. Diagnosis and treatment of rheumatic fever with special reference to early carditis. Postgrad Med J 29(336):493-497.
Thomsen, A. R., A. Nansen, A. N. Madsen, C. Bartholdy, and J. P. Christensen 2003. Regulation of T cell migration during viral infection: role of adhesion molecules and chemokines. Immunol Lett 85(2):119-127.
Toor, D., and H. Vohra 2012. Immune responsiveness during disease progression from acute rheumatic fever to chronic rheumatic heart disease. Microbes Infect 14(12):1111-1117.
Towbin, J. A. 2007. Scarring in the heart--a reversible phenomenon? N Engl J Med 357(17):1767-1768.
Towers, R. J., D. Gal, D. McMillan, K. S. Sriprakash, B. J. Currie, M. J. Walker, G. S. Chhatwal, and P. K. Fagan 2004. Fibronectin-binding protein gene recombination and horizontal transfer between group A and G streptococci. J Clin Microbiol 42(11):5357-5361.
Toyka, K. V., D. B. Brachman, A. Pestronk, and I. Kao 1975. Myasthenia gravis: passive transfer from man to mouse. Science 190(4212):397-399.
Tseng, S. P., Y. Y. Lin, J. C. Tsai, P. R. Hsueh, H. J. Chen, W. C. Hung, and L. J. Teng 2010. Distribution of emm types and genetic characterization of the mgc locus in group G *Streptococcus dysgalactiae* subsp. *equisimilis* from a hospital in northern Taiwan. J Clin Microbiol 48(8):2975-2977.
Tsujimura, E., H. Kusuoka, K. Fukughi, S. Hasegawa, K. Yufani, M. Hori, S. Hirono, T. Izumi, and T. Nishimura 2000. Changes in perfusion and fatty acid metabolism of rat heart with autoimmune myocarditis. Ann Nucl Med 14(5):361-367.
Tzartos, S., S. Hochschwender, P. Vasquez, and J. Lindstrom 1987. Passive transfer of experimental autoimmune myasthenia gravis by monoclonal antibodies to the main immunogenic region of the acetylcholine receptor. J Neuroimmunol 15(2):185-194.
Umapathy, S., and A. Saxena 2018. Acute rheumatic fever presenting as complete heart block: report of an adolescent case and review of literature. BMJ Case Rep 2018.
Unny, S. K., and B. L. Middlebrooks 1983. Streptococcal rheumatic carditis. Microbiol Rev 47(1):97-120.

Valentin-Weigand, P., J. Grulich-Henn, G. S. Chhatwal, G. Muller-Berghaus, H. Blobel, and K. T. Preissner 1988. Mediation of adherence of streptococci to human endothelial cells by complement S protein (vitronectin). Infect Immun 56(11):2851-2855.
Vanace, P. W. 1960. Experimental streptococcal infection in the rhesus monkey. Ann N Y Acad Sci 85:910-930.
Vandamme, P., B. Pot, E. Falsen, K. Kersters, and L. A. Devriese 1996. Taxonomic study of lancefield streptococcal groups C, G, and L (*Streptococcus dysgalactiae*) and proposal of *S. dysgalactiae* subsp. *equisimilis* subsp. *nov*. Int J Syst Bacteriol 46(3):774-781.
Vartian, C., P. I. Lerner, D. M. Shlaes, and K. V. Gopalakrishna 1985. Infections due to Lancefield group G streptococci. Medicine (Baltimore) 64(2):75-88.
Vashishtha, A., and V. A. Fischetti 1993. Surface-exposed conserved region of the streptococcal M protein induces antibodies cross-reactive with denatured forms of myosin. J Immunol 150(10):4693-4701.
Veasy, L. G., and H. R. Hill 1997. Immunologic and clinical correlations in rheumatic fever and rheumatic heart disease. Pediatr Infect Dis J 16(4):400-407.
Veasy, L. G., and L. Y. Tani 2005. A new look at acute rheumatic mitral regurgitation. Cardiol Young 15(6):568-577.
Veasy, L. G., L. Y. Tani, and H. R. Hill 1994. Persistence of acute rheumatic fever in the intermountain area of the United States. J Pediatr 124(1):9-16.
Veasy, L. G., S. E. Wiedmeier, G. S. Orsmond, H. D. Ruttenberg, M. M. Boucek, S. J. Roth, V. F. Tait, J. A. Thompson, J. A. Daly, E. L. Kaplan, and et al. 1987. Resurgence of acute rheumatic fever in the intermountain area of the United States. N Engl J Med 316(8):421-427.
Venezio, F. R., R. M. Gullberg, G. O. Westenfelder, J. P. Phair, and F. V. Cook 1986. Group G streptococcal endocarditis and bacteremia. Am J Med 81(1):29-34.
Vernino, S., L. G. Ermilov, L. Sha, J. H. Szurszewski, P. A. Low, and V. A. Lennon 2004. Passive transfer of autoimmune autonomic neuropathy to mice. J Neurosci 24(32):7037-7042.
Vijayalakshmi, I. B., R. O. Vishnuprabhu, N. Chitra, R. Rajasri, and T. V. Anuradha 2008. The efficacy of echocardiographic criterions for the diagnosis of carditis in acute rheumatic fever. Cardiol Young 18(6):586-592.
Virmani, R., and W. C. Roberts 1977. Aschoff bodies in operatively excised atrial appendages and in papillary muscles. Frequency and clinical significance. Circulation 55(4):559-563.

Visai, L., S. Bozzini, G. Raucci, A. Toniolo, and P. Speziale 1995. Isolation and characterization of a novel collagen-binding protein from *Streptococcus pyogenes* strain 6414. J Biol Chem 270(1):347-353.

Visentainer, J. E., F. C. Pereira, M. M. Dalalio, L. T. Tsuneto, P. R. Donadio, and R. A. Moliterno 2000. Association of HLA-DR7 with rheumatic fever in the Brazilian population. J Rheumatol 27(6):1518-1520.

Wahid, R. M., M. Yoshinaga, J. Nishi, N. Maeno, J. Sarantuya, T. Ohkawa, A. M. Jalil, K. Kobayashi, and K. Miyata 2005. Immune response to a laminin-binding protein (Lmb) in group A streptococcal infection. Pediatr Int 47(2):196-202.

Walter, F., M. Siegel, and H. Malke 1989. Nucleotide sequence of the streptokinase gene from a group-G *Streptococcus*. Nucleic Acids Res 17(3):1262.

Wang, B., T. Dileepan, S. Briscoe, K. A. Hyland, J. Kang, A. Khoruts, and P. P. Cleary 2010. Induction of TGF-beta1 and TGF-beta1-dependent predominant Th17 differentiation by group A streptococcal infection. Proc Natl Acad Sci USA 107(13):5937-5942.

Wang, B., N. Ruiz, A. Pentland, and M. Caparon 1997. Keratinocyte proinflammatory responses to adherent and nonadherent group A streptococci. Infect Immun 65(6):2119-2126.

Wang, J. R., and M. W. Stinson 1994a. M protein mediates streptococcal adhesion to HEp-2 cells. Infect Immun 62(2):442-448.

Wang, J. R., and M. W. Stinson 1994b. Streptococcal M6 protein binds to fucose-containing glycoproteins on cultured human epithelial cells. Infect Immun 62(4):1268-1274.

Wannamaker, L. W. 1954. The epidemiology of streptococcal infections. *In* Streptococcal Infections. M. McCarty, ed. New York: Columbia University Press.

Watanabe, S., S. Kumazaki, K. Kusunoki, T. Inoue, Y. Maeda, S. Usui, R. Shinohata, T. Ohtsuki, S. Hirohata, S. Kusachi, K. Kitamori, M. Mori, Y. Yamori, and H. Oka 2017. A High-Fat and High-Cholesterol Diet Induces Cardiac Fibrosis, Vascular Endothelial, and Left Ventricular Diastolic Dysfunction in SHRSP5/Dmcr Rats. J Atheroscler Thromb.

Watkins, D. A., C. O. Johnson, S. M. Colquhoun, G. Karthikeyan, A. Beaton, G. Bukhman, M. H. Forouzanfar, C. T. Longenecker, B. M. Mayosi, G. A. Mensah, B. R. Nascimento, A. L. P. Ribeiro, C. A. Sable, A. C. Steer, M. Naghavi, A. H. Mokdad, C. J. L. Murray, T. Vos, J. R. Carapetis, and G. A. Roth 2017. Global, Regional, and National Burden of Rheumatic Heart Disease, 1990-2015. N Engl J Med 377(8):713-722.

Watsky, K. L., N. Kollisch, and P. Densen 1985. Group G streptococcal bacteremia. The clinical experience at Boston University Medical Center and a critical review of the literature. Arch Intern Med 145(1):58-61.

Wegmann, K. W., W. Zhao, A. C. Griffin, and W. F. Hickey 1994. Identification of myocarditogenic peptides derived from cardiac myosin capable of inducing experimental allergic myocarditis in the Lewis rat. The utility of a class II binding motif in selecting self-reactive peptides. J Immunol 153(2):892-900.

Wen, Y., Z. Zeng, C. Gui, L. Li, and W. Li 2015. Changes in the expression of Th17 cell-associated cytokines in the development of rheumatic heart disease. Cardiovasc Pathol 24(6):382-387.

Wessels, M. R., and M. S. Bronze 1994. Critical role of the group A streptococcal capsule in pharyngeal colonization and infection in mice. Proc Natl Acad Sci USA 91(25):12238-12242.

Whatmore, A. M., and M. A. Kehoe 1994. Horizontal gene transfer in the evolution of group A streptococcal emm-like genes: gene mosaics and variation in Vir regulons. Mol Microbiol 11(2):363-374.

White, H., W. Walsh, A. Brown, T. Riddell, A. Tonkin, R. Jeremy, D. Brieger, C. Zeitz, and L. Kritharides 2010. Rheumatic heart disease in indigenous populations. Heart Lung Circ 19(5-6):273-281.

WHO 1987. WHO Global Programme for the Prevention of Rheumatic Fever/Rheumatic Heart Disease in Sixteen Developing Countries (AGFUND Supported). WHO Meeting of National Programme Managers, Geneva.

WHO 1988. Rheumatic fever and rheumatic heart disease. Report of a WHO Study Group. World Health Organ Tech Rep Ser 764:1-58.

WHO 2004. Rheumatic fever and rheumatic heart disease. Report of a WHO expert consultation. Geneva, 29 October – 1 November 2001. WHO Technical Report Series 923. [online].

Williams, G. S. 2003. Group C and G streptococci infections: emerging challenges. Clin Lab Sci 16(4):209-213.

Williamson, D. A., P. R. Smeesters, A. C. Steer, J. Morgan, M. Davies, P. Carter, A. Upton, S. Y. Tong, J. Fraser, and N. J. Moreland 2016. Comparative M-protein analysis of *Streptococcus pyogenes* from pharyngitis and skin infections in New Zealand: Implications for vaccine development. BMC Infect Dis 16(1):561.

Williamson, D. A., P. R. Smeesters, A. C. Steer, J. D. Steemson, A. C. Ng, T. Proft, J. D. Fraser, M. G. Baker, J. Morgan, P. E. Carter, and N. J. Moreland 2015. M-Protein Analysis of *Streptococcus pyogenes* Isolates Associated with Acute Rheumatic Fever in New Zealand. J Clin Microbiol 53(11):3618-3620.

Winram, S. B., and R. Lottenberg 1996. The plasmin-binding protein Plr of group A streptococci is identified as glyceraldehyde-3-phosphate dehydrogenase. Microbiology 142 ( Pt 8):2311-2320.
Woolcock, J. B. 1974. Purification and antigenicity of an M-like protein of *Streptococcus equi*. Infect Immun 10(1):116-122.
Woolley, K., and P. Stark 1999. Pulmonary parenchymal manifestations of mitral valve disease. Radiographics 19(4):965-972.
Wu, X., M. Li, S. Q. Chen, S. Li, and F. Guo 2017. Pin1 facilitates isoproterenolinduced cardiac fibrosis and collagen deposition by promoting oxidative stress and activating the MEK1/2ERK1/2 signal transduction pathway in rats. Int J Mol Med.
Wunderlich, N. C., R. Beigel, and R. J. Siegel 2013. Management of mitral stenosis using 2D and 3D echo-Doppler imaging. JACC Cardiovasc Imaging 6(11):1191-1205.
Xie, X., H. Zhou, J. Huang, H. Huang, Z. Feng, K. Mei, B. Yu, Z. Su, and J. Gu 2010. An animal model of chronic rheumatic valvulitis induced by formalin-killed streptococci. Rheumatol Int 30(12):1621-1625.
Yamaguchi, M., Y. Terao, and S. Kawabata 2013. Pleiotropic virulence factor - Streptococcus pyogenes fibronectin-binding proteins. Cell Microbiol 15(4):503-511.
Yamaguchi, T., R. Kawahara, C. Katsukawa, M. Kanki, T. Harada, S. Yonogi, S. Iwasaki, H. Uehara, S. Okajima, H. Nishimura, K. Motomura, M. Miyazono, Y. Kumeda, and K. Kawatsu 2018. Food-Borne Outbreak of Group G Streptococcal Pharyngitis in a School Dormitory in Osaka, Japan. J Clin Microbiol.
Yaman, I. H., A. Dagdemir, and K. Baysal 2003. Serum intercellular adhesion molecule-1 levels in acute rheumatic fever. Ann Trop Paediatr 23(3):167-171.
Yamauchi, R., M. Tanaka, N. Kume, M. Minami, T. Kawamoto, K. Togi, T. Shimaoka, S. Takahashi, J. Yamaguchi, T. Nishina, M. Kitaichi, M. Komeda, T. Manabe, S. Yonehara, and T. Kita 2004. Upregulation of SR-PSOX/CXCL16 and recruitment of CD8+ T cells in cardiac valves during inflammatory valvular heart disease. Arterioscler Thromb Vasc Biol 24(2):282-287.
Yang, L. C., P. R. Soprey, M. K. Wittner, and E. N. Fox 1977. Streptococcal-induced cell-mediated-immune destruction of cardiac myofibers in vitro. J Exp Med 146(2):344-360.
Yang, Z. 2007. PAML 4: phylogenetic analysis by maximum likelihood. Mol Biol Evol 24(8):1586-1591.
Yegin, O., M. Coskun, and H. Ertug 1997. Cytokines in acute rheumatic fever. Eur J Pediatr 156(1):25-29.

Yetkin, E., A. R. Erbay, M. Ileri, H. Turhan, M. Balci, S. Cehreli, G. Yetkin, and D. Demirkan 2001. Levels of circulating adhesion molecules in rheumatic mitral stenosis. Am J Cardiol 88(10):1209-1211.

Yoshizawa, N., K. Yamakami, M. Fujino, T. Oda, K. Tamura, K. Matsumoto, T. Sugisaki, and M. D. Boyle 2004. Nephritis-associated plasmin receptor and acute poststreptococcal glomerulonephritis: characterization of the antigen and associated immune response. J Am Soc Nephrol 15(7):1785-1793.

Zabriskie, J. B. 1967. Mimetic relationships between group A streptococci and mammalian tissues. Adv Immunol 7:147-188.

Zabriskie, J. B., and E. H. Freimer 1966. An immunological relationship between the group. A *Streptococcus* and mammalian muscle. J Exp Med 124(4):661-678.

Zabriskie, J. B., K. C. Hsu, and B. C. Seegal 1970. Heart-reactive antibody associated with rheumatic fever: characterization and diagnostic significance. Clin Exp Immunol 7(2):147-159.

Zachary, J. F., S. A. Hartleben, L. A. Frizzell, and W. D. O'Brien, Jr. 2002. Arrhythmias in rat hearts exposed to pulsed ultrasound after intravenous injection of a contrast agent. J Ultrasound Med 21(12):1347-1356.

Zaman, M. M., N. Yoshiike, M. A. Rouf, S. Haque, A. H. Chowdhury, T. Nakayama, and H. Tanaka 1998. Association of rheumatic fever with serum albumin concentration and body iron stores in Bangladeshi children: case-control study. Bmj 317(7168):1287-1288.

Zhang, P., C. J. Cox, K. M. Alvarez, and M. W. Cunningham 2009. Cutting edge: cardiac myosin activates innate immune responses through TLRs. J Immunol 183(1):27-31.

Zhang, Q. C., H. H. Yin, and B. L. Yin 2005. [Concentration and significance of s-ICAM-1, s-VCAM-1, and vWF in the plasma of patients with rheumatic heart disease]. Zhong Nan Da Xue Xue Bao Yi Xue Ban 30(4):407-409.

# APPENDIX 1
# MEDIA AND REAGENTS

Unless otherwise stated all chemicals of the highest grade, glass wares and plastic consumables were purchased from the following companies:

- Chemicals from Sigma, Australia.
- Bacterial culture media from Sigma and Acumedia, Australia.
- Plastic ware from Sarstedt, Australia.
- Micro plates and cell culture flasks from Thermo Scientific, Australia.

## 1.1 General buffers and solutions

1.1.1 Phosphate buffered saline (PBS, 10× stock, 1000 ml)

- NaCl (#CM0982B, *Thermo Scientific, Australia*): 80 g
- $KH_2PO_4$ (#10203, *AnalaR, Australia*): 2 g
- $Na_2HPO_4$ (#ALF011592.36, *Thermo Scientific, Australia*): 11.5 g
- Double $dH_2O$: to 1000 ml

  Combine ingredients with stirring until fully dissolved and adjust pH to 7.4. Autoclave at 121°C for 15 min. For working solution, add 100 ml of 10× stock to 900 ml double distilled water.

1.1.2 Tris buffered saline (TBS, 10× stock, 1000 ml)

- NaCl: 80 g
- KCl (#10198, *AnalaR, Australia*): 2 g
- Tris base (#2311-500G, *Thermo Scientific, Australia*): 30 g
- Double $dH_2O$: to 1000 ml

  Combine ingredients in 800 ml water and adjust pH to 6.8 using HCl. Autoclave at 121°C for 15 min. For working solution, add 100 ml of 10× stock to 900 ml double distilled water.

1.1.3 0.3% $H_2O_2$, 70% methanol in 1× TBS (100 ml)

- $H_2O_2$ (30%) (#10366, *Merck Millipore, Australia*): 1 ml
- Methanol (#2.5LTPL, *POCD Healthcare, Australia*): 69 ml
- TBS (1×, see 1.1.2): 30 ml. Mix well.

1.1.4 Tween-20 (0.1% in 1× TBS, 1000 ml) [50 mM Tris-Cl, pH 7.5, 150 mM NaCl]

- Tris: 6.05 g
- NaCl: 8.76 g
- $dH_2O$: to 800 ml

  Dissolve ingredients, adjust pH to 7.5 with 1 M HCl and make volume up to 1000 ml with distilled water. TBS is stable at 4°C for 3 m.

1.1.5 Paraformaldehyde (4% in PBS, 100 ml)

- PBS (1×, see 1.1.1): 100 ml
- Paraformaldehyde powder (#C007, *ProSciTech, Australia*): 4 g

  Boil until fully dissolved, use fume hood, filter sterilise (0.45 μm). Store at 2-8°C for up to 1 m.

1.1.6 Sodium azide (0.02%, 100 ml)

- Sodium azide (#SA189, *Chem-Supply Pty Ltd, Australia*): 2 g
- $dH_2O$: to 100 ml

  Stir until fully dissolved, filter sterilise (0.45 μm). Dilute 1:100 in distilled water to make 0.02%.

1.1.7 Permeabilisation solution (1×, 1% triton-PBS, 25 ml)

- Triton X-100: 0.25 ml
- PBS (1×, see 1.1.1): 24.75 ml

  Mix well, filter sterilise (0.45 μm).

1.1.8 Trypan blue stain (0.4%, 10 ml)

- Trypan blue crystal: 0.04 g
- $dH_2O$: 10 ml

  Mix well, filter sterilise (0.22 μm).

**1.2 Bacterial broths and agars**

1.2.1 Todd Hewitt broth with 0.2% yeast (THYB, 1000 ml)

- Todd Hewitt base (#7161, *Sigma, Australia*): 36.4 g
- Yeast extract: 2 g

- $dH_2O$: to 1000 ml

  Combine ingredients with stirring until completely dissolved. Autoclave at 121°C for 15 min. Store at 4°C.

1.2.2 Terrific broth (1000 ml)

- Tryptone: 12 g
- Yeast: 24 g
- $K_2HPO_4$: 9.4 g
- $KH_2PO_4$ (#10203, *AnalaR, Australia*): 2.2 g
- Glycerol: 4 ml
- $dH_2O$: to 1000 ml

  Combine ingredients with stirring until completely dissolved and adjust pH to 7.2. Autoclave at 121°C for 15 min. Store at 4°C.

1.2.3 Luria-Bertani (LB) medium (1000 ml)

- Tryptone: 10 g
- Yeast extract: 5 g
- NaCl: 10 g
- $dH_2O$: to 1000 ml

  Combine ingredients with stirring until completely dissolved. Autoclave at 121°C for 15 min. Store at 4°C.

1.2.4 Luria-Bertani (LB) agar (500 ml)

- LB medium (#7213, *Acumedia, Australia*): 500 ml
- Agar technical No. 3 (#LP0013, *Oxoid Ltd, Australia*): 15 g
- Antibiotics: as required

  Dissolve agar base in LB medium by boiling for 15 min. Autoclave at 121°C for 15 min, cool to 50°C and aseptically add antibiotics before pouring into petri dishes. Store at 4°C.

1.2.5 Sheep blood agar (5%, 1000 ml)

- Blood agar base no. 2 (#7266, *Acumedia, Australia*): 40 g
- Sheep blood, sterile defibrinated: 50 ml

- $dH_2O$: to 1000 ml

  Dissolve agar base in water and boil for 15 min until agar has completely dissolved. Autoclave at 121°C for 15 min, cool to 50°C and aseptically add blood and mix gently swirling and pour into petri dishes. Store at 4°C.

**1.3 Buffers and reagents for protein purification**

1.3.1 Lysis buffer (1000 ml)

- $NaH_2PO_4$: 6.9 g (final concentration 50 mM)
- NaCl: 17.54 g (final concentration 300 mM)
- Imidazole: 0.68 g (final concentration 10 mM
- Double $dH_2O$: to 1000 ml

  Combine ingredients with stirring until completely dissolved and adjust pH to 8.0 using NaOH. Autoclave at 121°C for 15 min. Store at 4°C.

1.3.2 Wash buffer (1000 ml)

- $NaH_2PO_4$: 6.9 g (final concentration 50 mM)
- NaCl: 17.54 g (final concentration 300 mM)
- Imidazole: 1.36 g (final concentration 20 mM
- Double $dH_2O$: to 1000 ml

  Combine ingredients with stirring until completely dissolved and adjust pH to 8.0 using NaOH. Autoclave at 121°C for 15 min. Store at 4°C.

1.3.3 Elution buffer (100 ml)

- $NaH_2PO_4$: 0.69 g (final concentration 50 mM)
- NaCl: 1.754 g (final concentration 300 mM)
- Imidazole: 0.136 g (final concentration 20 mM
- Double $dH_2O$: to 100 ml

  Combine ingredients with stirring until completely dissolved and adjust pH to 8.0 using NaOH. Autoclave at 121°C for 15 min. Store at 4°C.

1.3.4 Isopropyl ß-D-1-thiogalactopyranoside (IPTG, 1 M)

- IPTG (#R0392, *Thermo Scientific, Australia*): 2.383 g
- Double $dH_2O$: to 10 ml

Dissolve IPTG thoroughly in water. Filter sterilise (22 µm) and store in 1 ml aliquots at -20°C.

1.3.5 Lysozyme (100 mg/ml)

- Lysozyme (#1243004, *Roche, Australia*): 1 g
- Double $dH_2O$: to 10 ml

  Dissolve lysozyme thoroughly in water. Filter sterilise (0.22 µm) and store in 1 ml aliquots at -20°C.

1.3.6 NaOH (1 M, 1000 ml)

- NaOH (solid): 40 g
- $dH_2O$: enough to dissolve completely

  Add more distilled water to make the volume 1000 ml. Heat will be generated that may affect volume, cool and be slow.

**1.4 Antibiotic solutions**

1.4.1 Ampicillin (100 mg/ml)

- Ampicillin (#A9518, *Sigma, Australia*): 10 g
- Double $dH_2O$: 100 ml

  Dissolve ampicillin in the water. Filter sterilise (0.22 µm) and store at -20°C in 1 ml aliquots.

1.4.2 Kanamycin (25 mg/ml)

- Kanamycin sulphate (#K1377, *Sigma, Australia*): 2.5 g
- Double $dH_2O$: 100 ml

  Dissolve kanamycin in the water. Filter sterilise (0.22 µm) and store at -20°C in 1 ml aliquots.

**1.5 Reagents for electrophoresis**

1.5.1 Tris-HCl (0.5 M, pH 6.8, 50 ml)

- Tris: 3 g
- $dH_2O$: up to 50 ml

  Adjust pH 6.8 with HCl, autoclave and store at room temperature.

1.5.2 Tris-HCl (1.5 M, pH 8.8, 30 ml)

- Tris: 5.4 g
- HCl (concentrated): 0.4 ml
- $dH_2O$: 30 ml

  Adjust pH 8.8 with HCl, autoclave and store at room temperature.

1.5.3 SDS solution (10%, 50 ml)

- SDS: 5 g
- $dH_2O$: 50 ml

  Mix well. Heat in the water bath for well-mixing. Sterilise by filter sterilisation (0.45μm).

1.5.4 Ammonium persulphate solution (APS, 10%, 100 ml)

- Ammonium persulphate (#161-0700, *Bio-rad, Australia*): 100 mg
- $dH_2O$: 100 ml

  Combine ingredients, mix well. Use within 24 h.

1.5.5 Separating gel 12% (1 gel, 5 ml)

- Acrylamide/bis-acrylamide (30% w/v) (#A9926, *Sigma, Australia*): 2 ml
- Tris (1.5 M, pH 8.8): 1.3 ml
- SDS solution (10%, w/v, see 1.5.3): 50 μl
- Double $dH_2O$: 1.6 ml
- APS solution (10%, w/v, see 1.5.4): 50 μl
- TEMED (#T9281-25ML, *Sigma, Australia*): 5 μl

  Combine ingredients thoroughly except APS and TEMED. Add APS and TEMED immediately prior to pouring the gel.

1.5.6 Stacking gel (1 gel, 2.5 ml)

- Acrylamide/bis-acrylamide (30%, w/v): 0.335 ml
- Tris 0.5 M, pH 6.8): 0.625 ml
- SDS solution (10%, w/v, see 1.5.3): 25 μl
- Double $dH_2O$: 1.49 ml
- APS solution (10%, w/v, see 1.5.4): 25 μl

- TEMED: 1 µl

  Combine ingredients thoroughly except APS and TEMED. Add APS and TEMED immediately prior to pouring the gel.

1.5.7 Tris-HEPES running buffer (1×, 1000 ml)

- Tris: 12.1 g
- HEPES: 23.8 g
- SDS: 1 g (or 10 ml of 10% solution)
- $dH_2O$: 1000 ml

1.5.8 Coomassie destaining solution (1000 ml)

- Methanol: 100 ml
- Glacial acetic acid: 70 ml
- $dH_2O$: 830 ml

  Combine ingredients in fume hood. Store at room temperature away from direct light.

**1.6 Cell culture media and reagents**

(All media preparation was carried out in a biological laminar flow hood using ascetic techniques)

1.6.1 Transport medium (500 ml)

- RPMI 1640: 450 ml
- Penicillin: 5 ml (final concentration 100 IU/ml)
- Streptomycin: 5 ml (final concentration 100 µg/ml)

  Mix antibiotics thoroughly into RPMI and store at 4°C.

1.6.2 Rat splenic MNC culture medium (2×, 50 ml)

- Transport medium (with penicillin and streptomycin, see 1.6.1): 45.5 ml
- L-glutamine (200 mM stock): 1 ml (final concentration 2 mM)
- HEPES buffer (1 M stock): 1 ml (final concentration 10 mM)
- Rat serum: 2.5 ml (final concentration 2.5%)

  Mix all ingredients thoroughly and store at 4°C until required. Use within 24 h.

1.6.3 Heat inactivated rat serum

Heat rat serum at 56°c for 30 min. Check sterility by streaking onto blood agar and incubating at 37°C with 5% $CO_2$ for two days. Store at -20°C.

1.6.4 ConA (5 µg/ml, 400 µl)

- Stock ConA (93 mg/ml): 20 µl
- RPMI: 380 µl

  Prepare in a safety cabinet.

1.6.5 Staining buffer (100 ml)

- PBS (1×, see 1.1.1): 97.95 ml
- Foetal bovine serum: 2 ml
- NaN3: 0.05 ml

  Adjust pH 7.4, filter sterilise using a 0.22 µm filter.

1.6.6 Freezing medium

- DMSO: 5-10%
- Foetal bovine serum: 20%
- Endothelial cell culture medium: 70-75%

  Filter sterilise growth medium and FBS using a 0.22 µm filter, add DMSO (do not filter, it will dissolve the cellulose acetate membrane). Aliquot into tubes and store at -80°C for up to one year.

**1.7 Reagents for ELISA**

1.7.1 Carbonate bicarbonate coating buffer (1000 ml)

- $Na_2CO_3$: 3.18 g
- $NaHCO_3$: 5.86 g
- $NaN_3$: 0.4 g
- $dH_2O$: 950 ml

  Adjust pH 9.6 with HCl. Add more $dH_2O$ to make 1000 ml. Autoclave and store at 4°C.

1.7.2 Washing solution (1× PBS, pH 7.4, containing 0.05% Tween-20, 1000 ml)

- PBS (1×, see 1.1.1): 1000 ml
- Tween-20: 0.5 ml

  Mix well by gentle swirling the bottle. Use immediately or store at 4°C.

1.7.3 Blocking buffer or ELISA diluent (1%, 100 ml)

- Washing solution (see 1.7.2): 100 ml
- Bovine serum albumin: 1 gm

  Mix the ingredients thoroughly, filter sterilise (0.22 μm). Use immediately or store at 4°C.

## APPENDIX 2

## MANUFACTURER/SUPPLIER ADDRESSES

| Company | Address |
|---|---|
| Acumedia | : Michigan, USA |
| AD Instrument | : Gladstone Rd, Castle Hill, Sydney, Australia |
| Amersham Bioscience | : Australia |
| AnalaR | : Victoria, Australia |
| Astral Scientific Pty. Ltd. | : Taren Point, New South Wales, Australia |
| Australian Biostain | : Traralgon East, Victoria, Australia |
| Australian Biosearch | : Wangara, Western Australia, Australia |
| BD FACS | : Netherlands |
| BD Bioscience | : San Diego, California, USA |
| Becton Dickinson Bioscience | : San Jose, California, USA |
| BioLegend | : San Diego, California, USA |
| Bio-rad Laboratories | : Regents Park, New South Wales, Australia |
| Bio-strategy laboratory products | : Tingalpa, Queensland, Australia |
| Cell bioscience | : Heidelberg, Victoria, Australia |
| Chattagnooga, DJO Global Pty. Ltd. | : Normanhurst, New South Wales, Australia |
| Chem-Supply Pty Ltd | : Bedford St, Gillman South Australia, Australia |
| Corning Costar Corporation | : Cambridge, Massachusetts, USA |
| eBioscience | : San Diego, USA |
| Eppendorf | : Hamburg, Germany |
| G Bioscience | : Page Avenue St. Louis, Missouri, U.S.A. |
| GE Healthcare | : Baulkham Hills, New South Wales, Australia |
| Genlantis PrimaPure | : San Diego, USA |
| Goldmix Stockfeeds | : Queensland, Australia |
| Gradipore, Inc. | : Frenchs Forest, New South Wales, Australia |
| GraphPad Software Inc | : La Jolla, California, USA |
| Invitrogen Australia Pty Ltd | : Mt Waverley, Victoria, Australia |
| Jackson Immunoresearch | : West Grove, Pennsylvania, USA |
| Kingfisher Biotech, INC. | : Saint Paul, Minnesota, USA |

| Company | Address |
|---|---|
| KPL | : Milford, USA |
| LASER Animal Health | : Fison Avenue West, Eagle Farm, Queensland, Australia |
| Life Technologies | : Caribbean Drive, Scoresby, Victoria, Australia |
| Millipore corporation | : North Ryde, New South Wales, Australia |
| Nunc | : Roskilde, Denmark |
| NuSep | : Homebush West, New South Wales, Australia |
| Olympus | : Macquarie Park, New South Wales, Australia |
| Perkin Elmer | : Glen Waverley, Victoria, Australia |
| Pierce Biotechnology | : Rockford, IL, USA |
| ProSciTech | : Queensland, Australia |
| Qiagen | : Doncaster, Victoria, Australia |
| Roche | : Millers Point, New South Wales, Australia |
| Sapphire bioscience | : Redfern, New South Wales, Australia |
| Sarstedt | : Ingle Farm, South Australia, Australia |
| Shandon Southern Products Ltd | : Runcorn, Cheshire, UK |
| Sigma Alirich | : Castle Hill, New South Wales, Australia |
| Terumo | : Somerset, New Jersey, USA |
| Thermo fisher scientific | : Scoresby, Victoria, Australia |
| Vector Laboratories | : Burlingame, USA |
| VWR International Pty Ltd | : Brisbane, Queensland, Australia |

# APPENDIX 3
# HISTOLOGICAL STAINING PROTOCOLS

## 3.1 Haematoxylin Eosin (H&E) Staining

After preparation of sections:

- De-paraffinise sections through 2 changes of xylene, 2 min each.
- Dehydrate sections through a series of graded alcohols (2 min > 1 min > 1 min).
- Wash in running tap water for 1 min.
- Stain in Mayer's hematoxylin solution for 8 min.
- Wash in running tap water for 30 sec.
- Wash in Scott's Tap Water substitute for 30 sec.
- Wash running tap water for 2 min.
- Stain in Eosin 4 min.
- Differentiate Eosin by 4/5 dips in running tap water.
- Rinse in alcohol, 10 dips.
- Rinse in alcohol, 10 dips.
- Alcohol 1 min.
- Xylene 2 min.
- Xylene 1 min.
- Xylene until cover slipped.
- Mount sections with DPX
- Get rid of bubbles with a wooden stick
- Place in 37°C incubator for ~48hrs
- Examine under microscope
    - Nuclei: blue
    - Cytoplasm: pink to purple

## 3.2 Masson's trichrome staining

After preparation of sections:

- De-paraffinise sections through 2 changes of xylene, 2 min each.
- Dehydrate sections through a series of graded alcohols (2 min > 1 min > 1 min).
- Wash in running tap water for 1 min.
- Stain in Celestine blue for 5 min.

- Rinse in water.
- Stain in Mayer's hematoxylin solution for 5 min.
- Wash in running tap water for 30 sec.
- Wash in Scott's Tap Water substitute for 30 sec.
- Wash running tap water for 2 min.
- Stain with Acid Fuchin (Solution A) for 5 min.
- Rinse in distilled water.
- Treat with Phosphomolybdic Acid (Solution B) for 5 min.
- Drain.
- Stain with Methyl Blue (Solution C) for 2-5 min.
- Rinse in distilled water.
- Treat with 1% acetic acid for 2 min.
- Rinse quickly.
- Rinse in alcohol, 10 dips.
- Rinse in alcohol, 10 dips.
- Alcohol 1 min.
- Xylene 2 min.
- Xylene 1 min.
- Xylene until cover slipped.
- Mount sections with DPX
- Get rid of bubbles with a wooden stick
- Place in 37°C incubator for ~48hrs
- Examine under microscope
    - Nuclei: blue/black
    - Cytoplasm, muscle, RBC: red
    - Collagen: blue

# APPENDIX 4

# STATISTICAL ANALYSIS OF CHAPTER 4

## 4.1 Statistical analysis of Figure 4.1

| Nonlin fit | | A | B |
|---|---|---|---|
| | | SS2 | NW |
| | | Y | Y |
| 1 | Straight line | | |
| 2 | Best-fit values | | |
| 3 | YIntercept | -0.2656 | -0.08083 |
| 4 | Slope | 1.007 | 1.002 |
| 5 | Std. Error | | |
| 6 | YIntercept | 0.2443 | 0.2804 |
| 7 | Slope | 0.00616 | 0.007072 |
| 8 | 95% CI (asymptotic) | | |
| 9 | YIntercept | -0.9438 to 0.4126 | -0.8594 to 0.6978 |
| 10 | Slope | 0.99 to 1.024 | 0.982 to 1.021 |
| 11 | Goodness of Fit | | |
| 12 | Degrees of Freedom | 4 | 4 |
| 13 | R square | 0.9999 | 0.9998 |
| 14 | Absolute Sum of Squares | 0.00624 | 0.008225 |
| 15 | Sy.x | 0.0395 | 0.04535 |

## 4.2 Statistical analysis of Figure 4.9

Panel A: D'Agostino & Pearson normality test

| Col. stats | | A | B | C |
|---|---|---|---|---|
| | | Normality PBS | Normality rM5 | Normality Stg |
| | | Y | Y | Y |
| 1 | Number of values | 10 | 10 | 10 |
| 2 | | | | |
| 3 | D'Agostino & Pearson normality test | | | |
| 4 | K2 | 2.654 | 2.758 | 0.9014 |
| 5 | P value | 0.2652 | 0.2519 | 0.6372 |
| 6 | Passed normality test (alpha=0.05)? | Yes | Yes | Yes |
| 7 | P value summary | ns | ns | ns |

Panel A:

Unpaired t test between PBS 2% and PBS 5%

| Unpaired t test | | |
|---|---|---|
| 1 | Table Analyzed | VCAM 2%vs5% %+ve |
| 2 | | |
| 3 | Column B | PBS 5% |
| 4 | vs. | vs. |
| 5 | Column A | PBS 2% |
| 6 | | |
| 7 | Unpaired t test | |
| 8 | P value | 0.0074 |
| 9 | P value summary | ** |
| 10 | Significantly different (P < 0.05)? | Yes |
| 11 | One- or two-tailed P value? | Two-tailed |
| 12 | t, df | t=3.563 df=8 |

Unpaired t test between rM5 2% and rM5 5%

| Unpaired t test | | |
|---|---|---|
| 1 | Table Analyzed | VCAM 2%vs5% %+ve |
| 2 | | |
| 3 | Column D | rM5 5% |
| 4 | vs. | vs. |
| 5 | Column C | rM5 2% |
| 6 | | |
| 7 | Unpaired t test | |
| 8 | P value | 0.0216 |
| 9 | P value summary | * |
| 10 | Significantly different (P < 0.05)? | Yes |
| 11 | One- or two-tailed P value? | Two-tailed |
| 12 | t, df | t=2.845 df=8 |

Unpaired t test between Stg 2% and Stg 5%

| Unpaired t test | | |
|---|---|---|
| 1 | Table Analyzed | VCAM 2%vs5% %+ve |
| 2 | | |
| 3 | Column F | Stg 5% |
| 4 | vs. | vs. |
| 5 | Column E | Stg 2% |
| 6 | | |
| 7 | Unpaired t test | |
| 8 | P value | 0.4492 |
| 9 | P value summary | ns |
| 10 | Significantly different (P < 0.05)? | No |
| 11 | One- or two-tailed P value? | Two-tailed |
| 12 | t, df | t=0.7956 df=8 |

Panel B: D'Agostino & Pearson normality test

| Col. stats | | A | B | C |
|---|---|---|---|---|
| | | Normality PBS | Normality rM5 | Normality Stg |
| | | Y | Y | Y |
| 1 | Number of values | 12 | 12 | 12 |
| 2 | | | | |
| 3 | D'Agostino & Pearson normality test | | | |
| 4 | K2 | 0.9753 | 1.229 | 0.2861 |
| 5 | P value | 0.6141 | 0.5408 | 0.8667 |
| 6 | Passed normality test (alpha=0.05)? | Yes | Yes | Yes |
| 7 | P value summary | ns | ns | ns |

Panel B:

Unpaired t test between PBS 2% and PBS 5%

| Unpaired t test | |
|---|---|
| Table Analyzed | VCAM 2%vs5% MF |
| | |
| Column B | PBS 5% |
| vs. | vs. |
| Column A | PBS 2% |
| | |
| Unpaired t test | |
| P value | 0.0037 |
| P value summary | ** |
| Significantly different (P < 0.05)? | Yes |
| One- or two-tailed P value? | Two-tailed |
| t, df | t=4.044 df=8 |

Unpaired t test between rM5 2% and rM5 5%

| Unpaired t test | |
|---|---|
| Table Analyzed | VCAM 2%vs5% MFI |
| | |
| Column D | rM5 5% |
| vs. | vs. |
| Column C | rM5 2% |
| | |
| Unpaired t test | |
| P value | 0.0011 |
| P value summary | ** |
| Significantly different (P < 0.05)? | Yes |
| One- or two-tailed P value? | Two-tailed |
| t, df | t=4.983 df=8 |

Unpaired t test between Stg 2% and Stg 5%

| Unpaired t test | |
|---|---|
| Table Analyzed | VCAM 2%vs5% MFI |
| | |
| Column F | Stg 5% |
| vs. | vs. |
| Column E | Stg 2% |
| | |
| Unpaired t test | |
| P value | 0.0070 |
| P value summary | ** |
| Significantly different (P < 0.05)? | Yes |
| One- or two-tailed P value? | Two-tailed |
| t, df | t=3.595 df=8 |

Panel C: D'Agostino & Pearson normality test

| Col. stats | A | B | C |
|---|---|---|---|
| | Normality PBS | Normality rM5 | Normality Stg |
| | Y | Y | Y |
| Number of values | 10 | 10 | 10 |
| | | | |
| D'Agostino & Pearson normality test | | | |
| K2 | 2.535 | 1.157 | 3.656 |
| P value | 0.2816 | 0.5607 | 0.1608 |
| Passed normality test (alpha=0.05)? | Yes | Yes | Yes |
| P value summary | ns | ns | ns |

Panel C:

Unpaired t test between PBS 2% and PBS 5%

| Unpaired t test | |
|---|---|
| Table Analyzed | ICAM 2%vs5% %+ve |
| | |
| Column B | PBS 5% |
| vs. | vs. |
| Column A | PBS 2% |
| | |
| Unpaired t test | |
| P value | 0.0815 |
| P value summary | ns |
| Significantly different (P < 0.05)? | No |
| One- or two-tailed P value? | Two-tailed |
| t, df | t=1.992 df=8 |

Unpaired t test between rM5 2% and rM5 5%

| Unpaired t test | |
|---|---|
| Table Analyzed | ICAM 2%vs5% %+ve |
| | |
| Column D | rM5 5% |
| vs. | vs. |
| Column C | rM5 2% |
| | |
| Unpaired t test | |
| P value | 0.0646 |
| P value summary | ns |
| Significantly different (P < 0.05)? | No |
| One- or two-tailed P value? | Two-tailed |
| t, df | t=2.142 df=8 |

Unpaired t test between Stg 2% and Stg 5%

| Unpaired t test | |
|---|---|
| Table Analyzed | ICAM 2%vs5% %+ve |
| | |
| Column F | Stg 5% |
| vs. | vs. |
| Column E | Stg 2% |
| | |
| Unpaired t test | |
| P value | 0.0789 |
| P value summary | ns |
| Significantly different (P < 0.05)? | No |
| One- or two-tailed P value? | Two-tailed |
| t, df | t=2.013 df=8 |

Panel D: D'Agostino & Pearson normality test

| Col. stats | A | B | C |
|---|---|---|---|
| | Normality PBS | Normality rM5 | Normality Stg |
| | Y | Y | Y |
| Number of values | 10 | 10 | 10 |
| | | | |
| D'Agostino & Pearson normality test | | | |
| K2 | 4.576 | 2.95 | 0.48 |
| P value | 0.1015 | 0.2288 | 0.7866 |
| Passed normality test (alpha=0.05)? | Yes | Yes | Yes |
| P value summary | ns | ns | ns |

Panel D:

Unpaired t test between PBS 2% and PBS 5%

| Unpaired t test | |
|---|---|
| Table Analyzed | ICAM 2%vs5% MFI |
| | |
| Column B | PBS 5% |
| vs. | vs. |
| Column A | PBS 2% |
| | |
| Unpaired t test | |
| P value | 0.0109 |
| P value summary | * |
| Significantly different (P < 0.05)? | Yes |
| One- or two-tailed P value? | Two-tailed |
| t, df | t=3.299 df=8 |

Unpaired t test between rM5 2% and rM5 5%

| Unpaired t test | |
|---|---|
| Table Analyzed | ICAM 2%vs5% MFI |
| | |
| Column D | rM5 5% |
| vs. | vs. |
| Column C | rM5 2% |
| | |
| Unpaired t test | |
| P value | 0.0002 |
| P value summary | *** |
| Significantly different (P < 0.05)? | Yes |
| One- or two-tailed P value? | Two-tailed |
| t, df | t=6.412 df=8 |

Unpaired t test between Stg 2% and Stg 5%

| Unpaired t test | |
|---|---|
| Table Analyzed | ICAM 2%vs5% MFI |
| | |
| Column F | Stg 5% |
| vs. | vs. |
| Column E | Stg 2% |
| | |
| Unpaired t test | |
| P value | 0.0111 |
| P value summary | * |
| Significantly different (P < 0.05)? | Yes |
| One- or two-tailed P value? | Two-tailed |
| t, df | t=3.283 df=8 |

## 4.3 Statistical analysis of Figure 4.10

Panel A: D'Agostino & Pearson normality test

| Col. stats | A | B | C |
|---|---|---|---|
| | Normality PBS | Normality rM5 | Normality Stg |
| | Y | Y | Y |
| Number of values | 10 | 10 | 10 |
| | | | |
| D'Agostino & Pearson normality test | | | |
| K2 | 2.758 | 2.654 | 2.869 |
| P value | 0.2519 | 0.2652 | 0.2383 |
| Passed normality test (alpha=0.05)? | Yes | Yes | Yes |
| P value summary | ns | ns | ns |

Panel A:

Unpaired t test between PBS 2h and PBS 6h

| Unpaired t test | |
|---|---|
| Table Analyzed | VCAM 2hvs6h %+ve |
| | |
| Column B | PBS 6h |
| vs. | vs. |
| Column A | PBS 2h |
| | |
| Unpaired t test | |
| P value | 0.0082 |
| P value summary | ** |
| Significantly different (P < 0.05)? | Yes |
| One- or two-tailed P value? | Two-tailed |
| t, df | t=3.492 df=8 |

Unpaired t test between rM5 2h and rM5 6h

| Unpaired t test | |
|---|---|
| Table Analyzed | VCAM 2hvs6h %+ve |
| | |
| Column D | rM5 6h |
| vs. | vs. |
| Column C | rM5 2h |
| | |
| Unpaired t test | |
| P value | 0.0035 |
| P value summary | ** |
| Significantly different (P < 0.05)? | Yes |
| One- or two-tailed P value? | Two-tailed |
| t, df | t=4.093 df=8 |

Unpaired t test between Stg 2h and Stg 6h

| Unpaired t test | |
|---|---|
| Table Analyzed | VCAM 2hvs6h %+ve |
| | |
| Column F | Stg 6h |
| vs. | vs. |
| Column E | Stg 2h |
| | |
| Unpaired t test | |
| P value | 0.0056 |
| P value summary | ** |
| Significantly different (P < 0.05)? | Yes |
| One- or two-tailed P value? | Two-tailed |
| t, df | t=3.749 df=8 |

Panel B: D'Agostino & Pearson normality test

| Col. stats | A | B | C |
|---|---|---|---|
| | Normality PBS | Normality rM5 | Normality Stg |
| | Y | Y | Y |
| Number of values | 10 | 10 | 10 |
| | | | |
| D'Agostino & Pearson normality test | | | |
| K2 | 0.3878 | 4.785 | 1.145 |
| P value | 0.8238 | 0.0914 | 0.5642 |
| Passed normality test (alpha=0.05)? | Yes | Yes | Yes |
| P value summary | ns | ns | ns |

Panel B:

Unpaired t test between PBS 2h and PBS 6h

| Unpaired t test | |
|---|---|
| Table Analyzed | VCAM 2hvs6h MFI |
| | |
| Column B | PBS 6h |
| vs. | vs. |
| Column A | PBS 2h |
| | |
| Unpaired t test | |
| P value | 0.1192 |
| P value summary | ns |
| Significantly different (P < 0.05)? | No |
| One- or two-tailed P value? | Two-tailed |
| t, df | t=1.745 df=8 |

Unpaired t test between rM5 2h and rM5 6h

| Unpaired t test | |
|---|---|
| Table Analyzed | VCAM 2hvs6h MFI |
| | |
| Column D | rM5 6h |
| vs. | vs. |
| Column C | rM5 2h |
| | |
| Unpaired t test | |
| P value | <0.0001 |
| P value summary | **** |
| Significantly different (P < 0.05)? | Yes |
| One- or two-tailed P value? | Two-tailed |
| t, df | t=8.242 df=8 |

Unpaired t test between Stg 2h and Stg 6h

| Unpaired t test | |
|---|---|
| Table Analyzed | VCAM 2hvs6h MFI |
| | |
| Column F | Stg 6h |
| vs. | vs. |
| Column E | Stg 2h |
| | |
| Unpaired t test | |
| P value | 0.0007 |
| P value summary | *** |
| Significantly different (P < 0.05)? | Yes |
| One- or two-tailed P value? | Two-tailed |
| t, df | t=5.32 df=8 |

Panel C: D'Agostino & Pearson normality test

| Col. stats | A | B | C |
|---|---|---|---|
| | Normality PBS | Normality rM5 | Normality Stg |
| | Y | Y | Y |
| Number of values | 10 | 10 | 10 |
| | | | |
| D'Agostino & Pearson normality test | | | |
| K2 | 0.3262 | 2.145 | 4.923 |
| P value | 0.8495 | 0.3422 | 0.0853 |
| Passed normality test (alpha=0.05)? | Yes | Yes | Yes |
| P value summary | ns | ns | ns |

Panel C:

Unpaired t test between PBS 2h and PBS 6h

| Unpaired t test | |
|---|---|
| Table Analyzed | ICAM 2hvs6h %+ve |
| | |
| Column B | PBS 6h |
| vs. | vs. |
| Column A | PBS 2h |
| | |
| Unpaired t test | |
| P value | 0.0295 |
| P value summary | * |
| Significantly different (P < 0.05)? | Yes |
| One- or two-tailed P value? | Two-tailed |
| t, df | t=2.645 df=8 |

Unpaired t test between rM5 2h and rM5 6h

| Unpaired t test | |
|---|---|
| Table Analyzed | ICAM 2hvs6h %+ve |
| | |
| Column D | rM5 6h |
| vs. | vs. |
| Column C | rM5 2h |
| | |
| Unpaired t test | |
| P value | 0.0043 |
| P value summary | ** |
| Significantly different (P < 0.05)? | Yes |
| One- or two-tailed P value? | Two-tailed |
| t, df | t=3.946 df=8 |

Unpaired t test between Stg 2h and Stg 6h

| Unpaired t test | |
|---|---|
| Table Analyzed | ICAM 2hvs6h %+ve |
| | |
| Column F | Stg 6h |
| vs. | vs. |
| Column E | Stg 2h |
| | |
| Unpaired t test | |
| P value | 0.2429 |
| P value summary | ns |
| Significantly different (P < 0.05)? | No |
| One- or two-tailed P value? | Two-tailed |
| t, df | t=1.261 df=8 |

Panel D: D'Agostino & Pearson normality test

| Col. stats | A | B | C |
|---|---|---|---|
| | Normality PBS | Normality rM5 | Normality Stg |
| | Y | Y | Y |
| Number of values | 10 | 10 | 10 |
| | | | |
| D'Agostino & Pearson normality test | | | |
| K2 | 1.666 | 1.906 | 4.576 |
| P value | 0.4347 | 0.3857 | 0.1015 |
| Passed normality test (alpha=0.05)? | Yes | Yes | Yes |
| P value summary | ns | ns | ns |

Panel D:

Unpaired t test between PBS 2h and PBS 6h

| Unpaired t test | |
|---|---|
| Table Analyzed | ICAM 2hvs6h MFI |
| | |
| Column B | PBS 6h |
| vs. | vs. |
| Column A | PBS 2h |
| | |
| Unpaired t test | |
| P value | 0.0090 |
| P value summary | ** |
| Significantly different (P < 0.05)? | Yes |
| One- or two-tailed P value? | Two-tailed |
| t, df | t=3.425 df=8 |

Unpaired t test between rM5 2h and rM5 6h

| Unpaired t test | |
|---|---|
| Table Analyzed | ICAM 2hvs6h MFI |
| | |
| Column D | rM5 6h |
| vs. | vs. |
| Column C | rM5 2h |
| | |
| Unpaired t test | |
| P value | 0.0039 |
| P value summary | ** |
| Significantly different (P < 0.05)? | Yes |
| One- or two-tailed P value? | Two-tailed |
| t, df | t=4 df=8 |

Unpaired t test between Stg 2h and Stg 6h

| Unpaired t test | |
|---|---|
| Table Analyzed | ICAM 2hvs6h MFI |
| | |
| Column F | Stg 6h |
| vs. | vs. |
| Column E | Stg 2h |
| | |
| Unpaired t test | |
| P value | 0.0061 |
| P value summary | ** |
| Significantly different (P < 0.05)? | Yes |
| One- or two-tailed P value? | Two-tailed |
| t, df | t=3.695 df=8 |

## APPENDIX 5

## SUPPLEMENTARY FIGURES AND STATISTICAL ANALYSIS OF CHAPTER 5

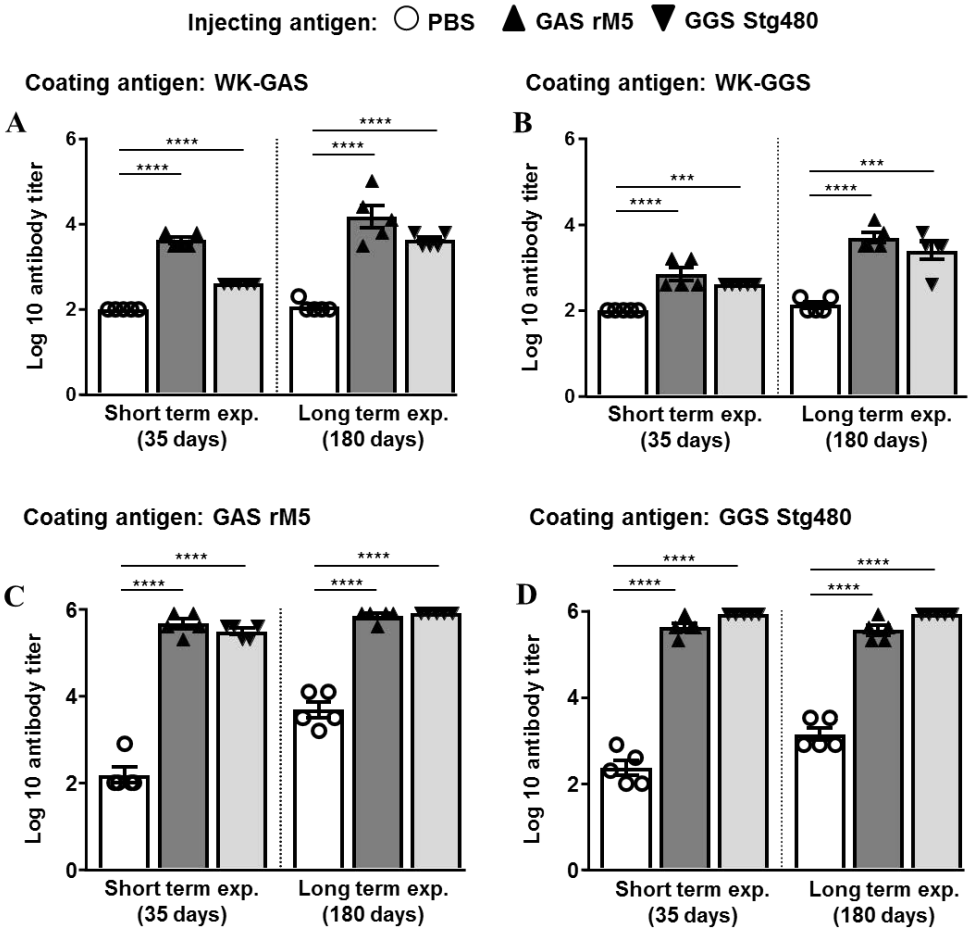


**Supplementary Figure 5.1** Antibodies generated following exposure to GGS Stg480 and GAS rM5 reacted with WK-GAS, WK-GGS and GAS and GGS M-proteins. Serum IgG in rats injected short term and long term with GGS Stg480 and GAS rM5 reacted with surface antigens of WK-GAS (A) and WK-GGS (B). Similarly, serum IgG in rats injected with GGS Stg480 reacted with GAS rM5 (C). Anti-GAS rM5 antibodies also reacted significantly against GGS Stg480 (D). In all experiments, serum from PBS injected rats was used as control. Error bars represent standard errors of the mean (SEM). Statistical difference by one-way ANOVA with Tukey's post hoc multiple comparison; ***p<0.001, ****p<0.0001.

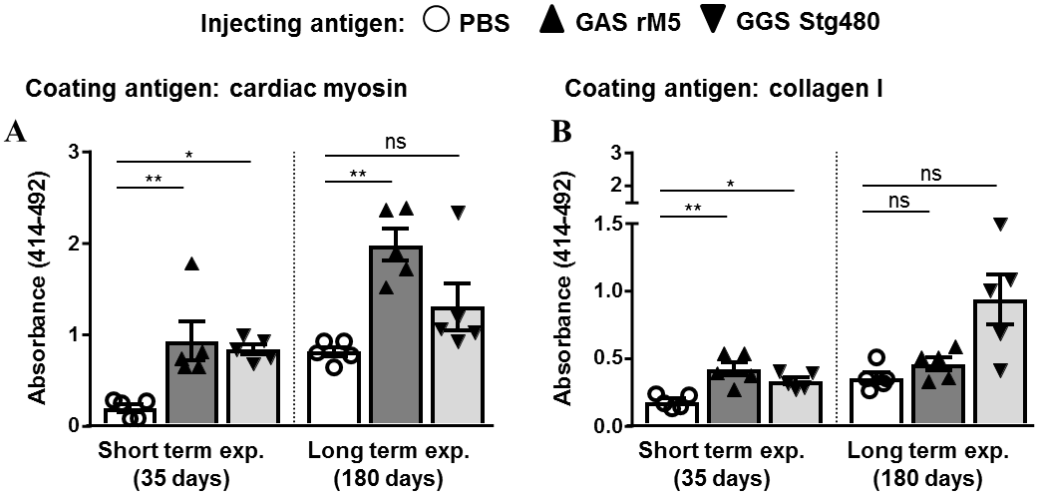


**Supplementary Figure 5.2** Antibodies generated following exposure to GGS Stg480 and GAS rM5 cross-reacted with cardiac myosin and collagen I. (A) Antisera at 1:100 dilution raised in rats following injection with GGS Stg480 and GAS rM5 reacted against cardiac myosin though the difference between absorbance values of sera from rats injected long term with PBS and GGS Stg480 was not significant. (B) Reactivity to collagen I was also observed though the sera from GGS Stg480 and GAS rM5 injected long term rats was not significantly higher compared to the sera from PBS injected control rats. In all experiments PBS injected control rats were included. Error bars represent standard errors of the mean (SEM). Statistical difference by one-way ANOVA with Tukey's post hoc multiple comparison (A, B left panel) and Kruskal-Wallis test (B right panel); *p<0.05, **p<0.01, ns: not significant.

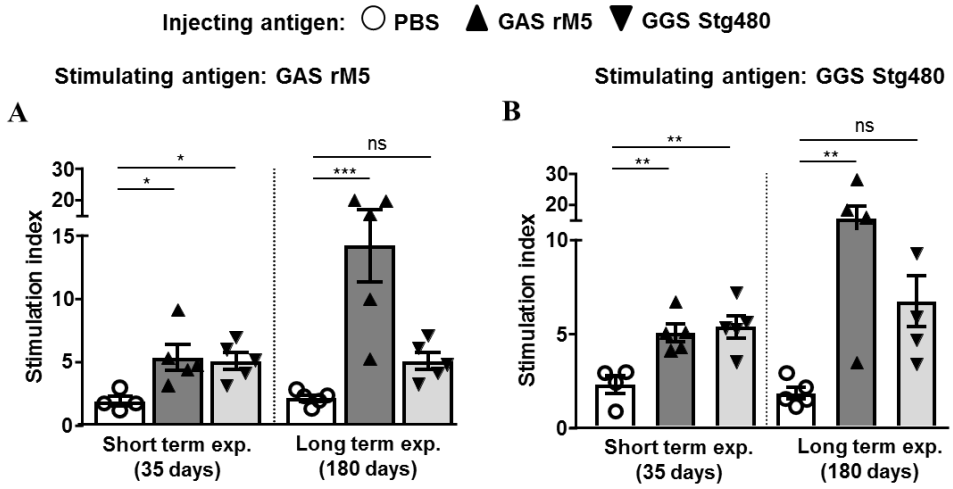


**Supplementary Figure 5.3** Splenic T-cells from GGS Stg480 and GAS rM5 injected rats proliferate in response to GGS and GAS M-proteins. The T-cells from rats injected short term and long term with GGS Stg480 proliferated in response to GAS rM5 though the proliferative response from long term injected rats was not significant compared to PBS injected control rats (A). The anti-GAS rM5 T-cells also proliferated significantly in response to GGS Stg480 (B). The T-cell proliferative response to GAS rM5 and GGS Stg480 was minimum in control rats injected with PBS. Error bars represent standard errors of the mean (SEM). Statistical difference by one-way ANOVA with Tukey's post hoc multiple comparison (A, B left panel) and Kruskal-Wallis test (B right panel); *p<0.05, **p<0.01, ***p<0.001, ns: not significant.

## 5.1 Statistical analysis of Figure 5.1

Panel A (short term exp.): Normality test and Tukey's multiple comparisons test

| Col. stats | A |
|---|---|
| | Normality check |
| | Y |
| Number of values | 20 |
| | |
| D'Agostino & Pearson normality test | |
| K2 | 5.679 |
| P value | 0.0585 |
| Passed normality test (alpha=0.05)? | Yes |
| P value summary | ns |

| 1way ANOVA Multiple comparisons | | | | | |
|---|---|---|---|---|---|
| Number of families | 1 | | | | |
| Number of comparisons per family | 3 | | | | |
| Alpha | 0.05 | | | | |
| | | | | | |
| Tukey's multiple comparisons test | Mean Diff. | 95.00% CI of diff. | Significant? | Summary | Adjusted P Value |
| | | | | | |
| PBS vs. GAS | -2.494 | -2.879 to -2.11 | Yes | **** | <0.0001 |
| PBS vs. GGS | -1.405 | -1.805 to -1.004 | Yes | **** | <0.0001 |
| GAS vs. GGS | 1.089 | 0.6891 to 1.49 | Yes | **** | <0.0001 |

Panel A (long term exp.): Normality test and Tukey's multiple comparisons test

| Col. stats | A |
|---|---|
| | Normality A |
| | Y |
| Number of values | 22 |
| | |
| D'Agostino & Pearson normality test | |
| K2 | 5.631 |
| P value | 0.0599 |
| Passed normality test (alpha=0.05)? | Yes |
| P value summary | ns |

| 1way ANOVA Multiple comparisons | | | | |
|---|---|---|---|---|
| Number of families | 1 | | | |
| Number of comparisons per family | 3 | | | |
| Alpha | 0.05 | | | |
| | | | | |
| Tukey's multiple comparisons test | Mean Diff. | 95.00% CI of diff. | Significant? | Summary |
| | | | | |
| PBS vs. GAS | -2.295 | -2.694 to -1.896 | Yes | **** |
| PBS vs. GGS | -0.9891 | -1.401 to -0.5771 | Yes | **** |
| GAS vs. GGS | 1.306 | 0.9073 to 1.705 | Yes | **** |

Panel B (short term exp.): Normality test and Tukey's multiple comparisons test

| Col. stats | A |
|---|---|
| | Normality A |
| | Y |
| Number of values | 18 |
| | |
| D'Agostino & Pearson normality test | |
| K2 | 5.12 |
| P value | 0.0773 |
| Passed normality test (alpha=0.05)? | Yes |
| P value summary | ns |

| 1way ANOVA Multiple comparisons | | | | |
|---|---|---|---|---|
| Number of families | 1 | | | |
| Number of comparisons per family | 3 | | | |
| Alpha | 0.05 | | | |
| | | | | |
| Tukey's multiple comparisons test | Mean Diff. | 95.00% CI of diff. | Significant? | Summary |
| | | | | |
| PBS vs. rM5 | -1.605 | -1.74 to -1.471 | Yes | **** |
| PBS vs. rGGSm | -0.6021 | -0.7367 to -0.4675 | Yes | **** |
| rM5 vs. rGGSm | 1.003 | 0.8688 to 1.138 | Yes | **** |

Panel B (long term exp.): Normality test and Tukey's multiple comparisons test

| Col. stats | A |
|---|---|
| | Normality A |
| | Y |
| Number of values | 15 |
| | |
| D'Agostino & Pearson normality test | |
| K2 | 4.194 |
| P value | 0.1228 |
| Passed normality test (alpha=0.05)? | Yes |
| P value summary | ns |

| 1way ANOVA Multiple comparisons | | | | | |
|---|---|---|---|---|---|
| Number of families | 1 | | | | |
| Number of comparisons per family | 3 | | | | |
| Alpha | 0.05 | | | | |
| | | | | | |
| Tukey's multiple comparisons test | Mean Diff. | 95.00% CI of diff. | Significant? | Summary | Adjusted P Value |
| | | | | | |
| PBS vs. rM5 | -2.468 | -3.04 to -1.897 | Yes | **** | <0.0001 |
| PBS vs. rGGSm | -1.144 | -1.716 to -0.5723 | Yes | *** | 0.0005 |
| rM5 vs. rGGSm | 1.325 | 0.7529 to 1.896 | Yes | *** | 0.0001 |

Panel C (short term exp.): Normality test and Tukey's multiple comparisons test

| Col. stats | A |
|---|---|
| | Normality check |
| | Y |
| Number of values | 20 |
| | |
| D'Agostino & Pearson normality test | |
| K2 | 5.679 |
| P value | 0.0585 |
| Passed normality test (alpha=0.05)? | Yes |
| P value summary | ns |

| 1way ANOVA Multiple comparisons | | | | | |
|---|---|---|---|---|---|
| Number of families | 1 | | | | |
| Number of comparisons per family | 3 | | | | |
| Alpha | 0.05 | | | | |
| | | | | | |
| Tukey's multiple comparisons test | Mean Diff. | 95.00% CI of diff. | Significant? | Summary | Adjusted P Value |
| | | | | | |
| PBS vs. GAS | -1.806 | -2.181 to -1.432 | Yes | **** | <0.0001 |
| PBS vs. GGS | -2.408 | -2.798 to -2.018 | Yes | **** | <0.0001 |
| GAS vs. GGS | -0.6021 | -0.992 to -0.2122 | Yes | ** | 0.0027 |

Panel C (long term exp.): Normality test and Tukey's multiple comparisons test

| Col. stats | A |
|---|---|
| | Normality G |
| | Y |
| Number of values | 22 |
| | |
| D'Agostino & Pearson normality test | |
| K2 | 5.631 |
| P value | 0.0599 |
| Passed normality test (alpha=0.05)? | Yes |
| P value summary | ns |

| 1way ANOVA Multiple comparisons | | | | | |
|---|---|---|---|---|---|
| Number of families | 1 | | | | |
| Number of comparisons per family | 3 | | | | |
| Alpha | 0.05 | | | | |
| | | | | | |
| Tukey's multiple comparisons test | Mean Diff. | 95.00% CI of diff. | Significant? | Summary | Adjusted P Value |
| | | | | | |
| PBS vs. GAS | -1.994 | -2.393 to -1.595 | Yes | **** | <0.0001 |
| PBS vs. GGS | -2.924 | -3.336 to -2.512 | Yes | **** | <0.0001 |
| GAS vs. GGS | -0.93 | -1.329 to -0.531 | Yes | **** | <0.0001 |

Panel D (short term exp.): Normality test and Tukey's multiple comparisons test

| Col. stats | A |
|---|---|
| | Normality G |
| | Y |
| Number of values | 18 |
| | |
| D'Agostino & Pearson normality test | |
| K2 | 0.2656 |
| P value | 0.8756 |
| Passed normality test (alpha=0.05)? | Yes |
| P value summary | ns |

| 1way ANOVA Multiple comparisons | | | | |
|---|---|---|---|---|
| Number of families | 1 | | | |
| Number of comparisons per family | 3 | | | |
| Alpha | 0.05 | | | |
| | | | | |
| Tukey's multiple comparisons test | Mean Diff. | 95.00% CI of diff. | Significant? | Summary |
| | | | | |
| PBS vs. rM5 | -0.8027 | -1.072 to -0.5336 | Yes | **** |
| PBS vs. rGGSm | -0.6021 | -0.8712 to -0.3329 | Yes | **** |
| rM5 vs. rGGSm | 0.2007 | -0.0685 to 0.4699 | No | ns |

Panel D (long term exp.): Normality test and Tukey's multiple comparisons test

| Col. stats | A |
|---|---|
| | Normality G |
| | Y |
| Number of values | 15 |
| | |
| D'Agostino & Pearson normality test | |
| K2 | 3.769 |
| P value | 0.1519 |
| Passed normality test (alpha=0.05)? | Yes |
| P value summary | ns |

| 1way ANOVA Multiple comparisons | | | | | |
|---|---|---|---|---|---|
| Number of families | 1 | | | | |
| Number of comparisons per family | 3 | | | | |
| Alpha | 0.05 | | | | |
| | | | | | |
| Tukey's multiple comparisons test | Mean Diff. | 95.00% CI of diff. | Significant? | Summary | Adjusted P Value |
| | | | | | |
| PBS vs. rM5 | -0.7225 | -1.423 to -0.02239 | Yes | * | 0.0430 |
| PBS vs. rGGSm | -1.325 | -2.025 to -0.6244 | Yes | *** | 0.0008 |
| rM5 vs. rGGSm | -0.602 | -1.302 to 0.09807 | No | ns | 0.0953 |

## 5.2 Statistical analysis of Figure 5.2

Panel A (short term exp.): Normality test and Tukey's multiple comparisons test

| Col. stats | A |
|---|---|
| | Normality |
| | Y |
| Number of values | 20 |
| | |
| D'Agostino & Pearson normality test | |
| K2 | 3.069 |
| P value | 0.2156 |
| Passed normality test (alpha=0.05)? | Yes |
| P value summary | ns |

| 1way ANOVA Multiple comparisons | | | | |
|---|---|---|---|---|
| Number of families | 1 | | | |
| Number of comparisons per family | 3 | | | |
| Alpha | 0.05 | | | |
| | | | | |
| Tukey's multiple comparisons test | Mean Diff. | 95.00% CI of diff. | Significant? | Summary |
| | | | | |
| PBS vs. GAS | -2.58 | -2.978 to -2.182 | Yes | **** |
| PBS vs. GGS | -1.57 | -1.984 to -1.156 | Yes | **** |
| GAS vs. GGS | 1.011 | 0.5966 to 1.425 | Yes | **** |

Panel A (long term exp.): Normality test and Tukey's multiple comparisons test

| Col. stats | A |
|---|---|
| | Normlality A |
| | Y |
| Number of values | 22 |
| | |
| D'Agostino & Pearson normality test | |
| K2 | 2.986 |
| P value | 0.2247 |
| Passed normality test (alpha=0.05)? | Yes |
| P value summary | ns |

| 1way ANOVA Multiple comparisons | | | | |
|---|---|---|---|---|
| Number of families | 1 | | | |
| Number of comparisons per family | 3 | | | |
| Alpha | 0.05 | | | |
| | | | | |
| Tukey's multiple comparisons test | Mean Diff. | 95.00% CI of diff. | Significant? | Summary |
| | | | | |
| PBS vs. rM5 | -2.211 | -2.69 to -1.732 | Yes | **** |
| PBS vs. rGGSm | -1.075 | -1.57 to -0.5803 | Yes | **** |
| rM5 vs. rGGSm | 1.136 | 0.6565 to 1.615 | Yes | **** |

Panel B (short term exp.): Normality test and Tukey's multiple comparisons test

| Col. stats | A |
|---|---|
| | Normlality |
| | Y |
| Number of values | 18 |
| | |
| D'Agostino & Pearson normality test | |
| K2 | 5.12 |
| P value | 0.0773 |
| Passed normality test (alpha=0.05)? | Yes |
| P value summary | ns |

1way ANOVA
Multiple comparisons

| | | | | | |
|---|---|---|---|---|---|
| Number of families | 1 | | | | |
| Number of comparisons per family | 3 | | | | |
| Alpha | 0.05 | | | | |
| | | | | | |
| Tukey's multiple comparisons test | Mean Diff. | 95.00% CI of diff. | Significant? | Summary | |
| | | | | | |
| PBS vs. rM5 | -3.412 | -3.768 to -3.056 | Yes | **** | |
| PBS vs. rGGSm | -2.408 | -2.764 to -2.052 | Yes | **** | |
| rM5 vs. rGGSm | 1.003 | 0.6473 to 1.36 | Yes | **** | |

Panel B (long term exp.): Normality test and Tukey's multiple comparisons test

| Col. stats | A |
|---|---|
| | Normality |
| | Y |
| Number of values | 15 |
| | |
| D'Agostino & Pearson normality test | |
| K2 | 5.28 |
| P value | 0.0714 |
| Passed normality test (alpha=0.05)? | Yes |
| P value summary | ns |

1way ANOVA
Multiple comparisons

| | | | | | |
|---|---|---|---|---|---|
| Number of families | 1 | | | | |
| Number of comparisons per family | 3 | | | | |
| Alpha | 0.05 | | | | |
| | | | | | |
| Tukey's multiple comparisons test | Mean Diff. | 95.00% CI of diff. | Significant? | Summary | Adjusted P Value |
| | | | | | |
| PBS vs. rM5 | -3.251 | -3.633 to -2.869 | Yes | **** | <0.0001 |
| PBS vs. rGGSm | -3.311 | -3.694 to -2.929 | Yes | **** | <0.0001 |
| rM5 vs. rGGSm | -0.0602 | -0.4426 to 0.3222 | No | ns | 0.9081 |

Panel C (short term exp.): Normality test and Tukey's multiple comparisons test

| Col. stats | A |
|---|---|
| | Normality |
| | Y |
| Number of values | 20 |
| | |
| D'Agostino & Pearson normality test | |
| K2 | 3.069 |
| P value | 0.2156 |
| Passed normality test (alpha=0.05)? | Yes |
| P value summary | ns |

1way ANOVA
Multiple comparisons

| | | | | | |
|---|---|---|---|---|---|
| Number of families | 1 | | | | |
| Number of comparisons per family | 3 | | | | |
| Alpha | 0.05 | | | | |
| | | | | | |
| Tukey's multiple comparisons test | Mean Diff. | 95.00% CI of diff. | Significant? | Summary | Adjusted P Value |
| | | | | | |
| PBS vs. GAS | -1.032 | -1.453 to -0.611 | Yes | **** | <0.0001 |
| PBS vs. GGS | -2.071 | -2.51 to -1.633 | Yes | **** | <0.0001 |
| GAS vs. GGS | -1.039 | -1.478 to -0.601 | Yes | **** | <0.0001 |

Panel C (long term exp.): Normality test and Tukey's multiple comparisons test

| Col. stats | A | B |
|---|---|---|
| | Data Set-A | Normality G |
| | Y | Y |
| Number of values | 0 | 22 |
| | | |
| D'Agostino & Pearson normality test | | |
| K2 | N too small | 5.194 |
| P value | | 0.0745 |
| Passed normality test (alpha=0.05)? | | Yes |
| P value summary | | ns |

1way ANOVA
Multiple comparisons

| | | | | |
|---|---|---|---|---|
| Number of families | 1 | | | |
| Number of comparisons per family | 3 | | | |
| Alpha | 0.05 | | | |
| | | | | |
| Tukey's multiple comparisons test | Mean Diff. | 95.00% CI of diff. | Significant? | Summary |
| | | | | |
| PBS vs. rM5 | -1.559 | -1.882 to -1.236 | Yes | **** |
| PBS vs. rGGSm | -2.451 | -2.785 to -2.118 | Yes | **** |
| rM5 vs. rGGSm | -0.8923 | -1.215 to -0.5695 | Yes | **** |

Panel D (short term exp.): Normality test and Tukey's multiple comparisons test

| Col. stats | A |
|---|---|
| | Normlality |
| | Y |
| Number of values | 18 |
| | |
| D'Agostino & Pearson normality test | |
| K2 | 5.12 |
| P value | 0.0773 |
| Passed normality test (alpha=0.05)? | Yes |
| P value summary | ns |

1way ANOVA
Multiple comparisons

| | | | | |
|---|---|---|---|---|
| Number of families | 1 | | | |
| Number of comparisons per family | 3 | | | |
| Alpha | 0.05 | | | |
| | | | | |
| Tukey's multiple comparisons test | Mean Diff. | 95.00% CI of diff. | Significant? | Summary |
| | | | | |
| PBS vs. rM5 | -2.458 | -2.736 to -2.181 | Yes | **** |
| PBS vs. rGGSm | -3.462 | -3.739 to -3.184 | Yes | **** |
| rM5 vs. rGGSm | -1.003 | -1.281 to -0.726 | Yes | **** |

Panel D (long term exp.): Normality test and Tukey's multiple comparisons test

| Col. stats | A |
|---|---|
| | Normality |
| | Y |
| Number of values | 15 |
| | |
| D'Agostino & Pearson normality test | |
| K2 | 5.949 |
| P value | 0.0511 |
| Passed normality test (alpha=0.05)? | Yes |
| P value summary | ns |

| 1way ANOVA Multiple comparisons | | | | | |
|---|---|---|---|---|---|
| Number of families | 1 | | | | |
| Number of comparisons per family | 3 | | | | |
| Alpha | 0.05 | | | | |
| | | | | | |
| Tukey's multiple comparisons test | Mean Diff. | 95.00% CI of diff. | Significant? | Summary | Adjusted P Value |
| | | | | | |
| PBS vs. rM5 | -2.95 | -3.332 to -2.568 | Yes | **** | <0.0001 |
| PBS vs. rGGSm | -3.552 | -3.935 to -3.17 | Yes | **** | <0.0001 |
| rM5 vs. rGGSm | -0.6021 | -0.9844 to -0.2197 | Yes | ** | 0.0033 |

## 5.3 Statistical analysis of Figure 5.3

Panel A (short term exp.): Normality test and Mann-Whitney test

| Col. stats | A |
|---|---|
| | Normality |
| | Y |
| Number of values | 20 |
| | |
| D'Agostino & Pearson normality test | |
| K2 | 22.21 |
| P value | <0.0001 |
| Passed normality test (alpha=0.05)? | No |
| P value summary | **** |

| Mann-Whitney test | |
|---|---|
| Table Analyzed | GGS1 CM absorbance 1:100 |
| | |
| Column B | GAS |
| vs. | vs. |
| Column A | PBS |
| | |
| Mann Whitney test | |
| P value | 0.0006 |
| Exact or approximate P value? | Exact |
| P value summary | *** |
| Significantly different (P < 0.05)? | Yes |
| One- or two-tailed P value? | Two-tailed |
| Sum of ranks in column A,B | 28 , 77 |
| Mann-Whitney U | 0 |

| Mann-Whitney test | |
|---|---|
| Table Analyzed | GGS1 CM absorbance 1:100 |
| | |
| Column C | GGS |
| vs. | vs. |
| Column A | PBS |
| | |
| Mann Whitney test | |
| P value | 0.0012 |
| Exact or approximate P value? | Exact |
| P value summary | ** |
| Significantly different (P < 0.05)? | Yes |
| One- or two-tailed P value? | Two-tailed |
| Sum of ranks in column A,C | 28 , 63 |
| Mann-Whitney U | 0 |

Panel A (long term exp.): Normality test and Mann-Whitney test

| Col. stats | A |
|---|---|
| | Normality CM |
| | Y |
| Number of values | 22 |
| | |
| D'Agostino & Pearson normality test | |
| K2 | 8.293 |
| P value | 0.0158 |
| Passed normality test (alpha=0.05)? | No |
| P value summary | * |

| Mann-Whitney test | |
|---|---|
| Table Analyzed | GGS2_CM_1:100 dilution |
| | |
| Column B | GAS |
| vs. | vs. |
| Column A | PBS |
| | |
| Mann Whitney test | |
| P value | 0.0003 |
| Exact or approximate P value? | Exact |
| P value summary | *** |
| Significantly different (P < 0.05)? | Yes |
| One- or two-tailed P value? | Two-tailed |
| Sum of ranks in column A,B | 28 , 92 |
| Mann-Whitney U | 0 |

| Mann-Whitney test | |
|---|---|
| Table Analyzed | GGS2_CM_1:100 dilution |
| | |
| Column C | GGS |
| vs. | vs. |
| Column A | PBS |
| | |
| Mann Whitney test | |
| P value | 0.0006 |
| Exact or approximate P value? | Exact |
| P value summary | *** |
| Significantly different (P < 0.05)? | Yes |
| One- or two-tailed P value? | Two-tailed |
| Sum of ranks in column A,C | 28 , 77 |
| Mann-Whitney U | 0 |

Panel B (short term exp.): Normality test and Mann-Whitney test

| Col. stats | A |
|---|---|
| | Normality |
| | Y |
| Number of values | 18 |
| | |
| D'Agostino & Pearson normality test | |
| K2 | 20.11 |
| P value | <0.0001 |
| Passed normality test (alpha=0.05)? | No |
| P value summary | **** |

| Mann-Whitney test | |
|---|---|
| Table Analyzed | GGS3 CM absorbance 1:100 |
| | |
| Column B | rM5 |
| vs. | vs. |
| Column A | PBS |
| | |
| Mann Whitney test | |
| P value | 0.0022 |
| Exact or approximate P value? | Exact |
| P value summary | ** |
| Significantly different (P < 0.05)? | Yes |
| One- or two-tailed P value? | Two-tailed |
| Sum of ranks in column A,B | 21 , 57 |
| Mann-Whitney U | 0 |

| Mann-Whitney test | |
|---|---|
| Table Analyzed | GGS3 CM absorbance 1:100 |
| | |
| Column C | rGGSm |
| vs. | vs. |
| Column A | PBS |
| | |
| Mann Whitney test | |
| P value | 0.0022 |
| Exact or approximate P value? | Exact |
| P value summary | ** |
| Significantly different (P < 0.05)? | Yes |
| One- or two-tailed P value? | Two-tailed |
| Sum of ranks in column A,C | 21 , 57 |
| Mann-Whitney U | 0 |

Panel B (long term exp.): Normality test and Mann-Whitney test

| Col. stats | A |
|---|---|
| | Normality CM |
| | Y |
| Number of values | 15 |
| | |
| D'Agostino & Pearson normality test | |
| K2 | 17.09 |
| P value | 0.0002 |
| Passed normality test (alpha=0.05)? | No |
| P value summary | *** |

| Mann-Whitney test | |
|---|---|
| Table Analyzed | CM 1:100 |
| | |
| Column B | rM5 |
| vs. | vs. |
| Column A | PBS |
| | |
| Mann Whitney test | |
| P value | 0.0079 |
| Exact or approximate P value? | Exact |
| P value summary | ** |
| Significantly different (P < 0.05)? | Yes |
| One- or two-tailed P value? | Two-tailed |
| Sum of ranks in column A,B | 15 , 40 |
| Mann-Whitney U | 0 |

| Mann-Whitney test | |
|---|---|
| Table Analyzed | CM 1:100 |
| | |
| Column C | rGGSm |
| vs. | vs. |
| Column A | PBS |
| | |
| Mann Whitney test | |
| P value | 0.0079 |
| Exact or approximate P value? | Exact |
| P value summary | ** |
| Significantly different (P < 0.05)? | Yes |
| One- or two-tailed P value? | Two-tailed |
| Sum of ranks in column A,C | 15 , 40 |
| Mann-Whitney U | 0 |

Panel C (short term exp.): Normality test and Mann-Whitney test

| Col. stats | A |
|---|---|
| | Normality |
| | Y |
| Number of values | 20 |
| | |
| D'Agostino & Pearson normality test | |
| K2 | 22.21 |
| P value | <0.0001 |
| Passed normality test (alpha=0.05)? | No |
| P value summary | **** |

| Mann-Whitney test | |
|---|---|
| Table Analyzed | GGS1 Col I absorbance 1:100 |
| | |
| Column B | GAS |
| vs. | vs. |
| Column A | PBS |
| | |
| Mann Whitney test | |
| P value | 0.0012 |
| Exact or approximate P value? | Exact |
| P value summary | ** |
| Significantly different (P < 0.05)? | Yes |
| One- or two-tailed P value? | Two-tailed |
| Sum of ranks in column A,B | 29 , 76 |
| Mann-Whitney U | 1 |

| Mann-Whitney test | |
|---|---|
| Table Analyzed | GGS1 Col I absorbance 1:100 |
| | |
| Column C | GGS |
| vs. | vs. |
| Column A | PBS |
| | |
| Mann Whitney test | |
| P value | 0.1375 |
| Exact or approximate P value? | Exact |
| P value summary | ns |
| Significantly different (P < 0.05)? | No |
| One- or two-tailed P value? | Two-tailed |
| Sum of ranks in column A,C | 38 , 53 |
| Mann-Whitney U | 10 |

Panel C (long term exp.): Normality test and Mann-Whitney test

| Col. stats | A |
|---|---|
| | Normality Col I |
| | Y |
| Number of values | 22 |
| | |
| D'Agostino & Pearson normality test | |
| K2 | 8.293 |
| P value | 0.0158 |
| Passed normality test (alpha=0.05)? | No |
| P value summary | * |

| Mann-Whitney test | |
|---|---|
| Table Analyzed | GGS2_Col I_1:100 dilution |
| | |
| Column B | GAS |
| vs. | vs. |
| Column A | PBS |
| | |
| Mann Whitney test | |
| P value | 0.0514 |
| Exact or approximate P value? | Exact |
| P value summary | ns |
| Significantly different (P < 0.05)? | No |
| One- or two-tailed P value? | Two-tailed |
| Sum of ranks in column A,B | 39 , 81 |
| Mann-Whitney U | 11 |

| Mann-Whitney test | |
|---|---|
| Table Analyzed | GGS2_Col I_1:100 dilution |
| | |
| Column C | GGS |
| vs. | vs. |
| Column A | PBS |
| | |
| Mann Whitney test | |
| P value | 0.3631 |
| Exact or approximate P value? | Exact |
| P value summary | ns |
| Significantly different (P < 0.05)? | No |
| One- or two-tailed P value? | Two-tailed |
| Sum of ranks in column A,C | 45 , 60 |
| Mann-Whitney U | 17 |

Panel D (short term exp.): Normality test and Mann-Whitney test

| Col. stats | A |
|---|---|
| | Normality |
| | Y |
| Number of values | 18 |
| | |
| D'Agostino & Pearson normality test | |
| K2 | 20.11 |
| P value | <0.0001 |
| Passed normality test (alpha=0.05)? | No |
| P value summary | **** |

| Mann-Whitney test | |
|---|---|
| Table Analyzed | GGS1 Col I absorbance 1:100 |
| | |
| Column B | rM5 |
| vs. | vs. |
| Column A | PBS |
| | |
| Mann Whitney test | |
| P value | 0.0087 |
| Exact or approximate P value? | Exact |
| P value summary | ** |
| Significantly different (P < 0.05)? | Yes |
| One- or two-tailed P value? | Two-tailed |
| Sum of ranks in column A,B | 23 , 55 |
| Mann-Whitney U | 2 |

| Mann-Whitney test | |
|---|---|
| Table Analyzed | GGS1 Col I absorbance 1:100 |
| | |
| Column C | rGGSm |
| vs. | vs. |
| Column A | PBS |
| | |
| Mann Whitney test | |
| P value | 0.0455 |
| Exact or approximate P value? | Exact |
| P value summary | * |
| Significantly different (P < 0.05)? | Yes |
| One- or two-tailed P value? | Two-tailed |
| Sum of ranks in column A,C | 26.5 , 51.5 |
| Mann-Whitney U | 5.5 |

Panel D (long term exp.): Normality test and Mann-Whitney test

| Col. stats | A |
|---|---|
| | Normality Col I |
| | Y |
| Number of values | 15 |
| | |
| D'Agostino & Pearson normality test | |
| K2 | 17.09 |
| P value | 0.0002 |
| Passed normality test (alpha=0.05)? | No |
| P value summary | *** |

| Mann-Whitney test | |
|---|---|
| Table Analyzed | Col I 1:100 |
| | |
| Column B | rM5 |
| vs. | vs. |
| Column A | PBS |
| | |
| Mann Whitney test | |
| P value | 0.0079 |
| Exact or approximate P value? | Exact |
| P value summary | ** |
| Significantly different (P < 0.05)? | Yes |
| One- or two-tailed P value? | Two-tailed |
| Sum of ranks in column A,B | 15 , 40 |
| Mann-Whitney U | 0 |

| Mann-Whitney test | |
|---|---|
| Table Analyzed | Col I 1:100 |
| | |
| Column C | rGGSm |
| vs. | vs. |
| Column A | PBS |
| | |
| Mann Whitney test | |
| P value | 0.0079 |
| Exact or approximate P value? | Exact |
| P value summary | ** |
| Significantly different (P < 0.05)? | Yes |
| One- or two-tailed P value? | Two-tailed |
| Sum of ranks in column A,C | 15 , 40 |
| Mann-Whitney U | 0 |

## 5.4 Statistical analysis of Figure 5.4

Panel A: Normality test and Tukey's multiple comparison test

| Col. stats | A |
|---|---|
| | Normality 96h |
| | Y |
| Number of values | 21 |
| | |
| D'Agostino & Pearson normality test | |
| K2 | 4.841 |
| P value | 0.0889 |
| Passed normality test (alpha=0.05)? | Yes |
| P value summary | ns |

| 1way ANOVA<br>Multiple comparisons | | | | | |
|---|---|---|---|---|---|
| Number of families | 1 | | | | |
| Number of comparisons per family | 3 | | | | |
| Alpha | 0.05 | | | | |
| | | | | | |
| Tukey's multiple comparisons test | Mean Diff. | 95.00% CI of diff. | Significant? | Summary | Adjusted P Value |
| | | | | | |
| 96P vs. 96A | -7.342 | -11.68 to -3.007 | Yes | ** | 0.0011 |
| 96P vs. 96G | -5.244 | -9.904 to -0.5837 | Yes | * | 0.0261 |
| 96A vs. 96G | 2.098 | -2.426 to 6.622 | No | ns | 0.4776 |

Panel B (short term exp.): Normality test and Tukey's multiple comparison test

| Col. stats | A |
|---|---|
| | Normality A |
| | Y |
| Number of values | 18 |
| | |
| D'Agostino & Pearson normality test | |
| K2 | 3.573 |
| P value | 0.1675 |
| Passed normality test (alpha=0.05)? | Yes |
| P value summary | ns |

| 1way ANOVA<br>Multiple comparisons | | | | |
|---|---|---|---|---|
| Number of families | 1 | | | |
| Number of comparisons per family | 3 | | | |
| Alpha | 0.05 | | | |
| | | | | |
| Tukey's multiple comparisons test | Mean Diff. | 95.00% CI of diff. | Significant? | Summary |
| | | | | |
| PBS vs. rM5 | -9.432 | -17.76 to -1.099 | Yes | * |
| PBS vs. rGGSm | -12.72 | -21.05 to -4.385 | Yes | ** |
| rM5 vs. rGGSm | -3.286 | -11.62 to 5.047 | No | ns |

Panel B (long term exp.): Normality test and Tukey's multiple comparison test

| Col. stats | A |
|---|---|
| | Normality |
| | Y |
| Number of values | 15 |
| | |
| D'Agostino & Pearson normality test | |
| K2 | 2.553 |
| P value | 0.2790 |
| Passed normality test (alpha=0.05)? | Yes |
| P value summary | ns |

| 1way ANOVA<br>Multiple comparisons | | | | | |
|---|---|---|---|---|---|
| Number of families | 1 | | | | |
| Number of comparisons per family | 3 | | | | |
| Alpha | 0.05 | | | | |
| | | | | | |
| Tukey's multiple comparisons test | Mean Diff. | 95.00% CI of diff. | Significant? | Summary | Adjusted P Value |
| | | | | | |
| PBS vs. rM5 | -4.071 | -7.244 to -0.8976 | Yes | * | 0.0130 |
| PBS vs. rGGSm | -4.108 | -7.282 to -0.9352 | Yes | * | 0.0123 |
| rM5 vs. rGGSm | -0.03757 | -3.211 to 3.136 | No | ns | 0.9995 |

Panel C: Normality test and Tukey's multiple comparison test

| Col. stats | A |
|---|---|
| | Normality 96h |
| | Y |
| Number of values | 21 |
| | |
| D'Agostino & Pearson normality test | |
| K2 | 4.633 |
| P value | 0.0986 |
| Passed normality test (alpha=0.05)? | Yes |
| P value summary | ns |

| 1way ANOVA<br>Multiple comparisons | | | | | |
|---|---|---|---|---|---|
| Number of families | 1 | | | | |
| Number of comparisons per family | 3 | | | | |
| Alpha | 0.05 | | | | |
| | | | | | |
| Tukey's multiple comparisons test | Mean Diff. | 95.00% CI of diff. | Significant? | Summary | Adjusted P Value |
| | | | | | |
| 96P vs. 96A | -4.9 | -9.656 to -0.1443 | Yes | * | 0.0428 |
| 96P vs. 96G | -6.583 | -11.7 to -1.471 | Yes | * | 0.0109 |
| 96A vs. 96G | -1.683 | -6.646 to 3.279 | No | ns | 0.6681 |

Panel D (short term exp.): Normality test and Tukey's multiple comparison test

| Col. stats | A |
|---|---|
| | Normality G |
| | Y |
| Number of values | 18 |
| | |
| D'Agostino & Pearson normality test | |
| K2 | 3.573 |
| P value | 0.1675 |
| Passed normality test (alpha=0.05)? | Yes |
| P value summary | ns |

| 1way ANOVA<br>Multiple comparisons | | | | |
|---|---|---|---|---|
| Number of families | 1 | | | |
| Number of comparisons per family | 3 | | | |
| Alpha | 0.05 | | | |
| | | | | |
| Tukey's multiple comparisons test | Mean Diff. | 95.00% CI of diff. | Significant? | Summary |
| | | | | |
| PBS vs. rM5 | -15.54 | -27.83 to -3.253 | Yes | * |
| PBS vs. rGGSm | -31.2 | -43.49 to -18.91 | Yes | **** |
| rM5 vs. rGGSm | -15.66 | -27.95 to -3.368 | Yes | * |

Panel D (long term exp.): Normality test and Tukey's multiple comparison test

| Col. stats | A |
|---|---|
| | Normality |
| | Y |
| Number of values | 15 |
| | |
| D'Agostino & Pearson normality test | |
| K2 | 2.553 |
| P value | 0.2790 |
| Passed normality test (alpha=0.05)? | Yes |
| P value summary | ns |

| 1way ANOVA<br>Multiple comparisons | | | | | |
|---|---|---|---|---|---|
| Number of families | 1 | | | | |
| Number of comparisons per family | 3 | | | | |
| Alpha | 0.05 | | | | |
| | | | | | |
| Tukey's multiple comparisons test | Mean Diff. | 95.00% CI of diff. | Significant? | Summary | Adjusted P Value |
| | | | | | |
| PBS vs. rM5 | -8.105 | -15.95 to -0.2642 | Yes | * | 0.0427 |
| PBS vs. rGGSm | -9.286 | -17.13 to -1.445 | Yes | * | 0.0208 |
| rM5 vs. rGGSm | -1.181 | -9.022 to 6.66 | No | ns | 0.9155 |

## 5.5 Statistical analysis of Figure 5.5

Panel A: Normality test and Tukey's multiple comparison test

| Col. stats | A |
|---|---|
| | Normality |
| | Y |
| Number of values | 12 |
| | |
| D'Agostino & Pearson normality test | |
| K2 | 5.316 |
| P value | 0.0701 |
| Passed normality test (alpha=0.05)? | Yes |
| P value summary | ns |

| 1way ANOVA<br>Multiple comparisons | | | | | |
|---|---|---|---|---|---|
| Number of families | 1 | | | | |
| Number of comparisons per family | 3 | | | | |
| Alpha | 0.05 | | | | |
| | | | | | |
| Tukey's multiple comparisons test | Mean Diff. | 95.00% CI of diff. | Significant? | Summary | Adjusted P Value |
| | | | | | |
| PBS-rM5 vs. GAS-rM5 | -4077 | -4225 to -3928 | Yes | **** | <0.0001 |
| PBS-rM5 vs. GGS-rM5 | -3921 | -4069 to -3772 | Yes | **** | <0.0001 |
| GAS-rM5 vs. GGS-rM5 | 156 | 7.615 to 304.4 | Yes | * | 0.0400 |

Panel B (short term exp.): Normality test and Tukey's multiple comparison test

| Col. stats | A |
|---|---|
| | Normality |
| | Y |
| Number of values | 12 |
| | |
| D'Agostino & Pearson normality test | |
| K2 | 5.344 |
| P value | 0.0691 |
| Passed normality test (alpha=0.05)? | Yes |
| P value summary | ns |

| 1way ANOVA<br>Multiple comparisons | | | | | |
|---|---|---|---|---|---|
| Number of families | 1 | | | | |
| Number of comparisons per family | 3 | | | | |
| Alpha | 0.05 | | | | |
| | | | | | |
| Tukey's multiple comparisons test | Mean Diff. | 95.00% CI of diff. | Significant? | Summary | Adjusted P Value |
| | | | | | |
| PBS-rM5 vs. rM5-rM5 | -2922 | -2991 to -2853 | Yes | **** | <0.0001 |
| PBS-rM5 vs. rGm-rM5 | -2876 | -2945 to -2807 | Yes | **** | <0.0001 |
| rM5-rM5 vs. rGm-rM5 | 46.15 | -22.78 to 115.1 | No | ns | 0.2028 |

Panel B (long term exp.): Normality test and Tukey's multiple comparison test

| Col. stats | A |
|---|---|
| | Normality |
| | Y |
| Number of values | 12 |
| | |
| D'Agostino & Pearson normality test | |
| K2 | 2.636 |
| P value | 0.2676 |
| Passed normality test (alpha=0.05)? | Yes |
| P value summary | ns |

| 1way ANOVA Multiple comparisons | | | | | |
|---|---|---|---|---|---|
| Number of families | 1 | | | | |
| Number of comparisons per family | 3 | | | | |
| Alpha | 0.05 | | | | |
| | | | | | |
| Tukey's multiple comparisons test | Mean Diff. | 95.00% CI of diff. | Significant? | Summary | Adjusted P Value |
| | | | | | |
| PBS-rM5 vs. rM5-rM5 | -2836 | -4371 to -1301 | Yes | ** | 0.0015 |
| PBS-rM5 vs. rGm-rM5 | -2416 | -3951 to -880.4 | Yes | ** | 0.0044 |
| rM5-rM5 vs. rGm-rM5 | 420.2 | -1115 to 1955 | No | ns | 0.7330 |

Panel C: Normality test and Tukey's multiple comparison test

| Col. stats | A |
|---|---|
| | Normality |
| | Y |
| Number of values | 12 |
| | |
| D'Agostino & Pearson normality test | |
| K2 | 5.348 |
| P value | 0.0690 |
| Passed normality test (alpha=0.05)? | Yes |
| P value summary | ns |

| 1way ANOVA Multiple comparisons | | | | | |
|---|---|---|---|---|---|
| Number of families | 1 | | | | |
| Number of comparisons per family | 3 | | | | |
| Alpha | 0.05 | | | | |
| | | | | | |
| Tukey's multiple comparisons test | Mean Diff. | 95.00% CI of diff. | Significant? | Summary | Adjusted P Value |
| | | | | | |
| PBS-rGm vs. GAS-rGm | -3918 | -3974 to -3861 | Yes | **** | <0.0001 |
| PBS-rGm vs. GGS-rGm | -3986 | -4043 to -3930 | Yes | **** | <0.0001 |
| GAS-rGm vs. GGS-rGm | -68.61 | -125 to -12.19 | Yes | * | 0.0196 |

Panel D (short term exp.): Normality test and Tukey's multiple comparison test

| Col. stats | A |
|---|---|
| | Normality |
| | Y |
| Number of values | 12 |
| | |
| D'Agostino & Pearson normality test | |
| K2 | 5.351 |
| P value | 0.0689 |
| Passed normality test (alpha=0.05)? | Yes |
| P value summary | ns |

| 1way ANOVA Multiple comparisons | | | | | |
|---|---|---|---|---|---|
| Number of families | 1 | | | | |
| Number of comparisons per family | 3 | | | | |
| Alpha | 0.05 | | | | |
| | | | | | |
| Tukey's multiple comparisons test | Mean Diff. | 95.00% CI of diff. | Significant? | Summary | Adjusted P Value |
| | | | | | |
| PBS-rGm vs. rM5-rGm | -2879 | -2911 to -2847 | Yes | **** | <0.0001 |
| PBS-rGm vs. rGm-rGm | -2838 | -2871 to -2806 | Yes | **** | <0.0001 |
| rM5-rGm vs. rGm-rGm | 40.92 | 8.693 to 73.15 | Yes | * | 0.0156 |

Panel D (long term exp.): Normality test and Tukey's multiple comparison test

| Col. stats | A |
|---|---|
| | Normality |
| | Y |
| Number of values | 12 |
| | |
| D'Agostino & Pearson normality test | |
| K2 | 4.933 |
| P value | 0.0849 |
| Passed normality test (alpha=0.05)? | Yes |
| P value summary | ns |

| 1way ANOVA Multiple comparisons | | | | | |
|---|---|---|---|---|---|
| Number of families | 1 | | | | |
| Number of comparisons per family | 3 | | | | |
| Alpha | 0.05 | | | | |
| | | | | | |
| Tukey's multiple comparisons test | Mean Diff. | 95.00% CI of diff. | Significant? | Summary | Adjusted P Value |
| | | | | | |
| PBS-rGm vs. rM5-rGm | -3209 | -5183 to -1235 | Yes | ** | 0.0036 |
| PBS-rGm vs. rGm-rGm | -3398 | -5372 to -1424 | Yes | ** | 0.0025 |
| rM5-rGm vs. rGm-rGm | -188.3 | -2162 to 1786 | No | ns | 0.9618 |

## 5.6 Statistical analysis of Figure 5.6

Panel A: Normality test and Tukey's multiple comparison test

| Col. stats | A |
|---|---|
| | Normality |
| | Y |
| Number of values | 12 |
| | |
| D'Agostino & Pearson normality test | |
| K2 | 4.486 |
| P value | 0.1061 |
| Passed normality test (alpha=0.05)? | Yes |
| P value summary | ns |

| 1way ANOVA Multiple comparisons | | | | | |
|---|---|---|---|---|---|
| Number of families | 1 | | | | |
| Number of comparisons per family | 3 | | | | |
| Alpha | 0.05 | | | | |
| | | | | | |
| Tukey's multiple comparisons test | Mean Diff. | 95.00% CI of diff. | Significant? | Summary | Adjusted P Value |
| | | | | | |
| PBS-rM5 vs. GAS-rM5 | -8715 | -9220 to -8210 | Yes | **** | <0.0001 |
| PBS-rM5 vs. GGS-rM5 | -2843 | -3348 to -2338 | Yes | **** | <0.0001 |
| GAS-rM5 vs. GGS-rM5 | 5873 | 5368 to 6378 | Yes | **** | <0.0001 |

Panel B (short term exp.): Normality test and Tukey's multiple comparison test

| Col. stats | A |
|---|---|
| | Normality |
| | Y |
| Number of values | 12 |
| | |
| D'Agostino & Pearson normality test | |
| K2 | 2.369 |
| P value | 0.3059 |
| Passed normality test (alpha=0.05)? | Yes |
| P value summary | ns |

1way ANOVA
Multiple comparisons

| | | | | | |
|---|---|---|---|---|---|
| Number of families | 1 | | | | |
| Number of comparisons per family | 3 | | | | |
| Alpha | 0.05 | | | | |
| | | | | | |
| Tukey's multiple comparisons test | Mean Diff. | 95.00% CI of diff. | Significant? | Summary | Adjusted P Value |
| | | | | | |
| PBS-rM5 vs. rM5-rM5 | -706.3 | -1008 to -404.5 | Yes | *** | 0.0003 |
| PBS-rM5 vs. rGm-rM5 | -681.8 | -983.6 to -380.1 | Yes | *** | 0.0004 |
| rM5-rM5 vs. rGm-rM5 | 24.43 | -277.3 to 326.2 | No | ns | 0.9723 |

Panel B (long term exp.): Normality test and Tukey's multiple comparison test

| Col. stats | A |
|---|---|
| | Normality |
| | Y |
| Number of values | 12 |
| | |
| D'Agostino & Pearson normality test | |
| K2 | 0.8167 |
| P value | 0.6648 |
| Passed normality test (alpha=0.05)? | Yes |
| P value summary | ns |

1way ANOVA
Multiple comparisons

| | | | | | |
|---|---|---|---|---|---|
| Number of families | 1 | | | | |
| Number of comparisons per family | 3 | | | | |
| Alpha | 0.05 | | | | |
| | | | | | |
| Tukey's multiple comparisons test | Mean Diff. | 95.00% CI of diff. | Significant? | Summary | Adjusted P Value |
| | | | | | |
| PBS-rM5 vs. rM5-rM5 | -3334 | -5408 to -1261 | Yes | ** | 0.0039 |
| PBS-rM5 vs. rGm-rM5 | -2508 | -4582 to -434.1 | Yes | * | 0.0202 |
| rM5-rM5 vs. rGm-rM5 | 826.7 | -1247 to 2900 | No | ns | 0.5304 |

Panel C: Normality test and Tukey's multiple comparison test

| Col. stats | A |
|---|---|
| | Normality |
| | Y |
| Number of values | 12 |
| | |
| D'Agostino & Pearson normality test | |
| K2 | 3.477 |
| P value | 0.1757 |
| Passed normality test (alpha=0.05)? | Yes |
| P value summary | ns |

1way ANOVA
Multiple comparisons

| | | | | | |
|---|---|---|---|---|---|
| Number of families | 1 | | | | |
| Number of comparisons per family | 3 | | | | |
| Alpha | 0.05 | | | | |
| | | | | | |
| Tukey's multiple comparisons test | Mean Diff. | 95.00% CI of diff. | Significant? | Summary | Adjusted P Value |
| | | | | | |
| PBS-rGm vs. GAS-rGm | -4317 | -7700 to -933.8 | Yes | * | 0.0152 |
| PBS-rGm vs. GGS-rGm | -7690 | -11073 to -4307 | Yes | *** | 0.0004 |
| GAS-rGm vs. GGS-rGm | -3373 | -6756 to 9.544 | No | ns | 0.0506 |

Panel D (short term exp.): Normality test and Tukey's multiple comparison test

| Col. stats | A |
|---|---|
| | Normality |
| | Y |
| Number of values | 12 |
| | |
| D'Agostino & Pearson normality test | |
| K2 | 1.379 |
| P value | 0.5019 |
| Passed normality test (alpha=0.05)? | Yes |
| P value summary | ns |

1way ANOVA
Multiple comparisons

| | | | | | |
|---|---|---|---|---|---|
| Number of families | 1 | | | | |
| Number of comparisons per family | 3 | | | | |
| Alpha | 0.05 | | | | |
| | | | | | |
| Tukey's multiple comparisons test | Mean Diff. | 95.00% CI of diff. | Significant? | Summary | Adjusted P Value |
| | | | | | |
| PBS-rGm vs. rM5-rGm | -938 | -1834 to -41.97 | Yes | * | 0.0408 |
| PBS-rGm vs. rGm-rGm | -1568 | -2464 to -672.4 | Yes | ** | 0.0022 |
| rM5-rGm vs. rGm-rGm | -630.5 | -1526 to 265.5 | No | ns | 0.1767 |

Panel D (long term exp.): Normality test and Tukey's multiple comparison test

| Col. stats | A |
|---|---|
| | Normality |
| | Y |
| Number of values | 12 |
| | |
| D'Agostino & Pearson normality test | |
| K2 | 1.053 |
| P value | 0.5908 |
| Passed normality test (alpha=0.05)? | Yes |
| P value summary | ns |

1way ANOVA
Multiple comparisons

| | | | | | |
|---|---|---|---|---|---|
| Number of families | 1 | | | | |
| Number of comparisons per family | 3 | | | | |
| Alpha | 0.05 | | | | |
| | | | | | |
| Tukey's multiple comparisons test | Mean Diff. | 95.00% CI of diff. | Significant? | Summary | Adjusted P Value |
| | | | | | |
| PBS-rGm vs. rM5-rGm | -2042 | -2361 to -1722 | Yes | **** | <0.0001 |
| PBS-rGm vs. rGm-rGm | -2323 | -2642 to -2004 | Yes | **** | <0.0001 |
| rM5-rGm vs. rGm-rGm | -281.1 | -600.4 to 38.24 | No | ns | 0.0841 |

## 5.7 Statistical analysis of Figure 5.7

Panel A: Normality test and Tukey's multiple comparison test

| Col. stats | A |
|---|---|
| | Normality |
| | Y |
| Number of values | 12 |
| | |
| D'Agostino & Pearson normality test | |
| K2 | 2.824 |
| P value | 0.2436 |
| Passed normality test (alpha=0.05)? | Yes |
| P value summary | ns |

1way ANOVA
Multiple comparisons

| | | | | | |
|---|---|---|---|---|---|
| Number of families | 1 | | | | |
| Number of comparisons per family | 3 | | | | |
| Alpha | 0.05 | | | | |
| | | | | | |
| Tukey's multiple comparisons test | Mean Diff. | 95.00% CI of diff. | Significant? | Summary | Adjusted P Value |
| | | | | | |
| PBS-rM5 vs. GAS-rM5 | -9.592 | -13.14 to -6.041 | Yes | **** | <0.0001 |
| PBS-rM5 vs. GGS-rM5 | -8.569 | -12.12 to -5.017 | Yes | *** | 0.0002 |
| GAS-rM5 vs. GGS-rM5 | 1.024 | -2.528 to 4.575 | No | ns | 0.7096 |

Panel B (short term exp.): Normality test and Tukey's multiple comparison test

| Col. stats | A |
|---|---|
| | Normality |
| | Y |
| Number of values | 12 |
| | |
| D'Agostino & Pearson normality test | |
| K2 | 2.043 |
| P value | 0.3601 |
| Passed normality test (alpha=0.05)? | Yes |
| P value summary | ns |

1way ANOVA
Multiple comparisons

| | | | | | |
|---|---|---|---|---|---|
| Number of families | 1 | | | | |
| Number of comparisons per family | 3 | | | | |
| Alpha | 0.05 | | | | |
| | | | | | |
| Tukey's multiple comparisons test | Mean Diff. | 95.00% CI of diff. | Significant? | Summary | Adjusted P Value |
| | | | | | |
| PBS-rM5 vs. rM5-rM5 | -7.479 | -12.52 to -2.433 | Yes | ** | 0.0064 |
| PBS-rM5 vs. rGm-rM5 | -5.982 | -11.03 to -0.9361 | Yes | * | 0.0223 |
| rM5-rM5 vs. rGm-rM5 | 1.497 | -3.548 to 6.543 | No | ns | 0.6957 |

Panel B (long term exp.): Normality test and Tukey's multiple comparison test

| Col. stats | A |
|---|---|
| | Normality |
| | Y |
| Number of values | 12 |
| | |
| D'Agostino & Pearson normality test | |
| K2 | 1.576 |
| P value | 0.4548 |
| Passed normality test (alpha=0.05)? | Yes |
| P value summary | ns |

1way ANOVA
Multiple comparisons

| | | | | | |
|---|---|---|---|---|---|
| Number of families | 1 | | | | |
| Number of comparisons per family | 3 | | | | |
| Alpha | 0.05 | | | | |
| | | | | | |
| Tukey's multiple comparisons test | Mean Diff. | 95.00% CI of diff. | Significant? | Summary | Adjusted P Value |
| | | | | | |
| PBS-rM5 vs. rM5-rM5 | -15.66 | -24.25 to -7.064 | Yes | ** | 0.0017 |
| PBS-rM5 vs. rGm-rM5 | -9.63 | -18.22 to -1.039 | Yes | * | 0.0295 |
| rM5-rM5 vs. rGm-rM5 | 6.026 | -2.566 to 14.62 | No | ns | 0.1784 |

Panel C: Normality test and Tukey's multiple comparison test

| Col. stats | A |
|---|---|
| | Normality |
| | Y |
| Number of values | 12 |
| | |
| D'Agostino & Pearson normality test | |
| K2 | 3.493 |
| P value | 0.1744 |
| Passed normality test (alpha=0.05)? | Yes |
| P value summary | ns |

1way ANOVA
Multiple comparisons

| | | | | | |
|---|---|---|---|---|---|
| Number of families | 1 | | | | |
| Number of comparisons per family | 3 | | | | |
| Alpha | 0.05 | | | | |
| | | | | | |
| Tukey's multiple comparisons test | Mean Diff. | 95.00% CI of diff. | Significant? | Summary | Adjusted P Value |
| | | | | | |
| PBS-rGm vs. GAS-rGm | -8.139 | -12.09 to -4.184 | Yes | *** | 0.0007 |
| PBS-rGm vs. GGS-rGm | -8.532 | -12.49 to -4.577 | Yes | *** | 0.0005 |
| GAS-rGm vs. GGS-rGm | -0.3934 | -4.348 to 3.561 | No | ns | 0.9586 |

Panel D (short term exp.): Normality test and Tukey's multiple comparison test

| Col. stats | A |
|---|---|
| | Normality |
| | Y |
| Number of values | 12 |
| | |
| D'Agostino & Pearson normality test | |
| K2 | 1.576 |
| P value | 0.4548 |
| Passed normality test (alpha=0.05)? | Yes |
| P value summary | ns |

1way ANOVA
Multiple comparisons

| | | | | | |
|---|---|---|---|---|---|
| Number of families | 1 | | | | |
| Number of comparisons per family | 3 | | | | |
| Alpha | 0.05 | | | | |
| | | | | | |
| Tukey's multiple comparisons test | Mean Diff. | 95.00% CI of diff. | Significant? | Summary | Adjusted P Value |
| | | | | | |
| PBS-rGm vs. rM5-rGm | -5.117 | -9.855 to -0.3795 | Yes | * | 0.0353 |
| PBS-rGm vs. rGm-rGm | -7.237 | -11.98 to -2.499 | Yes | ** | 0.0053 |
| rM5-rGm vs. rGm-rGm | -2.12 | -6.858 to 2.618 | No | ns | 0.4562 |

Panel D (long term exp.): Normality test and Tukey's multiple comparison test

| Col. stats | A |
|---|---|
| | Normality |
| | Y |
| Number of values | 12 |
| | |
| D'Agostino & Pearson normality test | |
| K2 | 4.2 |
| P value | 0.1225 |
| Passed normality test (alpha=0.05)? | Yes |
| P value summary | ns |

| 1way ANOVA<br>Multiple comparisons | | | | | |
|---|---|---|---|---|---|
| Number of families | 1 | | | | |
| Number of comparisons per family | 3 | | | | |
| Alpha | 0.05 | | | | |
| | | | | | |
| Tukey's multiple comparisons test | Mean Diff. | 95.00% CI of diff. | Significant? | Summary | Adjusted P Value |
| | | | | | |
| PBS-rGm vs. rM5-rGm | -8.878 | -12.48 to -5.278 | Yes | *** | 0.0002 |
| PBS-rGm vs. rGm-rGm | -24.15 | -27.75 to -20.55 | Yes | **** | <0.0001 |
| rM5-rGm vs. rGm-rGm | -15.27 | -18.87 to -11.67 | Yes | **** | <0.0001 |

## 5.8 Statistical analysis of Supplementary Figure 5.1

Panel A (short term exp.): Normality test and Tukey's multiple comparison test

| Col. stats | A |
|---|---|
| | Normality A |
| | Y |
| Number of values | 15 |
| | |
| D'Agostino & Pearson normality test | |
| K2 | 3.942 |
| P value | 0.1393 |
| Passed normality test (alpha=0.05)? | Yes |
| P value summary | ns |

| 1way ANOVA<br>Multiple comparisons | | | | |
|---|---|---|---|---|
| Number of families | 1 | | | |
| Number of comparisons per family | 3 | | | |
| Alpha | 0.05 | | | |
| | | | | |
| Tukey's multiple comparisons test | Mean Diff. | 95.00% CI of diff. | Significant? | Summary |
| | | | | |
| PBS vs. rM5 | -1.626 | -1.786 to -1.465 | Yes | **** |
| PBS vs. rGGSm | -0.6021 | -0.7627 to -0.4414 | Yes | **** |
| rM5 vs. rGGSm | 1.024 | 0.8629 to 1.184 | Yes | **** |

Panel A (long term exp.): Normality test and Tukey's multiple comparison test

| Col. stats | A |
|---|---|
| | Normality A |
| | Y |
| Number of values | 15 |
| | |
| D'Agostino & Pearson normality test | |
| K2 | 1.304 |
| P value | 0.5210 |
| Passed normality test (alpha=0.05)? | Yes |
| P value summary | ns |

| 1way ANOVA<br>Multiple comparisons | | | | |
|---|---|---|---|---|
| Number of families | 1 | | | |
| Number of comparisons per family | 3 | | | |
| Alpha | 0.05 | | | |
| | | | | |
| Tukey's multiple comparisons test | Mean Diff. | 95.00% CI of diff. | Significant? | Summary |
| | | | | |
| PBS vs. rM5 | -2.107 | -2.708 to -1.506 | Yes | **** |
| PBS vs. rGGSm | -1.565 | -2.166 to -0.9643 | Yes | **** |
| rM5 vs. rGGSm | 0.5419 | -0.05914 to 1.143 | No | ns |

Panel B (short term exp.): Normality test and Tukey's multiple comparison test

| Col. stats | A |
|---|---|
| | Normality G |
| | Y |
| Number of values | 15 |
| | |
| D'Agostino & Pearson normality test | |
| K2 | 0.8927 |
| P value | 0.6400 |
| Passed normality test (alpha=0.05)? | Yes |
| P value summary | ns |

| 1way ANOVA<br>Multiple comparisons | | | | |
|---|---|---|---|---|
| Number of families | 1 | | | |
| Number of comparisons per family | 3 | | | |
| Alpha | 0.05 | | | |
| | | | | |
| Tukey's multiple comparisons test | Mean Diff. | 95.00% CI of diff. | Significant? | Summary |
| | | | | |
| PBS vs. rM5 | -0.8429 | -1.164 to -0.5216 | Yes | **** |
| PBS vs. rGGSm | -0.6021 | -0.9233 to -0.2808 | Yes | *** |
| rM5 vs. rGGSm | 0.2408 | -0.08042 to 0.5621 | No | ns |

Panel B (long term exp.): Normality test and Tukey's multiple comparison test

| Col. stats | A |
|---|---|
| | Normality G |
| | Y |
| Number of values | 15 |
| | |
| D'Agostino & Pearson normality test | |
| K2 | 5.768 |
| P value | 0.0559 |
| Passed normality test (alpha=0.05)? | Yes |
| P value summary | ns |

| 1way ANOVA<br>Multiple comparisons | | | | |
|---|---|---|---|---|
| Number of families | 1 | | | |
| Number of comparisons per family | 3 | | | |
| Alpha | 0.05 | | | |
| | | | | |
| Tukey's multiple comparisons test | Mean Diff. | 95.00% CI of diff. | Significant? | Summary |
| | | | | |
| PBS vs. rM5 | -1.565 | -2.106 to -1.025 | Yes | **** |
| PBS vs. rGGSm | -1.264 | -1.805 to -0.7236 | Yes | *** |
| rM5 vs. rGGSm | 0.301 | -0.2397 to 0.8417 | No | ns |

Panel C (short term exp.): Normality test and Tukey's multiple comparison test

| Col. stats | A |
|---|---|
| | Normality A |
| | Y |
| Number of values | 15 |
| | |
| D'Agostino & Pearson normality test | |
| K2 | 5.48 |
| P value | 0.0646 |
| Passed normality test (alpha=0.05)? | Yes |
| P value summary | ns |

1way ANOVA
Multiple comparisons

| | | | | | | |
|---|---|---|---|---|---|---|
| Number of families | 1 | | | | | |
| Number of comparisons per family | 3 | | | | | |
| Alpha | 0.05 | | | | | |
| | | | | | | |
| Tukey's multiple comparisons test | Mean Diff. | 95.00% CI of diff. | Significant? | Summary | Adjusted P Value | |
| | | | | | | |
| PBS vs. rM5 | -3.492 | -3.983 to -3.001 | Yes | **** | <0.0001 | |
| PBS vs. rGGSm | -3.311 | -3.802 to -2.821 | Yes | **** | <0.0001 | |
| rM5 vs. rGGSm | 0.1806 | -0.3101 to 0.6713 | No | ns | 0.6015 | |

Panel C (long term exp.): Normality test and Tukey's multiple comparison test

| Col. stats | A |
|---|---|
| | Normality A |
| | Y |
| Number of values | 15 |
| | |
| D'Agostino & Pearson normality test | |
| K2 | 4.095 |
| P value | 0.1290 |
| Passed normality test (alpha=0.05)? | Yes |
| P value summary | ns |

1way ANOVA
Multiple comparisons

| | | | | |
|---|---|---|---|---|
| Number of families | 1 | | | |
| Number of comparisons per family | 3 | | | |
| Alpha | 0.05 | | | |
| | | | | |
| Tukey's multiple comparisons test | Mean Diff. | 95.00% CI of diff. | Significant? | Summary |
| | | | | |
| PBS vs. rM5 | -2.167 | -2.582 to -1.753 | Yes | **** |
| PBS vs. rGGSm | -2.228 | -2.642 to -1.813 | Yes | **** |
| rM5 vs. rGGSm | -0.06021 | -0.4749 to 0.3545 | No | ns |

Panel D (short term exp.): Normality test and Tukey's multiple comparison test

| Col. stats | A |
|---|---|
| | Normality G |
| | Y |
| Number of values | 15 |
| | |
| D'Agostino & Pearson normality test | |
| K2 | 5.382 |
| P value | 0.0678 |
| Passed normality test (alpha=0.05)? | Yes |
| P value summary | ns |

1way ANOVA
Multiple comparisons

| | | | | | |
|---|---|---|---|---|---|
| Number of families | 1 | | | | |
| Number of comparisons per family | 3 | | | | |
| Alpha | 0.05 | | | | |
| | | | | | |
| Tukey's multiple comparisons test | Mean Diff. | 95.00% CI of diff. | Significant? | Summary | Adjusted P Value |
| | | | | | |
| PBS vs. rM5 | -3.251 | -3.686 to -2.816 | Yes | **** | <0.0001 |
| PBS vs. rGGSm | -3.552 | -3.987 to -3.117 | Yes | **** | <0.0001 |
| rM5 vs. rGGSm | -0.301 | -0.736 to 0.1339 | No | ns | 0.1967 |

Panel D (long term exp.): Normality test and Tukey's multiple comparison test

| Col. stats | A |
|---|---|
| | Normality G |
| | Y |
| Number of values | 15 |
| | |
| D'Agostino & Pearson normality test | |
| K2 | 5.062 |
| P value | 0.0796 |
| Passed normality test (alpha=0.05)? | Yes |
| P value summary | ns |

1way ANOVA
Multiple comparisons

| | | | | |
|---|---|---|---|---|
| Number of families | 1 | | | |
| Number of comparisons per family | 3 | | | |
| Alpha | 0.05 | | | |
| | | | | |
| Tukey's multiple comparisons test | Mean Diff. | 95.00% CI of diff. | Significant? | Summary |
| | | | | |
| PBS vs. rM5 | -2.408 | -2.812 to -2.004 | Yes | **** |
| PBS vs. rGGSm | -2.769 | -3.174 to -2.365 | Yes | **** |
| rM5 vs. rGGSm | -0.3612 | -0.7655 to 0.04299 | No | ns |

## 5.9 Statistical analysis of Supplementary Figure 5.2

Panel A (short term exp.): Normality test and Tukey's multiple comparison test

| Col. stats | A |
|---|---|
| | Normality CM |
| | Y |
| Number of values | 15 |
| | |
| D'Agostino & Pearson normality test | |
| K2 | 5.621 |
| P value | 0.0602 |
| Passed normality test (alpha=0.05)? | Yes |
| P value summary | ns |

1way ANOVA
Multiple comparisons

| | | | | | |
|---|---|---|---|---|---|
| Number of families | 1 | | | | |
| Number of comparisons per family | 3 | | | | |
| Alpha | 0.05 | | | | |
| | | | | | |
| Tukey's multiple comparisons test | Mean Diff. | 95.00% CI of diff. | Significant? | Summary | Adjusted P Value |
| | | | | | |
| PBS vs. rM5 | -0.7398 | -1.237 to -0.2427 | Yes | ** | 0.0049 |
| PBS vs. rGGSm | -0.6471 | -1.144 to -0.15 | Yes | * | 0.0119 |
| rM5 vs. rGGSm | 0.0927 | -0.4044 to 0.5898 | No | ns | 0.8738 |

Panel A (long term exp.): Normality test and Tukey's multiple comparison test

| Col. stats | A |
|---|---|
| | Normality CM |
| | Y |
| Number of values | 15 |
| | |
| D'Agostino & Pearson normality test | |
| K2 | 2.898 |
| P value | 0.2348 |
| Passed normality test (alpha=0.05)? | Yes |
| P value summary | ns |

| 1way ANOVA<br>Multiple comparisons | | | | |
|---|---|---|---|---|
| Number of families | 1 | | | |
| Number of comparisons per family | 3 | | | |
| Alpha | 0.05 | | | |
| | | | | |
| Tukey's multiple comparisons test | Mean Diff. | 95.00% CI of diff. | Significant? | Summary |
| | | | | |
| PBS vs. rM5 | -1.17 | -1.861 to -0.4793 | Yes | ** |
| PBS vs. rGGSm | -0.4916 | -1.183 to 0.1995 | No | ns |
| rM5 vs. rGGSm | 0.6788 | -0.01225 to 1.37 | No | ns |

Panel B (short term exp.): Normality test and Tukey's multiple comparison test

| Col. stats | A |
|---|---|
| | Normality Col I |
| | Y |
| Number of values | 15 |
| | |
| D'Agostino & Pearson normality test | |
| K2 | 1.259 |
| P value | 0.5329 |
| Passed normality test (alpha=0.05)? | Yes |
| P value summary | ns |

| 1way ANOVA<br>Multiple comparisons | | | | | |
|---|---|---|---|---|---|
| Number of families | 1 | | | | |
| Number of comparisons per family | 3 | | | | |
| Alpha | 0.05 | | | | |
| | | | | | |
| Tukey's multiple comparisons test | Mean Diff. | 95.00% CI of diff. | Significant? | Summary | Adjusted P Value |
| | | | | | |
| PBS vs. rM5 | -0.243 | -0.3771 to -0.1089 | Yes | ** | 0.0011 |
| PBS vs. rGGSm | -0.155 | -0.2891 to -0.02087 | Yes | * | 0.0239 |
| rM5 vs. rGGSm | 0.088 | -0.04613 to 0.2221 | No | ns | 0.2275 |

Panel B (long term exp.): Normality test and Kruskal-Wallis test

| Col. stats | A |
|---|---|
| | Normality Col I |
| | Y |
| Number of values | 15 |
| | |
| D'Agostino & Pearson normality test | |
| K2 | 9.646 |
| P value | 0.0080 |
| Passed normality test (alpha=0.05)? | No |
| P value summary | ** |

| 1way ANOVA<br>Multiple comparisons | | | | |
|---|---|---|---|---|
| Number of families | 1 | | | |
| Number of comparisons per family | 3 | | | |
| Alpha | 0.05 | | | |
| | | | | |
| Dunn's multiple comparisons test | Mean rank diff. | Significant? | Summary | Adjusted P Value |
| | | | | |
| PBS vs. rM5 | -0.8 | No | ns | >0.9999 |
| PBS vs. rGGSm | -5.2 | No | ns | 0.1980 |
| rM5 vs. rGGSm | -4.4 | No | ns | 0.3594 |

## 5.10 Statistical analysis of Supplementary Figure 5.3

Panel A (short term exp.): Normality test and Tukey's multiple comparison test

| Col. stats | A |
|---|---|
| | Normality rM5 |
| | Y |
| Number of values | 14 |
| | |
| D'Agostino & Pearson normality test | |
| K2 | 1.378 |
| P value | 0.5020 |
| Passed normality test (alpha=0.05)? | Yes |
| P value summary | ns |

| 1way ANOVA<br>Multiple comparisons | | | | |
|---|---|---|---|---|
| Number of families | 1 | | | |
| Number of comparisons per family | 2 | | | |
| Alpha | 0.05 | | | |
| | | | | |
| Dunnett's multiple comparisons test | Mean Diff. | 95.00% CI of diff. | Significant? | Summary |
| | | | | |
| PBS vs. rM5 | -3.472 | -6.327 to -0.617 | Yes | * |
| PBS vs. rGGSm | -3.188 | -6.043 to -0.3327 | Yes | * |

Panel A (long term exp.): Normality test and Tukey's multiple comparison test

| Col. stats | A |
|---|---|
| | Normality rM5 |
| | Y |
| Number of values | 15 |
| | |
| D'Agostino & Pearson normality test | |
| K2 | 5.193 |
| P value | 0.0746 |
| Passed normality test (alpha=0.05)? | Yes |
| P value summary | ns |

| 1way ANOVA<br>Multiple comparisons | | | | |
|---|---|---|---|---|
| Number of families | 1 | | | |
| Number of comparisons per family | 2 | | | |
| Alpha | 0.05 | | | |
| | | | | |
| Dunnett's multiple comparisons test | Mean Diff. | 95.00% CI of diff. | Significant? | Summary |
| | | | | |
| PBS vs. rM5 | -12.06 | -18.18 to -5.945 | Yes | *** |
| PBS vs. rGGSm | -2.936 | -9.055 to 3.183 | No | ns |

Panel B (short term exp.): Normality test and Tukey's multiple comparison test

| Col. stats | A |
|---|---|
| | Normality Stg |
| | Y |
| 1 Number of values | 14 |
| 2 | |
| 3 D'Agostino & Pearson normality test | |
| 4 K2 | 4.067 |
| 5 P value | 0.1309 |
| 6 Passed normality test (alpha=0.05)? | Yes |
| 7 P value summary | ns |

| 1way ANOVA Multiple comparisons | | | | |
|---|---|---|---|---|
| 1 Number of families | 1 | | | |
| 2 Number of comparisons per family | 2 | | | |
| 3 Alpha | 0.05 | | | |
| 4 | | | | |
| 5 Dunnett's multiple comparisons test | Mean Diff. | 95.00% CI of diff. | Significant? | Summary |
| 6 | | | | |
| 7 PBS vs. rM5 | -2.765 | -4.676 to -0.8539 | Yes | ** |
| 8 PBS vs. rGGSm | -3.086 | -4.997 to -1.175 | Yes | ** |

Panel B (long term exp.): Normality test and Kruskal-Wallis test

| Col. stats | A |
|---|---|
| | Normality Stg |
| | Y |
| 1 Number of values | 15 |
| 2 | |
| 3 D'Agostino & Pearson normality test | |
| 4 K2 | 8.116 |
| 5 P value | 0.0173 |
| 6 Passed normality test (alpha=0.05)? | No |
| 7 P value summary | * |

| 1way ANOVA Multiple comparisons | | | | |
|---|---|---|---|---|
| 1 Number of families | 1 | | | |
| 2 Number of comparisons per family | 3 | | | |
| 3 Alpha | 0.05 | | | |
| 4 | | | | |
| 5 Dunn's multiple comparisons test | Mean rank diff. | Significant? | Summary | Adjusted P Value |
| 6 | | | | |
| 7 PBS vs. rM5 | -9.2 | Yes | ** | 0.0034 |
| 8 PBS vs. rGGSm | -5.8 | No | ns | 0.1209 |
| 9 rM5 vs. rGGSm | 3.4 | No | ns | 0.6880 |

## APPENDIX 6

## SUPPLEMENTARY FIGURES AND STATISTICAL ANALYSIS OF CHAPTER 6

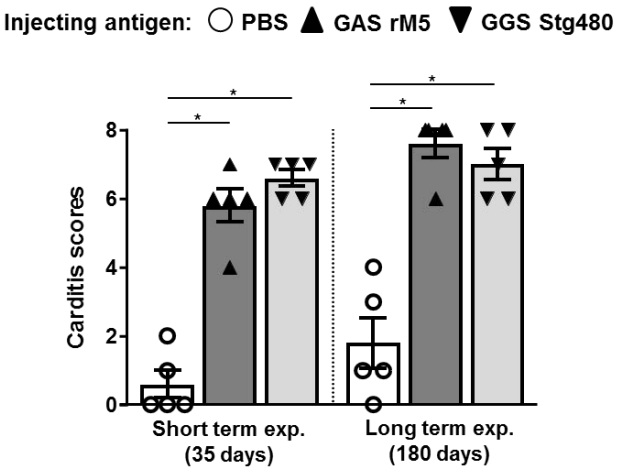


**Supplementary Figure 6.1** GGS and GAS induce identical histological changes in heart tissues. Higher carditis scores were determined in Lewis rats injected with M-proteins of GGS (n=5) and GAS (n=5) following 35 days (short term exp.) and 180 days (long term exp.) of priming injection compared to PBS injected control rats (n=5). Error bars represent standard errors of the mean (SEM). Statistical difference by 1-way ANOVA with Tukey's post hoc multiple comparison test; *p<0.0001.

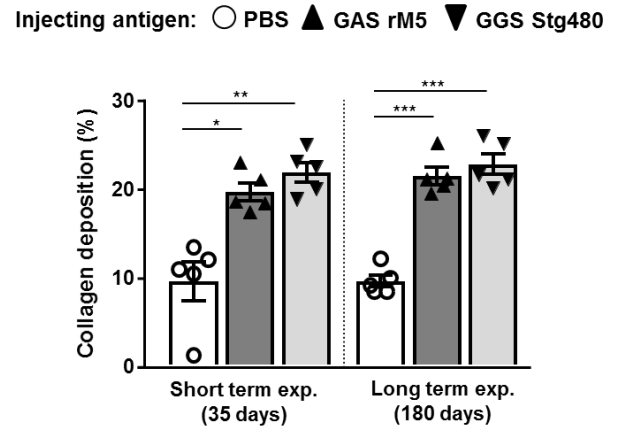


**Supplementary Figure 6.2** GGS and GAS M-proteins induce collagen deposition in the mitral valve and myocardium. Extensive collagen deposition was demonstrated in Lewis rats injected with M-proteins of GGS (n=5) and GAS (n=5) following 35 days (short term exp.) and 180 days (long term exp.) of priming injection compared to PBS injected control rats (n=5). Error bars represent standard errors of the mean (SEM). Statistical difference by 1-way ANOVA with Tukey's post hoc multiple comparison test; *p<0.01, **p<0.001, ***p<0.0001.

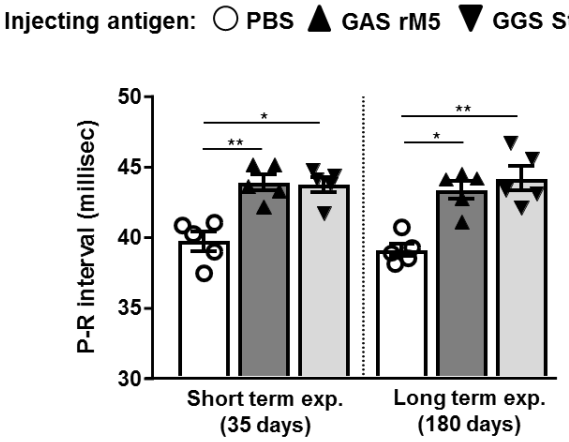


**Supplementary Figure 6.3** Electrocardiographic changes demonstrate cardiac dysfunction following exposure to GAS and GGS. Prolongation of P-R interval in rats injected with GAS rM5 (n=5) and GGS Stg480 (n=5) was observed following 35 days (short term exp.) and 180 days (long term exp.) of priming injection compared to the PBS injected control rats (n=5). Error bars represent standard errors of the mean (SEM). Statistical difference by 1-way ANOVA with Tukey's post hoc multiple comparison test; *p<0.01, **p<0.001.

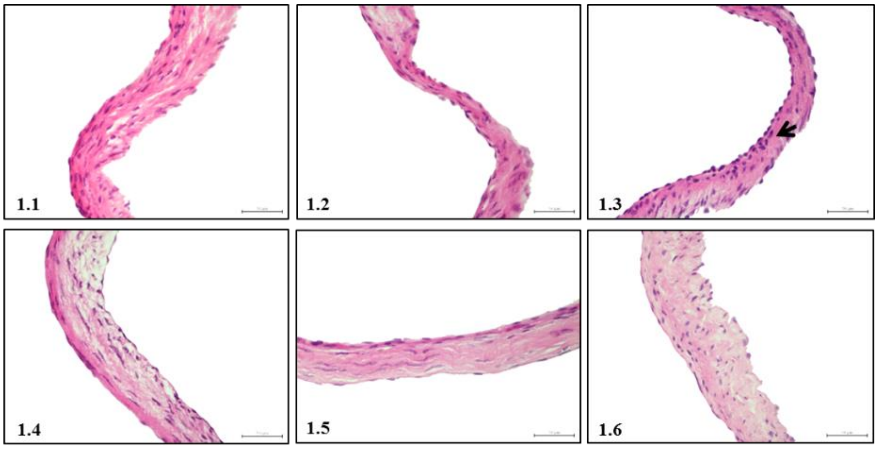


**Supplementary Figure 6.4A** H&E stained sections of mitral valves from rats injected with PBS (homologous boost short term exp., 60 days). Magnifications 400×. Arrow (→) indicates inflammatory focus.

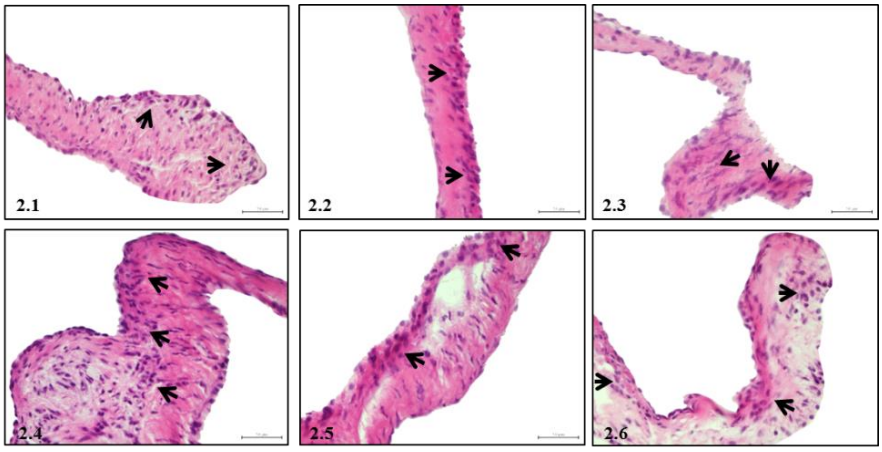


**Supplementary Figure 6.4B** H&E stained sections of mitral valves from rats injected with whole-killed GAS M5 (homologous boost short term exp., 60 days). Magnifications 400×. Arrows (→) indicate inflammatory foci.

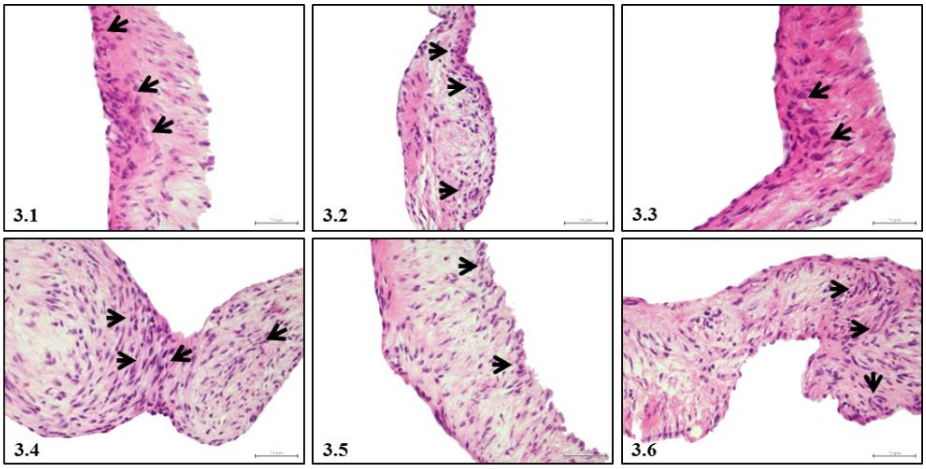


**Supplementary Figure 6.4C** H&E stained sections of mitral valves from rats injected with whole-killed GGS NS3396 (homologous boost short term exp., 60 days). Magnifications 400×. Arrows (→) indicate inflammatory foci.

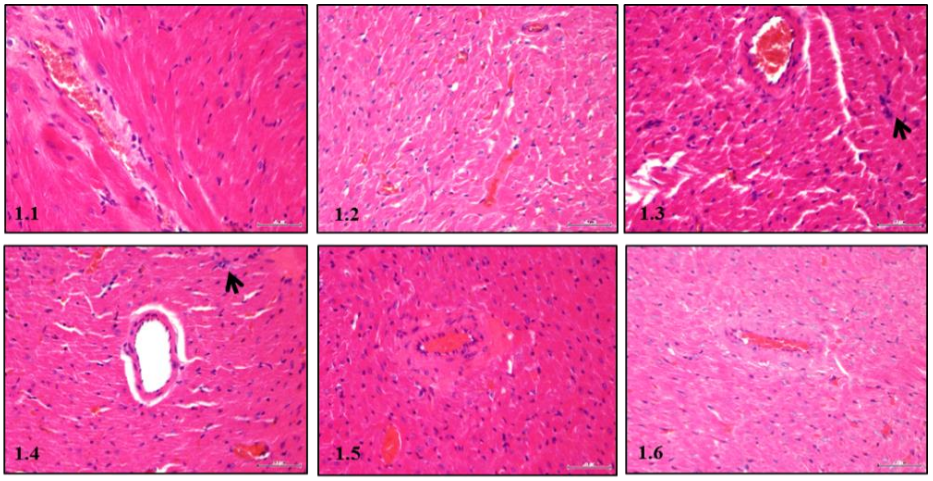


**Supplementary Figure 6.4D** H&E stained sections of myocardium from rats injected with PBS (homologous boost short term exp., 60 days). Magnifications 400×. Arrow (→) indicates inflammatory focus.

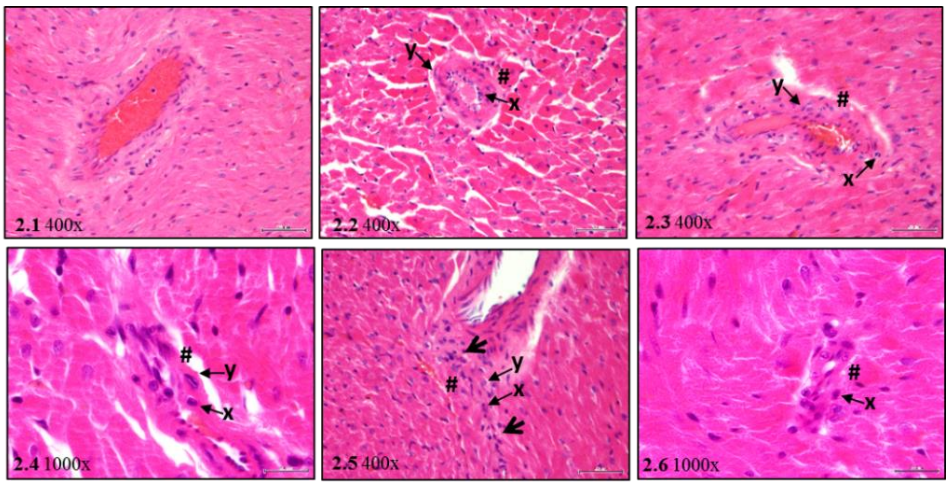


**Supplementary Figure 6.4E** H&E stained sections of myocardium from rats injected with whole-killed GAS M5 (homologous boost short term exp., 60 days). Magnifications as indicated. 'Aschoff nodule like' structure indicated by asterisk (#), x: Anitschkow like cells, y: Aschoff like cells. Arrows (→) indicate inflammatory foci.

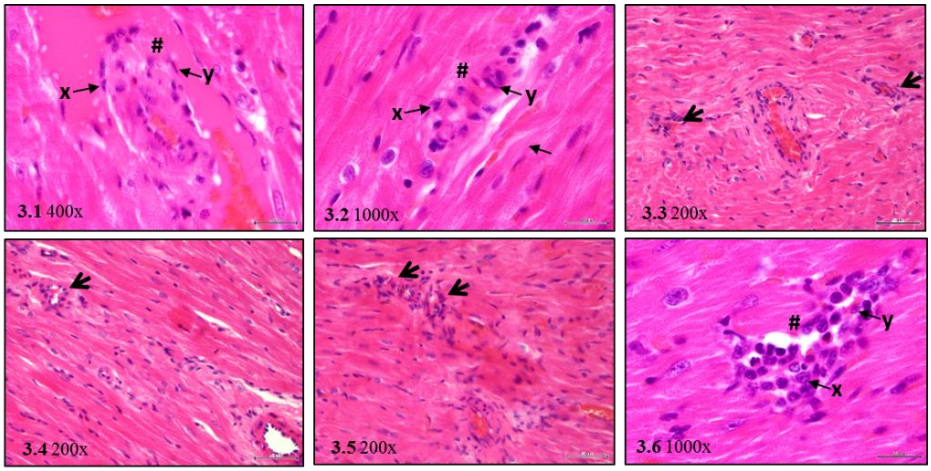


**Supplementary Figure 6.4F** H&E stained sections of myocardium from rats injected with whole-killed GGS NS3396 (homologous boost short term exp., 60 days). Magnifications as indicated. 'Aschoff nodule like' structure indicated by asterisk (#), x: Anitschkow like cells, y: Aschoff like cells. Arrows (→) indicate inflammatory foci.

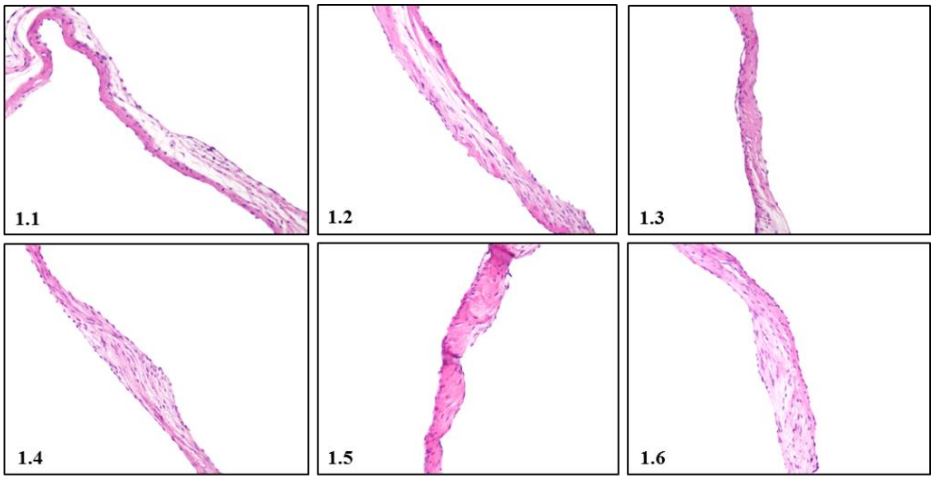


**Supplementary Figure 6.5A** H&E stained sections of mitral valves from rats injected with PBS (homologous boost long term exp., 240 days). Magnifications 200×. Arrow (→) indicates inflammatory focus.

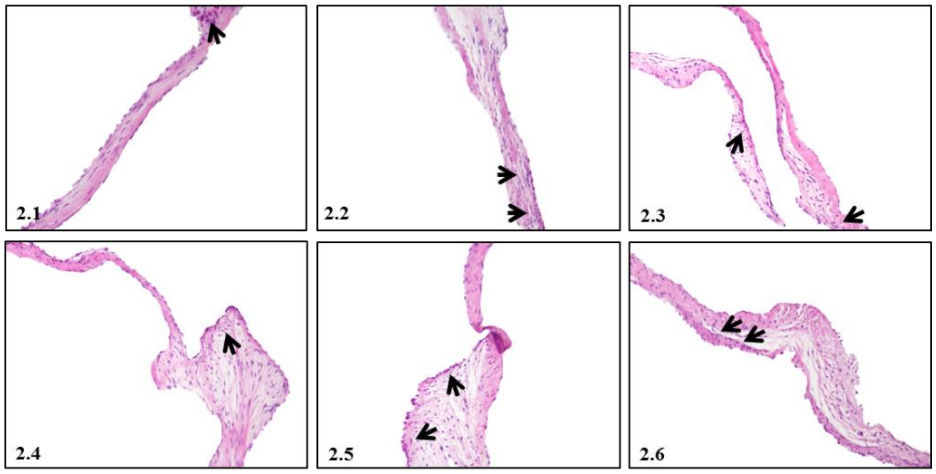


**Supplementary Figure 6.5B** H&E stained sections of mitral valves from rats injected with whole-killed GAS M5 (homologous boost short term exp., 240 days). Magnifications 200×. Arrows (→) indicate inflammatory foci.

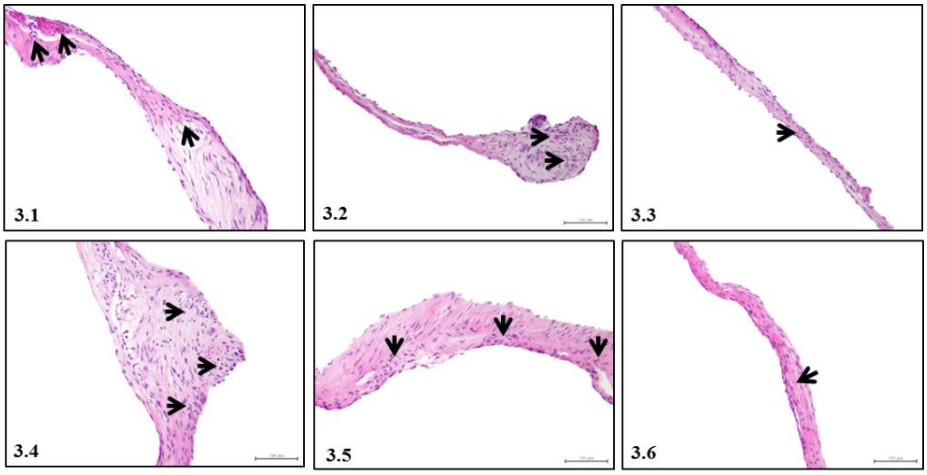


**Supplementary Figure 6.5C** H&E stained sections of mitral valves from rats injected with whole-killed GGS NS3396 (homologous boost long term exp., 240 days). Magnifications 200×. Arrows (→) indicate inflammatory foci.

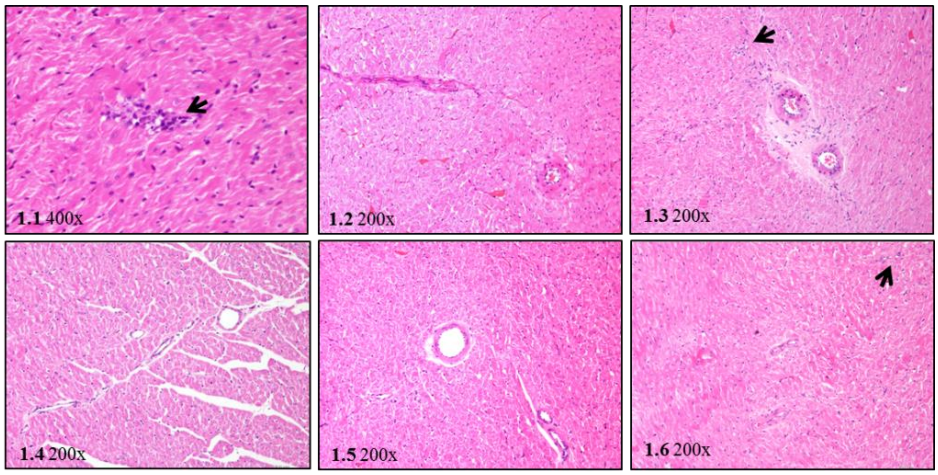


**Supplementary Figure 6.5D** H&E stained sections of myocardium from rats injected with PBS (homologous boost long term exp., 240 days). Magnifications as indicated. Arrows (→) indicate inflammatory foci.

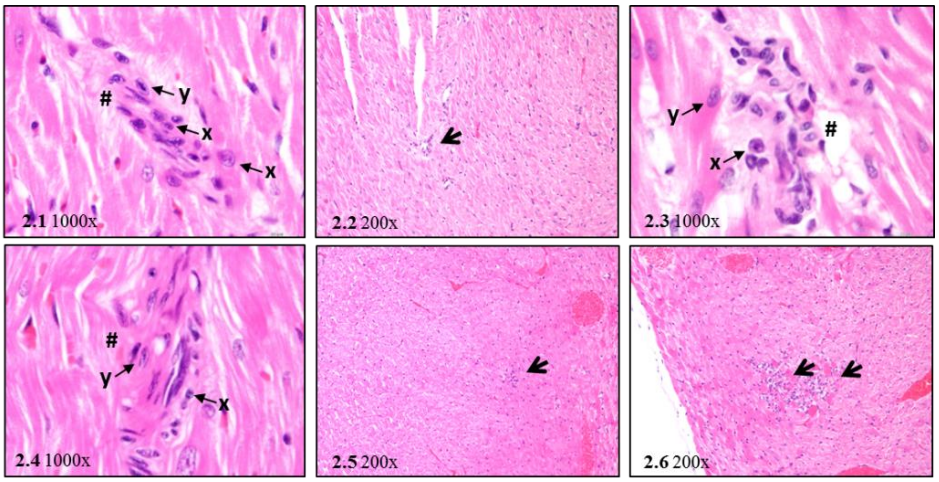


**Supplementary Figure 6.5E** H&E stained sections of myocardium from rats injected with whole-killed GAS M5 (homologous boost long term exp., 240 days). Magnifications as indicated. 'Aschoff nodule like' structure indicated by asterisk (#), x: Anitschkow like cells, y: Aschoff like cells. Arrows (→) indicate inflammatory foci.

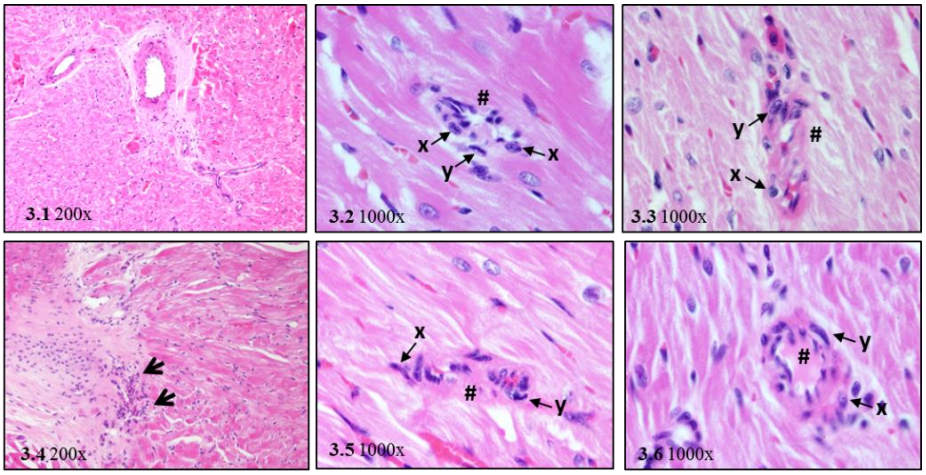


**Supplementary Figure 6.5F** H&E stained sections of myocardium from rats injected with whole-killed GGS NS3396 (homologous boost long term exp., 240 days). Magnifications as indicated. 'Aschoff nodule like' structure indicated by asterisk (#), x: Anitschkow like cells, y: Aschoff like cells. Arrows (→) indicate inflammatory foci.

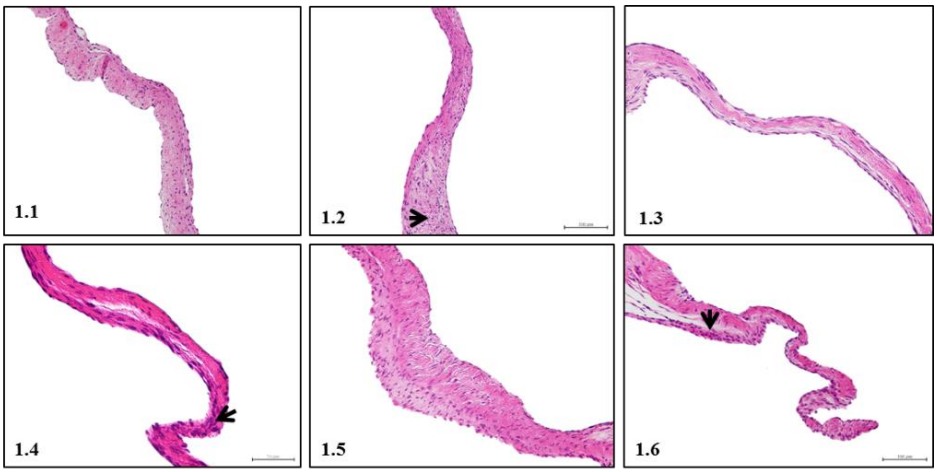


**Supplementary Figure 6.6A** H&E stained sections of mitral valves from rats injected with PBS (homologous boost short term exp., 35 days). Magnifications 200×. Arrows (→) indicate inflammatory foci.

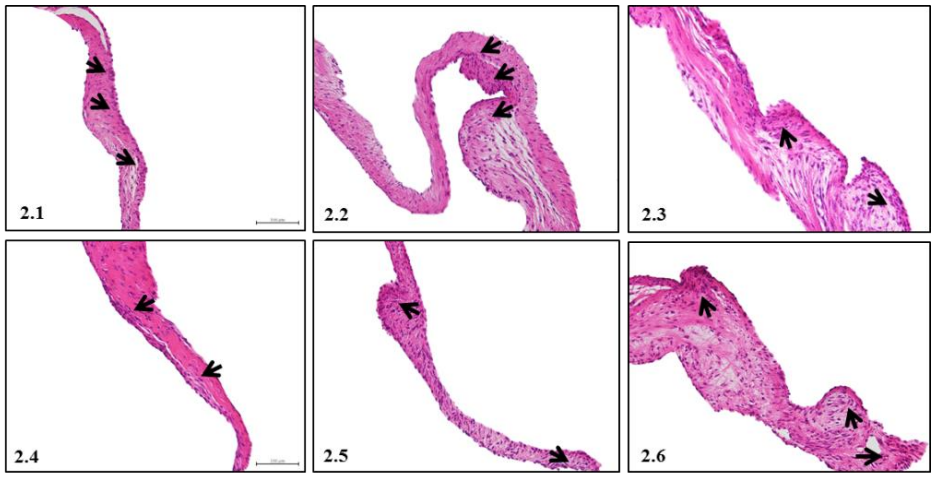


**Supplementary Figure 6.6B** H&E stained sections of mitral valves from rats injected with GAS rM5 (homologous boost short term exp., 35 days). Magnifications 200×. Arrows (→) indicate inflammatory foci.

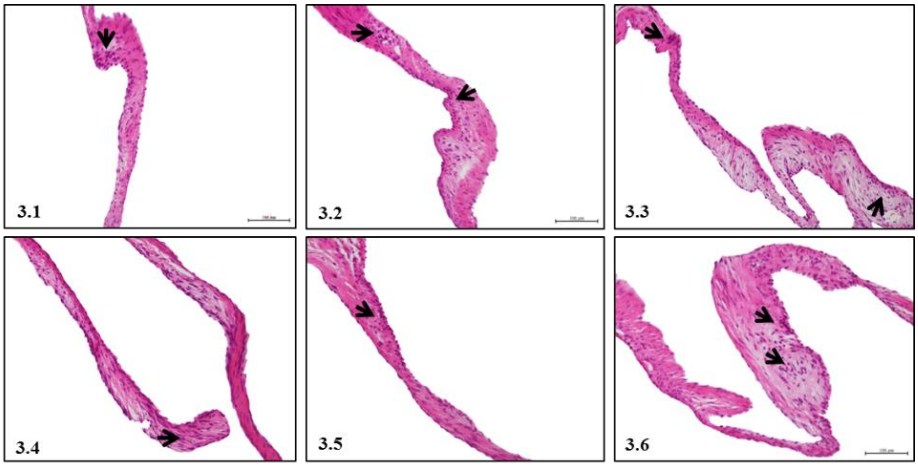


**Supplementary Figure 6.6C** H&E stained sections of mitral valves from rats injected with GGS Stg480 (homologous boost short term exp., 35 days). Magnifications 200×. Arrows (→) indicate inflammatory foci.

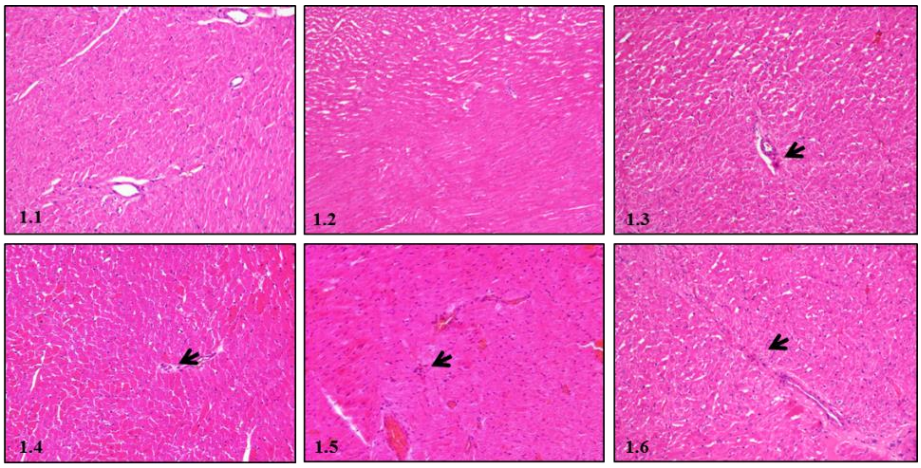


**Supplementary Figure 6.6D** H&E stained sections of myocardium from rats injected with PBS (homologous boost short term exp., 35 days). Magnifications 200×. Arrows (→) indicate inflammatory foci.

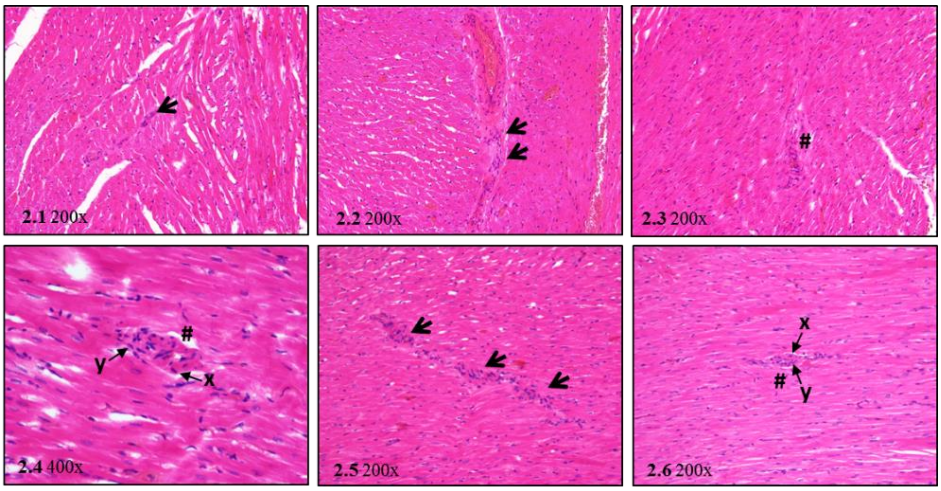


**Supplementary Figure 6.6E** H&E stained sections of myocardium from rats injected with GAS rM5 (homologous boost short term exp., 35 days). Magnifications as indicated. 'Aschoff nodule like' structure indicated by asterisk (#), x: Anitschkow like cells, y: Aschoff like cells. Arrows (→) indicate inflammatory foci.

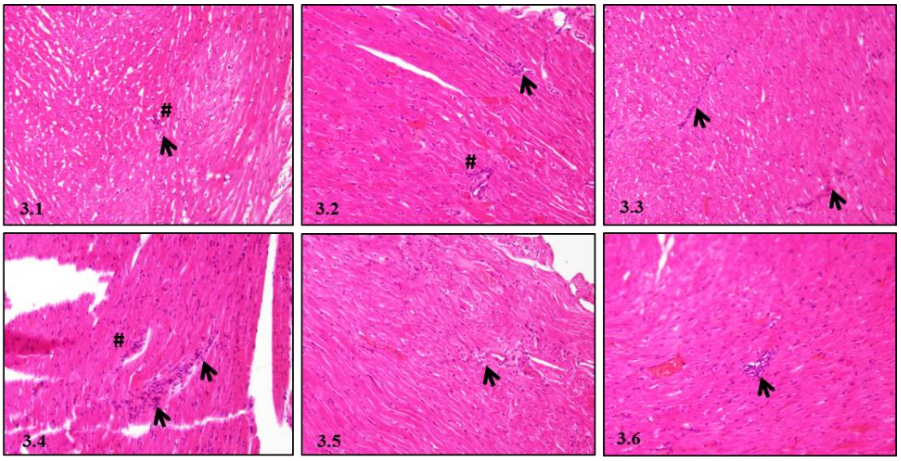


**Supplementary Figure 6.6F** H&E stained sections of myocardium from rats injected with GGS Stg480 (homologous boost short term exp., 35 days). Magnifications 200×. 'Aschoff nodule like' structure indicated by asterisk (#), x: Anitschkow like cells, y: Aschoff like cells. Arrows (→) indicate inflammatory foci.

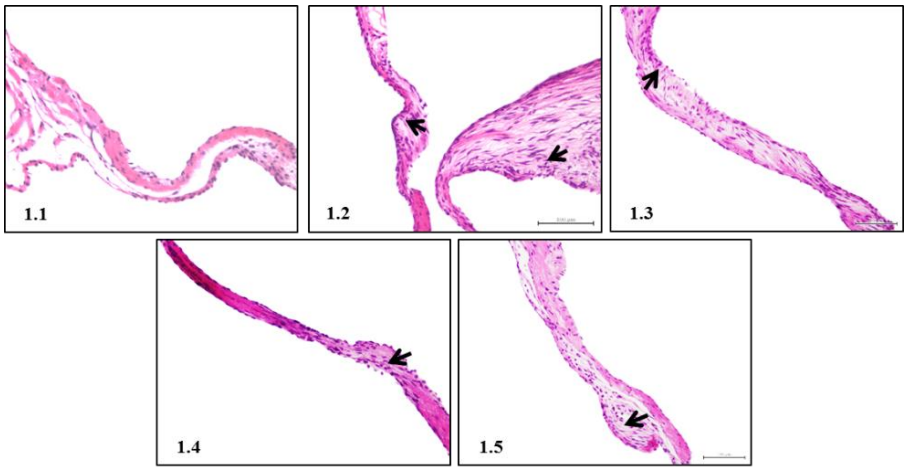


**Supplementary Figure 6.7A** H&E stained sections of mitral valves from rats injected with PBS (homologous boost short term repeat exp., 35 days). Magnifications 200×. Arrows (→) indicate inflammatory foci.

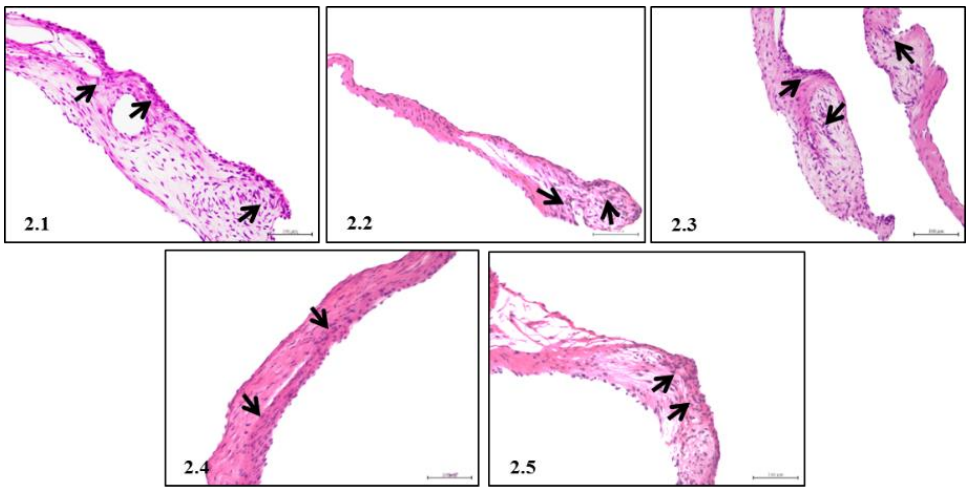


**Supplementary Figure 6.7B** H&E stained sections of mitral valves from rats injected with GAS rM5 (homologous boost short term repeat exp., 35 days). Magnifications 200×. Arrows (→) indicate inflammatory foci.

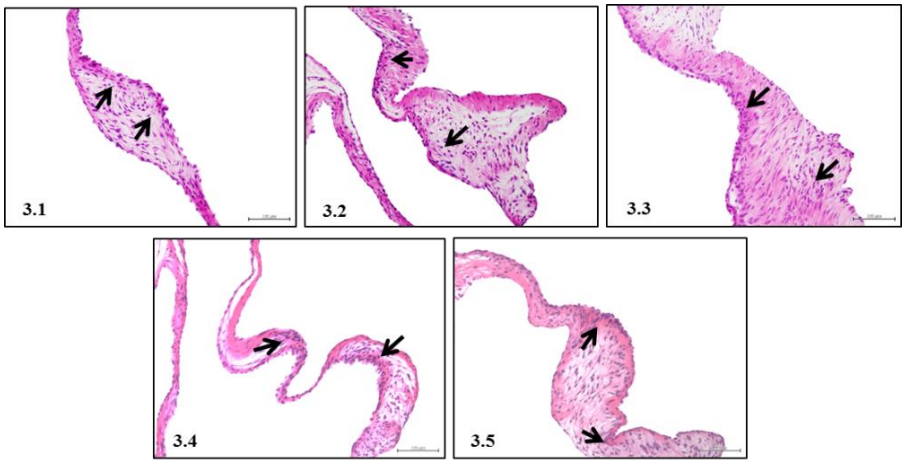


**Supplementary Figure 6.7C** H&E stained sections of mitral valves from rats injected with GGS Stg480 (homologous boost short term repeat exp., 35 days). Magnifications 200×. Arrows (→) indicate inflammatory foci.

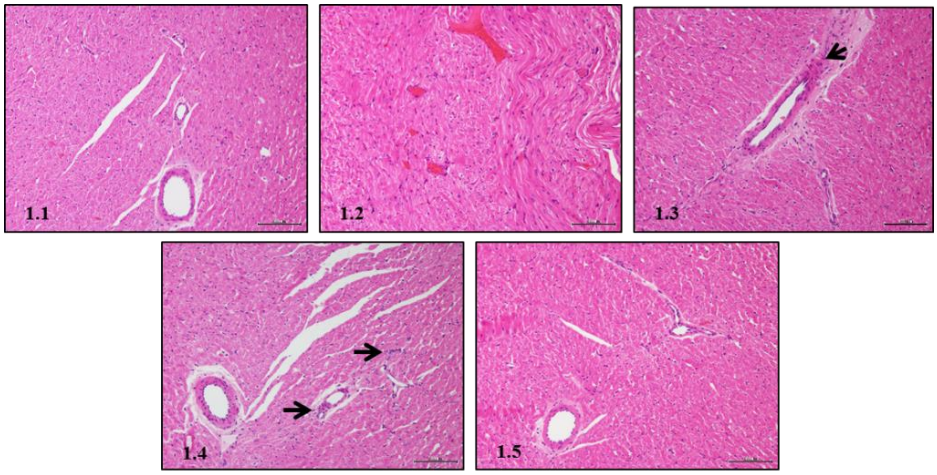


**Supplementary Figure 6.7D** H&E stained sections of myocardium from rats injected with PBS (homologous boost short term repeat exp., 35 days). Magnifications 200×. Arrows (→) indicate inflammatory foci.

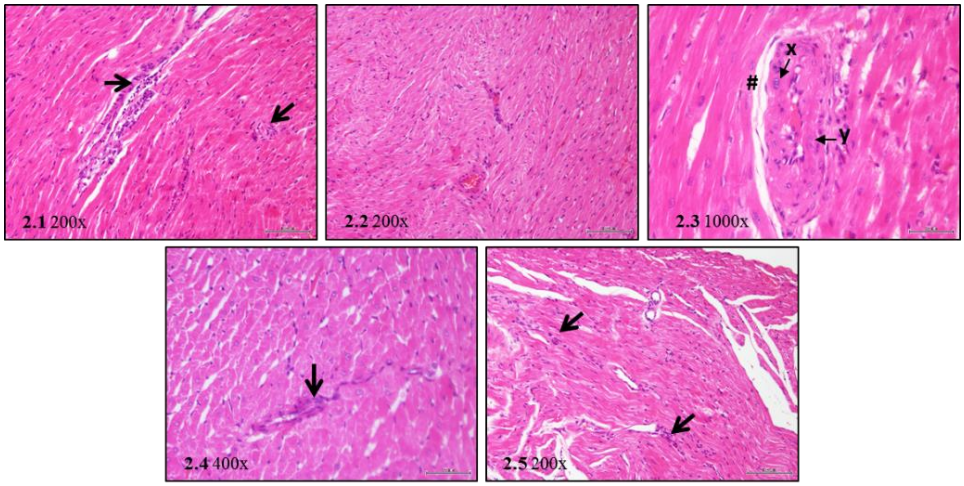


**Supplementary Figure 6.7E** H&E stained sections of myocardium from rats injected with GAS rM5 (homologous boost short term repeat exp., 35 days). Magnifications as indicated. 'Aschoff nodule like' structure indicated by asterisk (#), x: Anitschkow like cells, y: Aschoff like cells. Arrows (→) indicate inflammatory foci.

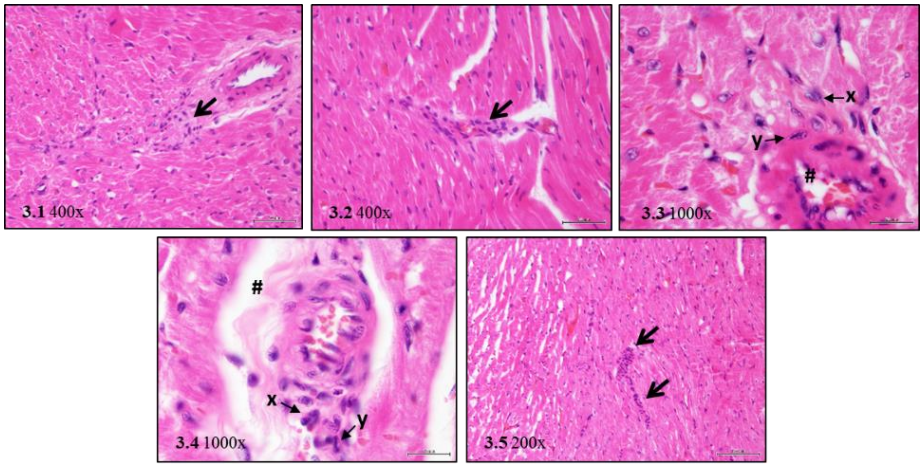


**Supplementary Figure 6.7F** H&E stained sections of myocardium from rats injected with GGS Stg480 (homologous boost short term repeat exp., 35 days). Magnifications 200×. 'Aschoff nodule like' structure indicated by asterisk (#), x: Anitschkow like cells, y: Aschoff like cells. Arrows (→) indicate inflammatory foci.

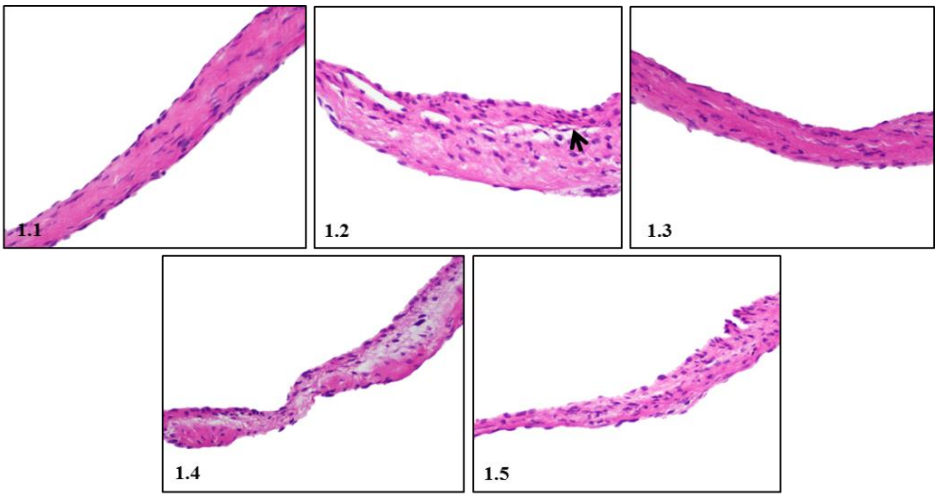


**Supplementary Figure 6.8A** H&E stained sections of mitral valves from rats injected with PBS (homologous boost long term exp., 225 days). Magnifications 400×. Arrows (→) indicate inflammatory foci.

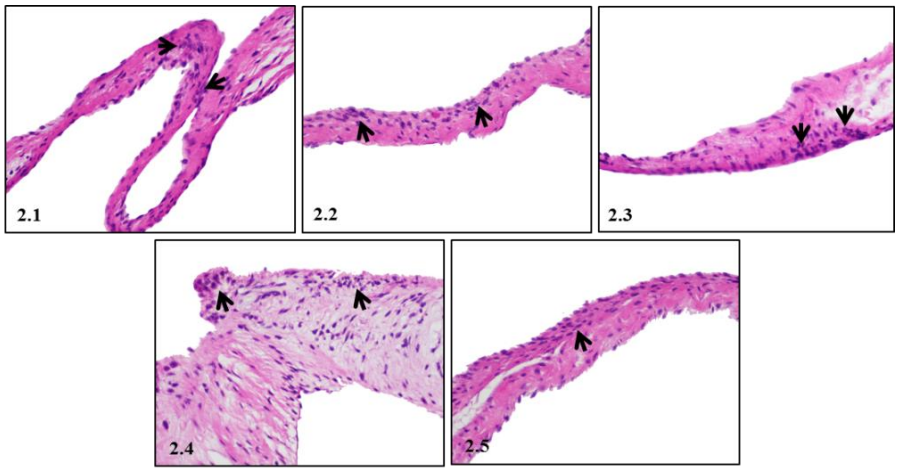


**Supplementary Figure 6.8B** H&E stained sections of mitral valves from rats injected with GAS rM5 (homologous boost long term exp., 225 days). Magnifications 400×. Arrows (→) indicate inflammatory foci.

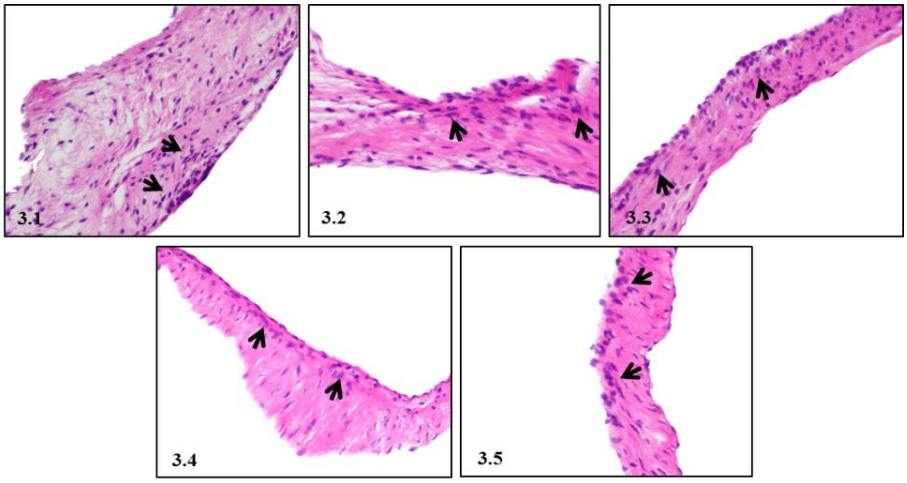


**Supplementary Figure 6.8C** H&E stained sections of mitral valves from rats injected with GGS Stg480 (homologous boost long term exp., 225 days). Magnifications 400×. Arrows (→) indicate inflammatory foci.

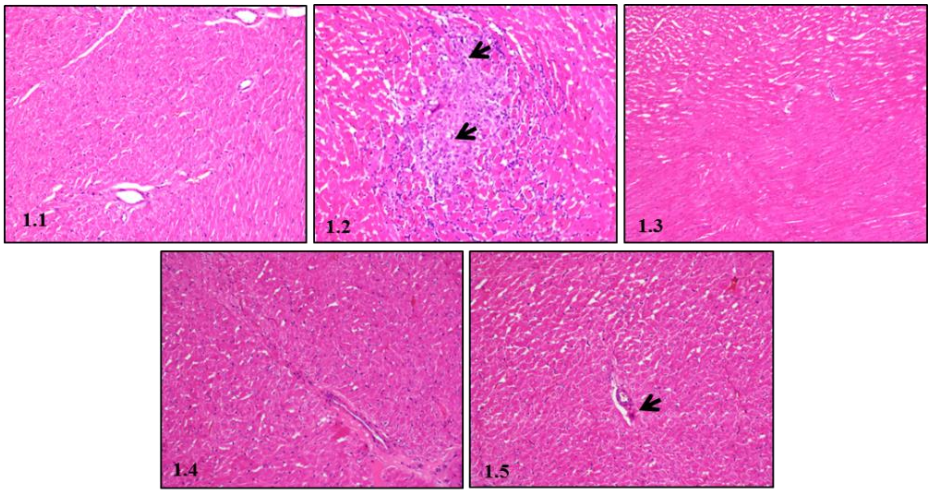


**Supplementary Figure 6.8D** H&E stained sections of myocardium from rats injected with PBS (homologous boost long term exp., 225 days). Magnifications 200×. Arrows (→) indicate inflammatory foci.

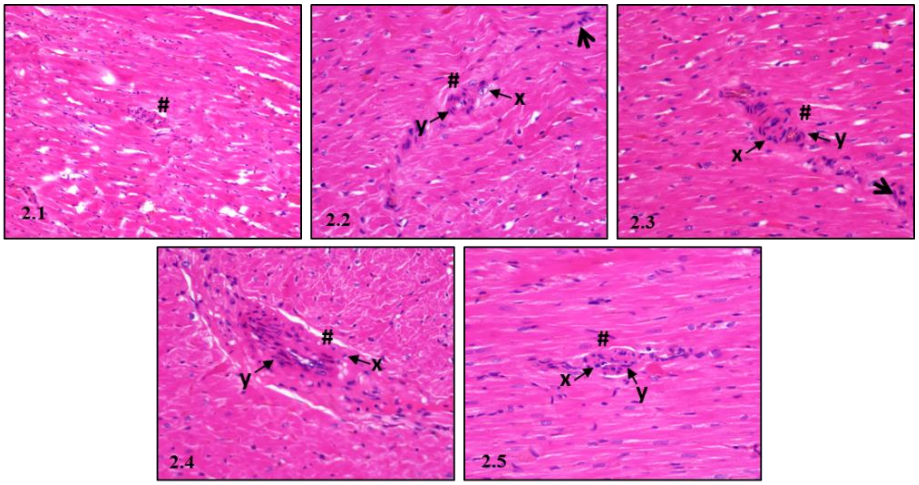


**Supplementary Figure 6.8E** H&E stained sections of myocardium from rats injected with GAS rM5 (homologous boost long term exp., 225 days). Magnifications 400×. 'Aschoff nodule like' structure indicated by asterisk (#), x: Anitschkow like cells, y: Aschoff like cells.

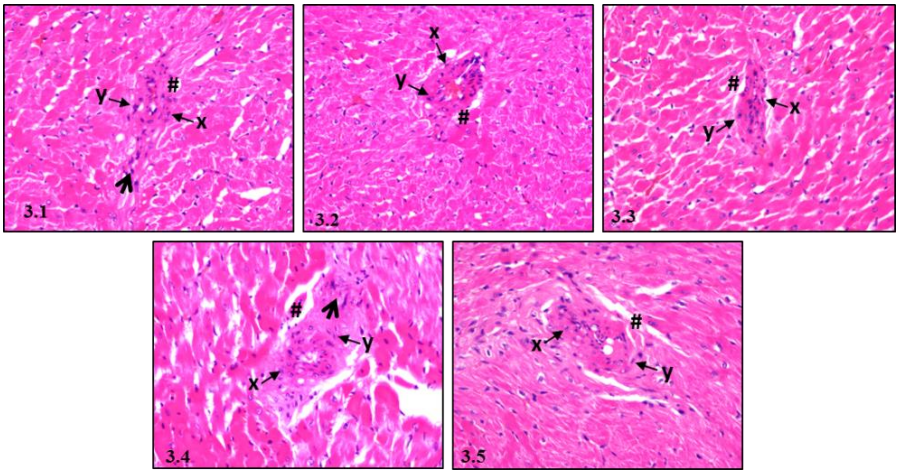


**Supplementary Figure 6.8F** H&E stained sections of myocardium from rats injected with GGS Stg480 (homologous boost long term exp., 225 days). Magnifications 400×. 'Aschoff nodule like' structure indicated by asterisk (#), x: Anitschkow like cells, y: Aschoff like cells.

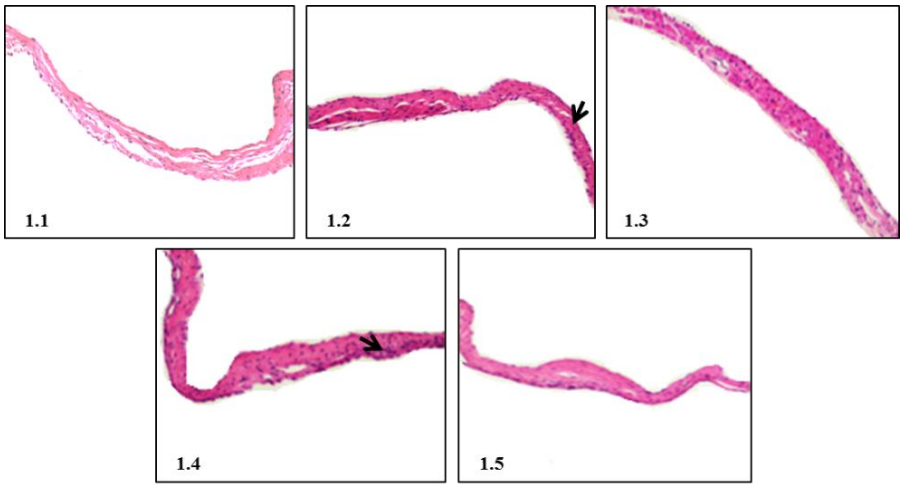


**Supplementary Figure 6.9A** H&E stained sections of mitral valves from rats injected with PBS (homologous boost long term repeat exp., 180 days). Magnifications 200×. Arrows (→) indicate inflammatory foci.

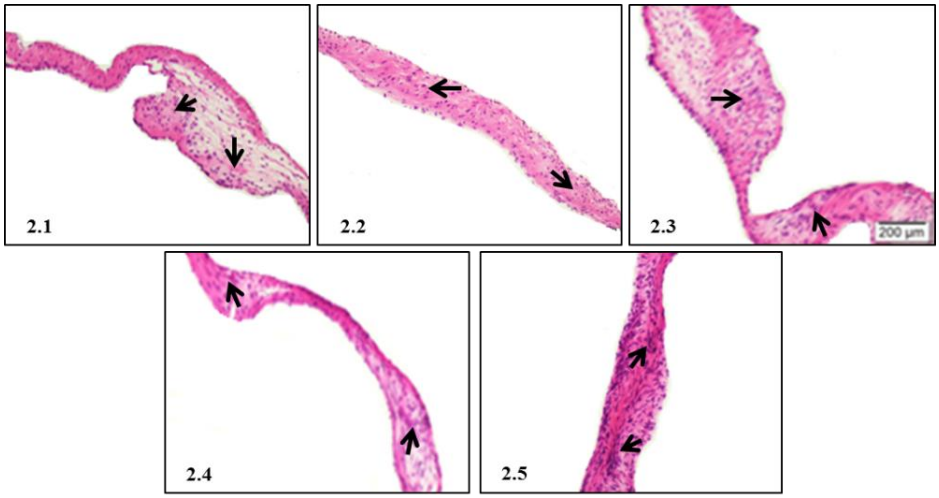


**Supplementary Figure 6.9B** H&E stained sections of mitral valves from rats injected with GAS rM5 (homologous boost long term repeat exp., 180 days). Magnifications 200×. Arrows (→) indicate inflammatory foci.

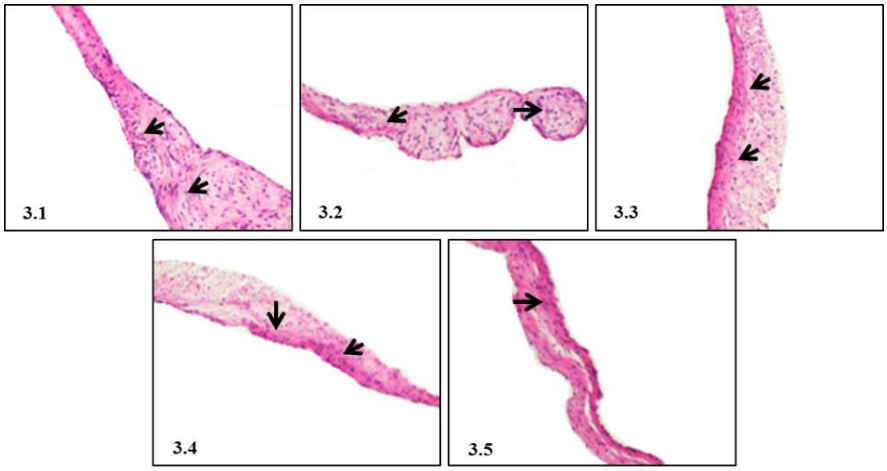


**Supplementary Figure 6.9C** H&E stained sections of mitral valves from rats injected with GGS Stg480 (homologous boost long term repeat exp., 180 days). Magnifications 200×. Arrows (→) indicate inflammatory foci.

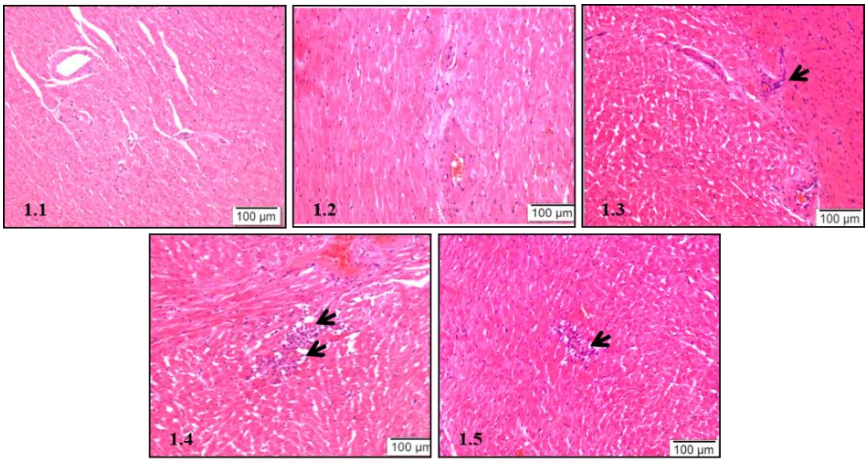


**Supplementary Figure 6.9D** H&E stained sections of myocardium from rats injected with PBS (homologous boost long term repeat exp., 180 days). Magnifications 200×. Arrows (→) indicate inflammatory foci.

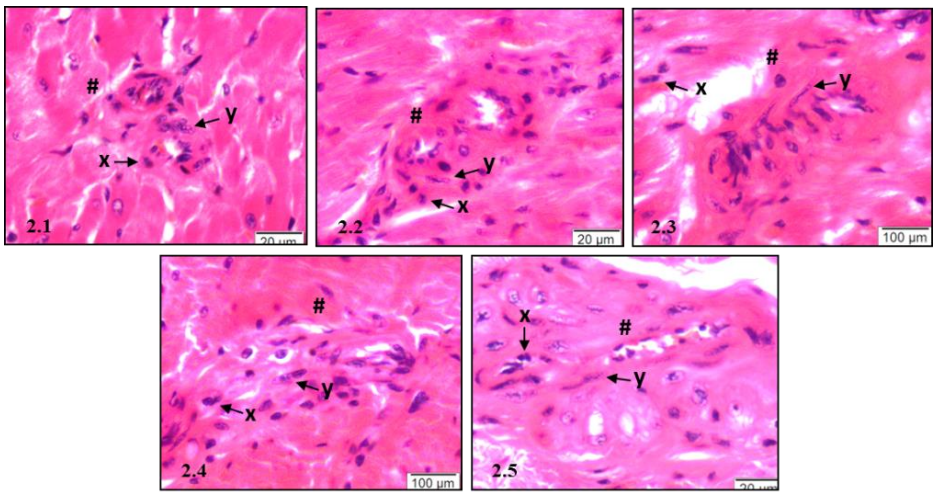


**Supplementary Figure 6.9E** H&E stained sections of myocardium from rats injected with GAS rM5 (homologous boost long term repeat exp., 180 days). Magnifications 1000×. 'Aschoff nodule like' structure indicated by asterisk (#), x: Anitschkow like cells, y: Aschoff like cells.

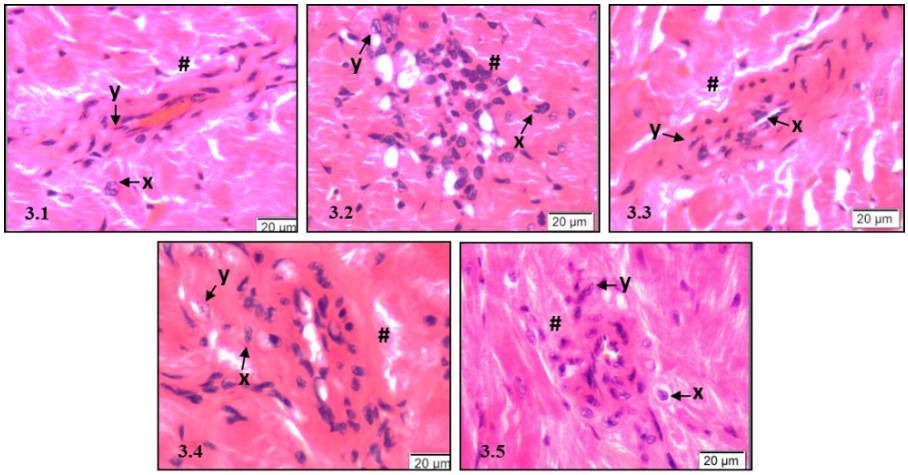


**Supplementary Figure 6.9F** H&E stained sections of myocardium from rats injected with GGS Stg480 (homologous boost long term repeat exp., 180 days). Magnifications 1000×. 'Aschoff nodule like' structure indicated by asterisk (#), x: Anitschkow like cells, y: Aschoff like cells.

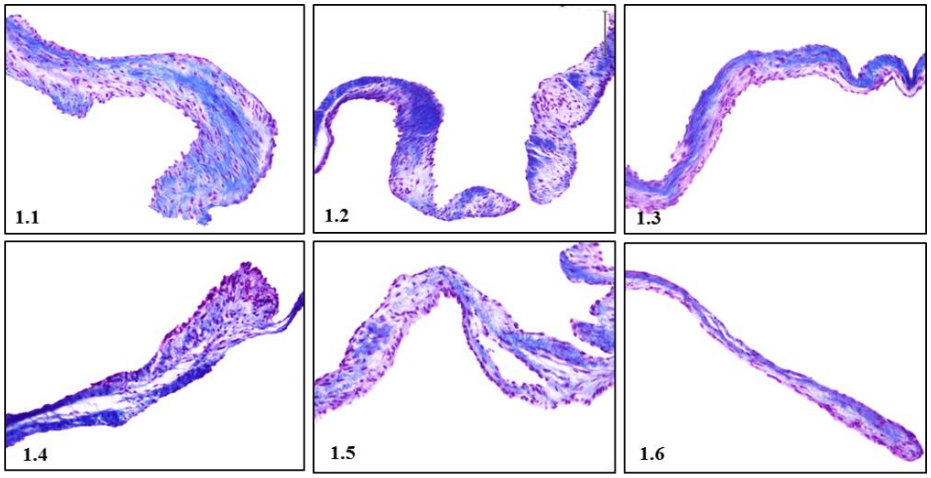


**Supplementary Figure 6.10A** Masson's trichrome stained sections of mitral valves from rats injected with PBS (homologous boost short term exp., 60 days). Magnifications 400×. Blue colour indicates collagen fibre deposition.

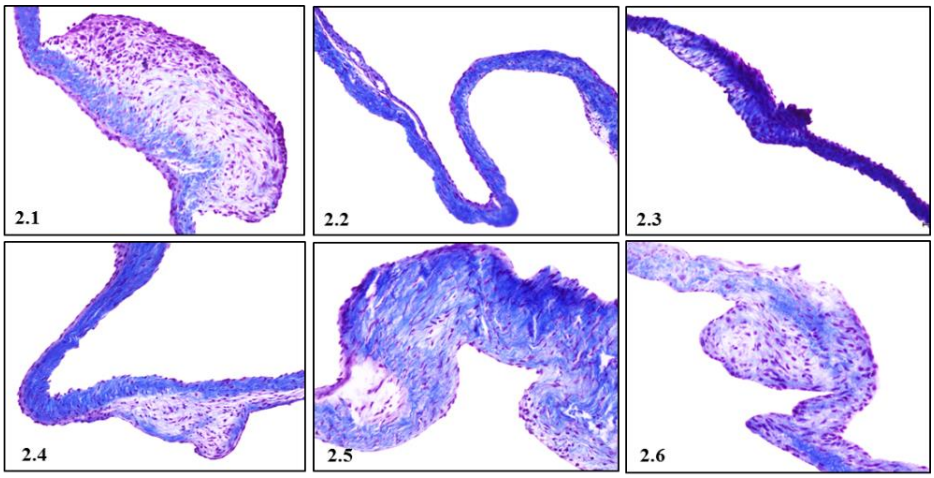


**Supplementary Figure 6.10B** Masson's trichrome stained sections of mitral valves from rats injected with whole-killed GAS M5 (homologous boost short term exp., 60 days). Magnifications 400×. Blue colour indicates collagen fibre deposition.

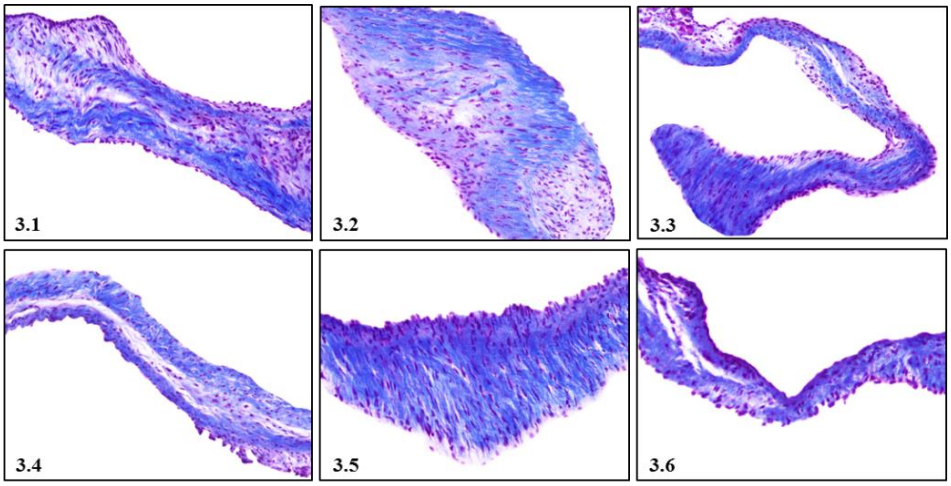


**Supplementary Figure 6.10C** Masson's trichrome stained sections of mitral valves from rats injected with whole-killed GGS NS3396 (homologous boost short term exp., 60 days). Magnifications 400×. Blue colour indicates collagen fibre deposition.

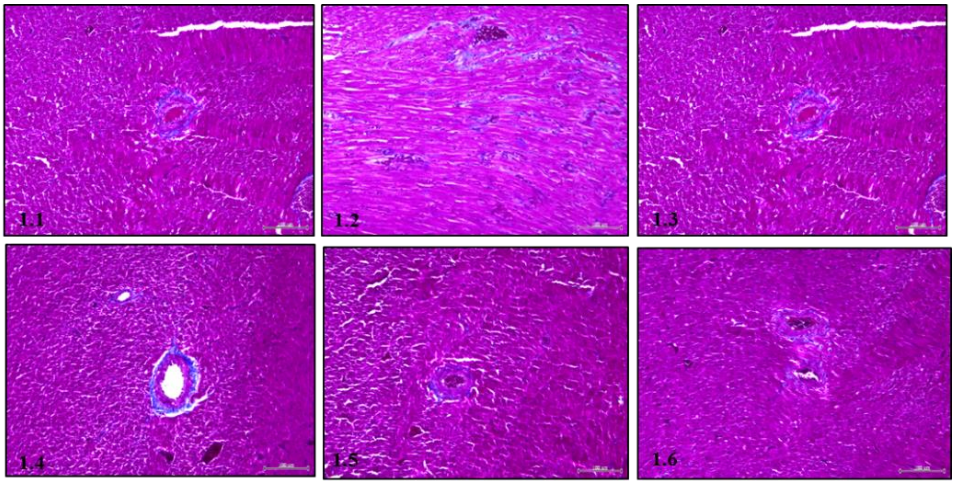


**Supplementary Figure 6.10D** Masson's trichrome stained sections of myocardium from rats injected with PBS (homologous boost short term exp., 60 days). Magnifications 200×. Blue colour indicates collagen fibre deposition.

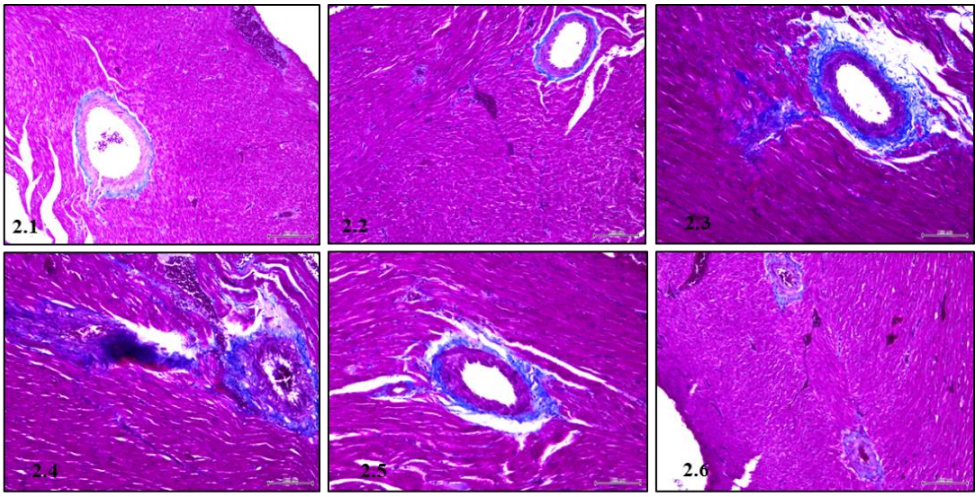


**Supplementary Figure 6.10E** Masson's trichrome stained sections of myocardium from rats injected with whole-killed GAS M5 (homologous boost short term exp., 60 days). Magnifications 200×. Blue colour indicates collagen fibre deposition.

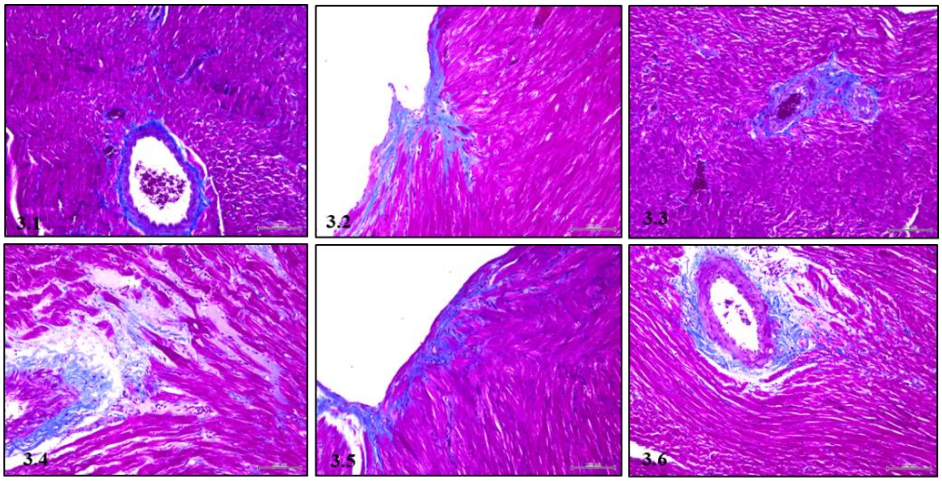


**Supplementary Figure 6.10F** Masson's trichrome stained sections of myocardium from rats injected with whole-killed GGS NS3396 (homologous boost short term exp., 60 days). Magnifications 200×. Blue colour indicates collagen fibre deposition.

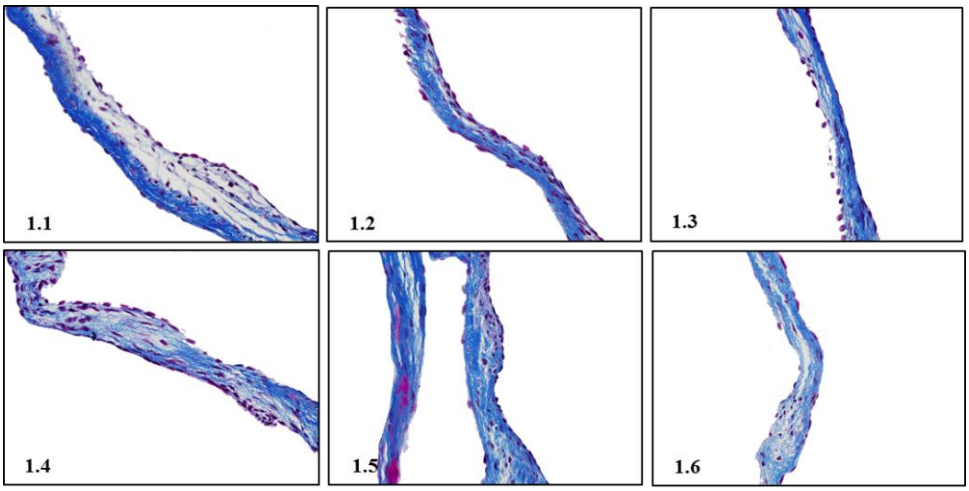


**Supplementary Figure 6.11A** Masson's trichrome stained sections of mitral valves from rats injected with PBS (homologous boost long term exp., 240 days). Magnifications 400×. Blue colour indicates collagen fibre deposition.

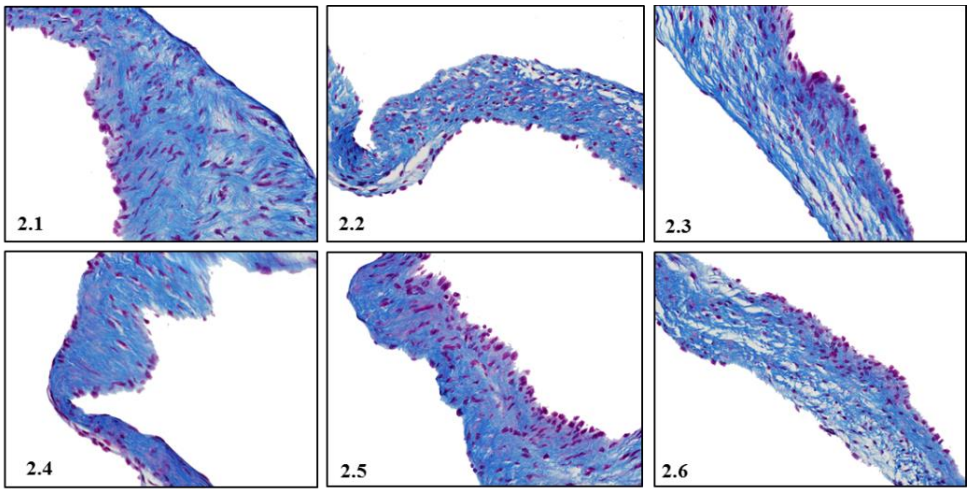


**Supplementary Figure 6.11B** Masson's trichrome stained sections of mitral valves from rats injected with whole-killed GAS M5 (homologous boost long term exp., 240 days). Magnifications 400×. Blue colour indicates collagen fibre deposition.

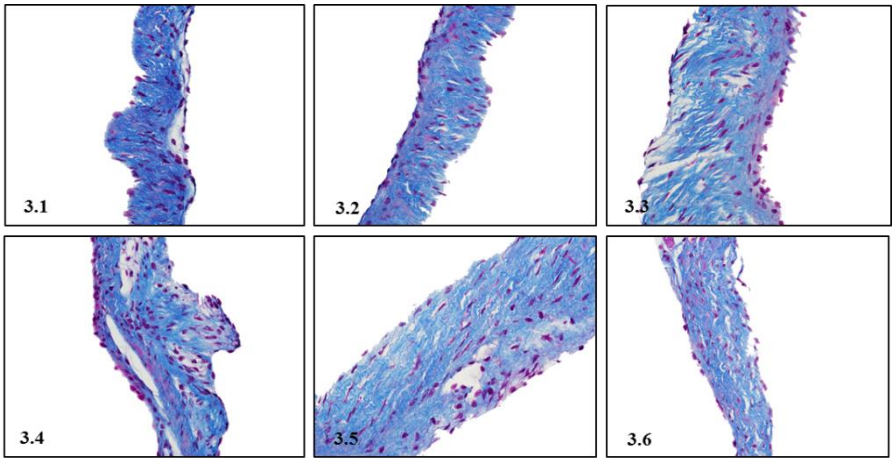


**Supplementary Figure 6.11C** Masson's trichrome stained sections of mitral valves from rats injected with whole-killed GGS NS3396 (homologous boost long term exp., 240 days). Magnifications 400×. Blue colour indicates collagen fibre deposition.

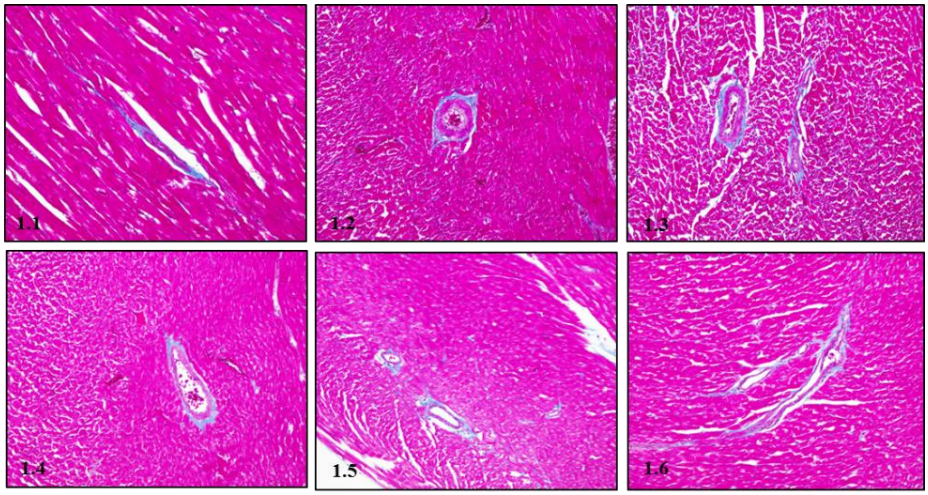


**Supplementary Figure 6.11D** Masson's trichrome stained sections of myocardium from rats injected with PBS (homologous boost long term exp., 240 days). Magnifications 200×. Blue colour indicates collagen fibre deposition.

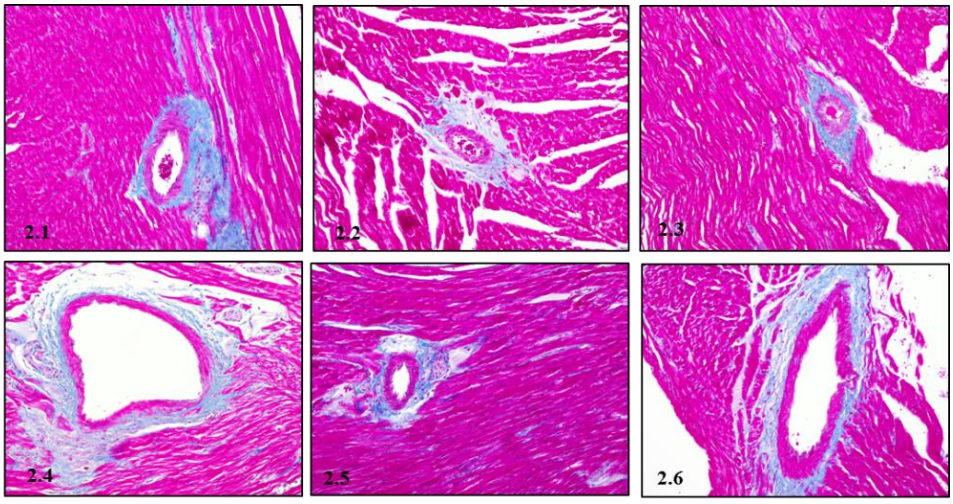


**Supplementary Figure 6.11E** Masson's trichrome stained sections of myocardium from rats injected with whole-killed GAS M5 (homologous boost long term exp., 240 days). Magnifications 200×. Blue colour indicates collagen fibre deposition.

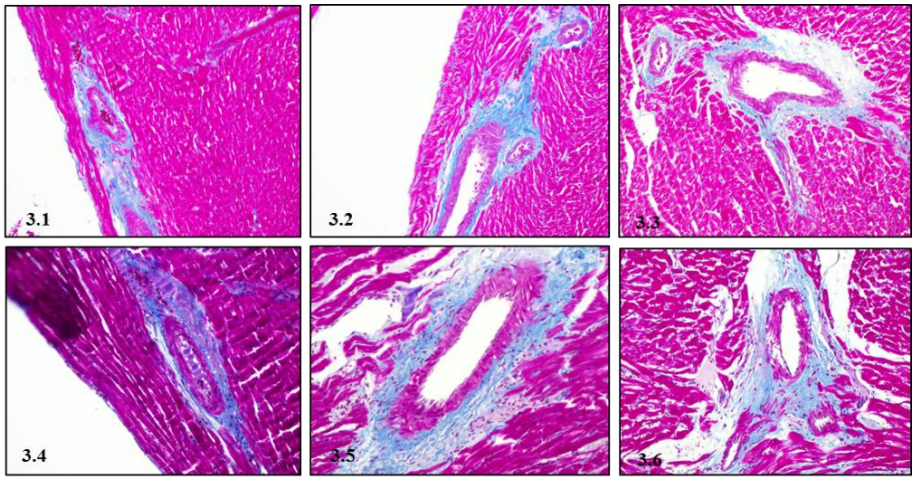


**Supplementary Figure 6.11F** Masson's trichrome stained sections of myocardium from rats injected with whole-killed GGS NS3396 (homologous boost long term exp., 240 days). Magnifications 200×. Blue colour indicates collagen fibre deposition.

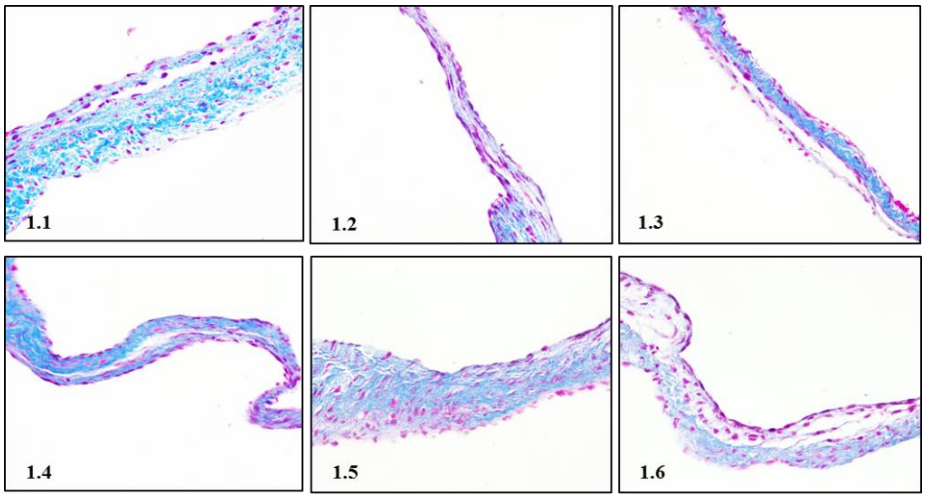


**Supplementary Figure 6.12A** Masson's trichrome stained sections of mitral valves from rats injected with PBS (homologous boost short term exp., 35 days). Magnifications 400×. Blue colour indicates collagen fibre deposition.

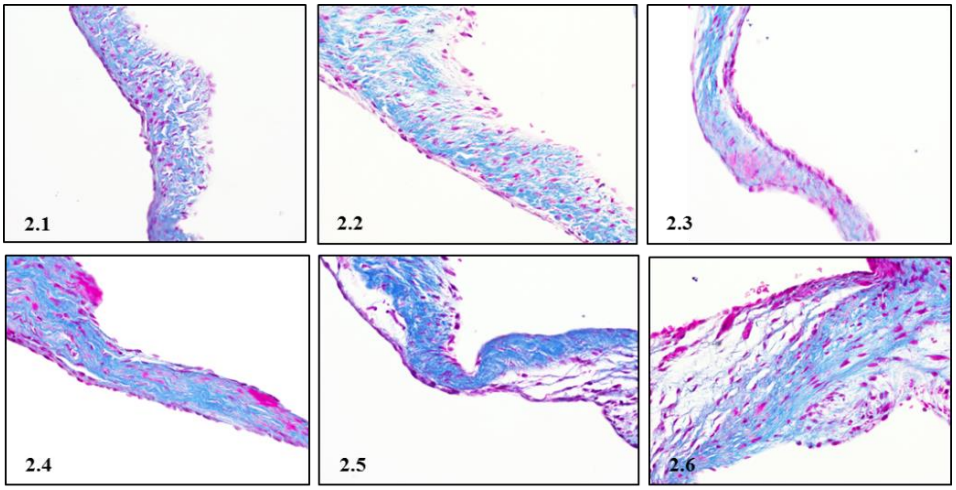


**Supplementary Figure 6.12B** Masson's trichrome stained sections of mitral valves from rats injected with GAS rM5 (homologous boost short term exp., 35 days). Magnifications 400×. Blue colour indicates collagen fibre deposition.

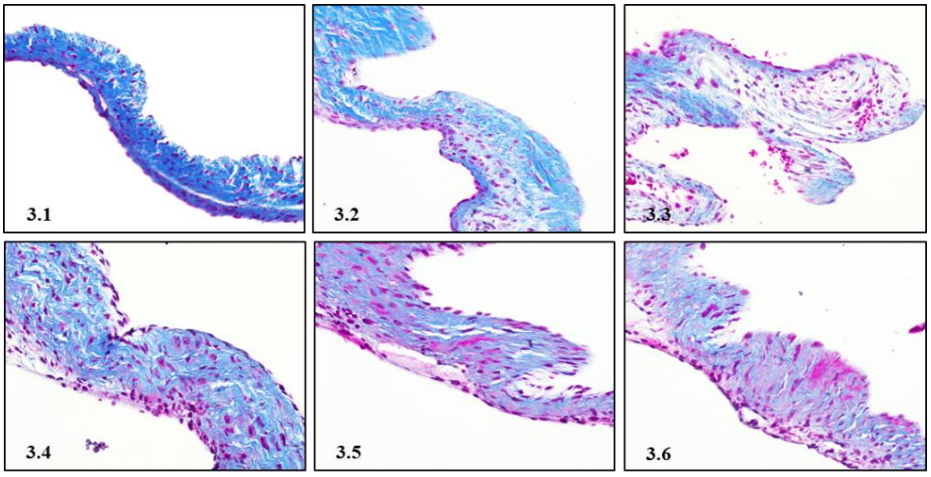


**Supplementary Figure 6.12C** Masson's trichrome stained sections of mitral valves from rats injected with GGS Stg480 (homologous boost short term exp., 35 days). Magnifications 400×. Blue colour indicates collagen fibre deposition.

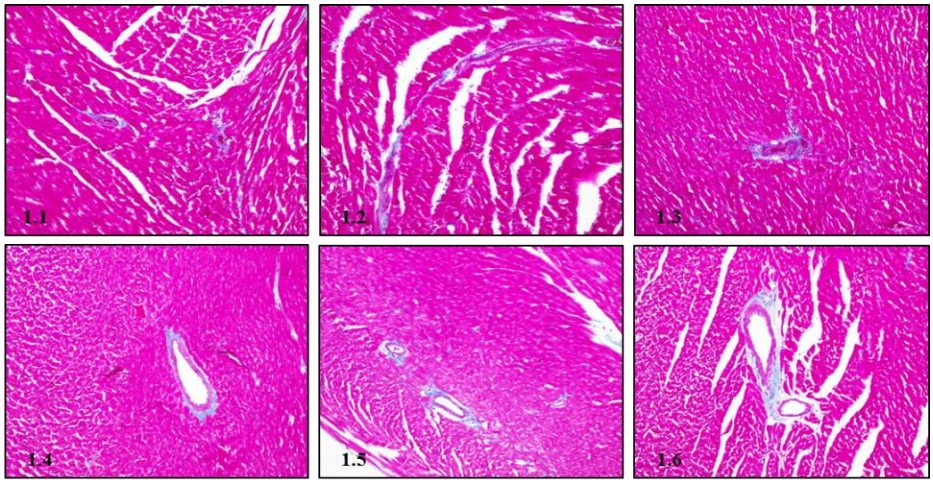


**Supplementary Figure 6.12D** Masson's trichrome stained sections of myocardium from rats injected with PBS (homologous boost short term exp., 35 days). Magnifications 200×. Blue colour indicates collagen fibre deposition.

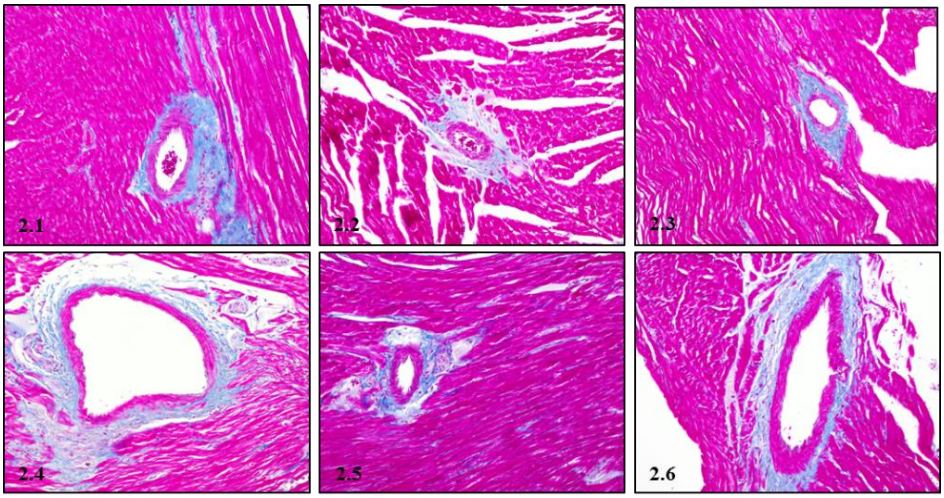


**Supplementary Figure 6.12E** Masson's trichrome stained sections of myocardium from rats injected with GAS rM5 (homologous boost short term exp., 35 days). Magnifications 200×. Blue colour indicates collagen fibre deposition.

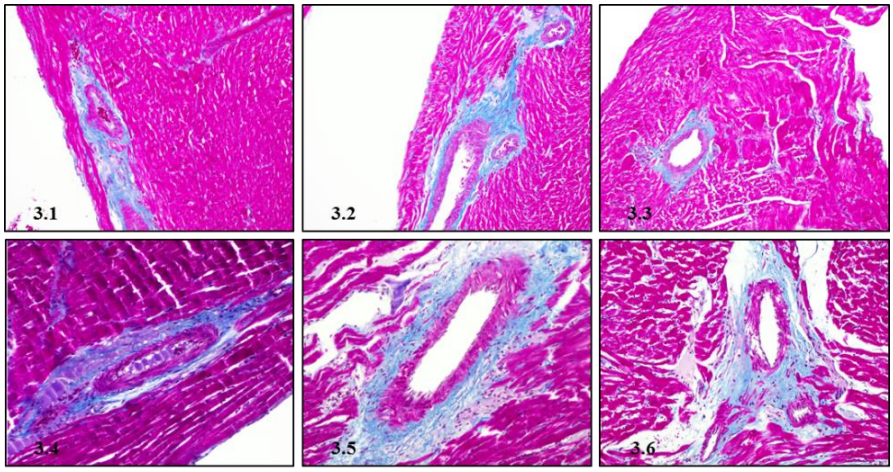


**Supplementary Figure 6.2F** Masson's trichrome stained sections of myocardium from rats injected with GGS Stg480 (homologous boost short term exp., 35 days). Magnifications 200×. Blue colour indicates collagen fibre deposition.

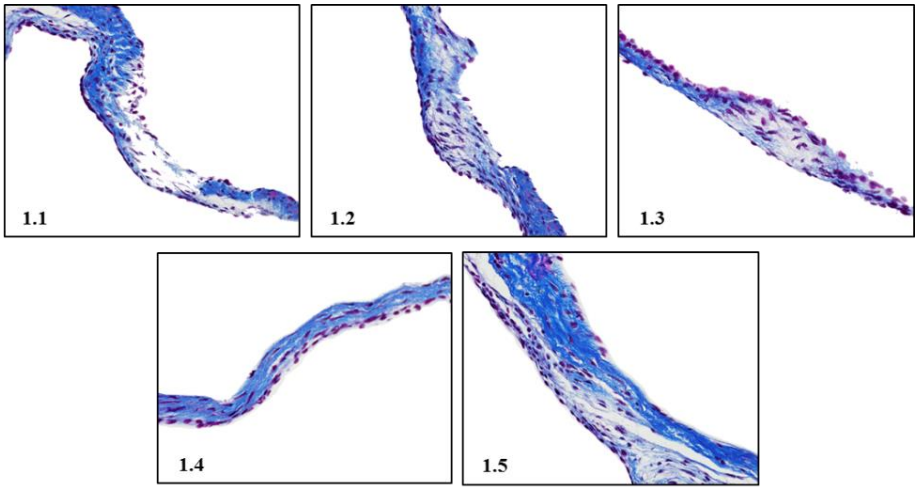


**Supplementary Figure 6.13A** Masson's trichrome stained sections of mitral valves from rats injected with PBS (homologous boost short term repeat exp., 35 days). Magnifications 400×. Blue colour indicates collagen fibre deposition.

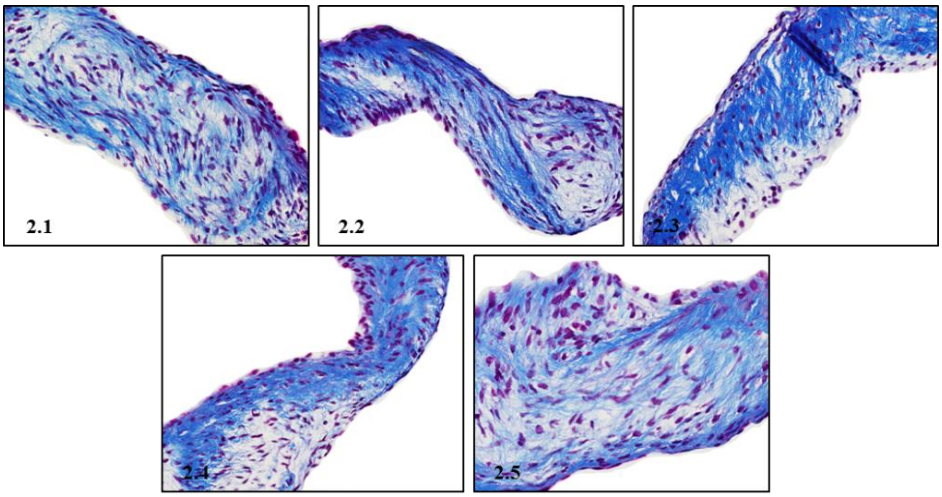


**Supplementary Figure 6.13B** Masson's trichrome stained sections of mitral valves from rats injected with GAS rM5 (homologous boost short term repeat exp., 35 days). Magnifications 400×. Blue colour indicates collagen fibre deposition.

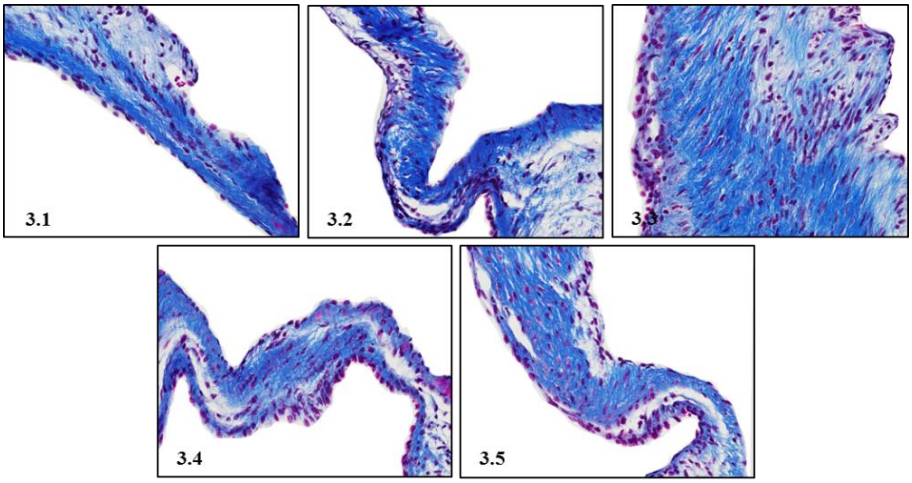


**Supplementary Figure 6.13C** Masson's trichrome stained sections of mitral valves from rats injected with GGS Stg480 (homologous boost short term repeat exp., 35 days). Magnifications 400×. Blue colour indicates collagen fibre deposition.

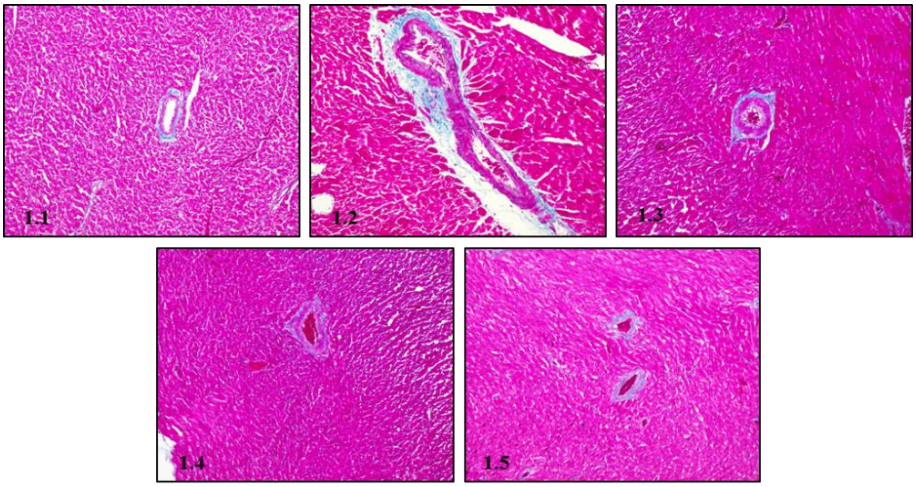


**Supplementary Figure 6.13D** Masson's trichrome stained sections of myocardium from rats injected with PBS (homologous boost short term repeat exp., 35 days). Magnifications 200×. Blue colour indicates collagen fibre deposition.

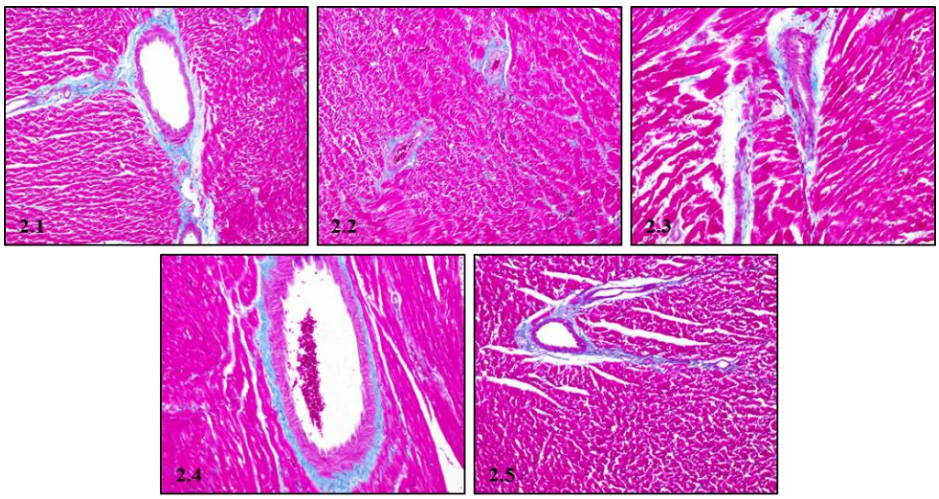


**Supplementary Figure 6.13E** Masson's trichrome stained sections of myocardium from rats injected with GAS rM5 (homologous boost short term repeat exp., 35 days). Magnifications 200×. Blue colour indicates collagen fibre deposition.

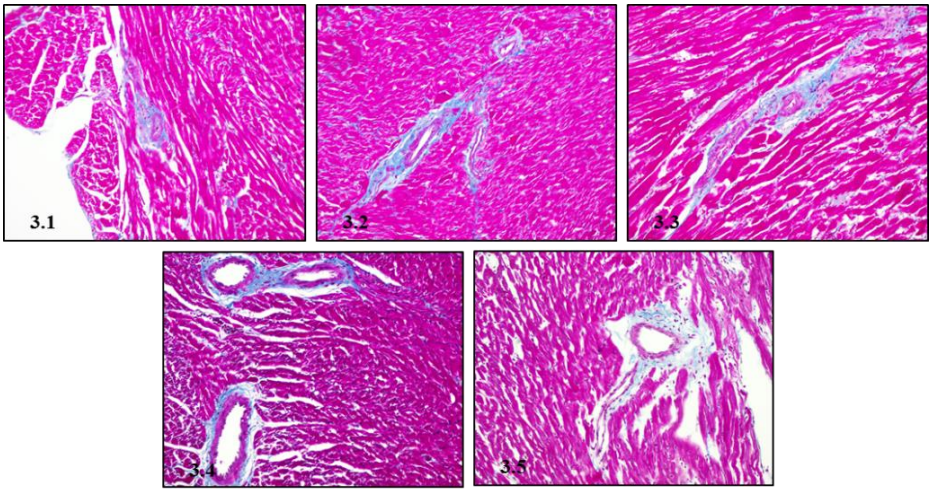


**Supplementary Figure 6.13F** Masson's trichrome stained sections of myocardium from rats injected with GGS Stg480 (homologous boost short term exp., 35 days). Magnifications 200×. Blue colour indicates collagen fibre deposition.

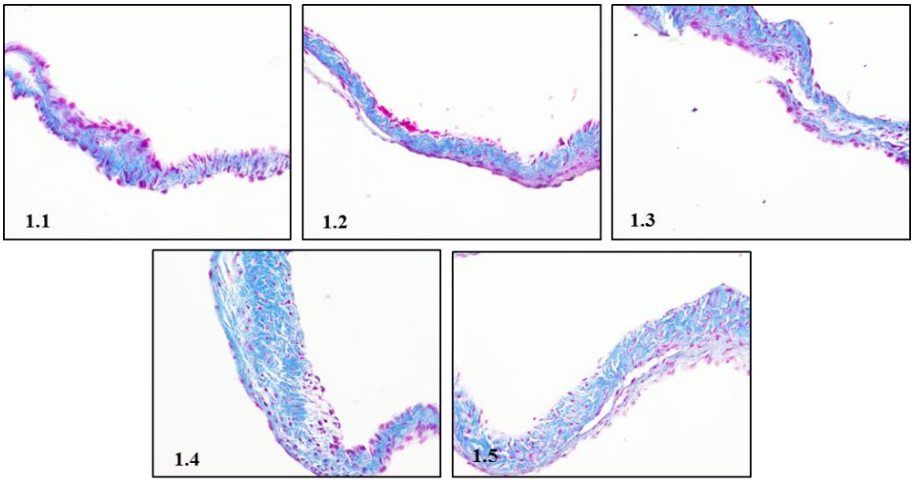


**Supplementary Figure 6.14A** Masson's trichrome stained sections of mitral valves from rats injected with PBS (homologous boost long term exp., 225 days). Magnifications 400×. Blue colour indicates collagen fibre deposition.

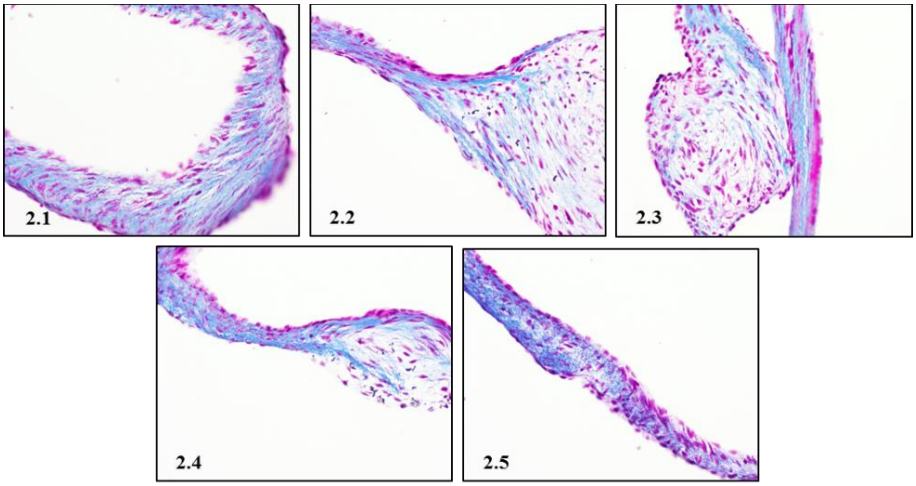


**Supplementary Figure 6.14B** Masson's trichrome stained sections of mitral valves from rats injected with GAS rM5 (homologous boost long term exp., 225 days). Magnifications 400×. Blue colour indicates collagen fibre deposition.

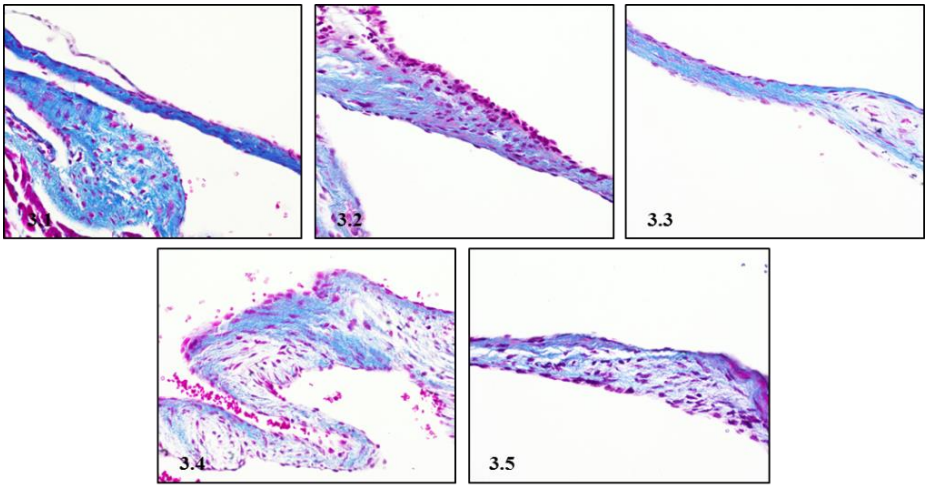


**Supplementary Figure 6.14C** Masson's trichrome stained sections of mitral valves from rats injected with GGS Stg480 (homologous boost long term exp., 225 days). Magnifications 400×. Blue colour indicates collagen fibre deposition.

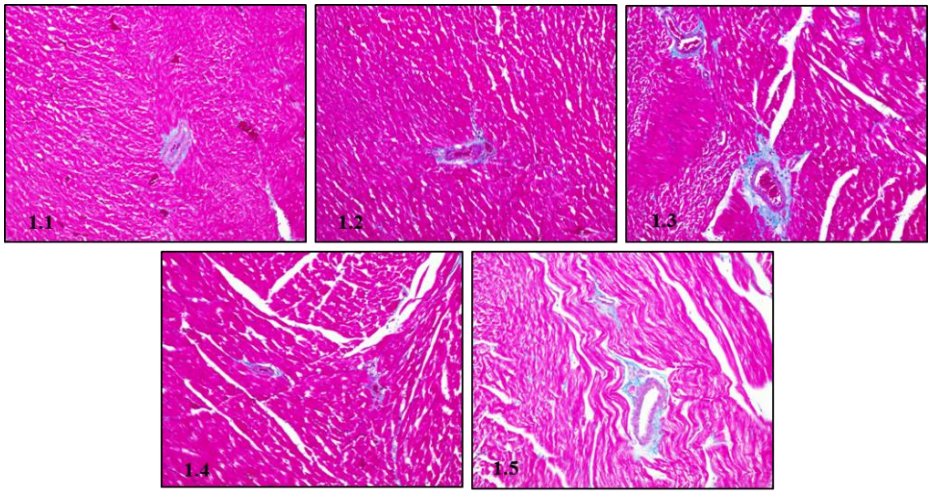


**Supplementary Figure 6.14D** Masson's trichrome stained sections of myocardium from rats injected with PBS (homologous boost long term exp., 225 days). Magnifications 200×. Blue colour indicates collagen fibre deposition.

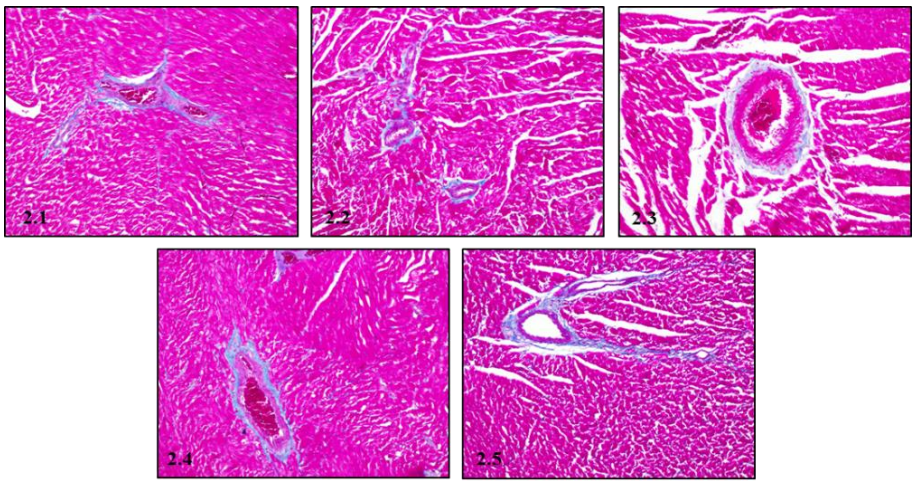


**Supplementary Figure 6.14E** Masson's trichrome stained sections of myocardium from rats injected with GAS rM5 (homologous boost long term exp., 225 days). Magnifications 200×. Blue colour indicates collagen fibre deposition.

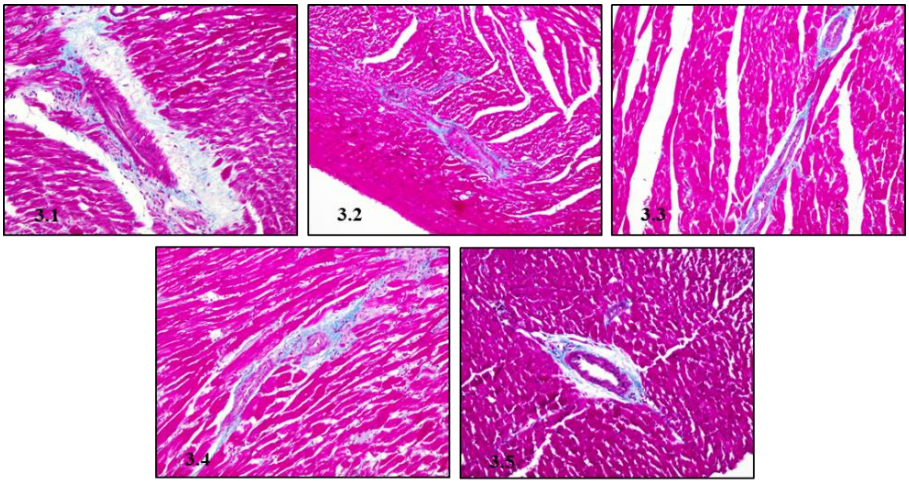


**Supplementary Figure 6.14F** Masson's trichrome stained sections of myocardium from rats injected with GGS Stg480 (homologous boost long term exp., 225 days). Magnifications 200×. Blue colour indicates collagen fibre deposition.

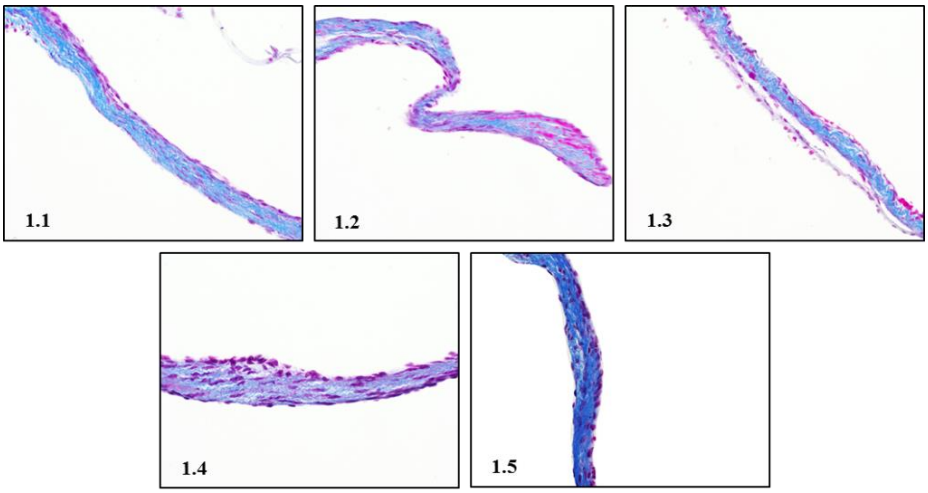


**Supplementary Figure 6.15A** Masson's trichrome stained sections of mitral valves from rats injected with PBS (homologous boost long term repeat exp., 180 days). Magnifications 400×. Blue colour indicates collagen fibre deposition.

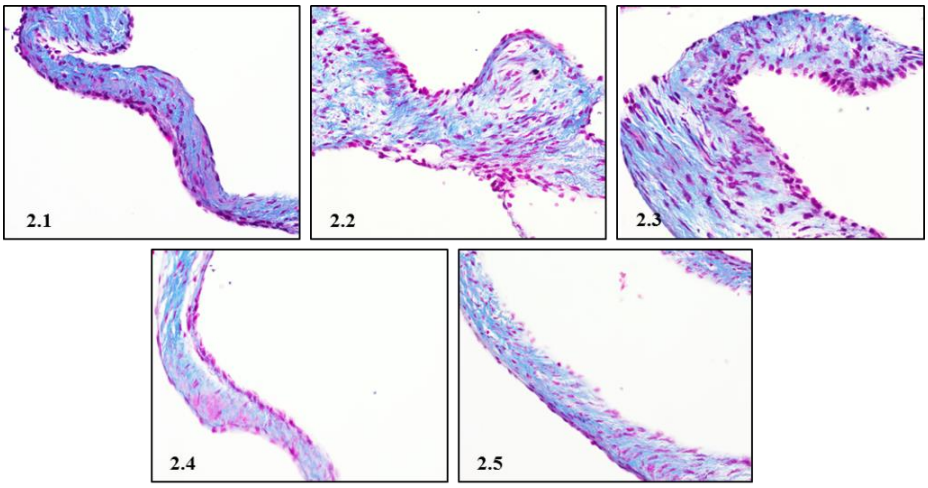


**Supplementary Figure 6.15B** Masson's trichrome stained sections of mitral valves from rats injected with GAS rM5 (homologous boost long term repeat exp., 180 days). Magnifications 400×. Blue colour indicates collagen fibre deposition.

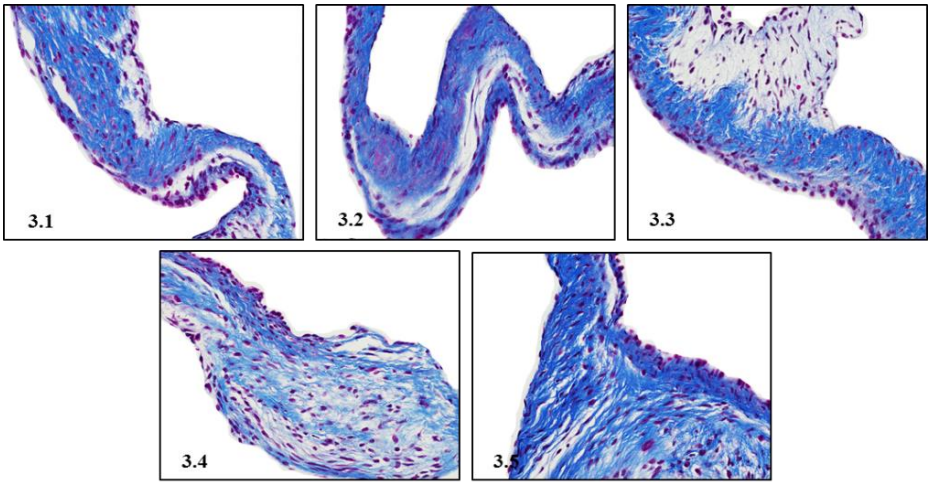


**Supplementary Figure 6.15C** Masson's trichrome stained sections of mitral valves from rats injected with GGS Stg480 (homologous boost long term repeat exp., 180 days). Magnifications 400×. Blue colour indicates collagen fibre deposition.

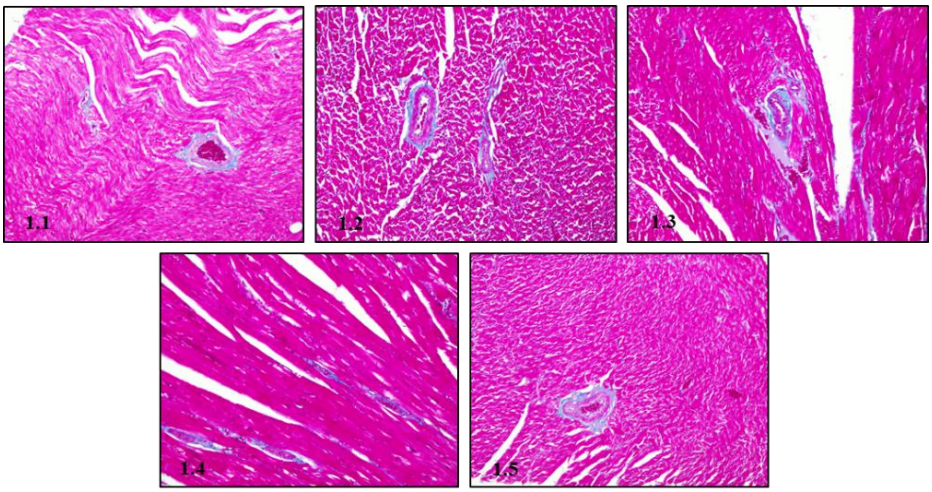


**Supplementary Figure 6.15D** Masson's trichrome stained sections of myocardium from rats injected with PBS (homologous boost long term repeat exp., 180 days). Magnifications 200×. Blue colour indicates collagen fibre deposition.

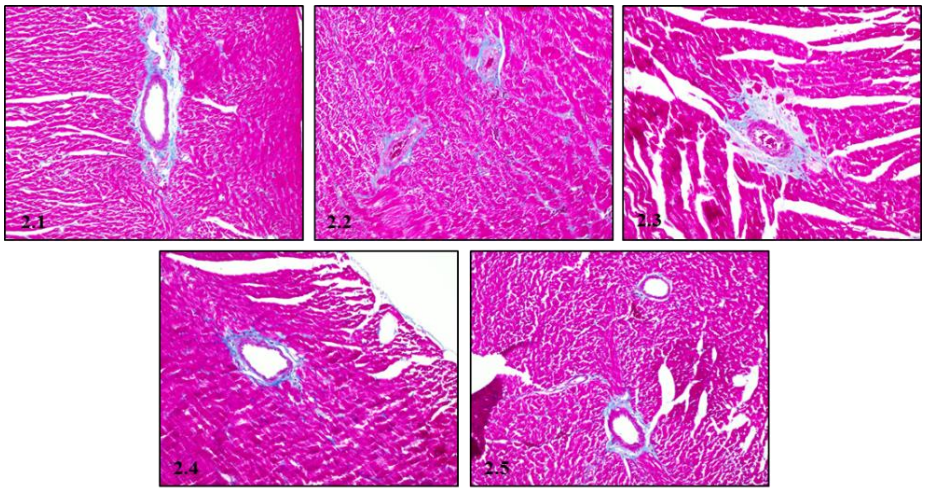


**Supplementary Figure 6.15E** Masson's trichrome stained sections of myocardium from rats injected with GAS rM5 (homologous boost long term repeat exp., 180 days). Magnifications 200×. Blue colour indicates collagen fibre deposition.

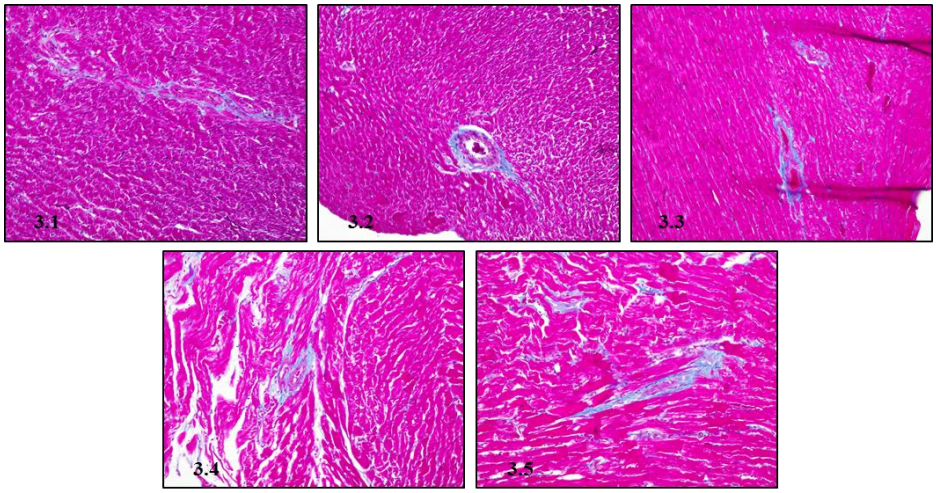


**Supplementary Figure 6.15F** Masson's trichrome stained sections of myocardium from rats injected with GGS Stg480 (homologous boost long term repeat exp., 180 days). Magnifications 200×. Blue colour indicates collagen fibre deposition.

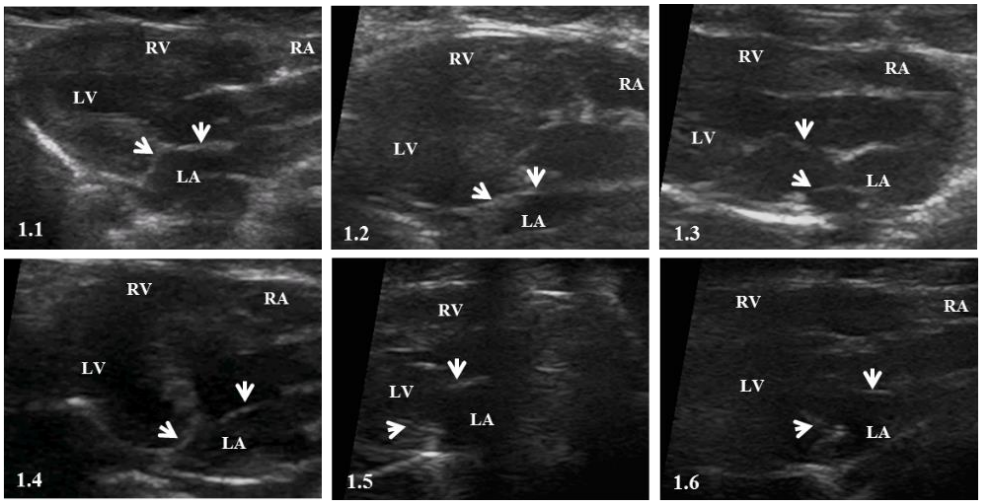


**Supplementary Figure 6.16A** Echocardiographic examination of mitral valves of control rats injected with PBS (homologous boost long term exp., 240 days). Arrows (→) indicate mitral valve leaflets. RA: right atrium, RV: right ventricle, LA: left atrium, LV: left ventricle.

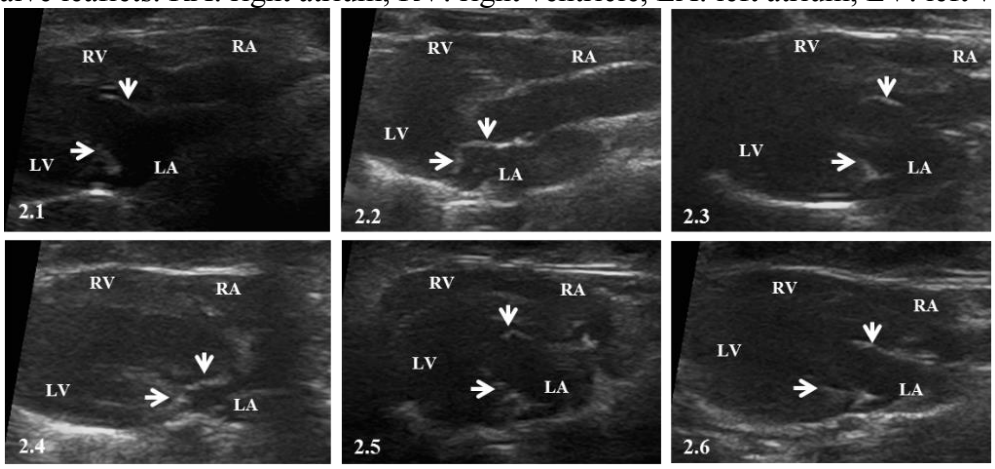


**Supplementary Figure 6.16B** Echocardiographic examination of mitral valves of rats injected with whole-killed GAS M5 (homologous boost long term exp., 240 days). Arrows (→) indicate mitral valve leaflets. RA: right atrium, RV: right ventricle, LA: left atrium, LV: left ventricle.

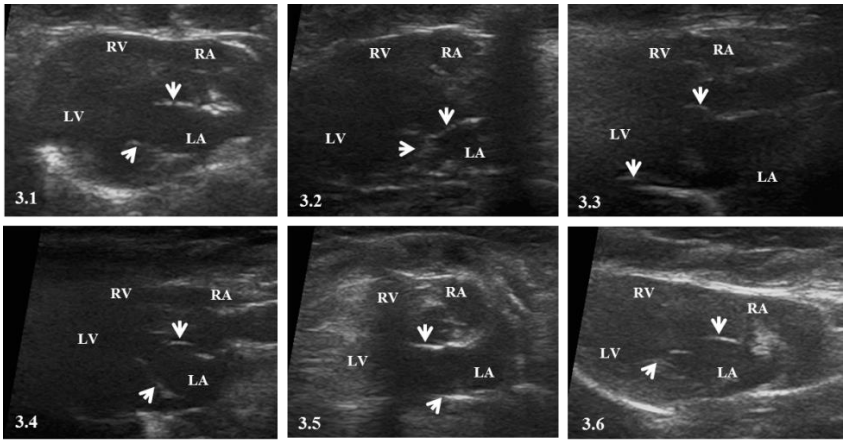


**Supplementary Figure 6.16C** Echocardiographic examination of mitral valves of rats injected with whole-killed GGS NS3396 (homologous boost long term exp., 240 days). Arrows (→) indicate mitral valve leaflets. RA: right atrium, RV: right ventricle, LA: left atrium, LV: left ventricle.

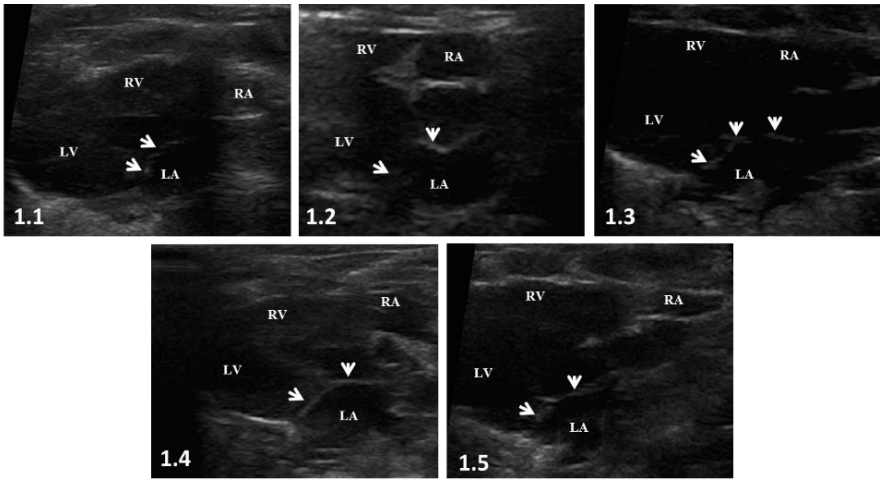


**Supplementary Figure 6.17A** Echocardiographic examination of mitral valves of control rats injected with PBS (homologous boost long term exp., 225 days). Arrows (→) indicate mitral valve leaflets. RA: right atrium, RV: right ventricle, LA: left atrium, LV: left ventricle.

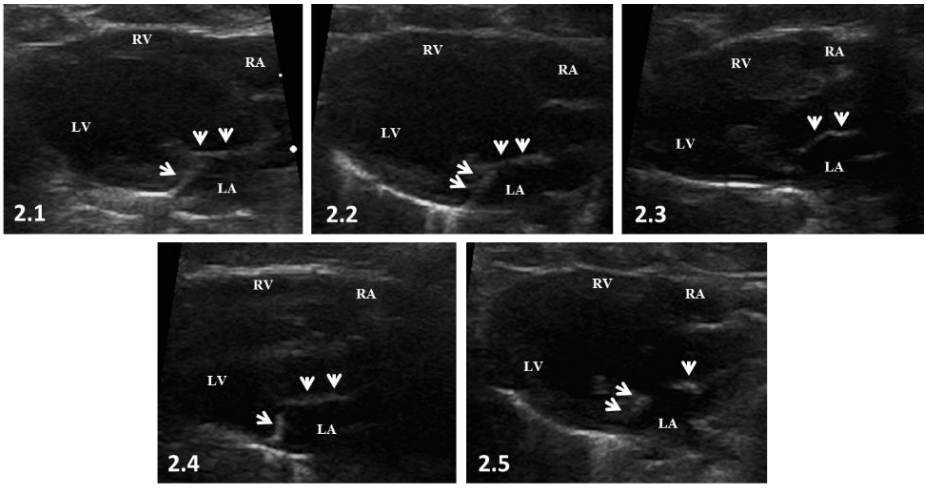


**Supplementary Figure 6.17B** Echocardiographic examination of mitral valves of rats injected with GAS rM5 (homologous boost long term exp., 225 days). Arrows (→) indicate mitral valve leaflets. RA: right atrium, RV: right ventricle, LA: left atrium, LV: left ventricle.

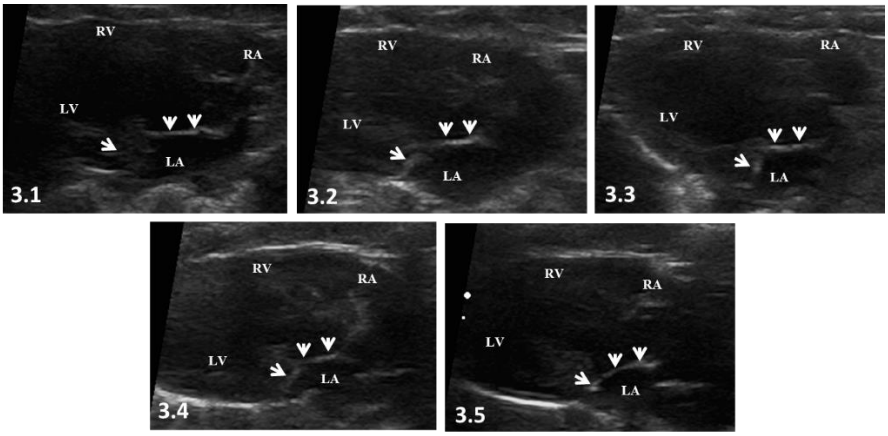


**Supplementary Figure 6.17C** Echocardiographic examination of mitral valves of rats injected with GGS Stg480 (homologous boost long term exp., 225 days). Arrows (→) indicate mitral valve leaflets. RA: right atrium, RV: right ventricle, LA: left atrium, LV: left ventricle.

## 6.1 Statistical analysis of Figure 6.1

Panel A (short term exp.): Normality test and Tukey's multiple comparisons test

| Col. stats | A |
|---|---|
| | Normlality |
| | Y |
| Number of values | 18 |
| | |
| D'Agostino & Pearson normality test | |
| K2 | 0.8961 |
| P value | 0.6389 |
| Passed normality test (alpha=0.05)? | Yes |
| P value summary | ns |

| 1way ANOVA<br>Multiple comparisons | | | | | |
|---|---|---|---|---|---|
| Number of families | 1 | | | | |
| Number of comparisons per family | 3 | | | | |
| Alpha | 0.05 | | | | |
| | | | | | |
| Tukey's multiple comparisons test | Mean Diff. | 95.00% CI of diff. | Significant? | Summary | Adjusted P Value |
| | | | | | |
| PBS vs. GAS | -4.286 | -5.752 to -2.82 | Yes | **** | <0.0001 |
| PBS vs. GGS | -5.286 | -6.811 to -3.76 | Yes | **** | <0.0001 |
| GAS vs. GGS | -1 | -2.526 to 0.5258 | No | ns | 0.2408 |

Panel A (long term exp.): Normality test and Tukey's multiple comparisons test

| Col. stats | A |
|---|---|
| | Normlality |
| | Y |
| Number of values | 18 |
| | |
| D'Agostino & Pearson normality test | |
| K2 | 0.8961 |
| P value | 0.6389 |
| Passed normality test (alpha=0.05)? | Yes |
| P value summary | ns |

| 1way ANOVA<br>Multiple comparisons | | | | | |
|---|---|---|---|---|---|
| Number of families | 1 | | | | |
| Number of comparisons per family | 3 | | | | |
| Alpha | 0.05 | | | | |
| | | | | | |
| Tukey's multiple comparisons test | Mean Diff. | 95.00% CI of diff. | Significant? | Summary | Adjusted P Value |
| | | | | | |
| PBS vs. GAS | -4.375 | -5.475 to -3.275 | Yes | **** | <0.0001 |
| PBS vs. GGS | -4.714 | -5.851 to -3.578 | Yes | **** | <0.0001 |
| GAS vs. GGS | -0.3393 | -1.439 to 0.7609 | No | ns | 0.7174 |

Panel B (short term exp.): Normality test and Tukey's multiple comparisons test

| Col. stats | A |
|---|---|
| | Normlality |
| | Y |
| Number of values | 18 |
| | |
| D'Agostino & Pearson normality test | |
| K2 | 0.8961 |
| P value | 0.6389 |
| Passed normality test (alpha=0.05)? | Yes |
| P value summary | ns |

| 1way ANOVA<br>Multiple comparisons | | | | | |
|---|---|---|---|---|---|
| Number of families | 1 | | | | |
| Number of comparisons per family | 3 | | | | |
| Alpha | 0.05 | | | | |
| | | | | | |
| Tukey's multiple comparisons test | Mean Diff. | 95.00% CI of diff. | Significant? | Summary | Adjusted P Value |
| | | | | | |
| PBS vs. GAS | -3.833 | -5.601 to -2.066 | Yes | *** | 0.0001 |
| PBS vs. GGS | -3.333 | -5.101 to -1.566 | Yes | *** | 0.0005 |
| GAS vs. GGS | 0.5 | -1.267 to 2.267 | No | ns | 0.7471 |

Panel B (long term exp.): Normality test and Tukey's multiple comparisons test

| Col. stats | A |
|---|---|
| | Normlality |
| | Y |
| Number of values | 15 |
| | |
| D'Agostino & Pearson normality test | |
| K2 | 3.835 |
| P value | 0.1469 |
| Passed normality test (alpha=0.05)? | Yes |
| P value summary | ns |

1way ANOVA
Multiple comparisons

| | | | | | |
|---|---|---|---|---|---|
| Number of families | 1 | | | | |
| Number of comparisons per family | 3 | | | | |
| Alpha | 0.05 | | | | |
| | | | | | |
| Tukey's multiple comparisons test | Mean Diff. | 95.00% CI of diff. | Significant? | Summary | Adjusted P Value |
| | | | | | |
| PBS vs. rM5 | -5.4 | -6.778 to -4.022 | Yes | **** | <0.0001 |
| PBS vs. rGGSm | -5.8 | -7.178 to -4.422 | Yes | **** | <0.0001 |
| rM5 vs. rGGSm | -0.4 | -1.778 to 0.9777 | No | ns | 0.7250 |

## 6.2 Statistical analysis of Figure 6.2

Panel A (short term exp.): Normality test and Tukey's multiple comparisons test

| Col. stats | A |
|---|---|
| | Normality |
| | Y |
| Number of values | 20 |
| | |
| D'Agostino & Pearson normality test | |
| K2 | 1.48 |
| P value | 0.4772 |
| Passed normality test (alpha=0.05)? | Yes |
| P value summary | ns |

1way ANOVA
Multiple comparisons

| | | | | | |
|---|---|---|---|---|---|
| Number of families | 1 | | | | |
| Number of comparisons per family | 3 | | | | |
| Alpha | 0.05 | | | | |
| | | | | | |
| Tukey's multiple comparisons test | Mean Diff. | 95.00% CI of diff. | Significant? | Summary | Adjusted P Value |
| | | | | | |
| PBS vs. rM5 | -7.224 | -11.13 to -3.315 | Yes | *** | 0.0005 |
| PBS vs. Stg480 | -8.662 | -12.73 to -4.593 | Yes | *** | 0.0001 |
| rM5 vs. Stg480 | -1.438 | -5.507 to 2.631 | No | ns | 0.6436 |

Panel A (long term exp.): Normality test and Tukey's multiple comparisons test

| Col. stats | A |
|---|---|
| | Normality |
| | Y |
| Number of values | 22 |
| | |
| D'Agostino & Pearson normality test | |
| K2 | 1.96 |
| P value | 0.3753 |
| Passed normality test (alpha=0.05)? | Yes |
| P value summary | ns |

1way ANOVA
Multiple comparisons

| | | | | | |
|---|---|---|---|---|---|
| Number of families | 1 | | | | |
| Number of comparisons per family | 3 | | | | |
| Alpha | 0.05 | | | | |
| | | | | | |
| Tukey's multiple comparisons test | Mean Diff. | 95.00% CI of diff. | Significant? | Summary | Adjusted P Value |
| | | | | | |
| PBS vs. rM5 | -9.407 | -12.41 to -6.406 | Yes | **** | <0.0001 |
| PBS vs. Stg480 | -7.738 | -10.84 to -4.639 | Yes | **** | <0.0001 |
| rM5 vs. Stg480 | 1.669 | -1.332 to 4.67 | No | ns | 0.3542 |

Panel B (short term exp.): Normality test and Tukey's multiple comparisons test

| Col. stats | A |
|---|---|
| | Normality |
| | Y |
| Number of values | 18 |
| | |
| D'Agostino & Pearson normality test | |
| K2 | 0.5807 |
| P value | 0.7480 |
| Passed normality test (alpha=0.05)? | Yes |
| P value summary | ns |

1way ANOVA
Multiple comparisons

| | | | | | |
|---|---|---|---|---|---|
| Number of families | 1 | | | | |
| Number of comparisons per family | 3 | | | | |
| Alpha | 0.05 | | | | |
| | | | | | |
| Tukey's multiple comparisons test | Mean Diff. | 95.00% CI of diff. | Significant? | Summary | Adjusted P Value |
| | | | | | |
| PBS vs. rM5 | -6.999 | -12.35 to -1.651 | Yes | * | 0.0104 |
| PBS vs. Stg480 | -11.2 | -16.55 to -5.85 | Yes | *** | 0.0002 |
| rM5 vs. Stg480 | -4.199 | -9.547 to 1.149 | No | ns | 0.1369 |

Panel B (long term exp.): Normality test and Tukey's multiple comparisons test

| Col. stats | A |
|---|---|
| | Normality |
| | Y |
| Number of values | 15 |
| | |
| D'Agostino & Pearson normality test | |
| K2 | 2.228 |
| P value | 0.3283 |
| Passed normality test (alpha=0.05)? | Yes |
| P value summary | ns |

1way ANOVA
Multiple comparisons

| | | | | | |
|---|---|---|---|---|---|
| Number of families | 1 | | | | |
| Number of comparisons per family | 3 | | | | |
| Alpha | 0.05 | | | | |
| | | | | | |
| Tukey's multiple comparisons test | Mean Diff. | 95.00% CI of diff. | Significant? | Summary | Adjusted P Value |
| | | | | | |
| PBS vs. rM5 | -9.544 | -13.87 to -5.22 | Yes | *** | 0.0002 |
| PBS vs. Stg480 | -11.26 | -15.59 to -6.94 | Yes | **** | <0.0001 |
| rM5 vs. Stg480 | -1.72 | -6.044 to 2.604 | No | ns | 0.5546 |

## 6.3 Statistical analysis of Figure 6.3

Panel A (short term exp.): Normality test and Tukey's multiple comparisons test

| Col. stats | A |
|---|---|
| | Normality Post |
| | Y |
| Number of values | 20 |
| | |
| D'Agostino & Pearson normality test | |
| K2 | 0.2296 |
| P value | 0.8915 |
| Passed normality test (alpha=0.05)? | Yes |
| P value summary | ns |

| 1way ANOVA<br>Multiple comparisons | | | | | |
|---|---|---|---|---|---|
| Number of families | 1 | | | | |
| Number of comparisons per family | 3 | | | | |
| Alpha | 0.05 | | | | |
| | | | | | |
| Tukey's multiple comparisons test | Mean Diff. | 95.00% CI of diff. | Significant? | Summary | Adjusted P Value |
| | | | | | |
| Post-PBS vs. Post-GAS | -5.343 | -7.99 to -2.696 | Yes | *** | 0.0002 |
| Post-PBS vs. Post-GGS | -4.152 | -6.907 to -1.397 | Yes | ** | 0.0034 |
| Post-GAS vs. Post-GGS | 1.19 | -1.564 to 3.945 | No | ns | 0.5219 |

Panel A (long term exp.): Normality test and Tukey's multiple comparisons test

| Col. stats | A |
|---|---|
| | Normality Post |
| | Y |
| Number of values | 23 |
| | |
| D'Agostino & Pearson normality test | |
| K2 | 1.291 |
| P value | 0.5245 |
| Passed normality test (alpha=0.05)? | Yes |
| P value summary | ns |

| 1way ANOVA<br>Multiple comparisons | | | | | |
|---|---|---|---|---|---|
| Number of families | 1 | | | | |
| Number of comparisons per family | 3 | | | | |
| Alpha | 0.05 | | | | |
| | | | | | |
| Tukey's multiple comparisons test | Mean Diff. | 95.00% CI of diff. | Significant? | Summary | Adjusted P Value |
| | | | | | |
| Cull-P vs. Cull-A | -3.915 | -5.609 to -2.221 | Yes | **** | <0.0001 |
| Cull-P vs. Cull-G | -4.315 | -6.009 to -2.621 | Yes | **** | <0.0001 |
| Cull-A vs. Cull-G | -0.4004 | -2.037 to 1.236 | No | ns | 0.8115 |

Panel B (short term exp.): Normality test and Tukey's multiple comparisons test

| Col. stats | A |
|---|---|
| | Normality Post |
| | Y |
| Number of values | 18 |
| | |
| D'Agostino & Pearson normality test | |
| K2 | 1.626 |
| P value | 0.4436 |
| Passed normality test (alpha=0.05)? | Yes |
| P value summary | ns |

| 1way ANOVA<br>Multiple comparisons | | | | | |
|---|---|---|---|---|---|
| Number of families | 1 | | | | |
| Number of comparisons per family | 3 | | | | |
| Alpha | 0.05 | | | | |
| | | | | | |
| Tukey's multiple comparisons test | Mean Diff. | 95.00% CI of diff. | Significant? | Summary | Adjusted P Value |
| | | | | | |
| PBS-Post vs. rM5-Post | -5.383 | -6.643 to -4.124 | Yes | **** | <0.0001 |
| PBS-Post vs. rGGSm-Post | -4.25 | -5.509 to -2.991 | Yes | **** | <0.0001 |
| rM5-Post vs. rGGSm-Post | 1.133 | -0.1259 to 2.393 | No | ns | 0.0810 |

Panel B (long term exp.): Normality test and Tukey's multiple comparisons test

| Col. stats | A |
|---|---|
| | Normality Post |
| | Y |
| Number of values | 15 |
| | |
| D'Agostino & Pearson normality test | |
| K2 | 3.66 |
| P value | 0.1604 |
| Passed normality test (alpha=0.05)? | Yes |
| P value summary | ns |

| 1way ANOVA<br>Multiple comparisons | | | | | |
|---|---|---|---|---|---|
| Number of families | 1 | | | | |
| Number of comparisons per family | 3 | | | | |
| Alpha | 0.05 | | | | |
| | | | | | |
| Tukey's multiple comparisons test | Mean Diff. | 95.00% CI of diff. | Significant? | Summary | Adjusted P Value |
| | | | | | |
| PBS-Cull vs. rM5-Cull | -3.455 | -4.56 to -2.349 | Yes | **** | <0.0001 |
| PBS-Cull vs. rGGSm-Cull | -3.54 | -4.645 to -2.434 | Yes | **** | <0.0001 |
| rM5-Cull vs. rGGSm-Cull | -0.08506 | -1.19 to 1.02 | No | ns | 0.9771 |

## 6.4 Statistical analysis of Figure 6.4

Panel A (whole killed exp.): Normality test and Tukey's multiple comparisons test

| Col. stats | A |
|---|---|
| | Normality |
| | Y |
| Number of values | 22 |
| | |
| D'Agostino & Pearson normality test | |
| K2 | 2.782 |
| P value | 0.2488 |
| Passed normality test (alpha=0.05)? | Yes |
| P value summary | ns |

| 1way ANOVA<br>Multiple comparisons | | | | | |
|---|---|---|---|---|---|
| Number of families | 1 | | | | |
| Number of comparisons per family | 3 | | | | |
| Alpha | 0.05 | | | | |
| | | | | | |
| Tukey's multiple comparisons test | Mean Diff. | 95.00% CI of diff. | Significant? | Summary | Adjusted P Value |
| | | | | | |
| PBS vs. GAS | -2.286 | -3.293 to -1.279 | Yes | **** | <0.0001 |
| PBS vs. GGS | -2.714 | -3.754 to -1.674 | Yes | **** | <0.0001 |
| GAS vs. GGS | -0.4286 | -1.435 to 0.5783 | No | ns | 0.5368 |

Panel B (M-protein exp.): Normality test and Tukey's multiple comparisons test

| Col. stats | A |
|---|---|
| | Normality |
| | Y |
| Number of values | 15 |
| | |
| D'Agostino & Pearson normality test | |
| K2 | 3.593 |
| P value | 0.1659 |
| Passed normality test (alpha=0.05)? | Yes |
| P value summary | ns |

1way ANOVA
Multiple comparisons

| | | | | | |
|---|---|---|---|---|---|
| Number of families | 1 | | | | |
| Number of comparisons per family | 3 | | | | |
| Alpha | 0.05 | | | | |
| | | | | | |
| Tukey's multiple comparisons test | Mean Diff. | 95.00% CI of diff. | Significant? | Summary | Adjusted P Value |
| | | | | | |
| PBS vs. rM5 | -3 | -3.924 to -2.076 | Yes | **** | <0.0001 |
| PBS vs. rGGSm | -3.2 | -4.124 to -2.276 | Yes | **** | <0.0001 |
| rM5 vs. rGGSm | -0.2 | -1.124 to 0.7242 | No | ns | 0.8345 |

## 6.5 Statistical analysis of Supplementary Figure 6.1

Short term exp.: Normality test and Tukey's multiple comparisons test

| Col. stats | A |
|---|---|
| | Normality check |
| | Y |
| Number of values | 15 |
| | |
| D'Agostino & Pearson normality test | |
| K2 | 4.707 |
| P value | 0.0950 |
| Passed normality test (alpha=0.05)? | Yes |
| P value summary | ns |

1way ANOVA
Multiple comparisons

| | | | | | |
|---|---|---|---|---|---|
| Number of families | 1 | | | | |
| Number of comparisons per family | 3 | | | | |
| Alpha | 0.05 | | | | |
| | | | | | |
| Tukey's multiple comparisons test | Mean Diff. | 95.00% CI of diff. | Significant? | Summary | Adjusted P Value |
| | | | | | |
| PBS vs. rM5 | -5.2 | -6.677 to -3.723 | Yes | **** | <0.0001 |
| PBS vs. rGGSm | -6 | -7.477 to -4.523 | Yes | **** | <0.0001 |
| rM5 vs. rGGSm | -0.8 | -2.277 to 0.6774 | No | ns | 0.3504 |

Long term exp.: Normality test and Tukey's multiple comparisons test

| Col. stats | A |
|---|---|
| | Normality check |
| | Y |
| Number of values | 15 |
| | |
| D'Agostino & Pearson normality test | |
| K2 | 2.705 |
| P value | 0.2586 |
| Passed normality test (alpha=0.05)? | Yes |
| P value summary | ns |

1way ANOVA
Multiple comparisons

| | | | | | |
|---|---|---|---|---|---|
| Number of families | 1 | | | | |
| Number of comparisons per family | 3 | | | | |
| Alpha | 0.05 | | | | |
| | | | | | |
| Tukey's multiple comparisons test | Mean Diff. | 95.00% CI of diff. | Significant? | Summary | Adjusted P Value |
| | | | | | |
| PBS vs. rM5 | -5.8 | -7.867 to -3.733 | Yes | **** | <0.0001 |
| PBS vs. Stg480 | -5.2 | -7.267 to -3.133 | Yes | **** | <0.0001 |
| rM5 vs. Stg480 | 0.6 | -1.467 to 2.667 | No | ns | 0.7250 |

## 6.6 Statistical analysis of Supplementary Figure 6.2

Short term exp.: Normality test and Tukey's multiple comparisons test

| Col. stats | A |
|---|---|
| | Normality |
| | Y |
| Number of values | 15 |
| | |
| D'Agostino & Pearson normality test | |
| K2 | 5.011 |
| P value | 0.0816 |
| Passed normality test (alpha=0.05)? | Yes |
| P value summary | ns |

1way ANOVA
Multiple comparisons

| | | | | | |
|---|---|---|---|---|---|
| Number of families | 1 | | | | |
| Number of comparisons per family | 3 | | | | |
| Alpha | 0.05 | | | | |
| | | | | | |
| Tukey's multiple comparisons test | Mean Diff. | 95.00% CI of diff. | Significant? | Summary | Adjusted P Value |
| | | | | | |
| PBS vs. rM5 | -10.1 | -15.82 to -4.376 | Yes | ** | 0.0014 |
| PBS vs. Stg480 | -12.27 | -18 to -6.55 | Yes | *** | 0.0003 |
| rM5 vs. Stg480 | -2.174 | -7.897 to 3.549 | No | ns | 0.5829 |

Long term exp.: Normality test and Tukey's multiple comparisons test

| Col. stats | A |
|---|---|
| | Normality |
| | Y |
| Number of values | 15 |
| | |
| D'Agostino & Pearson normality test | |
| K2 | 3.701 |
| P value | 0.1572 |
| Passed normality test (alpha=0.05)? | Yes |
| P value summary | ns |

1way ANOVA
Multiple comparisons

| | | | | | |
|---|---|---|---|---|---|
| Number of families | 1 | | | | |
| Number of comparisons per family | 3 | | | | |
| Alpha | 0.05 | | | | |
| | | | | | |
| Tukey's multiple comparisons test | Mean Diff. | 95.00% CI of diff. | Significant? | Summary | Adjusted P Value |
| | | | | | |
| PBS vs. rM5 | -11.87 | -15.5 to -8.24 | Yes | **** | <0.0001 |
| PBS vs. Stg480 | -13.17 | -16.8 to -9.542 | Yes | **** | <0.0001 |
| rM5 vs. Stg480 | -1.302 | -4.932 to 2.328 | No | ns | 0.6164 |

## 6.7 Statistical analysis of Supplementary Figure 6.3

Short term exp.: Normality test and Tukey's multiple comparisons test

| Col. stats | A |
|---|---|
| | Normality check |
| | Y |
| Number of values | 15 |
| | |
| D'Agostino & Pearson normality test | |
| K2 | 1.672 |
| P value | 0.4335 |
| Passed normality test (alpha=0.05)? | Yes |
| P value summary | ns |

| 1way ANOVA<br>Multiple comparisons | | | | | |
|---|---|---|---|---|---|
| Number of families | 1 | | | | |
| Number of comparisons per family | 3 | | | | |
| Alpha | 0.05 | | | | |
| | | | | | |
| Tukey's multiple comparisons test | Mean Diff. | 95.00% CI of diff. | Significant? | Summary | Adjusted P Value |
| | | | | | |
| PBS-Post vs. rM5-Post | -4.169 | -6.423 to -1.916 | Yes | *** | 0.0009 |
| PBS-Post vs. rGGSm-Post | -4.009 | -6.262 to -1.755 | Yes | ** | 0.0013 |
| rM5-Post vs. rGGSm-Post | 0.1607 | -2.093 to 2.414 | No | ns | 0.9803 |

Long term exp.: Normality test and Tukey's multiple comparisons test

| Col. stats | A |
|---|---|
| | Normality check |
| | Y |
| Number of values | 15 |
| | |
| D'Agostino & Pearson normality test | |
| K2 | 1.611 |
| P value | 0.4469 |
| Passed normality test (alpha=0.05)? | Yes |
| P value summary | ns |

| 1way ANOVA<br>Multiple comparisons | | | | | |
|---|---|---|---|---|---|
| Number of families | 1 | | | | |
| Number of comparisons per family | 3 | | | | |
| Alpha | 0.05 | | | | |
| | | | | | |
| Tukey's multiple comparisons test | Mean Diff. | 95.00% CI of diff. | Significant? | Summary | Adjusted P Value |
| | | | | | |
| PBS-Cull vs. rM5-Cull | -4.253 | -6.765 to -1.741 | Yes | ** | 0.0019 |
| PBS-Cull vs. rGGSm-Cull | -5.087 | -7.599 to -2.576 | Yes | *** | 0.0004 |
| rM5-Cull vs. rGGSm-Cull | -0.8344 | -3.346 to 1.677 | No | ns | 0.6587 |

## APPENDIX 7

## SUPPLEMENTARY FIGURES AND STATISTICFAL ANALYSIS OF CHAPTER 7

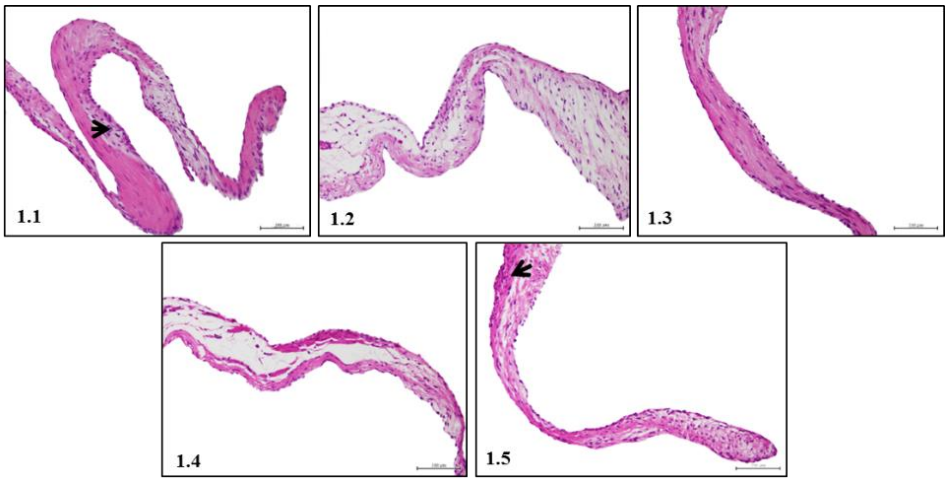


**Supplementary Figure 7.1A** H&E stained sections of mitral valves from rats injected with PBS (heterologous boost short term exp., 35 days). Magnifications 200×. Arrows (→) indicate inflammatory foci.

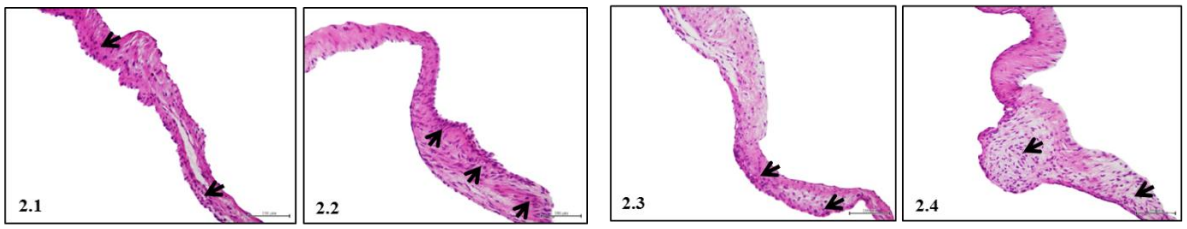


**Supplementary Figure 7.1B** H&E stained sections of mitral valves from rats primed with GAS rM5 and boosted with GGS Stg480 (heterologous boost short term exp., 35 days). Magnifications 200×. Arrows (→) indicate inflammatory foci.

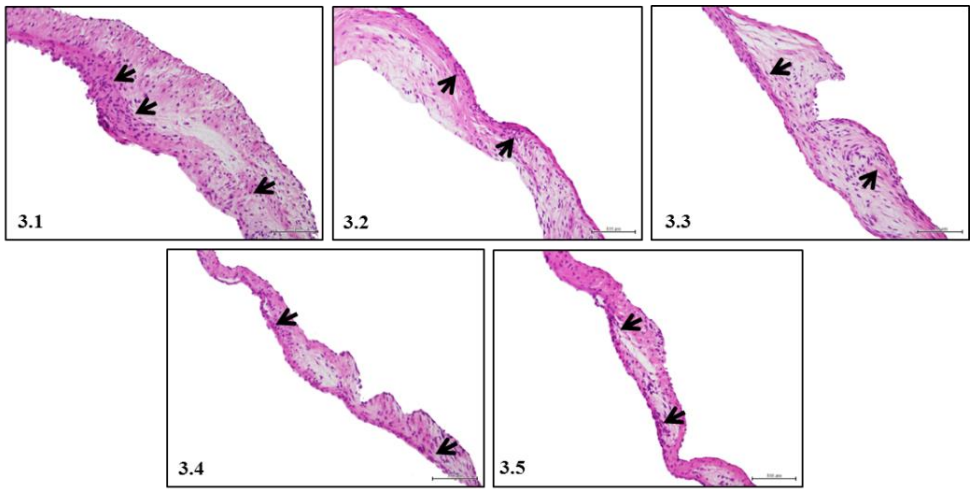


**Supplementary Figure 7.1C** H&E stained sections of mitral valves from rats primed with GGS Stg480 and boosted with GAS rM5 (heterologous boost short term exp., 35 days). Magnifications 200×. Arrows (→) indicate inflammatory foci.

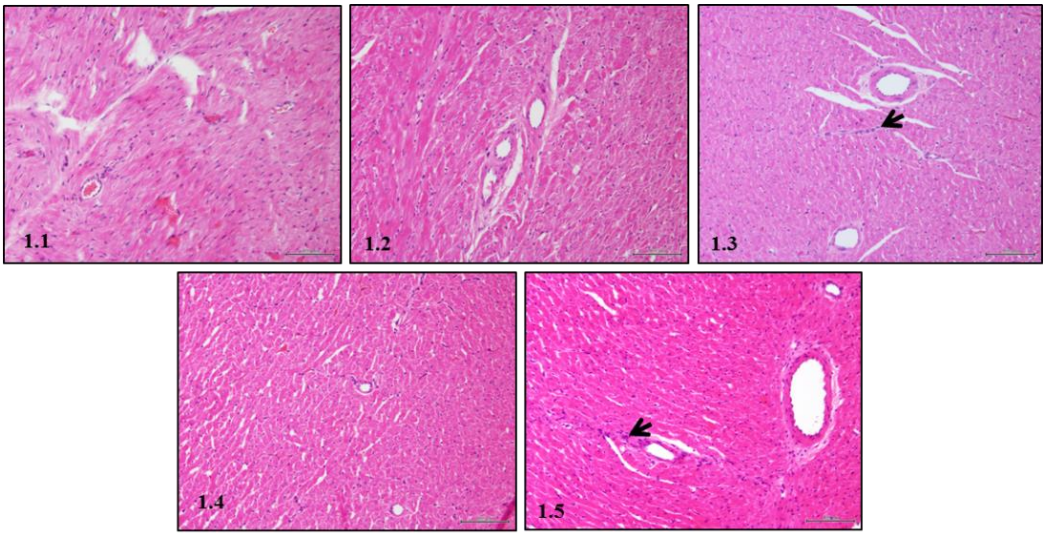


**Supplementary Figure 7.1D** H&E stained sections of myocardium from rats injected with PBS (heterologous boost short term exp., 35 days). Magnifications 200×. Arrows (→) indicate inflammatory foci.

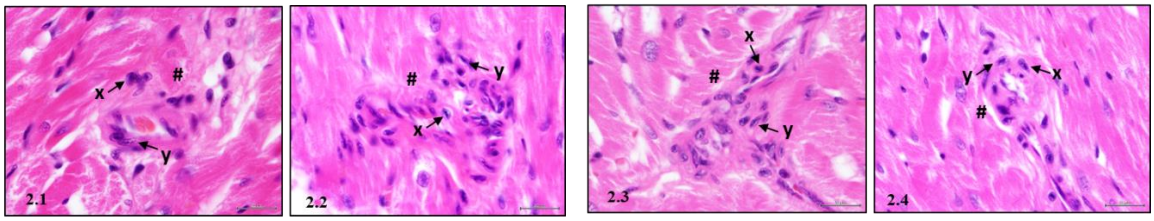


**Supplementary Figure 7.1E** H&E stained sections of myocardium from rats primed with GAS rM5 and boosted with GGS Stg480 (heterologous boost short term exp., 35 days). Magnifications 1000×. 'Aschoff nodule like' structure indicated by asterisk (#), x: Anitschkow like cells, y: Aschoff like cells.

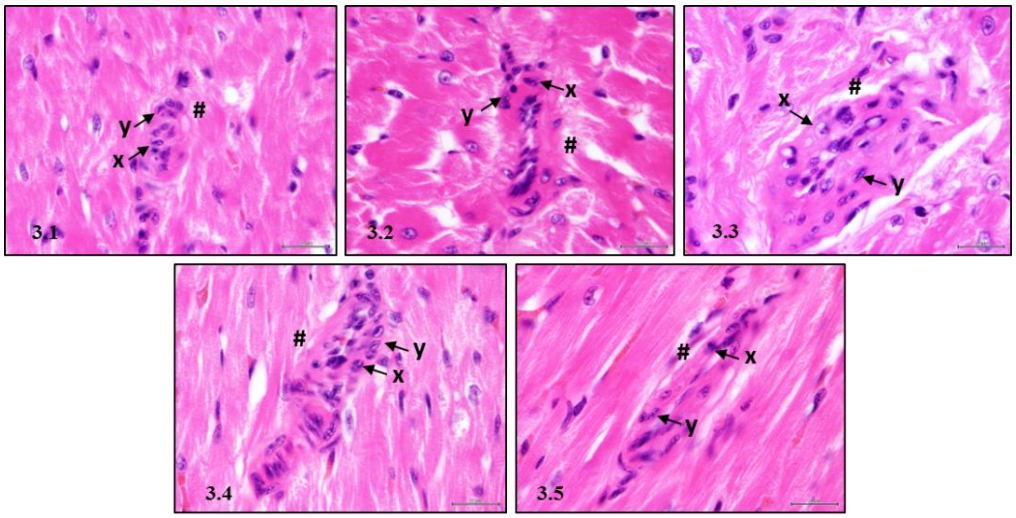


**Supplementary Figure 7.1F** H&E stained sections of myocardium from rats primed with GGS Stg480 and boosted with GAS rM5 (heterologous boost short term exp., 35 days). Magnifications 1000×. 'Aschoff nodule like' structure indicated by asterisk (#), x: Anitschkow like cells, y: Aschoff like cells.

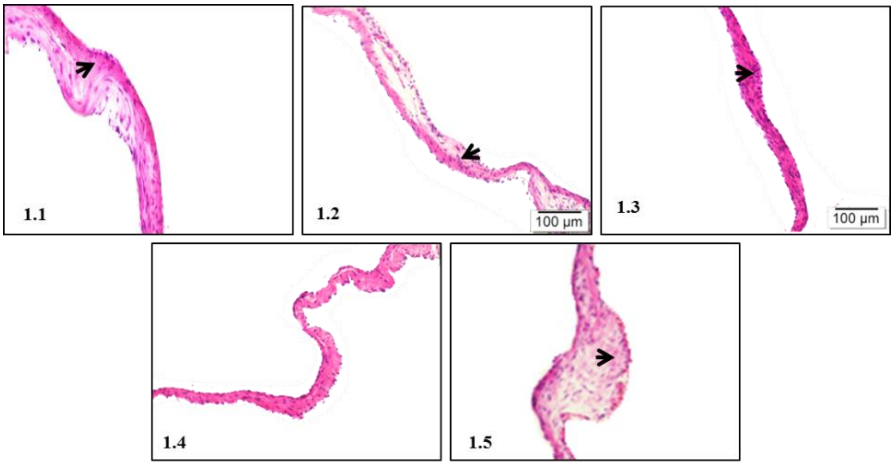


**Supplementary Figure 7.2A** H&E stained sections of mitral valves from rats injected with PBS (heterologous boost long term exp., 180 days). Magnifications 200×. Arrows (→) indicate inflammatory foci.

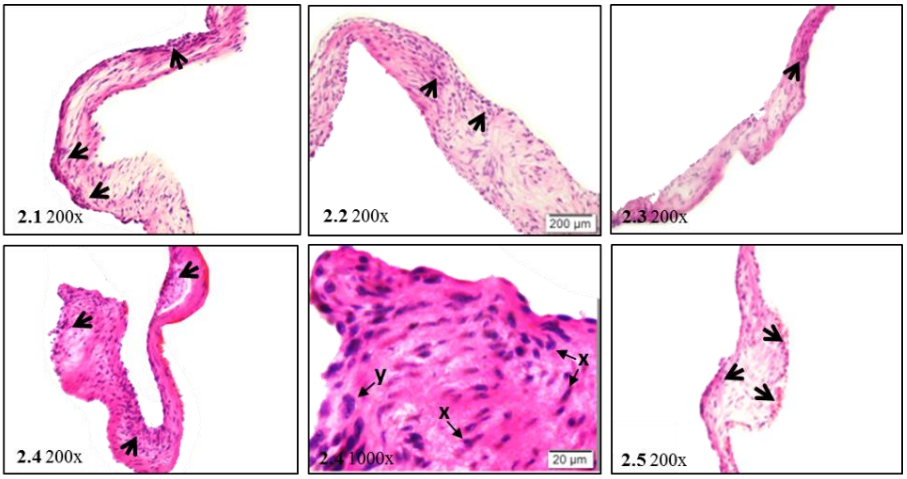


**Supplementary Figure 7.2B** H&E stained sections of mitral valves from rats primed with GAS rM5 and boosted with GGS Stg480 (heterologous boost long term exp., 180 days). Magnifications as indicated. x: Anitschkow like cells, y: Aschoff like cells. Arrows (→) indicate inflammatory foci.

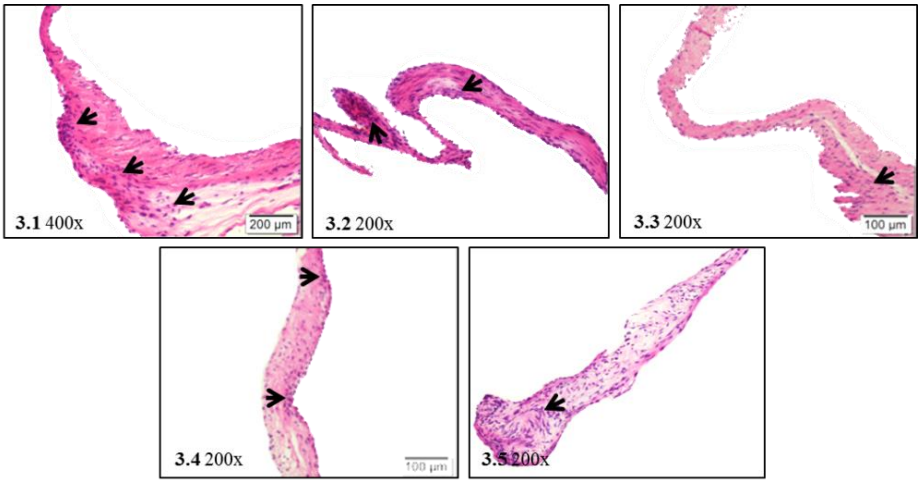


**Supplementary Figure 7.2C** H&E stained sections of mitral valves from rats primed with GGS Stg480 and boosted with GAS rM5 (heterologous boost long term exp., 180 days). Magnifications as indicated. Arrows (→) indicate inflammatory foci.

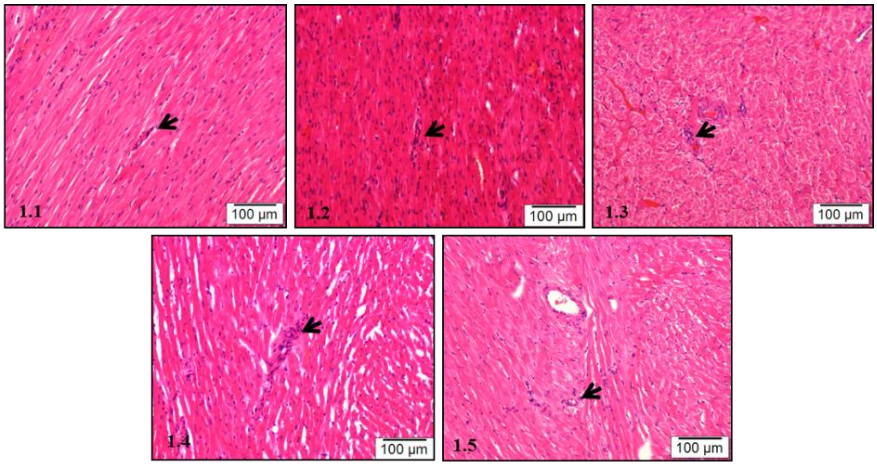


**Supplementary Figure 7.2D** H&E stained sections of myocardium from rats injected with PBS (heterologous boost long term exp., 180 days). Magnifications 200×. Arrows (→) indicate inflammatory foci.

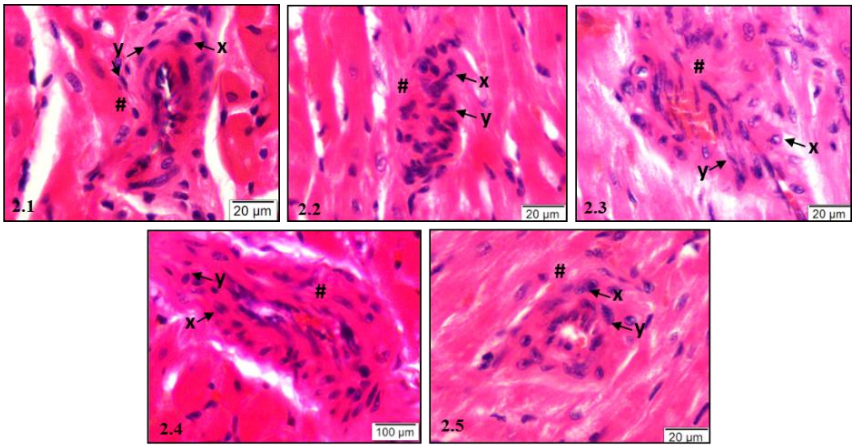


**Supplementary Figure 7.2E** H&E stained sections of myocardium from rats primed with GAS rM5 and boosted with GGS Stg480 (heterologous boost long term exp., 180 days). Magnifications 1000×. 'Aschoff nodule like' structure indicated by asterisk (#), x: Anitschkow like cells, y: Aschoff like cells.

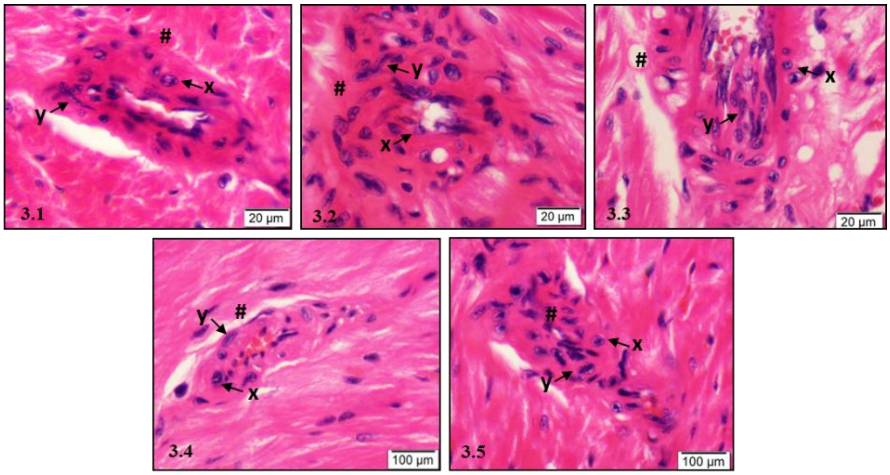


**Supplementary Figure 7.2F** H&E stained sections of myocardium from rats primed with GGS Stg480 and boosted with GAS rM5 (heterologous boost long term exp., 180 days). Magnifications 1000×. 'Aschoff nodule like' structure indicated by asterisk (#), x: Anitschkow like cells, y: Aschoff like cells.

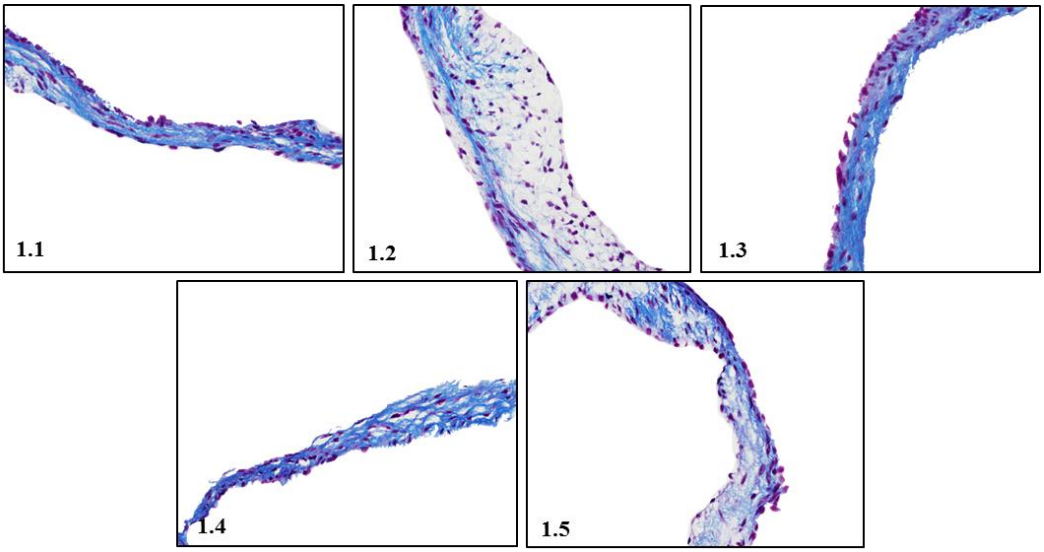


**Supplementary Figure 7.3A** Masson's trichrome stained sections of mitral valves from rats injected with PBS (heterologous boost short term exp., 35 days). Magnifications 400×. Blue colour indicates collagen fibre deposition.

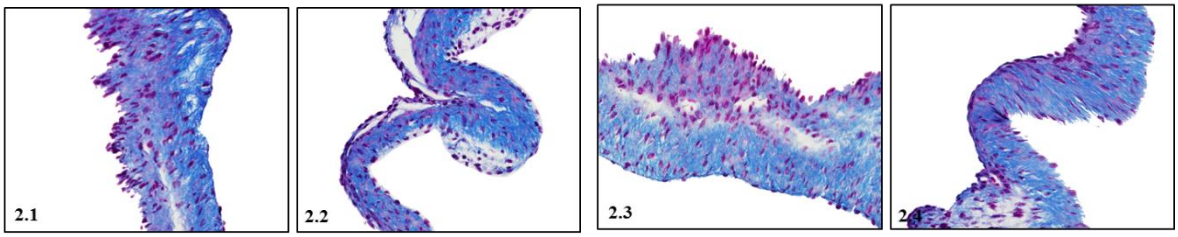


**Supplementary Figure 7.3B** Masson's trichrome stained sections of mitral valves from rats primed with GAS rM5 and boosted with GGS Stg480 (heterologous boost short term exp., 35 days). Magnifications 400×. Blue colour indicates collagen fibre deposition.

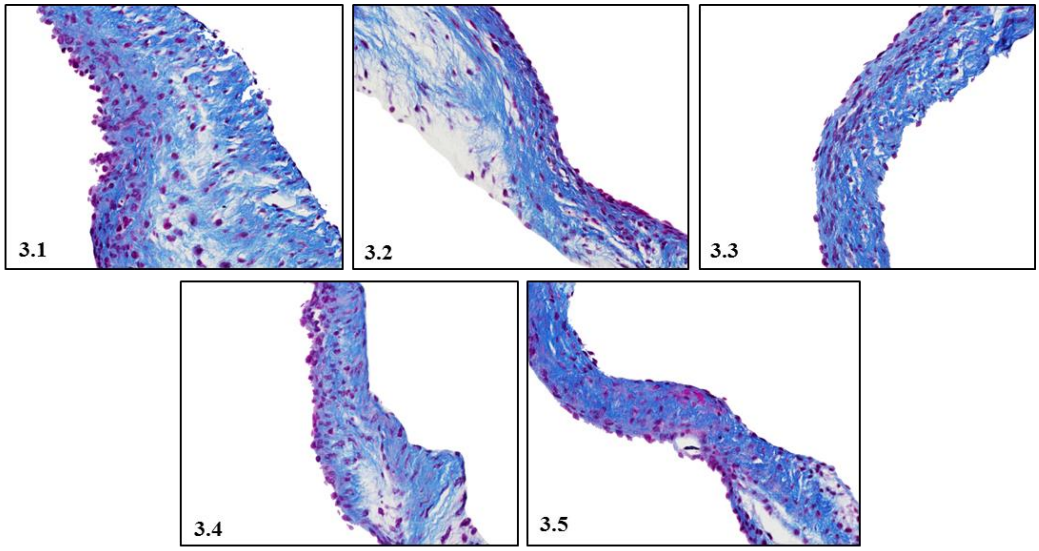


**Supplementary Figure 7.3C** Masson's trichrome stained sections of mitral valves from rats primed with GGS Stg480 and boosted with GAS rM5 (heterologous boost short term exp., 35 days). Magnifications 400×. Blue colour indicates collagen fibre deposition.

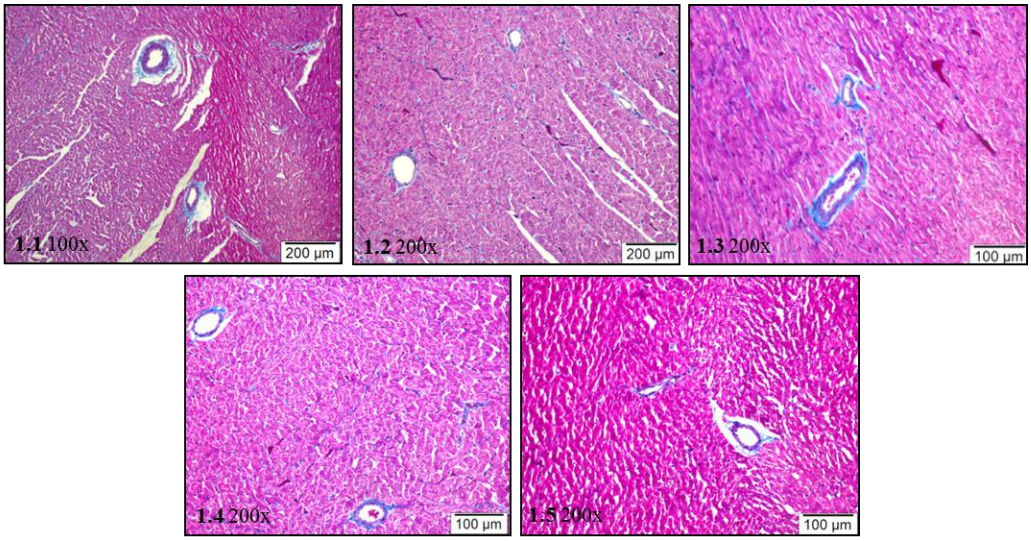


**Supplementary Figure 7.3D** Masson's trichrome stained sections of myocardium from rats injected with PBS (heterologous boost short term exp., 35 days). Magnifications as indicated. Blue colour indicates collagen fibre deposition.

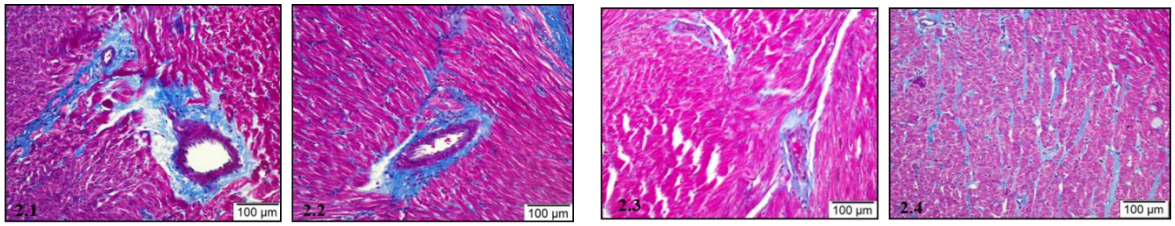


**Supplementary Figure 7.3E** Masson's trichrome stained sections of myocardium from rats primed with GAS rM5 and boosted with GGS Stg480 (heterologous boost short term exp., 35 days). Magnifications 200×. Blue colour indicates collagen fibre deposition.

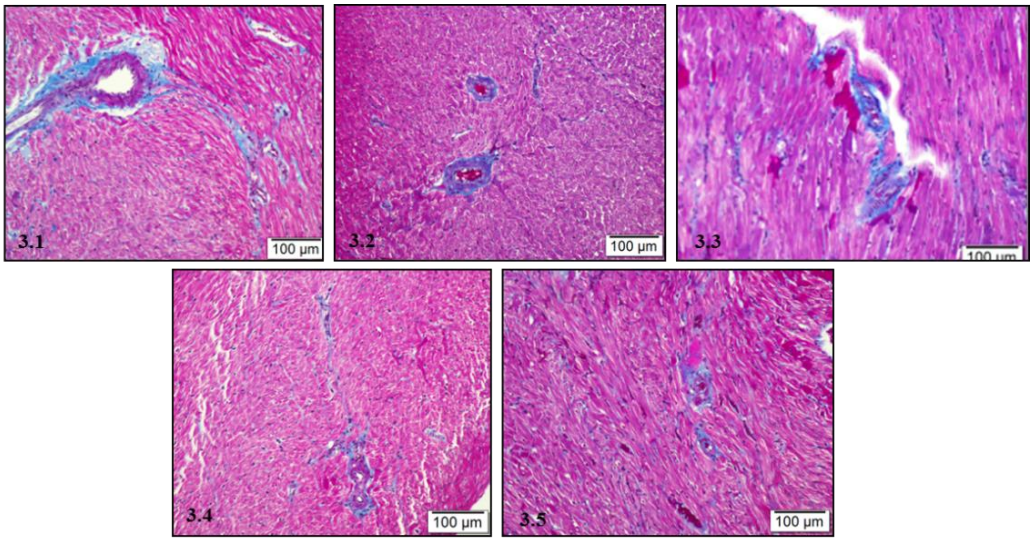


**Supplementary Figure 7.3F** Masson's trichrome stained sections of myocardium from rats primed with GGS Stg480 and boosted with GAS rM5 (heterologous boost short term exp., 35 days). Magnifications 200×. Blue colour indicates collagen fibre deposition.

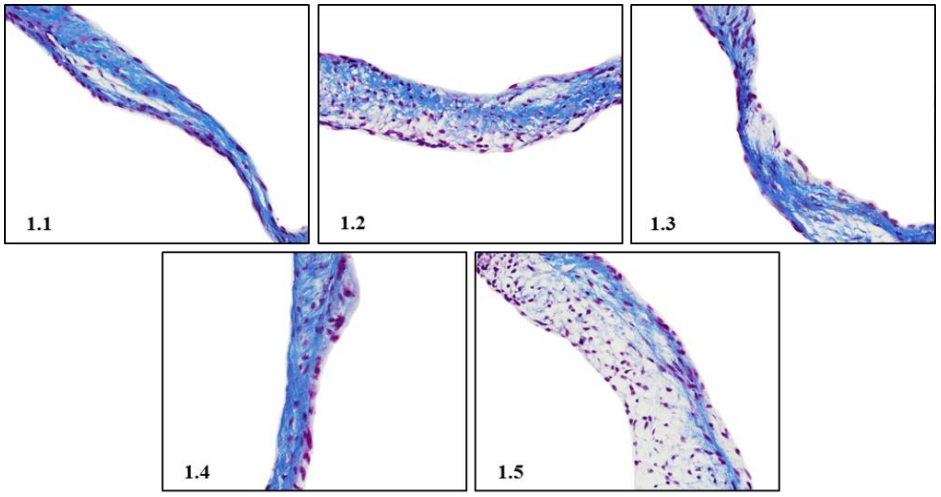


**Supplementary Figure 7.4A** Masson's trichrome stained sections of mitral valves from rats injected with PBS (heterologous boost long term exp., 180 days). Magnifications 400×. Blue colour indicates collagen fibre deposition.

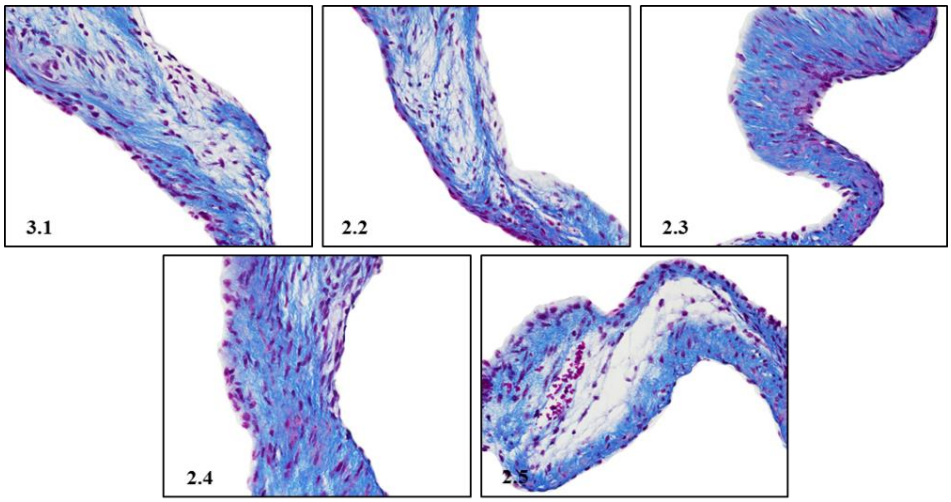


**Supplementary Figure 7.4B** Masson's trichrome stained sections of mitral valves from rats primed with GAS rM5 and boosted with GGS Stg480 (heterologous boost long term exp., 180 days). Magnifications 400×. Blue colour indicates collagen fibre deposition.

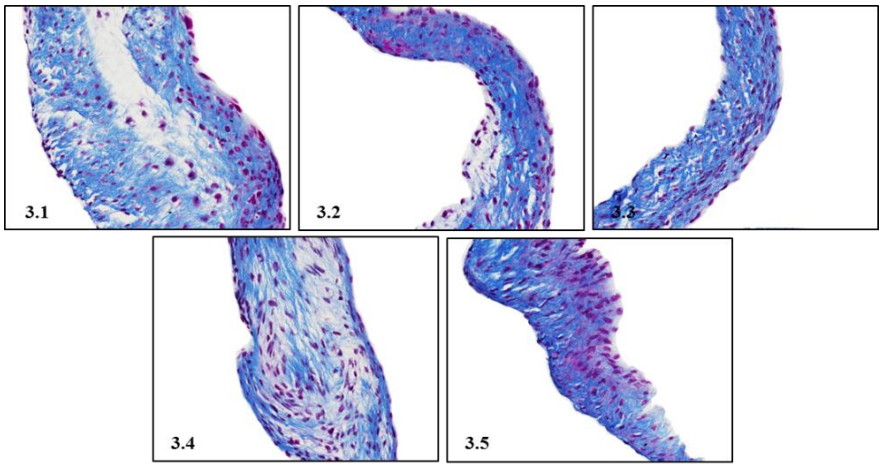


**Supplementary Figure 7.4C** Masson's trichrome stained sections of mitral valves from rats primed with GGS Stg480 and boosted with GAS rM5 (heterologous boost long term exp., 180 days). Magnifications 400×. Blue colour indicates collagen fibre deposition.

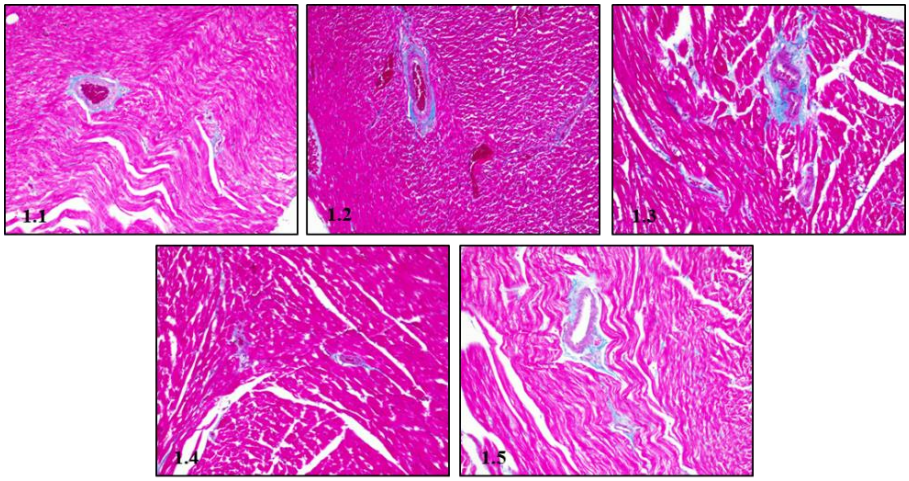


**Supplementary Figure 7.4D** Masson's trichrome stained sections of myocardium from rats injected with PBS (heterologous boost long term exp., 180 days). Magnifications 200×. Blue colour indicates collagen fibre deposition.

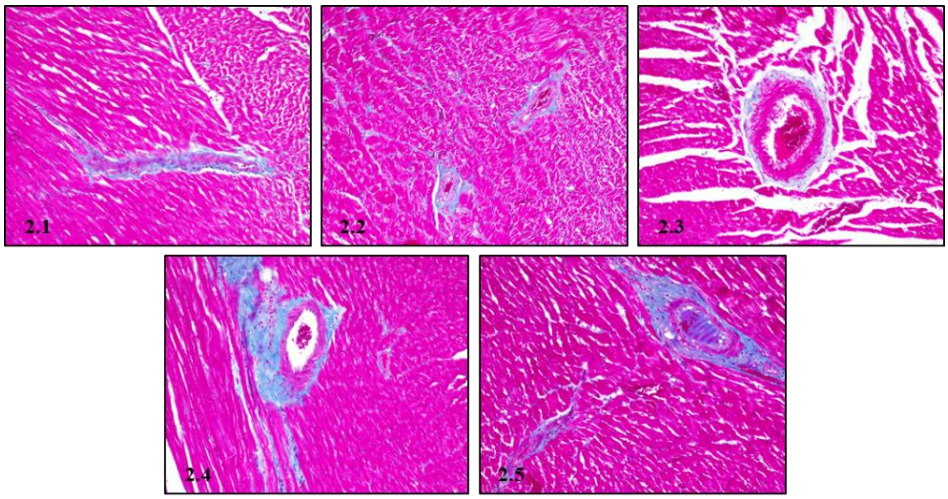


**Supplementary Figure 7.4E** Masson's trichrome stained sections of myocardium from rats primed with GAS rM5 and boosted with GGS Stg480 (heterologous boost long term exp., 180 days). Magnifications 200×. Blue colour indicates collagen fibre deposition.

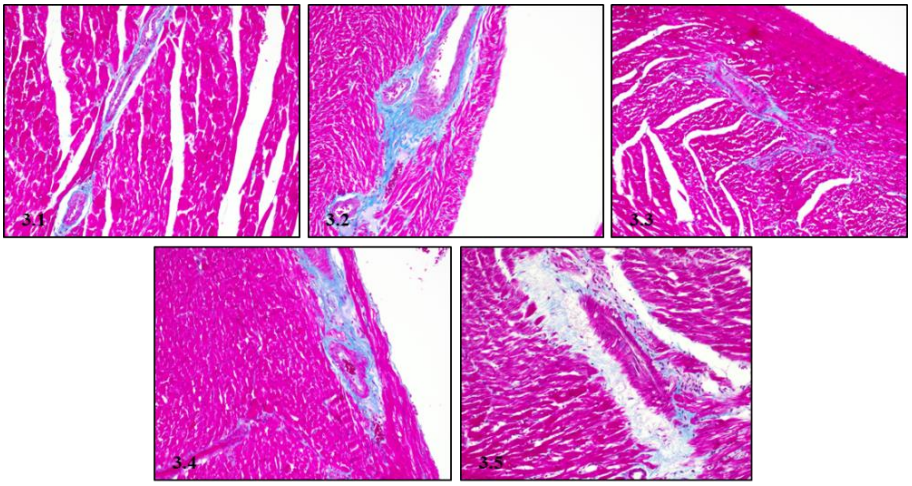


**Supplementary Figure 7.4F** Masson's trichrome stained sections of myocardium from rats primed with GGS Stg480 and boosted with GAS rM5 (heterologous boost long term exp., 180 days). Magnifications 200×. Blue colour indicates collagen fibre deposition.

## 7.1 Statistical analysis of Figure 7.1

Panel A (short term exp.): Normality test and Tukey's multiple comparison test

| Col. stats | A |
|---|---|
| | Normality rM5 |
| | Y |
| Number of values | 14 |
| | |
| D'Agostino & Pearson normality test | |
| K2 | 4.093 |
| P value | 0.1292 |
| Passed normality test (alpha=0.05)? | Yes |
| P value summary | ns |

1way ANOVA
Multiple comparisons

| | | | | | |
|---|---|---|---|---|---|
| Number of families | 1 | | | | |
| Number of comparisons per family | 3 | | | | |
| Alpha | 0.05 | | | | |
| | | | | | |
| Tukey's multiple comparisons test | Mean Diff. | 95.00% CI of diff. | Significant? | Summary | Adjusted P Value |
| | | | | | |
| PBS vs. rM5 | -2.122 | -2.549 to -1.695 | Yes | **** | <0.0001 |
| PBS vs. rGGSm | -1.024 | -1.426 to -0.6207 | Yes | **** | <0.0001 |
| rM5 vs. rGGSm | 1.099 | 0.6716 to 1.526 | Yes | **** | <0.0001 |

Panel A (long term exp.): Normality test and Tukey's multiple comparison test

| Col. stats | A |
|---|---|
| | Normality rM5 |
| | Y |
| Number of values | 15 |
| | |
| D'Agostino & Pearson normality test | |
| K2 | 1.751 |
| P value | 0.4167 |
| Passed normality test (alpha=0.05)? | Yes |
| P value summary | ns |

1way ANOVA
Multiple comparisons

| | | | | | |
|---|---|---|---|---|---|
| Number of families | 1 | | | | |
| Number of comparisons per family | 3 | | | | |
| Alpha | 0.05 | | | | |
| | | | | | |
| Tukey's multiple comparisons test | Mean Diff. | 95.00% CI of diff. | Significant? | Summary | Adjusted P Value |
| | | | | | |
| PBS vs. rM5 | -0.4214 | -0.7684 to -0.07443 | Yes | * | 0.0180 |
| PBS vs. rGGSm | -0.9633 | -1.31 to -0.6163 | Yes | **** | <0.0001 |
| rM5 vs. rGGSm | -0.5419 | -0.8888 to -0.1949 | Yes | ** | 0.0035 |

Panel B (short term exp.): Normality test and Tukey's multiple comparison test

| Col. stats | A |
|---|---|
| | Normality Stg |
| | Y |
| Number of values | 14 |
| | |
| D'Agostino & Pearson normality test | |
| K2 | 3.182 |
| P value | 0.2037 |
| Passed normality test (alpha=0.05)? | Yes |
| P value summary | ns |

1way ANOVA
Multiple comparisons

| | | | | | |
|---|---|---|---|---|---|
| Number of families | 1 | | | | |
| Number of comparisons per family | 3 | | | | |
| Alpha | 0.05 | | | | |
| | | | | | |
| Tukey's multiple comparisons test | Mean Diff. | 95.00% CI of diff. | Significant? | Summary | Adjusted P Value |
| | | | | | |
| PBS vs. rM5 | -0.9182 | -1.55 to -0.2866 | Yes | ** | 0.0061 |
| PBS vs. rGGSm | -0.9633 | -1.559 to -0.3679 | Yes | ** | 0.0029 |
| rM5 vs. rGGSm | -0.04515 | -0.6767 to 0.5864 | No | ns | 0.9797 |

Panel B (long term exp.): Normality test and Tukey's multiple comparison test

| Col. stats | A |
|---|---|
| | Normality Stg |
| | Y |
| Number of values | 15 |
| | |
| D'Agostino & Pearson normality test | |
| K2 | 2.879 |
| P value | 0.2370 |
| Passed normality test (alpha=0.05)? | Yes |
| P value summary | ns |

1way ANOVA
Multiple comparisons

| | | | | | |
|---|---|---|---|---|---|
| Number of families | 1 | | | | |
| Number of comparisons per family | 3 | | | | |
| Alpha | 0.05 | | | | |
| | | | | | |
| Tukey's multiple comparisons test | Mean Diff. | 95.00% CI of diff. | Significant? | Summary | Adjusted P Value |
| | | | | | |
| PBS vs. rM5 | -1.325 | -1.684 to -0.9654 | Yes | **** | <0.0001 |
| PBS vs. rGGSm | -0.7827 | -1.142 to -0.4236 | Yes | *** | 0.0002 |
| rM5 vs. rGGSm | 0.5418 | 0.1827 to 0.901 | Yes | ** | 0.0044 |

Panel C (short term exp.): Normality test and Tukey's multiple comparison test

| Col. stats | A |
|---|---|
| | Normlality rM5 |
| | Y |
| Number of values | 15 |
| | |
| D'Agostino & Pearson normality test | |
| K2 | 3.971 |
| P value | 0.1373 |
| Passed normality test (alpha=0.05)? | Yes |
| P value summary | ns |

1way ANOVA
Multiple comparisons

| | | | | | |
|---|---|---|---|---|---|
| Number of families | 1 | | | | |
| Number of comparisons per family | 3 | | | | |
| Alpha | 0.05 | | | | |
| | | | | | |
| Tukey's multiple comparisons test | Mean Diff. | 95.00% CI of diff. | Significant? | Summary | Adjusted P Value |
| | | | | | |
| PBS-rM5 vs. rM5-rGGSm | -3.462 | -3.871 to -3.052 | Yes | **** | <0.0001 |
| PBS-rM5 vs. rGGSm-rM5 | -3.131 | -3.517 to -2.745 | Yes | **** | <0.0001 |
| rM5-rGGSm vs. rGGSm-rM5 | 0.3311 | -0.07833 to 0.7406 | No | ns | 0.1181 |

Panel C (long term exp.): Normality test and Tukey's multiple comparison test

| Col. stats | A |
|---|---|
| | Normality rM5 |
| | Y |
| Number of values | 15 |
| | |
| D'Agostino & Pearson normality test | |
| K2 | 3.971 |
| P value | 0.1373 |
| Passed normality test (alpha=0.05)? | Yes |
| P value summary | ns |

| 1way ANOVA<br>Multiple comparisons | | | | | |
|---|---|---|---|---|---|
| Number of families | 1 | | | | |
| Number of comparisons per family | 3 | | | | |
| Alpha | 0.05 | | | | |
| | | | | | |
| Tukey's multiple comparisons test | Mean Diff. | 95.00% CI of diff. | Significant? | Summary | Adjusted P Value |
| | | | | | |
| PBS-rM5 vs. rM5-rGGSm | -2.167 | -2.986 to -1.348 | Yes | **** | <0.0001 |
| PBS-rM5 vs. rGGSm-rM5 | -1.866 | -2.685 to -1.047 | Yes | *** | 0.0002 |
| rM5-rGGSm vs. rGGSm-rM5 | 0.301 | -0.518 to 1.12 | No | ns | 0.6023 |

Panel D (short term exp.): Normality test and Tukey's multiple comparison test

| Col. stats | A |
|---|---|
| | Normality Stg |
| | Y |
| Number of values | 15 |
| | |
| D'Agostino & Pearson normality test | |
| K2 | 3.088 |
| P value | 0.2135 |
| Passed normality test (alpha=0.05)? | Yes |
| P value summary | ns |

| 1way ANOVA<br>Multiple comparisons | | | | | |
|---|---|---|---|---|---|
| Number of families | 1 | | | | |
| Number of comparisons per family | 3 | | | | |
| Alpha | 0.05 | | | | |
| | | | | | |
| Tukey's multiple comparisons test | Mean Diff. | 95.00% CI of diff. | Significant? | Summary | Adjusted P Value |
| | | | | | |
| PBS-rGGSm vs. rM5-rGGSm | -3.477 | -3.891 to -3.063 | Yes | **** | <0.0001 |
| PBS-rGGSm vs. rGGSm-rM5 | -3.913 | -4.304 to -3.523 | Yes | **** | <0.0001 |
| rM5-rGGSm vs. rGGSm-rM5 | -0.4365 | -0.8509 to -0.0221 | Yes | * | 0.0391 |

Panel D (long term exp.): Normality test and Tukey's multiple comparison test

| Col. stats | A |
|---|---|
| | Normality Stg |
| | Y |
| Number of values | 15 |
| | |
| D'Agostino & Pearson normality test | |
| K2 | 3.088 |
| P value | 0.2135 |
| Passed normality test (alpha=0.05)? | Yes |
| P value summary | ns |

| 1way ANOVA<br>Multiple comparisons | | | | | |
|---|---|---|---|---|---|
| Number of families | 1 | | | | |
| Number of comparisons per family | 3 | | | | |
| Alpha | 0.05 | | | | |
| | | | | | |
| Tukey's multiple comparisons test | Mean Diff. | 95.00% CI of diff. | Significant? | Summary | Adjusted P Value |
| | | | | | |
| PBS-rGGSm vs. rM5-rGGSm | -2.709 | -3.445 to -1.973 | Yes | **** | <0.0001 |
| PBS-rGGSm vs. rGGSm-rM5 | -2.95 | -3.686 to -2.214 | Yes | **** | <0.0001 |
| rM5-rGGSm vs. rGGSm-rM5 | -0.2408 | -0.9769 to 0.4952 | No | ns | 0.6668 |

## 7.2 Statistical analysis of Figure 7.2

Short term exp.: Normality test and Tukey's multiple comparison test

| Col. stats | A |
|---|---|
| | Normlality CM |
| | Y |
| Number of values | 14 |
| | |
| D'Agostino & Pearson normality test | |
| K2 | 2.825 |
| P value | 0.2436 |
| Passed normality test (alpha=0.05)? | Yes |
| P value summary | ns |

| 1way ANOVA<br>Multiple comparisons | | | | | |
|---|---|---|---|---|---|
| Number of families | 1 | | | | |
| Number of comparisons per family | 3 | | | | |
| Alpha | 0.05 | | | | |
| | | | | | |
| Tukey's multiple comparisons test | Mean Diff. | 95.00% CI of diff. | Significant? | Summary | Adjusted P Value |
| | | | | | |
| PBS-CM vs. rM5-rGGSm | -1.468 | -2.111 to -0.8256 | Yes | *** | 0.0002 |
| PBS-CM vs. rGGSm-rM5 | -0.6287 | -1.235 to -0.02277 | Yes | * | 0.0421 |
| rM5-rGGSm vs. rGGSm-rM5 | 0.8396 | 0.1969 to 1.482 | Yes | * | 0.0121 |

Long term exp.: Normality test and Tukey's multiple comparison test

| Col. stats | A |
|---|---|
| | Normality rM5 |
| | Y |
| Number of values | 15 |
| | |
| D'Agostino & Pearson normality test | |
| K2 | 4.555 |
| P value | 0.1025 |
| Passed normality test (alpha=0.05)? | Yes |
| P value summary | ns |

| 1way ANOVA<br>Multiple comparisons | | | | | |
|---|---|---|---|---|---|
| Number of families | 1 | | | | |
| Number of comparisons per family | 3 | | | | |
| Alpha | 0.05 | | | | |
| | | | | | |
| Tukey's multiple comparisons test | Mean Diff. | 95.00% CI of diff. | Significant? | Summary | Adjusted P Value |
| | | | | | |
| PBS-CM vs. rM5-rGGSm | -0.6891 | -1.028 to -0.35 | Yes | *** | 0.0004 |
| PBS-CM vs. rGGSm-rM5 | -0.5946 | -0.9337 to -0.2555 | Yes | ** | 0.0014 |
| rM5-rGGSm vs. rGGSm-rM5 | 0.0945 | -0.2446 to 0.4336 | No | ns | 0.7431 |

## 7.3 Statistical analysis of Figure 7.3

Panel A (short term exp.): Normality test and Tukey's multiple comparison test

| Col. stats | A |
|---|---|
| | Normality rM5 |
| | Y |
| Number of values | 14 |
| | |
| D'Agostino & Pearson normality test | |
| K2 | 2.03 |
| P value | 0.3624 |
| Passed normality test (alpha=0.05)? | Yes |
| P value summary | ns |

| 1way ANOVA Multiple comparisons | | | | | |
|---|---|---|---|---|---|
| Number of families | 1 | | | | |
| Number of comparisons per family | 3 | | | | |
| Alpha | 0.05 | | | | |
| | | | | | |
| Tukey's multiple comparisons test | Mean Diff. | 95.00% CI of diff. | Significant? | Summary | Adjusted P Value |
| | | | | | |
| PBS vs. rM5 | -1.789 | -3.018 to -0.5595 | Yes | ** | 0.0061 |
| PBS vs. rGGSm | -2.234 | -3.393 to -1.074 | Yes | *** | 0.0008 |
| rM5 vs. rGGSm | -0.4446 | -1.674 to 0.7849 | No | ns | 0.6058 |

Panel A (long term exp.): Normality test and Tukey's multiple comparison test

| Col. stats | A |
|---|---|
| | Normality rM5 |
| | Y |
| Number of values | 14 |
| | |
| D'Agostino & Pearson normality test | |
| K2 | 2.168 |
| P value | 0.3382 |
| Passed normality test (alpha=0.05)? | Yes |
| P value summary | ns |

| 1way ANOVA Multiple comparisons | | | | | |
|---|---|---|---|---|---|
| Number of families | 1 | | | | |
| Number of comparisons per family | 3 | | | | |
| Alpha | 0.05 | | | | |
| | | | | | |
| Tukey's multiple comparisons test | Mean Diff. | 95.00% CI of diff. | Significant? | Summary | Adjusted P Value |
| | | | | | |
| PBS vs. rM5/rGGSm | -3.194 | -5.9 to -0.4872 | Yes | * | 0.0217 |
| PBS vs. rGGSm/rM5 | -6.792 | -9.344 to -4.24 | Yes | **** | <0.0001 |
| rM5/rGGSm vs. rGGSm/rM5 | -3.599 | -6.305 to -0.8922 | Yes | * | 0.0108 |

Panel B (short term exp.): Normality test and Tukey's multiple comparison test

| Col. stats | A |
|---|---|
| | Normality Stg |
| | Y |
| Number of values | 14 |
| | |
| D'Agostino & Pearson normality test | |
| K2 | 0.07223 |
| P value | 0.9645 |
| Passed normality test (alpha=0.05)? | Yes |
| P value summary | ns |

| 1way ANOVA Multiple comparisons | | | | | |
|---|---|---|---|---|---|
| Number of families | 1 | | | | |
| Number of comparisons per family | 3 | | | | |
| Alpha | 0.05 | | | | |
| | | | | | |
| Tukey's multiple comparisons test | Mean Diff. | 95.00% CI of diff. | Significant? | Summary | Adjusted P Value |
| | | | | | |
| PBS vs. rM5/rGGSm | -3.194 | -5.9 to -0.4872 | Yes | * | 0.0217 |
| PBS vs. rGGSm/rM5 | -6.792 | -9.344 to -4.24 | Yes | **** | <0.0001 |
| rM5/rGGSm vs. rGGSm/rM5 | -3.599 | -6.305 to -0.8922 | Yes | * | 0.0108 |

Panel B (long term exp.): Normality test and Tukey's multiple comparison test

| Col. stats | A |
|---|---|
| | Normality Stg |
| | Y |
| Number of values | 14 |
| | |
| D'Agostino & Pearson normality test | |
| K2 | 5.014 |
| P value | 0.0815 |
| Passed normality test (alpha=0.05)? | Yes |
| P value summary | ns |

| 1way ANOVA Multiple comparisons | | | | | |
|---|---|---|---|---|---|
| Number of families | 1 | | | | |
| Number of comparisons per family | 3 | | | | |
| Alpha | 0.05 | | | | |
| | | | | | |
| Tukey's multiple comparisons test | Mean Diff. | 95.00% CI of diff. | Significant? | Summary | Adjusted P Value |
| | | | | | |
| PBS vs. rM5/rGGSm | -5.138 | -8.302 to -1.974 | Yes | ** | 0.0029 |
| PBS vs. rGGSm/rM5 | -11.51 | -14.5 to -8.531 | Yes | **** | <0.0001 |
| rM5/rGGSm vs. rGGSm/rM5 | -6.376 | -9.54 to -3.212 | Yes | *** | 0.0005 |

## 7.4 Statistical analysis of Figure 7.4

Panel A (short term exp.): Normality test and Tukey's multiple comparison test

| Col. stats | A |
|---|---|
| | Normality |
| | Y |
| Number of values | 15 |
| | |
| D'Agostino & Pearson normality test | |
| K2 | 2.408 |
| P value | 0.3000 |
| Passed normality test (alpha=0.05)? | Yes |
| P value summary | ns |

| 1way ANOVA Multiple comparisons | | | | | |
|---|---|---|---|---|---|
| Number of families | 1 | | | | |
| Number of comparisons per family | 3 | | | | |
| Alpha | 0.05 | | | | |
| | | | | | |
| Tukey's multiple comparisons test | Mean Diff. | 95.00% CI of diff. | Significant? | Summary | Adjusted P Value |
| | | | | | |
| PBS-mv vs. rM5/rGGSm | -6.85 | -8.041 to -5.659 | Yes | **** | <0.0001 |
| PBS-mv vs. rGGSm/rM5 | -6.8 | -7.922 to -5.678 | Yes | **** | <0.0001 |
| rM5/rGGSm vs. rGGSm/rM5 | 0.05 | -1.141 to 1.241 | No | ns | 0.9929 |

Panel A (long term exp.): Normality test and Tukey's multiple comparison test

| Col. stats | A |
|---|---|
| | Normality |
| | Y |
| Number of values | 15 |
| | |
| D'Agostino & Pearson normality test | |
| K2 | 2.408 |
| P value | 0.3000 |
| Passed normality test (alpha=0.05)? | Yes |
| P value summary | ns |

1way ANOVA
Multiple comparisons

| | | | | | |
|---|---|---|---|---|---|
| Number of families | 1 | | | | |
| Number of comparisons per family | 3 | | | | |
| Alpha | 0.05 | | | | |
| | | | | | |
| Tukey's multiple comparisons test | Mean Diff. | 95.00% CI of diff. | Significant? | Summary | Adjusted P Value |
| | | | | | |
| PBS vs. rM5/rGGSm | -4.8 | -6.622 to -2.978 | Yes | **** | <0.0001 |
| PBS vs. rGGSm/rM5 | -5.6 | -7.422 to -3.778 | Yes | **** | <0.0001 |
| rM5/rGGSm vs. rGGSm/rM5 | -0.8 | -2.622 to 1.022 | No | ns | 0.4916 |

## 7.5 Statistical analysis of Figure 7.5

Panel A (short term exp.): Normality test and Tukey's multiple comparison test

| Col. stats | A |
|---|---|
| | Normality |
| | Y |
| Number of values | 15 |
| | |
| D'Agostino & Pearson normality test | |
| K2 | 2.151 |
| P value | 0.3411 |
| Passed normality test (alpha=0.05)? | Yes |
| P value summary | ns |

1way ANOVA
Multiple comparisons

| | | | | | |
|---|---|---|---|---|---|
| Number of families | 1 | | | | |
| Number of comparisons per family | 3 | | | | |
| Alpha | 0.05 | | | | |
| | | | | | |
| Tukey's multiple comparisons test | Mean Diff. | 95.00% CI of diff. | Significant? | Summary | Adjusted P Value |
| | | | | | |
| PBS vs. rM5 | -10.56 | -15.16 to -5.958 | Yes | *** | 0.0001 |
| PBS vs. Stg480 | -10.82 | -15.42 to -6.223 | Yes | *** | 0.0001 |
| rM5 vs. Stg480 | -0.2644 | -4.864 to 4.335 | No | ns | 0.9871 |

Panel A (long term exp.): Normality test and Tukey's multiple comparison test

| Col. stats | A |
|---|---|
| | Normality |
| | Y |
| Number of values | 15 |
| | |
| D'Agostino & Pearson normality test | |
| K2 | 4.659 |
| P value | 0.0973 |
| Passed normality test (alpha=0.05)? | Yes |
| P value summary | ns |

1way ANOVA
Multiple comparisons

| | | | | | |
|---|---|---|---|---|---|
| Number of families | 1 | | | | |
| Number of comparisons per family | 3 | | | | |
| Alpha | 0.05 | | | | |
| | | | | | |
| Tukey's multiple comparisons test | Mean Diff. | 95.00% CI of diff. | Significant? | Summary | Adjusted P Value |
| | | | | | |
| PBS vs. rM5 | -13.98 | -17.57 to -10.4 | Yes | **** | <0.0001 |
| PBS vs. Stg480 | -13.36 | -16.95 to -9.78 | Yes | **** | <0.0001 |
| rM5 vs. Stg480 | 0.619 | -2.965 to 4.203 | No | ns | 0.8906 |

## 7.6 Statistical analysis of Figure 7.6

Short term exp.: Normality test and Tukey's multiple comparison test

| Col. stats | A |
|---|---|
| | Normality |
| | Y |
| Number of values | 15 |
| | |
| D'Agostino & Pearson normality test | |
| K2 | 2.311 |
| P value | 0.3149 |
| Passed normality test (alpha=0.05)? | Yes |
| P value summary | ns |

1way ANOVA
Multiple comparisons

| | | | | | |
|---|---|---|---|---|---|
| Number of families | 1 | | | | |
| Number of comparisons per family | 3 | | | | |
| Alpha | 0.05 | | | | |
| | | | | | |
| Tukey's multiple comparisons test | Mean Diff. | 95.00% CI of diff. | Significant? | Summary | Adjusted P Value |
| | | | | | |
| PBS-Cull vs. rM5-rGGSm-Cull | -3.098 | -5.108 to -1.088 | Yes | ** | 0.0038 |
| PBS-Cull vs. rGGSm-rM5-Cull | -5.233 | -7.243 to -3.222 | Yes | **** | <0.0001 |
| rM5-rGGSm-Cull vs. rGGSm-rM5-Cull | -2.135 | -4.145 to -0.1245 | Yes | * | 0.0373 |

Long term exp.: Normality test and Tukey's multiple comparison test

| Col. stats | A |
|---|---|
| | Normality |
| | Y |
| Number of values | 15 |
| | |
| D'Agostino & Pearson normality test | |
| K2 | 0.2021 |
| P value | 0.9039 |
| Passed normality test (alpha=0.05)? | Yes |
| P value summary | ns |

1way ANOVA
Multiple comparisons

| | | | | | |
|---|---|---|---|---|---|
| Number of families | 1 | | | | |
| Number of comparisons per family | 3 | | | | |
| Alpha | 0.05 | | | | |
| | | | | | |
| Tukey's multiple comparisons test | Mean Diff. | 95.00% CI of diff. | Significant? | Summary | Adjusted P Value |
| | | | | | |
| PBS-Cull vs. rM5-Cull | -4.823 | -7.268 to -2.379 | Yes | *** | 0.0005 |
| PBS-Cull vs. rGGSm-Cull | -5.975 | -8.42 to -3.531 | Yes | **** | <0.0001 |
| rM5-Cull vs. rGGSm-Cull | -1.152 | -3.597 to 1.292 | No | ns | 0.4442 |

## APPENDIX 8

## SUPPLEMENTARY FIGURES AND STATISTICAL ANALYSIS OF CHAPTER 8

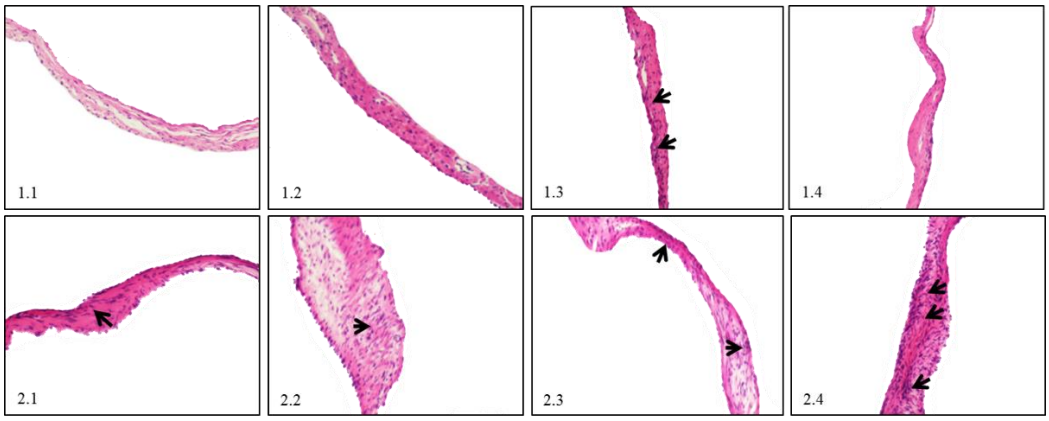


**Supplementary Figure 8.1A** H&E stained sections of mitral valves from donor rats injected with PBS (1.1-1.4) and GAS rM5 (2.1-2.4). Magnifications 200×. Arrows (→) indicate inflammatory foci.

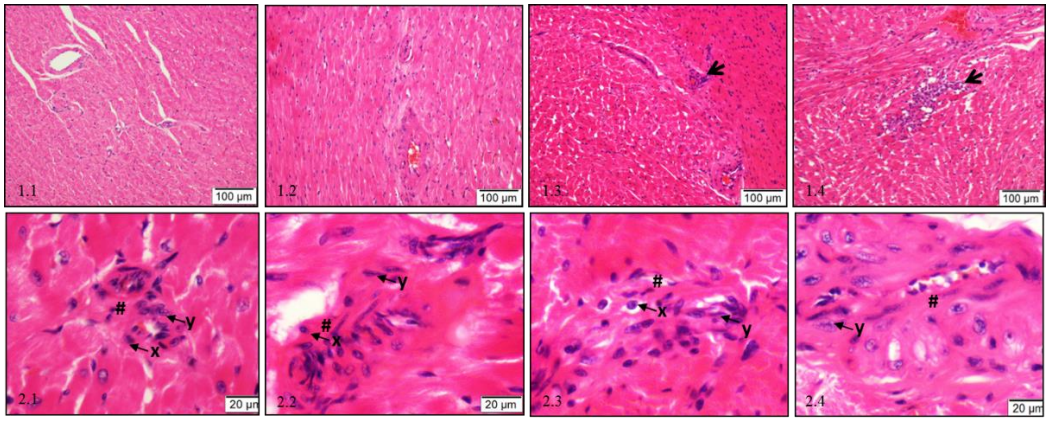


**Supplementary Figure 8.1B** H&E stained sections of myocardium from donor rats injected with PBS (1.1-1.4) and GAS rM5 (2.1-2.4). Magnifications 200× (1.1-1.4), 1000× (2.1-2.4). 'Aschoff nodule like' structure indicated by asterisk (#), x: Anitschkow like cells, y: Aschoff like cells. Arrows (→) indicate inflammatory foci.

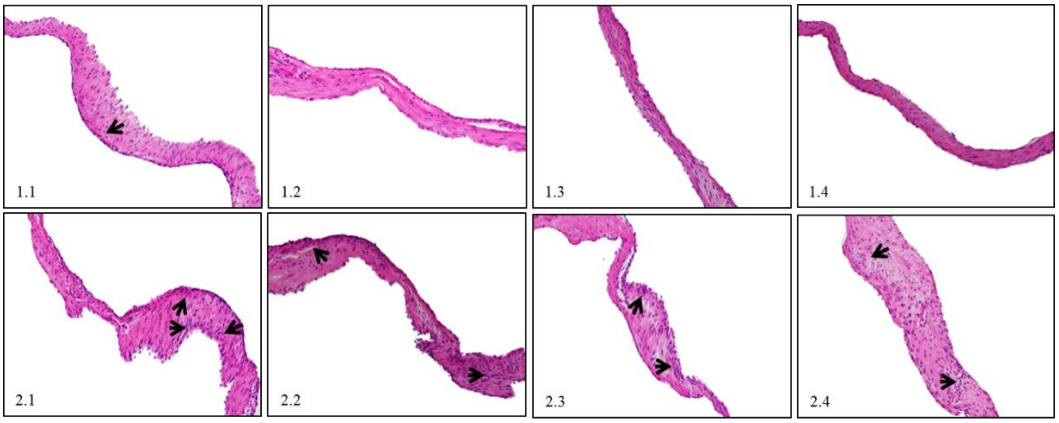


**Supplementary Figure 8.2A** H&E stained sections of mitral valves from recipient rats injected with serum from donor rats injected with PBS (1.1-1.4) and GAS rM5 (2.1-2.4). Magnifications 200×. Arrows (→) indicate inflammatory foci.

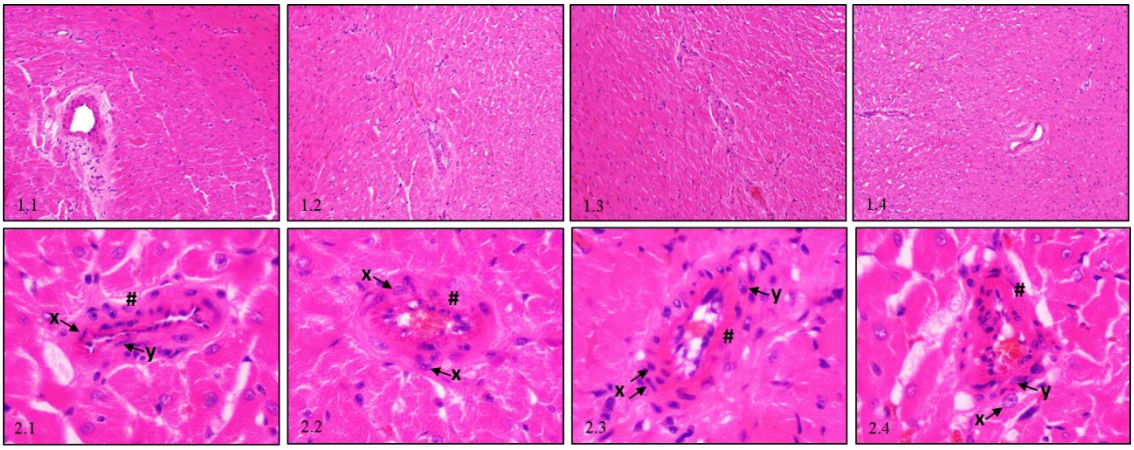


**Supplementary Figure 8.2B** H&E stained sections of myocardium from recipient rats injected with serum from donor rats injected with PBS (1.1-1.4) and GAS rM5 (2.1-2.4). Magnifications 200× (1.1-1.4), 1000× (2.1-2.4). Arrows (→) indicate inflammatory foci. 'Aschoff nodule like' structure indicated by asterisk (#), x: Anitschkow like cells, y: Aschoff like cells.

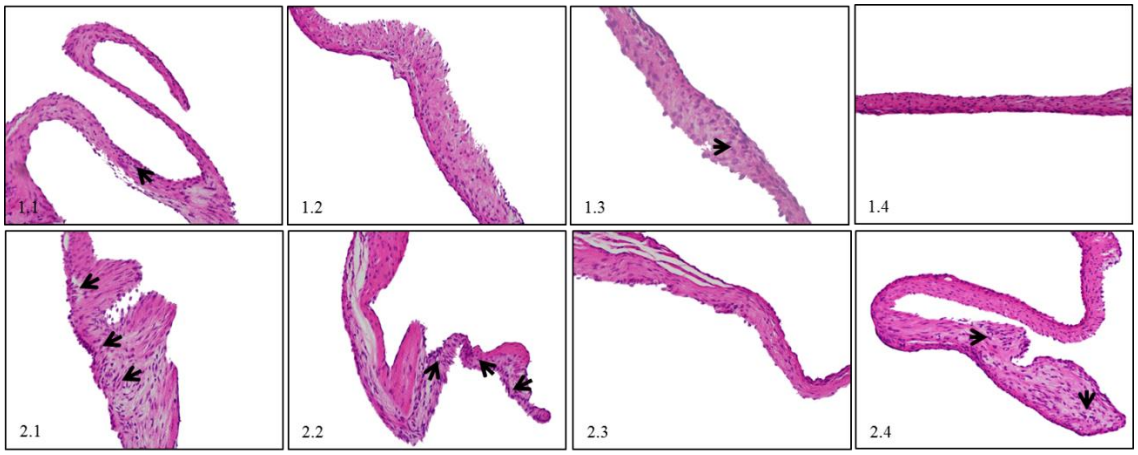


**Supplementary Figure 8.2C** H&E stained sections of mitral valves from recipient rats injected with splenocytes from donor rats injected with PBS (1.1-1.4) and GAS rM5 (2.1-2.4). Magnifications 200× except 1.3 (400×). Arrows (→) indicate inflammatory foci.

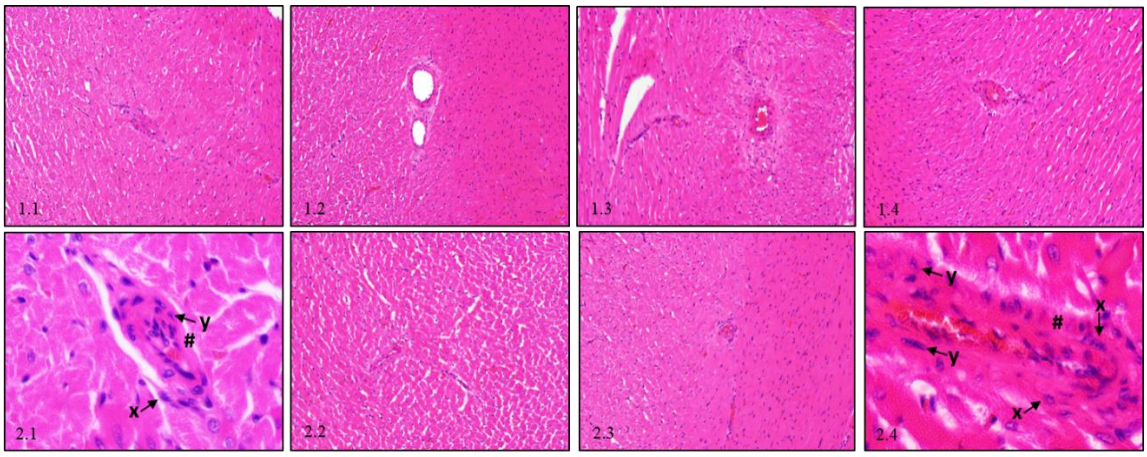


**Supplementary Figure 8.2D** H&E stained sections of myocardium from recipient rats injected with splenocyte from donor rats injected with PBS (1.1-1.4) and GAS rM5 (2.1-2.4). Magnifications 200× (1.1-1.4, 2.2-2.3), 1000× (2.1, 2.4). Arrows (→) indicate inflammatory foci. 'Aschoff nodule like' structure indicated by asterisk (#), x: Anitschkow like cells, y: Aschoff like cells.

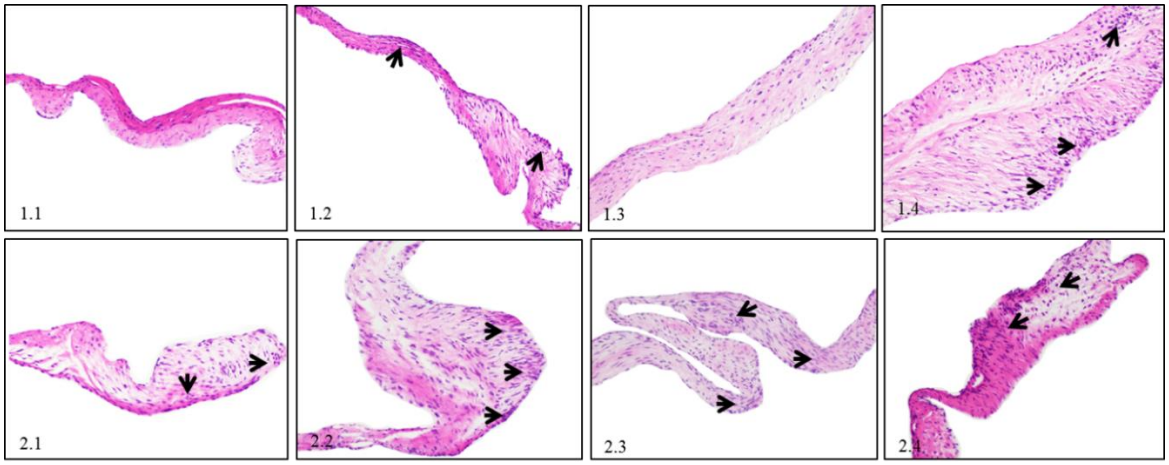


**Supplementary Figure 8.2E** H&E stained sections of mitral valves from recipient rats injected with serum and splenocytes from donor rats injected with PBS (1.1-1.4) and GAS rM5 (2.1-2.4). Magnifications 200×. Arrows (→) indicate inflammatory foci.

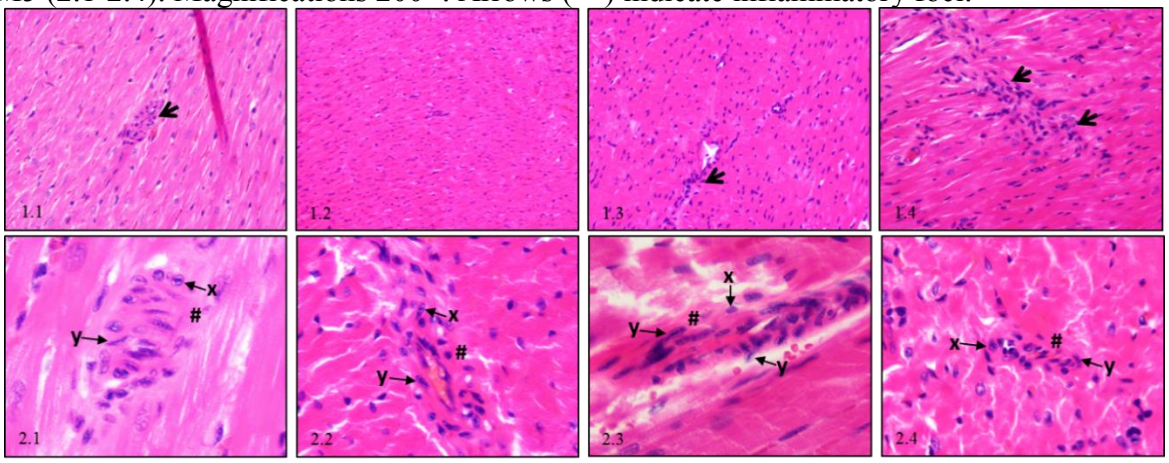


**Supplementary Figure 8.2F.** H&E staining of myocardium of serum and splenocyte recipient rats, magnifications as indicated. 'Aschoff nodule like' structure indicated by asterisk (#), x: Anitschkow like cells, y: Aschoff like cells. Arrows (→) indicate inflammatory foci.

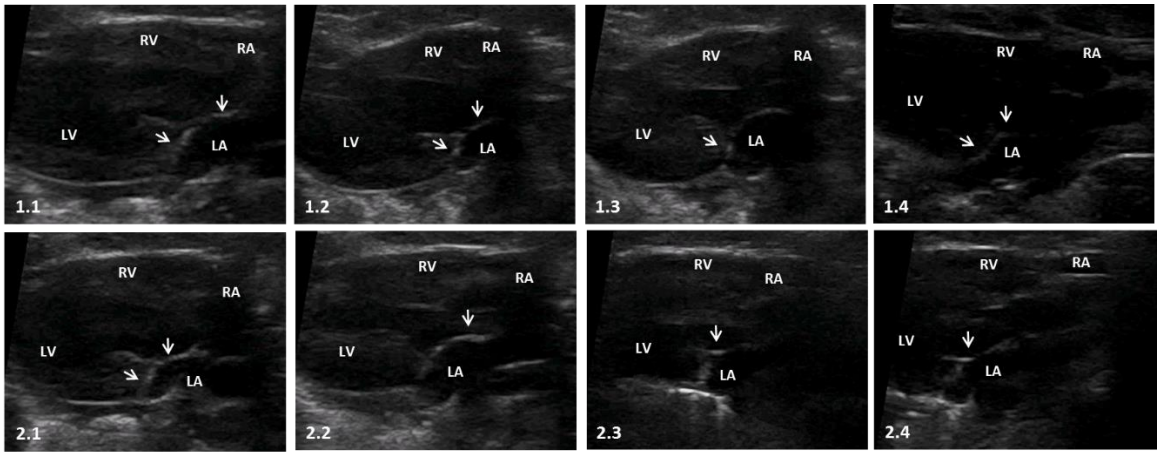


**Supplementary Figure 8.3A** Echocardiographic images of donor rats. Normal mitral leaflets with no evidence of thickening or nodules in the donor rats injected with PBS (1.1-1.4). Thickened leaflets observed as dense thick white and nodular structures in the mitral valve of rats injected with GAS rM5 (2.1-2.4). Arrows indicate mitral valves. LA: left atrium; LV: left ventricle; RA: right atrium; RV: right ventricle.

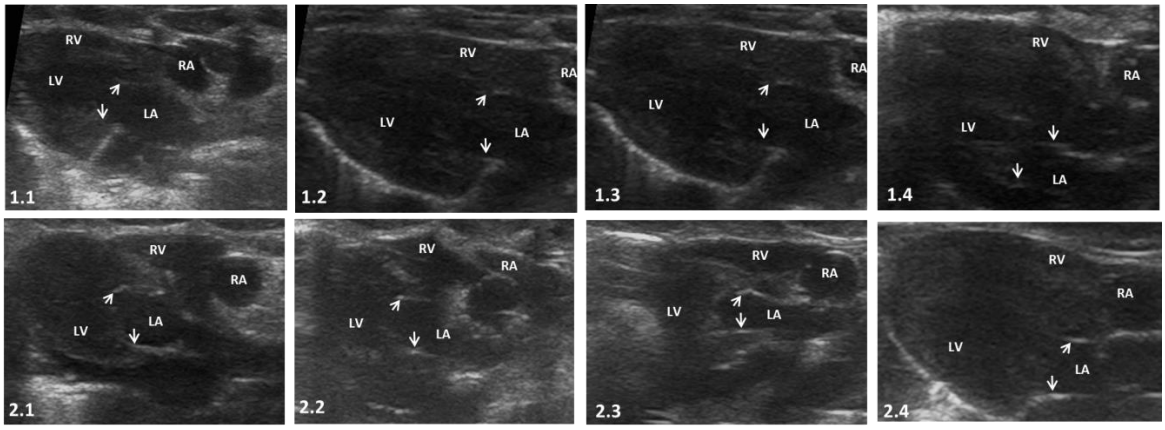


**Supplementary Figure 8.3B** Echocardiographic examination of mitral valves of serum and splenocyte recipient rats. Normal mitral leaflets with no evidence of thickening or nodules in the rats injected with serum and splenocyte from PBS injected rats (1.1-1.4). Thickened leaflets observed as dense white and nodular structures in the mitral valve of rats injected with serum and splenocyte from GAS rM5 injected rats (2.1-2.4). Arrows (→) indicate mitral valves. LA: left atrium; LV: left ventricle; RA: right atrium; RV: right ventricle.

## 8.1 Statistical analysis of Figure 8.2

Panel A (Donors): Normality test and Unpaired t test

| Col. stats | A |
|---|---|
| | Normality |
| | Y |
| 1 Number of values | 8 |
| 2 | |
| 3 D'Agostino & Pearson normality test | |
| 4 K2 | 3.874 |
| 5 P value | 0.1442 |
| 6 Passed normality test (alpha=0.05)? | Yes |
| 7 P value summary | ns |

| Unpaired t test | |
|---|---|
| 1 Table Analyzed | Score out of 8 |
| 2 | |
| 3 Column B | rM5 |
| 4 vs. | vs. |
| 5 Column A | PBS |
| 6 | |
| 7 Unpaired t test | |
| 8 P value | 0.0003 |
| 9 P value summary | *** |
| 10 Significantly different (P < 0.05)? | Yes |
| 11 One- or two-tailed P value? | Two-tailed |
| 12 t, df | t=7.385 df=6 |

Panel A (Serum recipients): Normality test and Unpaired t test

| Col. stats | A |
|---|---|
| | Serum |
| | Y |
| 1 Number of values | 8 |
| 2 | |
| 3 D'Agostino & Pearson normality test | |
| 4 K2 | 2.027 |
| 5 P value | 0.3629 |
| 6 Passed normality test (alpha=0.05)? | Yes |
| 7 P value summary | ns |

| Unpaired t test | |
|---|---|
| 1 Table Analyzed | Added |
| 2 | |
| 3 Column B | rM5 serum |
| 4 vs. | vs. |
| 5 Column A | PBS serum |
| 6 | |
| 7 Unpaired t test | |
| 8 P value | 0.0022 |
| 9 P value summary | ** |
| 10 Significantly different (P < 0.05)? | Yes |
| 11 One- or two-tailed P value? | Two-tailed |
| 12 t, df | t=5.093 df=6 |

Panel A (Splenocyte recipients): Normality test and Unpaired t test

| Col. stats | A |
|---|---|
| | Splenocyte |
| | Y |
| 1 Number of values | 8 |
| 2 | |
| 3 D'Agostino & Pearson normality test | |
| 4 K2 | 3.677 |
| 5 P value | 0.1591 |
| 6 Passed normality test (alpha=0.05)? | Yes |
| 7 P value summary | ns |

| Unpaired t test | |
|---|---|
| 1 Table Analyzed | Added |
| 2 | |
| 3 Column D | rM5 MNCs |
| 4 vs. | vs. |
| 5 Column C | PBS MNCs |
| 6 | |
| 7 Unpaired t test | |
| 8 P value | 0.1047 |
| 9 P value summary | ns |
| 10 Significantly different (P < 0.05)? | No |
| 11 One- or two-tailed P value? | Two-tailed |
| 12 t, df | t=1.91 df=6 |

Panel A (Serum and splenocyte recipients): Normality test and Unpaired t test

| Col. stats | A |
|---|---|
| | Scores |
| | Y |
| 1 Number of values | 8 |
| 2 | |
| 3 D'Agostino & Pearson normality test | |
| 4 K2 | 4.2 |
| 5 P value | 0.1225 |
| 6 Passed normality test (alpha=0.05)? | Yes |
| 7 P value summary | ns |

| Unpaired t test | |
|---|---|
| 1 Table Analyzed | Analysis |
| 2 | |
| 3 Column B | rM5 |
| 4 vs. | vs. |
| 5 Column A | PBS |
| 6 | |
| 7 Unpaired t test | |
| 8 P value | 0.0092 |
| 9 P value summary | ** |
| 10 Significantly different (P < 0.05)? | Yes |
| 11 One- or two-tailed P value? | Two-tailed |
| 12 t, df | t=3.781 df=6 |

## 8.2 Statistical analysis of Figure 8.3

Donors: Normality test and Unpaired t test

| Col. stats | A |
|---|---|
| | Normality |
| | Y |
| 1 Number of values | 8 |
| 2 | |
| 3 D'Agostino & Pearson normality test | |
| 4 K2 | 4.142 |
| 5 P value | 0.1261 |
| 6 Passed normality test (alpha=0.05)? | Yes |
| 7 P value summary | ns |

| Unpaired t test | |
|---|---|
| 1 Table Analyzed | Miliseconds |
| 2 | |
| 3 Column D | rM5-Cull |
| 4 vs. | vs. |
| 5 Column C | PBS-Cull |
| 6 | |
| 7 Unpaired t test | |
| 8 P value | 0.0004 |
| 9 P value summary | *** |
| 10 Significantly different (P < 0.05)? | Yes |
| 11 One- or two-tailed P value? | Two-tailed |
| 12 t, df | t=7.06 df=6 |

Serum recipients : Normality test and Unpaired t test

| Col. stats | A |
|---|---|
| | Normality |
| | Y |
| 1 Number of values | 8 |
| 2 | |
| 3 D'Agostino & Pearson normality test | |
| 4 K2 | 0.6822 |
| 5 P value | 0.7110 |
| 6 Passed normality test (alpha=0.05)? | Yes |
| 7 P value summary | ns |

| Unpaired t test | |
|---|---|
| 1 Table Analyzed | Sera |
| 2 | |
| 3 Column B | rM5 serum |
| 4 vs. | vs. |
| 5 Column A | PBS serum |
| 6 | |
| 7 Unpaired t test | |
| 8 P value | 0.0065 |
| 9 P value summary | ** |
| 10 Significantly different (P < 0.05)? | Yes |
| 11 One- or two-tailed P value? | Two-tailed |
| 12 t, df | t=4.082 df=6 |

Splenocyte recipients : Normality test and Unpaired t test

| Col. stats | A |
|---|---|
| | Normality |
| | Y |
| Number of values | 8 |
| | |
| D'Agostino & Pearson normality test | |
| K2 | 1.482 |
| P value | 0.4767 |
| Passed normality test (alpha=0.05)? | Yes |
| P value summary | ns |

| Unpaired t test | |
|---|---|
| Table Analyzed | MNCs |
| | |
| Column B | rM5 Splenocyte |
| vs. | vs. |
| Column A | PBS Splenocyte |
| | |
| Unpaired t test | |
| P value | 0.0452 |
| P value summary | * |
| Significantly different (P < 0.05)? | Yes |
| One- or two-tailed P value? | Two-tailed |
| t, df | t=2.521 df=6 |

Serum and splenocyte recipients : Normality test and Unpaired t test

| Col. stats | A |
|---|---|
| | Normality |
| | Y |
| Number of values | 8 |
| | |
| D'Agostino & Pearson normality test | |
| K2 | 0.261 |
| P value | 0.8776 |
| Passed normality test (alpha=0.05)? | Yes |
| P value summary | ns |

| Unpaired t test | |
|---|---|
| Table Analyzed | Data 1 |
| | |
| Column D | rM5-Cull |
| vs. | vs. |
| Column C | PBS-Cull |
| | |
| Unpaired t test | |
| P value | 0.0171 |
| P value summary | * |
| Significantly different (P < 0.05)? | Yes |
| One- or two-tailed P value? | Two-tailed |
| t, df | t=3.265 df=6 |

## 8.3 Statistical analysis of Figure 8.4

Panel A (Donors): Normality test and Unpaired t test

| Col. stats | A |
|---|---|
| | Normality |
| | Y |
| Number of values | 8 |
| | |
| D'Agostino & Pearson normality test | |
| K2 | 3.163 |
| P value | 0.2057 |
| Passed normality test (alpha=0.05)? | Yes |
| P value summary | ns |

| Unpaired t test | |
|---|---|
| Table Analyzed | Echo |
| | |
| Column B | rM5 |
| vs. | vs. |
| Column A | PBS |
| | |
| Unpaired t test | |
| P value | 0.0003 |
| P value summary | *** |
| Significantly different (P < 0.05)? | Yes |
| One- or two-tailed P value? | Two-tailed |
| t, df | t=7.348 df=6 |

Panel A (Serum and splenocyte recipients): Normality test and Unpaired t test

| Col. stats | A |
|---|---|
| | Normality |
| | Y |
| Number of values | 8 |
| | |
| D'Agostino & Pearson normality test | |
| K2 | 1.595 |
| P value | 0.4506 |
| Passed normality test (alpha=0.05)? | Yes |
| P value summary | ns |

| Unpaired t test | |
|---|---|
| Table Analyzed | Data 1 |
| | |
| Column B | rM5 |
| vs. | vs. |
| Column A | PBS |
| | |
| Unpaired t test | |
| P value | 0.0013 |
| P value summary | ** |
| Significantly different (P < 0.05)? | Yes |
| One- or two-tailed P value? | Two-tailed |
| t, df | t=5.657 df=6 |

## 8.4 Statistical analysis of Figure 8.5

Panel A (Donors): Normality test and Unpaired t test

| Col. stats | A |
|---|---|
| | Normality |
| | Y |
| Number of values | 8 |
| | |
| D'Agostino & Pearson normality test | |
| K2 | 4.048 |
| P value | 0.1321 |
| Passed normality test (alpha=0.05)? | Yes |
| P value summary | ns |

| Unpaired t test | |
|---|---|
| Table Analyzed | rM5_log |
| | |
| Column B | rM5 |
| vs. | vs. |
| Column A | PBS |
| | |
| Unpaired t test | |
| P value | 0.0001 |
| P value summary | *** |
| Significantly different (P < 0.05)? | Yes |
| One- or two-tailed P value? | Two-tailed |
| t, df | t=8.854 df=6 |

Panel A (Serum recipients): Normality test and Mann-Whitney test

| Col. stats | A |
|---|---|
| | Normality Serum |
| | Y |
| Number of values | 8 |
| | |
| D'Agostino & Pearson normality test | |
| K2 | 8.655 |
| P value | 0.0132 |
| Passed normality test (alpha=0.05)? | No |
| P value summary | * |

| Mann-Whitney test | |
|---|---|
| Table Analyzed | AT1_rM5_Log Ab titre |
| | |
| Column B | rM5-Serum |
| vs. | vs. |
| Column A | PBS-Serum |
| | |
| Mann Whitney test | |
| P value | 0.0286 |
| Exact or approximate P value? | Exact |
| P value summary | * |
| Significantly different (P < 0.05)? | Yes |
| One- or two-tailed P value? | Two-tailed |
| Sum of ranks in column A,B | 10 , 26 |
| Mann-Whitney U | 0 |

Panel A (Splenocyte recipients): Normality test and Unpaired t test

| Col. stats | A |
|---|---|
| | Normality Splenocyte |
| | Y |
| Number of values | 8 |
| | |
| D'Agostino & Pearson normality test | |
| K2 | 3.791 |
| P value | 0.1502 |
| Passed normality test (alpha=0.05)? | Yes |
| P value summary | ns |

| Unpaired t test | |
|---|---|
| Table Analyzed | AT1_rM5_Log Ab titre |
| | |
| Column D | rM5-Cell |
| vs. | vs. |
| Column C | PBS-Cell |
| | |
| Unpaired t test | |
| P value | 0.0003 |
| P value summary | *** |
| Significantly different (P < 0.05)? | Yes |
| One- or two-tailed P value? | Two-tailed |
| t, df | t=7.667 df=6 |

Panel A (Serum and splenocyte recipients): Normality test and Unpaired t test

| Col. stats | A |
|---|---|
| | Normlality-rM5 |
| | Y |
| Number of values | 8 |
| | |
| D'Agostino & Pearson normality test | |
| K2 | 2.329 |
| P value | 0.3121 |
| Passed normality test (alpha=0.05)? | Yes |
| P value summary | ns |

| Unpaired t test | |
|---|---|
| Table Analyzed | AT2_rM5-rGGSm_log |
| | |
| Column B | rM5 |
| vs. | vs. |
| Column A | PBS-rM5 |
| | |
| Unpaired t test | |
| P value | 0.0010 |
| P value summary | *** |
| Significantly different (P < 0.05)? | Yes |
| One- or two-tailed P value? | Two-tailed |
| t, df | t=5.96 df=6 |

Panel B (Donors): Normality test and Unpaired t test

| Col. stats | A |
|---|---|
| | CM |
| | Y |
| 1 Number of values | 8 |
| 2 | |
| 3 D'Agostino & Pearson normality test | |
| 4 K2 | 1.011 |
| 5 P value | 0.6032 |
| 6 Passed normality test (alpha=0.05)? | Yes |
| 7 P value summary | ns |

| Unpaired t test | |
|---|---|
| 1 Table Analyzed | RHD-AT2_CM-Col I |
| 2 | |
| 3 Column B | rM5-CM |
| 4 vs. | vs. |
| 5 Column A | PBS-CM |
| 6 | |
| 7 Unpaired t test | |
| 8 P value | 0.0324 |
| 9 P value summary | * |
| 10 Significantly different (P < 0.05)? | Yes |
| 11 One- or two-tailed P value? | Two-tailed |
| 12 t, df | t=2.771 df=6 |

Panel B (Serum recipients): Normality test and Mann-Whitney test

| Col. stats | A |
|---|---|
| | Normality Serum |
| | Y |
| 1 Number of values | 8 |
| 2 | |
| 3 D'Agostino & Pearson normality test | |
| 4 K2 | 18.41 |
| 5 P value | 0.0001 |
| 6 Passed normality test (alpha=0.05)? | No |
| 7 P value summary | *** |

| Mann-Whitney test | |
|---|---|
| 1 Table Analyzed | CM |
| 2 | |
| 3 Column D | rM5-Serum |
| 4 vs. | vs. |
| 5 Column C | PBS-Serum |
| 6 | |
| 7 Mann Whitney test | |
| 8 P value | >0.9999 |
| 9 Exact or approximate P value? | Exact |
| 10 P value summary | ns |
| 11 Significantly different (P < 0.05)? | No |
| 12 One- or two-tailed P value? | Two-tailed |
| 13 Sum of ranks in column C,D | 18 , 18 |
| 14 Mann-Whitney U | 8 |

Panel B (Splenocyte recipients): Normality test and Unpaired t test

| Col. stats | A |
|---|---|
| | Normality Splenocyte |
| | Y |
| 1 Number of values | 8 |
| 2 | |
| 3 D'Agostino & Pearson normality test | |
| 4 K2 | 1.698 |
| 5 P value | 0.4279 |
| 6 Passed normality test (alpha=0.05)? | Yes |
| 7 P value summary | ns |

| Unpaired t test | |
|---|---|
| 1 Table Analyzed | CM |
| 2 | |
| 3 Column F | rM5-Splenocyte |
| 4 vs. | vs. |
| 5 Column E | PBS-Splenocyte |
| 6 | |
| 7 Unpaired t test | |
| 8 P value | 0.3836 |
| 9 P value summary | ns |
| 10 Significantly different (P < 0.05)? | No |
| 11 One- or two-tailed P value? | Two-tailed |
| 12 t, df | t=0.9399 df=6 |

Panel B (Serum and splenocyte recipients): Normality test and Mann-Whitney test

| Col. stats | A |
|---|---|
| | Normality Serum and Splenocyte |
| | Y |
| 1 Number of values | 8 |
| 2 | |
| 3 D'Agostino & Pearson normality test | |
| 4 K2 | 21.05 |
| 5 P value | <0.0001 |
| 6 Passed normality test (alpha=0.05)? | No |
| 7 P value summary | **** |

| Mann-Whitney test | |
|---|---|
| 1 Table Analyzed | CM |
| 2 | |
| 3 Column H | rM5-Serum and Splenocyte |
| 4 vs. | vs. |
| 5 Column G | PBS-Serum and Splenocyte |
| 6 | |
| 7 Mann Whitney test | |
| 8 P value | 0.3429 |
| 9 Exact or approximate P value? | Exact |
| 10 P value summary | ns |
| 11 Significantly different (P < 0.05)? | No |
| 12 One- or two-tailed P value? | Two-tailed |
| 13 Sum of ranks in column G,H | 14 , 22 |
| 14 Mann-Whitney U | 4 |

## 8.5 Statistical analysis of Figure 8.6

Panel A (Donors): Normality test and Unpaired t test

| Col. stats | A |
|---|---|
| | Normality |
| | Y |
| 1 Number of values | 8 |
| 2 | |
| 3 D'Agostino & Pearson normality test | |
| 4 K2 | 3.397 |
| 5 P value | 0.1830 |
| 6 Passed normality test (alpha=0.05)? | Yes |
| 7 P value summary | ns |

| Unpaired t test | |
|---|---|
| 1 Table Analyzed | rM5 |
| 2 | |
| 3 Column B | rM5 |
| 4 vs. | vs. |
| 5 Column A | PBS |
| 6 | |
| 7 Unpaired t test | |
| 8 P value | 0.0010 |
| 9 P value summary | ** |
| 10 Significantly different (P < 0.05)? | Yes |
| 11 One- or two-tailed P value? | Two-tailed |
| 12 t, df | t=5.953 df=6 |

Panel A (Serum and splenocyte recipients): Normality test and Unpaired t test

| Col. stats | A |
|---|---|
| | Normality |
| | Y |
| 1 Number of values | 8 |
| 2 | |
| 3 D'Agostino & Pearson normality test | |
| 4 K2 | 1.291 |
| 5 P value | 0.5245 |
| 6 Passed normality test (alpha=0.05)? | Yes |
| 7 P value summary | ns |

| Unpaired t test | |
|---|---|
| 1 Table Analyzed | AT2_LPA_rM5 |
| 2 | |
| 3 Column B | rM5 |
| 4 vs. | vs. |
| 5 Column A | PBS |
| 6 | |
| 7 Unpaired t test | |
| 8 P value | 0.0056 |
| 9 P value summary | ** |
| 10 Significantly different (P < 0.05)? | Yes |
| 11 One- or two-tailed P value? | Two-tailed |
| 12 t, df | t=4.21 df=6 |

Panel B (Donors): Normality test and Unpaired t test

| Col. stats | A |
|---|---|
| | Normality Donors |
| | Y |
| 1 Number of values | 8 |
| 2 | |
| 3 D'Agostino & Pearson normality test | |
| 4 K2 | 5.798 |
| 5 P value | 0.0551 |
| 6 Passed normality test (alpha=0.05)? | Yes |
| 7 P value summary | ns |

| Unpaired t test | |
|---|---|
| 1 Table Analyzed | Data 1 |
| 2 | |
| 3 Column B | rM5-Donor |
| 4 vs. | vs. |
| 5 Column A | PBS-Donor |
| 6 | |
| 7 Unpaired t test | |
| 8 P value | <0.0001 |
| 9 P value summary | **** |
| 10 Significantly different (P < 0.05)? | Yes |
| 11 One- or two-tailed P value? | Two-tailed |
| 12 t, df | t=9.503 df=6 |

Panel B (Serum and splenocyte recipients): Normality test and Mann-Whitney test

| Col. stats | A |
|---|---|
| | Normality Recipients |
| | Y |
| 1 Number of values | 8 |
| 2 | |
| 3 D'Agostino & Pearson normality test | |
| 4 K2 | 8.605 |
| 5 P value | 0.0135 |
| 6 Passed normality test (alpha=0.05)? | No |
| 7 P value summary | * |

| Mann-Whitney test | |
|---|---|
| 1 Table Analyzed | Data 1 |
| 2 | |
| 3 Column D | rM5-Recipient |
| 4 vs. | vs. |
| 5 Column C | PBS-Recipient |
| 6 | |
| 7 Mann Whitney test | |
| 8 P value | 0.0286 |
| 9 Exact or approximate P value? | Exact |
| 10 P value summary | * |
| 11 Significantly different (P < 0.05)? | Yes |
| 12 One- or two-tailed P value? | Two-tailed |
| 13 Sum of ranks in column C,D | 10 , 26 |
| 14 Mann-Whitney U | 0 |

Panel C (Donors): Normality test and Unpaired t test

| Col. stats | A |
|---|---|
| | Normality Donors |
| | Y |
| 1 Number of values | 8 |
| 2 | |
| 3 D'Agostino & Pearson normality test | |
| 4 K2 | 2.385 |
| 5 P value | 0.3035 |
| 6 Passed normality test (alpha=0.05)? | Yes |
| 7 P value summary | ns |

| Unpaired t test | |
|---|---|
| 1 Table Analyzed | Data 1 |
| 2 | |
| 3 Column B | rM5-Donor |
| 4 vs. | vs. |
| 5 Column A | PBS-Donor |
| 6 | |
| 7 Unpaired t test | |
| 8 P value | 0.0003 |
| 9 P value summary | *** |
| 10 Significantly different (P < 0.05)? | Yes |
| 11 One- or two-tailed P value? | Two-tailed |
| 12 t, df | t=7.687 df=6 |

Panel C (Serum and splenocyte recipients): Normality test and Unpaired t test

| Col. stats | A |
|---|---|
| | Normality Recipients |
| | Y |
| 1 Number of values | 8 |
| 2 | |
| 3 D'Agostino & Pearson normality test | |
| 4 K2 | 3.088 |
| 5 P value | 0.2135 |
| 6 Passed normality test (alpha=0.05)? | Yes |
| 7 P value summary | ns |

| Unpaired t test | |
|---|---|
| 1 Table Analyzed | Data 1 |
| 2 | |
| 3 Column D | rM5-Recipient |
| 4 vs. | vs. |
| 5 Column C | PBS-Recipient |
| 6 | |
| 7 Unpaired t test | |
| 8 P value | 0.0008 |
| 9 P value summary | *** |
| 10 Significantly different (P < 0.05)? | Yes |
| 11 One- or two-tailed P value? | Two-tailed |
| 12 t, df | t=6.156 df=6 |

Panel D (Donors): Normality test and Unpaired t test

| Col. stats | A |
|---|---|
| | Normality Donors |
| | Y |
| 1 Number of values | 8 |
| 2 | |
| 3 D'Agostino & Pearson normality test | |
| 4 K2 | 2.635 |
| 5 P value | 0.2678 |
| 6 Passed normality test (alpha=0.05)? | Yes |
| 7 P value summary | ns |

| Unpaired t test | |
|---|---|
| 1 Table Analyzed | Data 1 |
| 2 | |
| 3 Column B | rM5-Donor |
| 4 vs. | vs. |
| 5 Column A | PBS-Donor |
| 6 | |
| 7 Unpaired t test | |
| 8 P value | 0.0011 |
| 9 P value summary | ** |
| 10 Significantly different (P < 0.05)? | Yes |
| 11 One- or two-tailed P value? | Two-tailed |
| 12 t, df | t=5.888 df=6 |

Panel D (Serum and splenocyte recipients): Normality test and Unpaired t test

| Col. stats | A |
|---|---|
| | Normality Recipients |
| | Y |
| 1 Number of values | 8 |
| 2 | |
| 3 D'Agostino & Pearson normality test | |
| 4 K2 | 3.857 |
| 5 P value | 0.1454 |
| 6 Passed normality test (alpha=0.05)? | Yes |
| 7 P value summary | ns |

| Unpaired t test | |
|---|---|
| 1 Table Analyzed | Data 1 |
| 2 | |
| 3 Column D | rM5-Recipient |
| 4 vs. | vs. |
| 5 Column C | PBS-Recipient |
| 6 | |
| 7 Unpaired t test | |
| 8 P value | 0.0130 |
| 9 P value summary | * |
| 10 Significantly different (P < 0.05)? | Yes |
| 11 One- or two-tailed P value? | Two-tailed |
| 12 t, df | t=3.489 df=6 |

## APPENDIX 9

## SUPPLEMENTARY FIGURES AND STATISTICAL ANALYSIS OF CHAPTER 9

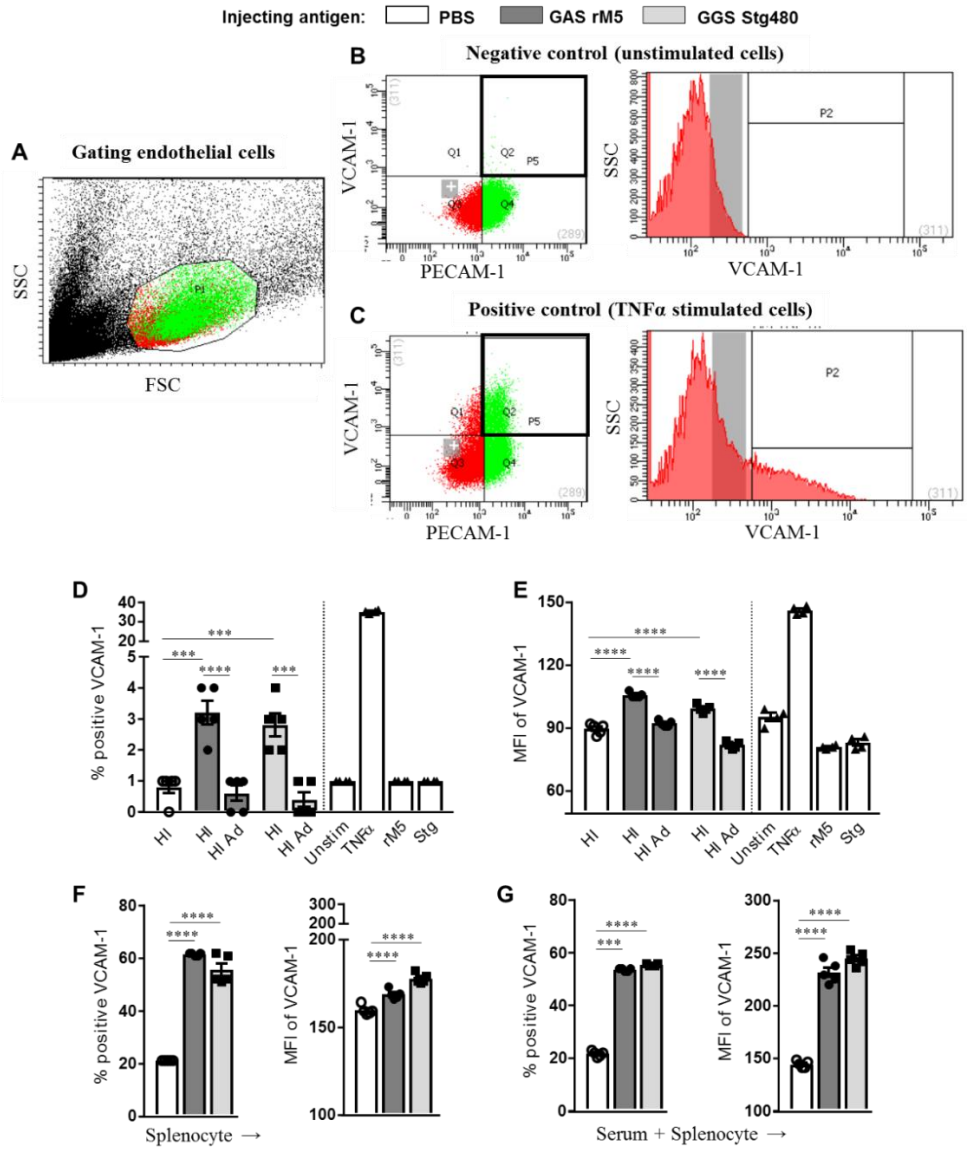


**Supplementary Figure 9.1** GAS and GGS M-protein specific antibodies and splenocytes induce expression of VCAM-1 in endothelial cells. (A) Dot plot showing the gating strategy used to determine the percentage of VCAM-1 positive endothelial cells. Unstimulated endothelial cells (negative control) showed low VCAM-1 expression (B, D-E). However, TNF-α stimulation (positive control) increased expression of VCAM-1 (C, D-E). Heat inactivated (HI) pooled serum from rats injected with GAS rM5 and GGS Stg480 induced VCAM-1 expression in a larger percentage of endothelial cells compared to serum from PBS injected control rats (D-E). VCAM-1 expression reduced after adsorption of GAS rM5 serum with GAS rM5 and GGS Stg480 serum with Stg480 (HI ad). The addition of rM5 or Stg480 M-proteins to endothelial cells did not influence endothelial cell VCAM-1 expression (D-E). Significantly higher expression of VCAM-1 was observed in the RAOEC stimulated with splenocytes from rats injected with GAS And GGS M-protein compared to controls (F) or when splenocytes and sera were added together (G). Error bars represent standard errors of the mean (SEM). Statistical differences were determined using one-way ANOVA with Tukey's post hoc multiple comparisons test; ***p<0.001, ****p<0.0001.

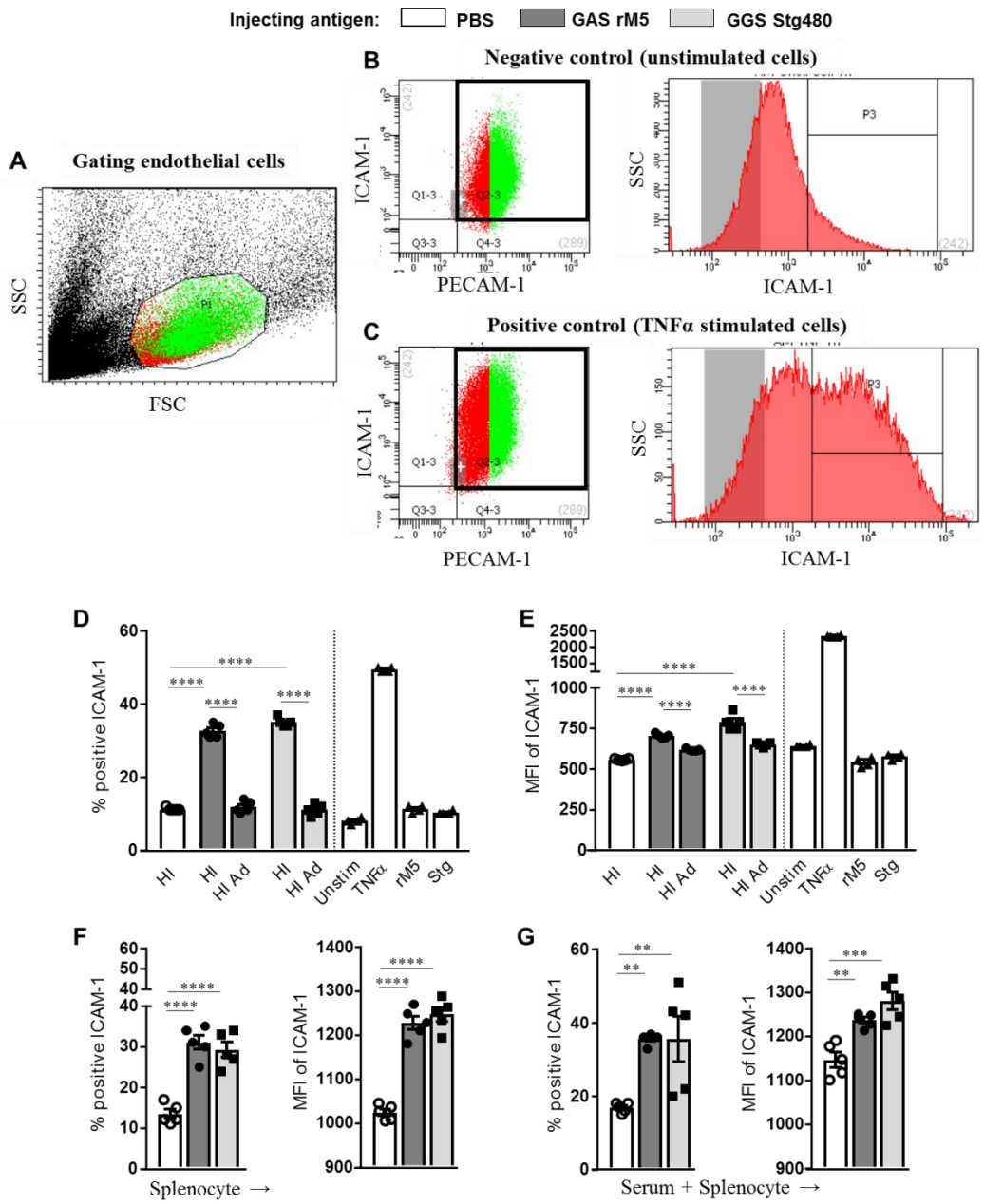


**Supplementary Figure 9.2** GAS and GGS M-protein specific antibodies and splenocytes induce expression of ICAM-1 in endothelial cells. (A) Dot plot showing the gating strategy used to determine the percentage of ICAM-1 positive endothelial cells. Unstimulated endothelial cells (negative control) showed low ICAM-1 expression (B, D-E). However, TNF-α stimulation (positive control) increased expression of ICAM-1 (C, D-E). Heat inactivated (HI) pooled serum from rats injected with GAS rM5 and GGS Stg480 induced ICAM-1 expression in a larger percentage of endothelial cells compared to serum from PBS injected control rats (D-E). ICAM-1 expression reduced after adsorption of GAS rM5 serum with GAS rM5 and GGS Stg480 serum with Stg480 (HI ad). The addition of rM5 or Stg480 M-proteins to endothelial cells did not influence endothelial cell ICAM-1 expression (D-E). Significantly higher expression of ICAM-1 was observed in the RAOEC stimulated with splenocytes from rats injected with GAS and GGS M-protein compared to controls (F) or when splenocytes and sera were added together (G). Error bars represent standard errors of the mean (SEM). Statistical differences were determined using one-way ANOVA with Tukey's post hoc multiple comparisons test; **p<0.01, ***p<0.001, ****p<0.0001.

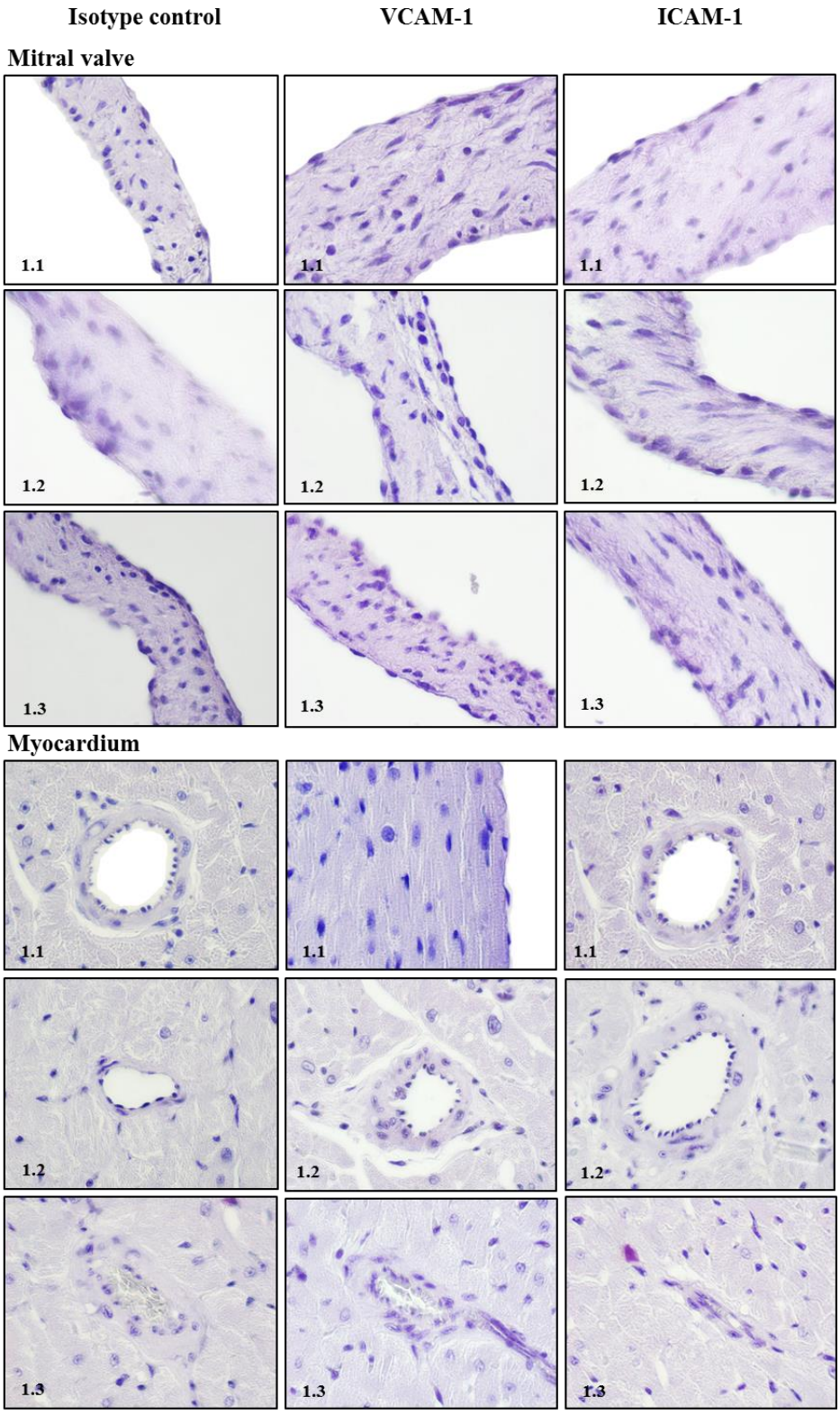


**Supplementary Figure 9.3** PBS injection of rats did not induce adhesion molecule expression in heart tissues. VCAM-1 and ICAM-1 levels in paraffin sections of heart tissues were assessed by immunohistochemical staining with monoclonal antibodies to VCAM-1 and ICAM-1. Mitral valve and myocardium sections from rats injected with PBS had no evidence of VCAM-1 or ICAM-1 positive cells. Isotype control antibody stained sections also had no positive cells. Magnifications 1000x.

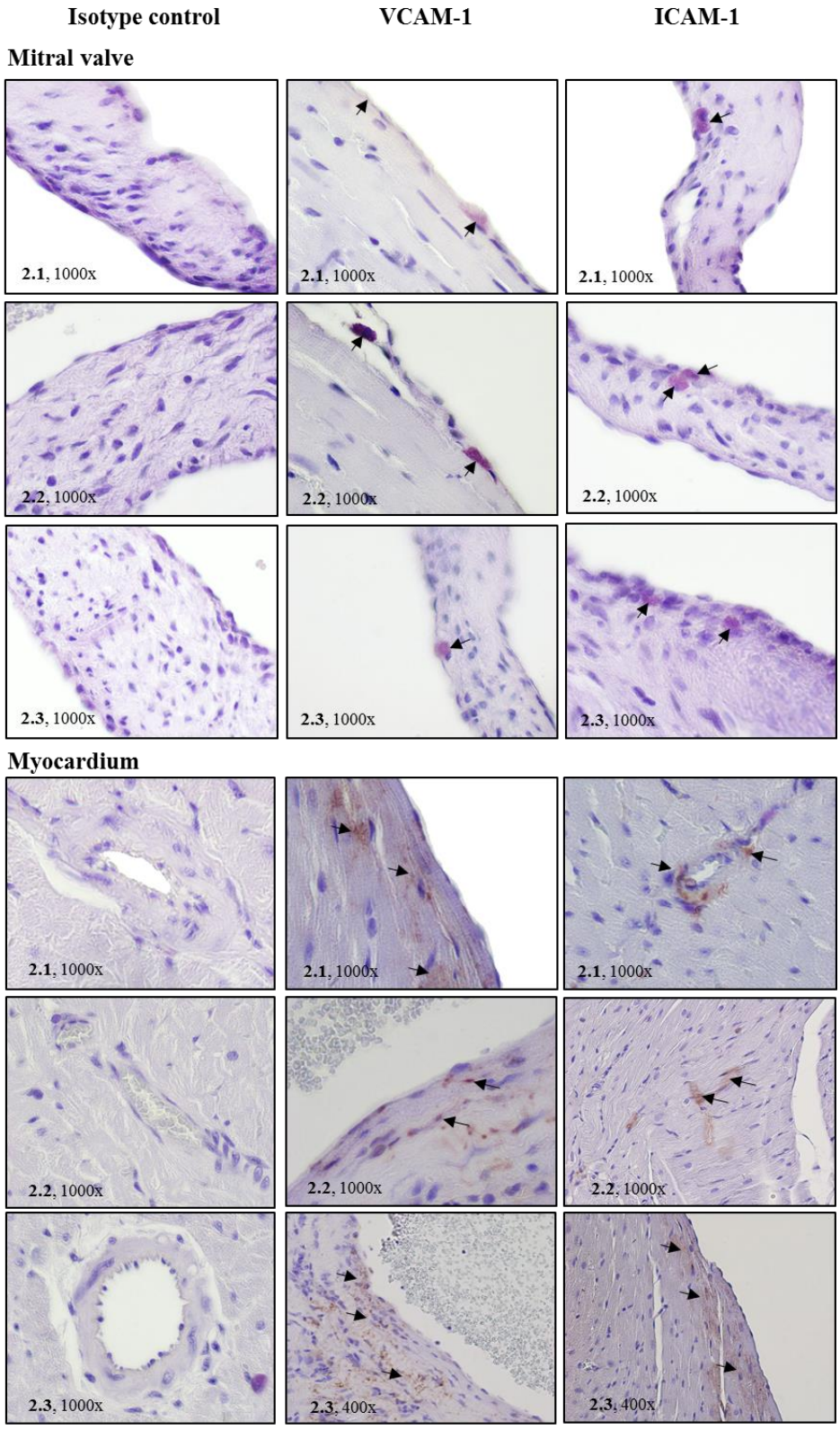


**Supplementary Figure 9.4** GAS M-protein injection induces adhesion molecule expression in heart tissues. VCAM-1 and ICAM-1 levels in paraffin sections of heart tissue were assessed by immunohistochemical staining with monoclonal antibodies to VCAM-1 and ICAM-1. VCAM-1 and ICAM-1 stained cells were found in the mitral valve and myocardium sections (indicated by arrows) of rats injected with GAS rM5. Isotype control antibody stained sections from the rats had no positive cells. Magnifications as indicated.

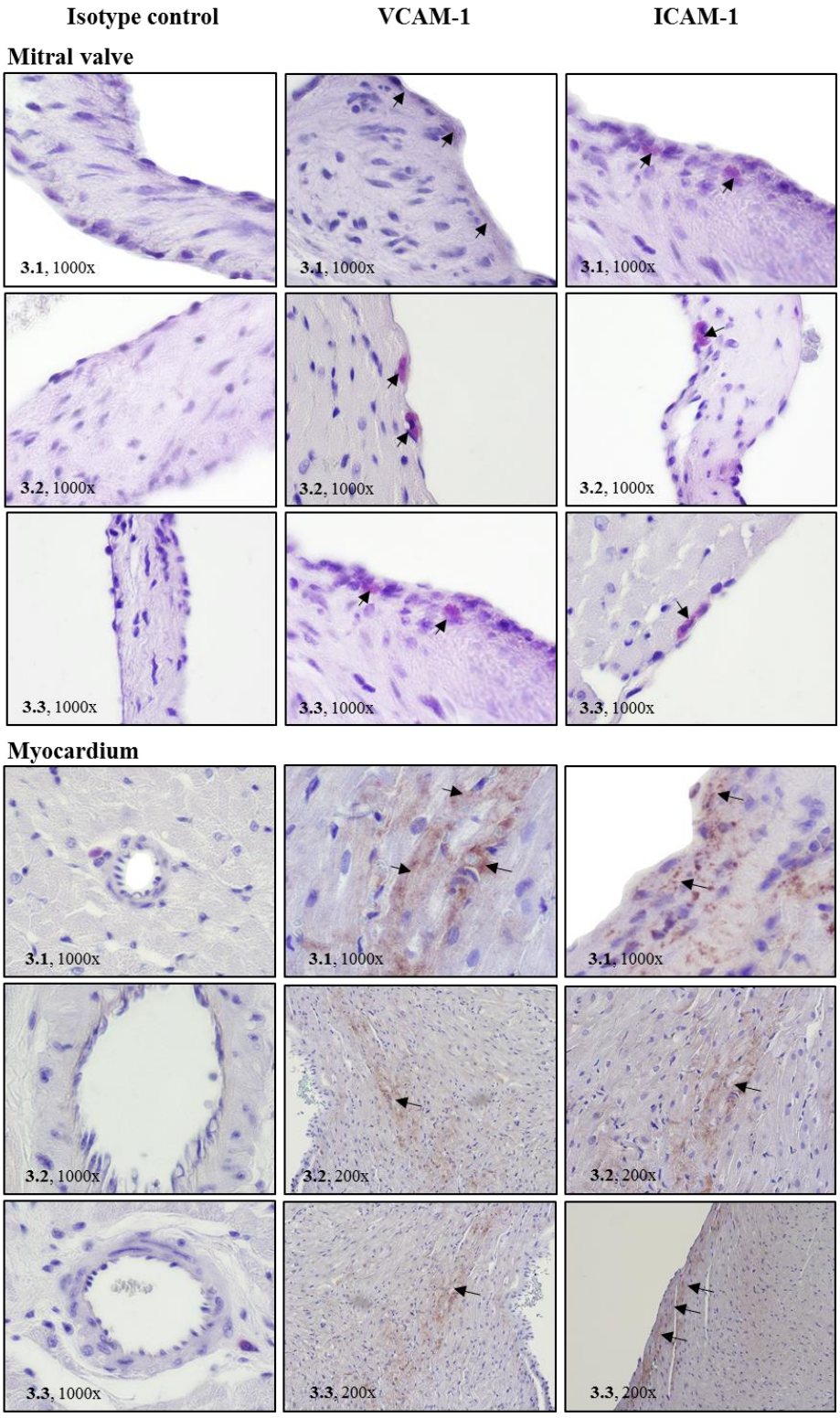


**Supplementary Figure 9.5** GGS M-protein injection induces adhesion molecule expression in heart tissues. VCAM-1 and ICAM-1 levels in paraffin sections of heart tissue were assessed by immunohistochemical staining with monoclonal antibodies to VCAM-1 and ICAM-1. VCAM-1 and ICAM-1 stained cells were found in the mitral valve and myocardium sections (indicated by arrows) of rats injected with GGS Stg480. Isotype control antibody stained sections from the rats had no positive cells. Magnifications as indicated.

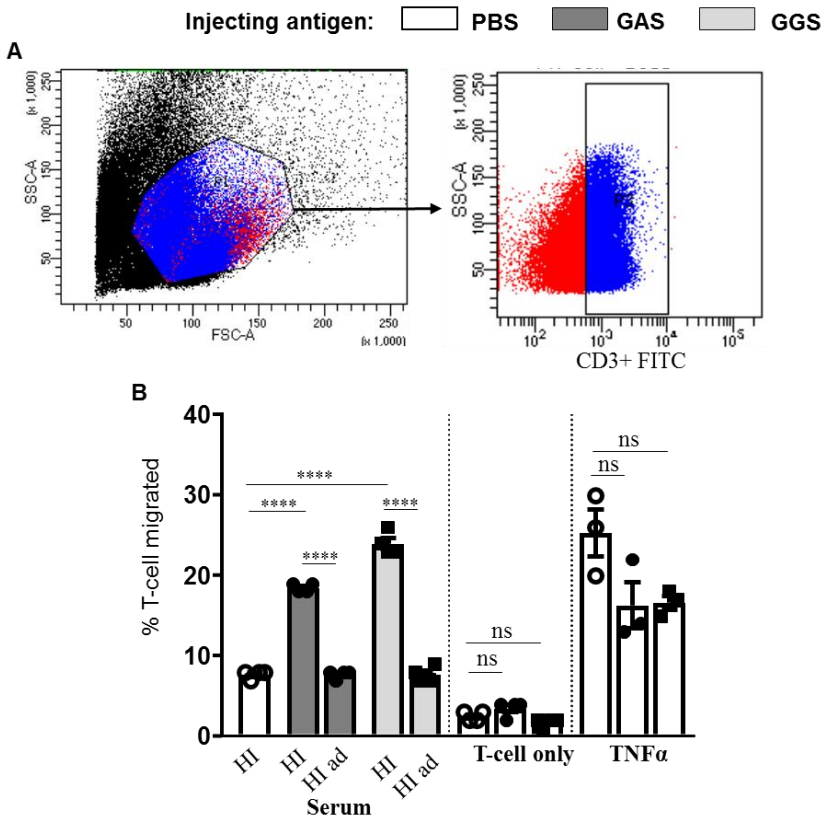


**Supplementary Figure 9.6** GAS and GGS M-protein specific antibodies induce T-cell migration across endothelial cell monolayers. Splenic MNCs from rats injected with rM5/Stg480/PBS was enumerated using Neubauer haemocytometer and $10^6$ cells were added to the respective upper chambers. The actual number of CD3+ T-cells provided in the upper chamber was enumerated as 180,781 for PBS, 564,718 for rM5 and 594,150 for Stg480 using 123count$^{TM}$ eBeads and flow cytometry. Heat-inactivated serum from rats injected with rM5/Stg480/PBS was added (rM5 serum to rM5 T-cell etc.) to the endothelial monolayer in upper chamber. Pooled serum from rM5 infected animals, pre-adsorbed with rM5 and pre-adsorbed serum from Stg480 injected rats was added in separate wells. Rat chemoattractant CXCL9 was added to the lower chambers. After 6 h of incubation, the total number of T-cells in the lower chamber was counted using 123count$^{TM}$ eBeads. (A) A representative dot plots show gating of MNCs in gate P1 and CD3+ T-cells in gate P3. (B) Heat inactivated (HI) sera from rM5- or Stg480-injected rats induced significantly higher T-cell migration to the lower chamber compared to the HI serum from PBS injected control rats. Pre-adsorption of rM5 serum (HI ad) with rM5 and Stg480 proteins significantly reduced T-cell migration. Few T-cells crossed the unstimulated endothelial monolayer (T-cell only). Stimulation of the endothelial monolayer with TNF-α (positive control) allowed the highest T-migration. Error bars represent standard errors of the mean (SEM). Statistical difference by one-way ANOVA with Tukey's post hoc multiple comparisons test; ****$p<0.0001$, ns: not significant.

## 9.1 Statistical analysis of Figure 9.3

Normality test and Tukey's multiple comparison test

| Col. stats | A |
|---|---|
| | Normality |
| | Y |
| Number of values | 25 |
| | |
| D'Agostino & Pearson normality test | |
| K2 | 1.859 |
| P value | 0.3947 |
| Passed normality test (alpha=0.05)? | Yes |
| P value summary | ns |

1way ANOVA
Multiple comparisons

| | | | | | |
|---|---|---|---|---|---|
| Number of families | 1 | | | | |
| Number of comparisons per family | 10 | | | | |
| Alpha | 0.05 | | | | |
| | | | | | |
| Tukey's multiple comparisons test | Mean Diff. | 95.00% CI of diff. | Significant? | Summary | Adjusted P Value |
| | | | | | |
| PBS-Un vs. rM5-Un | -1.339 | -1.793 to -0.8845 | Yes | **** | <0.0001 |
| PBS-Un vs. rM5-Ad | -0.2553 | -0.7094 to 0.1988 | No | ns | 0.4662 |
| PBS-Un vs. Stg-Un | -1.2 | -1.654 to -0.7455 | Yes | **** | <0.0001 |
| PBS-Un vs. Stg-Ad | -0.6464 | -1.101 to -0.1923 | Yes | ** | 0.0031 |
| rM5-Un vs. rM5-Ad | 1.083 | 0.6292 to 1.537 | Yes | **** | <0.0001 |
| rM5-Un vs. Stg-Un | 0.139 | -0.3151 to 0.5931 | No | ns | 0.8874 |
| rM5-Un vs. Stg-Ad | 0.6922 | 0.2381 to 1.146 | Yes | ** | 0.0016 |
| rM5-Ad vs. Stg-Un | -0.9443 | -1.398 to -0.4902 | Yes | **** | <0.0001 |
| rM5-Ad vs. Stg-Ad | -0.3911 | -0.8452 to 0.06301 | No | ns | 0.1130 |
| Stg-Un vs. Stg-Ad | 0.5532 | 0.09909 to 1.007 | Yes | * | 0.0124 |

## 9.2 Statistical analysis of Figure 9.4

Panel D: Normality test and Tukey's multiple comparison test

| Col. stats | A |
|---|---|
| | Normality |
| | Y |
| Number of values | 15 |
| | |
| D'Agostino & Pearson normality test | |
| K2 | 1.336 |
| P value | 0.5127 |
| Passed normality test (alpha=0.05)? | Yes |
| P value summary | ns |

1way ANOVA
Multiple comparisons

| | | | | | |
|---|---|---|---|---|---|
| Number of families | 1 | | | | |
| Number of comparisons per family | 10 | | | | |
| Alpha | 0.05 | | | | |
| | | | | | |
| Tukey's multiple comparisons test | Mean Diff. | 95.00% CI of diff. | Significant? | Summary | Adjusted P Value |
| | | | | | |
| HI PBS vs. HI rM5 | -1.46 | -1.823 to -1.097 | Yes | **** | <0.0001 |
| HI PBS vs. HI Ad rM5 | -0.12 | -0.4831 to 0.2431 | No | ns | 0.8571 |
| HI PBS vs. HI Stg | -1.5 | -1.863 to -1.137 | Yes | **** | <0.0001 |
| HI PBS vs. HI Ad Stg | 0 | -0.3631 to 0.3631 | No | ns | >0.9999 |
| HI rM5 vs. HI Ad rM5 | 1.34 | 0.9769 to 1.703 | Yes | **** | <0.0001 |
| HI rM5 vs. HI Stg | -0.04 | -0.4031 to 0.3231 | No | ns | 0.9972 |
| HI rM5 vs. HI Ad Stg | 1.46 | 1.097 to 1.823 | Yes | **** | <0.0001 |
| HI Ad rM5 vs. HI Stg | -1.38 | -1.743 to -1.017 | Yes | **** | <0.0001 |
| HI Ad rM5 vs. HI Ad Stg | 0.12 | -0.2431 to 0.4831 | No | ns | 0.8571 |
| HI Stg vs. HI Ad Stg | 1.5 | 1.137 to 1.863 | Yes | **** | <0.0001 |

Panel E: Normality test and Tukey's multiple comparison test

| Col. stats | A |
|---|---|
| | Normality |
| | Y |
| Number of values | 25 |
| | |
| D'Agostino & Pearson normality test | |
| K2 | 4.783 |
| P value | 0.0915 |
| Passed normality test (alpha=0.05)? | Yes |
| P value summary | ns |

1way ANOVA
Multiple comparisons

| | | | | | |
|---|---|---|---|---|---|
| Number of families | 1 | | | | |
| Number of comparisons per family | 10 | | | | |
| Alpha | 0.05 | | | | |
| | | | | | |
| Tukey's multiple comparisons test | Mean Diff. | 95.00% CI of diff. | Significant? | Summary | Adjusted P Value |
| | | | | | |
| HI PBS vs. HI rM5 | -22.8 | -26.32 to -19.28 | Yes | **** | <0.0001 |
| HI PBS vs. HI Ad rM5 | -5.2 | -8.72 to -1.68 | Yes | ** | 0.0022 |
| HI PBS vs. HI Stg | -39 | -42.52 to -35.48 | Yes | **** | <0.0001 |
| HI PBS vs. HI Ad Stg | -3.8 | -7.32 to -0.2797 | Yes | * | 0.0305 |
| HI rM5 vs. HI Ad rM5 | 17.6 | 14.08 to 21.12 | Yes | **** | <0.0001 |
| HI rM5 vs. HI Stg | -16.2 | -19.72 to -12.68 | Yes | **** | <0.0001 |
| HI rM5 vs. HI Ad Stg | 19 | 15.48 to 22.52 | Yes | **** | <0.0001 |
| HI Ad rM5 vs. HI Stg | -33.8 | -37.32 to -30.28 | Yes | **** | <0.0001 |
| HI Ad rM5 vs. HI Ad Stg | 1.4 | -2.12 to 4.92 | No | ns | 0.7569 |
| HI Stg vs. HI Ad Stg | 35.2 | 31.68 to 38.72 | Yes | **** | <0.0001 |

Panel F (left): Normality test and Tukey's multiple comparison test

| Col. stats | A |
|---|---|
| | Normality |
| | Y |
| Number of values | 15 |
| | |
| D'Agostino & Pearson normality test | |
| K2 | 5.604 |
| P value | 0.0607 |
| Passed normality test (alpha=0.05)? | Yes |
| P value summary | ns |

| 1way ANOVA<br>Multiple comparisons | | | | | |
|---|---|---|---|---|---|
| Number of families | 1 | | | | |
| Number of comparisons per family | 3 | | | | |
| Alpha | 0.05 | | | | |
| | | | | | |
| Tukey's multiple comparisons test | Mean Diff. | 95.00% CI of diff. | Significant? | Summary | Adjusted P Value |
| | | | | | |
| PBS vs. rM5 | -37.46 | -44.17 to -30.75 | Yes | **** | <0.0001 |
| PBS vs. Stg | -34.02 | -40.73 to -27.31 | Yes | **** | <0.0001 |
| rM5 vs. Stg | 3.44 | -3.266 to 10.15 | No | ns | 0.3870 |

Panel F (right): Normality test and Tukey's multiple comparison test

| Col. stats | A |
|---|---|
| | Normality |
| | Y |
| Number of values | 15 |
| | |
| D'Agostino & Pearson normality test | |
| K2 | 5.954 |
| P value | 0.0509 |
| Passed normality test (alpha=0.05)? | Yes |
| P value summary | ns |

| 1way ANOVA<br>Multiple comparisons | | | | | |
|---|---|---|---|---|---|
| Number of families | 1 | | | | |
| Number of comparisons per family | 3 | | | | |
| Alpha | 0.05 | | | | |
| | | | | | |
| Tukey's multiple comparisons test | Mean Diff. | 95.00% CI of diff. | Significant? | Summary | Adjusted P Value |
| | | | | | |
| PBS vs. rM5 | -2114 | -2590 to -1638 | Yes | **** | <0.0001 |
| PBS vs. Stg | -2064 | -2540 to -1588 | Yes | **** | <0.0001 |
| rM5 vs. Stg | 49.4 | -426.6 to 525.4 | No | ns | 0.9588 |

Panel G (left): Normality test and Tukey's multiple comparison test

| Col. stats | A |
|---|---|
| | Normality |
| | Y |
| Number of values | 15 |
| | |
| D'Agostino & Pearson normality test | |
| K2 | 5.275 |
| P value | 0.0715 |
| Passed normality test (alpha=0.05)? | Yes |
| P value summary | ns |

| 1way ANOVA<br>Multiple comparisons | | | | | |
|---|---|---|---|---|---|
| Number of families | 1 | | | | |
| Number of comparisons per family | 3 | | | | |
| Alpha | 0.05 | | | | |
| | | | | | |
| Tukey's multiple comparisons test | Mean Diff. | 95.00% CI of diff. | Significant? | Summary | Adjusted P Value |
| | | | | | |
| PBS vs. rM5 | -41.66 | -50.01 to -33.31 | Yes | **** | <0.0001 |
| PBS vs. Stg | -35.44 | -43.79 to -27.09 | Yes | **** | <0.0001 |
| rM5 vs. Stg | 6.22 | -2.129 to 14.57 | No | ns | 0.1577 |

Panel G (right): Normality test and Tukey's multiple comparison test

| Col. stats | A |
|---|---|
| | Normality |
| | Y |
| Number of values | 15 |
| | |
| D'Agostino & Pearson normality test | |
| K2 | 4.593 |
| P value | 0.1006 |
| Passed normality test (alpha=0.05)? | Yes |
| P value summary | ns |

| 1way ANOVA<br>Multiple comparisons | | | | | |
|---|---|---|---|---|---|
| Number of families | 1 | | | | |
| Number of comparisons per family | 3 | | | | |
| Alpha | 0.05 | | | | |
| | | | | | |
| Tukey's multiple comparisons test | Mean Diff. | 95.00% CI of diff. | Significant? | Summary | Adjusted P Value |
| | | | | | |
| PBS vs. rM5 | -2167 | -2314 to -2020 | Yes | **** | <0.0001 |
| PBS vs. Stg | -2016 | -2163 to -1869 | Yes | **** | <0.0001 |
| rM5 vs. Stg | 151.2 | 4.121 to 298.3 | Yes | * | 0.0438 |

## 9.3 Statistical analysis of Figure 9.5

Panel D: Normality test and Tukey's multiple comparison test

| Col. stats | A |
|---|---|
| | Normality |
| | Y |
| Number of values | 25 |
| | |
| D'Agostino & Pearson normality test | |
| K2 | 0.5973 |
| P value | 0.7418 |
| Passed normality test (alpha=0.05)? | Yes |
| P value summary | ns |

| 1way ANOVA<br>Multiple comparisons | | | | | |
|---|---|---|---|---|---|
| Number of families | 1 | | | | |
| Number of comparisons per family | 10 | | | | |
| Alpha | 0.05 | | | | |
| | | | | | |
| Tukey's multiple comparisons test | Mean Diff. | 95.00% CI of diff. | Significant? | Summary | Adjusted P Value |
| | | | | | |
| HI PBS vs. HI rM5 | -6.44 | -10.8 to -2.083 | Yes | ** | 0.0022 |
| HI PBS vs. HI Ad rM5 | 4.582 | 0.2252 to 8.939 | Yes | * | 0.0363 |
| HI PBS vs. HI Stg | -3.48 | -7.837 to 0.8768 | No | ns | 0.1589 |
| HI PBS vs. HI Ad Stg | 4.4 | 0.04324 to 8.757 | Yes | * | 0.0470 |
| HI rM5 vs. HI Ad rM5 | 11.02 | 6.665 to 15.38 | Yes | **** | <0.0001 |
| HI rM5 vs. HI Stg | 2.96 | -1.397 to 7.317 | No | ns | 0.2869 |
| HI rM5 vs. HI Ad Stg | 10.84 | 6.483 to 15.2 | Yes | **** | <0.0001 |
| HI Ad rM5 vs. HI Stg | -8.062 | -12.42 to -3.705 | Yes | *** | 0.0002 |
| HI Ad rM5 vs. HI Ad Stg | -0.182 | -4.539 to 4.175 | No | ns | >0.9999 |
| HI Stg vs. HI Ad Stg | 7.88 | 3.523 to 12.24 | Yes | *** | 0.0002 |

Panel E: Normality test and Tukey's multiple comparison test

| Col. stats | A |
|---|---|
| | Normality |
| | Y |
| Number of values | 25 |
| | |
| D'Agostino & Pearson normality test | |
| K2 | 4.783 |
| P value | 0.0915 |
| Passed normality test (alpha=0.05)? | Yes |
| P value summary | ns |

1way ANOVA
Multiple comparisons

| | | | | | | |
|---|---|---|---|---|---|---|
| 1 | Number of families | 1 | | | | |
| 2 | Number of comparisons per family | 10 | | | | |
| 3 | Alpha | 0.05 | | | | |
| 4 | | | | | | |
| 5 | Tukey's multiple comparisons test | Mean Diff. | 95.00% CI of diff. | Significant? | Summary | Adjusted P Value |
| 6 | | | | | | |
| 7 | HI PBS vs. HI rM5 | -656.8 | -819.9 to -493.7 | Yes | **** | <0.0001 |
| 8 | HI PBS vs. HI Ad rM5 | -19 | -182.1 to 144.1 | No | ns | 0.9966 |
| 9 | HI PBS vs. HI Stg | -719.4 | -882.5 to -556.3 | Yes | **** | <0.0001 |
| 10 | HI PBS vs. HI Ad Stg | -47 | -210.1 to 116.1 | No | ns | 0.9073 |
| 11 | HI rM5 vs. HI Ad rM5 | 637.8 | 474.7 to 800.9 | Yes | **** | <0.0001 |
| 12 | HI rM5 vs. HI Stg | -62.6 | -225.7 to 100.5 | No | ns | 0.7794 |
| 13 | HI rM5 vs. HI Ad Stg | 609.8 | 446.7 to 772.9 | Yes | **** | <0.0001 |
| 14 | HI Ad rM5 vs. HI Stg | -700.4 | -863.5 to -537.3 | Yes | **** | <0.0001 |
| 15 | HI Ad rM5 vs. HI Ad Stg | -28 | -191.1 to 135.1 | No | ns | 0.9850 |
| 16 | HI Stg vs. HI Ad Stg | 672.4 | 509.3 to 835.5 | Yes | **** | <0.0001 |

Panel F (left): Normality test and Tukey's multiple comparison test

| Col. stats | A |
|---|---|
| | Normality |
| | Y |
| Number of values | 15 |
| | |
| D'Agostino & Pearson normality test | |
| K2 | 3.403 |
| P value | 0.1824 |
| Passed normality test (alpha=0.05)? | Yes |
| P value summary | ns |

1way ANOVA
Multiple comparisons

| | | | | | | |
|---|---|---|---|---|---|---|
| 1 | Number of families | 1 | | | | |
| 2 | Number of comparisons per family | 3 | | | | |
| 3 | Alpha | 0.05 | | | | |
| 4 | | | | | | |
| 5 | Tukey's multiple comparisons test | Mean Diff. | 95.00% CI of diff. | Significant? | Summary | Adjusted P Value |
| 6 | | | | | | |
| 7 | PBS vs. rM5 | -25.64 | -32.91 to -18.37 | Yes | **** | <0.0001 |
| 8 | PBS vs. Stg | -22.3 | -29.57 to -15.03 | Yes | **** | <0.0001 |
| 9 | rM5 vs. Stg | 3.34 | -3.927 to 10.61 | No | ns | 0.4611 |

Panel F (right): Normality test and Tukey's multiple comparison test

| Col. stats | A |
|---|---|
| | Normality |
| | Y |
| Number of values | 15 |
| | |
| D'Agostino & Pearson normality test | |
| K2 | 2.289 |
| P value | 0.3184 |
| Passed normality test (alpha=0.05)? | Yes |
| P value summary | ns |

1way ANOVA
Multiple comparisons

| | | | | | | |
|---|---|---|---|---|---|---|
| 1 | Number of families | 1 | | | | |
| 2 | Number of comparisons per family | 3 | | | | |
| 3 | Alpha | 0.05 | | | | |
| 4 | | | | | | |
| 5 | Tukey's multiple comparisons test | Mean Diff. | 95.00% CI of diff. | Significant? | Summary | Adjusted P Value |
| 6 | | | | | | |
| 7 | PBS vs. rM5 | -4473 | -6126 to -2820 | Yes | **** | <0.0001 |
| 8 | PBS vs. Stg | -4429 | -6081 to -2776 | Yes | **** | <0.0001 |
| 9 | rM5 vs. Stg | 44.2 | -1608 to 1697 | No | ns | 0.9972 |

Panel G (left): Normality test and Tukey's multiple comparison test

| Col. stats | A |
|---|---|
| | Normality |
| | Y |
| Number of values | 15 |
| | |
| D'Agostino & Pearson normality test | |
| K2 | 3.403 |
| P value | 0.1824 |
| Passed normality test (alpha=0.05)? | Yes |
| P value summary | ns |

1way ANOVA
Multiple comparisons

| | | | | | | |
|---|---|---|---|---|---|---|
| 1 | Number of families | 1 | | | | |
| 2 | Number of comparisons per family | 3 | | | | |
| 3 | Alpha | 0.05 | | | | |
| 4 | | | | | | |
| 5 | Tukey's multiple comparisons test | Mean Diff. | 95.00% CI of diff. | Significant? | Summary | Adjusted P Value |
| 6 | | | | | | |
| 7 | PBS vs. rM5 | -26.48 | -36.19 to -16.77 | Yes | **** | <0.0001 |
| 8 | PBS vs. Stg | -22.04 | -31.75 to -12.33 | Yes | *** | 0.0002 |
| 9 | rM5 vs. Stg | 4.44 | -5.268 to 14.15 | No | ns | 0.4644 |

Panel G (right): Normality test and Tukey's multiple comparison test

| Col. stats | A |
|---|---|
| | Normality |
| | Y |
| Number of values | 15 |
| | |
| D'Agostino & Pearson normality test | |
| K2 | 3.703 |
| P value | 0.1570 |
| Passed normality test (alpha=0.05)? | Yes |
| P value summary | ns |

1way ANOVA
Multiple comparisons

| | | | | | | |
|---|---|---|---|---|---|---|
| 1 | Number of families | 1 | | | | |
| 2 | Number of comparisons per family | 3 | | | | |
| 3 | Alpha | 0.05 | | | | |
| 4 | | | | | | |
| 5 | Tukey's multiple comparisons test | Mean Diff. | 95.00% CI of diff. | Significant? | Summary | Adjusted P Value |
| 6 | | | | | | |
| 7 | PBS vs. rM5 | -6151 | -11354 to -947.9 | Yes | * | 0.0210 |
| 8 | PBS vs. Stg | -7731 | -12934 to -2528 | Yes | ** | 0.0049 |
| 9 | rM5 vs. Stg | -1580 | -6783 to 3623 | No | ns | 0.7040 |

## 9.4 Statistical analysis of Figure 9.7

VCAM-1: Normality test and Tukey's multiple comparison test

| Col. stats | A |
|---|---|
| | VCAM-Myo |
| | Y |
| Number of values | 9 |
| | |
| D'Agostino & Pearson normality test | |
| K2 | 3.114 |
| P value | 0.2108 |
| Passed normality test (alpha=0.05)? | Yes |
| P value summary | ns |

1way ANOVA
Multiple comparisons

| | | | | | |
|---|---|---|---|---|---|
| Number of families | 1 | | | | |
| Number of comparisons per family | 3 | | | | |
| Alpha | 0.05 | | | | |
| | | | | | |
| Tukey's multiple comparisons test | Mean Diff. | 95.00% CI of diff. | Significant? | Summary | Adjusted P Value |
| | | | | | |
| PBS-Myo vs. rM5-Myo | -0.21 | -0.4522 to 0.03217 | No | ns | 0.0832 |
| PBS-Myo vs. Stg-Myo | -1.627 | -1.869 to -1.384 | Yes | **** | <0.0001 |
| rM5-Myo vs. Stg-Myo | -1.417 | -1.659 to -1.174 | Yes | **** | <0.0001 |

ICAM-1: Normality test and Tukey's multiple comparison test

| Col. stats | A |
|---|---|
| | ICAM-Myo |
| | Y |
| Number of values | 9 |
| | |
| D'Agostino & Pearson normality test | |
| K2 | 3.478 |
| P value | 0.1757 |
| Passed normality test (alpha=0.05)? | Yes |
| P value summary | ns |

1way ANOVA
Multiple comparisons

| | | | | | |
|---|---|---|---|---|---|
| Number of families | 1 | | | | |
| Number of comparisons per family | 3 | | | | |
| Alpha | 0.05 | | | | |
| | | | | | |
| Tukey's multiple comparisons test | Mean Diff. | 95.00% CI of diff. | Significant? | Summary | Adjusted P Value |
| | | | | | |
| PBS-Myo vs. rM5-Myo | -2.524 | -3.317 to -1.731 | Yes | *** | 0.0002 |
| PBS-Myo vs. Stg-Myo | -3.254 | -4.047 to -2.461 | Yes | **** | <0.0001 |
| rM5-Myo vs. Stg-Myo | -0.7297 | -1.523 to 0.06349 | No | ns | 0.0679 |

## 9.5 Statistical analysis of Figure 9.8

Serum: Normality test and Tukey's multiple comparison test

| Col. stats | A |
|---|---|
| | Normality serum |
| | Y |
| Number of values | 20 |
| | |
| D'Agostino & Pearson normality test | |
| K2 | 2.254 |
| P value | 0.3239 |
| Passed normality test (alpha=0.05)? | Yes |
| P value summary | ns |

1way ANOVA
Multiple comparisons

| | | | | | |
|---|---|---|---|---|---|
| Number of families | 1 | | | | |
| Number of comparisons per family | 10 | | | | |
| Alpha | 0.05 | | | | |
| | | | | | |
| Tukey's multiple comparisons test | Mean Diff. | 95.00% CI of diff. | Significant? | Summary | Adjusted P Value |
| | | | | | |
| PBS-HI vs. rM5-HI | -11.25 | -15.09 to -7.406 | Yes | **** | <0.0001 |
| PBS-HI vs. rM5-HI Ad | 0.25 | -3.594 to 4.094 | No | ns | 0.9996 |
| PBS-HI vs. Stg-HI | -21.25 | -25.09 to -17.41 | Yes | **** | <0.0001 |
| PBS-HI vs. Stg-HI Ad | -7 | -10.84 to -3.156 | Yes | *** | 0.0004 |
| rM5-HI vs. rM5-HI Ad | 11.5 | 7.656 to 15.34 | Yes | **** | <0.0001 |
| rM5-HI vs. Stg-HI | -10 | -13.84 to -6.156 | Yes | **** | <0.0001 |
| rM5-HI vs. Stg-HI Ad | 4.25 | 0.4056 to 8.094 | Yes | * | 0.0270 |
| rM5-HI Ad vs. Stg-HI | -21.5 | -25.34 to -17.66 | Yes | **** | <0.0001 |
| rM5-HI Ad vs. Stg-HI Ad | -7.25 | -11.09 to -3.406 | Yes | *** | 0.0003 |
| Stg-HI vs. Stg-HI Ad | 14.25 | 10.41 to 18.09 | Yes | **** | <0.0001 |

T-cell only: Normality test and Tukey's multiple comparison test

| Col. stats | A |
|---|---|
| | Normality Cell only |
| | Y |
| Number of values | 12 |
| | |
| D'Agostino & Pearson normality test | |
| K2 | 1.7 |
| P value | 0.4273 |
| Passed normality test (alpha=0.05)? | Yes |
| P value summary | ns |

1way ANOVA
Multiple comparisons

| | | | | | |
|---|---|---|---|---|---|
| Number of families | 1 | | | | |
| Number of comparisons per family | 3 | | | | |
| Alpha | 0.05 | | | | |
| | | | | | |
| Tukey's multiple comparisons test | Mean Diff. | 95.00% CI of diff. | Significant? | Summary | Adjusted P Value |
| | | | | | |
| PBS-Cell vs. rM5-Cell | -1 | -2.396 to 0.396 | No | ns | 0.1678 |
| PBS-Cell vs. Stg-Cell | -0.75 | -2.146 to 0.646 | No | ns | 0.3358 |
| rM5-Cell vs. Stg-Cell | 0.25 | -1.146 to 1.646 | No | ns | 0.8731 |

TNF-α: Normality test and Tukey's multiple comparison test

| Col. stats | A |
|---|---|
| | Normaltiy TNF |
| | Y |
| Number of values | 12 |
| | |
| D'Agostino & Pearson normality test | |
| K2 | 1.7 |
| P value | 0.4273 |
| Passed normality test (alpha=0.05)? | Yes |
| P value summary | ns |

1way ANOVA
Multiple comparisons

| | | | | | |
|---|---|---|---|---|---|
| Number of families | 1 | | | | |
| Number of comparisons per family | 3 | | | | |
| Alpha | 0.05 | | | | |
| | | | | | |
| Tukey's multiple comparisons test | Mean Diff. | 95.00% CI of diff. | Significant? | Summary | Adjusted P Value |
| | | | | | |
| PBS-TNF vs. rM5-TNF | -4.5 | -12.41 to 3.411 | No | ns | 0.2992 |
| PBS-TNF vs. Stg-TNF | -9.75 | -17.66 to -1.839 | Yes | * | 0.0183 |
| rM5-TNF vs. Stg-TNF | -5.25 | -13.16 to 2.661 | No | ns | 0.2076 |

## 9.6 Statistical analysis of Supplementary Figure 9.1

Panel D: Normality test and Tukey's multiple comparison test

| Col. stats | A |
|---|---|
| | Normality |
| | Y |
| Number of values | 25 |
| | |
| D'Agostino & Pearson normality test | |
| K2 | 2.785 |
| P value | 0.2484 |
| Passed normality test (alpha=0.05)? | Yes |
| P value summary | ns |

| 1way ANOVA<br>Multiple comparisons | | | | | |
|---|---|---|---|---|---|
| Number of families | 1 | | | | |
| Number of comparisons per family | 10 | | | | |
| Alpha | 0.05 | | | | |
| | | | | | |
| Tukey's multiple comparisons test | Mean Diff. | 95.00% CI of diff. | Significant? | Summary | Adjusted P Value |
| | | | | | |
| HI PBS vs. HI rM5 | -2.4 | -3.655 to -1.145 | Yes | *** | 0.0001 |
| HI PBS vs. HI Ad rM5 | 0.2 | -1.055 to 1.455 | No | ns | 0.9886 |
| HI PBS vs. HI Stg | -2 | -3.255 to -0.7446 | Yes | *** | 0.0010 |
| HI PBS vs. HI Ad Stg | 0.4 | -0.8554 to 1.655 | No | ns | 0.8723 |
| HI rM5 vs. HI Ad rM5 | 2.6 | 1.345 to 3.855 | Yes | **** | <0.0001 |
| HI rM5 vs. HI Stg | 0.4 | -0.8554 to 1.655 | No | ns | 0.8723 |
| HI rM5 vs. HI Ad Stg | 2.8 | 1.545 to 4.055 | Yes | **** | <0.0001 |
| HI Ad rM5 vs. HI Stg | -2.2 | -3.455 to -0.9446 | Yes | *** | 0.0003 |
| HI Ad rM5 vs. HI Ad Stg | 0.2 | -1.055 to 1.455 | No | ns | 0.9886 |
| HI Stg vs. HI Ad Stg | 2.4 | 1.145 to 3.655 | Yes | *** | 0.0001 |

Panel E: Normality test and Tukey's multiple comparison test

| Col. stats | A |
|---|---|
| | Normality |
| | Y |
| Number of values | 25 |
| | |
| D'Agostino & Pearson normality test | |
| K2 | 2.866 |
| P value | 0.2386 |
| Passed normality test (alpha=0.05)? | Yes |
| P value summary | ns |

| 1way ANOVA<br>Multiple comparisons | | | | | |
|---|---|---|---|---|---|
| Number of families | 1 | | | | |
| Number of comparisons per family | 10 | | | | |
| Alpha | 0.05 | | | | |
| | | | | | |
| Tukey's multiple comparisons test | Mean Diff. | 95.00% CI of diff. | Significant? | Summary | Adjusted P Value |
| | | | | | |
| HI PBS vs. HI rM5 | -16.2 | -19.53 to -12.87 | Yes | **** | <0.0001 |
| HI PBS vs. HI Ad rM5 | -2.6 | -5.932 to 0.7322 | No | ns | 0.1751 |
| HI PBS vs. HI Stg | -9.8 | -13.13 to -6.468 | Yes | **** | <0.0001 |
| HI PBS vs. HI Ad Stg | 7.6 | 4.268 to 10.93 | Yes | **** | <0.0001 |
| HI rM5 vs. HI Ad rM5 | 13.6 | 10.27 to 16.93 | Yes | **** | <0.0001 |
| HI rM5 vs. HI Stg | 6.4 | 3.068 to 9.732 | Yes | *** | 0.0001 |
| HI rM5 vs. HI Ad Stg | 23.8 | 20.47 to 27.13 | Yes | **** | <0.0001 |
| HI Ad rM5 vs. HI Stg | -7.2 | -10.53 to -3.868 | Yes | **** | <0.0001 |
| HI Ad rM5 vs. HI Ad Stg | 10.2 | 6.868 to 13.53 | Yes | **** | <0.0001 |
| HI Stg vs. HI Ad Stg | 17.4 | 14.07 to 20.73 | Yes | **** | <0.0001 |

Panel F (left): Normality test and Tukey's multiple comparison test

| Col. stats | A |
|---|---|
| | Normality |
| | Y |
| Number of values | 15 |
| | |
| D'Agostino & Pearson normality test | |
| K2 | 5.275 |
| P value | 0.0715 |
| Passed normality test (alpha=0.05)? | Yes |
| P value summary | ns |

| 1way ANOVA<br>Multiple comparisons | | | | | |
|---|---|---|---|---|---|
| Number of families | 1 | | | | |
| Number of comparisons per family | 3 | | | | |
| Alpha | 0.05 | | | | |
| | | | | | |
| Tukey's multiple comparisons test | Mean Diff. | 95.00% CI of diff. | Significant? | Summary | Adjusted P Value |
| | | | | | |
| PBS vs. rM5 | -40.6 | -45.9 to -35.3 | Yes | **** | <0.0001 |
| PBS vs. Stg | -34.6 | -39.9 to -29.3 | Yes | **** | <0.0001 |
| rM5 vs. Stg | 6 | 0.7 to 11.3 | Yes | * | 0.0267 |

Panel F (right): Normality test and Tukey's multiple comparison test

| Col. stats | A |
|---|---|
| | Normality |
| | Y |
| Number of values | 15 |
| | |
| D'Agostino & Pearson normality test | |
| K2 | 1.953 |
| P value | 0.3766 |
| Passed normality test (alpha=0.05)? | Yes |
| P value summary | ns |

| 1way ANOVA<br>Multiple comparisons | | | | | |
|---|---|---|---|---|---|
| Number of families | 1 | | | | |
| Number of comparisons per family | 3 | | | | |
| Alpha | 0.05 | | | | |
| | | | | | |
| Tukey's multiple comparisons test | Mean Diff. | 95.00% CI of diff. | Significant? | Summary | Adjusted P Value |
| | | | | | |
| PBS vs. rM5 | -9.2 | -13.86 to -4.538 | Yes | *** | 0.0005 |
| PBS vs. Stg | -18.2 | -22.86 to -13.54 | Yes | **** | <0.0001 |
| rM5 vs. Stg | -9 | -13.66 to -4.338 | Yes | *** | 0.0007 |

Panel G (left): Normality test and Tukey's multiple comparison test

| Col. stats | A |
|---|---|
| | Normality |
| | Y |
| 1 Number of values | 15 |
| 2 | |
| 3 D'Agostino & Pearson normality test | |
| 4 K2 | 5.275 |
| 5 P value | 0.0715 |
| 6 Passed normality test (alpha=0.05)? | Yes |
| 7 P value summary | ns |

1way ANOVA
Multiple comparisons

| | | | | | | |
|---|---|---|---|---|---|---|
| 1 | Number of families | 1 | | | | |
| 2 | Number of comparisons per family | 3 | | | | |
| 3 | Alpha | 0.05 | | | | |
| 4 | | | | | | |
| 5 | Tukey's multiple comparisons test | Mean Diff. | 95.00% CI of diff. | Significant? | Summary | Adjusted P Value |
| 6 | | | | | | |
| 7 | PBS vs. rM5 | -32 | -33.34 to -30.66 | Yes | **** | <0.0001 |
| 8 | PBS vs. Stg | -33.8 | -35.14 to -32.46 | Yes | **** | <0.0001 |
| 9 | rM5 vs. Stg | -1.8 | -3.143 to -0.4572 | Yes | ** | 0.0099 |

Panel G (right): Normality test and Tukey's multiple comparison test

| Col. stats | A |
|---|---|
| | Normality |
| | Y |
| 1 Number of values | 15 |
| 2 | |
| 3 D'Agostino & Pearson normality test | |
| 4 K2 | 1.953 |
| 5 P value | 0.3766 |
| 6 Passed normality test (alpha=0.05)? | Yes |
| 7 P value summary | ns |

1way ANOVA
Multiple comparisons

| | | | | | | |
|---|---|---|---|---|---|---|
| 1 | Number of families | 1 | | | | |
| 2 | Number of comparisons per family | 3 | | | | |
| 3 | Alpha | 0.05 | | | | |
| 4 | | | | | | |
| 5 | Tukey's multiple comparisons test | Mean Diff. | 95.00% CI of diff. | Significant? | Summary | Adjusted P Value |
| 6 | | | | | | |
| 7 | PBS vs. rM5 | -87.6 | -99.94 to -75.26 | Yes | **** | <0.0001 |
| 8 | PBS vs. Stg | -100.8 | -113.1 to -88.46 | Yes | **** | <0.0001 |
| 9 | rM5 vs. Stg | -13.2 | -25.54 to -0.8584 | Yes | * | 0.0360 |

## 9.7 Statistical analysis of Supplementary Figure 9.2

Panel D: Normality test and Tukey's multiple comparison test

| Col. stats | A |
|---|---|
| | Normality |
| | Y |
| 1 Number of values | 25 |
| 2 | |
| 3 D'Agostino & Pearson normality test | |
| 4 K2 | 0.5973 |
| 5 P value | 0.7418 |
| 6 Passed normality test (alpha=0.05)? | Yes |
| 7 P value summary | ns |

1way ANOVA
Multiple comparisons

| | | | | | | |
|---|---|---|---|---|---|---|
| 1 | Number of families | 1 | | | | |
| 2 | Number of comparisons per family | 10 | | | | |
| 3 | Alpha | 0.05 | | | | |
| 4 | | | | | | |
| 5 | Tukey's multiple comparisons test | Mean Diff. | 95.00% CI of diff. | Significant? | Summary | Adjusted P Value |
| 6 | | | | | | |
| 7 | HI PBS vs. HI rM5 | -21.4 | -24.1 to -18.7 | Yes | **** | <0.0001 |
| 8 | HI PBS vs. HI Ad rM5 | -0.6 | -3.303 to 2.103 | No | ns | 0.9618 |
| 9 | HI PBS vs. HI Stg | -23.8 | -26.5 to -21.1 | Yes | **** | <0.0001 |
| 10 | HI PBS vs. HI Ad Stg | 0.2 | -2.503 to 2.903 | No | ns | 0.9994 |
| 11 | HI rM5 vs. HI Ad rM5 | 20.8 | 18.1 to 23.5 | Yes | **** | <0.0001 |
| 12 | HI rM5 vs. HI Stg | -2.4 | -5.103 to 0.3031 | No | ns | 0.0972 |
| 13 | HI rM5 vs. HI Ad Stg | 21.6 | 18.9 to 24.3 | Yes | **** | <0.0001 |
| 14 | HI Ad rM5 vs. HI Stg | -23.2 | -25.9 to -20.5 | Yes | **** | <0.0001 |
| 15 | HI Ad rM5 vs. HI Ad Stg | 0.8 | -1.903 to 3.503 | No | ns | 0.8989 |
| 16 | HI Stg vs. HI Ad Stg | 24 | 21.3 to 26.7 | Yes | **** | <0.0001 |

Panel E: Normality test and Tukey's multiple comparison test

| Col. stats | A |
|---|---|
| | Normality |
| | Y |
| 1 Number of values | 25 |
| 2 | |
| 3 D'Agostino & Pearson normality test | |
| 4 K2 | 1.638 |
| 5 P value | 0.4408 |
| 6 Passed normality test (alpha=0.05)? | Yes |
| 7 P value summary | ns |

1way ANOVA
Multiple comparisons

| | | | | | | |
|---|---|---|---|---|---|---|
| 1 | Number of families | 1 | | | | |
| 2 | Number of comparisons per family | 10 | | | | |
| 3 | Alpha | 0.05 | | | | |
| 4 | | | | | | |
| 5 | Tukey's multiple comparisons test | Mean Diff. | 95.00% CI of diff. | Significant? | Summary | Adjusted P Value |
| 6 | | | | | | |
| 7 | HI PBS vs. HI rM5 | -147.4 | -191.7 to -103.1 | Yes | **** | <0.0001 |
| 8 | HI PBS vs. HI Ad rM5 | -60.6 | -104.9 to -16.33 | Yes | ** | 0.0045 |
| 9 | HI PBS vs. HI Stg | -231 | -275.3 to -186.7 | Yes | **** | <0.0001 |
| 10 | HI PBS vs. HI Ad Stg | -93.4 | -137.7 to -49.13 | Yes | **** | <0.0001 |
| 11 | HI rM5 vs. HI Ad rM5 | 86.8 | 42.53 to 131.1 | Yes | **** | <0.0001 |
| 12 | HI rM5 vs. HI Stg | -83.6 | -127.9 to -39.33 | Yes | *** | 0.0001 |
| 13 | HI rM5 vs. HI Ad Stg | 54 | 9.728 to 98.27 | Yes | * | 0.0123 |
| 14 | HI Ad rM5 vs. HI Stg | -170.4 | -214.7 to -126.1 | Yes | **** | <0.0001 |
| 15 | HI Ad rM5 vs. HI Ad Stg | -32.8 | -77.07 to 11.47 | No | ns | 0.2139 |
| 16 | HI Stg vs. HI Ad Stg | 137.6 | 93.33 to 181.9 | Yes | **** | <0.0001 |

Panel F (left): Normality test and Tukey's multiple comparison test

| Col. stats | A |
|---|---|
| | Normality |
| | Y |
| Number of values | 15 |
| | |
| D'Agostino & Pearson normality test | |
| K2 | 3.997 |
| P value | 0.1356 |
| Passed normality test (alpha=0.05)? | Yes |
| P value summary | ns |

| 1way ANOVA<br>Multiple comparisons | | | | | |
|---|---|---|---|---|---|
| Number of families | 1 | | | | |
| Number of comparisons per family | 3 | | | | |
| Alpha | 0.05 | | | | |
| | | | | | |
| Tukey's multiple comparisons test | Mean Diff. | 95.00% CI of diff. | Significant? | Summary | Adjusted P Value |
| | | | | | |
| PBS vs. rM5 | -17.6 | -23.72 to -11.48 | Yes | **** | <0.0001 |
| PBS vs. Stg | -15.8 | -21.92 to -9.677 | Yes | **** | <0.0001 |
| rM5 vs. Stg | 1.8 | -4.323 to 7.923 | No | ns | 0.7193 |

Panel F (right): Normality test and Tukey's multiple comparison test

| Col. stats | A |
|---|---|
| | Normality |
| | Y |
| Number of values | 15 |
| | |
| D'Agostino & Pearson normality test | |
| K2 | 5.433 |
| P value | 0.0661 |
| Passed normality test (alpha=0.05)? | Yes |
| P value summary | ns |

| 1way ANOVA<br>Multiple comparisons | | | | | |
|---|---|---|---|---|---|
| Number of families | 1 | | | | |
| Number of comparisons per family | 3 | | | | |
| Alpha | 0.05 | | | | |
| | | | | | |
| Tukey's multiple comparisons test | Mean Diff. | 95.00% CI of diff. | Significant? | Summary | Adjusted P Value |
| | | | | | |
| PBS vs. rM5 | -203.2 | -254.5 to -151.9 | Yes | **** | <0.0001 |
| PBS vs. Stg | -222.8 | -274.1 to -171.5 | Yes | **** | <0.0001 |
| rM5 vs. Stg | -19.6 | -70.88 to 31.68 | No | ns | 0.5791 |

Panel G (left): Normality test and Tukey's multiple comparison test

| Col. stats | A |
|---|---|
| | Normality |
| | Y |
| Number of values | 15 |
| | |
| D'Agostino & Pearson normality test | |
| K2 | 2.883 |
| P value | 0.2366 |
| Passed normality test (alpha=0.05)? | Yes |
| P value summary | ns |

| 1way ANOVA<br>Multiple comparisons | | | | | |
|---|---|---|---|---|---|
| Number of families | 1 | | | | |
| Number of comparisons per family | 3 | | | | |
| Alpha | 0.05 | | | | |
| | | | | | |
| Tukey's multiple comparisons test | Mean Diff. | 95.00% CI of diff. | Significant? | Summary | Adjusted P Value |
| | | | | | |
| PBS vs. rM5 | -18.8 | -32.38 to -5.221 | Yes | ** | 0.0080 |
| PBS vs. Stg | -18.8 | -32.38 to -5.221 | Yes | ** | 0.0080 |
| rM5 vs. Stg | 0 | -13.58 to 13.58 | No | ns | >0.9999 |

Panel G (right): Normality test and Tukey's multiple comparison test

| Col. stats | A |
|---|---|
| | Normality |
| | Y |
| Number of values | 15 |
| | |
| D'Agostino & Pearson normality test | |
| K2 | 0.241 |
| P value | 0.8865 |
| Passed normality test (alpha=0.05)? | Yes |
| P value summary | ns |

| 1way ANOVA<br>Multiple comparisons | | | | | |
|---|---|---|---|---|---|
| Number of families | 1 | | | | |
| Number of comparisons per family | 3 | | | | |
| Alpha | 0.05 | | | | |
| | | | | | |
| Tukey's multiple comparisons test | Mean Diff. | 95.00% CI of diff. | Significant? | Summary | Adjusted P Value |
| | | | | | |
| PBS vs. rM5 | -90.4 | -149.7 to -31.14 | Yes | ** | 0.0041 |
| PBS vs. Stg | -133.8 | -193.1 to -74.54 | Yes | *** | 0.0002 |
| rM5 vs. Stg | -43.4 | -102.7 to 15.86 | No | ns | 0.1663 |

## 9.8 Statistical analysis of Supplementary Figure 9.6

Serum: Normality test and Tukey's multiple comparison test

| Col. stats | A |
|---|---|
| | Normality Serum |
| | Y |
| Number of values | 20 |
| | |
| D'Agostino & Pearson normality test | |
| K2 | 2.254 |
| P value | 0.3239 |
| Passed normality test (alpha=0.05)? | Yes |
| P value summary | ns |

| 1way ANOVA<br>Multiple comparisons | | | | | |
|---|---|---|---|---|---|
| Number of families | 1 | | | | |
| Number of comparisons per family | 10 | | | | |
| Alpha | 0.05 | | | | |
| | | | | | |
| Tukey's multiple comparisons test | Mean Diff. | 95.00% CI of diff. | Significant? | Summary | Adjusted P Value |
| | | | | | |
| PBS-HI vs. rM5-HI | -10.75 | -12.64 to -8.859 | Yes | **** | <0.0001 |
| PBS-HI vs. rM5-HI Ad | 0 | -1.891 to 1.891 | No | ns | >0.9999 |
| PBS-HI vs. Stg-HI | -16.25 | -18.14 to -14.36 | Yes | **** | <0.0001 |
| PBS-HI vs. Stg-HI Ad | 0 | -1.891 to 1.891 | No | ns | >0.9999 |
| rM5-HI vs. rM5-HI Ad | 10.75 | 8.859 to 12.64 | Yes | **** | <0.0001 |
| rM5-HI vs. Stg-HI | -5.5 | -7.391 to -3.609 | Yes | **** | <0.0001 |
| rM5-HI vs. Stg-HI Ad | 10.75 | 8.859 to 12.64 | Yes | **** | <0.0001 |
| rM5-HI Ad vs. Stg-HI | -16.25 | -18.14 to -14.36 | Yes | **** | <0.0001 |
| rM5-HI Ad vs. Stg-HI Ad | 0 | -1.891 to 1.891 | No | ns | >0.9999 |
| Stg-HI vs. Stg-HI Ad | 16.25 | 14.36 to 18.14 | Yes | **** | <0.0001 |

T-cell only: Normality test and Tukey's multiple comparison test

| Col. stats | A |
|---|---|
| | Normality Cell only |
| | Y |
| Number of values | 12 |
| | |
| D'Agostino & Pearson normality test | |
| K2 | 1.086 |
| P value | 0.5809 |
| Passed normality test (alpha=0.05)? | Yes |
| P value summary | ns |

| 1way ANOVA<br>Multiple comparisons | | | | | |
|---|---|---|---|---|---|
| Number of families | 1 | | | | |
| Number of comparisons per family | 3 | | | | |
| Alpha | 0.05 | | | | |
| | | | | | |
| Tukey's multiple comparisons test | Mean Diff. | 95.00% CI of diff. | Significant? | Summary | Adjusted P Value |
| | | | | | |
| PBS-Cell vs. rM5-Cell | -1 | -2.434 to 0.4343 | No | ns | 0.1814 |
| PBS-Cell vs. Stg-Cell | 0.75 | -0.6843 to 2.184 | No | ns | 0.3534 |
| rM5-Cell vs. Stg-Cell | 1.75 | 0.3157 to 3.184 | Yes | * | 0.0193 |

TNF-α: Normality test and Tukey's multiple comparison test

| Col. stats | A |
|---|---|
| | Normaltiy TNF |
| | Y |
| Number of values | 9 |
| | |
| D'Agostino & Pearson normality test | |
| K2 | 1.333 |
| P value | 0.5134 |
| Passed normality test (alpha=0.05)? | Yes |
| P value summary | ns |

| 1way ANOVA<br>Multiple comparisons | | | | | |
|---|---|---|---|---|---|
| Number of families | 1 | | | | |
| Number of comparisons per family | 3 | | | | |
| Alpha | 0.05 | | | | |
| | | | | | |
| Tukey's multiple comparisons test | Mean Diff. | 95.00% CI of diff. | Significant? | Summary | Adjusted P Value |
| | | | | | |
| PBS-TNF vs. rM5-TNF | 9 | -1.43 to 19.43 | No | ns | 0.0846 |
| PBS-TNF vs. Stg-TNF | 8.667 | -1.763 to 19.1 | No | ns | 0.0958 |
| rM5-TNF vs. Stg-TNF | -0.3333 | -10.76 to 10.1 | No | ns | 0.9947 |